

ACTA
PATHOLOGICA
ET MICROBIOLOGICA
SCANDINAVICA

A PATHOLOGY

EDITORIAL BOARD

STEEN OLSEN DENMARK

J RAPOLA FINLAND

O BJARNASON ICELAND

K ARNESEN NORWAY

J L E ERICSSON SWEDEN

EDITOR IN CHIEF

J CHR SHIM

ADVISORY BOARD

J RYGAARD DENMARK

J VISFELDT DENMARK

T NEVALAINEN FINLAND

L TEPPÖ FINLAND

G GEORGSSON ICELAND

J HALLGRÍMSSON ICELAND

T HOVIG NORWAY

O D LÆRUM NORWAY

T BERG SWEDEN

K NILSSON SWEDEN

VOL. 88 A, FASC 1 JANUARY 1980

ISSN 0165-4184

MUNKSGAARD COPENHAGEN

Founded 1924

Editor-in Chief	J CHR SIIM, M D, Copenhagen Denmark
Managing Editors	JAKOB VISFELDT, M D and ERIK BRUMMERSTEDT, D V M
Consultant for Illustrations	Mr AKSEL BIRCH-ANDERSEN
Editorial Office	c/o INGER DANIELSEN, Secretary, Johnstrups Allé 6, DK 1923 Copenhagen V, Denmark

Acta Pathologica et Microbiologica Scandinavica is intended for the prompt publication of original research in the fields of pathology, microbiology, and immunology. It is included in Current Contents, Excerpta Medica and Medlars.

Acta Pathologica et Microbiologica Scandinavica is a nonprofit making scientific journal. Since 1924, it has been published by the Scandinavian Societies for Medical Microbiology and Pathology. It appears in three sections: Section A Pathology, Section B Microbiology, and Section C Immunology.

Acta Pathologica et Microbiologica Scandinavica has subscribers in more than seventy countries throughout the world with a wide readership in the major research institutes, hospitals, laboratories, and specialist libraries.

EDITORIAL CORRESPONDENCE

All communications regarding manuscripts and editorial matters should be addressed to the Editorial Office, c/o Inger Danielsen, Secretary, Johnstrups Allé 6, DK-1923 Copenhagen V, Denmark.

SUBSCRIPTION

At present one annual volume of Section A, one of Section B, and one of Section C (each section consisting of 6 issues appearing bimonthly) will contain a total of approximately 1300 pages. During the past few years approximately four free supplements have been issued annually. These supplements will be delivered separately to the subscribers by surface mail at no extra charge. The subscription price is

Sect A, B and C	D kr 980 - plus postage	D kr 84 - (\$ 202.20 £ 90.45 DM 351.15)
Sect A	D kr 580 - plus postage	D kr 28 - (\$ 115.55 £ 51.70 DM 200.70)
Sect B	D kr 580 - plus postage	D kr 28 - (\$ 115.55 £ 51.70 DM 200.70)
Sect C	D kr 460 - plus postage	D kr 28 - (\$ 90.90 £ 41.50 DM 160.05)
Sect A and C (combined)	D kr 860 - plus postage	D kr 56 - (\$ 174.10 £ 77.90 DM 302.30)
Sect B and C (combined)	D kr 860 - plus postage	D kr 56 - (\$ 174.10 £ 77.90 DM 302.30)

Back numbers (whole volumes or single copies) are available.
NB: All prices are subject to exchange rate fluctuation.

© 1980 by Acta Pathologica et Microbiologica Scandinavica. All rights reserved.
Reproduction in any form, including microfilm, without written permission of the Editor is prohibited.

Second class postage paid at Jamaica, N.Y. Airfreight and mailing in the U.S. by Publications Expediting Inc., Elmont, N.Y. 11003. Printed in Denmark.

ACTA PATHOLOGICA ET MICROBIOLOGICA SCANDINAVICA

Section **A** PATHOLOGY

EDITORIAL BOARD

STEEN OLSEN DENMARK
J RAPOLA FINLAND
O BJARNASON ICELAND
K ARNESEN NORWAY
J L E ERICSSON SWEDEN

EDITOR IN-CHIEF

J CHR SIIM

ADVISORY BOARD

J RYGAARD DENMARK
J VISFELDT DENMARK
T NEVALAINEN FINLAND
L TEPPÖ FINLAND
G GEORGSSON ICELAND
J HALLGRÍMSSON ICELAND
T HOVIG NORWAY
O D LÆRUM NORWAY
T BERGE SWEDEN
K NILSSON SWEDEN

VOL 88 A FASC 1-6 1980

MUNKSGAARD COPENHAGEN

Published by the
Scandinavian Societies for Microbiology and Pathology



Acta Pathologica
et Microbiologica
Scandinavica

1980

All rights reserved

Reproduction in any form
including microfilm without written permission
of the Editor is prohibited

Distributed by Munksgaard
International Booksellers and Publishers Ltd
35 Norre Sogade DK 1370 Copenhagen N Denmark

Printed by
bording grafik a/s
Copenhagen

INDEX

VOL. 88 A FASC 1-6 1980

<i>Afelius Lars Erik</i>	5	<i>Halken S</i>	255
<i>Albrechtsen R</i>	175	<i>Hallgren Bo</i>	11
<i>Alumets J</i>	103	<i>Hamberg Hans</i>	231
<i>Andersson Ingvar</i>	416	<i>Hansen Ole Paaske</i>	25
<i>Anniko Matti</i>	19	<i>Hansen T Mørk</i>	143
<i>Arbogh Bengt</i>	341	<i>Helin G</i>	143
<i>Arro E</i>	327	<i>Helin Heikki</i>	75
<i>Auer G</i>	355	<i>Helin P</i>	143
<i>Benediktisdottir Kristrun</i>	161	<i>Helweg Larsen Karin</i>	307
<i>Birch Andersen Aksel</i>	397	<i>Hjelt L</i>	217
<i>Blom Erik</i>	397	<i>Holund B</i>	143
<i>Blom Jens</i>	25	<i>Holm Lars Erik</i>	251
<i>Blomquist E</i>	327	<i>Hultcrantz Rolf</i>	341
<i>Boeryd Bernt</i>	11	<i>Ihamaki T</i>	217
<i>Bojaeri Louis Jacques van</i>	415	<i>Jacobsen Marianne</i>	151
<i>Boquist Lennart</i>	201	<i>Jacobsen Marianne</i>	369
<i>Brunk U</i>	327	<i>Jakobsen A L</i>	119
<i>Brunk Ulf T</i>	231	<i>Jensen K Birger</i>	383
<i>Brandolin T</i>	291	<i>Jensen Mogens Krogh</i>	377
<i>Bremnitz J</i>	119	<i>Johansen Preben</i>	377
<i>Christensen Hans Ewald</i>	55	<i>Jung Bo</i>	231
<i>Christensen N</i>	285	<i>Juntti Berggren Lisa</i>	339
<i>Christensen Steen Bach</i>	61	<i>Keiding Niels</i>	307
<i>Christiansen L A</i>	383	<i>Kekki M</i>	217
<i>Clausen Per Prætorius</i>	225	<i>Kofod B</i>	143
<i>Clausen Per Prætorius</i>	299	<i>Kristensen Ingrid B</i>	89
<i>Clausen Per Prætorius</i>	369	<i>Kvinnslund Stener</i>	111
<i>Collins V P</i>	327	<i>Ladefoged Christian</i>	55
<i>Ehnbage Anita</i>	5	<i>Lagerberg Fredrik</i>	161
<i>Eide Tor J</i>	97	<i>Lambertsen G</i>	41
<i>Eide Tor J</i>	211	<i>Langmark F T</i>	41
<i>Ericsson Jan L E</i>	231	<i>Langmark F T</i>	179
<i>Ericsson Jan L E</i>	341	<i>Larsson S</i>	1
<i>Falkner S</i>	103	<i>Lindgren Jan</i>	49
<i>Forsberg John Gunnar</i>	111	<i>Linell F</i>	59
<i>Francis Dorihe</i>	151	<i>Linell F</i>	416
<i>Fredriksson B A</i>	327	<i>Ljungberg O</i>	59
<i>Fyhrquist Frej</i>	241	<i>Ljungberg O</i>	103
<i>Garbarsch C</i>	143	<i>Ljungberg O</i>	416
<i>Gram Niels</i>	307	<i>Lønning Per Eystein</i>	111
<i>Grimelius L</i>	103	<i>Lowhagen Torsten</i>	251
<i>Grimelius L</i>	125	<i>Lorenzen M</i>	255
<i>Grimelius L</i>	339	<i>Lorenzen I</i>	143
<i>Grossmann Gerlie</i>	359	<i>Lundell Lars</i>	161
	103	<i>Lundqvist Monalill</i>	339

Published by the
Scandinavian Societies for Microbiology and Pathology

©
Acta Pathologica
et Microbiologica
Scandinavica
1980
All rights reserved

Reproduction in any form
including microfilm without written permission
of the Editor is prohibited

Distributed by Munksgaard
International Booksellers and Publishers Ltd
35 Norre Sogade DK 1370 Copenhagen K Denmark

Printed by
bording grafik a/s
Copenhagen

Actin bone immunofluorescence transmission electron microscopy	129	Coronary heart disease atherosclerosis coronary artery Finnish men	167
Adenylate cyclase cervical carcinoma mouse neoplasm transplantation estradiol progesterone	111	DNA analyses human breast carcinoma	355
Alcohol consumption maternal fetal death growth retardation microscopic malformations	285	DOCA NaCl hypertension nephritis immune complexes rat	241
Alloxan diabetes alloxan antagonism pathogenesis inorganic phosphate intracellular pH mitochondrial lesion	201	Duodenal ulcer cimetidine gastric acid secretion serum gastrin gastrin-cell density	383
Alpha 1 antitrypsin deficiency alpha 1 antitrypsin globules cirrhosis liver biopsies	225	Endodermal sinus tumour hemoglobin A and F human yolk sac immunohistochemistry	175
Alpha 1 antitrypsin globules alpha 1 antitrypsin deficiency cirrhosis liver biopsies	225	Enkephalin β -endorphin rectal carcinoid mixed endocrine tumour immunocytochemistry	103
Alpha 1-antitrypsin liver tissue immunohistochemistry fixation	299	Fetal death alcohol consumption maternal growth retardation microscopic malformations	285
Antral gastrin producing cells immunohistochemistry quantitation	255	Fine needle aspiration renal biopsy glomerular diseases	75
Antrum human curvatures mucosal volume	417	Finnish men atherosclerosis coronary artery coronary heart disease	167
Aorta thoracic atherosclerosis	97	Fish oil rapeseed cardiac triglycerides heart lesions pigs	41
Articular cartilage osteoarthritis glycosaminoglycans	61	Fish oil rapeseed oil heart lesions rats	179
Atherosclerosis coronary artery coronary heart disease Finnish men	167	Gammopathy monoclonal enzymocytochemistry immunohistochemistry	377
Atherosclerosis thoracic aorta	97	Gastric carcinoma intestinal metaplasia premalignant lesions carcinogenesis histochemistry	217
Bacteroides fragilis lipopolysaccharide chemotactic factor bone resorption	263	Gastrin-cell density duodenal ulcer cimetidine gastric acid secretion serum gastrin	383
Basal cell carcinoma head and neck histological scoring system recurrences	5	Gastrin producing cells antral immunohistochemistry quantitation	255
β -endorphin enkephalin rectal carcinoid mixed endocrine tumour immunocytochemistry	103	Glial cell cultures ultrastructure	327
Bone resorption chemotactic factor Bacteroides fragilis lipopolysaccharide	263	Glomerular diseases fine needle aspiration renal biopsy	75
Breast carcinoma human DNA analyses	355	Glomerulonephritis nephrotic syndrome renal biopsy survival	319
Breast carcinoma tubular carcinoma sclerosing lesions classification	59	Glycosaminoglycans articular cartilage osteoarthritis	61
Breast osteogenic sarcoma	161		285
Bronchiolar epithelial lesions artificial ventilation hyaline membrane disease IRDS premature newborn rabbit	359		175
Bursa of Fabricius chemical bursectomy colchicine	407		55
Carcinoembryonic antigen fetal tissue maternal serum	49	Urynx carcinoma	307
Carcinoid rectal mixed endocrine tumour enkephalin β -endorphin immunocytochemistry	103		195
Carrageenan colon stereomicroscopy histology	135	bronchiolar epithelial lesions IRDS premature newborn rabbit	359
Cartilage immobilization osteoarthritis scanning electron microscopy	291	Hypertension nephritis DOCA NaCl immune complexes rat	241
C-cells thyroid silver staining technique	339	Immunoglobulin immunoperoxidase fixation trypsinization lymphoid tissue	369
Cervical carcinoma neoplasm transplantation mouse adenylate cyclase estradiol progesterone	111	Immunoperoxidase immunoglobulin fixation trypsinization lymphoid tissue	369
Cimetidine duodenal ulcer gastric acid secretion serum gastrin gastrin-cell density	383	Inflammatory cells non lymphoid tumours	387
Cirrhosis liver biopsies alpha 1 antitrypsin deficiency alpha 1 antitrypsin globules	225	Inner ear degeneration genetic old English sheep-dog meninges labyrinth	19
Colchicine bursa of Fabricius chemical bursectomy	407	Intercostal artery orifices intimal folds rabbit aorta	69
Colon carrageenan stereomicroscopy histology	135		217
Congophilic substance hip joints autopsy material	55		217

<i>Mansa Bendi</i>	25	<i>Siurala M</i>	217
<i>Mark J</i>	189	<i>Smidth Susanne</i>	369
<i>Melsen Flemming</i>	83	<i>Søndergaard Knud</i>	269
<i>Miettinen Aaro</i>	241	<i>Søndergaard Knud</i>	275
<i>Møller Jens Chr</i>	89	<i>Sorvari Tapani E</i>	407
<i>Mosekilde Leif</i>	83	<i>Stalsberg Helge</i>	211
<i>Nielsen H Overgaard</i>	255	<i>Sundler F</i>	103
<i>Nielsen H Overgaard</i>	383	<i>Sundstrom C</i>	189
<i>Nielsen H Overgaard</i>	417	<i>Svaar H</i>	41
<i>Nilsen Rune</i>	129	<i>Svaar H</i>	179
<i>Nilsson R</i>	359	<i>Sveen Kjell</i>	263
<i>Nordgren Hans</i>	5	<i>Svendsen Einar</i>	69
<i>Nyberg Marcus</i>	319	<i>Svendsen Einar</i>	97
<i>Olsen Grete</i>	275	<i>Svennevig J L</i>	387
<i>Olsen P Skov</i>	135	<i>Tallqvist Gustav</i>	319
<i>Olsson Tomas</i>	195	<i>Thulin Anders</i>	161
<i>Olsson Yngve</i>	125	<i>Tikkaenen Ilkka</i>	241
<i>Opstvedt J</i>	41	<i>Tornroth Tom</i>	241
<i>Pasternack Amos</i>	319	<i>Tribukait B</i>	355
<i>Pettersson Erna</i>	319	<i>van Bogaert Louis Jacques</i>	415
<i>Poulsen S Seier</i>	135	<i>Varis A</i>	217
<i>Rasmussen B Bruun</i>	285	<i>Videman T</i>	291
<i>Reimann Inge</i>	61	<i>Westermarck B</i>	189
<i>Ridell B</i>	1	<i>Wewer U</i>	175
<i>Rismyhr Bjørn</i>	211	<i>Wilander E</i>	103
<i>Rissanen Viljo</i>	167	<i>Wilander E</i>	339
<i>Robertson B</i>	359	<i>Wimberley P D</i>	175
<i>Romppanen Timo</i>	407	<i>Wroblewski Romulad</i>	341
<i>Seppala K</i>	217		
<i>Silfversward Claes</i>	251		
<i>Sipponen P</i>	217		
		A See Ae Æ See Ae Ö See Oe	
		Ø See Oe Å See Aa	

COEXISTENCE OF A THYMOMA AND HODGKIN'S DISEASE OF THE THYMUS

A Case Report

B RIDELL and S LARSSON

The Departments of Pathology I and Thoracic Surgery Sahlgrenska sjukhuset, University of Goteborg Sweden

Ridell B & Larsson S Coexistence of a thymoma and Hodgkin's disease of the thymus. A case report. Acta path microbiol scand Sect A 88 1-4, 1980

A case of simultaneous occurrence of a thymoma and Hodgkin's disease of the thymus is described

Key words Thymoma Hodgkin's disease of the thymus

B Ridell Department of Pathology Sahlgrenska sjukhuset 413 45 Goteborg Sweden

Received 27 xii 78 Accepted 11 vi 79

In most instances thymic tumours have a characteristic mode of growth and microscopical picture. Some tumours of the thymus, however, have long been a challenge to pathologists, owing to their granulomatous appearance, and have been considered variously as a variant of thymoma or Hodgkin's disease of the thymus. The present report deals with a thymic mass that contained two distinct tumours, one of which was a thymoma and the other Hodgkin's disease of the thymus.

CASE HISTORY

A 58-year-old man was admitted to Sahlgrenska sjukhuset in 1972 owing to severe pruritus. His general condition was good and no abnormalities were noted at the physical examinations. A radiological examination of the chest revealed an abnormal shadow at the level of the arch of the aorta, which was considered to be a tumour of mediastinal origin. At mediastinoscopy a few enlarged lymph nodes were found under the carina. Histologically these lymph nodes were anthracotic and without

Fig 1 Hodgkin's disease of the thymus. Tumour nodules surrounded by sclerotic bands (Originally paraffin-embedding. Specimen re-embedded in methacrylate May-Grunwald Giemsa $\times 30$)



IRDS artificial ventilation bronchiolar epithelial lesions hyaline membrane disease premature newborn rabbit	359	Plasma cells multiple myeloma ultrastructure nuclear/cytoplasmic asynchrony	25
Iron overload liver ultrastructure histochemistry	341	Prostate carcinoma transurethral resectates histology overlooking	211
Larynx carcinoma variance component models histological grading	307	Proteoglycans nucleic acids granulation tissue rats	143
Liver biopsies cirrhosis alpha 1 antitrypsin deficiency alpha 1 antitrypsin globules	225	Pulmonary blastoma frequency	151
Liver iron overload ultrastructure histochemistry	341	Pyelonephritis xanthogranulomatous clinicopathological study pathogenesis	89
Liver tissue alpha 1 antitrypsin immunohistochemistry fixation	299	Rapeseed oil fish oil cardiac triglycerides heart lesions pigs	41
Malignant melanoma cutaneous classification	269	Rapeseed oil fish oil heart lesions rats	179
Malignant melanoma cutaneous foot classification	275	Renal biopsy fine needle aspiration glomerular diseases	75
Methoxy substituted glycerol ethers tumour growth and metastases lipids chemotherapy	11	Renal biopsy glomerulonephritis nephrotic syndrome survival	319
Microfilaments X irradiation cultured human cells transmission electron microscopy cell motility microtubules	231	Silver gold histochemical technique muscle soft tissue tumours	125
Microtubules X irradiation cultured human cells transmission electron microscopy cell motility microfilaments	231	Silver staining technique thyroid parafollicular C cells	339
Mineralization lag time bone histomorphometry tetracycline double labeling	83	Sperm defect tail stump sterility in bulls spermiogenesis distal centriole adjunct granules centriolar adjunct	397
Monoclonal gammopathy enzymocytochemistry immunohistochemistry	377	Suspension culture tumour cells vacuoles TFM microtubules	119
Myeloma multiple plasma cells ultrastructure nuclear/cytoplasmic asynchrony	25	Swedish Cancer Registry malignant thyroid tumour diagnosis	251
Neoplasm transplantation cervical carcinoma mouse adenylate cyclase estradiol progesterone	111	Teratoma malignant established cell line	189
Nephritis hypertension DOCA NaCl immune complexes rat	241	Thymoma Hodgkins diverse thymus	1
Nephrotic syndrome glomerulonephritis renal biopsy survival	319	Thyroid parafollicular C cells silver staining technique	339
Nerve transection horseradish peroxidase axons	195	Thyroid tumour malignant diagnosis Swedish Cancer Registry	251
Non lymphoid tumours inflammatory cells	387	Transurethral resectates prostate carcinoma histology overlooking	211
Nucleic acids proteoglycans granulation tissue rats	143	Tubular carcinoma breast carcinoma sclerosing lesions classification	59
Old English sheepdog genetic inner ear degeneration meningitis labyrinth	19	Vacuoles tumour cells suspension culture TFM microtubules	119
Osteoarthritis articular cartilage glycosaminoglycans	61	Variance component models histological grading larynx carcinoma	307
Osteoarthritis cartilage immobilization scanning electron microscopy	291	Xanthogranulomatous pyelonephritis clinicopathological study pathogenesis	89
Osteogenic sarcoma breast	161	X irradiation cultured human cells transmission electron microscopy cell motility microtubules microfilaments	231

SUPPLEMENTS

Supplement 272	<i>Linnell Folke Ljungberg, Otto and Andersson Ingvor</i> Breast Carcinoma Aspects of early stages progression and related problems Pp 233 1980 (Section A)
Supplement 273	<i>Nilsen Henrik</i> Circulating Immune Complexes Properties Methods for Detection and Disease Models Pp 56 1980 (Section C)

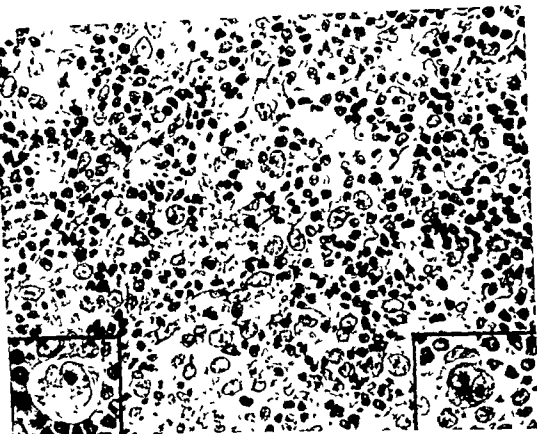


Fig 3 Accumulations of large atypical cells in a mediastinal lymph node ($\times 460$) Lacunar giant cell (left inset) and Reed Sternberg cell (right inset) in the same node ($\times 720$) (Originally paraffin-embedding Specimen re-embedded in methacrylate May Grunwald Giemsa)

tumour and supplementary radiotherapy is an efficacious mode of therapy in Hodgkin's disease of the thymus (Bergh *et al* 1978 b)

It has been stated that a second malignancy is found in 21 per cent of individuals with a thymoma when followed up over a 20 year period (Soadjian *et al* 1968). In our material of thymomas (Bergh *et al* 1978 a) there has not been any other case of a second malignant tumour during a mean observation period of 10 years. The coexistence of a thymoma and Hodgkin's disease must be considered a pure coincidence.

The present case provides an interesting contribution to the discussion about granulomatous lesions in the thymic region. The simultaneous occurrence of an epithelial thymoma and Hodgkin's disease of the thymus as separate tumours supports the view that Hodgkin's disease of the thymus is a distinct : thymomas

REFERENCES

- Bergh N P, Gatzinsky P, Larsson S, Lundin P and Ridell B. Tumours of the thymus and thymic region. I Clinicopathological studies on thymomas. *Annals of thoracic surgery* 25: 91-98, 1978.
- Bergh N P, Gatzinsky P, Larsson S, Lundin P and Ridell B. Tumours of the thymus and thymic region. II Clinicopathological studies on Hodgkin's disease of the thymus. *Annals of thoracic surgery* 25: 99-106, 1978.
- Bloodworth Jr J M B, Hiratsuka H, Hickey R C and Wu J. Ultrastructure of the human thymus. *Thymic tumours and myasthenia gravis. Pathology annual* 10, 1975. Appleton-Century-Crofts/N.Y.
- Burke W A, Burford T H and Dorfman R F. Hodgkin's disease of the mediastinum. *Annals of thoracic surgery* 3: 287-296, 1967.
- Katz A and Lattes R. Granulomatous thymoma or Hodgkin's disease of thymus. A clinical and

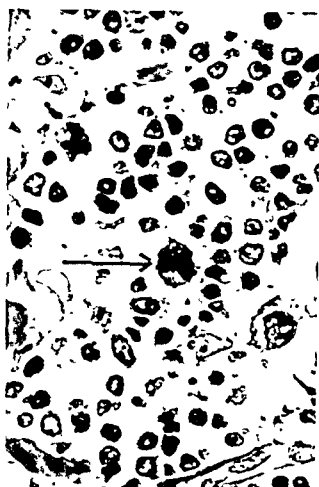


Fig 2 Reed-Sternberg cell in thymic tumour (arrow) (Originally paraffin embedding. Specimen re-embedded in methacrylate. May-Grunwald-Giemsa $\times 720$)

signs of tumour. Bronchoscopy did not reveal any primary lung tumour. At thoracotomy the tumour was located at the mediastinum. It partly enclosed the left subclavian and common carotid arteries. The tumour reached the posterior surface of the sternum and infiltrated the pericardium and the left anonymous vein and vagal nerve. The tumour was removed, together with the remnants of the thymus. The anonymous vein, the vagal nerve and parts of the pericardium and pleura had to be resected. The postoperative course was uneventful. Immediately after the operation the patient spontaneously remarked that the pruritus had completely disappeared.

The operation specimen weighed 275 g. The cut surface of the tumour had solid nodular areas surrounded by thick fibrous bands with a vague demarcation in the periphery. Remnants of the upper thymus horns were seen in the upper part of the specimen. On the left lateral side of the specimen a separate, well-demarcated soft tumour with a diameter of 4 cm was seen.

Microscopically, the large tumour was nodular with the tumour nodules surrounded by sclerotic bands of varying breadth (Fig. 1). The nodular areas had a varying cell density with a mixed cellular composition. Most of

the cells were small lymphocytes but thymic epithelial cells and occasional eosinophils and plasma cells were also present. In the nodules there was an irregular distribution of large multinucleated cells, some of which were Reed-Sternberg cells (Fig. 2). In the periphery of the tumour remnants of thymic tissue were found. In some areas, thymic epithelium was identified in the tumour. A lymph node taken at the pulmonary artery contained vaguely nodular tumour tissue with scattered atypical giant cells, some of which were lacunar cells, others Reed-Sternberg cells (Fig. 3). The picture here was considered to be consistent with Hodgkin's disease nodular sclerosis.

Three other lymph nodes taken from the vicinity of the trachea were normal. The separate, well-demarcated tumour was microscopically an epithelial thymoma (Fig. 4).

The patient received full-course radiotherapy postoperatively. He is alive and well, free from clinical disease six years after the operation.

COMMENT

The present case was found in a retrospective analysis of patients with primary tumours in the thymic region operated upon at Sahlgrenska sjukhuset during the period 1954-1975 (Bergh *et al.* 1978 a & b). This series comprised 43 thymomas and 17 cases of Hodgkin's disease of the thymus.

A thymic origin of the present tumour seems likely judging by findings of thymic tissue in the periphery of and in the tumour, and the macroscopic findings of two separate tumours with different microscopic patterns were interpreted as evidence that the mediastinal mass was composed of two different tumours.

The controversial problem of the classification of some tumours of the thymus as granulomatous thymomas or Hodgkin's disease of the thymus has been debated for many years (Lowenhaupt 1961, Bloodworth 1975, Rosai 1976). However, reviews of these tumours have established that there is often recurrent disease in other parts of the lymphatic system, which microscopically is Hodgkin's disease (Latiz and Lattes 1969, Keller and Castelman 1974). The traditional reluctance to use the term Hodgkin's disease might partly be due to the fact that otherwise characteristic thymomas have been reported to contain granulomatous areas (Thomson and Thackray 1957) without sclerosis and that the localized tumours with a granulomatous appearance had a better prognosis than Hodgkin's disease usually has. Some reports have established, however, that the prognosis for Hodgkin's disease limited to one site is good (Burke *et al.* 1967). Surgical removal of the

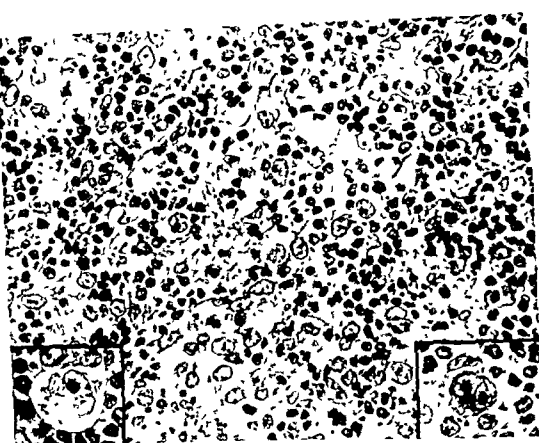


Fig 3 Accumulations of large atypical cells in a mediastinal lymph node ($\times 460$) Lacunar giant cell (left inset) and Reed-Sternberg cell (right inset) in the same node ($\times 720$) (Originally paraffin-embedding. Specimen re-embedded in methacrylate. May Grunwald-Gemsa)

tumour and supplementary radiotherapy is an efficacious mode of therapy in Hodgkin's disease of the thymus (Bergh *et al.* 1978 b).

It has been stated that a second malignancy is found in 21 per cent of individuals with a thymoma when followed up over a 20 year period (Soadjian *et al.* 1968). In our material of thymomas (Bergh *et al.* 1978 a) there has not been any other case of a second malignant tumour during a mean observation period of 10 years. The coexistence of a thymoma and Hodgkin's disease must be considered a pure coincidence.

The present case provides an interesting contribution to the discussion about granulomatous lesions in the thymic region. The simultaneous occurrence of an epithelial thymoma and Hodgkin's disease of the thymus as separate tumours supports the view that Hodgkin's disease of the thymus is a distinct entity from thymomas.

REFERENCES

- Bergh N P, Gatzinsky P, Larsson S, Lund n P and Ridell B. Tumours of the thymus and thymic region I Clinicopathological studies on thymomas. *Annals of thoracic surgery* 25 91-98 1978.
- Bergh N P, Gatzinsky P, Larsson S, Lund n P and Ridell B. Tumours of the thymus and thymic region II Clinicopathological studies on Hodgkin's disease of the thymus. *Annals of thoracic surgery* 25 99-106 1978.
- Bloodworth Jr J M B, Hiratsuka H, Hickey R C and *et al.*
- Burke
- Hodgkin's disease of the mediastinum. *Annals of thoracic surgery* 3 287-296 1967.
- Karr A and Laties R. Granulomatous thymoma or Hodgkin's disease of thymus. A clinical and

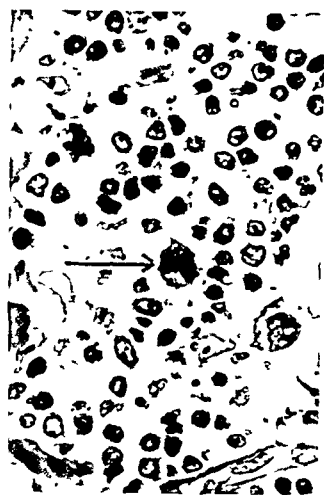


Fig 2 Reed Sternberg cell in thymic tumour (arrow) (Originally paraffin embedding. Specimen re embedded in methacrylate May Grunwald Giemsa $\times 720$)

signs of tumour. Bronchoscopy did not reveal any primary lung tumour. At thoracotomy the tumour was located to the mediastinum. It partly enclosed the left subclavian and common carotid arteries. The tumour reached the posterior surface of the sternum and infiltrated the pericardium and the left anomalous vein and vagal nerve. The tumour was removed together with the remnants of the thymus. The anomalous vein the vagal nerve and parts of the pericardium and pleura had to be resected. The postoperative course was uneventful. Immediately after the operation the patient spontaneously remarked that the pruritus had completely disappeared.

The operation specimen weighed 275 g. The cut surface of the tumour had solid nodular areas surrounded by thick fibrous bands with a vague demarcation in the periphery. Remnants of the upper thymus horns were seen in the upper part of the specimen. On the left lateral side of the specimen a separate well-demarcated soft tumour with a diameter of 4 cm was seen.

Microscopically the large tumour was nodular with the tumour nodules surrounded by sclerotic bands of varying breadth (Fig. 1). The nodular areas had a varying cell density with a mixed cellular composition. Most of

the cells were small lymphocytes but thymic epithelial cells and occasional eosinophils and plasma cells were also present. In the nodules there was an irregular distribution of large multinucleated cells some of which were Reed-Sternberg cells (Fig. 2). In the periphery of the tumour remnants of thymic tissue were found. In some areas thymic epithelium was identified in the tumour. A lymph node taken at the pulmonary artery contained vaguely nodular tumour tissue with scattered atypical giant cells some of which were lacunar cells others Reed-Sternberg cells (Fig. 3). The picture here was considered to be consistent with Hodgkin's disease nodular sclerosis.

Three other lymph nodes taken from the vicinity of the trachea were normal. The separate well-demarcated tumour was microscopically an epithelial thymoma (Fig. 4).

The patient received full course radiotherapy postoperatively. He is alive and well free from clinical disease six years after the operation.

COMMENT

The present case was found in a retrospective analysis of patients with primary tumours in the thymic region operated upon at Sahlgrenska sjukhuset during the period 1954-1975 (Bergh *et al* 1978 a & b). This series comprised 43 thymomas and 17 cases of Hodgkin's disease of the thymus.

A thymic origin of the present tumour seems likely judging by findings of thymic tissue in the periphery of and in the tumour and the macroscopic findings of two separate tumours with different microscopic patterns were interpreted as evidence that the mediastinal mass was composed of two different tumours.

The controversial problem of the classification of some tumours of the thymus as granulomatous thymomas or Hodgkin's disease of the thymus has been debated for many years (Lowenhaupt 1961 Bloodworth 1975 Rosai 1976). However reviews of these tumours have established that there is often recurrent disease in other parts of the lymphatic system which microscopically is Hodgkin's disease (Katz and Lattes 1969 Keller and Castleman 1974). The traditional reluctance to use the term Hodgkin's disease might partly be due to the fact that otherwise characteristic thymomas have been reported to contain granulomatous areas (Thomson and Thackray 1957) without sclerosis and that the localized tumours with a granulomatous appearance had a better prognosis than Hodgkin's disease usually has. Some reports have established however that the prognosis for Hodgkin's disease limited to one site is good (Burke *et al* 1967). Surgical removal of the

BASAL CELL CARCINOMA IN THE HEAD AND NECK

The Importance of Location and Histological Picture Studied with a New Scoring System in Predicting Recurrences

LARS-ERIK AFZELIUS ANITA EHNHAGE and HANS NORDGREN

The Departments of Otorhinolaryngology and Pathology University Hospital Lund Sweden

Afzelius L. E. Ehnhage A. & Nordgren H. Basal cell carcinoma in the head and neck. The importance of location and histological picture studied by a new scoring system in predicting recurrences. *Acta path microbiol scand Sect. A 88* 5-9 1980

A scoring system for judging the aggressiveness of basal cell carcinomas of the head and neck is devised based upon 258 tumours from 123 patients. This system is discussed and we suggest using the depth of growth, the degree of palisading and the narrow epithelial strand formation (narrow strands) as a scoring basis. It is shown that tumours located on the ear are more aggressive than tumours in other places. Tumours on the nose often recur even though their histological picture is not that aggressive. This phenomenon is also discussed. For proper scoring, an excisional biopsy should be performed unless the tumour is very small. Recurrent tumours and tumours treated with X-ray also have a higher score.

Key words: Basal cell carcinoma, head and neck, histological scoring system, recurrences.

Hans Nordgren, Department of Pathology, Central Hospital, S-631 88 Eskilstuna, Sweden.

Received 17.1.79 Accepted 26.6.79

During recent years an impression has grown among clinicians as well as among pathologists that some basal cell carcinomas of the head and neck region are more aggressive than most other basal cell carcinomas and that these were usually located in the middle of the face and on the ear. These tumours also seem to have a higher rate of recurrence.

In the literature these problems have been discussed to some extent. *Mora and Robins* (1978) found basal cell carcinoma growing in the triangle of the face (formed by lines drawn from the outer canthi to the philtrum of the lip) tended to be more invasive, more destructive, more recurrent and more difficult to treat than those in other sites. *Bari et al* (1978) noted a higher rate of recurrence in tumours located on the ear and lips (very few cases) periocularly and on the nose and scalp than on other sites. *Jackson and Adams* (1973) denied any differences according to the location but their tables indicate a slight tendency towards more horrifying basal cell carcinomas located on the scalp, ears, lips and canthi and nose compared with other sites.

Some reports have touched upon the correlation between prognosis and histology. *Thackray* (1951) made up a classification system and found a correlation only with infiltrative growth. *Teloh* (1953) postulated that the only two significant factors were the degree of histology inflammatory reaction and the degree of histological invasion. *Jackson and Adams* (1973) could not find any correlation between the histological picture and the biological behaviour. *Sloane* (1977) also devised a classification system and found a correlation between infiltrative growth and outcome. *Dellon* (1978) showed that the more aggressive tumours had a greater differentiation to the squamous epithelium and more irregular palisading than less aggressive.

The aim of the present study is firstly to create a histological classification system of basal cell

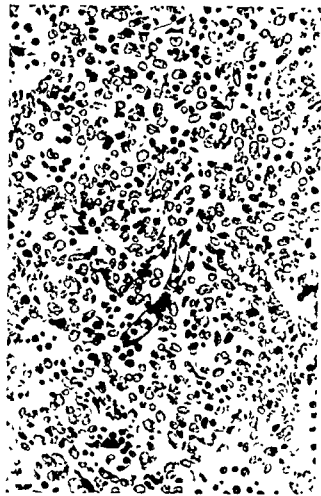


Fig 4. Epithelial thymoma (Originally paraffin-embedding Specimen re-embedded in methacrylate May-Grünwald-Giemsa $\times 310$)

histologic study and a re-evaluation *Cancer* 23 1-15, 1969

Keller, A R and Castleman, B Hodgkin's disease of the thymus gland *Cancer* 33 1615-1623, 1974

Lowenhaupt, E and Brown, R Carcinoma of the thymus of granulomatous type, a clinical and pathological study *Cancer* 4 1193-1209, 1961

Rosal J and Levine, G D Tumours of the thymus Armed Forces Institute of Pathology Bethesda MD 1976

Souadjian J V, Silverstein M N and Titus J L Thymoma and cancer *Cancer* 22 1221-1225, 1968

Thomson, A D and Thackray A C The histology of tumours of the thymus *Brit J Cancer* 11 348-357 1957

BASAL CELL CARCINOMA IN THE HEAD AND NECK

The Importance of Location and Histological Picture, Studied with a New Scoring System in Predicting Recurrences

LARS ERIK AFZELIUS ANITA EHNHAGE and HANS NORDGREN

The Departments of Otorhinolaryngology and Pathology University Hospital Lund Sweden

Afzelius L E Ehnbage A & Nordgren H Basal cell carcinoma in the head and neck The importance of location and histological picture studied by a new scoring system in predicting recurrences Acta path microbiol scand Sect. A 88 5-9 1980

A scoring system for judging the aggressiveness of basal cell carcinomas of the head and neck is devised based upon 258 tumours from 123 patients This system is discussed and we suggest using the depth of growth the degree of palisading and the narrow epithelial strand formation (narrow strands) as a scoring basis It is shown that tumours located on the ear are more aggressive than tumours in other places Tumours on the nose often recur even though their histological picture is not that aggressive This phenomenon is also discussed For proper scoring an excisional biopsy should be performed unless the tumour is very small Recurrent tumours and tumours treated with X ray also have a higher score

Key words Basal cell carcinoma head and neck histological scoring system recurrences

Hans Nordgren Department of Pathology Central Hospital S-631 88 Eskilstuna Sweden

Received 17 iii 79 Accepted 26 vi 79

During recent years an impression has grown among clinicians as well as among pathologists that some basal cell carcinomas of the head and neck region are more aggressive than most other basal cell carcinomas and that these were usually located in the middle of the face and on the ear These tumours also seem to have a higher rate of recurrence

In the literature these problems have been discussed to some extent *Mora and Robins* (1978) found basal cell carcinoma growing in the triangle of the face (formed by lines drawn from the outer canthi to the philtrum of the lip) tended to be more invasive more destructive more recurrent and more difficult to treat than those in other sites *Bari et al* (1978) noted a higher rate of recurrence in tumours located on the ear and lips (very few cases) periocularly and on the nose and scalp than on other sites *Jackson and Adams* (1973) denied any differences according to location in basal cell carcinoma of the face and ear and nose compared with other sites

Some reports have touched upon the correlation between prognosis and histology *Thackray* (1951) made up a classification system and found a correlation only with infiltrative growth *Teloh* (1953) postulated that the only two significant factors were the degree of histological inflammatory reaction and the degree of histological invasion *Jackson and Adams* (1973) could not find any correlation between the histological picture and the biological behaviour *Sloane* (1977) also devised a classification system and found a correlation between infiltrative growth and outcome *Dellon* (1978) showed that the more aggressive tumours had a greater differentiation to the squamous epithelium and more irregular palisading than less aggressive

The aim of the present study is firstly to create a histological classification system of basal cell carcinoma and secondly on the basis of this system to discuss the histological variation of the tumours related to location recurrence and X ray treatment thirdly to give some guidelines for the treatment of such tumours

MATERIAL AND METHOD

The material consists of 123 patients treated for basal cell carcinomas of the head and neck during a 6 year period (1971-1976) at the ENT Department University Hospital Lund Sweden. Sixty per cent of the patients were males and 40% females. The total number of tumours was 258.

This is a retrospective study consisting of patients referred to surgery for primary treatment and patients previously treated surgically and/or radiologically with recurrent tumours.

Eight of the patients were treated many years ago with radiotherapy to the head and neck region for other reasons, mostly tuberculosis. The head and neck region was divided into 7 locations: *ear* - ear and 1 cm around it; *front* - the forehead from the scalp down to and including the eyebrows; *eye* - the eyelids and canthi; *nose* - the nose and $\frac{1}{2}$ cm around it except the canthi; *mouth* - the lips and 1 cm around; *cheek* - cheeks with a lower margin at the lower part of the mandible; the other

margins at the aforementioned locations *miscellaneous* - the rest of the head and neck.

All histological examinations were carried out on sections from paraffin embedded formalin fixed tissue stained with hematoxylin and erythrosin.

The excised specimens were revised by one of us (HN) and a scoring system was created. In this scoring system the depth of the growth (using Clark's system (1968) for malignant melanomas), multifocality, palisading, amount of squamous epithelial differentiation, cell differentiation (Broders 1941), degrees of fibroplasia of the stroma and growth in narrow epithelial strands (narrow strands) were judged (Table 1, Fig 1 A, B). Recurrences were defined as new tumour growth in the old operation site after radical surgical excision or adequate (according to ICRU report 29 (1978)) X ray treatment.

For statistical analysis of the difference between the different scores, the non parametric Mann-Whitney U test was used and the calculations were carried out on a Compucord computer (327).

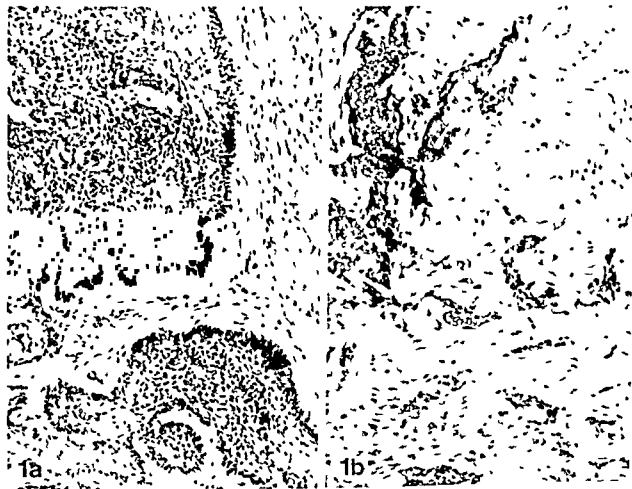


Fig 1 a Basal cell carcinoma with well defined borders, well developed palisading, score 1, and slight fibroplasia in the stroma, score 1. Haematoxylin and erythrosin $\times 125$.

Fig 1 b Basal cell carcinoma infiltrating in narrow epithelial strands, showing nearly complete loss of basal cell palisades, score 3. Marked fibroplasia in the stroma, score 3. Haematoxylin and erythrosin $\times 125$.

TABLE 1 *The Different Parameters and Their Respective Scores*

Parameter	Score range ^{a)}
Depth of Growth	1 - 5
Loss of Palisading	1 - 3
Fibroplasia	0 - 3
Narrow Strands	0 - 3
Multifocality	0 - 1
Squamous Epithelial Differentiation	0 - 3
Cell Differentiation	1 - 4
Maximum score	22

^{a)} Increasing score with increasing degree of change

RESULTS

The most common location for the basal cell carcinoma was on and around the ear, followed by the nose (Table 2). This table also gives the mean for different parameters in the scoring system and the mean of the total score from the different locations. Tumours located in the ear region have a significantly ($p < 0.01$) higher score than tumours from the other locations.

It is shown in Table 3 that the scoring done on the whole excised tumour is higher than on the biopsy.

TABLE 3 *The Mean of Total Score for Biopsy and Whole Excised Tumours in Different Locations*

Location	Biopsy	
	Limited	Excision
Ear	12.0	15.3
Nose	10.5	12.8
Eye	10.9	12.0
Cheek	10.2	10.4
Front	11.8	11.7
Mouth	9.9	11.9
Miscell	10.9	11.2

Thirty two recurrences were noted in the material. Most of the recurrences were found in the ear and nose locations and occurred mostly after X ray treatment (Table 4). The mean score for the recurrences 14.6 is significantly higher ($p < 0.01$) than the mean score for the non recurrence group, 10.8. Even the mean score for the biopsies taken before the recurrences gives a higher but not significant value 11.6. The tumours from the ear and nose locations were further analyzed in order to find parameters in the scoring system of importance in predicting recurrences. The depth of growth, the narrow strands and the degrees of fibroplasia and loss of palisading were found to be most relevant (Table 5). These 4 parameters have significantly higher scores ($p < 0.01$) on the ear in the recurrence group than in the non recurrence group. Concerning the nose the differences are not that

TABLE 2 *The Mean Score for the Different Parameters in the Scoring System, the Number of Tumours and the Mean of Total Score in the Different Locations*

Parameter	Location						
	Ear	Nose	Eye	Cheek	Front	Mouth lip	Miscellaneous
Depth of growth	3.5	3.6	3.0	3.0	3.2	3.0	3.0
Loss of palisading	2.4	2.1	2.1	2.1	2.2	1.8	2.0
Fibroplasia	1.6	1.4	1.3	1.2	1.6	1.2	1.3
Narrow strand	1.6	1.0	1.2	0.8	1.4	1.0	1.0
Multifocality	0.8	0.6	0.6	0.7	0.6	0.6	0.7
Squamous epithelial differentiation	0.9	0.8	1.0	0.5	0.9	0.7	0.9
Cell differentiation	2.4	2.2	2.2	2.2	1.9	1.9	2.1
Mean total score	13.2	11.7	11.4	10.6	11.8	10.2	11.0
Number of tumours	66	65	27	24	16	15	47

$M = 11.4$

TABLE 4 *Number of Recurrences after X-Ray and Radical Excision in Different Locations*

Location	Number of recurrences after		Total
	X-ray	Radical excision	
Ear	4	3	7
Eye	1	1	2
Cheek	3	1	4
Mouth-lip	1	0	1
Front	0	0	0
Nose	10	1	11
Miscellaneous	5	2	7
Total	24	8	32

convincing, except for narrow strands ($p < 0.01$). In the tumours prior to the recurrences the scores of these parameters were slightly higher than for the non-recurrences, except for the depth of growth in the nose region. All except one of these recurrences

TABLE 5 *Total Mean Score for the Different Parameters in the Scoring System for Tumours Prior to the Recurrences (Prior) the Recurrences (Rec) and the Non-Recurrences (Non-Rec) in the Ear and Nose Locations*

Location		Ear	Nose
Parameter			
Depth of growth	Prior	3.9	3.2
	Rec	4.4	3.7
	Non-rec	3.6	3.6
Loss of palisading	Prior	2.6	2.2
	Rec	3.0	2.3
	Non-rec	2.3	2.1
Fibroplasia	Prior	1.8	1.1
	Rec	2.3	1.4
	Non-rec	1.5	1.0
Narrow strand	Prior	1.7	1.1
	Rec	2.6	1.6
	Non-rec	1.4	0.9
Multifocality	Prior	0.9	0.5
	Rec	1.0	0.6
	Non-rec	0.8	0.5
Squamous epithelial differentiation	Prior	0.6	0.7
	Rec	1.0	0.8
	Non-rec	0.9	0.7
Cell differentiation	Prior	2.1	2.0
	Rec	2.4	2.1
	Non-rec	2.5	2.0

came after X-ray treatment and diagnoses were made on limited biopsies.

It seems as if X-radiation makes the scores higher. In 24 tumours scoring was made before and after X-ray. The mean score before X-ray was 11.1 and after 13.6.

DISCUSSION

The impetus for this study came from the impression that some basal cell carcinomas of the head and neck region were more aggressive than others and that such tumours were preferably located around the nose and ear. We searched for a scoring system to make it possible to judge the aggressiveness of each tumour. The literature is rather confusing on this issue and previously no definitive scoring system has been published. We, therefore, suggest a system covering all the important parameters in the histological assessment of the basal cell carcinoma.

It is important to create a scoring system easy to use by every pathologist. As each interpretation of a specimen is somewhat subjective it would be advantageous to have many criteria. On the other hand an extensive system can be too impractical for the pathologist and thus not be accepted in the routine work.

Our scoring system is constructed of parameters which express the growth pattern of the tumours, such as depth of growth, multifocality, narrow strands, loss of palisading and degree of fibroplasia, and by parameters reflecting the cell appearance, such as the cell differentiation and degree of squamous epithelial maturity. The last parameter was chosen in order to detect the so-called metatypical carcinoma (Selidam *et al* 1974).

The material is to some extent selective, in that only a part of it consists of new untreated cases, a great number are recurrences after earlier treatment with surgery and/or X-ray. This fact makes it impossible to estimate the frequency of recurrence in this material, consequently no comparisons with other case materials can be made in this report.

On the basis of our scoring system it is evident that tumours on and around the ear are the histologically most aggressive. In accordance with this there are many recurrences seen on the ear.

What is the reason for this? The structure of the tissue in this very special localization? A longer case history? The thickness of the skin on the ear is sparse and practically no subcutaneous fat is present. These facts can contribute to a higher Clark score. The location as such can increase the patient's delay, and the time factor could be a reason for the more aggressive behaviour of the tumour. The

medical records unfortunately often do not record adequate information about the age of the neoplasm.

The localization with the greatest problems from a clinical point of view (most often recurrences) is on the nose. Tumours located there had however a score not significantly different from the material as a whole. The explanation may be technical reasons: the margins are often narrower than in other places where a good cosmetic result can be achieved even though ample margin is taken.

The evaluation of the scoring parameters in Table 5 clearly shows that the parameters concerning the cell appearance have no influence on the recurrences. This finding is in accordance with Headington (1974). The parameters of growth pattern especially depth palisading fibroplasia and narrow strands are the most important factors in the development of a recurrence. The last two parameters are well correlated and used by some authors in the morphea concept (Caro and Howell 1951). Multifocality thought to be of importance for recurrence (Sloane 1977) is a somewhat obscure concept, since it is dependent on the section technique. It was not found relevant in this study.

To make the scoring system more convenient it could be restricted to the three parameters mentioned above and our proposed scoring system would then be based upon a score with a maximum of 11 (depth - 5 loss of palisading - 3 and narrow strands - 3).

It thus seems that in our material the following conclusions can be drawn: basal cell carcinoma localized on the ear should generally be regarded as potentially more malignant than on other locations in the head and neck region. In accordance with this we advise more extensive excision margins like those taken around squamous-cell carcinoma of tumours in this location. Further in this location we advocate excisional biopsies unless the tumour is very small because limited biopsies give less information and a falsely low score. Recurrent tumours and tumours treated earlier with X rays should also be treated with wider margins as above.

REFERENCES

1. Bart R S, Schrager D, Kopf A W, Bromberg J & Dubin N. Scalpel excision of basal cell carcinomas. *Arch. Dermatol.* 114: 787-783 1978.
2. Broders A C. The microscopic grading of cancer. Mayo Clinic Number Surg. Clin. North Am. 71: 947-961 1941.
3. Caro M R., Howell J B. Morphea like epithelioma. *A.M.A. Arch. Dermatol. Syphilol.* 65: 471 1952.
4. Clark W H Jr, From L, Bernardino E A & Mihm M C Jr. The histogenesis and biologic behaviour of primary human malignant melanomas of the skin. *Cancer Res.* 29: 705-727 1969.
5. Dell n, A L. Host tumor relationships in basal cell and squamous cell cancer of the skin. *Plast. Reconstr. Surg.* 67: 37 1978.
6. Headington J T. Epidermal carcinomas of the integument of the nose and ear. In: Basajns, J G (Ed.) Tumors of the Head and Neck. Clinical and Pathological Considerations. Williams & Wilkins Co. Baltimore 1974 p 370-331.
7. ICRU Report 29. Dose specification for reporting external beam therapy with photons and electrons. International Commission on Radiation Units and Measurements, Washington, D.C. 1978.
8. Jackson R & Adams H A. Horrifying basal cell carcinoma. A study of 33 cases and a comparison with 435 non-horror cases and a report on four metastatic cases. *J. Surg. Oncol.* 5: 431-463 1973.
9. Mora R G & Roberts P. Basal-cell carcinomas in the center of the face. Special diagnosis, prognostic, and therapeutic considerations. *J. Dermatol. Surg. Oncol.* 4: 315-371 1978.
10. Seldam R E J, Helwig E B, Sobin L H & Tarlon H. Histological typing of skin tumours. International Histological Classification of Tumours No 17. WHO 1974.
11. Sloane J P. The value of typing basal cell carcinomas in predicting recurrence after surgical excision. *Br. J. Dermatol.* 95: 127-132, 1977.
12. Teloh H A. Correlation of rate of growth with histologic characteristics of basal cell carcinoma. *Arch. Dermatol. Syphilol.* 69: 403-418 1953.
13. Thackray A C. Histological classification of rodent ulcers and its bearing on their prognosis. *Br. J. Cancer* 17: 113-124 1951.

TABLE 4 Number of Recurrences after X Ray and Radical Excision in Different Locations

Location	Number of recurrences after		Total
	X ray	Radical excision	
Ear	4	3	7
Eye	1	1	2
Cheek	3	1	4
Mouth lip	1	0	1
Front	0	0	0
Nose	10	1	11
Miscellaneous	5	2	7
Total	24	8	32

convincing except for narrow strands ($p < 0.01$). In the tumours prior to the recurrences the scores of these parameters were slightly higher than for the non recurrences except for the depth of growth in the nose region. All except one of these recurrences

TABLE 5 Total Mean Score for the Different Parameters in the Scoring System for Tumours Prior to the Recurrences (Prior), the Recurrences (Rec) and the Non Recurrences (Non Rec) in the Ear and Nose Locations

Parameter \ Location		Ear	Nose
Depth of growth	Prior	3.9	3.2
	Rec	4.4	3.7
	Non rec	3.6	3.6
Loss of palisading	Prior	2.6	2.2
	Rec	3.0	2.3
	Non rec	2.3	2.1
Fibroplasia	Prior	1.8	1.1
	Rec	2.3	1.4
	Non rec	1.5	1.0
Narrow strand	Prior	1.7	1.1
	Rec	2.6	1.6
	Non rec	1.4	0.9
Multifocality	Prior	0.9	0.5
	Rec	1.0	0.6
	Non rec	0.8	0.5
Squamous epithelial differentiation	Prior	0.6	0.7
	Rec	1.0	0.8
	Non rec	0.9	0.7
Cell differentiation	Prior	2.1	2.0
	Rec	2.4	2.1
	Non rec	2.5	2.0

came after X ray treatment and diagnoses were made on limited biopsies.

It seems as if X radiation makes the scores higher. In 24 tumours scoring was made before and after X ray. The mean score before X ray was 11.1 and after 13.6.

DISCUSSION

The impetus for this study came from the impression that some basal cell carcinomas of the head and neck region were more aggressive than others and that such tumours were preferably located around the nose and ear. We searched for a scoring system to make it possible to judge the aggressiveness of each tumour. The literature is rather confusing on this issue and previously no definitive scoring system has been published. We therefore suggest a system covering all the important parameters in the histological assessment of the basal cell carcinoma.

It is important to create a scoring system easy to use by every pathologist. As each interpretation of a specimen is somewhat subjective it would be advantageous to have many criteria. On the other hand an extensive system can be too impractical for the pathologist and thus not be accepted in the routine work.

Our scoring system is constructed of parameters which express the growth pattern of the tumours such as depth of growth, multifocality, narrow strands, loss of palisading and degree of fibroplasia and by parameters reflecting the cell appearance such as the cell differentiation and degree of squamous epithelial maturity. The last parameter was chosen in order to detect the so-called metatypical carcinoma (Selidam *et al.* 1974).

The material is to some extent selective in that only a part of it consists of new untreated cases; a great number are recurrences after earlier treatment with surgery and/or X ray. This fact makes it impossible to estimate the frequency of recurrence in this material; consequently no comparisons with other case materials can be made in this report.

On the basis of our scoring system it is evident that tumours on and around the ear are the histologically most aggressive. In accordance with this there are many recurrences seen on the ear.

What is the reason for this? The structure of the tissue in this very special localization? A longer case history? The thickness of the skin on the ear is sparse and practically no subcutaneous fat is present. These facts can contribute to a higher Clark score. The location as such can increase the patient's delay and the time factor could be a reason for the more aggressive behaviour of the tumour. The

medical records unfortunately often do not record adequate information about the age of the neoplasm.

The localization with the greatest problems from a clinical point of view (most often recurrences) is on the nose. Tumours located there had however a score not significantly different from the material as a whole. The explanation may be technical reasons: the margins are often narrower than in other places where a good cosmetic result can be achieved even though ample margin is taken.

The evaluation of the scoring parameters in Table 5 clearly shows that the parameters concerning the cell appearance have no influence on the recurrences. This finding is in accordance with *Headington* (1974). The parameters of growth pattern especially depth palisading fibroplasia and narrow strands are the most important factors in the development of a recurrence. The last two parameters are well correlated and used by some authors in the morphea concept (*Caro and Howell* 1951). Multifocality thought to be of importance for recurrence (*Sloane* 1977) is a somewhat obscure concept since it is dependent on the section technique. It was not found relevant in this study.

To make the scoring system more convenient it could be restricted to the three parameters mentioned above and our proposed scoring system would then be based upon a score with a maximum of 11 (depth - 5 loss of palisading - 3 and narrow strands - 3).

It thus seems that in our material the following conclusions can be drawn: basal cell carcinoma localized on the ear should generally be regarded as potentially more malignant than on other locations in the head and neck region. In accordance with this we advise more extensive excision margins like those taken around squamous-cell carcinoma of tumours in this location. Further in this location we advocate excisional biopsies unless the tumour is very small because limited biopsies give less information and a falsely low score. Recurrent tumours and tumours treated earlier with X rays should also be treated with wider margins as above.

REFERENCES

1. *Bart R S, Schrager D, Kopf A W, Bromberg J & Dubin N* Scalpel excision of basal cell carcinoma. *Arch Dermatol* 114 782-783 1978
2. *Broders A C* The microscopic grading of cancer. Mayo Clinic Number Surg Clin North Am 21 947-961 1941
3. *Caro M R, Howell J B* Morphea like epithelioma. *AMA Arch Dermatol Syphilol* 65 471 1952
4. *Clark W H Jr, From L, Bernadino E A & Mihm M C Jr* The histogenesis and biologic behaviour of primary human malignant melanomas of the skin. *Cancer Res* 29 705-727 1969
5. *Dellon A L* Host tumor relationships in basal cell and squamous cell cancer of the skin. *Plast Reconstr Surg* 62 37 1978
6. *Headington J T* Epidermal carcinomas of the integument of the nose and ear. In *Batsakis J G* (Ed) Tumors of the Head and Neck. Clinical and Pathological Considerations. Williams & Wilkins Co Baltimore 1974 p 320-331
7. *ICRU Report 29* Dose specification for reporting external beam therapy with photons and electrons. International Commission on Radiation Units and Measurements. Washington DC 1978
8. *Jackson R & Adams H A* Horrifying basal cell carcinoma. A study of 33 cases and a comparison with 435 non horror cases and a report on four metastatic cases. *J Surg Oncol* 5 431-463 1973
9. *Mora R G & Robins P* Basal-cell carcinomas in the center of the face. Special diagnostic, prognostic and therapeutic considerations. *J Dermatol Surg Oncol* 4 315-321 1978
10. *Seldam R E J, Helwig E B, Sobin L H & Torloni H* Histological typing of skin tumours. International Histological Classification of Tumours No 12. WHO 1974
11. *Sloane J P* The value of typing basal cell carcinomas in predicting recurrence after surgical excision. *Br J Dermatol* 96 127-137 1977
12. *Teloh H A* Correlation of rate of growth with histologic characteristics of basal cell carcinoma. *Arch Dermatol Syphilol* 68 408-418 1953
13. *Thackray A C* Histological classification of rodent ulcers and its bearing on their prognosis. *Br J Cancer* 12 213-224 1951

ACTION ON VARIOUS EXPERIMENTAL TUMOUR-HOST SYSTEMS OF METHOXY-SUBSTITUTED GLYCEROL ETHERS INCORPORATED INTO THE FEED

BERNT BOERYD and BO HALLGREN

Department of Pathology I University of Linköping Linköping and Astra Research Laboratories
Mölndal Sweden

Boeryd B & Hallgren B Action on various experimental tumour host systems of methoxy substituted
glycerol ethers incorporated into the feed Acta path microbiol scand Sect A 88 11-18 1980

formation from Melanoma B16 and two MCA sarcomas was inhibited

Key words Chemotherapy lipids methoxy substituted glycerol ethers tumour growth and metastases

B Boeryd Department of Pathology I Regional Hospital 581 85 Linköping Sweden

Accepted as submitted 7 vii 79

Lipids are essential constituents of all cells and
major components of all cell membranes Among
the cell lipids the most important are the

Fatty acids have a central role in the nutrition of
tumours and for their growth The metabolic
pathways of lipids in tumour cells are essentially the
same as in normal cells These circumstances have
raised the question whether chemotherapy interfere
ring with fatty acid metabolism could be a possible
means of cancer control (Spector 1975) However
anti tumour activity by lipids has been reported
(Boeryd *et al* 1971 Weitel *et al* 1972 Ando *et al*
1972) It has also been possible to alter the fatty acid
composition of an animal

substituted glycerol ethers isolated from Greenland
shark liver oil (Hallgren and Ståhlberg 1967)
inhibited metastasis formation from a MCA
induced sarcoma (Boeryd *et al* 1971) and in
preliminary studies the synthetic compound 1 0-(2
methoxy hexadecyl) glycerol (MGE 16 0) inhibited
the growth of some experimental tumours (Boeryd
et al 1974) Furthermore the methoxy substituted
glycerol ethers have been shown to stimulate the
plaque forming cell response (PFC) against sheep
red blood cells (SRBC) and to increase the ability of
parental spleen cells to induce graft versus host re
action (GVHR) (Boeryd *et al* 1975 1978) The stu
dies of the effect of methoxy-substituted glycerol
ethers (MGE) on experimental tumours have now
been extended to include several tumour host
systems The compounds tested have been mainly
synthetic 1 0-(2 methoxy hexadecyl) glycerol
MGE 16 0 1 0-(2 methoxy hexadecenyl) glycerol
MGE 16 1 and 1 0-(2 methoxy-dodecyl) glycerol
MGE 12 0 The mixture of methoxy-substituted
glycerol ethers isolated from Greenland shark liver
oil was tested in one tumour host system

In previous studies the mixture of 2 methoxy

Animals and tumours All strains of mice used were inbred. In the separate experiments the animals were of similar age and of similar weight, varying between 22–28 g in the different experiments. Each group comprised 10–20 mice.

The tumours used were in C57BL/6J mice Melanoma B16, Mammary carcinoma Ca 755, Lewis Lung Tumour LLT, Myeloid leukemia C1498 and MCA-induced sarcoma MCG101 (Boerjrd and Suurkula 1973), in DBA/2J mice Leukemia L1210, Leukemia P388 in ascitic form and Lymphatic leukemia P1534, in A/Sn mice lymphoma LAA, in C3H mice Spontaneous mammary carcinoma MaCal, in CBA mice MCA-induced sarcoma MCG1 in its solid form, MCG1-SS, in its ascitic form, MCG1-AA, and in its solid ascitic form, MCG1-AS (Helligren *et al* 1966), MCA-induced sarcoma MCG12 and the MCA-induced epidermoid carcinoma EpCal (Suurkula and Boerjrd 1975).

Ca 775 and P388 were obtained from Dr A. Goldin, National Institute of Health, Bethesda, MD, USA, L1210 from Dr T. Connors, Chester Beatty Research Institute, London, England, and LLT from Dr K. Hellman, Cancer Chemotherapy Department, Imperial Cancer Research Fund, London, England, LAA from Dr G. Klein, Institute of Tumour Biology, Stockholm, Sweden, P1534 and C1498 from The Jackson Laboratory, Bar Harbor, Maine, USA.

For the transplantation of the tumours standard procedures were adopted. The solid tumours and C1498, P1534 and LAA were transplanted with a small piece of tumour tissue subcutaneously into the flank. The ascitic tumours P388 and MCG1-AA were transplanted intraperitoneally with 10^5 and 2×10^6 cells, respectively. For transplantation of L1210 the spleen of a donor was minced and diluted 1:10 in saline, of this suspension 0.2 ml was given subcutaneously into the flank. When the intention primarily was to study influences on spontaneous metastasis formation, the solid tumour was transplanted subcutaneously to the tail (Hagmar and Boerjrd 1968). By amputation of the tail with the tumour the survival time of the animals could be prolonged. Tail tumours including 2 cm of the tail were weighed at amputation.

In two tumour-host systems, MCG101 in C57BL/6J mice and MCG12 in CBA-mice, an immunization transplantation resistance test was performed in mice differently fed during immunization (See Tables 7 and 8).

The investigation also included combination treatment with MGE 160 and Cyclophosphamide, Methotrexate and Thiotepa of B16, MaCal, P388, MCG1-SS and C1498.

All animals were observed during the whole observation period. Weight changes and deaths were noted.

Feed The methoxy-substituted glycerol ethers were given in the pelleted feed in a concentration of 0.1%, 0.25%, 0.50%, 1.0%, 1.5% or 2% per cent. The treatment was usually started the day after tumour transplantation (day +1) and continued during the whole observation period if not otherwise stated.

In a preliminary study, the ability of parental spleen

cells to induce GVHR was increased by MGE 160 in a concentration of 0.1 per cent in the feed given to the donors 44 days before the test (Boerjrd *et al* 1978). Therefore, in some experiments MGE was given about 1½ month before tumour transplantation and during the whole observation period. Furthermore the substance was given intermittently in a few experiments.

The controls were given pelleted feed with the same composition as the test feed but without the glycerol ethers. Water was available *ad libitum*.

At the end of the observation period the animals were killed by ether. The solid tumours were carefully dissected out and weighed. In mice transplanted with C1498, P1534 and P388 the survival time was noted. The growth of the ascitic tumour MCG1-AA was determined by measuring the total packed cell volume (TPCV) (Tarnowski and Bross 1958). At autopsy of animals transplanted with solid tumour, lymph node metastases were noted. From some experiments the lungs were prepared for histological investigation according to Boerjrd (1965), and the incidence of metastases was determined.

Differences in tumour weight between groups were tested according to Wilcoxon's two-sample rank test. Differences in incidence of metastases between groups were tested by 2×2 contingency table test. $P < 0.05$ was accepted as significant. In the tables, only the experiments which resulted in a change in tumour growth or in spread will be presented.

RESULTS

Melanoma B16 The growth of melanoma B16 was inhibited by 0.5% MGE 160 in the feed given day +1 and tended to be inhibited by 2% of the compound given intermittently. In a concentration of 0.1%, MGE 160 given day -43 tended to stimulate the tumour growth. Furthermore, MGE 161 and MGE 120 in a concentration of 0.5% in the feed inhibited the growth of B16, but at the same time the average body weight of the mice decreased. However, feed restriction resulting in a similar body weight change did not influence significantly the tumour growth (Table 1). Spontaneous metastases to the lungs from melanoma B16 transplanted to the tail tended to be inhibited in mice given 0.1% MGE 160 for 43 days before tumour transplantation (Table 2).

LLT The growth of this tumour was inhibited by MGE 160 given in a concentration of 0.1% 43 days before tumour transplantation while in a concentration of 0.25% it had no effect. The incidence of pulmonary metastases was not influenced by the substance in either concentration (Table 3). Treatment of the animals with the substance the day after tumour transplantation did not affect the tumour growth (results not given in tables).

TABLE 1 Effect on the growth of Melanoma B16 by different Methoxy substituted glycerol ethers

Groups and treatment	No of animals	Test diet (days) ¹⁾	Observ period (days)	No of mice dead ²⁾	Average body weight change (g)	Average tumour weight (g)	P
Controls	10		14	1	+0.4	0.93	
0.5% MGE 16.0	10	+1	14		-0.7	0.52	<0.05
Controls	15		18		-0.8	0.36	
2% MGE 16.0	15	+1-4 8-13	18	2	-1.8	0.21	<0.15
Controls	20		21	1	+1.5	1.61	
0.1% MGE 16.0	20	-43	21	2	+0.5	2.13	
0.25% MGE 16.0	20	-43	21		+2.2	1.56	<0.10
Controls	15		17		+0.3	1.10	
0.25% MGE 16.1	15	+1	17		-0.5	0.90	
0.5% MGE 16.1	15	+1	17	1	-3.2	0.61	<0.05
Feed restriction 2.5 g/day	15		17		-2.7	0.91	
Controls	15		17		+1.3	0.8	
0.25% MGE 12.0	15	+1	17		-0.5	0.8	
0.5% MGE 12.0	15	+1	17		-2.9	0.5	<0.05

1) Indication of one day only means the day the treatment started and that it lasted for the whole observation period

2) Mice dead before termination of experiment

MCG101 The growth of this sarcoma tended to be inhibited by 1% MGE 16.0 in the diet given the day after tumour transplantation (Table 3)

LAA The local growth of this tumour was significantly inhibited by 1% MGE 16.0 given the day after tumour transplantation. Interval treatment with 2% was also effective (Table 3)

tion of 2% given intermittently inhibited the growth of the carcinoma (Table 3) The synthetic compound, MGE 16.0 given intermittently during the last 2 weeks of the observation period tended to

TABLE 2 Effect of MGE 16.0 on Spontaneous Metastasis Formation from Melanoma B16 and MCG1 SS Amputation of Tail Tumours after 30 and 13 Days Respectively

Tumour	Groups and treatment	No of animal	Test diet (days)	Observ period (days)	Average body weight change	Average tumour weight with 2 cm of the tail	Incidence of metastases			
							to lymph nodes		Total	
							Gluteal	Lumbar		
B16	Controls	25 ¹⁾		56	-0.2	0.70	12/23	3/23	15/23	15/23
	0.1% MGE	25 ²⁾	-45	56	+0.8	0.68	12/22	1/22	8/22 ³⁾	13/22
MCG1 SS	Controls	20		24	+1.8	0.20	15/20	10/20	10/20	15/20
	0.5% MGE	20	+1	24	+1.1	0.16	8/20 ⁴⁾	5/20	5/20	9/20

1) 2) 2 and 3 mice respectively died before the end of observation period

3) 8/22 # 15/23 P = 0.10

4) 8/20 # 15/20 P = 0.10

MATERIAL AND METHODS

Animals and tumours All strains of mice used were inbred. In the separate experiments the animals were of similar age and of similar weight, varying between 22–28 g in the different experiments. Each group comprised 10–20 mice.

The tumours used were in C57BL/6J mice Melanoma B16, Mammary carcinoma Ca 755, Lewis Lung Tumour LLT, Myeloid leukemia C1498 and MCA-induced sarcoma MCG101 (Boeryd and Suurkula 1973), in DBA/2J mice Leukemia L1210, Leukemia P388 in ascitic form and Lymphatic leukemia P1534, in A/Sn mice lymphoma LAA, in C3H mice Spontaneous mammary carcinoma MaCa1, in CBA mice MCA-induced sarcoma MCG1 in its solid form, MCG1-SS, in its ascitic form, MCG1-AA, and in its solid ascitic form, MCG1-AS (Mellgren *et al.* 1966), MCA-induced sarcoma MCG12 and the MCA-induced epidermoid carcinoma EpCa1 (Suurkula and Boeryd 1975).

Ca 775 and P388 were obtained from Dr A Goldin National Institute of Health, Bethesda, MD, USA, L1210 from Dr T Connors, Chester Beatty Research Institute, London, England, and LLT from Dr K Hellman, Cancer Chemotherapy Department, Imperial Cancer Research Fund, London, England, LAA from Dr G Klein Institute of Tumour Biology, Stockholm, Sweden, P1534 and C1498 from The Jackson Laboratory, Bar Harbor, Maine, USA.

For the transplantation of the tumours standard procedures were adopted. The solid tumours and C1498, P1534 and LAA were transplanted with a small piece of tumour tissue subcutaneously into the flank. The ascitic tumours P388 and MCG1-AA were transplanted intraperitoneally with 10^5 and 2×10^6 cells, respectively. For transplantation of L1210 the spleen of a donor was minced, and diluted 1:10 in saline, of this suspension 0.2 ml was given subcutaneously into the flank. When the intention primarily was to study influences on spontaneous metastasis formation, the solid tumour was transplanted subcutaneously to the tail (Hagmar and Boeryd 1968). By amputation of the tail with the tumour the survival time of the animals could be prolonged. Tail tumours including 2 cm of the tail were weighed at amputation.

In two tumour-host systems, MCG101 in C57BL/6J mice and MCG12 in CBA-mice, an immunization/transplantation resistance test was performed in mice differently fed during immunization (See Tables 7 and 8).

The investigation also included combination treatment with MGE 160 and Cyclophosphamide, Methotrexate and Thiotepa of B16 MaCa1 P388, MCG1-SS and C1498.

All animals were observed during the whole observation period. Weight changes and deaths were noted.

Feed The methoxy-substituted glycerol ethers were given in the pelleted feed in a concentration of 0.1%, 0.25, 0.50, 1.0, 1.5 or 2 per cent. The treatment was usually started the day after tumour transplantation (day + 1) and continued during the whole observation period if not otherwise stated.

In a preliminary study, the ability of parental spleen

cells to induce GVHR was increased by MGE 160 in a concentration of 0.1 per cent in the feed given to donors 44 days before the test (Boeryd *et al.* 197). Therefore, in some experiments MGE was given about 1½ month before tumour transplantation and during the whole observation period. Furthermore the substance was given intermittently in a few experiments.

The controls were given pelleted feed with the same composition as the test feed but without the glycerol ethers. Water was available *ad libitum*.

At the end of the observation period the animals were killed by ether. The solid tumours were carefully dissected out and weighed. In mice transplanted with C1498, P1534 and P388 the survival time was noted. The growth of the ascitic tumour MCG1-AA was determined by measuring the total packed cell volume (TPCV) (Tarnowski and Bross 1958). At autopsy of animals transplanted with solid tumour, lymph node metastases were noted. From some experiments the lungs were prepared for histological investigation according to Boeryd (1965), and the incidence of metastases was determined.

Differences in tumour weight between groups were tested according to Wilcoxon's two sample rank test. Differences in incidence of metastases between groups were tested by 2×2 contingency table test. $P < 0.05$ was accepted as significant. In the tables only the experiments which resulted in a change in tumour growth or in spread will be presented.

RESULTS

Melanoma B16 The growth of melanoma B16 was inhibited by 0.5% MGE 160 in the feed given day + 1 and tended to be inhibited by 2% of the compound given intermittently. In a concentration of 0.1%, MGE 160 given day -43 tended to stimulate the tumour growth. Furthermore, MGE 161 and MGE 120 in a concentration of 0.5% in the feed inhibited the growth of B16, but at the same time the average body weight of the mice decreased. However, feed restriction resulting in a similar body weight change did not influence significantly the tumour growth (Table 1). Spontaneous metastases to the lungs from melanoma B16 transplanted to the tail tended to be inhibited in mice given 0.1% MGE 160 for 43 days before tumour transplantation (Table 2).

LLT The growth of this tumour was inhibited by MGE 160 given in a concentration of 0.1% 43 days before tumour transplantation, while in a concentration of 0.25% it had no effect. The incidence of pulmonary metastases was not influenced by the substance in either concentration (Table 3). Treatment of the animals with the substance the day after tumour transplantation did not affect the tumour growth (results not given in tables).

TABLE 6 Spontaneous Metastasis Formation from MCG12 after Treatment with MGE 16-0 Animals Allowed to Die of Metastases until Day 156 Amputation of Tail Tumour after 18 Days Treatment Day + 1 - + 18

Groups and treatment	No of mice	Average tumour weight with 2 cm of the tail	of spontaneous dead of metastases	Incidence of metastases at autopsy after 156 days	of metastases totally
Controls	8	0.71	3/8	1/5	4/8
0.1% MGE	8	1.04 ¹⁾	3/8	1/5	4/8
0.5% MGE	7	0.25 ²⁾	0/7	0/7	0/7

1) 1.04 # 0.71 P < 0.15

2) 0.25 # 0.71 P < 0.05

stimulate the tumour growth. This occurred in mice whose average body weight decreased (Table 4). MGE 16.0 given the day after tumour transplantation did not affect the tumour growth (Results not given in the table).

P1534 Some prolongation of the survival time of mice transplanted with this tumour was noted after treatment with 1% MGE 16.0 (Table 5). Lower concentration of the substance had no effect.

MCG1-SS The local growth of this tumour transplanted subcutaneously to the tail was not affected by MGE 16.0. However, 0.5% of the substance in the feed tended to inhibit the spontaneous metastases to the regional lymph nodes from tail tumours (Table 2).

MCG12 MGE 16.0 in a concentration of 0.5% inhibited the growth of MCG12 transplanted to the tail. None of these mice died of metastases within an

TABLE 7 Immunization - Resistance Test with MCG 101 Immunization with Tumours Transplanted to the Tail Amputation of Tail Tumours 17 days and challenge 25 Days after Tumour Transplantation Test Diet Days + 1 - + 25

Challenge cell dose	Nonimmunized	Incidence of takes after challenge		
		Immunized ¹⁾	1% MGE	Immunized ²⁾ + 1% MGE
10 ⁷		5/5		5/5
10 ⁶		3/4		5/5
10 ⁵	5/5	3/4	5/5	5/5
10 ⁴	5/5	3/5	5/5	1/5
10 ³	5/5	1/5	4/4	0/5
10 ²	5/5	2/5	4/4	2/5

1) 2) Average weight of tail tumours including 2 cm of the tail 0.45 g and 0.33 g respectively 0.45 # 0.33 P < 0.10

TABLE 8 Immunization - Resistance Test with MCG12 Immunization with Tumours Transplanted to the Tail Amputation 21 Days and Challenge 30 days after Tumour Transplantation Test Diet Days + 1 - + 21

Challenge cell dose	Nonimmunized	Incidence of takes		
		Immunized ¹⁾	Immunized ²⁾ + 0.1% MGE	Immunized ³⁾ + 0.5% MGE
10 ⁵	8/8	7/7	8/8	8/8
10 ⁴	7/8	6/7	7/8	7/7
10 ³	7/8	0/4	3/7	3/8
10 ²	6/8	0/6	1/7	3/8

1) 2) 3) Average weight of tail tumours including 2 cm of the tail 0.73 g 0.54 g and 0.33 g respectively 0.73 # 0.33 P < 0.05

TABLE 3 *Effect of MGE 16-0 on the Growth of LLT, MCG 101 and LAA*

Tumour	Groups and treatment	No of mice	Test diet (days)	Observ period (days)	Average body weight change	Average tumour weight	P
LLT	Controls	20 ¹⁾		17	+ 3.7	1.48 ²⁾	<0.01
	0.1 % MGE	20	- 43	17	+ 3.5	0.97 ³⁾	
	0.25 % MGE	20	- 43	17	+ 3.6	1.36 ⁴⁾	
MCG101	Controls	10		14	+ 2.3	1.84	<0.10
	0.5 % MGE	10	+ 1	14	+ 2.9	1.43	
	1.0 % MGE	10	+ 1	14	- 0.7	1.16	
LAA	Controls	10		15	+ 1.5	1.37	<0.05
	0.5 % MGE	10	+ 1	15	+ 1.7	1.06	
	1.0 % MGE	10	+ 1	15	- 0.4	0.78	
	Controls	15		17	+ 2.1	1.63	<0.01
	2 % MGE	15	+ 1-5	17	- 0.3	1.04	
			8-12 15-16				

1) 3 mice died before the end of the observation period

2 3 4) Incidence of pulmonary metastases was 13/17, 18/20, 17/20, respectively

TABLE 4 *Effect of the Mixture of MGE Isolated from Greenland Shark Liver Oil and MGE 16-0 on the Growth of MaCal*

Groups and treatment	No of mice	Test diet (days)	Observ period (days)	No of mice dead	Average body weight change	Average tumour weight	P
Groups	20		29		- 0.1	0.60	<0.02
2.0 % MGE _{mix}	20	+ 1-14 16-21	29		+ 0.2	0.22	
Controls	10		31		+ 2.0	0.34	<0.15
1.5 % MGE 16-0	10	18-22 26-31	31	1	- 1.2	0.69	
1.5 % MGE 16-0	10	15-18 22-26	31	2	+ 1.2	0.38	<0.10
1.5 % MGE 16-0	10	18-31	31	1	- 2.5	0.71	

TABLE 5 *Effect of MGE 16-0 on Survival Time of Mice Transplanted with P1534*

Groups and treatment	No of mice	Test diet (days)	Average body weight change on 18th day	Average time (days)
Controls	10		- 0.7	18.8
1 % MGE	10	+ 1	- 1.3	30.5

observation period of 156 days and at autopsy none of the mice had metastases (Table 6). The growth of MCG12 transplanted subcutaneously into the flank was not influenced by MGE 16 0 in concentrations of 0.1%, 0.25 or 0.5% (Results not given in tables).

In the immunization-resistance test with MCG101 the C57 mice were treated with 1.0% MGE 16 0 until challenge. The average weight of the tail tumours tended to be inhibited by MGE but the resistance against the challenge tumour cells in these preimmunized mice was not increased. Pre-treatment with the same concentration of MGE but without immunization did not affect the incidence of takes from the challenged tumour cells compared to controls. In the similar immunization-resistance test with MCG12 in CBA-mice treated with 0.1% or 0.5% MGE 16 0, the growth of the immunizing tail tumour was inhibited by 0.5% of the compound. However, the resistance against the challenged tumour cells in these pre-immunized mice given MGE was, if anything, decreased compared to the preimmunized mice not given MGE.

The combination treatment with the different chemotherapeutics and MGE 16 0 did not accentuate the effect of any drug included.

The tumours not influenced by MGE were Ca755, C1498, L1210, P388, MCG1-AA, MCG1-AS and EpCal.

DISCUSSION

For the evaluation of the anti-tumour effects of synthetic methoxy-substituted glycerol ethers, a broad spectrum of tumour-host systems has been used, including carcinomas, sarcomas, lymphomas and leukemias on different inbred strains of mice. MGE 16 0 has been tested on all tumour-host systems included, MGE 16 1 on B16 and Ca755, and MGE 12 0 on B16, MaCal and P1534. Of these compounds, MGE 16 0 was most effective and less toxic, and in various concentrations and treatment schedules inhibited the growth of several tumours, although to different degrees. Of the systems affected by MGE there seems to be no preference for any type of tumour. However, none of the two ascitic tumours tested was influenced.

The spontaneous metastases formation tended to be inhibited by MGE 16 0 in three systems. In a previous study the mixture of methoxy substituted glycerol ethers inhibited significantly spontaneous metastases to the lymph nodes from MCG1-SS (Boerjé *et al.* 1971). In the present study, the synthetic MGE 16 0 tended to inhibit the dissemination of the same tumour to regional lymph nodes.

The PFC response to SRBC was stimulated in CBA mice by MGE 16 0 in concentrations of 0.5% in the diet for 4 days before SRBC injection and in C57BL/6J mice in a concentration of 0.1% given for 14 days before SRBC. The ability of parental spleen cells to induce GVHR was stimulated by 0.1% MGE 16 0 given for 44 days to spleen cell donors before the spleen cell transfer (Boerjé *et al.* 1978). The PFC response is T cell dependent (Canor 1972) and the GVHR is mediated by T cells (Gowans *et al.* 1965). Pre-treatment of mice with 0.1% MGE 16 0 for 43–45 days before tumour transplantation and during the whole observation period inhibited the growth of LLT, tended to stimulate the growth of B16, but tended to inhibit the dissemination of B16 transplanted to the tail. This low concentration of MGE 16 0 was effective only when it was given for about 1½ months before tumour transplantation. In view of the effect of MGE 16 0 on the GVHR, it seems probable that the effect of the substance on B16 and LLT, at least in part, is immune mediated.

On the other hand, in the immunization transplantation resistance test with MCG101, treatment with 1% MGE 16 0 during immunization did not increase the transplantation resistance against MCG101 challenged cells. Similar experiments with MCG12 resulted, if anything, in a decreased transplantation resistance in mice treated with 0.1% and 0.5% MGE 16 0 during immunization. In these experiments, however, the treatment started the day after transplantation of the immunizing tumour, i.e. similar to most of the experiments in which the antitumour effects by MGE were studied. Thus the results of these transplantation resistance tests do not indicate that the effect of MGE 16 0 on MCG101 transplanted s.c. in the flank (Table 3) or the protective effect against MCG12 metastases from tail tumour (Table 6) is immune mediated.

Fatty acids are required for the growth and division of tumour cells (Henderson and LePage 1959, Spector 1975). The sources of tumour fatty acids can be i) biosynthesis by the tumour itself (Medes *et al.* 1957), ii) the host (Mays 1969) and iii) the diet (Littman *et al.* 1966).

Non substituted glycerol ethers, alkyl and alk-1-enyl ones, occur in membrane phospholipids (Horrocks 1972). Snyder and Wood (1968, 1969) found that alkyl- and alk-1-enyl glycerol ethers were significantly higher in several experimental tumours and in human tumours studied than in normal tissues, in which these glycerol ethers occur in minor amounts. The amount of ether-linked phospholipids was also higher in the tumours than in most normal tissues. Furthermore Albert and

Andersson (1977) demonstrated a higher content of ether linked phospholipids in human brain tumour than in normal brain gray matter. Howard et al (1972) found a correlation between growth and differentiation of transplanted hepatomas and levels of ether linked lipids. The most rapidly growing tumours had the highest levels and the less rapidly growing and more highly differentiated ones had progressively lower levels of ether linked lipids. The authors also generally found an inverse relationship between the levels of ether lipids and the levels of a glycerol phosphate dehydrogenase.

Unsubstituted alkoxy lipids have been described as having bacteriostatic properties, hematopoietic effects and protective properties against radiation damages (Mangold 1972). The effect of methoxy substituted glycerol ethers on biological systems is however totally unknown (Mangold 1972). The substitution of the glycerol ethers by a methoxy group might change the activity of the glycerol ethers. Unsubstituted glycerol ethers have been described as stimulating certain bacteria (Brohult 1960) while methoxy-substituted ones have an antibiotic effect against several bacteria (Boeryd et al 1971).

There are probably several mechanisms behind the effect of the methoxysubstituted glycerol ethers on tumour growth and spread but they cannot be decided on the basis of the present results. The substances included in the feed are adjuvants (Boeryd et al 1978) and may influence the tumours by immune mediated mechanisms. However in some of the experiments discussed above non immunological effects on the tumours seem more reasonable. Methoxy substituted glycerol ethers occur normally in man e.g. in bone marrow although in trace quantities. It might be that the supply of MGE in the feed interferes with host resistance against tumours but not necessarily by immune mechanisms.

The host lipid metabolism can be profoundly altered during the growth of tumours both in animals and man (Costa 1977). Alteration of the fatty acid composition of experimental tumours cells by changing the content of fat in the diet has also been described (Rao and Abraham 1975). The methoxy substituted glycerol ethers may possibly be incorporated into the tumour cell lipids and/or membranes phospholipids (Friedberg and Halpert 1978) and thereby change the ability of the tumour cells to grow.

In conclusion it has been possible to demonstrate influences although not dramatic ones on tumour growth or spread by lipids normally occurring in man when these substances are incorporated into the feed. Depending on the treatment schedules and

concentration of the substances the effect varied. In a few experiments the growth of the tumours tended to be stimulated but in most systems affected the growth or spread of the tumours was inhibited.

REFERENCES

- Albert H A & Anderson D E. Ether linked glycerol lipids in human brain tumours. *Lipids* 12: 188-192 1977.
- Ando K, Kodama K, Kato A, Tamura G & Arima K. Antitumour activity of glycerol ethers. *Cancer Res* 32: 125-129 1972.
- Boeryd B, Hallgren B & Ståhlberg G. Studies on the effect of methoxy substituted glycerol ethers on tumour growth and metastasis formation. *Brit J exp Path* 52: 221-230 1971.
- Boeryd B & Suurkula M. Tumour metastasis in mice with reduced immune reactivity. I. Studies with two MCA induced sarcomas in radiation and thymectomized radiation C57BL/6J chimeras. *Int J Cancer* 12: 722-727 1973.
- Boeryd B, Hallgren B & Ståhlberg G. Antitumour activity of methoxy substituted glycerol ethers. Abstracts from the XIth International Cancer Congress Florence Italy 1974.
- Boeryd B, Hallgren B, Lange S, Lindholm L & Ståhlberg G. Biological activities of substituted glycerol ethers. Abstracts from 18th International Conference on the Biochemistry of lipids, Graz Austria 1975.
- Boeryd B, Nilsson T, Lindholm L, Lange S, Hallgren B & Ståhlberg G. Stimulation of immune reactivity by Methoxy substituted glycerol ethers. *Eur J Immunol* 8: 678-680 1978.
- Brohult A. Alkylglycerols as growth stimulating substances. *Nature* 188: 591-592 1960.
- Canfor H. The effects of *anthesis antiserum* upon graft versus host activity of spleen and lymph node cells. *Cell Immunol* 3: 461-469 1972.
- Costa G. Cachexia: the metabolic component of neoplastic diseases. *Cancer Res* 37: 2327-2335 1977.
- Friedberg S J & Halpert M. Ehrlich ascites tumour cell surface membranes: an abnormality in ether lipid content. *J Lipid Res* 19: 57-64 1978.
- Gowans J L & McGregor P D. The immunological activities of lymphocytes. *Progr Allergy* 9: 1 1965.
- Hagmar B & Boeryd B. Effect of heparin, aminocaproic acid and protamine on spontaneous metastasis formation from resectable tail tumours. *Path europ* 3: 509-520 1968.
- Hallgren B & Ståhlberg G. Methoxy substituted glycerol ethers isolated from Greenland shark liver oil. *Acta Chem Scand* 21: 1519-1529 1967.
- Henderson J F & LePage G A. The nutrition of tumours. A Review. *Cancer Res* 9: 887-902 1959.
- Horrocks L A. Content composition and metabolism of mammalian and avian lipids that contain ether groups. In: *Ether Lipids. Chemistry and Biology*. Ed

- F Snyder, pp 177-272 New York and London Academic Press, 1972
- Howard, B V, Morris, H P & Bailey, J M Etherlipids, a-glycerol phosphate dehydrogenase, and growth rate in tumours and cultured cells *Cancer Res* 32 1533-1538, 1972
- Lutman M K, Taguchi T & Mosbach, E H Effect of cholesterol-free fat-free diet and hypocholesterolemic agents on growth of transplantable animal tumours *Cancer Chemoter Res* 50 25-45, 1966
- Mangold H K Biological effects and biomedical applications of alkoxylipids In *Ether lipids, Chemistry and Biology*, Ed F Snyder pp 157-176 New York and London Academic Press, 1972
- Mays E T Serum lipids in human cancer *J Surg Res* 9 273-277, 1969
- Medes, G, Paden G & Weinhouse, S Metabolism of neoplastic tissues XI Absorption and oxidation of dietary fatty acids by implanted tumours *Cancer Res* 17 127-133 1957
- Mellgren J, Bartholdsson, E Boeryd B, & Norrby, K A spontaneously 20 methylcholanthrene-induced rhabdomyosarcoma and its transformation to ascites form in the CBA mouse *Acta pathol microbiol scandinav* 68 535-546, 1966
- Rao G S & Abraham S Dietary alterations of fatty acid composition of lipid classes in mouse mammary adenocarcinoma *Lipids* 10 641-643, 1975
- Snyder, F & Wood R The occurrence and metabolism of alkyl and alk-1-enyl ethers of glycerol in transplantable rat and mouse tumours *Cancer Res* 28 972-978, 1968
- Snyder, F & Wood, R Alkyl and alk-1-enyl ethers of glycerol in lipids from normal and neoplastic human tissue *Cancer Res* 29 251-257, 1969
- Snyder, F & Snyder, I Glycerolipids and cancer *Progr biochem Pharmacol* 10 1-41, 1975
- Spector, A A Fatty acid metabolism in tumours *Progr biochem Pharmacol* 10 42-75, 1975
- Suurkula M & Boeryd B Tumour metastasis in mice with reduced immune reactivity III Studies with three weakly antigenic tumours in thymectomized and/or sublethally irradiated mice *Int J Cancer* 16 404-412, 1975
- Tarnowski, G A & Bross, J D J Evaluation of the performance of indices of growth in the testing of tumour growth inhibition against the Nelson ascites tumour *Ann N Y Acad Sci* 75 586 1958
- Weitzel G, Jackisch R Mier-Gewert H & Zinser D Cystostatische Eigenschaften alkylverzweigter Alkohole und Aldehyde der Kettenlänge C₈ Hoppe Seyler's Physiol Chem 353 641-653 1972

SENSORINEURAL HEARING LOSS IN A SCANDINAVIAN OLD ENGLISH SHEEPDOG

A Case Report

MATTI ANNIKO

Department of Otorhinolaryngology, Karolinska Sjukhuset and King Gustaf V Research Institute,
Karolinska Institutet Stockholm, Sweden

Sensorineural hearing loss in a Scandinavian old English sheepdog. A case report. Acta path
microbiol scand Sect A 88 19-23 1980

Inner ear disease is extremely rare in the old English sheepdog. The present case would constitute the second known case in Scandinavia and the first one observed in Norway. The morphological investigation revealed complete degeneration of the organ of Corti. A single layer of cells was covering the anatomical location of the stria vascularis. The dog did not show clinical signs of vestibular dysfunction. Hair cells were present in the cristae ampullares and macula utriculi. The histopathological features support a genetic basis for the sensorineural hearing loss, though other (rare) causes of exogenously induced inner ear degeneration cannot be completely excluded on the morphological findings alone. The brain revealed signs of chronic meningitis.

Key words: Old English sheepdog, genetic inner ear degeneration, meningitis, labyrinth.

M Anniko, Department of Otorhinolaryngology, Karolinska sjukhuset, S 10401 Stockholm 60, Sweden.

Accepted as submitted 11 vii 79

Inner ear deafness occurs both in animals and in man and is caused either by genetic defects or environmental factors. A detailed analysis of the etiology is often difficult in individual cases. In maternal life, disease (viral infections, erythroblastosis foetalis and others) can be diagnosed early whereas the identification of genetic penetration of various characteristics requires thorough investigation and an extensive material. It is well established that genetic deafness occurs in many animals, including the mouse, guinea pig, cat and dog (Altman 1950).

Anderson *et al.* (1968) described in detail the inheritance pattern and histopathology/ultrastructure of cochlear deafness in the Dalmatian dog. A corresponding study was performed by Ernstson (1972) concerning the waltzing guinea pig, in which the vestibular part of the inner ear was also included. Otherwise, several reports have been published dealing with various aspects of inner-ear

dysfunction in animals and man (Lurie 1948, Bosher and Hallpike 1965, Mair and Elverland 1977).

Inner ear disease is extremely rare in the old English sheepdog. Anniko *et al.* (1977) analysed the first case of inner ear deafness in Sweden and suspected it to have a hereditary background. The present case was found in Norway and would therefore, according to my knowledge, constitute only the second old English sheepdog in Scandinavia with clinical manifestations of complete deafness.

MATERIAL AND METHODS

Material

The old English sheepdog subject to this study was 5 months old, i.e. not fully grown at the time of this investigation. Prior to sacrifice for morphological analysis of the temporal bones, the dog was clinically investigated with regard to the startle reflex, signs of

- F Snyder, pp 177-272 New York and London Academic Press, 1972
- Howard B V, Morris, H P & Bailey, J M Etherlipids, a-glycerol phosphate dehydrogenase, and growth rate in tumours and cultured cells *Cancer Res* 32 1533-1538, 1972
- Littman, M K, Taguchi, T & Mosbach E H Effect of cholesterol-free fat-free diet and hypocholesterolemic agents on growth of transplantable animal tumours *Cancer Chemoter Res* 50 25-45, 1966
- Mangold H K Biological effects and biomedical applications of alkoxylipids In *Ether lipids, Chemistry and Biology*, Ed F Snyder pp 157-176 New York and London Academic Press, 1972
- Mays, E T Serum lipids in human cancer *J Surg Res* 9 273-277, 1969
- Medes G, Paden G & Weinhouse S Metabolism of neoplastic tissues XI Absorption and oxidation of dietary fatty acids by implanted tumours *Cancer Res* 17 127-133, 1957
- Mellgren J, Bartholdsson E, Boeryd B, & Norrby, K A spontaneously 20-methylcholanthrene-induced rhabdomyosarcoma and its transformation to ascites form in the CBA mouse *Acta pathol microbiol scandinav* 68 535-546, 1966
- Rao G S & Abraham S Dietary alterations of fatty acid composition of lipid classes in mouse mammary adenocarcinoma *Lipids* 10 641-643, 1975
- Snyder, F & Wood, R The occurrence and metabolism of alkyl and alk-1-enyl ethers of glycerol in transplantable rat and mouse tumours *Cancer Res* 28 972-978, 1968
- Snyder, F & Wood, R Alkyl and alk-1-enyl ethers of glycerol in lipids from normal and neoplastic human tissue *Cancer Res* 29 251-257, 1969
- Snyder, F & Snyder, I *Glycerolipids and cancer* *Prog biochem Pharmacol* 10 1-41, 1975
- Spector, A A Fatty acid metabolism in tumours *Prog biochem Pharmacol* 10 42-75, 1975
- Suurkula, M & Boeryd B Tumour metastasis in mice with reduced immune reactivity III Studies with three weakly antigenic tumours in thymectomized and/or sublethally irradiated mice *Int J Cancer* 16 404-412, 1975
- Tarnowski, G A & Bross J D J Evaluation of the performance of indices of growth in the testing of tumour growth inhibition against the Nelson ascites tumour *Ann N Y Acad Sci* 75 586, 1958
- Weitzel G, Jackisch R, Mier-Gewert, H & Zinser D Cystostatische Eigenschaften alkylverzweigter Alkohole und Aldehyde der Kettenlänge C₈ *Hoppe Seyler's Physiol Chem* 353 641-653 1972

RESULTS

Clinical Observations

At the veterinary examination the animal was found to be healthy except for its hearing defect. The hearing was tested with short sound clicks at frequencies of 1, 2, 4 and 8 kHz following stimulation with intensities of 85, 100, 125 and 140 dB respectively. The startle reflex could not be provoked with any of the stimuli. The animal had a normal balance. There were no signs of nystagmus at rest or other signs of vestibular dysfunction, but nystagmus could be provoked by caloric testing (both sides). The middle ear cavity was morphologically normal prior to further handling.

Morphological Investigation

The inner ear sections were taken from each vestibular organ of the animal and four sections from each coil of the two cochleae.

Cochlea

In several sections Reissner's membrane had collapsed, narrowing the lumen of the cochlear duct. It was adherent to the stria vascularis and lay over the remnants of the organ of Corti (Fig. 1). In some specimens the degenerated organ of Corti/scar tissue was loosened from the basilar membrane. The tunnel of Corti was collapsed and the tectorial membrane dislodged from the organ of Corti. Hair cells could not be identified at any level in the cochlea. The type of supporting tissue in general could not be identified. Ganglion cells were present in great numbers, as also were myelinated nerves between the cochlear ganglion and the habenula perforata. The stria vascularis consisted of a single cell layer devoid of blood vessels (Fig. 2).

Vestibular Organs

Hair cells type I and type II were both identified and without obvious signs to decrease in number.

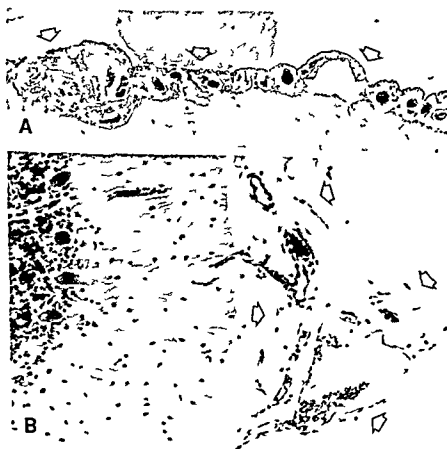


Fig. 3 LM A & B. The meninges (arrows) reveal a mild accumulation of histiocytic cells indicative of chronic meningitis. $\times 40$ and $\times 120$ respectively.

vestibular dysfunction and of nystagmus at rest and after caloric testing

Methods

Following an intravenous overdose of barbiturate the animal was decapitated and the temporal bones removed. The inner ear was reached through an access via the mastoid process and tympanic cavity. The basal coil of the cochlea was bulging slightly into the middle ear (containing the auditory ossicles) and it could be easily identified. The stapedial footplate was extracted and the round window membrane was removed allowing a gentle perfusion of the perilymphatic space with the fixative a technique often used in inner ear research (Wersall 1956 Anniko 1978). Thereafter the bone wall of the cochlea was taken away in approximately 1/3 of each coil removing also the stria vascularis to allow a direct flow of the fixative into the endolymphatic partition. A hole was drilled in the horizontal semicircular canal to perfuse also the vestibular part of the inner

ear. For both temporal bones this procedure took less than 5 minutes before fixation a period of time not causing post mortem artefacts even at the ultrastructural level (Wersall *et al* 1965 Anniko and Bagger-Sjöberg 1977).

A solution of 3% glutaraldehyde in 0.133 M sodium phosphate buffer (pH 7.4) was used as the initial fixative (2 hours) followed by postfixation in 2% osmic tetroxide (2 hours) during which the fixative was gently perfused several times through the membranous labyrinth. After dehydration in alcohol to 70% the specimens were dissected separating the cochlear and vestibular parts of the inner ear. The cochlea and each vestibular organ (3 cristae ampullares, utricle and saccule) were separately embedded in epon mixture and sectioned for light microscopy (staining toluidine blue).

The remaining part of the animal underwent ordinary autopsy including fixation of the brain and meninges with 4% formaldehyde (pH 7.4).



Fig 1 Light microscopy (LM) 1st coil of the cochlea. Complete degeneration of the organ of Corti. Reissner's membrane (indicated by arrows) is depressed, obstructing the endolymphatic space and lying close to the stria vascularis (SV). The region between the inner hair cell and the outer hair cells is marked with a filled arrow. 140 \times . *Inset*: Higher magnification of the location of the organ of Corti. Hair cells cannot be identified. 320 \times .

Fig 2 LM 2nd coil. Stria vascularis of the cochlea. A single cell layer covers the anatomical location of the stria vascularis. RM: Reissner's membrane. SP: spiral prominence. SV: stria vascularis. 320 \times .

- 7 Anniko M Nordemar H Van De Water T R Embryogenesis of the inner ear I Development and differentiation of the mammalian crista ampullaris *in vivo* and *in vitro* Arch Oto-Rhino-Laryng 224 285-299 1979
- 8 Bosher S K Hallpike C S Observations of the histological features development and pathogenesis of the inner ear degeneration of the deaf white cat Proc roy Soc B 162 147-170 1965
- 9 Dohlman G F Secretion and absorption of endolymph Ann Otol Rhinol Laryng 73 708-723 1964
- 10 Dohlman G F The mechanism of secretion and absorption of endolymph in the vestibular apparatus Acta Otolaryngol (Stockh) 59 275-288 1965
- 11 Erntson S The waltzing guinea pig A study on inherited inner ear degeneration Boktryckeri AB Thule Stockholm Sweden Monograph pp 1-16 1972
- 12 Johansson B Wedenberg E Westin B Measurement of tone response by the human fetus Acta Otolaryngol (Stockh) 57 188-197 1964
- 13 Lurie M H The membranous labyrinth in the congenitally deaf collie and dalmatian dog Laryngoscope 58 279-288 1948
- 14 Mair I W S Elverland H H Hereditary Deafness in the Cat. An Electron Microscopic Study of the Stria Vascularis and Reissner's Membrane Arch Oto-Rhino-Laryng 217 199-217 1977
- 15 Rebillard G Rebillard M Carlier E Fujol R Histophysiological relationships in the deaf white cat auditory system Acta Otolaryngol (Stockh) 82 48-56 1976
- 16 Schuknecht H F Pathology of the ear Harvard Press Cambridge 1974
- 17 Suga F Hattler K W Physiological and histopathological correlates of hereditary deafness in animals Laryngoscope (St Louis) 72 435-455 1970
- 18 Ylikoski J Correlative studies on the cochlear pathology and hearing loss in guinea pigs after intoxication with ototoxic antibiotics Acta Otolaryngol (Stockh) Suppl 326 1-62 1974
- 19 Versall J Studies on the structure and innervation of the sensory epithelium of the cristae ampullares in the guinea pig Acta Otolaryngol (Stockh) Suppl 126 1-85 1956
- 20 Versall J Kimura R Lundquist P-G Early postmortem changes in the organ of Corti (guinea pig) Z Zellforsch 65 220-237 1965
- 21 Anggård L An electrophysiological study of the development of cochlear functions in the rabbit Acta Otolaryngol (Stockh) Suppl 203 1-64 1965

Morphometrical methods were however not used. The secretory/re absorptive region around the vestibular organs revealed a normal morphology.

The Brain

The brain underwent ordinary autopsy. Gross morphologic/pathologic changes were not found. Fifteen pieces comprising brain and adjacent meninges taken from different parts of the cerebrum were analysed at the light microscopic level. All specimens revealed an increased thickness of the meninges and also a slight to moderate degree of histiocytic cell proliferation indicative of a chronic meningitis (Fig. 3A & B).

DISCUSSION

The present study reveals a selective degeneration of the auditory partition of the inner ear leaving the vestibular organs intact. This is in agreement with the previous report by Anniko *et al* (1977) describing a similar type of histopathology.

According to clinical observations the animal was deaf from birth thus indicating a pre natal inner ear damage but without vestibular dysfunction. The stria vascularis was composed of a single layer of undifferentiated cells. Such a feature can be observed either in genetic disorders or in inner ear disease later in life (Anderson *et al* 1968, Schuknecht and Igarashi 1964). However the corresponding epithelium around the vestibular organs and also most of the vestibular hair cells had a normal appearance. Independent systems for endolymph turnover (production/reabsorption) occur in the cochlea and vestibular organs (Dohlman 1964, 1965) - which thus can explain a normal/sufficient function of balance.

During embryogenesis and cytodifferentiation hair cells develop completely independently of other structures (Anniko *et al* 1979). A morphologically developed organ of Corti may precede its degeneration at a later stage before or after the physiological maturation and function of the organ as a whole. In the present case there occurred no signs of partial or complete aplasia of the inner ear thus indicating that the labyrinth has passed its organogenesis before damage took place. Either the cochlea had failed to develop hair cells and specialized cells in the stria vascularis during cytodifferentiation or these structures had undergone a regressive degeneration after morphologic differentiation. Such a transformation can occur both pre natally and after birth. Independently of the stage at which injury took place such inner ear pathology is frequently

connected with hereditary disorders (Suga and Hattler 1970, Rebillard *et al* 1976).

In the present case the whole organ of Corti had disintegrated at the time of investigation so the question of where in the cochlea the process has started cannot be solved. A large number of genetic hearing defects begin in the middle range of hearing both in animals and in man (Johansson *et al* 1964, Anggård 1965, Bosher and Hallpike 1964) in contrast to hair-cell degeneration caused by exogenous agents (Ylikoski 1974, Wersall 1978, personal communication) with primarily a high frequency loss with damage of the hair cells in the basal part of the cochlea. Primary lesions at the apex are extremely few (Anniko 1976).

The occurrence of meningitis in the present animal is obscure and might be coincidental. However, meningitis with or without involvement of inner ear physiology/morphology has been reported (review Schuknecht 1974). It appears unlikely that an infection of the labyrinth would be restricted only to the cochlear partition especially as there are no anatomical or physiological barriers between the auditory and vestibular parts. On the contrary, the endolymph is in continuous contact with both parts of the inner ear.

In conclusion the histopathologic appearance of the present case strongly supports a genetic basis for the sensorineural hearing loss.

Supported by grants from Karolinska Institutet and The Swedish Medical Research Council (grant no. 12X 720).

REFERENCES

- Altman F. Histologic picture of inherited nerve deafness in man and animals. *Arch Otolaryng* 51: 852-890 1950.
- Anderson H, Henrikson B, Lundquist P, G. Wedenborg E, Wersall J. Genetic hearing impairment in the Dalmatian dog. *Acta Otolaryngol* (Stockh) Suppl. 232: 1-34 1968.
- Anniko M. The cytochrome c oxidase in atoxyl treated guinea pigs. *Acta Otolaryngol* (Stockh) 82: 70-81 1976.
- Anniko M. Atoxyl induced pathological changes of the inner ear. A model system for the study of ototoxicity. Tryckeri: Balder AB Stockholm Sweden. Monograph pp 1-49 1978.
- Anniko M, Fabiansson E, Nilsson O. Deafness in an old English sheepdog. A case report. *Arch Oto Rhino Laryng* 218: 1-7 1977.
- Anniko M, Bagger Sjöback D. Early post mortem change of the crista ampullaris. A light and electron microscopic study of the guinea pig. *Virchows Arch B Cell Path* 25: 137-149 1977.

THE ULTRASTRUCTURE OF BONE MARROW PLASMA CELLS OBTAINED FROM PATIENTS WITH MULTIPLE MYELOMA DURING THE CLINICAL COURSE OF THE DISEASE

JENS BLOM¹ OLE PAASKE HANSEN² and BENDT MANSÅ¹

Department of Biophysics¹ Statens Seruminstitut, and Division of Haematology² Department of
Medicine Hvidovre University Hospital Copenhagen Denmark

Blom J Hansen O Paaske & Mansa B The ultrastructure of bone marrow plasma cells obtained from patients with multiple myeloma during the clinical course of the disease *Acta path microbiol scand Sect A* 88 25-39 1980

The ultrastructure of plasma cells from 65 consecutive bone marrow specimens from 13 patients with multiple myeloma is described. Biopsies were taken from 12 of the patients prior to and after initiation of treatment. The study was undertaken with the aim of correlating ultrastructural characteristics of the myeloma cells with biochemical and clinical parameters including the survival time after treatment of the patients with cytostatics. Intracellular inclusions were only seen in the plasma cells of 7 patients, of whom had rather long survival times. These cells are characterized by a low degree of differentiation. Nuclear bodies were observed in 10 patients, respectively. Nuclear bodies were observed in 10 patients, respectively. Nuclear bodies were observed in 10 patients, respectively.

0.004). A nuclear/cytoplasmic asymmetry was a characteristic feature of the ultrastructure of the myeloma cells. During treatment a significant increase from 34 to 54 per cent ($2P = 0.03$) was observed in the number of plasma cells with slight asymmetry. No correlation could be established between any ultrastructural features and the values obtained with clinical tests considered of major prognostic significance at the time of diagnosis e.g. the concentrations of serum creatinine, haemoglobin, serum albumin and serum calcium.

Key words Plasma cells multiple myeloma ultrastructure nuclear/cytoplasmic asynchrony

Jens Blom Department of Biophysics Statens Seruminstitut Artager Boulevard 80 DK 2300 Copenhagen S Denmark

Accepted as submitted 16 vii 79

Several papers (5, 23, 28) have presented detailed descriptions of the pleomorphic ultrastructure of the bone marrow plasma cells from patients with multiple myeloma. The cells have been characterized (16, 32) by an asynchronous maturation of nuclear chromatin and cellular cytoplasm. However, in another study (34) it was concluded that there was no characteristic plasma cell abnormality.

The present investigation was initiated with the intention of following a group of patients with

multiple myeloma throughout the clinical course of their disease and simultaneously studying the ultrastructure of their bone marrow plasma cells and the concentration of the M components in their sera

The study comprises the examination of 65 bone marrow biopsies and serum samples from 13 patients. These patients were examined at intervals throughout the clinical course of their disease and the first biopsy was taken at the time of the diagnosis prior to any treatment with cytostatics.

THE ULTRASTRUCTURE OF BONE MARROW PLASMA CELLS OBTAINED FROM PATIENTS WITH MULTIPLE MYELOMA DURING THE CLINICAL COURSE OF THE DISEASE

JENS BLOM¹ OLE PAASKE HANSEN² and BENDT MANSÅ¹

Department of Biophysics¹ Statens Seruminstitut, and Division of Haematology² Department of
Medicine Hvidovre University Hospital Copenhagen Denmark

Blom J, Hansen O, Paaske & Manså B. The ultrastructure of bone marrow plasma cells obtained from patients with multiple myeloma during the clinical course of the disease. *Acta path microbiol scand Sect. A* 88 25-39 1980

The ultrastructure of plasma cells from 65 consecutive bone marrow specimens from 13 patients with multiple myeloma is described. Biopsies were taken from 12 of the patients prior to and after initiation of treatment. The study was undertaken with the aim of correlating ultrastructural characteristics of the myeloma cells with biochemical and clinical parameters including the survival time after treatment of the patients with cytostatics. Intracellular inclusions were only seen in the cells of four patients, all of whom had rather long survival times. Two of these are still alive and furthermore their plasma cells are characterized by a low mean number of mitochondria in each sectioned cell studied ($P = 0.004$). A nuclear/cytoplasmic asynchrony was a characteristic feature of the ultrastructure of the myeloma cells. During treatment a significant increase from 34 to 54 per cent ($P = 0.03$) was observed in the number of plasma cells with slight asynchrony. No correlation could be established between any ultrastructural features and the values obtained with clinical tests considered of major prognostic significance at the time of diagnosis, e.g. the concentrations of serum creatinine, haemoglobin, serum albumin and serum calcium.

Key words: Plasma cells, multiple myeloma, ultrastructure, nuclear/cytoplasmic asynchrony.

Jens Blom, Department of Biophysics, Statens Seruminstitut, Artager Boulevard 80, DK 2300 Copenhagen S, Denmark.

Accepted as submitted 16 vii 79

Several papers (5, 23, 28) have presented detailed descriptions of the pleomorphic ultrastructure of the bone marrow plasma cells from patients with multiple myeloma. The cells have been characterized (16, 32) by an asynchronous maturation of nuclear chromatin and cellular cytoplasm. However, in another study (34) it was concluded that there was no characteristic plasma cell abnormality.

The present investigation was initiated with the intention of following a group of patients with

multiple myeloma throughout the clinical course of their disease and simultaneously studying the ultrastructure of their bone marrow plasma cells and the concentration of the M components in their sera.

The study comprises the examination of 65 bone marrow biopsies and serum samples from 13 patients. These patients were examined at intervals throughout the clinical course of their disease and the first biopsy was taken at the time of the diagnosis prior to any treatment with cytostatics.

MATERIAL AND METHODS

The criteria used for the diagnosis multiple myeloma were as follows (18): 1) Presence of at least 3 per cent atypical plasma cells in a bone marrow smear or a histological proof of a plasmacytoma or either of these conditions combined with a high concentration of a serum M component i.e. IgG ≥ 30 g/l (≥ 373 units/ml) IgA ≥ 20 g/l (≥ 1190 units/ml) or combined with excretion of high concentrations (> 60 mg/l) (9) of light chains in the urine. 2) Presence of at least 3 per cent atypical plasma cells in a bone marrow smear or a histological proof of a plasmacytoma or either of these conditions combined with the presence of osteolytic bone lesions on an X ray photograph.

Immunoelectrophoresis Qualitative immunoelectrophoretic analysis and determination of the concentrations of the serum M components were carried out as described previously (6).

Patients

Clinical and Laboratory Findings

Thirteen patients (5 men and 8 women) with multiple myeloma were studied (Table 1). The average age of the men was 58 years (range 41–70) and that of the women 61 years (range 43–76). Five of the patients had an M component of the IgG λ type (lambda* four an IgG λ kappa, one an IgG λ lambda, one an IgA kappa and two patients had Bence Jones protein of the type kappa in their serum).

Seven of the patients (54 per cent) were found to have osteolytic bone lesions when the multiple myeloma was diagnosed. The first sign of the disease in two of the patients (OB, ES) who had M components of kappa light chains in their sera was a plasmacytoma localized to the lumbar vertebra. A plasmacytoma was also found in a third patient (GH) but in that case it was present in the mandible. The tumours were surgically removed from patients OB and ES who were subsequently treated by X ray irradiation. When the plasmacytoma was discovered in these three patients the disease had disseminated to the bone marrow.

Bone marrow material from a patient with no sign of multiple myeloma was also studied in order to obtain some control plasma cells for comparison with plasma cells from the

per cent of the patients but only one (IN) showed a definite hypercalcaemia with a value of 4.13 mmol/l (normal range 2.27–2.55 mmol/l).

The Period of Observation

The patients were examined at intervals during the course of their disease (Table 1). Two patients are still alive. During the period of observation a total number of 65 bone marrow aspirations (range 2–15 per patient) were examined. The first bone marrow sample from a patient was taken prior to the initiation of treatment with cytostatics (melphalan or cyclophosphamide). Although one patient (EH) had been treated with melphalan before the first biopsy was taken, she was included in the study because she had Russell bodies in her plasma cells (6).

Methods for Electron Microscopy

The methods used for fixation and further preparation for electron microscopy of the bone marrow aspirations are described previously (6). Sections were made of three or more marrow particles from each of the 65 biopsies. The number of plasma cells on the individual micrographs of our survey fields at a magnification of 15 000 \times varied from specimen to specimen but a mean number of 25 different plasma cells from each biopsy was chosen for evaluation. A total number of 1600 plasma cells was selected from this material for further evaluation. The cells were selected so that they contained an abundance of the rough endoplasmic reticulum and were sectioned through their central region in such a way that the nucleus was included in the section. In most cases the Golgi complex was also present in cells sectioned in this way. The selection of cells for the evaluation was made by a technician considered to be less biased than any of the authors. Evaluation of the micrographs was carried out by one of the authors (JB) who was unaware of the results of the laboratory tests at this stage of the study. Approximately 5000 electron micrographs were examined.

Plasma Cell Evaluation

Each plasma cell included in a section was evaluated at a magnification of 15 000 \times and for more detailed study at 90 000 \times . The following parameters were taken into account.

Presence of the rough endoplasmic reticulum was registered as a PS.

Rough endoplasmic reticulum (ER) It was noted whether the reticulum was of lamellar or globular type. Intracisternal bodies (Russell bodies) were registered.

Mitochondria Number was counted and length and diameter measured when possible.

Cytoplasmic inclusions Number was counted and diameter measured.

Golgi complexes Number of centrioles in Golgi complexes was registered.

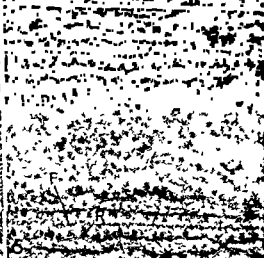
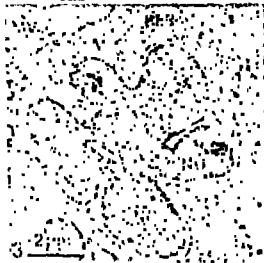
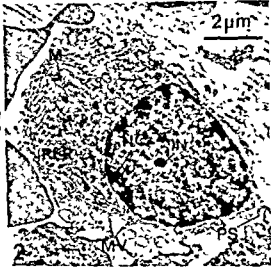
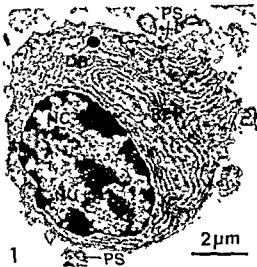
Contact zones Number of these between plasma cells

* The IgG subclasses were kindly determined by Dr S Skerfving, Bern, Switzerland.

TABLE 1 Results of Laboratory Tests Performed at the Time when the First Bone Marrow Biopsy was Taken

Patient	Age/sex	Serum monoclonal protein	Serum conc of M component (units/ml) ^b	HB (mmol/l) ^b	Se creatinine (μ mol/l) ^b	Se calcium (mmol/l) ^b	Se albumin (mmol/l) ^b	Survival time (months)	% plasma cells of nucleated cells in bone marrow
GH ^a	47/M	IgG ₁ κ	341	8.0	199	2.71	0.46	2.5	13
MN ^a	68/F	IgG ₁ λ	1129	5.6	113	2.32	0.37	3.5	31
LB	76/F	IgG ₁ λ	729	5.9	200	2.38	0.49	7	28
VS ^a	67/M	IgG ₁ λ	1258	6.5	143	2.59	0.27	13	61
KC	75/F	IgG ₁ κ	1255	5.1	120	2.35	0.47	20	20
CB ^a	67/M	IgG ₁ κ	971	6.8	87	2.67	0.28	24	66
EJ	43/F	IgG ₁ λ	690	6.8	121	2.39	0.42	29	46
JN ^a	63/F	IgG ₂ λ	416	3.3	87	4.13	0.35	29	87
EH	60/F	IgA κ	2610	4.9	170	2.55	0.47	29	24
GC	47/F	IgG ₁ λ	662	7.8	87	2.51	0.61	53	22
OB	41/M	Kappa	c	8.6	104	2.50	0.62	> 62	10
ES ^a	70/M	Kappa	c	9.0	116	1.36	0.59	63	5
AS ^a	54/F	IgG ₁ κ	775	7.8	87	1.63	0.32	> 78	30

^a Osteolytic lesions^b Normal range see Material and Methods^c 1-2 g/l



and dendritic bone marrow macrophages was counted (see ref 8 for details)

Shape of the nucleus Round ovoid or irregular

Nucleoli Number was counted and diameter measured

Nuclear inclusions and nuclear bodies Numbers were counted (for a detailed definition see ref 15 and later in the text) and structures examined in detail

Nuclear/cytoplasmic asynchrony Bernier & Graham (3) have described nuclear/cytoplasmic asynchrony of plasma cells at the ultrastructural level and their classification (slight moderate or marked asynchrony) has been used throughout this study

For the individual patients the incidence of the different parameters was registered in all the plasma cells selected and for each biopsy the percentage of each parameter was estimated and compared with the result obtained for the other biopsies

Statistics

The Wilcoxon test for pair differences was used (14) for comparison of the numbers of nuclear bodies found

Text to Figures

Except for Fig 1 all figures show electron micrographs of sections obtained from bone marrow specimens from patients with multiple myeloma. The bar on each micrograph represents 100 nm unless otherwise stated

in individual plasma cells from untreated and treated patients and for the evaluation of slight asynchrony

RESULTS

The ultrastructure of 1600 plasma cells from the bone marrow of the 13 myeloma patients was studied according to the principles mentioned at considerable variation from patient to patient was found. In contrast, the morphology of the cell appeared to change very little for each individual patient during the clinical course of the disease.

Most of the cells had a round or ovoid shape with slender, thin microvilli like extensions (MV) on the surface (Figs 2, 3, 17) and frequently also a small number of blunt cytoplasmic projections or pseudopods (PS) (Fig 2). In one patient (OB) > 30% of the cells showed PS in every biopsy and on these cells the PS were more frequent than the MV. For this particular patient - who is still alive - the γ component of the serum was found to contain light chains only.

Rough Endoplasmic Reticulum

The cisternae of the rough endoplasmic reticulum (RER) in the plasma cells from individual patients usually presented one of two morphological types:

Fig 1 A survey of a bone marrow plasma cell from a patient without any sign of multiple myeloma. The nuclear chromatin (NC) shows a characteristic peripheral clumping and a small nucleolus (NU). A parallel arrangement of the cisternae of flattened rough endoplasmic reticulum (RER) is seen in the cytoplasm. There is no evidence of nuclear cytoplasmic asynchrony. On the cell surface a few pseudopod like (PS) extensions of the cytoplasm are seen. DB denotes a dense body. 7 500 \times

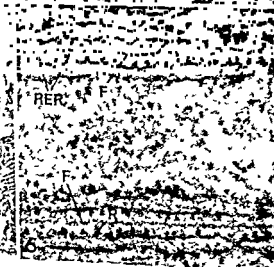
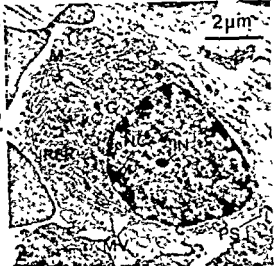
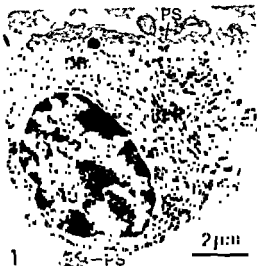
Fig 2 A survey of a plasma cell from patient AS. The nuclear chromatin (NC) shows small areas of condensation distributed through the nucleus and only slight aggregation at the periphery. An intranuclear inclusion (IN) is also present. This is given in higher magnification in Fig 16. The cytoplasm contains parallel cisternae of the rough endoplasmic reticulum (RER) and several mitochondria (M) are seen around the well developed Golgi complex (G). This cell demonstrates slight nuclear cytoplasmic asynchrony. Microvilli like (MV) as well as pseudopod like (PS) extensions are present on the cell surface. 7 500 \times

Fig 3 A survey of a part of a plasma cell from patient VS. The nucleus is very irregular and the nuclear chromatin (NC) is well dispersed with little or no aggregation. A small eccentrically located nucleolus (NU) is present. The cytoplasm contains parallel cisternae of the rough endoplasmic reticulum (RER) and several mitochondria (M) are seen. This cell demonstrates a moderate nuclear cytoplasmic asynchrony. MV denotes microvilli like extensions. 7 500 \times

Fig 4 A survey of a part of a plasma cell from patient EJ. The nucleus appears immature with well dispersed non aggregated chromatin. A moderately large nucleolus (NU) is present. The mature well differentiated cytoplasm contains an abundance of dilated cisternae of the rough endoplasmic reticulum (RER). Russell bodies (Rb) are found in a few of the RER cisternae. A well developed Golgi complex (G) is seen together with several mitochondria (M). This cell demonstrates marked nuclear cytoplasmic asynchrony. 7 500 \times

Fig 5 A survey of a plasma cell from patient OB. A longitudinal section through a concentric arrangement of the rough endoplasmic reticulum (RER₁) is seen. This structure is situated close to the Golgi complex (G). A similar structure (RER₂) is shown in cross section close to the nucleus. A nucleolus (NU) of moderate size is present in the slightly irregular nucleus. The cell presents slight nuclear-cytoplasmic asynchrony. 7 500 \times

Fig 6 High power view of part of the RER₁ from the plasma cell shown in Fig 5. Note filaments (F) between the parallel cisternae of the rough endoplasmic reticulum (RER) and their contact with the ribosomes (R) of the reticulum. 90 000 \times



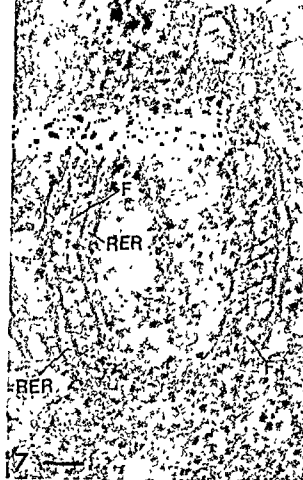


Fig 7 Part of a plasma cell from patient OB. A concentric arrangement of two cisternae of the rough endoplasmic reticulum (RER) is seen. Note the filament (F) located in the cytoplasm between the cisternae and its contact with the ribosomes (R) of the RER at certain points (arrows). 90 000 \times

Fig 8 Part of a plasma cell from patient ES. The cisternae of the annulate lamellae (AL) are continuous with the cisternae of the rough endoplasmic reticulum (RER). AN denotes the annuli formed where fusion of the paired membranes of the cisternae of the annulate lamellae has occurred. 90 000 \times

Fig 9 Part of a plasma cell from patient FH showing an abnormal mitochondrion with a concentric arrangement of the cristae. 90 000 \times

Fig 10 Part of a plasma cell from patient AS showing a dense body (DB) limited by a unit membrane (UM). The DB is an inhomogeneous structure composed of an amorphous and a crystalline region (CS) together with a lipid like inclusion (L). RER denotes rough endoplasmic reticulum. 90 000 \times

mina. Dilated cisternae of the rough endoplasmic reticulum (RER) are also seen. 7 500 \times

Fig. 12 High power view of part of the plasma cell

the plasma cell and the endothelial cell. Note the presence of vesicles (V) in the endothelial cell and the rough endoplasmic reticulum (RER) with dilated cisternae in the plasma cell. 90 000 \times

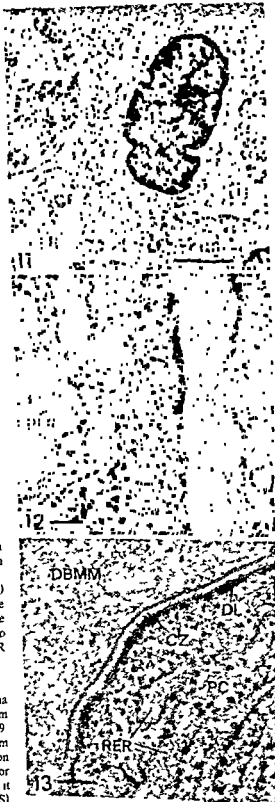
Fig. 13 Part of a plasma cell from patient JN. A contact zone (CZ) between the plasma cell (PC) and a cytoplasmic extension of a dendritic bone marrow macrophage (DBMM) is seen. Note the dense layer (DL) attached to the inner leaflet of the cell membrane of the plasma cell in the contact region. RER denotes rough endoplasmic reticulum. 90 000 \times

regular array of parallel, flattened cisternae (Figs 2, 3, 5, 17) or a globular type with dilated cisternae (Figs 4, 11). The former was the most common whereas the latter was found in most of the cells from four patients (MN, EJ, EH, OB) and in three of these (EJ, EH, OB) the cells contained Russell bodies (Fig. 4), i.e. electron-dense structures situated within the cisternae of the rough ER (6).

In addition to the rough ER some plasma cells contained different unusual structures situated in the cytoplasm close to the ER. Some cells from two of the patients (MN, ES) showed structure resembling annulate lamellae (21) (Fig. 8) these were often found in direct continuation of the rough ER. In four patients (KC, CB, OB, AS) there was an unusual circular arrangement of the rough ER (Fig. 5) which was seen both in cross sections (Figs 5, 7) and in longitudinal sections (Figs 5, 6). In the cytoplasmic matrix between the individual cisternae of the rough ER one to three filaments were seen to be in contact with the ribosomes of the rough ER (Figs 6, 7).

Mitochondria

The mean number of mitochondria in the plasma cell sections of individual biopsies varied from patient to patient with a range from 7 to 39 whereas the variation from biopsy to biopsy from each patient was very small. Any correlation between the number of mitochondria and clinical or biochemical findings was not apparent. However it should be noted that two of the patients (OB, AS) have lived for a long period after confirmation of the



diagnosis and both show a low mean number of mitochondria, *i.e.* 7 and 14, respectively. The diameter of the mitochondria was rather constant, between 0.3–0.4 μm , whereas the length varied from 0.5–2.0 μm . Only five of the patients (GH, VS, CB, EH, ES) showed morphological abnormalities in a few mitochondria in their plasma cells, where longitudinal, parallel or concentric arrangements of the cristae were present (Fig. 9). These changes were found throughout the clinical course of their disease.

Cytoplasmic Inclusions

Electron-dense bodies surrounded by a smooth membrane were observed in the cytoplasm of numerous plasma cells from nearly all patients (Fig. 17). The diameter of these inclusions varied from 0.5–1.0 μm . Often the dense core of the bodies presented a regular or crystalloid substructure and some lipid like material could also be seen (Fig. 10).

Golgi complexes

A well-developed Golgi complex was found in most of the plasma cells (Figs. 2, 4, 5). The usual components – stacks of flattened sacs, vesicles and vacuoles – were seen together with granules of variable size, shape and density. One or more centrioles were observed in about one third of the Golgi complexes studied.

Contact Zones

As previously published (7, 8), a number of contact zones between plasma cells and dendritic bone marrow macrophages were seen in biopsies of all of the patients with multiple myeloma (Fig. 13). Only one patient (VS), in whom the nuclei of the plasma cells were markedly irregular (Fig. 3), had a low number of such contact zones. In some patients (MN, LB, CB, OB) contact zones were seen in association with a strip of basement membrane or lamina densa like material instead of the contact with a macrophage extension (Fig. 11). Plasma cells presenting this type of zone were often situated in the perivascular compartment of the bone marrow (Figs. 11, 12).

Nuclei

Seventy-five per cent of the plasma cells studied had round or ovoid nuclei most of which were eccentrically located in the cytoplasm (Figs. 2, 4, 17). In three patients (VS, FH, OB), more than 50 per cent of the cells in the first biopsy showed a markedly irregular shape of the nucleus (Figs. 3, 5). These cells were often characterized by having many cytoplasmic filaments and microtubules localized to the cytoplasmic invaginations of the

nuclei (Fig. 14). Binucleate plasma cells were seen in 2 per cent of the cells.

Nucleoli with a diameter from 0.7–1.9 μm were found in about 40 per cent of the plasma cells (Figs. 3, 4, 5). Neither morphology nor size of the nucleoli could be correlated with any of the clinical or biochemical parameters studied.

Nuclear inclusions were found in the nuclei of cells from four of the patients (EJ, EH, OB, AS). Plasma cells from three of these contained Russell bodies in the nuclei as described earlier (6). Such Russell bodies were characterized by their homogeneous structure and their being surrounded by a single unit membrane (Figs. 10, 11 in ref. 6). The cells of the fourth patient (AS) had two kinds of intranuclear inclusions *i.e.* a crystalline and a fibrillar type (Figs. 2, 15, 16), both without a limiting membrane. These types were found in all of the 15 biopsies obtained from this patient. The crystalline type (Figs. 15, 21) appeared as a lattice of tubular structures each with an outer diameter of 11–12 nm. The fibrillar type consisted of a bundle of almost parallel fibrils, each with a diameter of 9–11 nm (Fig. 16).

In this report the term «nuclear bodies» is used to describe a group of intranuclear globules with different types of substructure (15). The diameter of these globular structures varied from 0.3–0.7 μm . In most nuclei they were easily recognized because of a surrounding clear halo (Fig. 17). Three morphologically distinguishable types were found: 1) a type composed of fibrils arranged in a concentric formation (Fig. 18); 2) a type of a fibrillogranular body consisting of a few small granules surrounded by randomly arranged fibrils (Fig. 19); and 3) a type with a dense core surrounded by fibrils (Figs. 17, 20). All fibrils found in the nuclear bodies were 6–8 nm in diameter. The two first types were the most common. Some plasma cells contained two nuclear bodies which generally belonged to the same morphological type. The nuclear bodies did not seem to be structurally related to the nucleoli although a nuclear body and a nucleolus were often found within the same nucleus. Occasionally, nuclear bodies were seen to surround the crystalline (Fig. 21) or fibrillar nuclear inclusions previously described to be present in the cells of the patient (AS).

Table 2 shows a comparison of the percentage of nuclear bodies in the plasma cells obtained from the patients before and during their treatment. During treatment this percentage increased from 7 to 16 which is significant ($2P = 0.004$). The three different morphological types of nuclear bodies were seen in the cells from the patients both before and during their treatment and no difference in size



Fig 14 Part of a plasma cell from patient VS who had very lobulated nuclei (cf Fig 3). The perinuclear space (PNS) is shown at a region of two lobules. Note the transversally cut filaments (F) and microtubules (MT) present in the cytoplasm within the lobules. NC denotes nuclear chromatin. 90 000 \times

Fig 15 Part of a plasma cell nucleus from patient AS. The crystalline type of an intranuclear inclusion is shown. NC denotes nuclear chromatin. 90 000 \times

Fig 16 High power view of part of the plasma cell nucleus shown in survey in Fig 2. The fibrillar type of an intranuclear inclusion is shown in detail. 90 000 \times

Fig 17 A survey of a plasma cell from patient AS. This cell shows slight nuclear-cytoplasmic asynchrony. Several microvilli-like extensions (MV) of the cytoplasm are observed and a dense body (DB) and several mitochondria (M) are present in the cytoplasm. Note the nuclear body (NB) surrounded by a clear halo within the nuclear chromatin (NC). 7 500 \times

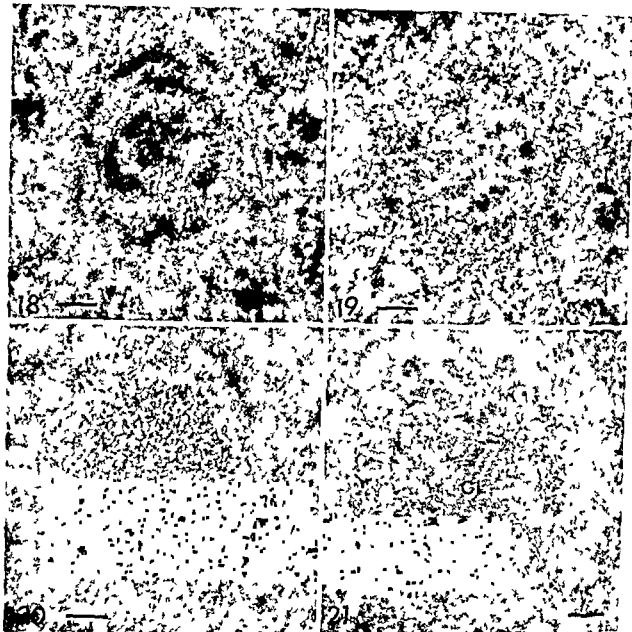


Fig 18 Part of a plasma cell nucleus from patient OB. A nuclear body composed of fibrils arranged concentrically is shown. 90 000 \times .

Fig 19 Part of a plasma cell nucleus from patient JN. A nuclear body composed of small granules surrounded by fibrils is shown. 90 000 \times .

Fig 20 Part of the nucleus of the plasma cell seen in Fig 17. A nuclear body with a central electron dense mass surrounded by fibrils is shown. 90 000 \times .

Fig 21 Part of a plasma cell nucleus from patient AS. A nuclear body surrounding a crystalline intranuclear inclusion (CI) is shown. 90 000 \times .

was observed in relation to survival time. Further more the presence of nuclear bodies had no relationship to the degree of nuclear/cytoplasmic asynchrony.

Nuclear/Cytoplasmic Asynchrony

Assessment of the asynchrony by the criteria described in Material and Methods is illustrated by

the following figures. A plasma cell without asynchrony is shown in Fig 1. The cell contains a mature looking nucleus with chromatin clumped in a cartwheel like arrangement. Parallel cisternae of the rough ER are seen in the mature appearing well organized cytoplasm. Occasionally nucleoli of moderate size are seen in the cells without asynchrony. Plasma cells with slight asynchrony

TABLE 2 The Frequency of Nuclear Bodies in Plasma Cells from Patients before and during Treatment

Plasma cells from 12 patients	Total number of plasma cells	Number of sections of plasma cell nuclei with nuclear bodies	% nuclear bodies of plasma cells (range)
Before treatment ^a	298	20	6.7 (0-13.3)
During treatment	1217	192	15.8 (8.2-23.3)

^aOne patient (EH) is omitted due to treatment at the time of the first biopsy.
The Wilcoxon test for pair differences was used: untreated versus treated (14) (2P = 0.004)

(Figs 2.5.17) have a mature appearing well organized cytoplasm with parallel stacks of rough ER and a nucleus with scattered small aggregates of chromatin. Nucleoli of moderate size are seen in many of these cells. Cells with moderate asynchrony (Fig. 3) show a nucleus with small amounts of chromatin aggregates and a cytoplasm containing stacks of flattened rough ER. In some cells with moderate asynchrony a nucleus with similar distribution of chromatin is present together with dilated rough ER in the cytoplasm. Cells with marked asynchrony (Fig. 4) show a nucleus with evenly distributed rather electron lucent chromatin and a cytoplasm containing dilated cisternae of the rough ER.

When the plasma cells were evaluated with respect to nuclear/cytoplasmic asynchrony it was found that cells without asynchrony were seen only occasionally in the patients. Marked asynchrony however was found in cells of the first biopsy from seven of the patients (GH, MN, CB, EJ, JN, EH, AS). After treatment was initiated marked asynchrony could be found only in a small number of cells.

that the cisternae of the rough ER were dilated and accordingly the plasma cells were most frequently classified as cells with marked asynchrony. Slight asynchrony (Figs 2.5.17) was seen in 34 per cent of the cells from the untreated patients. A total number of 298 cells were studied. An equal number of cells (292) obtained from the last biopsy of the same patients obtained during treatment showed that this percentage had increased to 54, i.e. a significant increase (2P = 0.03).

Clinical Staging and Course

No correlation could be found between the variation within the intracellular structures found in

the plasma cells of the patients and the clinical values of the major tests with prognostic significance obtained at the time of diagnosis, i.e. the concentrations of serum creatinine, haemoglobin, serum albumin and serum calcium. All the patients were treated with alkylating agents (melphalan or cyclophosphamide) but the schedules used for individual patients differed to some extent. Nine patients had a lower M component concentration in serum samples taken during the treatment than at the time of diagnosis. This decrease was most evident for patients with a short survival time (VN, LB, VS, KC) as described previously (17). For five patients the irregular intervals (2-26 months) at which blood samples were obtained did not permit a time related evaluation of changes in the M component concentration. Serum samples from three patients (KC, AS, GC) showed a marked increase in the serum concentration of the M component during the course of the disease. Plasma cells from patients who developed either a decrease or an increase of the M component showed no evident morphological changes as compared to the plasma cells obtained at the time of diagnosis except for the described increase in the number of nuclear bodies.

Six of the patients (VN, VS, KC, GH, JN, AS) were treated intermittently with cytostatics intravenously in doses which were calculated in relation to the body weight of the patients, i.e. melphalan 30-50 mg, cyclophosphamide 1000-2000 mg. The plasma cells obtained from these patients 1 to 30 days after treatment were evaluated and their ultrastructure was compared with that of cells from the first biopsy.

When the plasma cells showing slight nuclear/cytoplasmic asynchrony were evaluated, an increase in the percentage of cells with nuclear bodies was also noted.

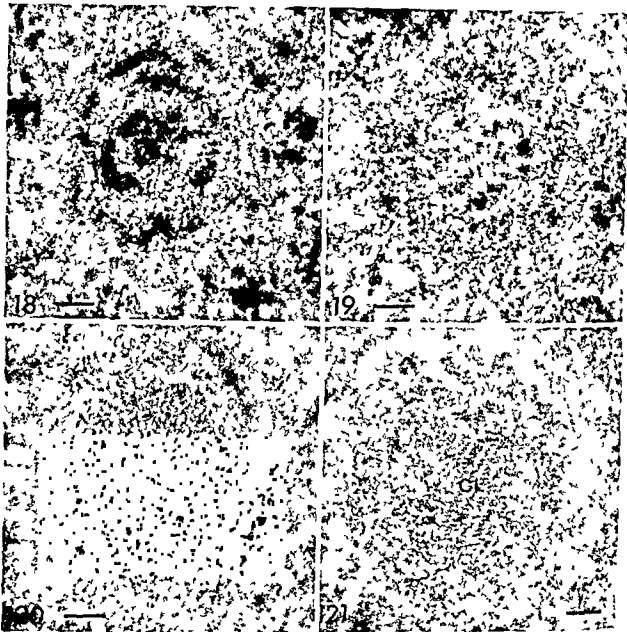


Fig 18 Part of a plasma cell nucleus from patient OB. A nuclear body composed of fibrils arranged concentrically is shown. 90 000 \times .

Fig 19 Part of a plasma cell nucleus from patient JN. A nuclear body composed of small granules surrounded by fibrils is shown. 90 000 \times .

Fig 20 Part of the nucleus of the plasma cell seen in Fig. 17. A nuclear body with a central electron dense mass surrounded by fibrils is shown. 90 000 \times .

Fig 21 Part of a plasma cell nucleus from patient AS. A nuclear body surrounding a crystalline intranuclear inclusion (CL) is shown. 90 000 \times .

was observed in relation to survival time. Furthermore, the presence of nuclear bodies had no relationship to the degree of nuclear/cytoplasmic asynchrony.

Nuclear/Cytoplasmic Asynchrony

Assessment of the asynchrony by the criteria described in Material and Methods is illustrated by

the following figures. A plasma cell *without* asynchrony is shown in Fig. 1. The cell contains a mature looking nucleus with chromatin clumped in a cartwheel like arrangement. Parallel cisternae of the rough ER are seen in the mature appearing well-organized cytoplasm. Occasionally nucleoli of moderate size are seen in the cells without asynchrony. Plasma cells with *slight* asynchrony

TABLE 2 *The Frequency of Nuclear Bodies in Plasma Cells from Patients before and during Treatment*

Plasma cells from 12 patients	Total number of plasma cells	Number of sections of plasma cell nuclei with nuclear bodies	% nuclear bodies of plasma cells (range)
Before treatment*	298	20	6.7 (0-13.3)
During treatment	1217	192	15.8 (8.2-23.3)

*One patient (EH) is omitted due to treatment at the time of the first biopsy

The Wilcoxon test for pair differences was used untreated versus treated (14) ($2P = 0.004$)

(Figs. 2, 5, 17) have a mature appearing, well-organized cytoplasm with parallel stacks of rough ER and a nucleus with scattered small aggregates of chromatin. Nucleoli of moderate size are seen in many of these cells. Cells with moderate asynchrony (Fig. 3) show a nucleus with small amounts of chromatin aggregates and a cytoplasm containing stacks of flattened rough ER. In some cells with moderate asynchrony a nucleus with similar distribution of chromatin is present together with dilated rough ER in the cytoplasm. Cells with marked asynchrony (Fig. 4) show a nucleus with evenly distributed, rather electron lucent chromatin and a cytoplasm containing dilated cisternae of the rough ER. Prominent nucleoli are seen frequently in the cells showing moderate and marked asynchrony.

When all the plasma cells available were evaluated with respect to nuclear/cytoplasmic asynchrony it was found that cells without asynchrony were seen only occasionally in the patients. Marked asynchrony, however, was found in cells of the first biopsy from seven of the patients (GH, MN, CB, EJ, JN, EH, AS). After treatment was initiated marked asynchrony could be found only in a small percentage of plasma cells in four of these seven patients (MN, CB, EH, EJ). Cells from two of them (EH, EJ) contained Russell bodies, which means that the cisternae of the rough ER ...

the plasma cells of the patients and the clinical values of the major tests with prognostic significance obtained at the time of diagnosis, i.e. the concentrations of serum creatinine, haemoglobin, serum albumin and serum calcium. All the patients were treated with alkylating agents (melphalan or cyclophosphamide), but the schedules used for individual patients differed to some extent. Nine patients had a lower M component concentration in serum samples taken during the treatment than at the time of diagnosis. This decrease was most evident for patients with a short survival time (MN, LB, VS, KC) as described previously (17). For five patients the irregular intervals (2-26 months) at which blood samples were obtained did not permit a time related evaluation of changes in the M component concentration. Serum samples from three patients (KC, AS, GC) showed a marked increase in the serum concentration of the M component during the course of the disease. Plasma cells from patients who developed either a decrease or an increase of the M component showed no evident morphological changes as compared to the plasma cells obtained at the time of diagnosis, except for the described increase in the number of nuclear bodies.

Six of the patients (GH, VS, KC, GH, JN, AS) were treated intermittently with cytostatics intravenously in doses which were calculated in relation to the body weight of the patients, i.e. melphalan 30-50 mg, cyclophosphamide 1000-2000 mg. The plasma cells obtained from these patients 1 to 30 days after treatment were evaluated and their ultrastructure was compared with that of cells from the first biopsy. The only common morphological difference observed, irrespective of the time interval after initiation of treatment, was a definite increase in the percentage of plasma cells showing slight nuclear/cytoplasmic asynchrony. An increase in the percentage of cells with nuclear bodies was also noted.

of the cells from the untreated patients. A total number of 298 cells were studied. An equal number of cells (292) obtained from the last biopsy of the same patients obtained during treatment, showed that this percentage had increased to 5.4, i.e. a significant increase ($2P = 0.03$).

Clinical Staging and Course

No correlation could be found between the variation within the intracellular structures found in

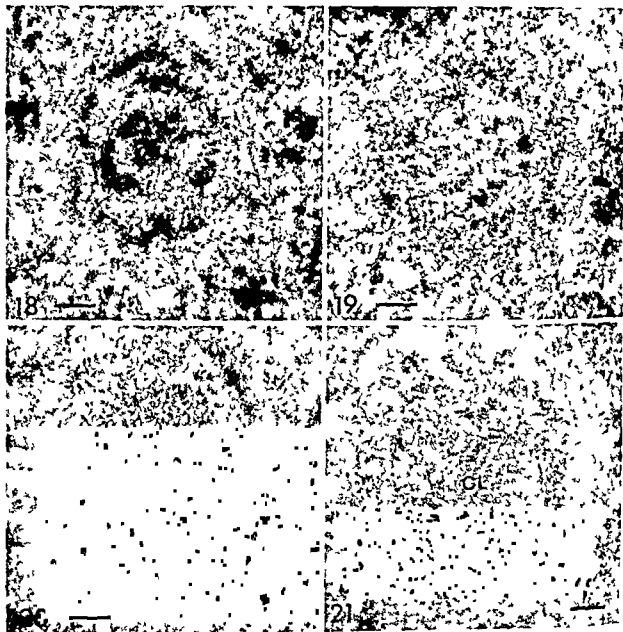


Fig 18 Part of a plasma cell nucleus from patient OB. A nuclear body composed of fibrils arranged concentrically is shown. 90 000 \times .

Fig 19 Part of a plasma cell nucleus from patient JN. A nuclear body composed of small granules surrounded by fibrils is shown. 90 000 \times .

Fig 20 Part of the nucleus of the plasma cell seen in Fig. 17. A nuclear body with a central electron dense mass surrounded by fibrils is shown. 90 000 \times .

Fig 21 Part of a plasma cell nucleus from patient AS. A nuclear body surrounding a crystalline intranuclear inclusion (CL) is shown. 90 000 \times .

was observed in relation to survival time. Furthermore, the presence of nuclear bodies had no relationship to the degree of nuclear/cytoplasmic asynchrony.

Nuclear/Cytoplasmic Asynchrony

Assessment of the asynchrony by the criteria described in Material and Methods is illustrated by

the following figures. A plasma cell *without* asynchrony is shown in Fig. 1. The cell contains a mature looking nucleus with chromatin clumped in a cartwheel like arrangement. Parallel cisternae of the rough ER are seen in the mature appearing, well organized cytoplasm. Occasionally nucleoli of moderate size are seen in the cells without asynchrony. Plasma cells with *slight* asynchrony

shown that their occurrence is not restricted to myeloma cells as contact zones have been found in plasma cells from patients without a serum M component (Blom, unpublished work). Our earlier hypothesis that the contact zones were most frequent in the bone marrow of patients at the terminal stage of their disease (8) could not be corroborated in this study. Another type of contact zones was observed between bone marrow plasma cells and a strip of basement membrane or a lamina densa like material. Plasma cells with such contact zones were often seen close to a small vessel. A structurally similar intimate contact with small vessels has been described in perivascular plasma cells of brain tissue from patients with multiple sclerosis (26).

Only a few myeloma cells in this study showed nuclei with markedly irregular contours. It has been suggested that such a nuclear lobulation is produced by a contraction of the microfibrils and microtubules which are accumulated in close association with the nucleus at the region of a nuclear lobulation (2, 4).

Three different morphological types of intranuclear inclusions were observed in the biopsies from four of our patients and it should be noted that these patients all had a rather long survival time. The intranuclear Russell body was seen in three patients and this observation has been described in detail previously (6). A fourth patient (AS) had two kinds of intranuclear inclusions: a crystalline and a fibrillar. The fibrillar type has been described in myeloma cells by Smetana *et al* (30) who called them rodlets and by Oikawa (25). The crystalline type has to the best of our knowledge not been described before in any plasma cell. The nature and significance of these nuclear inclusions are unknown.

Nuclear bodies were first described by De Thé *et al* (10) in tumour cells from a rabbit. Since then these structures have been observed in several different types of both normal and tumour cells (15). Some papers have described these globular structures in plasma cells (19, 29) but only a few observations on their presence in myeloma cells have been made (1, 31). The morphology and size of the nuclear bodies found in our study were identical to those already found (e.g. ref. 1, 15). Experiments with antigenically stimulated mice showed that the percentage of sections of lymphnode plasma cells containing one or more nuclear bodies increased parallel to the concentration of circulating antibodies (19, 29). This result led to a presumed relationship between the number of nuclear bodies in plasma cells and the concentration of serum antibodies. Simar (29) demonstrated by enzyme

digestion of plasma cell sections that the fibrillar component of nuclear bodies contains RNA, whereas the dense granular component contains DNA.

Recent studies by means of high resolution autoradiography have shown that nuclear bodies in spleen cells of immunized mice incorporated significantly more radioactive material than the surrounding nucleoplasm (13). Drewinko *et al* (11) and Salmon (27) have performed growth kinetic studies on myeloma cells. They measured the labelling index (LI) of bone marrow myeloma cells as an indication of the fraction of cells which synthesized DNA and thus could be considered to be a proliferating subpopulation of the myeloma cells. It was found that the LI of the myeloma cells increased from approximately 3 per cent before treatment to within the range of 15–40 per cent after administration of alkylating agents to the patients. In a later paper, however, Drewinko & Alexanian (12) concluded that the LI may not accurately reflect the growth fraction of the tumour mass in patients with multiple myeloma. On the other hand, that study showed that the LI for patients observed during the first 3 months of treatment was significantly higher than for untreated patients but after longer periods of treatment the LI declined. In our material we noted an increase in the number of nuclear bodies in the plasma cells during treatment of the patients (Table 2). Therefore it seems likely to us that it is the plasma cells with nuclear bodies which are in a proliferative phase. If so it should be possible to demonstrate a correlation between the number of nuclear bodies and the LI of the myeloma cells.

Snapper & Kahn (32) have considered that the immaturity of the nucleus in relation to the cytoplasm seen in myeloma cells is of diagnostic value. Graham & Bernier (16) classified nuclear/cytoplasmic asynchrony from ultrastructural studies on plasma cells and concluded that this asynchrony is the most consistent and reliable criterion for distinguishing myeloma cells from plasma cells obtained from patients without any sign of multiple myeloma. They also found that the degree of asynchrony correlated well with the clinical score they determined for their patients.

Our results support those of Graham & Bernier.

con

a n

166 myeloma cells we studied were slightly to markedly asynchronous.

With respect to clinical stage versus degree of asynchrony, we have compared the survival time with the degree of asynchrony. Except for patient AS, who is still alive and in whom most myeloma cells are only slightly asynchronous we were unable to demonstrate any pronounced relationship.

DISCUSSION

This paper describes the ultrastructure of myeloma cells, i.e. plasma cells from patients with multiple myeloma. Consecutive bone marrow specimens were obtained from 13 patients during the clinical course of their disease. A total of 65 biopsies were available for study, and from these 1600 sectioned plasma cells were examined.

The clinical course of multiple myeloma varies from patient to patient and in most cases is unpredictable. Several investigators (1, 3, 5, 16) have attempted to correlate a number of ultrastructural characteristics of myeloma cells with different biochemical and clinical parameters of the patients in order to achieve a reliable prognosis for the disease. The present time-related investigation of samples from 11 patients during their survival period is a further attempt to evaluate this possibility.

The morphological analysis of the plasma cells from the individual patients was carried out during the course of the disease. In addition, it was considered valuable to compare the morphology of plasma cells from the first biopsy of untreated patients with that of cells from biopsies of the same patients during their treatment. We can thus confirm earlier described morphological differences between myeloma cells (16, 23, 28) obtained from different patients. However, each individual patient presented a characteristic and rather constant «myeloma cell picture».

The size of the myeloma cells varied considerably between individual patients. Most of these cells possessed microvilli-like extensions on their surface together with a varying number of pseudopods and it is tempting to speculate whether the pseudopods participate in the movement of the cell (4) or if they represent the morphological basis for the secretion of immunoglobulins, clasmotosis (33). On the other hand, since only one patient (OB) showed a substantial number of myeloma cells with pseudopods in all biopsies, these structures do not seem to be absolutely necessary for the secretion of the immunoglobulins produced by the cells.

The main part of the cytoplasm in the myeloma cell is occupied by cisternae of the rough ER. Several investigators (1, 23, 28) have grouped the myeloma cells into as many as six different types based on the morphology of the rough ER. The results of an attempt to correlate these morphological differences with the class of M component produced have been of limited value. In our study, the lamellar type of the rough ER was the most common in the myeloma cells. Apart from the patients with Russell bodies (EH, EJ, OB), only one

patient (MN) had plasma cells where most of the rough ER was of the globular type. This patient had a very short survival time.

Annulate lamellae (21) were found in close relation to the cisternae of the rough ER in plasma cells from two patients (MN, ES). Such lamellae have been described previously in myeloma cells (16), but their significance and origin have not been clarified (15).

Circular arrangements of the rough ER with one to three filaments interposed between the cisternae were occasionally found in plasma cells from four of the patients (KC, OB, CB, AS). This type of structure has been described by Krull *et al.* (22) in bone marrow plasma cells of a patient who secreted Bence Jones protein of the kappa type. Fig. 12 in the paper of Graham & Bernier (16) shows a longitudinal section of a similar structure in a plasma cell from a patient secreting monoclonal IgG type kappa. These structures bear some resemblance to the «ribosome-lamellae-complex» described in hairy cells (20) and myeloma cells (25). In contrast to the last mentioned complexes, those in our study always presented their filaments interposed between two cisternae of the rough ER. Neither did we find a regular attachment of ribosomes to the concentric membranes of the rough ER, as described for the hairy cell complex (20). Similar filaments were found between the cylindrical arrangement of cisternae of the rough ER in some plasma cells of a patient with a serum M component of the IgG type lambda (Blom, unpublished work). This M component was shown to possess antistreptolysin O activity (24).

Some mitochondria with an abnormal morphology were observed in the myeloma cells of some patients, but their presence could not be correlated with presence or absence of other characteristic structures. However, the mean number of mitochondria in the sectioned plasma cells was very low for the two patients who are still alive. This can probably be taken as an indication of the low activity level of these myeloma cells. This again could be a sign of a better prognosis but a significant correlation could not be found between the survival time and the mean number of mitochondria in the myeloma cells of the other patients.

The ultrastructure of contact zones between plasma cells and dendritic bone marrow macrophages in patients with multiple myeloma has been described previously (7, 8). These contact zones were found in plasma cells in all the biopsies, except in cells with very irregular nuclei where they only occurred occasionally. The significance of the contact zones is still unknown. However, it has been

shown that their occurrence is not restricted to myeloma cells, as contact zones have been found in plasma cells from patients without a serum M component (Blom, unpublished work). Our earlier hypothesis that the contact zones were most frequent in the bone marrow of patients at the terminal stage of their disease (8) could not be corroborated in this study. Another type of contact zones was observed between bone marrow plasma cells and a strip of basement membrane or a lamina densa like material. Plasma cells with such contact zones were often seen close to a small vessel. A structurally similar intimate contact with small vessels has been described in perivascular plasma cells of brain tissue from patients with multiple sclerosis (26).

Only a few myeloma cells in this study showed nuclei with markedly irregular contours. It has been suggested that such a nuclear lobulation is produced by a contraction of the microfibrils and microtubules which are accumulated in close association with the nucleus at the region of a nuclear lobulation (2, 4).

Three different morphological types of intranuclear inclusions were observed in the biopsies from four of our patients and it should be noted that these patients all had a rather long survival time. The intranuclear Russell body was seen in three patients and this observation has been described in detail previously (6). A fourth patient (AS) had two kinds of intranuclear inclusions, a crystalline and a fibrillar. The fibrillar type has been described in myeloma cells by Smetana *et al.* (30), who called them rodlets, and by Okawa (25). The crystalline type has to the best of our knowledge not been described before in any plasma cell. The nature and significance of these nuclear inclusions are unknown.

Nuclear bodies were first described by De Thé *et al.* (10) in tumour cells from a rabbit. Since then these structures have been observed in several different types of both normal and tumour cells (15). Some papers have described these globular structures in plasma cells (19, 29), but only a few observations on their presence in myeloma cells have been made (1, 31). The morphology and size of the nuclear bodies found in our study were identical to those already found (e.g. ref. 1, 15). Experiments with antigenically stimulated mice showed that the percentage of sections of lymphnode plasma cells containing one or more nuclear bodies increased parallel to the concentration of circulating antibodies (19, 29). This result led to a presumed relationship between the number of nuclear bodies in plasma cells and the concentration of serum antibodies. Since (20) demonstrated by enzyme

digestion of plasma cell sections that the fibrillar component of nuclear bodies contains RNA, whereas the dense granular component contains DNA.

Recent studies by means of high resolution autoradiography have shown that nuclear bodies in spleen cells of immunized mice incorporated significantly more radioactive material than the surrounding nucleoplasm (13). Drewinko *et al.* (11) and Salmon (27) have performed growth kinetic studies on myeloma cells. They measured the labelling index (LI) of bone marrow myeloma cells as an indication of the fraction of cells which synthesized DNA and thus could be considered to be a proliferating subpopulation of the myeloma cells. It was found that the LI of the myeloma cells increased from approximately 3 per cent before treatment to within the range of 15–40 per cent after administration of alkylating agents to the patients. In a later paper, however, Drewinko & Alexanian (12) concluded that the LI may not accurately reflect the growth fraction of the tumour mass in patients with multiple myeloma. On the other hand, that study showed that the LI for patients observed during the first 3 months of treatment was significantly higher than for untreated patients, but after longer periods of treatment the LI declined. In our material we noted an increase in the number of nuclear bodies in the plasma cells during treatment of the patients (Table 2). Therefore it seems likely to us that it is the plasma cells with nuclear bodies which are in a proliferative phase. If so, it should be possible to demonstrate a correlation between the number of nuclear bodies and the LI of the myeloma cells.

Snapper & Kahn (32) have considered that the immaturity of the nucleus in relation to the cytoplasm seen in myeloma cells is of diagnostic value. Graham & Bernier (16) classified nuclear/cytoplasmic asynchrony from ultrastructural studies on plasma cells and concluded that this asynchrony is the most consistent and reliable criterion for distinguishing myeloma cells from plasma cells obtained from patients without any sign of multiple myeloma. They also found that the degree of asynchrony correlated well with the clinical score they determined for their patients.

Our results support those of Graham & Bernier concerning the nuclear/cytoplasmic asynchrony as a reliable criterion for myeloma cells. Most of the 1600 myeloma cells we studied were slightly to markedly asynchronous.

With respect to clinical stage versus degree of asynchrony, we have compared the survival time with the degree of asynchrony.

...to demonstrate any pronounced relationship

However, our study has shown that plasma cells with slight asynchrony constitute a significantly greater fraction of the cells in patients under than before treatment

In nine of the patients where the serum contained monoclonal IgG, the response to chemotherapy was associated with a reduction of the concentration of the serum M component as well as of the degree of nuclear/cytoplasmic asynchrony. This observation is in agreement with the findings reported for two of the patients studied by *Graham & Bernier* (16) and is compatible with the conception that cells with a high degree of asynchrony are especially susceptible to chemotherapy

We are indebted to civing *Aksel Birch-Andersen*, Department of Biophysics, Statens Seruminstitut, for his sustained support and advice through the years. We wish to thank *Joan M Rhodes* Ph.D., WHO Collaborative Centre for Reference and Research on Escherichia, Statens Seruminstitut, for her valuable and constructive criticism of the manuscript. The excellent and patient technical assistance of Mrs *Jytte Berg* and Mrs *Anne Grethe Caspersen* is gratefully acknowledged. Mr *Finn Laursen* and Miss *Anne Grethe Overgaard* are thanked for their expert photographic work.

We wish to thank the chiefs of the Medical Department of Finsen Hospital, Copenhagen, and the Medical Department B of Hillerød County Hospital, respectively, for providing us bone marrow aspirations from some of the patients

REFERENCES

- 1 *Asano, M., Kawahara, I. & Koiani, M.* Electron microscopic characteristics of myeloma cells with special reference to their correlation with myeloma globulin types. *Med J Shinshu Univ* 14 103-121, 1969
- 2 *Beltran, G. & Stuckey, W. J.* Nuclear lobulation and cytoplasmic fibrils in leukemic plasma cells. *Amer J clin Path* 58 159-164, 1972
- 3 *Bernier, G. M. & Graham, R. C. Jr.* Plasma cell asynchrony in myeloma. Correlation of light and electron microscopy. *Semin Hematol* 13 239-245 1976
- 4 *Bessis, M.* Living blood cells and their ultrastructure. Springer, Berlin 1973, p. 21 and 41
- 5 *Brecher, G., Tanaka, Y., Malmgren, R. A. & Fahey, J. L.* Morphology and protein synthesis in multiple myeloma and macroglobulinemia. *Ann NY Acad Sci* 131 642-653, 1964
- 6 *Blom, J., Mansa, B. & Hunk, A.* A study of Russell bodies in human monoclonal plasma cells by means of immunofluorescence and electron microscopy. *Acta path microbiol scand Sect A*, 84 335-349, 1976
- 7 *Blom, J.* The ultrastructure of macrophages found in contact with plasma cells in the bone marrow of patients with multiple myeloma. *Acta path microbiol scand Sect A*, 85 335-344, 1977
- 8 *Blom, J.* The ultrastructure of contact zones between plasma cells and macrophages in the bone marrow of patients with multiple myeloma. *Acta path microbiol scand Sect A*, 85 345-355, 1977
- 9 *Dammacco, F. & Waldenström, J.* Bence Jones proteinuria in benign monoclonal gammopathies. *Acta med scand* 184 403-409, 1968
- 10 *De The, G., Riviere, M. & Bernhard, W.* Examen au microscope électronique de la tumeur VX2 du lapin domestique dérivée du papillome de Shope. *Bull Cancer* 47 570-584, 1960
- 11 *Drewinko, B., Brown, B. W., Humphrey, R. & Alexanian, R.* Effect of chemotherapy on the labelling index of myeloma cells. *Cancer* 34 526-531, 1974
- 12 *Drewinko, B. & Alexanian, R.* Growth kinetics of plasma cell myeloma. *J nat Cancer Inst* 58 1247-1253, 1977
- 13 *Dupuy-Coin, A. M. & Bouteille, M.* Protein renewal in nuclear bodies, as studied by quantitative ultrastructural autoradiography. *Exp Cell Res* 90 111-118, 1975
- 14 *Geigy Scientific tables*, 7th ed 1970, p. 192
- 15 *Ghadially, F. N.* Ultrastructural pathology of the cell. Butterworths, London and Boston 1975 pp 80-83 and 283-289
- 16 *Graham, R. C. Jr. & Bernier, G. M.* The bone marrow in multiple myeloma. Correlation of plasma cell ultrastructure and clinical state. *Medicine (Baltimore)* 54 225-243, 1975
- 17 *Hansen, O., Paaske, Jessen, B. & Videbæk, A.* Prognosis of myelomatosis on treatment with prednisone and cytostatics. *Scand J Haematol* 10 282-290, 1973
- 18 *Hansen, O., Paaske, Thorling, E. B. & Drivsholm, A.* Serum erythropoietin in myelomatosis. *Scand J Haematol* 19 106-110, 1977
- 19 *Ishii, Y., Mori, M. & Onoé, T.* Electron microscopic study of nuclear bodies in plasma cells of mouse lymph nodes during the primary immune response. *J electron Microscopy* 20 182-190, 1971
- 20 *Katayama, I., Li, C. Y. & Yam, L. T.* Ultrastructural characteristics of the «hairy cells» of leukemic reticuloendotheliosis. *Amer J clin Path* 67 361-370, 1972
- 21 *Kessel, R. G.* Annulate lamellae. *J Ultrastruct Res Suppl* 10 1968
- 22 *Krull, P., Luciano, L. & Reale, E.* Über neuartige zylindrische Formationen in Plasmazellen eines gutartig verlaufenden Bence-Jones Plasmacytoms (BJP). *Klin Wschr* 50 552-556 1972
- 23 *Maldonado, J. E., Brown, A. L. Jr., Bayrd, E. D. & Pease, G. L.* Ultrastructure of the myeloma cell. *Cancer* 19 1613-1627 1966
- 24 *Mansa, B. & Kjems, E.* High titres of specific antibodies with the M-components of

- Research on Group A Streptococcus Excerpta Medica Monograph Amsterdam 1968 pp 218-224
- 25 *Okawa K* Electron microscopic observation of inclusion bodies in plasma cells of multiple myeloma and Waldenström's macroglobulinemia *Tohoku J exp Med* 117 257-281 1975
 - 26 *Prineas J W & Wright R C* Macrophages, lymphocytes and plasma cells in the perivascular compartment in chronic multiple sclerosis *Lab Invest* 38 409-421 1978
 - 27 *Salmon S E* Expansion of the growth fraction in multiple myeloma with alkylating agents *Blood* 45 119-129 1975
 - 28 *Shigematsu T* The fine structure of various types of myeloma cells as revealed by electron microscopy *Arch Histol Jap* 30 375-400 1969
 - 29 *Siman I J* Ultrastructure et constitution des corps nucléaires dans les plasmocytes *Z Zellforsch* 99 235-251 1969
 - 30 *Smetana K Gyorkey F Gyorkey P & Busch H* Ultrastructural studies on human myeloma plasmocytes *Cancer Res* 33 2300-2309 1973
 - 31 *Smetana K Hermansky F Kobliková H & Pospisil V* A further note on the ultrastructure of myeloma plasmacytes *Neoplasma* 18 3-13 1971
 - 32 *Snapper I & Kahn A I* Multiple myeloma *Semin Hematol* 1 87-143 1964
 - 33 *Thiery J P* Ultrastructure et fonctions des cellules impliquées dans la réaction immunitaire *Bull Soc Chim biol (Paris)* 50 1077-1100 1968
 - 34 *Zucker Frankl n D* Structural features of cells associated with the paraproteinemias *Semin Hematol* 1 165-198 1964

However, our study has shown that plasma cells with slight asynchrony constitute a significantly greater fraction of the cells in patients under than before treatment

In nine of the patients where the serum contained monoclonal IgG the response to chemotherapy was associated with a reduction of the concentration of the serum M component as well as of the degree of nuclear/cytoplasmic asynchrony. This observation is in agreement with the findings reported for two of the patients studied by *Graham & Bernier* (16) and is compatible with the conception that cells with a high degree of asynchrony are especially susceptible to chemotherapy

We are indebted to civing *Aksel Birch Andersen* Department of Biophysics Statens Seruminstitut for his sustained support and advice through the years. We wish to thank *Joan M Rhodes* Ph D WHO Collaborative Centre for Reference and Research on Escherichia Statens Seruminstitut for her valuable and constructive criticism of the manuscript. The excellent and patient technical assistance of *Mrs Jytte Berg* and *Mrs Anne Grethe Caspersen* is gratefully acknowledged. Mr *Finn Laursen* and Miss *Anne Grethe Overgaard* are thanked for their expert photographic work.

We wish to thank the chiefs of the Medical Department of Finsen Hospital Copenhagen and the Medical Department B of Hillerød County Hospital respectively for providing us bone marrow aspirations from some of the patients

REFERENCES

- 1 *Asano M Kawahara I & Kotani M* Electron microscopic characteristics of myeloma cells with special reference to their correlation with myeloma globulin types *Med J Shinshu Univ* 14 103-121 1969
- 2 *Beltran G & Stuckey W J* Nuclear lobulation and cytoplasmic fibrils in leukemic plasma cells *Amer J clin Path* 58 159-164 1972
- 3 *Bernier G M & Graham R C Jr* Plasma cell asynchrony in myeloma. Correlation of light and electron microscopy *Semin Hematol* 13 239-245 1976
- 4 *Bessis M* Living blood cells and their ultrastructure *Springer* Berlin 1973 p 21 and 41
- 5 *Brecher G Tanaka Y Malmgren R A & Fahey J L* Morphology and protein synthesis in multiple myeloma and macroglobulinemia *Ann NY Acad Sci* 131 642-653 1964
- 6 *Blom J Mansa B & Wuk A* A study of Russell bodies in human monoclonal plasma cells by means of immunofluorescence and electron microscopy *Acta path microbiol scand Sect A* 84 335-349 1976
- 7 *Blom J* The ultrastructure of macrophages found in contact with plasma cells in the bone marrow of patients with multiple myeloma *Acta path microbiol scand Sect A* 85 335-344 1977
- 8 *Blom J* The ultrastructure of contact zones between plasma cells and macrophages in the bone marrow of patients with multiple myeloma *Acta path microbiol scand Sect A* 85 345-355 1977
- 9 *Dammacco F & Waldenström J* Bence Jones proteinuria in benign monoclonal gammopathies *Acta med scand* 184 403-409 1968
- 10 *De Thé G Riviere M & Bernhard W* Examen au microscope électronique de la tumeur VX2 du lapin domestique dérivée du papillome de Shope *Bull Cancer* 47 570-584 1960
- 11 *Drewinko B Brown B W Humphrey R & Alexanian R* Effect of chemotherapy on the labelling index of myeloma cells *Cancer* 34 526-531 1974
- 12 *Drewinko B & Alexanian R* Growth kinetics of plasma cell myeloma *J nat Cancer Inst* 38 1247-1253 1977
- 13 *Dupuy Coin A M & Bouteille M* Protein renewal in nuclear bodies as studied by quantitative ultrastructural autoradiography *Exp Cell Res* 90 111-118, 1975
- 14 *Geigy* Scientific tables 7th ed 1970 p 192
- 15 *Ghadially F N* Ultrastructural pathology of the cell *Butterworths* London and Boston 1975 pp 80-83 and 283-289
- 16 *Graham R C Jr & Bernier G M* The bone marrow in multiple myeloma. Correlation of plasma cell ultrastructure and clinical state *Medicine (Baltimore)* 54 225-243 1975
- 17 *Hansen O Paaske Jessen B & Videbæk Aa* Prognosis of myelomatosis on treatment with prednisone and cytostatics *Scand J Haematol* 10 282-290 1973
- 18 *Hansen O Paaske Thorling E B & Drinsholm Aa* Serum erythropoietin in myelomatosis *Scand J Haematol* 19 106-110 1977
- 19 *Ishii Y Mori M & Onoé T* Electron microscopic study of nuclear bodies in plasma cells of mouse lymph nodes during the primary immune response *J electron Microscopy* 20 182-190 1971
- 20 *Katayama I Li C Y & Yam L T* Ultrastructural characteristics of the "hairy cells" of leukemic reticuloendotheliosis *Amer J clin Path* 67 361-370 1972
- 21 *Kessel R G* Annulate lamellae *J Ultrastruct Res Suppl* 10 1968
- 22 *Krull P Luciano L & Reale E* Über neuartige zylindrische Formationen in Plasmazellen eines gutartig verlaufenden Bence Jones Plasmacytoms (BJP) *Klin Wschr* 50 552-556 1972
- 23 *Maldonado J E Brown A L Jr Bayrd E D & Pease G L* Ultrastructure of the myeloma cell *Cancer* 19 1613-1627 1966
- 24 *Mansa B & Kjems E* High titres of specific antistreptolysin O activity within M components of human sera studied by a special immunoelectrophoretic technique *In Caravano R (Ed.) Current*

- Research on Group A Streptococcus Excerpta Medica Monograph Amsterdam 1968 pp 218-224
- 25 Okawa K Electron microscopic observation of inclusion bodies in plasma cells of multiple myeloma and Waldenstrom's macroglobulinemia Tohoku J exp Med 117 257-281 1975
- 26 Preuss J W & Wright R C Macrophages, lymphocytes and plasma cells in the perivascular compartment in chronic multiple sclerosis Lab Invest 38 409-421 1978
- 27 Salmon S E Expansion of the growth fraction in multiple myeloma with alkylating agents Blood 45 119-129 1975
- 28 Shigematsu T The fine structure of various types of myeloma cells as revealed by electron microscopy Arch Histol Jap 30 375-400 1969
- 29 Simar L J Ultrastructure et constitution des corps nucleaires dans les plasmocytes Z Zellforsch 99 235-251 1969
- 30 Smetana K Gyorkey F Gyorkey P & Busch H Ultrastructural studies on human myeloma plasmocytes Cancer Res 33 2300-2309 1973
- 31 Smetana K Hermansky F Koblikova H & Pospisil V A further note on the ultrastructure of myeloma plasmacytes Neoplasma 18 3-13 1971
- 32 Snapper I & Kahn A I Multiple myeloma Semin Hematol 1 87-143 1964
- 33 Thiery J P Ultrastructure et fonctions des cellules impliquees dans la reaction immunitaire Bull Soc Chim biol (Paris) 50 1077-1100 1968
- 34 Zucker Franklin D Structural features of cells associated with the paraproteinemias Semin Hematol 1 165-198 1964

MORPHOLOGICAL CHANGES AND FATTY ACID COMPOSITION IN HEARTS FROM PIGS FED RAPESEED OIL, FISH OIL, PARTIALLY HYDROGENATED FISH OIL, PARTIALLY HYDROGENATED SOYBEAN OIL AND LARD

H SVAAR¹ F T LANGMARK² G LAMBERTSEN³ and J OPSTVEDT⁴

¹Department of Pathology Ullevål Hospital Oslo Norway ²Department of Pathology The Norwegian Radium Hospital Oslo Norway ³Institute of Vitamin Research Bergen Norway
⁴Norwegian Herring Oil and Meal Industry Research Institute Bergen Norway

Svaar H Langmark F T Lambertsen G & Opstvedt J Morphological changes and fatty acid composition in hearts from pigs fed rapeseed oil fish oil partially hydrogenated fish oil partially hydrogenated soybean oil and lard *Acta path microbiol scand Sect A 88 41-48 1980*

Female pigs fed diets in which 42% of the caloric intake came from either rapeseed oil fish oil partially hydrogenated fish oil partially hydrogenated soybean oil or lard were killed after one week, five weeks six months and one year. Type of fat or length of feeding did not affect the cardiac content of total fat which was normal in all animals. The fatty acid pattern of tissue triglycerides only partly reflected the fatty acid pattern of diets. The relative amounts of C22:1 and C20:1 were greatest after six months and levelled off during the following six months. The content of C22:1 in cardiac triglycerides never exceeded one fifth of the dietary concentration. Microscopic lipidosis was found in some pigs after one week five weeks and six months. Minor heart lesions consisting of focal necrosis of muscle cells were found after one week and more frequently after six months and one year. No relationship between incidence and severity of the heart lesions and any particular type of fat in the diet could be found.

Key words: Rapeseed oil fish oil cardiac triglycerides heart lesions pigs

H Svaar Patologisk anatomisk afdeling Sentralsykehuset 1 Akershus 1474 Nordbyhagen Norge

Received 10 vi 79 Accepted 25 vii 79

When moderate to high levels of rapeseed oil are included in experimental diets certain myocardial effects may occur depending on the species employed and the length of the feeding period. Most experiments have been carried out with rats but some also with ducklings miniature pigs gerbils and monkeys (1, 2, 3, 6, 7, 15). In the weanling rat the initial effect is an accumulation of fat in the heart muscle cells which appears after a few hours and reaches a maximum after one week. Later it declines gradually in spite of continuous feeding with rapeseed oil. The myocardial lipidosis is dose

related to the erucic acid content in rapeseed oil when erucic acid constitutes more than 2% (w/w) of the diet (6). When rapeseed oil is given continuously to weanling rats for weeks and months increasing numbers of focal myocardial cell necrosis and cardiac fibrosis are found. The severity of the cardiac lesion may be dependent on the dietary level of erucic acid but identical changes have been found in rats receiving rapeseed oil with low erucic acid content (15).

It is of interest to examine whether fish oils containing small amounts of erucic acid and other

long-chain mono unsaturated fatty acids cause the same heart changes as rapeseed oil

In the first scientific report on cardiac effects of rapeseed oil *Raine et al* (13) described the findings in rats and pigs. In rats cardiac lesions were found after 2-8 weeks. In pigs, the changes were much less pronounced, and similar changes were observed when soybean oil was the fat source. Pigs are omnivorous like humans and they are fairly similar to man as regards plasma lipoproteins (10) and coronary circulation (17).

In the present study, domestic pigs were fed fat rich diets containing rapeseed oil, fish oil, partially hydrogenated fish oil, partially hydrogenated soybean oil or lard for 1, 5, 27 and 52 weeks, and their hearts were examined at each stage for evidence of lipidosis and cardiac lesions and for alterations in fatty acid composition by chemical analysis.

MATERIAL AND METHODS

Animals and Experimental design

Female piglets of the Norwegian landrace breed aged between 40 and 80 days (body weight range 10-17 kg) were obtained directly from local breeders. A total of 42 piglets came from 8 litters. Two piglets were killed before the start of the experiment. The remaining 5 piglets from each litter were randomly allocated to the five experimental groups to a total of 8 piglets per group. Piglets in each experimental group were kept in two separate pens of four piglets in each. Pen temperature and humidity were controlled.

Diets

Prior to the experiment the piglets had been nursed by their mothers and in addition received a commercial creep feed given *ad lib* and consisting of 2% dried skim milk, 3% herring meal, 11% soybean meal, 15% maize, 25% barley, 24% wheat, 12% molasses, 15% sugar, 4% grass meal and 2.5% minerals and vitamins.

The pigs were fed the experimental diets without an adaptation period. The five different diets contained 16% (w/w) from the following fats: rapeseed oil (RO), partially hydrogenated capelin oil (HCO) or capelin oil (CO), partially hydrogenated soybean oil (HSO) or lard (L). The composition of the diets was (all figures in % (w/w)): barley 39, solvent extracted soybean meal 26, ground oat hulls 15, sunflower oil 15, fat 16, mineral mixture 3, potassium monophosphate 0.5, vitamin mixture 0.45. The mineral mixture consisted of (all figures per kg of the diet): Ca 7.5 g, P 1.8 g, NaCl 4.73 g, Fe 48 mg, Mn 60 mg, Zn 51 mg, Se 0.1 mg, I 2.2 mg. The vitamin mixture consisted of (all figures per kg of the diet): Vit A 2800 IU, Vit D3 400 IU, Vit E 100 IU, Thiamine HCl 2.6 mg, Riboflavin 6 mg, Nicotin 44 mg, Pantothenic acid 26 mg, Choline Cl 15 mg, Vit B12 0.044 mg, Pyridoxin Cl 3 mg, Ethoxy quine 300 mg, DL methionine 400 mg. The composition

of the diets gives 3330 kcal per kg diet in metabolizable energy of which 42 % comes from fat. Protein constituted 17 % (w/w) of the diet and the concentrations of lysine and methionine were 0.9% and 0.5% (w/w) respectively.

The rapeseed oil was obtained in an unrefined form. The unrefined (raw) and partially hydrogenated capelin oils were processed from winter caught capelin (*Mallotus villosus*) under commercial conditions. The partially hydrogenated soybean oil was also a commercial sample and like the partially hydrogenated capelin oil was hydrogenated to a melting point of 31-33 °C.

Hydrogenated soybean oil was included in the study for its content of trans fatty acids as a control for the hydrogenated fish oils. Lard does not contain C22 fatty acids or trans fatty acids and served as a control fat.

Table 1 gives the composition of the fatty acids extracted from the feed. Batches of feed were prepared at the start of the experiment and again after 150, 180 and 240 days. Immediately after mixing the diets were stored in sealed polyethylene bags at ambient temperature (0-20 °C). Each bag contained feed for a maximum of 3 days consumption.

During the first two weeks the piglets had access to feed twice a day, each of one hour duration. Later a feeding schedule based on live weight was introduced, increasing from 1 kg per pig per day at 35 kg to 3 kg per pig per day at 100 kg and above. Individual feed intakes were recorded daily. Water was available *ad lib*. Live weights were recorded on arrival, once a week and prior to killing. Two pigs per treatment group were slaughtered after 1, 5, 27, 37 (treatment group CO only) and 52 weeks.

Complete autopsies were performed and all organs were weighed after dissection of attached fat. Tissue samples were taken from the heart, liver, kidneys, lungs, adrenals, spleen, small and large intestines, skeletal muscle (from the left thigh), adipose tissue (from below the right shoulder) and aorta. The hearts were cut transversally in 5 mm thick sections from the apex to the base. Every second section was fixed for morphological examination, the rest was frozen for chemical lipid analysis.

Morphological Examination

The hearts were examined by light microscopy for presence of lipidosis and for cardiac lesions. Standardized blocks from the left anterior wall were frozen, sectioned and stained with Oil Red O for demonstration of fat and the findings were graded as follows: 0 = negative, grade 1 = lipid droplets in less than 25% of the muscle cells, grade 2 = lipid droplets in 25-50% of muscle cells, grade 3 = lipid droplets in 50-75% of muscle cells and grade 4 = lipid droplets in more than 75% of the cells.

Three complete transverse sections from each heart were embedded in paraffin and stained with Hematoxylin, Phloxine, Saffron (14). This method was chosen to make a good distinction between connective tissue and other cardiac structures. Cardiac lesions consisted of muscle cell necrosis, accumulation of inflammatory cells

TABLE 1 Fatty Acid Composition of the Dietary Fats Extracted from the Feed

Fatty acids	Lard	HSD Hydrogenated soybean oil	HCO Hydrogenated capelin oil	CO Capelin oil	RO Rapeseed oil
14:0	1.9	0.3	6.8	5.7	—
16:0	20.9	11.5	12.0	9.2	4.2
16:1	3.8	0.4	7.1	6.1	0.1
18:0	14.8	8.1	3.9	1.5	1.4
18:1	40.7	62.1	15.9	13.0	13.1
18:2	12.6	13.2	7.6	6.3	17.4
18:3	1.6	0.9	—	1.5	10.3
18:4	—	—	—	3.6	—
20:0	—	—	3.0	—	—
20:1	1.5	0.5	15.2	14.4	8.3
20:2-3	—	—	2.4	—	—
20:4	0.2	—	—	—	—
20:5	—	—	—	8.0	—
22:0	—	0.5	2.2	—	—
22:1	—	0.5	17.8	18.0	42.2
22:2-4	—	—	3.1	—	—
22:5	—	—	—	1.0	—
22:6	—	—	—	8.7	—
Others	2.0	2.0	3.0	3.0	3.0
Ratio of unsaturated/ saturated fatty acids	1.6	3.8	2.5	4.9	16.3

and areas of connective scar tissue. The cardiac findings were graded as follows: grade 1 = one focal lesion consisting of necrotic muscle cells and inflammatory cells or a small focal scar; grade 2 = two or three focal lesions of grade 1 type; grade 3 = more than three focal lesions or larger confluent lesions covering more than one high power microscopical field. Frozen sections from the liver, adrenals, skeletal muscle, kidneys, and spleen were stained for fat with Oil Red O. Sections from all organs were stained with Hematoxylin Eosin. All specimens were studied independently by two pathologists without prior knowledge of the dietary group.

Method of Analysis

Chemical analysis of feed ingredients was done by conventional methods. Each diet was sampled and a composite was stored at -20°C in a sealed box pending analysis. The samples were extracted with chloroform/methanol to give total lipids from which fatty acid methyl esters were prepared and analysed by gas liquid chromatography.

Pieces of 5 g were taken from frozen samples of each heart, liver and skeletal muscle and pooled for each experimental group; thus 10 g samples were processed per organ per group.

Lipids were extracted from the ground samples with chloroform/methanol (7/3). The lipid extracts were

diluted to give a 5% solution for gas chromatography. These samples were stored in closed vials at -20°C until analysed.

These samples were analysed by gas chromatography using a 5% solution for gas chromatography. These samples were stored in closed vials at -20°C until analysed. The peaks were identified by standard runs of saturated acids and by semilog plots. The results were given as 20:2-3 and 22:2-4.

long-chain mono unsaturated fatty acids cause the same heart changes as rapeseed oil

In the first scientific report on cardiac effects of rapeseed oil, *Roine et al* (13) described the findings in rats and pigs. In rats, cardiac lesions were found after 2-8 weeks. In pigs, the changes were much less pronounced, and similar changes were observed when soybean oil was the fat source. Pigs are omnivorous like humans and they are fairly similar to man as regards plasma lipoproteins (10) and coronary circulation (17).

In the present study domestic pigs were fed fat-rich diets containing rapeseed oil, fish oil, partially hydrogenated fish oil, partially hydrogenated soybean oil or lard for 1, 5, 27 and 52 weeks and their hearts were examined at each stage for evidence of lipidosis and cardiac lesions and for alterations in fatty acid composition by chemical analysis.

MATERIAL AND METHODS

Animals and Experimental design

Female piglets of the Norwegian landrace breed aged between 40 and 80 days (body weight range 10-17 kg) were obtained directly from local breeders. A total of 42 piglets came from 8 litters. Two piglets were killed before the start of the experiment. The remaining 5 piglets from each litter were randomly allocated to the five experimental groups to a total of 8 piglets per group. Piglets in each experimental group were kept in two separate pens of four piglets in each. Pen temperature and humidity were controlled.

Diets

Prior to the experiment the piglets had been nursed by their mothers and in addition received a commercial creep feed given *ad lib* and consisting of 2% dried skim milk, 3% herring meal, 11% soybean meal, 15% maize, 25% barley, 24% wheat, 12% molasses, 1.5% sugar, 4% grass meal and 2.5% minerals and vitamins.

The pigs were fed the experimental diets without an adaptation period. The five different diets contained 16% (w/w) from the following fats: rapeseed oil (RO), partially hydrogenated capelin oil (HCO) or capelin oil (CO), partially hydrogenated soybean oil (HSO) or lard (L). The composition of the diets was (all figures in % (w/w)): barley 39, solvent extracted soybean meal 26, ground oat hulls 15, sunflower oil 1.5, fat 16, mineral mixture 3, potassium monophosphate 0.5, vitamin mixture 0.45. The mineral mixture consisted of (all figures per kg of the diet): Ca 7.5 g, P 1.8 g, NaCl 4.73 g, Fe 48 mg, Mn 60 mg, Zn 51 mg, Se 0.1 mg, 12.2 mg. The vitamin mixture consisted of (all figures per kg of the diet): Vit A 2800 IU, Vit D₃ 400 IU, Vit E 100 IU, Thiamine HCl 2.6 mg, Riboflavin 6 mg, Niacin 44 mg, Pantothenic acid 26 mg, Choline Cl 1.5 mg, Vit B₁₂ 0.044 mg, Pyridoxin Cl 3 mg, Ethoxy quine 300 mg, DL methionine 400 mg. The composition

of the diets gives 3330 kcal per kg diet in metabolizable energy of which 42% comes from fat. Pro constituted 17% (w/w) of the diet and the concentration of lysine and methionine were 0.9% and 0.5% (w/w) respectively.

The rapeseed oil was obtained in an unrefined form. The unrefined (raw) and partially hydrogenated capelin oils were processed from winter caught capelin (*Mallotus villosus*) under commercial conditions. The partially hydrogenated soybean oil was also a commercial sample and like the partially hydrogenated capelin oil hydrogenated to a melting point of 31-33°C.

Hydrogenated soybean oil was included in the diet for its content of trans fatty acids as a control for hydrogenated fish oils. Lard does not contain C22 fatty acids or trans fatty acids and served as a control fat.

Table 1 gives the composition of the fatty acids extracted from the feed. Batches of feed were prepared at the start of the experiment and again after 150, 180, 240 days. Immediately after mixing the diets were stored in sealed polyethylene bags at ambient temperature (0-20°C). Each bag contained feed for a maximum of 3 days consumption.

During the first two weeks the piglets had access to feed twice a day, each of one hour duration. Later the feeding schedule based on live weight was introduced, increasing from 1 kg per pig per day at 35 kg to 3 kg per pig per day at 100 kg and above. Individual feed intake was recorded daily. Water was available *ad lib*. Live weights were recorded on arrival, once a week and prior to killing. Two pigs per treatment group were slaughtered after 1, 5, 27, 37 (treatment group CO only) and 52 weeks.

Complete autopsies were performed and all organs were weighed after dissection of attached fat. Tissue samples were taken from the heart, liver, kidneys, lungs, adrenals, spleen, small and large intestines, skeletal muscle (from the left thigh), adipose tissue (from below the right shoulder) and aorta. The hearts were transversally in 5 mm thick sections from the apex to base. Every second section was fixed for morphological examination; the rest was frozen for chemical analysis.

Morphological Examination

The hearts were examined by light microscopy. The presence of lipidosis and for cardiac lesions. Standardized blocks from the left anterior wall were frozen, sectioned and stained with Oil Red O for demonstration of fat and the findings were graded as follows: 0 = negative, grade 1 = lipid droplets in less than 25% of the muscle cells, grade 2 = lipid droplets in 25-50% of the muscle cells, grade 3 = lipid droplets in 50-75% of the muscle cells and grade 4 = lipid droplets in more than 75% of the cells.

Three complete transverse sections from each heart were embedded in paraffin and stained with Hematoxylin-Phloxine-Saffron (14). This method was chosen to make a good distinction between connective tissue and other cardiac structures. Cardiac lesions consisted of muscle cell necrosis, accumulation of inflammatory cells...

TABLE 3 Fatty acid composition (%) of the heart triglycerides of pigs on a 42 cal% fat diet

TABLE 3 Fatty acid composition (%) of the heart infarctures of pigs																														
Fatty acids	L						HSO						HCO						CO						RO					
	(weeks)						(weeks)						(weeks)						(weeks)						(weeks)					
	1	5	27	52	1	5	27	52	1	5	27	52	1	5	27	52	1	5	27	52	1	5	27	52						
at start																														
140	19	05	19	07	15	14	09	05	22	12	38	19	54	18	35	20	10	04	11	04	10	04	11	04						
150	12	73	09	49	18	12	25	25	05	48	32	32	19	41	12	65	18	27	—	23	18	27	—	23						
155	187	203	193	160	199	156	148	126	200	112	163	156	138	146	178	158	166	118	127	139	166	118	127	139						
160	60	18	44	20	69	46	35	18	84	38	86	50	42	41	49	38	50	16	26	09	50	16	26	09						
161	—	—	—	—	—	—	—	—	—	—	—	—	—	10	—	38	—	—	—	—	—	—	—	—						
170	125	195	96	131	107	103	90	119	85	127	62	119	125	122	77	153	115	113	49	121	115	113	49	121						
180	296	250	349	313	291	389	403	367	286	148	281	193	164	216	230	232	229	144	261	192	229	144	261	192						
181	158	168	164	146	167	184	201	198	134	284	155	213	143	128	106	114	172	284	210	260	172	284	210	260						
182	05	07	03	07	07	11	16	09	11	10	25	09	07	10	11	08	23	42	57	34	23	42	57	34						
183	07	07	11	09	07	09	12	05	35	32	90	56	42	32	103	67	24	44	85	54	24	44	85	54						
201	14	07	09	04	09	01	—	03	08	09	15	11	06	04	—	08	12	11	08	14	12	11	08	14						
202-3	69	11	50	83	64	36	36	69	26	91	12	74	105	48	11	38	69	46	17	40	69	46	17	40						
204	04	—	04	05	04	03	05	05	20	08	08	04	55	94	63	07	12	09	—	02	12	09	—	02						
205	—	05	—	—	—	—	03	—	20	22	24	12	38	14	42	17	54	98	105	06	54	98	105	06						
221	03	05	05	03	03	02	04	03	05	04	—	05	11	08	09	07	07	10	08	06	07	10	08	06						
222-4	04	—	06	03	04	02	04	01	09	02	06	02	05	08	12	—	04	04	05	—	04	04	05	—						
225	05	—	04	04	06	02	03	01	20	—	—	01	16	30	32	—	05	—	—	—	05	—	—	—						
226	—	—	—	—	—	—	—	—	—	—	—	—	—	—	—	—	—	—	—	—	—	—	—	—						

Pooled data from 2 pigs per sampling

TABLE 2 Number of Pigs with Microscopical Lipidosis and Heart Muscle Necrosis

Dietary fat	Lipidosis				Heart muscle necrosis			
	1	5	27	52	1	5	27	52
			(weeks)				(weeks)	
Lard	0	0	0	0	0	0	1	1
Hydrogenated soy bean oil	0	0	0	0	1	0	1*	1
Hydrogenated capelin oil	1	0	1	0	0	0	1	1
Raw capelin oil	0	0	0	~	0	0	0	~
Rapeseed oil	1	2*	1*	0	1	0	1	2

2 pigs per sampling and group. All positive hearts had grade 1 lipidosis or grade 1 heart muscle necrosis except those marked with a * = one heart with grade 2 findings

RESULTS

General Conditions and Growth

In general all pigs showed normal appearance throughout the experimental period and had adequate growth rate and feed consumption. In the initial part of the experiment a few episodes of diarrhoea occurred. At the later stages some cases of limb weakness were seen. None of these conditions are



Figure 1 Grade 1 cardiac lesion with necrosis of individual muscle cells and infiltration of leucocytes and histiocytes. HPS 400x

unusual among pigs and there was no relationship between the conditions and the diets. After 37 weeks the remaining two pigs in the CO group suffered from mechanical bone fractures and had to be killed earlier than planned. All diets were readily consumed although the pigs fed RO and HSO had a slightly lower feed consumption compared to the other pigs during the first 2 weeks when they had free access to the feeds. The pigs fed rapeseed oil grew at a lower rate compared to the other groups ($p < 0.01$) the first half year consuming 13% more feed per kg live weight gain than the other groups. In the last half year no differences in growth rate were seen. The weight range after one year was 178–257 kg.

Morphological Results

Heart No macroscopic changes were found at autopsy in pigs killed after 1 or 5 weeks. The amount of epicardial fat was markedly increased after 27 and 52 (or 37) weeks in all groups.

Table 2 gives the result of the histological examination. Lipidosis was found in individual heart muscle cells in all parts of the heart walls but more frequently in the sub-epicardial areas. The lipid droplets were small also in grade 2 hearts. In the hearts taken at one year no lipidosis was found. Cardiac lesions were all small and focal and consisted of individual muscle cell necrosis with focal accumulation of leucocytes and histiocytes (Fig. 1). Some muscle cells with vacuolization and disintegration of myofibrils could be found around the lesions. Large groups of mature fat cells surrounded by atrophic muscle fibers were seen in all parts of the heart walls. This lipomatosis appeared more frequently in the older pigs and was found in all dietary groups.

Other organs In the aorta small foci of fatty streaks were found in most

TABLE 3 Fatty acid composition (%) of the heart triglycerides of pigs on a 42 cal% fat diet

Fatty acids	at start	L						HCO						CO						RO					
		5			27			1			5			1			5			1			5		
		(weeks)			(weeks)			(weeks)			(weeks)			(weeks)			(weeks)			(weeks)			(weeks)		
14:0	0.6	19	0.5	19	0.7	15	14	0.9	0.5	22	12	3.8	1.9	54	18	3.5	20	10	0.4	11	0.4	11	0.4	11	0.4
15:-	-	12	7.3	0.9	4.9	18	12	-	2.5	0.5	4.8	0.6	3.2	1.9	4.1	1.2	6.5	18	2.7	-	18	2.7	-	18	2.7
16:0	14.5	18.7	20.3	19.3	16.0	19.9	15.6	14.8	12.6	20.0	11.2	16.3	15.6	13.8	14.6	17.8	15.8	16.6	11.8	12.3	13.9	16.6	11.8	12.3	13.9
16:1	1.6	6.0	1.8	4.4	2.0	6.9	4.6	3.5	1.8	8.4	3.8	8.6	5.0	4.2	4.1	4.9	3.8	5.0	1.6	2.6	0.9	5.0	1.6	2.6	0.9
17:-	-	-	2.0	-	2.7	-	-	-	1.6	-	2.3	-	1.4	-	1.0	-	3.8	-	-	-	-	-	-	-	-
18:0	15.0	12.5	19.5	9.6	13.1	10.7	10.3	9.0	11.9	8.5	12.7	6.2	11.9	12.5	12.2	7.7	15.3	11.5	11.3	4.9	12.1	11.5	11.3	4.9	12.1
18:1	15.6	29.6	25.0	34.9	31.3	29.1	38.9	40.3	36.7	28.6	14.8	28.1	19.3	16.4	21.6	23.0	23.2	22.9	14.4	26.1	19.2	22.9	14.4	26.1	19.2
18:2	26.8	15.8	16.8	16.4	14.6	16.7	18.4	20.1	19.8	13.4	28.4	15.5	21.3	14.3	12.8	10.6	11.4	17.2	28.4	21.0	26.0	17.2	28.4	21.0	26.0
18:3	0.5	0.7	0.3	0.7	0.6	0.7	1.1	1.6	0.9	1.1	1.0	2.5	0.9	0.7	1.0	1.1	0.8	2.3	4.2	5.7	3.4	2.3	4.2	5.7	3.4
20:1	0.7	0.7	0.7	1.1	0.9	0.7	0.9	1.2	0.5	3.5	3.2	9.0	5.6	4.2	3.2	10.3	6.7	2.4	4.4	8.5	5.4	2.4	4.4	8.5	5.4
20:2-3	0.6	1.4	0.7	0.9	0.4	0.9	0.1	-	0.3	0.8	0.9	1.5	1.1	0.6	0.4	-	0.8	1.2	1.1	0.8	1.4	1.2	1.1	0.8	1.4
20:4	13.0	6.9	1.1	5.0	8.3	6.4	3.6	3.6	6.9	2.6	9.1	12.7	7.4	10.5	4.8	1.1	3.8	6.9	4.6	1.7	4.0	6.9	4.6	1.7	4.0
20:5	2.4	0.4	-	0.4	0.5	0.4	0.3	0.5	0.5	2.0	0.8	0.8	0.4	5.5	9.4	6.3	0.7	1.2	0.9	-	0.2	1.2	0.9	-	0.2
22:1	-	-	0.5	-	-	-	-	0.3	-	2.0	2.2	2.4	1.2	3.8	1.4	4.2	1.7	5.4	9.8	10.5	6.4	5.4	9.8	10.5	6.4
22:2-4	0.8	0.3	0.5	0.5	0.3	0.3	0.2	0.4	0.3	0.5	0.4	-	0.5	1.1	0.8	0.9	0.7	0.7	1.0	0.8	0.6	0.7	1.0	0.8	0.6
22:5	1.8	0.4	-	0.6	0.3	0.4	0.2	0.4	0.1	0.9	0.2	0.6	0.2	0.5	0.8	1.2	-	0.4	0.4	0.5	-	0.4	0.4	0.5	-
22:6	3.1	0.5	-	0.4	0.4	0.6	0.2	0.3	0.1	2.0	-	-	0.1	1.6	3.0	3.2	-	0.5	-	-	-	0.5	-	-	-

Pooled data from 2 pigs per sampling

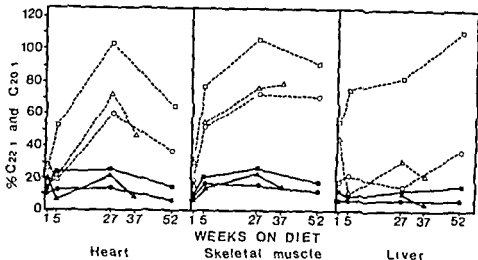


Figure 2 The relative amounts of C22:1 and C20:1 in the heart, liver and skeletal muscle. The amount of C22:1 and C20:1 in the diets is given as 100% — = C22:1 - - - = C20:1 ■ = Rapeseed oil ▲ = Rapa capelin oil ○ ● = Partly hydrogenated capelin oil

weeks. Fibrous or advanced lesions were not seen. No relation was found between appearance or number of fatty streaks and dietary fats. In skeletal muscle, trace amounts of lipid droplets were seen in all groups. No significant morphological changes were found in the lungs, kidneys, livers, spleens, adrenals, intestines or the adipose tissue, and the relative organ weights were similar in all groups.

Lipid in the Hearts

The amount of total lipids extracted varied somewhat at different periods without any tendency to increased accumulation in any particular diet. The average amount extracted from all hearts was 48 mg/g heart.

Fatty Acid Patterns in Hearts

Table 3 gives the fatty acid composition in the heart triglycerides as weight percentages.

The levels of C22:1 and C20:1 were of primary interest in this study. Both C22:1 and C20:1 increased in the hearts, but the peaks were not reached before 27 weeks on RO or fish oils. Fig. 2 shows the relative amounts of these acids in the hearts, livers and thigh muscles at different sampling times. The values are the concentration of C22:1 and C20:1 in the heart triglycerides as a percentage of the concentration of C22:1 and C20:1 in the respective dietary fats. Much higher levels of C20:1 than of C22:1 were evident in all tissues. The C22:1 was never found in the tissue lipids in concentrations above 25% of the dietary level. The relative concentrations of both monoenes were higher in the tissue triglycerides from the rapeseed oil group than from the two fish oil groups. Heart muscle and skeletal muscle tissue had similar levels

of the two acids during the experiment. The concentration of C22:1 and C20:1 increased through the first half year and showed lower values at the one year sampling compared to the value at 52 months.

The essential fatty acids, C18:2 omega-6 (linoleic acid) and C20:4 omega-6 (arachidonic acid), were found as major acids in most of the samples of the heart, liver and skeletal muscle.

C18:1 was higher in the hearts in the fish oil and RO groups than in the other groups. The average tissue levels (all sampling periods together) were 7% higher than the dietary levels of C18:1 in these groups. C18:1 was the major acid in HSO and L, and although the tissue levels of this acid were high they were lower than the dietary levels in HSO (~26%) and L (~10%). Similar results were found in the liver and thigh muscle samples. Detailed analytic data of the fatty acid patterns in skeletal muscle and liver may be obtained on request (G.L.).

DISCUSSION

The pigs fed rapeseed oil had a lower growth rate and a poorer efficiency of feed conversion than pigs fed the other fats, which is in line with previous findings (5). The digestibility however was not determined and it is therefore not possible to conclude whether differences in absorption or in metabolism of the absorbed fatty acids account for this.

There was no increase in total fat content in the hearts in any dietary group. But lipidosis of grade 1-2 (slight to moderate) was found in pigs fed rapeseed oil or hydrogenated fish oil. The lipidosis

probably reflects an altered distribution of the lipids in the heart muscle cells with formation of larger lipid droplets than normally present

The type of rapeseed oil used caused a grade 4 lipidosis in rats after one week, and the findings indicate considerable species differences between pigs and rats (12)

The fatty acid composition of the triglycerides of the hearts livers and skeletal muscles of the pigs partly reflected the fatty acid composition of the dietary fats. Heart triglycerides from pigs fed fish oils and rapeseed oil contained on an average 2.4% and 8.0% of C22:1 respectively which is about 1/5-1/6 of the concentrations in the respective dietary fats. On rapeseed oil the content of C22:1 in the heart triglycerides after 5 and 27 weeks of feeding was about twice that found after 1 and 52 weeks. This protracted peaking in C22:1 content is in agreement with other observations in pigs (7, 16). Further the maximum levels of C22:1 found in triglycerides of the heart and other tissues in the pigs were much lower than those found in rats after one week of feeding on rapeseed oil (12). On fish oil the content of C22:1 in heart triglycerides showed no clear-cut relation to the time of feeding.

In general the concentrations of C22:1 and C20:1 in tissue triglycerides as a percentage of the corresponding dietary lipids were higher on the rapeseed oil than on the fish oils. This result may arise from differences in double bond position in the monoene fatty acids in rapeseed oil and fish oil. In rapeseed oil 100% of the C22:1 is erucic acid (C22:1 omega-9) while hydrogenated fish oil contains a wide range of positional and geometrical isomeric forms of C22:1 fatty acids of which erucic acid constitutes approximately 1/10 (11). The concentration in tissue triglycerides as a percentage of the dietary concentration was higher for C20:1 than for C22:1. It is possible that the absorption rates of C22:1 and C20:1 are different in the pig but this does not seem very likely. The data probably indicate that C22:1 is more readily metabolized to its lower homologues in the pig than in other animals studied. The relative high content of C18:1 in tissue triglycerides compared with that of the dietary fat in pigs fed rapeseed oil and fish oils may also support this assumption.

It is fairly well established that the continuous feeding of rapeseed oil rich in erucic acid like that used in this study causes extensive and numerous heart muscle lesions in rats when fed for periods longer than 6 months. In this study on pigs definite cardiac lesions were found in all dietary groups and more frequently after 27 and 52 weeks than after shorter feeding periods. The appearances of the lesions were identical with those found in rats fed

similar fats but the relatively low incidence and mildness of the lesions contrast with the findings in rat experiments (3, 8).

It is noteworthy that identical lesions were found in the lard and soybean oil groups (i.e. the controls) as those found in the rapeseed oil groups. *Roine et al.* (13) described «myocarditis like» lesions in pigs fed 28% of calories from rapeseed oil for 2 months, but found the same amount and severity of lesions in pigs fed soybean oil as control fat. Similar findings have been reported by *Friend et al.* (9) and *Aherne et al.* (4). The pathogenesis of these lesions remains unknown but at the present time it seems more probable that they are caused by factors other than the consumption of C22:1 fatty acids by the pigs.

In the present study the dietary concentrations of C22:1 fatty acids were 7.4% and 3.2% in the rapeseed oil and fish oil diets respectively and only a mild degree of lipidosis was found. The data from this study as well as other studies on pigs cited above do not suggest that dietary C22:1 and C20:1 are cardiotoxic in pigs.

This work was supported by grants from the Royal Norwegian Council for Scientific and Industrial Research and the Norwegian Research Association for Edible Fats.

REFERENCES

1. Abdellatif A. M. M. & Vies R. O. Pathological effects of dietary rapeseed oil in rats. *Nutr. Metabol.* 12: 285-295, 1970.
2. Abdellatif A. M. M. & Vies R. O. Pathological effects of dietary rapeseed oil in ducklings. *Nutr. Metabol.* 12: 296-305, 1970.
3. Abdellatif A. M. M. & Vies R. O. Short term and long term pathological effects of glyceryl trierucate and of increasing levels of dietary rapeseed oil in rats. *Nutr. Metabol.* 15: 219-231, 1973.
4. Aherne F., Bowland P., Christian R. C. & Hardin R. T. Performance of myocardial and blood serum changes in pigs fed diets containing high or low erucic rapeseed oils. *Can. J. Anim. Sci.* 56: 275-284, 1976.
5. Appelquist L. A. & Ohlsson R. Rapeseed Cultivation, composition, processing and utilization. Rapeseed. Am. Elsevier, 1972.
6. Beare Rogers J. L. & Nera E. A. Cardiac lipids in rats and gerbils fed rapeseed oil. *Lipids* 7: 548-552, 1972.
7. Beare Rogers J. L. & Nera E. A. Cardiac fatty acids and histopathology of rats, pigs, monkeys and gerbils fed rapeseed oil. *Comp. Biochem. Physiol.* 41B: 793-800, 1972.
8. Charlton K. M., Corner A. H., Davey K., Kramer J. A. G., Mahadevan S. & Sauer F. D. Cardiac

- lesions in rats fed rapeseed oil *Can J Comp Med* 39 262-269, 1975
- 9 *Friend, D W, Corner, A H, Kramer, J K G, Charlton, K M, Gilka F & Sauer, F* Growth, cardiopathology and cardiac fatty acids of swine fed diets containing soybean oil or low erucic rapeseed oil *Can J Anim Sci* 55 275-284, 1976
 - 10 *Jackson, R L, Baker, H N, Taunton, O D, Smith, L C, Gatner, C W & Gotto A M* A comparison of the major apolipoprotein from pig and human high density lipoproteins *J Biol Chem* 348 2639-2644, 1973
 - 11 *Lambertsen G, Myklestad, H & Braekkan O R* Studies on monoene fatty acid isomers in HMF *J Amer Oil Chem Soc* 48 389-391, 1971
 - 12 *Opstvedt, J, Svaar, H, Hansen P, Pettersen, J, Langmark, F T & Barlow, S M* Comparison of lipid status in the hearts of piglets and rats on short term feeding of marine oils and rapeseed oils *Lipids*, 14 356-371, 1979
 - 13 *Roine, P, Uksila E, Teir, H & Rapola J* Histopathological changes in rats and pigs fed rapeseed oil *Z Ernahrungswiss* 1 118-124, 1960
 - 14 *Romeis B* Mikroskopisches Farbenteknik, Oldenburg Verlag, 1968
 - 15 *Roquelin, G & Leclerc, J* L'huile de colza riche en acide erucique et l'huile de colza sans acide erucique *Ann Biol Anim Biochim Biophys* 9 413-426 1969
 - 16 *Roquelin, G, Cluzan R, Vodovar, N & Levillain R* Recherches recentes sur les effets physiopathologiques des huiles de colza et de canbra au niveau du myocarde et d'autres organes *Cah Nutr Diet* 8 103-116, 1973
 - 17 *Schape, W* The collateral circulation of the heart North Holland Publ Comp 1971

CARCINOEMBRYONIC ANTIGEN IN FETAL TISSUES AND IN MATERNAL SERUM

JAN LINDGREN

Department of Bacteriology and Immunology University of Helsinki Finland

Lindgren J Carcinoembryonic antigen in fetal tissues and in maternal serum Acta path microbiol scand Sect A 88 49-53 1980

The occurrence of CEA was studied by radioimmunoassay and the triple bridge immunoperoxidase technique in tissues of human fetuses and by radioimmunoassay in fetal and maternal serum. The antiserum to CEA was extensively adsorbed to eliminate cross reactions with CEA related antigens. After the first trimester of pregnancy CEA was found throughout the gastrointestinal tract by both techniques whereas the other fetal tissues and fetal serum did not contain detectable amounts of CEA. The CEA level of all 69 sera of pregnant women was below 2.5 ng/ml. The excretory nature of CEA was suggested by the localization of CEA in the luminal border of the alimentary tract and by the finding that the CEA concentration in the content of fetal gastrointestinal canal was higher than in the surrounding tissue. Gel filtration on Sepharose 4B showed that molecular weight of CEA immunoreactive material of the fetal gut was similar to that of CEA purified from colon cancer but a minor component with a higher molecular weight was eluted in the void volume. When tested in radioimmunoassay the CEA immunoreactive material in both peaks gave an inhibition curve parallel to that of purified CEA.

Key words: Carcinoembryonic antigen, fetal tissue, maternal serum.

J. Lindgren, Department of Bacteriology and Immunology, University of Helsinki, Haartmaninkatu 3, 00290 Helsinki, Finland.

Received 15 vii 79 Accepted 9 viii 79

Carcinoembryonic antigen (CEA) was originally described by Gold & Freedman (1965) in the carcinomatous and fetal colon. The expression of CEA in tissue and blood of patients with malignant and nonmalignant disease has been widely documented (for review see Burin *et al.* 1978).

CEA appears also in normal gastrointestinal tissues (Go *et al.* 1975; Isaacson & Judd 1977; Shively *et al.* 1978). Furthermore adult normal human tissues contain glycoproteins that cross react immunologically with CEA (Burin *et al.* 1978). One of these, the normal cross reacting antigen (NCA; von Kleist *et al.* 1972; Mach & Pusztaszki 1972) has been well characterized and the influence of NCA in the CEA assay must be eliminated. Other cross reacting antigens such as NCA 2

(Burin *et al.* 1973), biliary glycoprotein I (BGP I; Svenberg 1976) and CEA like antigen of gastric secretions (CEA-like antigen; Vuento *et al.* 1976) are closely related to CEA and hence may interfere with the CEA assay. After the original papers on CEA were published little has been done to establish the occurrence of CEA in fetal tissues and serum during development.

In this report the expression of CEA in fetal organs was studied both immunohistochemically and by radioimmunoassay.

Materials and Methods
Fetal tissues were obtained from the Department of Pathology, University of Helsinki, Finland. The tissues were fixed in Bouin's fluid and embedded in paraffin. The tissues were sectioned and stained with hematoxylin and eosin. The tissues were also stained with periodic acid-Schiff (PAS) and with PAS after treatment with CEA antiserum.

- lesions in rats fed rapeseed oil *Can J Comp Med* 39 262-269, 1975
- 9 Friend, D W, Corner, A H, Kramer, J A G, Charlton, A M, Gilka, F & Sauer, F Growth, cardiopathology and cardiac fatty acids of swine fed diets containing soybean oil or low erucic rapeseed oil *Can J Anim Sci* 55 275-284, 1976
 - 10 Jackson, R L, Baker, H N, Taunton, O D, Smith, L C, Gainer, C W & Gotto, A M A comparison of the major apolipoprotein from pig and human high density lipoproteins *J Biol Chem* 248 2639-2644, 1973
 - 11 Lambertsen G, Mykkestad H & Bracklan, O R Studies on monoene fatty acid isomers in HMF *J Amer Oil Chem Soc* 48 389-391, 1971
 - 12 Opstvedt J, Svaar, H, Hansen P, Pettersen J, Langmark, F T & Barlow, S M Comparison of lipid status in the hearts of piglets and rats on short term feeding of marine oils and rapeseed oils *Lipids*, 14 356-371, 1979
 - 13 Roine, P, Uksila, E, Teur, H & Rapola J Histopathological changes in rats and pigs fed rapeseed oil *Z Ernahrungswiss* 1 118-124, 1960
 - 14 Romeis, B *Mikroskopisches Farbtechnik*, Oldenburg Verlag, 1968
 - 15 Roquelin G & Leclerc J L'huile de colza riche en acide erucique et l'huile de colza sans acide erucique *Ann Biol Anim Biochim Biophys* 9 413-426 1969
 - 16 Roquelin G, Cluzan R, Iodovar, N & Levilain R Recherches recentes sur les effets physiopathologiques des huiles de colza et de canbra au niveau du myocarde et d'autres organes *Cah Nutr Diet* 8 103-116, 1973
 - 17 Schape, W The collateral circulation of the heart North Holland Publ Comp 1971

CARCINOEMBRYONIC ANTIGEN IN FETAL TISSUES AND IN MATERNAL SERUM

JAN LINDGREN

Department of Bacteriology and Immunology University of Helsinki Finland

Lindgren J Carcinoembryonic antigen in fetal tissues and in maternal serum Acta path microbiol scand Sect A 88 49-53 1980

The occurrence of CEA was studied by radioimmunoassay and the triple bridge immunoperoxidase technique in tissues of human fetuses and by radioimmunoassay in fetal and maternal serum. The antiserum to CEA was extensively adsorbed to eliminate cross reactions with CEA related antigens. After the first trimester of pregnancy CEA was found throughout the gastrointestinal tract by both techniques, whereas the other fetal tissues and fetal serum did not contain detectable amounts of CEA. The CEA level of all 69 sera of pregnant women was below 2.5 ng/ml. The excretory nature of CEA was suggested by the localization of CEA in the luminal border of the alimentary tract and by the finding that the CEA concentration in the content of fetal gastrointestinal canal was higher than in the surrounding tissue. Gel filtration on Sepharose 4B showed that molecular weight of CEA immunoreactive material of the fetal gut was similar to that of CEA purified from colon cancer, but a minor component with a higher molecular weight was eluted in the void volume. When tested in radioimmunoassay the CEA immunoreactive material in both peaks gave an inhibition curve parallel to that of purified CEA.

Key words: Carcinoembryonic antigen, fetal tissue, maternal serum.

J Lindgren, Department of Bacteriology and Immunology, University of Helsinki, Haartmaninkatu 3, 00290 Helsinki, Finland.

Received 15 vi 79 Accepted 9 viii 79

Carcinoembryonic antigen (CEA) was originally described by Gold & Freedman (1965) in the carcinomatous and fetal colon. The expression of CEA in tissue and blood of patients with malignant and nonmalignant disease has been widely documented (for review see Burtin *et al.* 1978).

CEA appears also in normal gastrointestinal tissues (Go *et al.* 1975; Isaacson & Judd 1977; Shvely *et al.* 1978). Furthermore, adult normal human tissues contain glycoproteins that cross react immunologically with CEA (Burtin *et al.* 1978). One of these, the normal cross reacting antigen (NCA; von Kleist *et al.* 1972; Mach & Pusztaszeri 1972), has been well characterized, and the influence of NCA in the CEA assay must be eliminated, as such as NCA 2

(Burtin *et al.* 1973), biliary glycoprotein I (BGP I; Svenberg 1976), and CEA like antigen of gastric secretions (CELIA; Vuento *et al.* 1976) are closely related to CEA and hence may interfere with the CEA assay. After the original papers on CEA were published little has been done to establish the occurrence of CEA in fetal tissues and serum during development.

In this report the expression of CEA in fetal organs was studied both immunohistochemically and by radioimmunoassay. The presence of CEA in maternal serum at different stages of gestation was also determined. Molecular weight and immunological properties of fetal CEA reactive material were studied and compared with the CEA purified from liver metastases of human colon cancer.

- lesions in rats fed rapeseed oil *Can J Comp Med* 39 262-269, 1975
- 9 Friend, D W, Corner, A H, Kramer, J A G, Charlton, K M, Gilka, F & Sauer, F Growth, cardiopathology and cardiac fatty acids of swine fed diets containing soybean oil or low erucic rapeseed oil *Can J Anim Sci* 55 275-284, 1976
- 10 Jackson, R L, Baker, H N, Taunton O D, Smith, L C, Gainer, C W & Gutto, A M A comparison of the major apolipoprotein from pig and human high density lipoproteins *J Biol Chem* 248 2639-2644, 1973
- 11 Lambertsen, G, Myklestad, H & Braekkan, O R Studies on monoene fatty acid isomers in HMF *J Amer Oil Chem Soc* 48 389-391, 1971
- 12 Opsvædt, J, Skaar, H, Hansen, P, Pettersen J, Langmark, F T & Barlow, S M Comparison of lipid status in the hearts of piglets and rats on short term feeding of marine oils and rapeseed oils *Lipids* 14 356-371, 1979
- 13 Roine, P, Uksila E, Teir, H & Rapola J Histopathological changes in rats and pigs fed rapeseed oil *Z Ernahrungswiss* 1 118-124 1960
- 14 Romeis, B *Mikroskopisches Farbentechnik*, Olden burg Verlag, 1968
- 15 Roquelin G & Leclerc, J L'huile de colza riche en acide erucique et l'huile de colza sans acide erucique *Ann Biol Anim Biochim Biophys* 9 413-426 1969
- 16 Roquelin, G, Cluzan, R, Vodovar, N & Leclerc R Recherches recentes sur les effets physiopathologiques des huiles de colza et de canbra au niveau du myocarde et d'autres organes *Cah Nutr Diet* 8 103-116, 1973
- 17 Schape, W The collateral circulation of the heart *North Holland Publ Comp* 1971

CARCINOEMBRYONIC ANTIGEN IN FETAL TISSUES AND IN MATERNAL SERUM

JAN LINDGREN

Department of Bacteriology and Immunology University of Helsinki Finland

Lindgren J Carcinoembryonic antigen in fetal tissues and in maternal serum Acta path microbiol scand Sect A 88 49-53 1980

The occurrence of CEA was studied by radioimmunoassay and the triple bridge immunoperoxidase technique in tissues of human fetuses and by radioimmunoassay in fetal and maternal serum. The antiserum to CEA was extensively adsorbed to eliminate cross reactions with CEA related antigens. After the first trimester of pregnancy CEA was found throughout the gastrointestinal tract by both techniques whereas the other fetal tissues and fetal serum did not contain detectable amounts of CEA. The CEA level of all 69 sera of pregnant women was below 2.5 ng/ml. The excretory nature of CEA was suggested by the localization of CEA in the luminal border of the alimentary tract and by the finding that the CEA concentration in the content of fetal gastrointestinal canal was higher than in the surrounding tissue. Gel filtration on Sepharose 4B showed that molecular weight of CEA immunoreactive material of the fetal gut was similar to that of CEA purified from colon cancer but a minor component with a higher molecular weight was eluted in the void volume. When tested in radioimmunoassay the CEA immunoreactive material in both peaks gave an inhibition curve parallel to that of purified CEA.

Key words: Carcinoembryonic antigen, fetal tissue, maternal serum.

J Lindgren, Department of Bacteriology and Immunology, University of Helsinki, Haartmaninkatu 3, 00290 Helsinki, Finland.

Received 15 vi 79 Accepted 9 viii 79

Carcinoembryonic antigen (CEA) was originally described by Gold & Freedman (1965) in the carcinomatous and fetal colon. The expression of CEA in tissue and blood of patients with malignant and nonmalignant disease has been widely documented (for review see Burtin *et al* 1978).

CEA appears also in normal gastrointestinal tissues (Go *et al* 1975; Isaacson & Judd 1977; Shively *et al* 1978). Furthermore adult normal human tissues contain glycoproteins that cross react immunologically with CEA (Burtin *et al* 1978). One of these, the normal cross reacting antigen (NCA) von Kleist *et al* 1972; Mach & Pustjensen 1972) has been well characterized and the influence of NCA in the CEA assay must be eliminated. Other cross reacting antigens such as NCA 2

(Burtin *et al* 1973) biliary glycoprotein I (BGP I; Svenberg 1976) and CEA like antigen of gastric secretions (CELIA; Vuento *et al* 1976) are closely related to CEA and hence may interfere with the CEA assay. After the original papers on CEA were published little has been done to establish the occurrence of CEA in fetal tissues and serum during development.

In this report the expression of CEA in fetal organs was studied both immunohistochemically and by radioimmunoassay. The presence of CEA in

- lesions in rats fed rapeseed oil *Can J Comp Med* 39 262-269, 1975
- 9 Friend D W, Corner A H, Kramer J K G, Charlton K M, Gilka F & Sauer F Growth, cardiopathology and cardiac fatty acids of swine fed diets containing soybean oil or low erucic rapeseed oil *Can J Anim Sci* 55 275-284, 1976
 - 10 Jackson R L, Baker H N, Taunton O D, Smith L C, Gainer C W & Gotto A M A comparison of the major apolipoprotein from pig and human high density lipoproteins *J Biol Chem* 248 2639-2644, 1973
 - 11 Lambertsen G, Myklestad H & Braekkan O R Studies on monoene fatty acid isomers in HMF *J Amer Oil Chem Soc* 48 389-391, 1971
 - 12 Opstvedt J, Svaar H, Hansen P, Pettersen J, Langmark F T & Barlow S M Comparison of lipid status in the hearts of piglets and rats on short term feeding of marine oils and rapeseed oils *Lipids* 14 356-371, 1979
 - 13 Roine P, Uksila E, Teir H & Rapola J Histopathological changes in rats and pigs fed rapeseed oil *Z Ernahrungswiss* 1 118-124 1966
 - 14 Romeis B *Mikroskopisches Farbenteknik* Olden burg Verlag 1968
 - 15 Roquelin G & Leclerc J L'huile de colza riche e acide erucique et l'huile de colza sans acide erucique *Ann Biol Anim Biochim Biophys* 9 413-426 1969
 - 16 Roquelin G, Cluzan R, Vadovar A & Leclerc J R Recherches recentes sur les effets physiopathologiques des huiles de colza et de canbra au niveau du myocarde et d'autres organes *Cah Nutr Diet* 8 103-116, 1973
 - 17 Schape W The collateral circulation of the heart. North Holland Publ Comp 1971

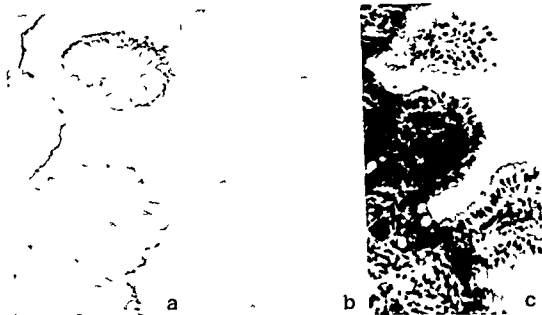


Fig 1 Demonstration of CEA on the secretory border of the fetal stomach a Immunoperoxidase staining with antiserum to CEA b Staining with antiserum to CEA adsorbed with CEA c Hematoxylin-eosin

tissues did not contain detectable amounts of CEA (Table 1). In fetus No 4 the contents of the intestine at different sites were studied separately. The highest CEA concentrations up to 283 ng/mg protein were found in the luminal contents of the jejunum and colon (Table 2).

CEA in fetal and maternal serum. No demonstrable CEA (< 1.0 ng/ml) was found in any of the seven serum samples from fetuses between the 21st and 32nd weeks of gestation. In one out of the 69 sera of pregnant women between the 8th and 42nd weeks the serum CEA level was 1.4, all the other levels being less than 1.0 ng/ml.

Immunoperoxidase staining of CEA. After the 12th week of gestation a positive staining reaction was seen at the luminal border of all parts of the gastrointestinal tract from the esophagus to the rectum. No cytoplasmic staining was seen and the goblet cells were consistently negative (Fig 1).

Molecular weight of CEA immunoreactive material. The main peak of CEA reactivity eluted in the same volume as purified CEA when chromatographed on a Sepharose 4B column. A minor peak of CEA immunoreactivity appeared in the void volume (Fig 2).

Immunological characterization of the CEA reactive material. A precipitation line of complete identity was seen in immunodiffusion when concen-

tested with purified CEA against the adsorbed antiserum to CEA. Gel filtration fractions containing high CEA concentrations gave inhibition curves parallel to that of purified CEA in radioimmunoassay (Fig 3).

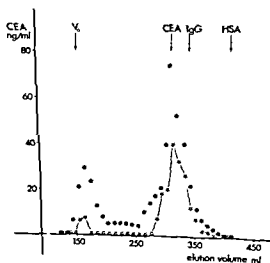


Fig 2 Gel C

MATERIALS AND METHODS

Antigens and antisera The purification of CEA and the generation and characterization of antisera have been described (Hammarström *et al* 1975, Lindgren *et al* 1979). CEA was purified from liver metastases of colon carcinoma using ion exchange chromatography, gel filtration and affinity chromatography. The antiserum to CEA was raised in rabbits with purified CEA. To eliminate reactivity with cross-reacting antigens the serum was adsorbed with A, B, and O human red blood cells, normal human serum coupled to CNBr-activated Sepharose 4B (Pharmacia, Uppsala, Sweden) and with Sepharose-coupled 1 M perchloric acid (PCA)-extracts of normal human spleen (NCA), meconium (NCA 2), and gastric juice (CELIA).

Fetal tissue specimens for radioimmunoassay Tissue samples including the rectum, colon, small intestine, stomach, esophagus, pancreas, liver, spleen, lung, kidney, thymus, muscle, brain, and adrenal gland were dissected from four apparently normal fetuses legally aborted at the 10th, 13th, 18th, and 20th weeks of pregnancy (numbers 1, 2, 3, and 4, respectively). Fetus No 5, born at the 31st week of gestation, presented with an adrenogenital syndrome and died at the age of one week. The specimens were taken into phosphate buffered saline, pH 7.4 (PBS). After freezing and thawing the specimens were sonicated at 70 W for two minutes, centrifuged at $1000 \times g$ for 15 minutes and the supernatants collected for CEA and protein determinations.

Serum samples Serum samples were taken by cardiac puncture from seven stillborn fetuses between the 21st and 32nd weeks of gestation. 69 maternal serum samples were obtained from pregnancies between the 8th and 42nd weeks. All sera were inactivated at 56 °C for 30 minutes and stored at -20 °C until tested.

Radioimmunoassay for CEA Double antibody assay was used as described (Rutanen *et al* 1978). Supernatants from tissue sonicates were diluted 1:2 with normal human serum and serum samples 1:2 with PBS. Greater dilutions were done with 1:2 diluted normal human serum. The sensitivity of the assay was 1.0 ng/ml.

Determination of protein The protein content of tissue sonicates was estimated according to Lowry *et al* (1951).

Immunohistochemical staining of CEA Tissue specimens of the rectum, colon, small intestine, stomach, esophagus, pancreas, liver, spleen, lung, kidney, thymus, muscle, brain, and adrenal gland were taken from eight apparently normal legally aborted fetuses between the 12th and 18th weeks of pregnancy. Tissue samples were fixed with formalin and embedded into paraffin. The triple-bridge immunoperoxidase method was applied as described (Lindgren *et al* 1979). Briefly after deparaffinization and rehydration the tissue sections were incubated sequentially with the adsorbed antiserum to CEA, sheep anti-rabbit IgG, rabbit anti-horse radish peroxidase, peroxidase and finally the substrate. To minimize nonspecific staining the sections were first treated with cold methanol containing 0.5% hydrogen peroxide and with 2% normal sheep serum between each step. Two adjacent control sections were stained either with the

same antiserum completely adsorbed with purified CEA or with hematoxylin-eosin. A positive reaction for CEA was a brown colour which appeared in the test slide but not in the adjacent control section. The staining characteristics of the antiserum have been described (Lindgren *et al* 1979).

Gel filtration Colonic and esophageal extracts of fetus No 4 were chromatographed on a Sepharose 4B column (82 x 2.5 cm, Pharmacia) equilibrated with 0.05 M Tris HCl buffer, pH 7.5. The column was calibrated with human IgG, albumin (Kabi, Stockholm, Sweden) and 125I-labelled purified CEA. The CEA concentration of fractions was measured by radioimmunoassay as described above. For radioimmunoassay the fractions were 5-10 times concentrated by lyophilization.

RESULTS

CEA concentration in fetal tissue CEA was found by radioimmunoassay throughout the fetal gastrointestinal tract in all fetuses studied, whereas other

TABLE 1 The CEA Content of Fetal Tissues ng/mg Protein

No of fetus	1	2	3	4	5
Age*	10	13	18	20	31
Esophagus		1.1	21.0	47.5	1.4
Ventricle		1.6	14.3	3.7	0.2
Duodenum	5.0**	0.8	2.4	1.8	0.6
Jejunum		2.1	20.0	23.7	4.6
Colon		2.5	8.3	1.2	17.0
Rectum		10.5	NT***	12.5	19.2
Other tissues****	<0.5	<0.5	<0.5	<0.5	<0.5

* weeks of gestation

** tested altogether

*** not tested

**** pancreas, liver, spleen, lung, kidney, thymus, muscle, brain and adrenal gland

TABLE 2 CEA Concentration in the Luminal Contents and the Corresponding Tissue at Different Sites of the Fetal Gastrointestinal Tract. The Values are ng/mg Protein

Tissue	Luminal content
Esophagus	47.5
Ventricle	3.7
Duodenum	1.8
Jejunum	23.7
Colon	1.2
Rectum	12.5
	NT*
	85
	16.3
	240
	283
	45.5

* not tested

- Mack J P & Pus tas eri G Demonstration of a partial identity between CEA and a normal glycoprotein. *Immunochimistry* 9 1031-1034 1972
- Martin F & Devant J Carcinoembryonic antigen in normal human saliva *J natl Cancer Inst* 50 1375-1379 1973
- Rutanen E M Lindgren J Sponen P Stenman U H Saksela E & Seppala M Carcinoembryonic antigen in malignant and nonmalignant gynecologic tumors Circulating levels and tissue localization. *Cancer* 42 581-590 1978
- Shively J E Todd C W Go V L W & Egan M L Am no terminal sequence of a carcinoembryonic antigen like glycoprotein isolated from the colonic lavages of healthy individuals *Cancer Res* 38 503-505 1978
- Sienberg T Carcinoembryonic antigen like substances of human bile Isolation and partial characterization *Int. J Cancer* 17 588-596 1976
- Von Kleist S Chavanel G & Burtin P Identification of an antigen from normal human tissue that cross reacts with the carcinoembryonic antigen. *Proc nat Acad Sci (Wash)* 69 2492-2494 1972
- Vuorio M Engvall E Seppala M & Ruoslahti E Isolation from human gastric juice of an antigen closely related to the carcinoembryonic antigen *Int. J Cancer* 18 156-160 1976

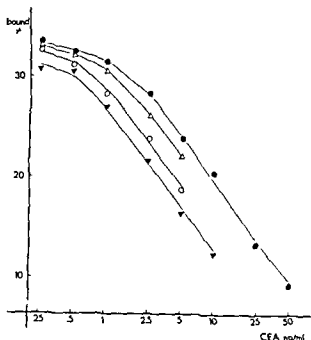


Fig 3 Inhibition of the gel filtration peaks presented in figure 2 in the radioimmunoassay for CEA ●—● purified CEA ▼—▼ fetal colonic CEA main peak △—△ fetal colonic CEA void peak ○—○ fetal esophageal CEA main peak

DISCUSSION

CEA is a normal constituent of the fetal gastrointestinal tract after the first trimester of pregnancy. Like in adult tissues (Go *et al* 1975, Isaacson & Judd 1977, Martin & Devant 1973) CEA is found throughout the fetal gastrointestinal tract from the esophagus to the rectum. However, high amounts of CEA were found in the esophagus and the jejunum during mid pregnancy, whereas the colon and the rectum became more dominant sites of CEA synthesis during the latter half of gestation.

The immunological properties, molecular weight and the immunohistochemical staining pattern suggest that the fetal CEA reactive material is closely related, if not identical to the CEA from colon cancer and different from the known cross reacting substances.

Gold & Freedman (1965) and Khoo *et al* (1973) reported the occurrence of CEA like activity in the fetal colon, pancreas and liver. This was not confirmed in the present study, and the discrepancy may be due to differences in the specificities of the antisera used.

The excretory nature of CEA (Go *et al* 1975) is suggested by the fact that the CEA concentration of the intestinal contents is higher than that of the corresponding tissues. Therefore, it is not surprising that the CEA level in fetal and maternal serum is negligible.

A minor high molecular weight CEA reactive component was seen in gel filtration. This has also been found by other workers (Keep *et al* 1978, Kimball & Brattain 1978). The absence of this material from purified preparations of CEA is likely to be due to exclusion during purification utilizing molecular sieving and selection of the major CEA peak only.

This work was supported by a grant from The Finnish Cultural Foundation. I thank Ms S. Kuisma and H. Kurppa for excellent technical assistance and Drs M. Seppälä and P. Sipponen for discussions.

REFERENCES

- Burtin P, Chavanel G & Hirsch Marie H. Characterization of a second normal antigen that cross reacts with CEA. *J Immunol* 111: 1926-1928, 1973.
- Burtin P, Gold P, Chu T M, Hammarstrom S G, Hansen H J, Johansson B G, Von Kleist S, Mach J P, Neville A M, Shively J E, Strocck P & Zamcheck N. Carcinoembryonic antigen. *Scand J Immunol* 8 suppl 8: 27-38, 1978.
- Gold P & Freedman S O. Specific carcinoembryonic antigens of the human digestive system. *J Exp Med* 122: 467-481, 1965.
- Go V L W, Ammon H V, Holtmüller A H, Krag E & Phillips S F. Quantification of carcinoembryonic antigen like activities in normal human gastrointestinal secretions. *Cancer* 36: 2346-2350, 1975.
- Hammarstrom S, Engvall E, Johansson B G, Svensson S, Sundblad G & Goldstein I J. Nature of the tumor associated determinant(s) of carcinoembryonic antigen. *Proc nat Acad Sci (Wash)* 72: 1528-1532, 1975.
- Isaacson P & Judd M A. Carcinoembryonic antigen (CEA) in the normal human small intestine. A light and electron microscopic study. *Gut* 18: 786-791, 1977.
- Keep P A, Leake B A & Rogers G T. Extraction of CEA from tumour tissue, fetal colon and patients sera and the effect of perchloric acid. *Br J Cancer* 37: 171-182, 1978.
- Khoo S K, Warner N L, Lie J T & Mackay J R. Carcinoembryonic antigenic activity of tissue extracts. A quantitative study of malignant and benign neoplasms, cirrhotic liver, normal adult and fetal organs. *Int J Cancer* 11: 681-687, 1973.
- Kimball P M & Brattain M G. A comparison of methods for the isolation of carcinoembryonic antigen. *Cancer Res* 38: 619-623, 1978.
- Lindgren J, Wahlstrom T & Seppälä M. Tissue CEA in premalignant epithelial lesions and epidermoid carcinoma of the uterine cervix. Prognostic significance. *Int J Cancer* 23: 448-453, 1979.
- Lowry O H, Rosebrough N J, Farr A L & Randall R J. Protein measurement with the Folin phenol reagent. *J Biol Chem* 193: 265-275, 1951.

- Mach J P & Pusztas eri G Demonstration of a partial identity between CEA and a normal glycoprotein. *Immunochimistry* 9 1031-1034 1972
- Martin F & Devant J Carcinoembryonic antigen in normal human saliva. *J natl Cancer Inst* 50 1375-1379 1973
- Rutanen E M Lindgren J Sipponen P Stenman U H Saksela E & Seppala M Carcinoembryonic antigen in malignant and nonmalignant gynecologic tumors. Circulating levels and tissue localization. *Cancer* 42 581-590 1978
- Shively J E Todd C W Go V L W & Egan M L Amino terminal sequence of a carcinoembryonic antigen like glycoprotein isolated from the colonic lavages of healthy individuals. *Cancer Res* 38 503-505 1978
- Svenberg T Carcinoembryonic antigen like substances of human bile. Isolation and partial characterization. *Int J Cancer* 17 588-596 1976
- Von Kleist S Chavanel G & Burtin P Identification of an antigen from normal human tissue that cross reacts with the carcinoembryonic antigen. *Proc nat Acad Sci (Wash)* 69 2492-2494 1972
- Vuento M Engvall E Seppala M & Ruoslahti E Isolation from human gastric juice of an antigen closely related to the carcinoembryonic antigen. *Int J Cancer* 18 156-160 1976

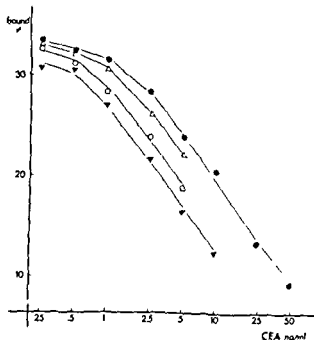


Fig. 3 Inhibition of the gel filtration peaks presented in figure 2 in the radioimmunoassay for CEA ●—● purified CEA ▼—▼ fetal colonic CEA main peak △—△ fetal colonic CEA void peak ○—○ fetal esophageal CEA main peak

DISCUSSION

CEA is a normal constituent of the fetal gastrointestinal tract after the first trimester of pregnancy. Like in adult tissues (Go *et al* 1975, Isaacson & Judd 1977, Martin & Devant 1973) CEA is found throughout the fetal gastrointestinal tract from the esophagus to the rectum. However, high amounts of CEA were found in the esophagus and the jejunum during mid pregnancy, whereas the colon and the rectum became more dominant sites of CEA synthesis during the latter half of gestation.

The immunological properties, molecular weight and the immunohistochemical staining pattern suggest that the fetal CEA reactive material is closely related if not identical to the CEA from colon cancer and different from the known cross reacting substances.

Gold & Freedman (1965) and Khoo *et al* (1973) reported the occurrence of CEA like activity in the fetal colon, pancreas and liver. This was not confirmed in the present study and the discrepancy may be due to differences in the specificities of the antisera used.

The excretory nature of CEA (Go *et al* 1975) is suggested by the fact that the CEA concentration of the intestinal contents was higher than that of the corresponding tissues. Therefore it is not surprising that the CEA level in fetal and maternal serum is negligible.

A minor high molecular weight CEA reactive component was seen in gel filtration. This has also been found by other workers (Keop *et al* 1978, Kimball & Brattain 1978). The absence of this material from purified preparations of CEA is likely to be due to exclusion during purification utilizing molecular sieving and selection of the major CEA peak only.

This work was supported by a grant from The Finnish Cultural Foundation. I thank Mrs S. Auisma and H. Kurppa for excellent technical assistance and Drs M. Seppälä and P. Sipponen for discussions.

REFERENCES

- Burtin P, Chavanel G & Hirsch Marie H. Characterization of a second normal antigen that cross reacts with CEA. *J Immunol* 111: 1926-1928, 1973.
- Burtin P, Gold P, Chu T M, Hammarstrom S G, Hansen H J, Johansson B G, Van Alost S, Mach J P, Neville A M, Shively J E, Strubel P & Zamcheck N. Carcinoembryonic antigen. *Scand J Immunol* 8 suppl 8: 27-38, 1978.
- Gold P & Freedman S O. Specific carcinoembryonic antigens of the human digestive system. *J Exp Med* 122: 467-481, 1965.
- Go V L W, Ammon H V, Holtmüller A H, Krag E & Phillips S F. Quantification of carcinoembryonic antigen like activities in normal human gastrointestinal secretions. *Cancer* 36: 2346-2350, 1975.
- Hammarstrom S, Engvall E, Johansson B G, Svensson S, Sundblad G & Goldstein J J. Nature of the tumor associated determinant(s) of carcinoembryonic antigen. *Proc nat Acad Sci (Wash)* 72: 1528-1532, 1975.
- Isaacson P & Judd M A. Carcinoembryonic antigen (CEA) in the normal human small intestine. A light and electron microscopic study. *Gut* 18: 786-791, 1977.
- Keop P A, Ickes B A & Rogers G T. Extraction of CEA from tumour tissue, fetal colon and patients sera and the effect of perchloric acid. *Br J Cancer* 37: 171-182, 1978.
- Khoo S K, Warner N L, Lie J T & Mackay I R. Carcinoembryonic antigenic activity of tissue extracts. A quantitative study of malignant and benign neoplasms, cirrhotic liver, normal adult and fetal organs. *Int J Cancer* 11: 681-687, 1973.
- Kimball P M & Brattain M G. A comparison of methods for the isolation of carcinoembryonic antigen. *Cancer Res* 38: 619-623, 1978.
- Lindgren J, Wahlstrom T & Seppälä M. Tissue CEA in premalignant epithelial lesions and epidermoid carcinoma of the uterine cervix. Prognostic significance. *Int J Cancer* 23: 448-453, 1979.
- Lowry O H, Rosebrough N J, Farr A L & Randall R J. Protein measurement with the Folin phenol reagent. *J Biol Chem* 193: 265-275, 1951.

TABLE 1 CS GD in Cartilage (Cart) and Amyloid Deposition in Capsule (Caps) in Different Age Groups

Age (years)	Grade of deposits									
	0		+		++		+++		Total	
	cart	caps	cart	caps	cart	caps	cart	caps	cart	caps
41-50		1			1				1	1
51-60	1	3			2				3	3
61-70	1	7	4	1	4	1			9	9
71-80		3	2	2	4	1	3	3	9	9
81-90		2	1		2	2	3	2	6	6
91-100		1		1	1		1		2	2
Total	2	17	7	4	14	4	7	5	30	30

TABLE 2 CS GD in Articular Cartilage at the Upper and Lower Parts of the Femoral Head (Right + Left Side)

	0	+	++	+++	Total
Upper pole	7 (14)	21 (42)	17 (34)	5 (10)	50
Lower pole	5 (10)	23 (46)	17 (34)	5 (10)	50
Total	12	44	34	10	100

The figures in parentheses are per cent

the cases. The deposits were mostly seen as a narrow rim just below the outer limit of the articular cartilage (Fig. 1 and 2). Single chondrocytes and small lacunas of atrophic chondrocytes often surrounded by a zone of the material (Fig. 3 and 4) were another characteristic feature. In some cases it was seen as round or irregular masses in the outer zone of the articular cartilage. At times these showed confluence between the superficial rim

(Fig. 1 and 2) and the congophilia surrounded chondrocytes (Fig. 3 and 4). This phenomenon is illustrated in Fig. 5.

Amyloid deposits were found in the fibrous joint capsule in 13 of the 30 cases i.e. in 43 per cent of the autopsies, often bilaterally (Fig. 6).

Relation to age. The CS-GD in the cartilage as well as the amyloid deposits in the capsules were larger the higher the age of the patient. This is shown in Table 1. There is a significant age relation with Spearman's Rho test ($0.001 < P < 0.01$) in both cases.

TABLE 3 CS GD in Articular Cartilage Versus Amyloid Substance in Capsule (Right + Left Side)

	Capsule		Total
	amyloid pos	amyloid neg	
	CS-GD pos	CS-GD neg	
CS-GD pos	17	29	46
CS-GD neg	0	4	4
Total	17	33	50

The relationship between the presence of CS GD in articular cartilage and amyloid deposits in the capsule is illustrated in Table 3.

Notice that when amyloid was found in the capsule, cartilage always contained CS-GD.

DISCUSSION

The frequency of amyloid positive fibrous capsules in a previous work (Christensen & Sørensen 1972) was 37 per cent. This figure is a little lower than the



Fig 1



Fig 2



Fig 3



Fig 4

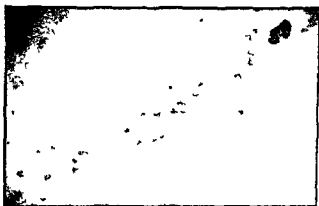


Fig 5



Fig 6

Fig 1 Congophilic deposits seen as a narrow rim just below the surface of the articular cartilage (Alkaline Congo red $\times 125$)

Fig 2 The same area as in Fig 1 showing green dichroism using polarized light (Alkaline Congo red $\times 125$)

Fig 3 Lacunas and single chondrocytes surrounded by a zone of congophilic material (Alkaline Congo red $\times 350$)

Fig 4 The same area as in Fig 3 showing green dichroism using polarized light (Alkaline Congo red $\times 350$)

Fig 5 Congophilic deposits in rounded or irregular masses in the outer zone of the articular cartilage (Alkaline Congo red $\times 250$)

Fig 6 Amyloid deposits in the fibrous joint capsule (Alkaline Congo red $\times 250$)

BRIEF REPORT

BREAST CARCINOMA PROGRESSION OF TUBULAR CARCINOMA
AND A NEW CLASSIFICATION

F Linell and O Ljungberg

Institute of Pathology General Hospital Malmö Sweden

Linell F & Ljungberg O Breast carcinoma Progression of tubular carcinoma and a new classification Acta path microbiol scand Sect A 88 59-60 1980

On histologic and statistic basis a new classification of ductal breast carcinoma is proposed. One group consists of five types representing different stages in a continuous progression from tubular carcinoma to pure ductal type. Another group is comprised by invasive comedo carcinoma which is derived from intraductal carcinoma. The development of tubular carcinoma from sclerosing lesions is stressed.

Key words: Breast carcinoma, classification, tubular carcinoma, sclerosing lesions.

F Linell, Institute of Pathology, General Hospital S 214 01 Malmö, Sweden.

Accepted as submitted 5 xi 79

The most common classification of breast carcinoma was developed by Foote & Stewart (6) in the 1940's. In most materials of invasive carcinoma the infiltrating lobular carcinoma comprises approximately 10 per cent. The remaining 90 per cent represent ductal carcinomas of which 65-80 per cent are not otherwise specified (NOS). Fisher *et al* (4). The rare tubular ductal carcinoma occurred in about 1 per cent in the large material of Fisher *et al* (4) based on 1000 cases. Also in Rosen's (12) material from Memorial Hospital (941 cases from 1976-1978) tubular carcinoma comprised only one per cent.

We have studied all breast carcinomas from the city of Malmö during the period 1976-1978. The material consists of 590 cases. Fifty seven of these were non-invasive. Of the remaining 533 invasive carcinomas 35 were not classified for various reasons (inadequate amount of tissue or derangement of histologic structure due to preoperative radiation). The study thus comprises 498 cases of invasive carcinoma. We have studied them personally macro- and microscopically and the histologic examination has been extensive. Owing to mammographic screening of a large proportion of the population of Malmö during 1977-1978 a relatively large number of small tumours were received for diagnosis.

The classification and relative frequency of the carcinomas is given in Table 1.

TABLE 1

Tubular carcinoma	21 %
Duct carcinoma NOS	56.2%
Medullary carcinoma with lymphoid stromal infiltration	5.6%
Mucinous carcinoma	4.2%
Lobular infiltrating carcinoma	12.9%

Patelchsky *et al* (11) in a mammographic screening study found 9 per cent tubular carcinomas. A high frequency of tubular carcinoma in screened material is also reported by Andersson *et al* (1).

During this study ample histologic evidence was obtained (Linell *et al* (10)) that tubular carcinoma

The high frequency of tubular carcinoma in our series may be ascribed to the fact that a large

frequency found in the present publication, which was 43 per cent. A possible explanation of the difference is that the patients in Christensen and Sørensen's material had a lower mean age than the autopsy material in the present study (63.1 against 72.7 years).

Amyloid substance in the surface layers of articular cartilage was briefly recorded by *Gamarski and Netto* (1959) in a case of primary amyloidosis. *Bywaters and Dorling* (1970) made the same findings in two cases exhibiting primary amyloidosis and multiple myeloma respectively. These are the only reports of the presence of amyloid substance in articular cartilage.

It is not surprising that amyloid substance could be found in the joint cartilage in these two reports, where the diagnoses were primary amyloidosis and multiple myeloma.

In our study, no known predisposition to amyloidosis was present in any of the cases and therefore we prefer to use the term CS GD for the compound found in the joint cartilage, at least until the results of histochemical and electron microscopic studies of the compound are available.

The tabulated relation to age indicates that CS-GD accumulates in articular cartilage with age. However, the same characteristic age relation has been described for amyloid disease in many earlier reports (*Thung* 1957), (*Buerger and Braunstein* 1960) (*Wright et al* 1969), (*Pirani* 1976). The age relation is as mentioned statistically significant ($0.001 < P < 0.01$).

The fact that there is no difference between the content of CS GD in cartilage from the upper and lower parts of the articular surface of the femoral head presumably indicated that the substance is equally distributed all over the cartilage surface and that stresses such as pressure and friction cannot be if at all, the only factors in its pathogenesis. Further, the diffuse spreading inside the joint and the typical deposition just below the articular surface indicate

that the substance is conveyed by the synovial fluid.

The observation that amyloid material in the capsule was never found when the joint cartilage was negative for CS GD, may also be of some importance with regard to the relationship between the two substances.

Electron microscopic investigations as well as chemical analysis designed to clarify this problem are in progress in our laboratory.

REFERENCES

- 1 *Buerger L & Braunstein H* Senile Cardiac Amyloidosis. *Am J Med* 28: 357 1960
- 2 *Bywaters E G & Dorling J* Amyloid deposits in articular cartilage. *Ann Rheum Dis* 29: 294 1970
- 3 *Christensen H E & Sørensen A H* Local amyloid formation of capsula fibrosa in arthrosis corae. *Acta path microbiol scand Sect A* 80 suppl 223 page 128-131 1972
- 4 *Cohen A S* In *Laboratory Diagnostic Methods in the Rheumatic Diseases*. Little Brown and Co Boston 295-412 1975
- 5 *Gamarski J & Netto M B* Osteoarticular manifestations in primary amyloidosis case presentation. *Arch interamer Rheum* 2: 651 1959
- 6 *Pirani C L* Tissue distribution of amyloid. In *Wickelius O & Pasternack A* (Eds.) *Amyloidosis*. Academic Press London 1976 page 33-49
- 7 *Puchner H, Sweet F & Levine M* On the binding of congo red by amyloid. *J Histochem Cytochem* 100: 355-364 1962
- 8 *Teglbjærk P S, Ladefoged C, Sørensen A H & Christensen H E* Local articular amyloid deposition in pyrophosphate arthritis. *Histological aspects*. *Acta path microbiol scand Sect A* 87: 307-311 1979
- 9 *Thun, P J* Amyloid and ageing. *Proc 14th Congr Int Ass Gerontol* 1: 175-179 1957
- 10 *Wright J R, Calkins E, Brann W J, Sjölie G & Schulz R T* Relationship of amyloid to aging. *Medicine* 45: 39-60 1969

DIFFERENTIAL HISTOCHEMICAL STAINING OF GLYCOSAMINOGLYCANS IN THE MATRIX OF OSTEOARTHRITIC CARTILAGE

STEEN BACH CHRISTENSEN and INGE REIMANN

Department of Orthopaedic Surgery Calcified Tissue Research Laboratory Rigshospitalet Copenhagen
Denmark

Christensen S B & Reimann I Differential histochemical staining of glycosaminoglycans in the matrix of osteoarthritic cartilage *Acta path microbiol scand Sect A* 88 61-68 1980

The distribution of chondroitin sulphate and keratan sulphate in osteoarthritic cartilage is analysed in a histochemical study using Safranin O Alcian Blue-CEC and Toluidin Blue O at different pH values. The material consisted of six femoral heads obtained during replacement surgery from patients with osteoarthritis and six control femoral heads from patients who were operated on because of either fracture or tumour. The heterogeneous distribution of from the osteoarthritic and control patients is described, which first was seen at the surface osteoarthritic staining of chondroitin sulphate especially around the cell clusters. This was a constant finding even in cartilage with only slight osteoarthritic changes. In the control patients this phenomenon was found only in the weightbearing area in very old cartilage or in cartilage with morphological signs of osteoarthritis. Finally the cartilage of osteophytes contained practically only chondroitin sulphate. These histochemical findings are in accordance with the increase in the rate of $^{35}\text{SO}_4$ incorporation despite the loss of glycosaminoglycans in osteoarthritis as described by others and they reflect probably an accelerated synthesis of glycosaminoglycans.

Key words: Articular cartilage osteoarthritis glycosaminoglycans.

Steen Bach Christensen Department of Orthopaedic Surgery Rigshospitalet 9 Blegdamsvej DK 2100 Copenhagen Denmark

Received 7 vii 79 Accepted 23 ix 79

Hyaline articular cartilage is a highly specialized connective tissue characterized by the matrix content of collagen and proteoglycans. These proteoglycans are composed of a central core to which a large number of negatively charged polymeric sugar chains are attached giving macromolecules stiffly extended in space with an enormous negative field (Rosenberg *et al* 1970; McDevitt 1973). Aggregates of proteoglycans linked together by hyaluronate and stabilized by a glycoprotein component (Uthardingham & Muir 1972; Hassell & Heinegård 1974; Heinegård & Hassell 1974) are responsible for the resiliency and resistance to deformation of the cartilage. This ability of the cartilage to act as a shock absorber

becomes weakened when glycosaminoglycans are depleted resulting in an impaired biomechanic function of the joint (Kempson *et al* 1970; Harris *et al* 1972).

In osteoarthritis biochemical studies have detected a decrease in glycosaminoglycan levels on dry weight hexosamine concentration (Matthews 1953; Mankin & Lippitt 1970, 1971; Bjelle *et al* 1972; Lust & Pronsky 1972) but parallel with the reduction an increased production of glycosami-

TABLE 2

Carcinoma type	No of cases	Mean diameter cm	Per cent with axillary metastases
Tubular carcinoma ++++	39	0.8	10.8
Tubular carcinoma +++	56	1.4	31
Tubular carcinoma ++	50	1.7	36
Tubular carcinoma +	70	2.0	51
Tubular carcinoma 0	47	2.5	52

proportion of the tumours were small it is well known that pure tubular carcinoma is always a small lesion (Taylor & Norris (14) Carstens (2))

The low frequency in old materials can be explained if the tubular carcinomas progress to another type Carstens (2) has emphasized that the larger tubular carcinomas have a component of a different histologic type. We have found that more than half of the tubular carcinomas have a more or less prominent zone of a more undifferentiated (ductal) type in their periphery. We call the pure tubular carcinomas »tubular carcinoma ++++» and the latter type »tubular carcinoma +++». Further histologic studies disclosed a third type which was mainly »ductal» but contained a distinct small proportion of tubular structures (»tubular carcinoma ++») and a fourth type with only occasional tubules mostly located in the central part of the lesion (»tubular carcinoma +») The tumours described above have a rather distinctive histologic structure with comparatively small relatively inconspicuous cribriform or solid intraductal proliferates and a striking sclerotic central part with abundant elastoid tissue. On these grounds we were able to discern still another type of »ductal» carcinoma which was devoid of tubules (»tubular carcinoma 0») yet probably derived from tubular carcinoma.

We thus believe - on histologic grounds - that the different types of tumours described here represent stages in a gradual progression to a less differentiated neoplasm (i.e. tubular carcinoma ++++ → tubular carcinoma 0). This is further supported by statistic evidence. A grouping of the cases according to the afore mentioned principles is given in Table 2.

These data strongly suggest that the histologic grouping really describes a progression to tumours with increasing size and higher frequency of nodal metastases.

In our original group of ductal carcinomas NOS there remains 112 cases (22.5% of the whole material) which cannot be included in the aforementioned groups. This remainder represents tumours which we designate as invasive »comedo» carcinomas. They are characterized by rather large atypical cells, widespread intraductal growth and out growth in the lobules (»cancerisation of lobules»). Elastoid stromal tissue is inconspicuous or absent in these tumours and they evidently progress from intraductal carcinomas. This type of duct carcinoma is clearly defined by Hultborn & Tornberg (8).

- References 1 Andersson J, Andrén L & Linell F. Radiology. In press. 2 Carstens P H B. Am J Clin Path 70: 204-210 1978. 3 Fenoglio C & Lanes R. Cancer 33: 691-700 1974. 4 Fisher E R, Gregorio R M & Fisher B. Cancer 36: 1-84 1975. 5 Fisher E R, Pritchard A S, Kotwal N & Lipman N. Am J Surg 130: 1-10 1970. 6 Fisher E R & Hutter R V. J Clin Oncol 1: 1-10 1983. 7 Hamperl H. Virch Arch A 369: 55-68 1975. 8 Hultborn K A & Tornberg B. Acta Radiol Suppl 196: 1960. 9 Ingier A. Virch Arch 198: 338-345 1910. 10 Linell F, Ljungberg O & Andersson I. To be published. 11 Paschevsky A S, Shaber G S, Schwartz G F, Feig S A & Nerlinger R E. Cancer 40: 1659-1670 1977. 12 Rosen P P. Ann Clin Lab Sci 9: 144-156 1979. 13 Semb C. Acta Chir Scand 64 Suppl X: 1928. 14 Taylor H B & Norris H J. Cancer 25: 687-692 1970.

DIFFERENTIAL HISTOCHEMICAL STAINING OF GLYCOSAMINOGLYCANS IN THE MATRIX OF OSTEOARTHRITIC CARTILAGE

STEEN BACH CHRISTENSEN and INGE REIMANN

Department of Orthopaedic Surgery Calcified Tissue Research Laboratory Rigshospitalet Copenhagen
Denmark

Christensen S B & Reimann I Differential histochemical staining of glycosaminoglycans in the matrix of osteoarthritic cartilage Acta path microbiol scand Sect A 88 61-68 1980

The distribution of chondroitin sulphate and keratan sulphate in osteoarthritic cartilage is analysed in a histochemical study using Safranin O Alcian Blue CEC and Toluidin Blue O at different pH values. The material consisted of six femoral heads obtained during replacement surgery from patients with osteoarthritis and six control femoral heads from patients who were operated on because of either fracture or tumour. The heterogeneous distribution of glycosaminoglycans in the matrix of cartilage from the osteoarthritic and control patients is described. In addition to the depletion of glycosaminoglycans which first was seen at the surface osteoarthritic cartilage was characterized by increasing territorial staining of chondroitin sulphate especially around the cell clusters. This was a constant finding even in cartilage with only slight osteoarthritic changes. In the control patients this phenomenon was found only in the weightbearing area in very old cartilage or in cartilage with morphological signs of osteoarthritis. Finally the cartilage of osteophytes contained practically only chondroitin sulphate. These histochemical findings are in accordance with the increase in the rate of $^{35}\text{SO}_4$ incorporation despite the loss of glycosaminoglycans in osteoarthritis as described by others and they reflect probably an accelerated synthesis of glycosaminoglycans.

Key words: Articular cartilage osteoarthritis glycosaminoglycans

Steen Bach Christensen Department of Orthopaedic Surgery Rigshospitalet, 9 Blegdamsvej DK 2100 Copenhagen Denmark

Received 7 vii 79 Accepted 23 ix 79

Hyaline articular cartilage is a highly specialized connective tissue characterized by the matrix content of collagen and proteoglycans. These proteoglycans are composed of a central core to which a large number of negatively charged polymeric sugar chains are attached giving macromolecules suffly extended in space with an enormous negative field (Rosenberg *et al* 1970 McDevitt 1973). Aggregates of proteoglycans linked together by hyaluronate and stabilized by a glucoprotein component (Hardingham & Muir 1972 Hascall & Heinegard 1974 Heinegard & Hascall 1974) are responsible for the resiliency and resistance to deformation of the cartilage. This structure is responsible for the cartilage's function as a shock absorber.

becomes weakened when glycosaminoglycans are depleted resulting in an impaired biomechanic function of the joint (Kempson *et al* 1970 Harris *et al* 1972).

In osteoarthritis biochemical studies have detected a decrease in glycosaminoglycan levels on dry weight hexosamine concentration (Matthews 1953 Mankin & Lippello 1970 1971 Bjelle *et al* 1972 Lust & Pronskey 1972) but parallel with the reduction an increased production of glycosaminoglycans has been observed (Kempson *et al* 1970).

The present study was designed to investigate the distribution of glycosaminoglycans in the matrix of osteoarthritic cartilage using differential histochemical staining. The results are compared with those obtained in control cartilage.

reduction was found to be proportional to the severity of the disease (Mankin *et al* 1971)

The histochemical reaction in these studies was based on the total amount of polyanions in the cartilage

The intention of the present study was to apply to osteoarthritic cartilage histochemical methods which permit differential staining of chondroitin and keratan sulphate sulphated and carboxylated glycosaminoglycans

MATERIALS AND METHODS

Cartilage specimens from 12 femoral heads were used. In the osteoarthritic group six heads were obtained during replacement surgery (mean age 64 range 50-79 years). In the control group five heads were obtained from patients with fracture of the femoral neck and one from a patient with a tumour in the knee who was exarticulated at the hip joint. This patient (age 22 years) was included in order to increase the range of age (mean age 69 range 22-88 years).

The specimens were fixed in 4% neutral buffered formaldehyde for 8 weeks and decalcified in 22% formic acid with 10% sodium citrate for 3 weeks (Morse 1945). Following decalcification the specimens were washed in running tap water, dehydrated in graded alcohol, cleared in methylsalicylate and double embedded in celloidin-paraffin. Sections were cut at 6 micra.

The paraffin sections were deparaffinized in xylene, hydrated through graded alcohols to distilled water, stained, hydrated again through alcohols, cleared in xylene and mounted in Eukitt.

Staining Methods

1. Safranin O fast green iron haematoxylin (Lillie 1965). In permanently mounted sections this dye is transformed to the orthochromatic form where it obeys Beer's law and can be used in quantification of polyanions (Rosenberg 1971). The Safranin O stained sections were used to classify the degree of osteoarthritic changes in an area in the cartilage according to the histological histochemical grading system of Mankin *et al* (1971).

2. Alcian Blue with the critical electrolyte concentration (CEC) principle (Scott and Doring, 1965).

Sections were stained with Alcian Blue 8GX (IC 1) 0.05 per cent in 0.025 M acetate buffer pH 5.8 containing 0.4 or 0.9 M $MgCl_2$. In control studies concentrations of 0.05, 0.2, 0.5, 0.6, 0.8, 1.0, 1.2 and 1.5 M $MgCl_2$ were also used. The sections were stained for 24 hours at room temperature. In cartilage Alcian Blue 0.4 M $MgCl_2$ will stain both chondroitin 4/6 sulphate and keratan sulphate while at 0.9 M $MgCl_2$ only staining of high molecular weight keratan sulphate remains (Laurenti and Scott 1964, Scott 1967).

3. Metachromatic staining with Toluidine Blue at different pH values. Sections were stained for one minute in 0.01 per cent Toluidine Blue O (Merck) in Walpole

buffer (pH 1.0, 2.0, 3.0, 4.0, 5.0). The interaction between cationic dyes and polyanions is of electrostatic nature and as the pK values of the carboxyl group and the sulphate group are different the reaction will depend on the hydrogen ion concentration in the medium. Metachromasia persisting at pH 1.5 indicates the presence of sulphated glycosaminoglycans while carboxyl groups will lose their metachromasia at pH 3 (Krygier & Kasprzak 1961, Spicer 1962).

Chemical Modification Experiments

1. Active methylation in 0.1 N HCl in methanol for 4 hours at 56 °C (Lillie 1958). This procedure should abolish the metachromasia since methylation removes the sulphate groups with formation of free methyl sulphate esters and since carboxyl groups become esterified.

2. Methylation saponification sequence. Methylated sections were saponified in 1% aqueous NaOH in 70% alcohol at 22 °C for 30 min (Spicer 1960). The methyl esters are removed and metachromasia is now based only on carboxyl groups.

3. Oxidative deamination with ninhydrin (0.5 per cent in absolute alcohol) at 37 °C for 30 min (Pearse 1960, Yosuma & Ichikawa 1953). This was done to elucidate any competitive effect of protein especially at low pH values (Andersen & Ehlers 1967).

4. Enzyme digestion experiments. Sections were digested with 0.1 per cent bovine testicular hyaluronidase.

sulphate but not keratan sulphate, dermatan sulphate and heparin sulphate (Meyer *et al* 1956, Lippi & Stoward 1965).

In order to control the effect of the fixation and decalcification procedures on the different staining methods, specimens from non calcified costal cartilage obtained post mortem from a young person were stained

weeks decalcification

The intercellular matrix is divided into zones according to the relation to the cell lacuna. In this paper the area surrounding one cell is named territorial and the interterritorial matrix is the area between territorial zones. In gross terms the articular cartilage is composed of the tangential layer at the surface, the intermediate layer and the calcified layer beneath the tidemark.

RESULTS

Osteoarthritic Cartilage

The degree of cartilage degeneration evaluated on the basis of the Safranin O stained preparation varied considerably from site to site within the same femoral head. Pronounced changes were seen in

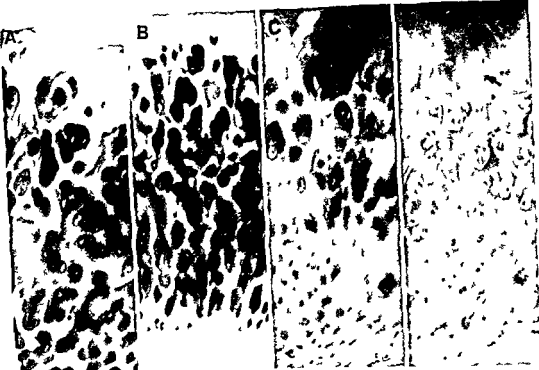


Figure 1 A Safranin O B Toluidine Blue pH 1 C Alcian Blue 0.4 M $MgCl_2$ D Alcian Blue 0.9 M $MgCl_2$ (serial sections) Magnification $\times 100$ Osteoarthritic cartilage (grade 8) from the femoral head of a patient aged 50 years. Superficial loss of staining intensity by Safranin O and an intense territorial staining is seen (A). By Toluidine Blue at pH 1 staining of sulphated glycosaminoglycans is present (B) and by Alcian Blue 0.4 M $MgCl_2$ this staining of territorial glycosaminoglycans is seen especially high around cell clusters (Arrows). However with Alcian Blue 0.9 M $MgCl_2$ (D) the staining has disappeared indicating the territorial glycosaminoglycans to be chondroitin sulphate.

weightbearing areas whereas less severe changes were present in non weightbearing areas. The reduction in the staining ability was first seen and most distinctly at the surface (Fig. 1A-4A).

The osteoarthritic cartilage was characterized not only by loss of staining for glycosaminoglycans but also by increasing territorial staining with Alcian Blue 0.4 M $MgCl_2$ especially around cell clusters (Fig. 1C-4B). This was also seen in cartilage with slight osteoarthritic changes.

By staining with Alcian Blue 0.9 M $MgCl_2$ mostly interterritorial staining was seen except for the most basal part of the radial zone and the calcified cartilage where territorial staining was present (Fig. 1D). The area around the cell clusters showed insignificant staining with Alcian Blue 0.9 M $MgCl_2$ but contained sulphated glycosaminoglycans as shown with Toluidine Blue at low pH values (Fig. 1B).

Furthermore it was observed that the cartilage on the osteophytes was hardly stained at all with Alcian Blue 0.9 M $MgCl_2$ (Fig. 1E).

Control Cartilage

The distribution of glycosaminoglycans in matrix varied in this group: two different patterns were observed.

One group (cartilage from 3 patients aged 22-69 and 73 years) showed the following features. By Safranin-O staining the histological histochemical grading showed no significant signs of osteoarthritis and especially no loss of staining ability (Grade 0-2) (Fig. 3A).

Staining with Alcian Blue 0.4 and 0.9 M $MgCl_2$ confirmed these findings: the highest staining intensity was seen interterritorially at the surface and in the territorial zone in the basal part of the cartilage (Fig. 3C,D). However staining at 0.9 M $MgCl_2$ differed from staining at 0.4 M $MgCl_2$. At 0.9 M $MgCl_2$ it was seen that the area with the highest intensity was located more basally than by staining at 0.4 M $MgCl_2$ (Fig. 3C,D). Staining by Toluidine Blue showed at pH 1 the degree of sulphated glycosaminoglycans was increased basally.

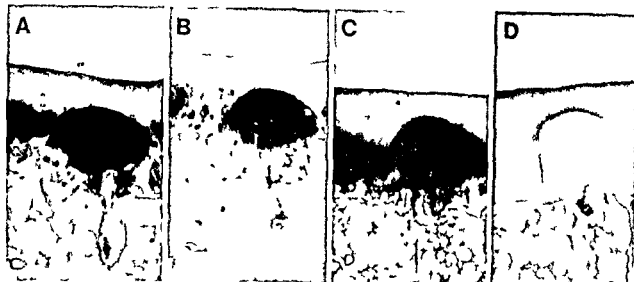


Figure 2 A Safranin O B Toluidine Blue pH 1 C Alcian Blue 0.4 M $MgCl_2$ D Alcian Blue 0.9 M $MgCl_2$ Magnification $\times 25$ Osteophyte cartilage from a patient aged 68 years. The glycosaminoglycans in the osteophytes cartilage are mainly chondroitin sulphate as metachromatic staining with Toluidine Blue at pH 1 (B) disappeared after hyaluronidase digest on and staining with Alcian Blue showed very low intensity at 0.9 M $MgCl_2$ (D)

In the other group of control cartilage (from 3 patients aged 72, 87 and 88 years) the staining with Alcian Blue 0.9 M $MgCl_2$ did not differ from the group mentioned above but in the weightbearing area there was increased territorial staining with Alcian Blue 0.4 M $MgCl_2$. The cartilage from the patient aged 72 showed a smaller area with

unmistakable degenerative changes (grade 5) in Safranin obtained preparation

Chemical Modification Experiments

Following active methylation the metachromatic reaction with Toluidine Blue at pH 5 disappeared. After saponification no colour reaction was seen

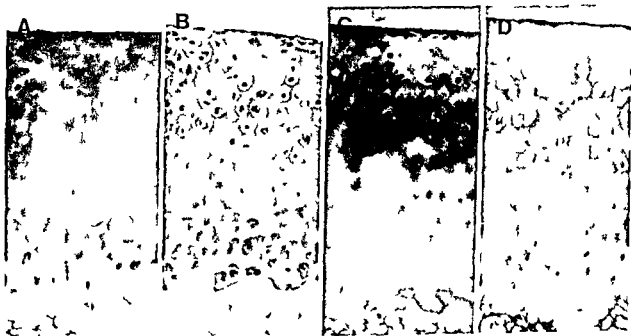


Figure 3 A Safranin O B Toluidine Blue pH 5 C Alcian Blue 0.4 M $MgCl_2$ D Alcian Blue 0.9 M $MgCl_2$ Magnification $\times 25$ Control cartilage from a patient aged 72 years. The glycosaminoglycans in the control cartilage are mainly chondroitin sulphate as metachromatic staining with Toluidine Blue at pH 5 (B) disappeared after hyaluronidase digest on and staining with Alcian Blue showed very low intensity at 0.9 M $MgCl_2$ (D)

see the concentrated deposit in the cartilage at 0.4 M

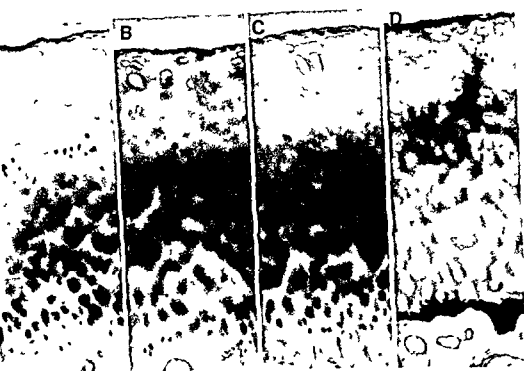


Figure 4. A Safranin O B Alcian Blue 0.4 M $MgCl_2$ C Hyaluronidase digestion and Alcian Blue 0.4 M $MgCl_2$ D Methylation and saponification Toluidine Blue pH 5 Magnification $\times 100$ Osteoarthritic cartilage from a patient aged 68 (grade 4) By Safranin O a superficial loss of staining is seen (A) By Alcian Blue 0.4 M $MgCl_2$ an increased territorial staining is shown even in the superficial area unstained by Safranin O This territorial staining disappears – except basally – after digestion with hyaluronidase prior to staining with Alcian Blue 0.4 M $MgCl_2$ (C) this indicates the territorial glycosaminoglycan to be chondroitin sulphate After methylation and saponification sequences only orthochromatic interterritorial staining is present (D) This staining was unaffected by hyaluronidase digestion and is probably due to collagen staining

with Toluidine Blue at pH values below 4 but at pH 5 only interterritorial orthochromatic staining was seen both in osteoarthritic and control cartilage

In osteoarthritic cartilage some superficial loss of staining was also seen after these procedures (Fig 4D) and this staining was not altered by preceding hyaluronidase digestion

Oxidative deamination with ninhydrin was followed by slightly increasing metachromasia but the distribution of the reaction was the same

It was confirmed by digestion with bovine testicular hyaluronidase and subsequent staining with Alcian Blue 0.4 M $MgCl_2$ that the glycosaminoglycans localized territorially in osteoarthritic cartilage was mainly chondroitin sulphate since loss of staining was seen following enzyme digestion (Fig 4BC) After hyaluronidase digestion no metachromatic staining with Toluidine Blue pH 1 was found in the osteophytes indicating that the sulphate groups in osteophytes cartilage (Fig 2B) derived from chondroitin sulphate

The investigations to control the effect of fixation and decalcification showed that the frozen sections had the highest staining intensity especially with Alcian Blue The critical electrolyte concentration for chondroitin sulphate in the decalcified sections was found at the same level as in the formalin fixated sections (between 0.6 and 0.8 M $MgCl_2$) The distribution in matrix was not changed and no difference was seen in preparations fixed for 8 days or 3 months After staining with Alcian Blue the decalcified preparations showed only a thin light staining at all surfaces both normal surfaces and surfaces cut during the preparation This surface staining was unaffected by high salt concentrations (1.5 M $MgCl_2$) and active methylation

DISCUSSION

Histochemical methods with selective precipitation of the polyanions by cationic dyes such as Alcian

Blue are relatively specific to characterize and locate chondroitin and keratan sulphate in cartilage. Thus Alcian Blue as used in this study will stain both keratan sulphate and chondroitin sulphate at 0.4 M $MgCl_2$ but only keratan sulphate at 0.9 M $MgCl_2$. Hyaluronic acid may only contribute to the metachromatic reaction at pH above 4, but as the relative content is only about one per cent (Hardingham & Muir 1973, Hascall & Heinegard 1974) the metachromasia of hyaluronic acid is poor and as fixation with formalin probably will extract some hyaluronic acid as shown in other tissue (Hale 1946) it was suggested that hyaluronic acid did not contribute to the metachromatic reaction.

In the present study increased territorial staining of chondroitin sulphate was found especially around the cell clusters in osteoarthritic cartilage. This is in accordance with a production of glycosaminoglycans resembling that which is seen in immature cartilage as described in biochemical studies on osteoarthritic cartilage (Mankin & Lippiello 1971, Bayliss & Ali 1978) and it is consistent with the increased frequency of mitosis of the chondrocytes in osteoarthritis (Hulth *et al.* 1972, Telhag 1972).

In normal cartilage a distribution of chondroitin sulphate and keratan sulphate corresponding to the one found in this study has been described (Stockwell & Scott 1965). However by staining aging cartilage with Alcian Blue 0.4 M $MgCl_2$ they found the most intense staining territorially. In the present study this was only seen in cartilage from very old persons (aged 87 and 88) in the weightbearing area and from a patient with incipient degenerative changes. Normal cartilage from patients of an age corresponding to 'osteoarthritic age' (50–75 years) seemed to have the same distribution of glycosaminoglycans as younger adults. Probably the increased territorial content of chondroitin sulphate is a very early sign of degenerative changes but not specific for osteoarthritis and it may perhaps occur in other joint diseases.

Stockwell (1970) reported that the staining of the tangential layer by Alcian Blue 0.9 M $MgCl_2$ increased with age and degenerative changes and attributed it to substances similar to keratan sulphate. The tangential staining by Alcian Blue found in this study was suggested not to arise from polyanions as this staining was unaffected by methylation.

The interpretation of the methylated and saponified sections (Fig. 4D) is not clear. The metachromatic reaction after these procedures may be based on carboxyl groups and as only interterritorial orthochromatic staining was seen in all layers of the cartilage carboxyl groups of chondroitin sulphate were not thought to contribute to the reaction. The

reason for this is probably diminished charge density after desulphatation where the necessary interchange distance is exceeded (Sykes 1958).

As further hyaluronidase digestion prior to methylation and saponification did not change the orthochromatic reaction at pH 5 it is agreed with Spicer & Lillie (1959) that the reaction in cartilage was based on staining of collagen. However it is remarkable that some superficial loss of staining was seen in osteoarthritic cartilage (Fig. 4D).

Biochemical studies on normal and osteoarthritic cartilage have first of all shown that hyaline cartilage undergoes striking changes with increasing age (Kaplan & Mayer 1959, Matthews & Glagov 1966). In neonatal cartilage chondroitin 4- and 6-sulphate are the only glycosaminoglycans present approximately in equal proportions. During development stage the composition changes from a low degree of sulphatation towards a complete degree of sulphatation of chondroitin sulphate and from a high ratio of 6 sulphate to 4 sulphate periods to a ratio of 0.25 or less in the fourth decade. Keratan sulphate is found in cartilage within a few years after birth and rises to a plateau value in the fourth decade remaining approximately constant thereafter.

In osteoarthritis the monomers are found to be smaller primarily due to alterations in the protein core. The chondroitin sulphate rich region is smaller and the monomers appear to lack the hyaluronic acid binding region. These monomers have lost their ability to bind to hyaluronic acid and form aggregates. This results in a looser network of proteoglycans (Unerot *et al.* 1978).

The decrease in glycosaminoglycans in osteoarthritic cartilage has been described as a loss of mainly chondroitin sulphate (Bollet *et al.* 1963, Bollet & Nance 1966), keratan sulphate (Mankin & Lippiello 1971, Benmaman *et al.* 1969, McDevitt *et al.* 1973) or both (Bjelle *et al.* 1972, Kuhn & Leppelmann 1958, Lust & Pronska 1972). This discrepancy might be explained by the problems connected with tissue sampling. In cartilage with minor degenerative changes and only superficial depletion of glycosaminoglycans primarily chondroitin sulphate is lost while in cartilage with severe depletion clusters of chondrocytes with high territorial contents of chondroitin sulphate the chondroitin sulphate/keratan sulphate ratios will be high.

Samples from cartilage with slight and severe osteoarthritic changes might therefore have different chondroitin sulphate/keratan sulphate ratios.

It is still not known whether the changes in the proteoglycan contents of osteoarthritic cartilage are due to increased degradation of normal proteogly-

cans by hyaluronidase (Bollet 1967 Bollet & Nance 1966) Catepsin D (Dingle et al 1971 Sapolsky et al 1973 Ali & Evans 1973) or neutral proteases (Sapolsky et al 1974) or whether the synthesized proteoglycans are altered (Bayliss & Ali 1978)

From the present study it is suggested that the synthesis mostly is characterized by an attempt to repair with a production modus of more immature nature

This work was supported by a grant from the Danish Medical Research Council project number 512 8704 The authors wish to thank dr H Andersen and Dr C Garbarsch Laboratory of Histochemistry and Cytochemistry Anatomy Department A University of Copenhagen for their helpful discussions and Ms K E Sonderlev for careful technical assistance

REFERENCES

- 1 Ali S Y & Evans L Enzyme degradation of cartilage in osteoarthritis Fed Proc 32 1494-1498 1973
- 2 Andersen H & Ehlers N Deamination to prevent the competitive effect of protein in metachromatic staining of sections at low pH values Histochemie 8 252-263 1967
- 3 Bayliss M T & Ali S Y Isolation of proteoglycans from human articular cartilage Biochem J 169 123-132 1978
- 4 Benmaman J D Ludewig J J & Anderson C E Glucosamine and galactosamine distribution in human cartilage Relationship to age and degenerative joint disease Clin Biochem 7 461-464 1969
- 5 Bielle A O Antonopoulos C A Engfeldt B & Hjerquist S O Fractioning of the glycosaminoglycans of human articular cartilage on Ecteola cellulose in aging and in osteoarthritis Calcif Tissue Res 8 237-246 1977
- 6 Bollet A J Hands J R & Sturgill B C Chondroitin sulphate concentration and protein polysaccharide composition of articular cartilage in osteoarthritis J Clin Invest 42 853-859 1963
- 7 Bollet A J & Nance J L Biochemical findings in normal and osteoarthritic articular cartilage II Chondroitin sulphate concentration and chain length water and ash content J Clin Invest 45 1170-1177 1966
- 8 Bollet A J Connective tissue polysaccharide metabolism and pathogenesis of osteoarthritis Adv Intern Med 13 33-60 1967
- 9 Collins D H The pathology of articular and spinal diseases Edward Arnold & Co London 1949 p 74
- 10 Collins D H & McElligott T F Sulphate ($^{35}\text{SO}_4$) uptake by articular cartilage in normal and osteoarthritic tissue J Clin Invest 45 1178-1184 1966
- 11 Dingle J T Barret A J & Weston P D Catepsin D Characteristics of immunoinhibition and confirmation of a role in cartilage breakdown Biochem J 123 1-13 1971
- 12 Eronen I Videman T Friman C & Michelsson J E Glycosaminoglycan metabolism in experimental osteoarthritis caused by immobilization Acta Orthop Scand 49 329-334 1978
- 13 Hale C B Histochemical demonstration of acid polysaccharides in animal tissue Nature 157 802 1946
- 14 Hardingham T E & Muir H The specific interaction of hyaluronic acid with cartilage proteoglycans Biochem Biophys Acta 279 401-405 1972
- 15 Hardingham T E & Muir H Hyaluronic acid in cartilage Trans Biochem Soc 1 282-284 1973
- 16 Harris E D Jr Parker H G & Radin E L Effects of proteolytic enzymes on structural and mechanical properties of cartilage Arthritis Rheum 15 497-503 1972
- 17 Hascall V C & Heinegard D Aggregation of cartilage proteoglycans The role hyaluronic acid J Biol Chem 249 4232-4241 1974
- 18 Heinegard D & Hascall V C Characteristics of the protein isolated from trypsin digests of aggregates J Biol Chem 249 4250-4256 1974
- 19 Hulth A Lindberg L & Telhag J Mitosis in human osteoarthritic cartilage Clin Orthop 84 197-199 1972
- 20 Inerot S Heinegard D Audell L & Olsson S E Articular cartilage proteoglycans in aging and osteoarthritis Biochem J 169 143-156 1978
- 21 Kaplan D & Mayer K Ageing of human cartilage Nature 183 1267-1269 1959
- 22 Kempson G E Muir H Swansson S A F & Freeman M A R Correlation between stiffness and the chemical constituents of cartilage on the human head Biochem Biophys Acta 215 70-77 1970
- 23 Krygier A & Kasprzyk K The influence of hydrogen ion concentrations and some other ions on metachromasia in staining mucopolysaccharides with toluidine blue Acta Med Pol 2 123-145 1961
- 24 Kuhn R & Leppelman H J Galaktosamin und Glukosamin im Knorpel in Abhängigkeit vom Lebensalter Justus Liebig's Annalen der Chemie 611 254-258 1958
- 25 Laurent T C & Scott J E Molecular weight fractionation of polyanions by Cetylpyridinium chloride in salt solutions Nature 202 661-662 1964
- 26 Leppi T J & Stoward P S On the use of testicular hyaluronidase for identifying acid mucins in tissue sections J Histochem Cytochem 13 406-407 1965
- 27 Lillie R D Methylation and alkali demethylation J Histochem Cytochem 6 398-399 1958
- 28 Lillie R D Histopathologic technique and practical histochemistry 3 ed McGraw Hill Book Company New York 1965 p 285

- 29 *Lust C & Pronsky H* Glycosaminoglycan content of normal and degenerative articular cartilage from dogs *Clin Chim Acta* 39 281-286 1972
- 30 *Mankin H J & Lippiello L* Biochemical and metabolic abnormalities in articular cartilage from human osteoarthritic hips *J Bone Joint Surg* 52 A 424-434 1970
- 31 *Mankin H J & Lippiello L* The glycosaminoglycans in normal and arthritic cartilage *J Clin Invest* 50 1712-1719 1971
- 32 *Mankin H J, Dorfman H, Lippiello L & Zarins A* Biochemical and metabolic abnormalities in articular cartilage from osteoarthritic human hips II Correlation of morphology with biochemical and metabolic data *J Bone Joint Surg* 53 A 525-537 1971
- 33 *Matthews B F* Composition of articular cartilage in osteoarthritis *Changes in collagen chondroitin sulphate ratio* *Br Med J* 2 660-661 1953
- 34 *Matthews B F & Glagov S* Acid mucopolysaccharide pattern in aging human cartilage *J Clin Invest* 45 1103-1111 1966
- 35 *McDevitt C A, Muir H & Pond M S* Canine articular cartilage in natural and experimentally induced osteoarthritis *Biochem Soc Trans* 1 287-289 1973
- 37 *Meyer A, Davidson E, Linker A & Hoffmann P* Acid mucopolysaccharides of connective tissue *Biochem Biophys Acta* 21 506-518 1956
- 38 *Morse A* Formic acid sodium citrate decalcification and butyl alcohol dehydration of teeth and bones for sectioning in paraffin *J Dent Res* 24 143-153 1945
- 39 *Pearse A C E* *Histochemistry Theoretical and applied* 3 ed Churchill Livingstone London 1968 pp 116 & 610
- 40 *Rosenberg L* Chemical basis for the histological use of Safranin O in the study of articular cartilage *J Bone Joint Surg* 53 A 69-82 1971
- 41 *Rosenberg L, Hellmann W & Kleinschmidt A K* Macromolecular models of proteinpolysaccharides from bovine nasal cartilage based on electron microscopic studies *J Biol Chem* 245 4123-4130 1970
- 42 *Sapolsky A J, Altman R D & Howell D S* Cathepsin D activity in normal and osteoarthritic human cartilage *Fed Proc* 32 1489-1493 1973
- 43 *Sapolsky A J, Howell D S & Woessner J F* Neutral proteases and Cathepsin D in human articular cartilage *J Clin Invest* 53 1044-1053 1974
- 44 *Scott J E & Döring J* Differential staining of acid glycosaminoglycans (mucopolysaccharides) by Alcian Blue in salt solutions *Histochemie* 5 211-233 1965
- 45 *Scott J E* On the use and abuse of the critical electrolyte concentration approach to the localization of tissue polyanions *J Histochem Cytochem* 15 111-113 1967
- 46 *Spicer S S* A correlative study of the histochemical properties rodent acid mucopolysaccharides *J Histochem Cytochem* 8 18-34 1960
- 47 *Spicer S S* Histochemical differentiation of sulfated rodent mucins *Ann Histochem* 7 23-28 1962
- 48 *Spicer S S & Little R D* Saponification as a means of selectively reversing the methylation blockade of tissue basophilia *J Histochem Cytochem* 7 123-125 1959
- 49 *Stockwell R A & Scott J E* Observation on the acid glycosaminoglycan (mucopolysaccharide) content of the matrix of aging cartilage *Ann Rheum Dis* 24 341-349 1965
- 50 *Stockwell R A* Changes in the acid glycosaminoglycan content of the matrix of aging human articular cartilage *Ann Rheum Dis* 29 500-515 1970
- 51 *Sylvén B* On the interaction between metachromatic dyes and various substrates of biological *Acta Histochem (Jena)* suppl 1 56-78 1958
- 52 *Telhag H* Mitosis of chondrocytes in experimental osteoarthritis in rabbits *Clin Orthop* 86 224-229 1972
- 53 *Yosuma A & Tchikava T* Ninhydrin schiff and alloxan schiff staining *J Lab Clin Med* 41 296-299 1953

PATTERN OF INTIMAL FOLDS AROUND INTERCOSTAL ARTERY ORIFICES IN RABBIT AORTA

A Reflection of Pattern of Blood Flow?

EINAR SVENDSEN

Institute of Medical Biology University of Tromsø Norway

Svensden E. Pattern of intimal folds around intercostal artery orifices in rabbit aorta. A reflection of pattern of blood flow? Acta path microbiol scand Sect. A 88 69-74 1980

The pattern of intimal folds was studied around intercostal artery orifices in rabbit aorta by scanning electron microscopy and light microscopy. The area just proximal and distal to the orifices revealed a smooth surface lacking folds reflected by a stretched internal elastic membrane which showed no undulation. Lateral as well as further proximal and distal well preserved folds were observed. It is reasonable to suppose that the pattern of intimal folds in this area reflects the special flow conditions prevailing in and at the intercostal artery orifices.

Key words: Intimal folds, intercostal artery orifices, rabbit aorta.

E. Svensden, Institute of Medical Biology, Box 977, University of Tromsø, 9001 Tromsø, Norway.

Received 1 vi 79 Accepted 25 ix 79

Earlier reports have shown that there is reason to believe that blood flow has an influence upon the pattern of the intimal folds created by the internal elastic lamina in human and rabbit arteries (2, 14). Flaherty *et al.* (4) showed that even orientation of the endothelial cells depends on the local flow situation. Crawford *et al.* (2) observed that the formative influence of blood flow upon the folds in arteries of man was most striking at branching sites and bends.

Svensden and Jørgensen (14) showed compression of folds and shallow pits in the distal part of the minor curvature of the aortic arch and lateral to the intercostal artery orifices. In the area between two intercostal artery orifices on the same side however a regular pattern of folds was seen (14, 15). They suggested that the pits could be imprints of eddies.

The aim of the present study was to obtain further information about the possible formative influence of blood flow upon the folds of the internal elastic lamina. For that purpose a study of the pattern of folds around the intercostal artery

orifices in rabbit aortas as seen by light microscopy and scanning electron microscopy seemed appropriate since the flow in association with such orifices is known from model studies (5, 9).

MATERIAL AND METHODS

6 New Zealand white male rabbits weighing about 3.5 kg each were used. The animals were raised on a low fat diet without addition (Kanin Pellets Felleskjøpet Trondheim). Sacrifice was made by a perfusion technique described earlier (15). The blood was washed out with buffered Tyrode solution with pH 7.4 and osmolality of 300 mOsm/kg followed by perfusion with 2% buffered glutaraldehyde, pH 7.4 for 5 minutes at a pressure of 80 mm Hg at room temperature. Then the aortas were carefully dissected free and postfixed by immersion in buffered glutaraldehyde 2% for 2 hours, dehydrated in increasing concentrations of alcohol and dried by the

scanning electron microscopy was performed with a Hitachi HHS-2R scanning electron microscope. After the scan

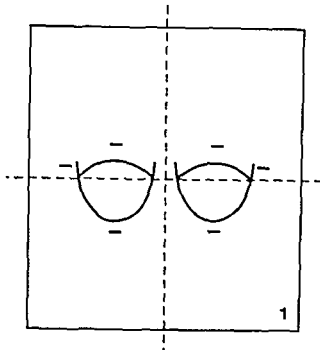


Fig 1 Schematic representation of a specimen from the area around intercostal artery orifices prepared for scanning electron microscopy. The dotted lines indicate how the specimens were sectioned for light microscopy after removal from their stubs. The bars indicate the sampled areas for light microscopy.

ning electron microscopy had been accomplished the specimens were carefully removed from their stubs and samples for light microscopy were taken out with a sharp razor blade in a standardized manner from the sites shown in Fig 1. The samples were embedded in Epon and semithin sections were cut. The sections were stained for elastin with *Victoria blue* and examined and photographed in a Zeiss photomicroscope.

RESULTS

Grossly the same pattern of folds was seen in the second pair of the intercostal artery orifices (Fig 2) as in the eight pair (Fig 3).

Immediately proximally and distally to the intercostal artery ostia the intimal folds were lacking (Figs 2 and 3). The proximal area gave an impression of a smooth intundibulum with lateral folds which curved towards the ostium. In proximal direction this area continued into regularly parallel folds (Figs 2 and 3). The extent of the smooth area downstream to the ostia could vary somewhat. The

smooth area merged with an area of regularly parallel folds still further distal (Figs 2 and 4). In some cases the folds just distal to the smooth area were somewhat wavy (Fig 3).

Light microscopy showed that the intimal folds were mainly dependent on folds in the internal elastic lamina. In the smooth areas proximal and distal to the ostia the internal elastic lamina revealed almost no undulation (Figs 5 and 6). Lateral to the ostia, however, where marked folds appeared on scanning electron micrographs (Fig 4) a distinct undulation of the innermost elastic membrane was observed (Figs 5 and 6).

DISCUSSION

The present study has shown that the intimal folds are mainly created by the folds of the internal elastic lamina. This is in agreement with previous work (14). It appears that the folds proximal and lateral to the ostia merge towards the ostium, following a stream-line pattern which should be expected in this area (9). The central part appears smooth. This may reflect a disturbed flow situation possibly vortices which level the folds. Flow experiments with model tubes have indicated this type of flow disturbance at such sites (7, 12).

Just distal to the ostia is an area where the special flow condition suggested at this site creates a small angle between the vessel wall and the tangent of the velocity profile. This means increased dragging forces parallel with the vascular interface expressed as shear stress in the work of Fry (6). At this site folds seem to be lacking. Further distally and proximally to the ostia the flow is expected to be regular and laminar (9) which may be reflected by regular parallel folds as shown in this paper and previous work (14). Crawford *et al* (2) also suggested formative influence of blood flow upon intimal folds demonstrated by casts of arteries in human bodies.

There has been conflicting evidence as to whether intimal folds exist (1, 2, 10, 13) or not (3, 8) *in vivo*. This work does not give any definite answer to that question. However, the pattern of the intimal folds suggesting an influence of blood flow upon the height and direction of the folds may be an indirect indication that intimal folds do exist *in vivo*. Results obtained by Svendsen & Tindall (13) with arterial casts during continuous monitoring of the diameter

Fig 2 Scanning electron micrograph of one ostium from the second pair of intercostal arteries. There is a longer distance between the ostia at this level than for the 8 pair. Lateral to and between the ostia wellpreserved folds are seen. No folds are present just proximal and distal to the ostium. The arrow indicates the direction of blood flow. 180x.



Fig 3 Scanning electron micrograph of ostium from the 8th pair of intercostal arteries. The very proximal and distal area to the ostium reveal a smooth surface. Further proximally and distally as well as laterally wellpreserved folds are seen the distal ones somewhat wavy. The arrow indicates the direction of blood flow. 110x

of the abdominal aorta of rabbits under anesthesia however, strongly indicate their existence at least in the diastolic phase

Endothelial cell injury is commonly found at the lower lip of intercostal artery ostia (15-16). This area merges with the smooth area downstream to the ostia. In the same area early development of atherosclerosis is seen (17). Mechanical stress may probably be one factor in introducing atherosclerosis (11).

In conclusion this work makes it reasonable to assume that the pattern of the intimal folds around intercostal artery orifices reflects the special flow conditions prevailing in and at the intercostal artery orifices.

I owe my gratitude to Prof. Leif Jørgensen and Dr. Alex Tindall for professional advice and for reading the manuscript. Mrs. Anne Gro Grøthe for technical assistance and Mrs. Dagny Madsen Fauske for typing the manuscript.

REFERENCES

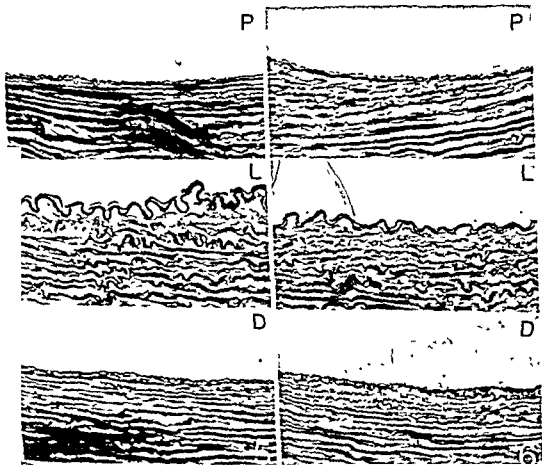
1. Boatman J B, Carter S D, Dorsey B O & White R R. Topographical features of the endothelial surface of the aorta. *Fed Proc (Abstract)* 31: 219 Abs. 1972.
2. Crawford D W, Barndt R & Back L H. Surface characteristics of normal and atherosclerotic human arteries including observations suggesting interaction between flow and intimal morphology. *Lab Invest* 34: 463-470. 1976.
3. Davis P F & Bowler D E. Scanning electron microscopy. Arterial endothelial integrity after fixation at physiological pressure. *Atherosclerosis* 21: 463-469. 1975.
4. Flaherty J T, Pierce J E, Ferrans V J, Patel D J, Tucker W A & Fry D L. Endothelial nuclear patterns in the canine arterial tree with particular reference to hemodynamic events. *Circ Res* 30: 23-33. 1972.



Fig 4 Scanning electron micrograph of the 8th pair of intercostal artery orifices. Note the smooth area proximal and distal to the ostia. Note also that the crest between the ostia has a smooth appearance. Horizontal bars represent regions sectioned for light microscopy. Arrow indicates direction of blood flow. 110x.

Fig 5 Light micrographs of semithin sections from the indicated sites around the left hand ostium in Fig 4. P, L, and D indicate the proximal, lateral and distal areas respectively. Note the distended internal elastic membranes just proximal and distal to the ostium. Laterally a marked undulation of the internal elastic lamina is seen. Victoria blue stain. 460x.

Fig 6 Light micrographs of semithin sections from the indicated sites around the right hand ostium in Fig 4. P, L, and D indicate the same sites as mentioned in Fig 5. The same appearance of the internal elastic membrane as described in Fig 5 is seen. 460x.



- 5 Fox J A & Hugh A E Localization of atheroma. A theory based on boundary layer separation. *Brit Heart J* 28 388-399 1966
- 6 Fry D L Certain chemorheologic considerations regarding the blood vascular interface with particular reference to coronary artery disease. *Circulation Suppl IV* 38-57 1969
- 7 Guistein W H, Schneck D J & Marks J O In vitro studies of local blood flow disturbance in a region of separation. *J Atheroscler Res* 8 381-388 1968
- 8 Haudenschild C, Baumgartner H R & Studer A Significance of fixation procedure for preservation of arteries. *Experientia* 28 828-831 1972
- 9 Pinchak A C & Osirach S Blood flow in branching vessels. *J Applied Phys* 41 646-658 1976
- 10 Shimamoto T, Yamashita Y & Sunaga T Scanning electron microscopic observation of endothelial surface of heart and blood vessels. *Proc Japan Acad* 45 507-511 1969
- 11 Stehbens W E A new concept of the aetiology of atherosclerosis. *Med J Austr* 2 934-935 1974
- 12 Stehbens W E Flow in glass models of arterial bifurcations and berry aneurysms at low Reynolds numbers. *Quart J Exper Phys* 60 181-192 1975
- 13 Svendsen E & Tindall A R The intimal surface of the rabbit aorta. Communication. Physiological Society Meeting London April 20 1979
- 14 Svendsen E & Jørgensen L Intimal pits of aorta in rabbits. Imprints of vortices of blood flow? *Acta path microbiol scand Sect A* 85 25-32 1977
- 15 Svendsen E & Jørgensen L Focal, spontaneous alterations and loss of endothelial cells in rabbit aorta. *Acta path microbiol scand Sect A* 86 1-13 1978
- 16 Svendsen E Focal endothelial cell injury in rabbit aorta. aggravation of injury by 2 days of cholesterol feeding. *Acta path microbiol scand Sect A* 87 123-130 1979
- 17 Texon M The hemodynamic basis of atherosclerosis. Further observations. The ostial lesion. *Bull NY Acad* 48 733-740 1972

DIAGNOSTIC VALUE OF MODIFIED FINE-NEEDLE ASPIRATION BIOPSY OF THE KIDNEY IN GLOMERULAR DISEASES

HEIKKI HELIN

Department of Biomedical Sciences University of Tampere Tampere Finland

Helin H Diagnostic value of modified fine needle aspiration biopsy of the kidney in glomerular diseases Acta path microbiol scand Sect A 88 75-81 1980

43 renal fine needles aspirates obtained with a modified sampling technique were subjected to ultrastructural examination with the aim of assessing the diagnostic value of this method in various glomerular diseases Findings in the aspiration specimens consisting of solitary glomeruli were regarded as diagnostic in 35% of the cases When considered together with clinical data the fine needle aspiration biopsies were suggestive of diagnosis or provided valuable information in a further 49% of the cases Due to the small outer diameter of the fine needle 0.7 mm complications following this kind of biopsy are practically negligible Thus it offers a safe alternative to the conventional renal biopsy methods utilizing large bore cutting needles in cases where biopsies with these methods are contraindicated

Key words: Fine needle aspiration renal biopsy glomerular diseases

Heikki Helin Department of Biomedical Sciences University of Tampere Box 607 SF 33101 Tampere 10 Finland

Received 23 vi 79 Accepted 1 x 79

A modified fine needle aspiration method for biopsy of the kidney has recently been introduced for use in the diagnostics of glomerular diseases (8) With this technique single glomeruli can be obtained for electron microscopical examination The advantage of the fine needle method is its atraumatic nature for due to the small outer diameter of the biopsy needle (0.7 mm) it can be used without fear of clinically relevant complications in situations where conventional biopsy with one of the large bore needles is contraindicated

To assess the value of the morphological information obtained by this method 43 fine needle aspiration biopsies (FNA) from 42 patients were subjected to ultrastructural examination The resulting information was correlated to that provided by data from clinical and laboratory investigations and in 29 out of the 43 cases to findings in parallel conventional biopsies

MATERIAL AND METHODS

43 consecutive FNA specimens from 42 patients with various clinical signs of renal disease (Table I) were available for morphological evaluation The ages of the patients ranged from 5 to 74 years (x 34) Nine patients were under 15 years of age In 29 cases a control specimen from a conventional renal biopsy was examined

The FNAs were performed according to a previously described technique (8) using a modified fine needle of 0.7 mm outer diameter The aspirates were processed according to a technically simple rapid schedule (1)

Light microscopy and stained with toluidine blue and Jones periodic acid silver methenamine Ultrathin sections were stained with lead citrate and uranyl acetate and examined in the JEM 100C electron microscope The FNA specimens were examined independently without knowing the results of the conventional biopsies performed simultaneously

The conventional biopsies were carried out with the Tru Cut® needle (Travenol Laboratories Inc Deerfield Illinois USA) One portion of the biopsy specimen was embedded in paraffin and sectioned for light microscopy and another processed for immunofluorescence examination

RESULTS

Indications of the biopsies are shown in Table 1 The diagnostic information on the FNA specimens was divided into four categories (Table 2) each of which is considered in greater detail in the following

TABLE 1 Indications of 43 Renal Fine Needle Aspiration Biopsies

nephrotic syndrome	3
acute renal failure	4
chronic renal failure	5
proteinuria	15
hematuria	8
diabetes with proteinuria	3
transplantation with renal failure	2
systemic lupus erythematosus	3
Total 43	

FNA establishing the diagnosis (15 cases) In this group the FNA as such was considered conclusive as to diagnosis These diagnoses were verified by light and immunofluorescence microscopical examination of the conventional biopsy specimens available in 9 cases Moreover a more precise morphological analysis was in some cases made possible by ultrastructural examination of the FNA specimens In the cases of membranous glomerulonephritis for example the stage of evolution of the membranous process could be accurately assessed (Fig 1) In 2 out of the 6 patients subjected to FNA only membranous glomerulonephritis was diagnosed Both patients presented clinically with SLE and marked proteinuria The FNA of a diabetic biopsied for proteinuria and renal failure showed the characteristic alteration of nodular diabetic glomerulosclerosis In a patient with rheumatoid arthritis heavy proteinuria and moderate renal failure the FNA revealed glomerular amyloidosis (Fig 2) FNA was performed on a renal transplant with moderately declined function in two patients In one of them the FNA finding was regarded as diagnostic of chronic rejection (Fig 3) In the other patient with Goodpasture's syndrome before transplantation alterations consistent with this diagnosis were seen in the FNA specimen

TABLE 2 Diagnostic Information Provided by 43 Renal Fine Needle Aspiration Biopsies (FNA) (gn = glomerulonephritis)

		Diagnosis or essential finding			
		biopsies	FNA with Tru Cut needle biopsy		FNA only
Diagnosis established by FNA	15	membranous gn	4	membranous gn in SLE	2
		mesangiocapillary gn	1	nodular diabetic	1
		minimal change nephropathy	1	glomerulosclerosis	1
		acute > poststreptococcal gn	2	chronic rejection	
		nodular diabetic		gn in Goodpasture's	
		glomerulosclerosis	1	syndrome	1
Diagnosis suggested by FNA	14			glomerular amyloidosis	1
		IgA nephropathy	6	residual changes after gn	1
		focal and segmental gn in SLE	1	focal glomerular sclerosis	1
		diffuse diabetic		mesangioproliferative gn	1
		glomerulosclerosis	1		
		focal and segmental gn	1		
		residual changes after			
		> poststreptococcal gn	1		
FNA providing useful information	7	focal glomerular sclerosis	1		
		normal ultrastructure	4	minor segmental changes	2
FNA providing little or no information	7	minor segmental changes	1		
		normal ultrastructure	3	normal ultrastructure	3
		unspecific scarring	1		
Total	43		29		14



Fig 1 a Portion of glomerular capillary wall in membranous glomerulonephritis in stage II. This field of view shows subepithelial electron-dense deposits (D) with spikes (arrow). U=urinary space. CL=capillary lumen. $\times 22,400$.

1 b Section from a repeat fine needle aspiration biopsy of the same patient after 21 months. A stage IV alteration is shown with deposition of electron lucent (D) and occasionally electron-dense (arrows) material within the widened basement membrane. U=urinary space. CL=capillary lumen. $\times 16,800$.

FNA suggestive of a diagnosis (14 cases). Examination of the FNA specimens in these 14 patients provided information which when considered together with the clinical data was suggestive of a histopathological diagnosis. Thus a mesangial sclerosing and proliferative glomerulonephropathy with characteristic electron-dense deposits suggested the presence of IgA nephropathy in 6 patients with either microscopic hematuria or recurrent macroscopic hematuria following infections (Fig 4). In

the 11 patients with a parallel conventional biopsy a good correlation between the findings in these and the FNA specimens was observed. Again the electron microscopical study of the FNA specimens allowed a more accurate analysis in some instances.

Three patients were biopsied with FNA only. One of them had a single kidney with moderate failure. In the FNA specimen residual changes after glomerulonephritis suggested a previous acute glomerulonephritis agreeing well with the history

The conventional biopsies were carried out with the Tru Cut® needle (Travenol Laboratories Inc Deerfield Illinois USA) One portion of the biopsy specimen was embedded in paraffin and sectioned for light microscopy and another processed for immunofluorescence examination

RESULTS

Indications of the biopsies are shown in Table 1 The diagnostic information on the FNA specimens was divided into four categories (Table 2) each of which is considered in greater detail in the following

TABLE 1 Indications of 43 Renal Fine Needle Aspiration Biopsies

nephrotic syndrome	3
acute renal failure	4
chronic renal failure	5
proteinuria	15
hematuria	8
diabetes with proteinuria	3
transplantation with renal failure	2
systemic lupus erythematosus	3
Total 43	

FNA establishing the diagnosis (15 cases) In this group the FNA as such was considered conclusive as to diagnosis These diagnoses were verified by light and immunofluorescence microscopical examination of the conventional biopsy specimens available in 9 cases Moreover a more precise morphological analysis was in some cases made possible by ultrastructural examination of the FNA specimens In the cases of membranous glomerulonephritis for example the stage of evolution of the membranous process could be accurately assessed (Fig 1) In 2 out of the 6 patients subjected to FNA only, membranous glomerulonephritis was diagnosed Both patients presented clinically with SLE and marked proteinuria The FNA of a diabetic biopsied for proteinuria and renal failure showed the characteristic alteration of nodular diabetic glomerulosclerosis In a patient with rheumatoid arthritis heavy proteinuria and moderate renal failure the FNA revealed glomerular amyloidosis (Fig 2) FNA was performed on a renal transplant with moderately declined function in two patients In one of them the FNA finding was regarded as diagnostic of chronic rejection (Fig 3) In the other patient with Goodpasture's syndrome before transplantation alterations consistent with this diagnosis were seen in the FNA specimen

TABLE 2 Diagnostic Information Provided by 43 Renal Fine Needle Aspiration Biopsies (FNA) (gn = glomerulonephritis)

		Diagnosis or essential finding		
	biopsies	FNA with Tru Cut needle biopsy	FNA only	
Diagnosis established by FNA	15	membranous gn 4 mesangiocapillary gn 1 minimal change nephropathy 1 acute poststreptococcal gn 2 nodular diabetic glomerulosclerosis 1	membranous gn in SLE 2 nodular diabetic glomerulosclerosis 1 chronic rejection gn in Goodpasture's syndrome 1 glomerular amyloidosis 1 residual changes after gn 1 focal glomerular sclerosis 1 mesangioproliferative gn 1	
Diagnosis suggested by FNA	14	IgA nephropathy 6 focal and segmental gn in SLE 1 diffuse diabetic glomerulosclerosis 1 focal and segmental gn 1 residual changes after poststreptococcal gn 1 focal glomerular sclerosis 1		
FNA providing useful information	7	normal ultrastructure 4 minor segmental changes 1	minor segmental changes 2	
FNA providing little or no information	7	normal ultrastructure 3 unspecific scarring 1	normal ultrastructure 3	
Total	43	29		14



Fig 1 a Portion of glomerular capillary wall in membranous glomerulonephritis in stage II. This field of view shows subepithelial electron-dense deposits (D) with spikes (arrow). U = urinary space. CL = capillary lumen. $\times 22,400$.

1 b Section from a repeat fine needle aspiration biopsy of the same patient after 21 months. A stage IV alteration is shown with deposition of electron-lucent (D) and occasionally electron-dense (arrows) material within the widened basement membrane. U = urinary space. CL = capillary lumen. $\times 16,800$.

FNA suggestive of a diagnosis (14 cases) Examination of the FNA specimens in these 14 patients provided information which when considered together with the clinical data was suggestive of a histopathological diagnosis. Thus a mesangial sclerosing and proliferative glomerulonephropathy with characteristic electron-dense deposits suggested the presence of IgA nephropathy in 6 patients with either microscopic hematuria or recurrent macroscopic hematuria following infections (Fig 4). In

the 11 patients with a parallel conventional biopsy, a good correlation between the findings in these and the FNA specimens was observed. Again the electron microscopical study of the FNA specimens allowed a more accurate analysis in some instances.

Three patients were biopsied with FNA only. One of them had a single kidney with moderate failure. In the FNA specimen residual changes after glomerulonephritis suggested a previous acute glomerulonephritis, agreeing well with the history



Fig 2 Renal fine-needle aspiration biopsy from a patient with rheumatoid arthritis and nephrotic syndrome. Note the subepithelial deposition of amyloid with spicule formation (arrows) in the glomerular basement membrane. U = urinary space. CL = capillary lumen. $\times 14,600$.



Fig 3 This section shows a glomerular capillary loop in a 2-year-old renal allograft showing chronic transplant nephropathy. Marked widening of lamina rara interna (arrows) of the basement membrane containing lamellae of newly formed lamina densa and endothelial cytoplasmic projections. Capillary lumen (CL) considerably narrowed. En = endothelial cells. $\times 11,600$.



Fig 4 Sect on from a fine needle aspirat on biopsy suggest ng IgA nephropathy in a patient with recurrent macroscopic hematuria. The field illustrates a glomerular mesangial area with large electron-dense deposits within the mesangial matrix (D) and beneath the glomerular basement membrane (arrows) $\times 6930$

of the patient. The remaining two patients, both children 12 years of age, were biopsied for proteinuria. In one of them, with a chronic course of corticoid-resistant heavy proteinuria, the FNA findings were suggestive of focal glomerular sclerosis, and in the other, with relatively mild proteinuria, changes fitting well with the diagnosis mesangio-proliferative glomerulonephritis were observed.

FNA providing useful information (7 cases) This category consisted of cases in which the FNA finding offered an explanation for the clinical setting without having features specific enough to suggest a diagnosis. Four of the 5 patients in this group biopsied with both methods had acute renal failure clinically. In all FNA specimens the glomerular morphology was essentially normal. Two of these four were suspected of epidemic nephropathy, and in the other two the clinical data spoke in favour of tubulointerstitial rather than glomerular disease. The conventional biopsies showed changes of acute tubulointerstitial nephritis in all 4 patients. In the fifth case, the FNA of a patient with rheumatoid arthritis and mild proteinuria revealed minor segmental changes in the mesangium, including matrix increase and small deposits. Focal and segmental glomerulonephritis was diagnosed in the control Tru-Cut biopsy.

In two cases FNA was the only biopsy available. Both demonstrated segmental mesangial alterations comparable to those described above. The indication of the biopsy in both cases was mild asymptomatic proteinuria.

FNA providing little or no information (7 cases) Included in this group were biopsies with normal morphology from 3 patients, two of whom presented clinically with slight asymptomatic proteinuria and one with asymptomatic microscopic hematuria. Out of these 3 patients, only one, a girl of 14 years with proteinuria, showed mild segmental changes in less than 10% of the glomeruli in the conventional biopsy. The glomeruli in the FNA of a fourth patient showed unspecific scarring. Unclassifiable chronic glomerulonephritis was diagnosed in the parallel biopsy in this patient with chronic renal failure.

In three children of 9, 10, and 15 years with asymptomatic proteinuria less than 1.0 g/24 h, the FNA performed as the only biopsy disclosed a normal glomerular ultrastructure. This, though expected (3), did not add to the information gained by clinical examinations.

DISCUSSION

Percutaneous renal biopsy, though a relatively safe procedure (2, 13), is not without risks and should therefore be performed only when medical contraindications are not present. Of equal importance are ethical limitations, whereby biopsies for such as pure «scientific» purposes are not acceptable (11). To overcome the disadvantage of lacking morphological information in the cases mentioned, the present method has been developed for adoption in the study of glomerular diseases.

According to previous experiences (7, 8) the modified FNA method provides an adequate sample, consisting of 1 to 12 glomeruli, usually 1 to 4, in 79.1% of cases. It is preferably used in diffuse glomerular diseases, which are known to affect all or nearly all glomeruli simultaneously (5).

As indicated by this study the information gained by the examination of FNA specimens was diagnostic in 35% of the cases. These included diseases which present a characteristic ultrastructural picture. A further 49% proved of value when the morphological information was correlated with that of clinical data. Correlation like this is also a known prerequisite for the successful use of fine-needle aspiration biopsy in diagnostic cytology (14). Normal findings in FNA specimens must be interpreted with care, because of the possibility of obtaining unaffected glomeruli in focal conditions. When electron microscopy is used however, some diseases, appearing focal in light microscopy, in fact show diffuse alterations. Thus for instance, the lesions in IgA nephropathy, a disease accounting for more than 25% of all cases of primary glomerulopathies in several materials published (6) show diffuse distribution in electron microscopy (1). Diffuse ultrastructural changes have also been reported in focal glomerular sclerosis (10). As to the electron microscopical analysis in general it has been found to increase considerably the precision and objectivity of renal biopsy information (12).

The risk of complications involved in percutaneous renal biopsy has been shown to relate to the caliber of the needle used (15, 16). In this respect the modified fine needle with an outer diameter of 0.7 mm and with a sharp inner edge of 0.43 mm compares favourably with the commonly used large bore needles of 1.4–1.9 mm diameter. In 37 patients so far biopsied with the modified fine-needle only, no complications except transient microhematuria have been seen. This agrees well with Soderstrom's (14) experiences concerning renal aspiration biopsy with a fine needle (0.7 mm outer diameter) in cytodiagnosics. These biopsies like the 182 described by Pasternack et al. (9) and

performed with a fine needle of the same caliber were not followed by any noteworthy complications.

The present FNA method is not meant to concur with the techniques generally used utilizing large bore needles. It is however a safe alternative when the last-mentioned can not be performed without exposing the patient to an undesired risk. An area of application of both clinical and scientific interest is repeat follow-up biopsy to assess the histological evolution of a disease process. Conditions without or with only minor renal symptoms following glomerular injury are seldom clarified by renal biopsy but are of undoubted interest. Such conditions are for instance malignant tumors or infectious diseases with secondary asymptomatic renal involvement.

REFERENCES

- Berger J, Yanava H, Nabarra B & Barbanel C. Recurrence of mesangial deposition of IgA after renal transplantation. *Kidney Int* 7: 232–241, 1975.
- Diaz-Buxo J A & Donadio J V. Complications of percutaneous renal biopsy. *Clinical Nephrology* 10: 223–227, 1975.
- Habib R. Value of renal biopsy in diagnosis, prognosis and management of glomerular diseases. In: Strauss J (Ed.) *Pediatric Nephrology* vol. 3. Plenum Press, New York etc. 1976, p. 9–26.
- Helin H, Pasternack A & Rantala I. Rapid processing of renal glomeruli for electron microscopy. *J Clin Path* 32: 516–520, 1979.
- Kellow W F, Coissonas N J, Chomet B & Zimmerman H J. Evaluation of the adequacy of needle biopsy specimens of the kidney. *Arch Intern Med* 104: 353–359, 1959.
- Lowance D C, Mullins J D & McPhaul J J. IgA associated glomerulonephritis. *Int Rev Exp Pathol* vol. 17. Academic Press, New York etc. 1977, p. 143–172.
- Pasternack A, Helin H & Rantala I. Clinical application of renal aspiration biopsy with a modified fine needle. In: *Dialysis Transplantation Nephrology. Proceedings of the European Dialysis and Transplant Association* vol. 14. Pitman, Tunbridge Wells 1977, p. 463–471.
- Pasternack A, Helin H, Tornroth T, Rantala I, Vaisanen J & Rahka R. Aspiration biopsy of the kidney with a modified fine needle. A way to obtain glomeruli for morphological study. *Clinical Nephrology* 10: 79–84, 1978.
- Pasternack A, Virolainen M & Haver P. Fine needle aspiration biopsy in the diagnosis of human allograft rejection. *J Urol* 109: 167–172, 1973.
- Rumpelt H J & Thoenes H. Focal and segmental sclerosing glomerulopathy. *Virchows Arch A* 302: 265–282, 1974.

- 11 *Schutterle G & Frisch H* Todliche Komplikationen nach Nierenblindpunktion *Med Klin* 60 184-189 1965
- 12 *Segel N J Spargo B H Kashgarian M & Hayslett J P* An evaluation of routine electron microscopy in the examination of renal biopsies *Nephron* 10 209-215 1973
- 13 *Slotkin E A & Madsen P O* Complications of renal biopsy. Incidence in 5000 reported cases *J Urol* 87 13-15 1962
- 14 *Soderstrom A* Fine Needle Aspiration Biopsy *Almqvist & Wiksell* Stockholm 1966
- 15 *Thaler H* Die Nierenbiopsie *Wien klin Wschr* 79 425-427 1967
- 16 *Thieler H Meister H Meyer W & Hesse P* Erfahrungen bei 250 Nierenbiopsien mit der Menghini Technik *Dtsch Ges Wesen* 23 881-886 1968

DISCUSSION

Percutaneous renal biopsy though a relatively safe procedure (2, 13) is not without risks and should therefore be performed only when medical contraindications are not present. Of equal importance are ethical limitations whereby biopsies for such as pure «scientific» purposes are not acceptable (11). To overcome the disadvantage of lacking morphological information in the cases mentioned the present method has been developed for adoption in the study of glomerular diseases.

According to previous experiences (7, 8) the modified FNA method provides an adequate sample consisting of 1 to 12 glomeruli usually 1 to 4 in 79.1% of cases. It is preferably used in diffuse glomerular diseases which are known to affect all or nearly all glomeruli simultaneously (5).

As indicated by this study the information gained by the examination of FNA specimens was diagnostic in 35% of the cases. These included diseases which present a characteristic ultrastructural picture. A further 49% proved of value when the morphological information was correlated with that of clinical data. Correlation like this is also a known prerequisite for the successful use of fine needle aspiration biopsy in diagnostic cytology (14). Normal findings in FNA specimens must be interpreted with care because of the possibility of obtaining unaffected glomeruli in focal conditions. When electron microscopy is used however some diseases appearing focal in light microscopy in fact show diffuse alterations. Thus for instance the lesions in IgA nephropathy, a disease accounting for more than 25% of all cases of primary glomerulopathies in several materials published (6) show diffuse distribution in electron microscopy (1). Diffuse ultrastructural changes have also been reported in focal glomerular sclerosis (10). As to the electron microscopical analysis in general it has been found to increase considerably the precision and objectivity of renal biopsy information (12).

The risk of complications involved in percutaneous renal biopsy has been shown to relate to the caliber of the needle used (15, 16). In this respect the modified fine needle with an outer diameter of 0.7 mm and with sharp inner edge of 0.43 mm compares favourably with the commonly used large bore needles of 1.4–1.9 mm diameter. In 87 patients so far biopsied with the modified fine needle only no complications except transient microhematuria have been seen. This agrees well with Soderstrom's (14) experiences concerning renal aspiration biopsy with a fine needle (0.7 mm outer diameter) in cytodiagnostics. These biopsies like the 182 described by Pasternack et al (9) and

performed with a fine needle of the same caliber were not followed by any noteworthy complications.

The present FNA method is not meant to compete with the techniques generally used utilizing large bore needles. It is however a safe alternative when the last mentioned can not be performed without exposing the patient to an undesired risk. An area of application of both clinical and scientific interest repeat follow up biopsy to assess the histologic evolution of a disease process. Conditions with or without only minor renal symptoms followed by glomerular injury are seldom clarified by renal biopsy but are of undoubted interest. Such conditions are for instance malignant tumors or infectious diseases with secondary asymptomatic renal involvement.

REFERENCES

- Berger J, Yaney H, Nabarra B & Barbanel C. Recurrence of mesangial deposition of IgA after renal transplantation. *Kidney Int* 7: 232–241, 1975.
- Diaz Buxo J A & Donadio J V. Complications of percutaneous renal biopsy. *Clinical Nephrology* 4: 223–227, 1975.
- Habib R. Value of renal biopsy in diagnosis, prognosis and management of glomerular diseases. In Strauss J (Ed.) *Pediatric Nephrology* vol 3. Plenum Press, New York etc, 1976, p. 9–26.
- Helin H, Pasternack A & Rantala I. Rapid processing of renal glomeruli for electron microscopy. *J Clin Path* 37: 516–520, 1979.
- Kellow H F, Coissonas N J, Chomet B & Zimmerman H J. Evaluation of the adequacy of needle biopsy specimens of the kidney. *Arch Intern Med* 104: 353–359, 1959.
- Lowance D C, Mullins J D & McPhaul J J. IgA associated glomerulonephritis. *Int Rev Exp Pathol* vol 17. Academic Press, New York etc, 1977, p. 143–177.
- Pasternack A, Helin H & Rantala I. Clinical application of renal aspiration biopsy with a modified fine needle. In *Dialysis Transplantation Nephrology Proceedings of the European Dialysis and Transplant Association* vol 14. Pitman, Tunbridge Wells, 1977, p. 463–471.
- Pasternack A, Helin H, Tornroth T, Rantala I, Vaisanen J & Rahka R. Aspiration biopsy of the kidney with a modified fine needle. A way to obtain glomeruli for morphological study. *Clinical Nephrology* 10: 79–84, 1978.
- Pasternack A, Virolainen M & Haver P. Fine-needle aspiration biopsy in the diagnosis of human allograft rejection. *J Urol* 109: 167–172, 1973.
- Rumpelt H J & Thoenes H. Focal and segmental sclerosing glomerulopathy. *Virchows Arch* A 362: 265–282, 1974.

TRABECULAR BONE MINERALIZATION LAG TIME DETERMINED BY TETRACYCLINE DOUBLE-LABELING IN NORMAL AND CERTAIN PATHOLOGICAL CONDITIONS

FLEMMING MELSEN and LEIF MOSEKILDE

University Institute of Pathology and Medical Department III Aarhus Amtssygehus and Department
of Neurology Aarhus Kommunehospital Aarhus Denmark

Melsen F & Mosekilde L. Trabecular bone mineralization lag time determined by tetracycline double labeling in normal and certain pathological conditions Acta path microbiol scand Sect A 88 83-88 1980

Quantitative histomorphometric analyses of iliac crest biopsy specimens were performed after tetracycline double labeling in 41 normal individuals 20 hyper and 10 hypothyroid patients 18 patients with primary hyperparathyroidism 20 epileptic patients receiving long term anticonvulsant therapy and 17 patients after jejunioileal bypass for morbid obesity The mineralization lag time in trabecular bone or the period of time between apposition and subsequent mineralization of osteoid was calculated from the bone formation rate at BMU level (Basic Multicellular Unit) and the mean width of osteoid seams The mineralization lag time was 8-52 days (median 21 days) in normal individuals and showed no variation with sex or age The mineralization lag time was shortened in hyperthyroidism normal in anticonvulsant bone disease and in primary hyperparathyroidism and markedly prolonged in hypothyroidism and following jejunioileal bypass Among all individuals an inverse hyperbolic relation ($r = 0.94$ $p < 0.001$) was found between the mineralization lag time and the average cellular activity of the osteoblasts

Key words Mineralization lag time bone histomorphometry tetracycline double labeling

F Melsen University Institute of Pathology Aarhus Amtssygehus 8000 Aarhus C Denmark

Accepted as submitted 1 x 79

Unmineralized bone matrix is laid down by osteoblasts as osteoid seams on the bone surfaces. That the osteoid seams have a certain thickness shows that there is a delay between the formation of bone matrix by osteoblasts and the subsequent mineralization. During this period a sequential change in the staining properties of the osteoid is observed. A distinct band which lies adjacent to the calcified matrix and stains with acid dyes has been termed the calcification front (Matrajt *et al* 1967) and has been taken as evidence of early mineralization. Tetracycline antibiotics will deposit *in vivo* in these sites of active mineralization (Milch *et al* 1958 Frost 1969).

In a steady state situation with regard to osteoid

thickness the rate of apposition of osteoid equals the rate of mineralization because any systematical change in this proportion will result in a change in the thickness of the osteoid.

The mineralization lag time or the time interval between apposition and subsequent mineralization of osteoid

The aim of the present investigation was to describe this calculation for trabecular bone and to report normal values. Furthermore the mineralization lag time has been calculated in certain pathological conditions.

TRABECULAR BONE MINERALIZATION LAG TIME DETERMINED BY TETRACYCLINE DOUBLE-LABELING IN NORMAL AND CERTAIN PATHOLOGICAL CONDITIONS

FLEMMING MIELSEN and LEIF MOSEKILDE

University Institute of Pathology and Medical Department III Aarhus Amtssygehus and Department
of Neurology Aarhus Kommunehospital Aarhus Denmark

Melsen F & Mosekilde L. Trabecular bone mineralization lag time determined by tetracycline double labeling in normal and certain pathological conditions Acta path microbiol scand Sect. A 88 83-88 1980

Quantitative histomorphometric analyses of iliac crest biopsy specimens were performed after tetracycline double labeling in 41 normal individuals 20 hyper and 10 hypothyroid patients 18 patients with primary hyperparathyroidism 20 epileptic patients receiving long term anticonvulsant therapy and 17 patients after jejunioileal bypass for morbid obesity The mineralization lag time in trabecular bone of the iliac crest was determined by double labeling with tetracycline and

showed no variation with sex or age The mineralization lag time was shortened in hyperthyroidism normal in anticonvulsant bone disease and in primary hyperparathyroidism and markedly prolonged in hypothyroidism and following jejunioileal bypass Among all individuals an inverse hyperbolic relation ($r = 0.94$ $p < 0.001$) was found between the mineralization lag time and the average cellular activity of the osteoblasts

Key words Mineralization lag time bone histomorphometry tetracycline double labeling

F Melsen University Institute of Pathology Aarhus Amtssygehus 8000 Aarhus C Denmark

Accepted as submitted 1 x 79

Unmineralized bone matrix is laid down by osteoblasts as osteoid seams on the bone surfaces. That the osteoid seams have a certain thickness shows that there is a delay between the formation of bone matrix by osteoblasts and the subsequent mineralization. During this period a sequential change in the staining properties of the osteoid is observed. A distinct band which lies adjacent to the calcified matrix and stains with acid dyes has been termed the calcification front (Matrajt *et al* 1967) and has been taken as evidence of early mineralization. Tetracycline antibiotics will deposit *in vivo* in these sites of active mineralization (Milch *et al* 1958 Frost 1969).

In a steady state situation with regard to osteoid

thickness the rate of apposition of osteoid equals the rate of mineralization because any systematical change in this proportion will result in a bone disease.

This assumption allows the calculation of the mineralization lag time or the time interval between apposition and subsequent mineralization of osteoid.

The aim of the present investigation was to describe this calculation for trabecular bone and to report normal values. Furthermore the mineralization lag time has been calculated in certain pathological conditions including hyper and hypothyroidism primary hyperparathyroidism anticonvulsant bone disease and osteomalacia following jejunioileal bypass for obesity.

NORMAL POPULATION

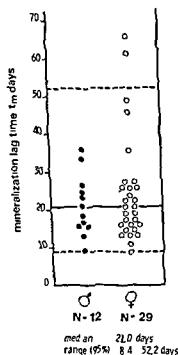


Fig 1 Mineralization lag time (t_m days) in normal males and females. Median and normal range (95%) are indicated

width of the osteoid seams (*W_1) was normal because of an increase in the appositional rate of osteoid ($=^*V_1(BVU)$) and a simultaneous decrease in the mineralization lag time (t_m). The osteoblastic activity was decreased in the hypothyroid patients both at active cellular level and at BVU level. The mean width of the osteoid seams was reduced because of a marked decrease in the appositional rate of osteoid and in spite of a prolongation of the mineralization lag time.

The osteoblastic activity was slightly decreased in the hyperparathyroid patients at cellular level and at BVU level. The mean osteoid seam width was normal. The osteoid appositional rate was slightly reduced and the mineralization lag time was slightly but insignificantly, prolonged ($p < 0.10$).

The epileptic patients receiving anticonvulsants showed a normal osteoblastic activity at active cellular level whereas the activity at BVU level was slightly increased. The mean osteoid seam width was increased because of the increased appositional rate of osteoid and in spite of the normal mineralization lag time.

The osteoblastic activity was reduced in the intestinal bypass patients at both active cellular level and BVU level. The mean width of the osteoid seams was increased because of a marked prolongation of the mineralization lag time and in spite of a reduction in the appositional rate of osteoid.

TABLE 1 Measured and Calculated Histomorphometric Values in Normal Individuals and in Certain Pathological Conditions

		$S_{frac}(n)$ $\mu m^2/\mu m^2$	$S_{frac}(tbl)$ $\mu^2/\mu m^2$	$^*V_1/t$ $\mu m/day$	$^*V_1(BVU)$ $\mu m^3/\mu m^2/day$	*W_1 μm	t_m days
Normal individuals	\bar{x}	0.179	0.135	0.65	0.50	9.6	23.5
	SE	0.011	0.010	0.02	0.02	0.4	2.5
Hyperthyroid patients	\bar{x}	0.173	0.144	0.94**	0.86**	9.3	13.1**
	SE	0.019	0.013	0.05	0.08	0.6	1.1
Hypothyroid patients	\bar{x}	0.149	0.032**	0.036**	0.12**	6.3**	92.3**
	SE	0.020	0.009	0.08	0.05	0.7	26.4
Hyperparathyroid patients	\bar{x}	0.281**	0.204**	0.56*	0.41*	9.9	28.6
	SE	0.023	0.019	0.03	0.03	0.6	2.8
Epileptics	\bar{x}	0.281**	0.247**	0.66	0.58*	12.2**	21.3
	SE	0.014	0.012	0.02	0.02	0.4	1.0
Intestinal bypass patients	\bar{x}	0.234*	0.117	0.46**	0.25**	12.3**	42.7**
	SE	0.032	0.014	0.03	0.03	1.4	6.4

Significance of difference from normal mean: * $p < 0.05$, ** $p < 0.01$ (Wilcoxon test for two pairs)

MATERIAL AND METHODS

The investigation comprised the following classes of normal individuals and patients who had all given informed consent to participate

41 normal volunteers 12 males aged 23 to 56 years (mean 32) and 29 females aged 19 to 53 years (mean 29) Entry into the investigation was based on normal thyroid parathyroid kidney and liver function None received tranquilizers anticonvulsants or other chronic medication

20 patients with untreated hyperthyroidism aged 24 to 46 years (mean 33) and 10 patients with untreated primary hypothyroidism aged 33 to 75 years (mean 54) The diagnosis was based on clinical symptoms and signs measurements of total serum thyroxine serum triiodo thyronine uptake test serum TSH and ^{131}I iodine uptake

18 patients with untreated primary hyperparathyroidism aged 29 to 74 years (mean 46) The diagnosis was based upon determination of serum immunoreactive parathyroid hormone (Christensen 1976) and total calcium corrected for individual variations in serum albumin In all cases a parathyroid adenoma was later found by neck exploration

20 adult epileptic outpatients aged 20 to 52 years (mean 29) who all received diphenylhydantoin some of them in combination with other anticonvulsants All had been treated for more than 10 years The patients were selected from a group of 60 epileptics in whom bone biopsy was performed (Mosekilde and Melsen 1976) The selection was based on the occurrence of an increased amount of osteoid and/or an increase in the mean size of the periosteocytic lacunae None of the patients had symptoms of bone disease

17 patients aged 29 to 64 years (mean 38) who 3 to 8 years (mean 5.2) previously had undergone jejunoileal bypass for morbid obesity The mean preoperative weight was 121 kg (range 102–173 kg) During operation 35 cm of jejunum was anastomosed end to side to 15 cm of the distal ileum The average weight loss was 39 kg (range 20–77) None of the patients had bone pains or bone tenderness

Transcortical iliac crest biopsies with a diameter of 8 mm (Border *et al* 1964) were obtained after doublelabeling with tetracycline (600 mg of demethyl chlorotetracycline given orally 14 13 4 and 3 days before biopsy) The bone specimens were embedded undecalcified in methylmethacrylate 8 mm thick sections were cut and stained with Masson trichrome for quantification of osteoid (Melsen *et al* 1978) and 20 μm thick unstained sections were mounted for quantification of dynamic parameters by fluorescent microscopy (Melsen and Mosekilde 1978) The following measurements were performed in trabecular bone using the point count principle and simple measurements with a micrometric eyepiece*)

Fractional formation surfaces ($S_{\text{frac}(f)}$) $\mu\text{m}^2/\mu\text{m}^2$ – the extent of osteoid covered surfaces in decimal fraction of the total trabecular bone surface

Fractional labeled surfaces ($S_{\text{frac}(lab)}$) $\mu\text{m}^2/\mu\text{m}^2$ – the extent of single and double tetracycline labeled surfaces

in decimal fraction of the total trabecular bone surface

Appositional rate ($^{45}\text{M}/t$) $\mu\text{m}/\text{day}$ – the mean distance between the lines in all zones double labeled with tetracycline (^{45}M) divided by the interval of days (t) between the labelings This value expresses the bone formation rate at active cellular level uncorrected (u) for fortuitous obliquity of the plane of section**)

Mean width of osteoid seams (^{45}W) μm – the mean of four extreme almost equally spaced measurements in all surfaces covered with osteoid uncorrected (u) for obliquity of the plane of section

The following parameters were calculated

Bone formation rate BMU level surface referent ($^{45}\text{V}_{\text{f}(BMU)}$) $\mu\text{m}^3/\mu\text{m}^2/\text{day}$ as

$$^{45}\text{V}_{\text{f}(BMU)} = \frac{S_{\text{frac}(lab)} \times ^{45}\text{M}/t}{S_{\text{frac}(f)}}$$

which expresses the amount of new bone mineralized in unit time per unit osteoid covered surfaces In a steady state situation with regard to osteoid thickness $^{45}\text{V}_{\text{f}(BMU)}$ is numerical identical to the appositional rate of osteoid ($^{45}\text{O}_{\text{f}(BMU)}$) $\mu\text{m}/\text{day}$ defined as the average thickness of osteoid laid down in unit time and reflecting the average activity of active and inactive osteoblasts

Mineralization lag time (t_m) days (Baylink *et al* 1970) as

$$t_m = \frac{^{45}\text{W}}{^{45}\text{V}_{\text{f}(BMU)}}$$

This calculation is based on the relations

$$^{45}\text{W} = t_m \times ^{45}\text{O}_{\text{f}(BMU)} \quad ^{45}\text{O}_{\text{f}(BMU)} = ^{45}\text{V}_{\text{f}(BMU)}$$

which express that the mean width of osteoid seams at steady state equals the mean thickness of osteoid laid down per day multiplied by the average number of days with osteoid formation before mineralization starts

RESULTS

The individual values of the mineralization lag (t_m) from the normal males and females are shown in Fig 1 No significant differences were found between the sexes ($p > 0.10$ (Wilcoxon test)) and t_m was unrelated to age ($R = 0.28$ $p > 0.10$ (Spearman

Table 1 gives the arithmetic mean values ($\pm \text{SE}$) of t_m and of the parameters involved in the calculation of t_m in the normal individuals and in the different patient groups The distribution of the individual t_m values in the different groups is shown in Fig 2

The hyperthyroid patients showed an increased activity of the osteoblasts both at active cellular ($^{45}\text{M}/t$) and at BMU level ($^{45}\text{V}_{\text{f}(BMU)}$) The mean

Among all individuals a highly significant inverse hyperbolic relation ($r = 0.94$ $p < 0.001$) was found between the mineralization lag time and the activity of the osteoblasts at BMU level (Fig. 3). A similar but less significant relation ($r = 0.75$, $p < 0.01$) was found between the mineralization lag time and the osteoblastic activity at active cellular level.

DISCUSSION

The present study has demonstrated that the mineralization lag time in trabecular bone in normal individuals is 8 to 52 days with a median of 21 days. This period of time is longer than the 10 days previously reported by Lacroix (1970) who analyzed active bone formation surfaces in cortical bone. It should however be noticed that the mineralization lag time in the present study represent an average value for both active (tetracycline labeled) and inactive (osteoid covered unlabeled) bone formation surfaces because both the bone formation rate and the mean width of osteoid seams are averaged over the total surface covered with osteoid. This calculation gives more information about the background of variations in the observed mean width of osteoid seams than determinations at active bone formation surface alone.

Both the appositional rate ($\mu\text{M}/t$) and the mean width of osteoid seams (μM) were uncorrected for fortuitous obliquity of the plane of section. This correction involves however a multiplication of both parameters by 0.73** and will therefore not change the calculated mineralization lag time.

It appears from the present study that excess thyroid hormone(s) shortens and deficient thyroid hormone(s) prolongs the mineralization lag time. This is in accordance with the finding that thyroid

and the longer life span of bone forming sites (Melssen et al 1977, Meunier et al 1978).

The observed normal mineralization lag time in anticonvulsant bone disease and the markedly prolonged lag time in intestinal bypass patients supports the concept that anticonvulsant bone disease differs from vitamin D deficient states (Schultz and Dellung 1974, Mosekilde et al 1977). This is in accordance with the findings of low levels of 1,25-dihydroxycholecalciferol, the ultimate metabolically active vitamin D metabolite in intestinal bypass patients (Lund et al 1979) and slightly increased values in epileptic patients receiving anticonvulsants (Urbiz et al 1977).

In the present study a high cellular activity of the osteoblasts was associated with a short mineralization lag time and vice versa. This supports the concept that the osteoblasts on the bone surface are in some way associated with the deposition of mineral at the calcification fronts (Arnot and Pautard 1967, Bunucci 1971).

The calculation of the mineralization lag time is based on a steady state situation with regard to bone remodeling. The bone remodeling period (sigma) or the period of time between the activation of new remodeling unit and its completion of the resorptive and subsequent formative phases equals the shortest time following a stimulus that a new steady state characteristic for that stimulus can exist (Frost 1969). The normal bone remodeling period in iliac crest trabecular bone can be estimated to about 4 months from the mean thickness of completed remodeling units (Lips et al 1978). The bone formation rate at BMU level (Melsen and Rosenkilde 1978) and the proportion of formative to resorptive surface (Melsen et al 1978). This period of time in trabecular bone equals the previously reported

lag time and less rapid at the end (Frost 1962, Lacroix 1970). In order to avoid sampling errors a relatively large number of osteoid seams should therefore be examined in each individual or in each test group.

We conclude that the mineralization lag time is a

* The symbols and notations used in the paper are to a great extent identical with those suggested by H. M. Frost (1977).

BMU - Basic Multicellular Unit. The functional entity of cells responsible for the turn-over of a remodeling unit of bone (Frost 1969).

** An orientation correction factor (0.73) has been computed by H. M. Frost (Cosine integration between variable bounds) on Hewlett Packard HP 65 program.

never contribute to the shortened mineralization lag time by inducing mineralization at an earlier stage of the maturation of osteoid.

The bone changes in primary hyperparathyroidism are among other factors characterized by an increased amount of osteoid (Melsen et al 1977, Meunier et al 1978) because of an increased extent of osteoid covered surfaces. The increase in the amount of unmineralized bone is not due to a mineralization defect because of the normal mean osteoid seam width and the normal mineralization lag time. The increased extent of bone forming surfaces may be explained by the high bone turn over with an increased number of remodeling units

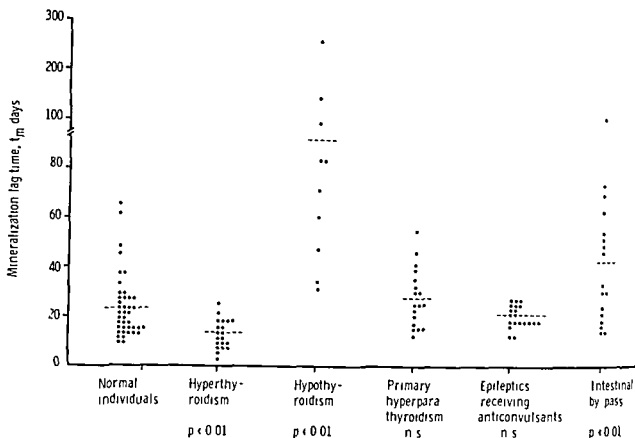


Fig 2 Distribution of t_m values in normal individuals and in various pathological conditions. The dotted lines indicate the arithmetic mean values

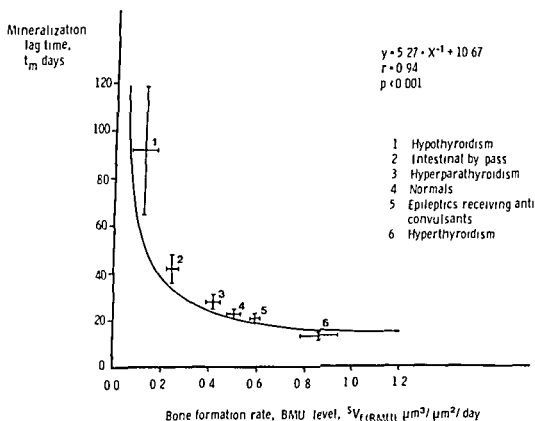


Fig 3 The relation between the mineralization lag time and the bone formation rate at BMU level in normal and pathological states. Mean and standard error of the mean are indicated for the different groups investigated

XANTHOGRANULOMATOUS PYELONEPHRITIS

A Clinico pathological Study with Special Reference to Pathogenesis

JENS CHR MØLLER and INGRID B KRISTENSEN

University Institute of Pathology Kommunehospitalet Aarhus and the Institute of Pathology Centralsygehuset Randers

Møller J C F & Kristensen I B Xanthogranulomatous pyelonephritis A clinico pathological study with special reference to pathogenesis Acta path microbiol scand Sect A 88 89-96 1980

Nineteen cases of xanthogranulomatous pyelonephritis (XP) were studied. There was a close relation to pyonephrosis and urinary tract obstruction was present in all cases but one which represented the tumorous variety of XP. The degree of xanthogranulomatous involvement was correlated to the severity of the acute inflammatory affection as evidenced by the clinical findings and the urographical excretory function. The topography of the xanthogranulomas was related to the level of urinary tract obstruction in accordance with the pattern of reaction common to obstructive pyelonephritis. Haemorrhage and considerable fibrous thickening and stenosis of arteries surrounding the xanthogranulomatous foci were conspicuous features. Based upon a morphological staging it was shown that the structural changes (towards fibrosis) were paralleled by a series of cellular events indicating removal of intracellular lipids in xanthoma cells by transformation to lipofuscin and transport in PAS-positive interstitial macrophages. This was comparable to the findings in experimental XP suggesting a similar and simple way of pathogenesis. It is concluded that XP - with the possible exception of the tumorous variety - can be ascribed to local resorption phenomena caused by concurrent factors usually involved in pyelonephritis urinary tract obstruction being the essential precondition focal haemorrhage and ischaemia contributory elements.

Key words: pyelonephritis xanthogranulomatous clinicopathological study pathogenesis

J C F Møller Patologisk Anatomisk Institut, Kommunehospitalet, DK 8000 Århus, Denmark

Accepted as submitted 9 x 79

The term xanthogranulomatous pyelonephritis (XP) denotes a morphological sub-type of pyelonephritis which is characterized by the presence of yellowish nodules and pericalyceal streaks of granulation tissue the essential feature of which is lipid laden macrophages. In spite of the unusual and often impressive appearance which may cause confusion with renal carcinoma (Selzer *et al* 1957) it appears from both casuistic reports and large retrospective series (Gingell *et al* 1973 Gammill *et al* 1975 Malek & Elder 1978) that the clinical findings and the pre-disposing factors are not fundamentally different from those of suppurative nephritis in general. The mechanisms involved in the xanthogranulomatous reaction are not known in detail but prolonged suppuration in addition to

urinary tract obstruction have been suggested as the most likely causal factors (Selzer *et al* 1957, Friedenberg & Spjut 1963).

The present work was undertaken in order to further investigate the basis for the xanthogranulomatous reaction by 1) correlating clinical and pathological findings and 2) comparing the morphological changes in the xanthogranulomas with studies in experimental models (Povysil & Konickova 1972).

MATERIALS AND METHODS

Nineteen cases representing one autopsy and eighteen nephrectomy specimens were studied. Thirteen of these had been previously diagnosed and recorded at six institutes of pathology. An additional six cases were

characteristic feature of different metabolic bone diseases and that observed changes in the mean width of osteoid seams may be explained by variations in the appositional rate of osteoid and in the mineralization lag time

REFERENCES

- Arnott H J & Paulard F G E Osteoblast function and fine structure *Israel J Med Sci* 3 657-670 1967
- Baylink D Stauffer M Wergedal J & Rich C Formation mineralization and resorption of bone in vitamin D deficient rats *J Clin Invest* 49 1122-1134 1970
- Bonucci E The locus of initial calcification in cartilage and bone *Clin Orthop* 78 108-139 1971
- Bordur P Matrajt H Miravet L & Hicco D Mesure histologique de la masse et de la resorption des travees osseuses *Path Biol* 12 1238-1243 1964
- Christensen M S A sensitive radioimmunoassay of parathyroid hormone in human serum using a specific extraction procedure *Scand J Clin Lab Invest* 36 313-322 1976
- Frost H M Tetracycline labelling and the zone of demarcation of osteoid seams *Canad J Biochem Physiol* 40 485-489 1962
- Frost H M Tetracycline based histological analysis of bone remodelling *Calc Tiss Res* 3 211-237 1969
- Frost H M A method of analysis of trabecular bone dynamics In Meunier P J Bone Histomorphometry ed Societe de la Nouvelle Imprimerie Fournie Toulouse France 1977 pp 445-476
- Jubin W Haussler M R McCain T A & Tolman K Plasma 1,25 dihydroxyvitamin D levels in patients receiving anticonvulsant drugs *J Clin Endocrinol Metab* 44 617-621 1977
- Lacroix P Recherche sur le remaniement interne des os *Arch Biol (Liege)* 81 275-304 1970
- Lips P Coupré P & Meunier P Mean wall thickness of trabecular bone packets in human iliac crest Changes with age *Calcif Tiss Res* 26 13-17 1978
- Lund B Christensen M S Hey H Lund B Norman A W & Sorensen O H Bone mineral content and vitamin D metabolites in patients treated with jejunoileal bypass for obesity *Calcif Tiss Res* 27S 96 1979
- Matrajt H Bordier P & Hicco D Mesures histologiques semi-quantitatives dans 17 observations d'osteomalacies nutritionnelles et renales In D. Hicco ed Influence de la Vitamin D Masson et Co Paris 1967
- Melsen F Mosekilde L & Christensen M S Interrelationships between bone histomorphometry, SiPTH and calcium phosphorus metabolism in primary hyperparathyroidism *Calcif Tiss Res* 24 16 1977
- Melsen F & Mosekilde L Tetracycline double label in iliac trabecular bone in 41 normal adults *Calcif Tiss Res* 26 99-102 1978
- Melsen F Melsen B Mosekilde L & Bergmann S Histomorphometric analysis of normal bone from the iliac crest *Acta Pathol Microbiol Scand Sect A* 86 70-81 1978
- Meunier P J Bresson C & Edouard C Dynamics of bone remodeling in primary hyperparathyroidism In Copp D H Talmage R V ed Excerpta Medica Amsterdam Oxford 1978 p 415
- Milch R A Rall D P & Tobie J E Fluorescence of tetracycline antibiotics in bone *J Bone Joint Surg* 40A 897-910 1958
- Mosekilde L & Christensen M S Decreased parathyroid function in hyperthyroidism Interrelationships between serum parathyroid hormone, calcium, phosphorus metabolism and thyroid function *Acta Endocr* 84 566-575 1977
- Mosekilde L & Melsen F Anticonvulsant osteomalacia determined by quantitative analyses of bone changes Population study and possible risk factors *Acta med Scand* 199 349-355 1976
- Mosekilde L Melsen F Christensen M S Lund B & Sorensen O H Effect of long term vitamin D₂ treatment on bone morphometry and biochemical values in anticonvulsant osteomalacia *Acta med Scand* 201 303-307 1977
- Schulz A & Dellng G Zur Histomorphologie und Morphometrie der Rachitis und ihrer Sonderformen *Vehr Dtsch Ges Pathol* 58 354-361 1974

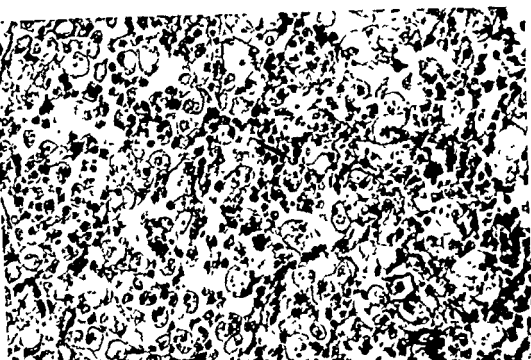


Fig 1 Early xanthogranulomatous reaction (stage I) Large vacuolated and granulated xanthoma cells mixed with polymorphonuclear leucocytes

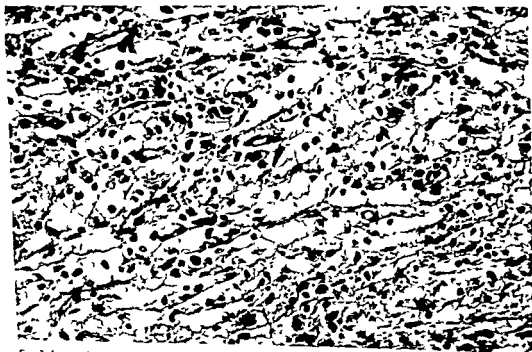


Fig 2 Intermediate xanthogranulomatous reaction (stage III) Sheets of xanthoma cells among slender capillaries. Rather few inflammatory cells

collected prospectively representing 5.4 per cent of all nephrectomies performed during one year

The extent of xanthogranulomatous involvement was macroscopically graded according to the following criteria

- I Slight degree of involvement focal changes in the perilymphatic renal tissue
- II Moderate degree of involvement diffuse perilymphatic changes (i.e. limited to the renal medulla)
- III Severe degree of involvement changes involving the whole kidney

Paraffin sections were stained with haematoxylin-eosin, van Gieson, PAS, Perl's, Prussian blue and Ziehl-Neelsen modified for staining of lipofuscin

For comparison with experimentally produced XP a morphological staging was done based upon the well known pattern of inflammatory reactions in general and upon the presumed dynamics of human XP in particular (Tonelli & Gianotti 1969; Putschar 1934)

Stage I maximal necrosis and granulocytic infiltration. Xanthoma cells loosely arranged (Fig. 1)

Stage II xanthoma cells organized in more solid formations along capillaries. Sporadic necroses

Stage III xanthoma cells closely packed in a well vascularized stroma (Fig. 2)

Stage IV decrease and splitting up of xanthoma cells due to fibrosis (Fig. 3)

In each stage the staining reaction for PAS positive substances, lipofuscin and iron was given a score from 0 to +++ 0 representing no or doubtful positive reaction, +++ maximal reaction

RESULTS

Clinical observations Relevant data are recorded in Table 1. There was a slight female preponderance (11 ♀/8 ♂) and a mean age of 56 years at the time of nephrectomy.

Eight patients had no previous symptoms of urinary tract disease and nephrectomy was performed after a relatively short period of acute illness with septic fever and flank pain. In 9 patients nephrectomy was preceded by several years' urinary tract disease and signs of acute pyelonephritis were present in only half of the cases.

Three patients had or developed malignancy of the urogenital tract (carcinoma of the cervix, uterine (1), carcinoma of the bladder (1) and carcinoma of the ureter (1)). One patient developed XP in relation to pregnancy and one patient was diabetic.

TABLE 1 *Xanthogranulomatous Pyelonephritis: Clinical Summary*

Case no	Age (years)	Sex	Chronic urological disease	Acute disease (duration)	Obstructive lesion	Bacteriological findings (urine)
I	73	M	+	6 weeks	Ureteral stone	Unknown
II	64	M	-	3 months	Ureteral stone	Gram - rods
III	55	F	+	-	Pelvic stone	Gram - rods
IV	72	M	+	-	Carcinoma of the bladder	Gram + rods
V	58	F	+	-	Pelvic stone	Proteus
VI	81	M	-	5 weeks	Pelvic stones	Proteus/E. coli
VII	30	M	-	4 weeks	-	Gram + cocci
VIII	70	M	+	-	Pelvic stone	Gram - rods
IX	22	F	-	4 months	Pelvic stone	Unknown
X	79	F	-	2 weeks	Pelvic stone	Unknown
XI	69	F	?	?	Ureteral stone	Unknown
XII	61	F	-	4 weeks	Ureteral stone	E. coli
XIII	40	M	-	4 months	Aberrant vessel	Unknown
XIV	8	F	+	4 weeks	Uretero-pelvic stenosis	E. coli
XV	67	F	+	3 months	Pelvic stone	E. coli
XVI	65	F	+	3 months	Pelvic stone	E. coli
XVII	57	F	?	?	Ureteral carcinoma	E. coli
XVIII		F	+	-	Pelvic stones	E. coli
XIX	26	M	-	4 weeks	Pelvic stone	Gram - rods



Fig 4



Fig 5

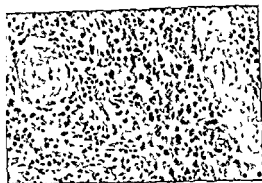


Fig 6



Fig 7

Fig 4 Part of kidney with typical pericalyceal xanthogranulomatous changes. Note haemorrhage in relation to xanthogranulomatous foci

Fig 5 Focal 'tumefactive' type of XP

Fig 6 Marginal xanthogranulomatous area with accumulation of macrophages giving the red brown PVS reaction of lipofuscin

Fig 7 Section of xanthogranuloma with areas of haemorrhage and conspicuous amounts of haemosiderin in xanthoma cells and other macrophages (Perl's Prussian blue)

in staining intensity between central and marginal areas

The various staining reactions as correlated to stage are illustrated in Fig 8

Clinico pathological relations From Table 2 it appears that in 3 groups of patients differing as to clinical course in most cases the presence of the acute phase was correlated to a high degree of xanthogranulomatous involvement and vice versa. No correlation was found between the clinical course (the duration from onset of clinical symptoms to nephrectomy in particular) and the microscopic stage of xanthogranulomatous change.

Seventy five per cent of kidneys with moderate and severe degree of xanthogranulomatous involve

TABLE 2 Quantitative Xanthogranulomatous Changes in Relation to Clinical Course of Urological Disease

	Macroscopic degree of renal involvement		
	I	II	III
Acute disease only (< 1/2 year) (8)	0	3	5
Chronic disease with acute phase (4)	0	1	3
Chronic disease without acute phase (5)	3	1	1
Unknown clinical course (2)	1	0	1

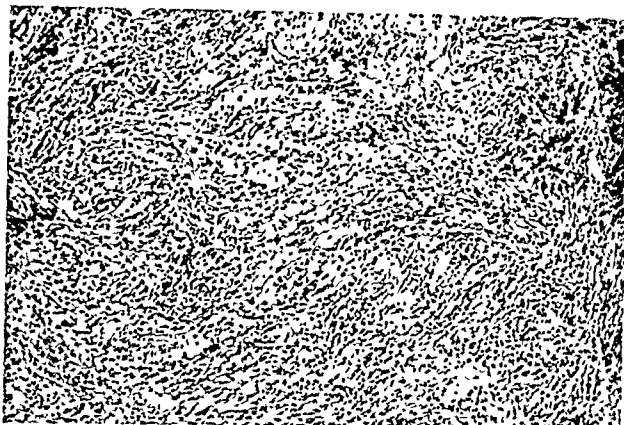


Fig. 3. Advanced xanthogranulomatous reaction (stage IV). Scattered xanthoma cells in a fibrillary stroma.

Bacteriuria was present in the majority of cases and *E. coli* was the organism most frequently isolated. Significant bacteriuria ($> 1 \times 10^5$ colonies/ml) however, was present only in a minor part of the series. Urinary tract obstruction was demonstrable in all cases but one. This was usually due to pelvic and ureteral stones (74 per cent).

An excretory urogram (IVP) was obtained in only 8 cases since 11 kidneys showed no function.

On account of the radiological findings renal tumour was suspected in 6 cases.

Pathological findings. Typically the xanthogranulomatous kidney was enlarged. 17 cases presenting varying degrees of pyonephrosis. The xanthogranulomatous changes varied from focal festoon-like yellowish streaks or easily missed small nodules in the pericalyceal renal tissue to more generalized lesions. Hemorrhage in relation to the xanthogranulomatous foci was a conspicuous feature of several cases (Fig. 4).

One case (no. VII) represented the localized tumorous form of XP (Fig. 5).

Microscopic examination of renal tissue adjoining the xanthogranulomatous foci showed signs of acute and chronic interstitial nephritis in all cases. There was an obvious predilection of the xanthogranulomas to segments with the most severe inflammation — especially in relation to the pelvic fornices and renal papillae.

Varying and at times pronounced degrees of luminal narrowing due to intimal thickening and fibrosis were observed in arteries situated at the periphery of the xanthogranulomas. Venous changes or thromboses were not seen.

The xanthogranulomas showed only slight mutual structural variation which made a morphological staging of the individual case possible.

Initially (stage I) the xanthoma cells appeared vacuolated and contained mostly small PAS-positive granules and partly degraded cellular elements (mainly polymorphonuclear leucocytes). Later (stage III) the PAS-positivity and the phagocytized elements disappeared, and the cytoplasm appeared more homogeneous (compare Fig. 1 and 2).

Macrophages differing from typical xanthoma cells due to a slightly smaller size, absence of cytoplasmic vacuoles and a more pronounced PAS-positive reaction were observed sporadically at stage I and mainly in the central xanthogranulomatous area. These cells made up a more conspicuous feature of stage II. At stage III macrophages of a similar type appeared in clusters at the periphery of the xanthogranulomas and showed the staining reaction of lipofuscin (Fig. 6).

In some cases striking amounts of haemosiderin were present in both xanthoma cells and smaller macrophages (Fig. 7) often with a zonal difference.

(Hooper *et al* 1962) This is in accordance with the pattern of inflammatory reaction in both human and experimental pyelonephritis (Heptinstall 1969) In this connection the tumorous or localized form of XP presents a special problem since urinary tract obstruction seems to be the exception rather than the rule in these cases (Selzer *et al* 1957 Noyes & Palubinskas 1969) Microscopically nothing indicates a morphogenesis basically different from that of the diffuse form and theoretically some sort of intrarenal obstruction might be at work This could not however be substantiated from the present study

In three cases with staghorn pelvic calculi (cases no III V and XVIII) nephrostomy with drainage of pus was done prior to nephrectomy This might explain the disproportionately slight xanthogranulomatous reaction in these cases indirectly pointing to the possible significance of varying degrees of urinary tract obstruction to the quantitative xanthogranulomatous response

Vascular changes mostly in the form of intimal and medial thickening have been observed in a number of cases (Tonelli & Gianotti 1969 Hooper *et al* 1962 Clay *et al* 1969 Schopfer 1967) The possible significance of ischaemic necrosis has been emphasized by Habib *et al* (1968) in a paper dealing with 4 paediatric cases characterized by an almost selective affection of the renal papillae This would be in agreement with both experimental and clinical observations that increased intrapelvic pressure (due to urinary tract obstruction) and narrowing of vessels (in relation to chronic pyelonephritis or diabetes) seem to favour the development of papillary necroses (Sheehan & Davis 1969 Heptinstall 1974) This might explain the high incidence of diabetes mellitus in some series (Gammill *et al* 1975) Papillary necrosis however is probably not the trigger mechanism of xanthogranuloma formation since XP so far has not been described in relation to so-called analgesic nephropathy

matory changes in the kidney Consequently it seems justified to believe that the pathogenic mechanisms are similar and rather simple ones with emphasis on urinary tract obstruction This is further illustrated by the findings of Tan & Heptinstall (1969) who under similar experimental conditions using however temporary occlusion of ureter found an inflammatory reaction with a corresponding time-correlated change in quantity and staining reactions of PAS positive interstitial cells but no formation of typical xanthomatous foci

Ultrastructural investigations have given some evidence that the PAS positive interstitial cells are in some way linked with (ineffective?) bacterial break-down (Tan & Heptinstall 1969) As to the xanthoma cells these are not specific to XP but may be present anywhere inflammation and obstruction coexists - 'obstructive pneumonia' being the classical example The origin of the fatty substance is disputed Cholesterol esters which make up part of the lipids (Saeed & Fine 1963) might derive from lysis of erythrocytes in relation to haemorrhage which applies to the macroscopic appearance and the presence of great amounts of haemosiderin in some cases of the present series

Provided the xanthoma cell and the PAS-positive interstitial cell represent different functional states of the same cell the series of events in the established xanthogranuloma can be explained simply in terms of a normal macrophage response with transformation of intracellular lipids to lipofuscin (Povysil & Konickova 1972 Tan & Heptinstall 1969)

In conclusion it seems obvious to consider the xanthogranulomatous reaction a post inflammatory resorption phenomenon representing a possible stage in the course of suppurative nephritis (Tonelli & Gianotti 1969) As to pathogenesis both the present and previous clinical observations in addition to experimental findings point to factors which may increase locally the need for or interfere with disposal of inflammatory waste products As far as urinary tract obstruction haemorrhage in the renal pelvis and focal renal ischaemia represent common denominators in ascending inflammatory kidney disease one might consider the xanthogranulomatous reaction a matter of concurrence and varying degrees of these factors Considering this and the various morphological expressions of the 'disease' and its temporary character (as indicated by both the present observations and the fact that XP is a very rare autopsy finding) it is not surprising to find overt xanthogranulomatous changes only in a minor part of cases of suppurative nephritis

the time-correlated structural transformation was accompanied by a series of cellular changes indicating no permanent data

experimental findings and the present observations strongly suggests that they are of basically identical character the only difference being a more constant presence and irregular distribution of PAS positive cells This might be due to differences in respect to route of infection or preexistent inflam

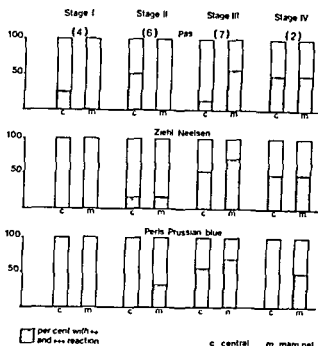


Fig 8 Semiquantitatively estimated staining reactions in central and marginal areas of xanthogranulomas as correlated to morphological stage

ment showed no function on excretory urography, the excretory function being largely inversely proportional to the degree of xanthogranulomatous affection

The type and degree of xanthogranulomatous reaction was found to some extent correlated to the level of urinary tract obstruction, obstructions distal to the renal pelvis being associated with more generalized xanthogranulomatous changes as compared with obstructions above the ureteropelvic junction (Table 3)

TABLE 3 Quantitative Xanthogranulomatous Changes in Relation to Type and Level of Urinary Tract Obstruction

	Macroscopic degree of renal involvement		
	I	II	III
Pelvic stone(s) (9)	3	4	2
Uretero pelvic stenosis			
aberrant vessel (2)	0	0	2
Ureteral stone			
ureteral carcinoma (6)	1	1	4
Carcinoma of the urinary bladder (1)	0	0	1
No obstructive lesion demonstrated (1)	0	0	1*

* Tumorous form of XP

In one case (no XVIII) partial resection of kidney was followed half a year later by nephrectomy. In the resected part obvious xanthogranulomatous changes were present. In the nephrectomy specimen however, no such changes could be demonstrated.

DISCUSSION

In spite of an increasing number of reports on xanthogranulomatous pyelonephritis it is still considered a rare affection (Chutkara & Singh 1976). The frequency reported varies considerably depending on the type of material investigated. Thus in a series of 3000 consecutive biopsies with chronic pyelonephritis Malek *et al* (1972) found xanthogranulomatous changes in only six per thousand. Concerning pyonephrosis Watt & Roylance (1971) in a series of 40 cases found XP in almost 25 per cent. The fact that one third of the present series (6 cases) was diagnosed prospectively during a relatively short period indicates that the frequency of XP to some degree depends on the attention paid to it. This too, is illustrated by the series reported by Hooper *et al* (1962).

The clinical appearance, age and sex distribution and bacteriological findings as well as the association of single cases with diabetes, pregnancy and obstructive malignant lesions of the urogenital tract are in line with previous observations (Malek & Elder 1978, Hooper *et al* 1962, Friedenberg & Spjut 1963) and point to a common aetiological and pathogenic basis for XP and pyelonephritis in general.

The close connection with pyonephrosis or suppurative nephritis suggests that the xanthogranulomatous reaction is a sequel to local necrosis and abscess formation. This is further supported by the observed concordance between different degrees of xanthogranulomatous involvement and the severity of inflammatory kidney disease as indicated by clinical and radiological findings. The lack of correlation between the microscopic stage of xanthogranulomatous change and the duration of the clinically acute stage however indicates that the xanthogranulomatous reaction is probably not a direct consequence of tissue break-down but to some extent depends on additional factors.

Calculi predominantly of the staghorn type represent a potent obstructive factor in a high percentage of cases (Chutkara & Singh 1976, Malek & Elder 1978) which is in agreement with the present findings. The observation that the xanthogranulomatous changes are to some extent topographically correlated to the level of calculous (and noncalculous) obstruction has been made by others

DISTRIBUTION OF ATHEROSCLEROSIS IN HUMAN DESCENDING THORACIC AORTA

A Morphometric Study

EINAR SVENDSEN and TOR J EIDE

Institute of Medical Biology University of Tromsø Norway

Svensen E & Eide T J Distribution of atherosclerosis in human descending thoracic aorta A morphometric study Acta path microbiol scand Sect A 88 97-101 1980

A morphometric study of 49 randomly selected human aortas is reported with regard to the distribution of atherosclerotic lesions in the descending thoracic aorta (DTA). The intercostal artery area (ICA area) revealed a higher degree of atherosclerosis compared with the remaining part of the DTA. The difference was more striking at overall lower grades of atherosclerosis of the DTA. The ventral aspect of the DTA in the proximal and caudal thirds showed a higher degree of atherosclerosis compared with the middle third. The atherosclerotic indices of the proximal and distal areas correlated significantly with increasing heart weights but not for the middle third. The explanation of this is presumably irregular flow conditions. For the distal part a possible effect of continuous pounding of an enlarged heart upon the ventral aspect of the descending thoracic aorta is discussed.

Key words: Atherosclerosis, thoracic aorta.

E Svendsen, Institute of Medical Biology, University of Tromsø, Box 977, 9001 Tromsø, Norway.

Received 25 v 79 Accepted 14 x 79

Experimentally induced atherosclerosis in the aorta has shown a focal occurrence (2, 21). The sites of occurrence correspond to sites with endothelial cell injury (27, 28, 29), increased permeability (16), increased platelet deposition (9, 11), as well as increased replication (32) and presumed flow disturbance (7, 10, 18, 26). In the literature there are indications that also in the human aorta certain areas are more susceptible to atherosclerotic development (1, 3, 4, 12, 20, 23). Fatty streaks occur early in the proximity of intercostal artery orifices (23). It is widely accepted that raised blood pressure increases atherosclerotic development and heart weight. Alteration of the flow situation may occur (5, 13, 14), and the enlarged heart gets a closer relation to the ventral aspect of the aorta. As all the experimentally recorded phenomena have been demonstrated in the descending thoracic aorta (DTA), a more detailed morphometric study of the atherosclerosis in human DTA seemed appropriate.

The following questions were asked:

1. Are there differences in the occurrence of atherosclerotic lesions in the intercostal artery area (ICA area) versus the remaining part of the DTA? If so, are the differences consistent at different overall degrees of atherosclerosis in the DTA?
2. How is the distribution of atherosclerosis in the non intercostal artery area? Does the heart weight influence this distribution?

MATERIAL AND METHODS

Forty nine aortas, all from males, were randomly selected from autopsies at the Department of Pathology.

The aortas were pinned out on a cork board and fixed in 4% buffered formalin. The aortas were slightly dried, photographed (dias) and subjected to a

The authors are indebted to the chief pathologists at the departments of pathology at Skive Sygehus Vejle Sygehus Sønderborg Sygehus and Aarhus County Hospital for placing specimens at our disposal

REFERENCES

- Chitkara, Y A & Singh A Xanthogranulomatous pyelonephritis *Int Surg* 61 357-360, 1976
- Clay, A, Dupont A Houcke, M, Gosselin B & Delobelle-Deroide, A Les nephrites xantho granulomateuses Etude anatomique de 15 observations *Lille med* 14 577-583, 1969
- Friedenberg, M J & Spjut, H J Xanthogranulomatous pyelonephritis *Am J Roentgenol Radium Ther Nucl Med* 90 97-108, 1963
- Gammill, S, Rabinowitz, J G Peace, R, Sorgen S, Hurwitz L & Himmelfarb E New thoughts concerning xanthogranulomatous pyelonephritis *Am J Roentgenol Radium Ther Nucl Med* 125 154-163 1975
- Gingell J C, Roylance, J Davies R & Penny J B Xanthogranulomatous pyelonephritis *Brit J Radiol* 46 99-109, 1973
- Habib R, Levy M & Royer P La Pyelonephrite chronique xanthogranulomateuse chez l'enfant *Arch Franc Ped* 25 489-510 1968
- Heptinstall R H The enigma of chronic pyelonephritis *J Infect Dis* 120 104-107 1969
- Heptinstall R H Pathology of the kidney 2nd ed vol 1 Little Brown and Company Boston 1974 pp 247-257
- Hooper R G Kempson R L & Schlegel J U Xanthogranulomatous pyelonephritis *J Urol* 88 585-593 1962
- Malek, R S, Greene, L F, De Weerd J H & Farrow G M Xanthogranulomatous pyelonephritis *Brit J Urol* 44 296-308, 1972
- Malek, R S & Elder, J S Xanthogranulomatous pyelonephritis A critical analysis of 26 cases and of the literature *J Urol* 119 589-593 1978
- Noves W E & Palubinskas A J Xanthogranulomatous pyelonephritis *J Urol* 101 132-136 1969
- Povysil C & Konickova L Experimental xanthogranulomatous pyelonephritis *Invest Urol* 9 313-318 1972
- Putschar, W Die entzündlichen Erkrankungen der ableitenden Harnwege und der Nierenhüllen einschließlich der Pyelonephritis und der Pyonephrose In Lubarsch O & Henke, F Handbuch der speziellen pathologischen Anatomie und Histologie 1st ed vol 6 J Springer Verlag Berlin 1934 pp 333-564
- Saeed S M & Fine G Xanthogranulomatous pyelonephritis *Am J Clin Path* 39 616-625 1963
- Schopfer, P Lesions veineuses dans la pyelonephrite xanthogranulomateuse *Urol Int* 22 68-83 1967
- Selzer, D W, Dahlin D C & De Weerd J H Tumefactive xanthogranulomatous pyelonephritis *Surgery* 42 874-883 1957
- Sheehan H L & Davis J C Experimental hydronephrosis *Arch Path* 68 185-225 1959
- Tan H K & Heptinstall H Experimental pyelonephritis A light and electron microscopic study of the periodic acid-Schiff positive interstitial cell *Lab Invest* 29 62-69, 1969
- Tonelli S & Gianotti P On the nature of xanthogranulomatous pyelonephritis *Urol Int* 24 330-343 1969
- Watt I & Roylance J Pyonephrosis *Clin Radiol* 27 513-519 1975

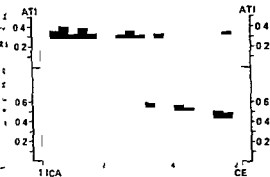


Fig 3 Graphical representation of the atherosclerotic lesions in the non ICA area of the DTA (uppermost diagram) and the ICA area (lower diagram) comprising all cases. Each of the twenty-one columns represent the mean atherosclerotic index at the actual level of the aorta. I ICA = first intercostal artery. CE = celiac trunk.

middle third however no significant correlation was found. In the same figure the mean atherosclerotic indices for each of the non ICA areas are estimated for four groups based on heart weights (200–299, 300–399, 400–499 and 500 grams and above). The most marked increase of atherosclerosis is observed between the first two groups in all three areas. In the group with heart weights above 500 grams there is further marked increase of atherosclerosis in the distal area. In the proximal and middle area however the increase is slight.

Table 1 shows the mean systolic pressure of the highest blood pressure encountered in the clinical journal of those with heart weight above and below 425 g. Mean pulse pressure, mean heart weight, mean age, the number of cases in each group as well as the atherosclerotic indices of the proximal, middle and distal thirds of the non ICA area of the DTA are given in the same table. The mean systolic pressure and the pulse pressure are somewhat higher in the group with heart weight above 425 g.

DISCUSSION

We present strong evidence that the ICA area is more prone to atherosclerosis than the remaining part of the DTA. This finding is in agreement with the work of Bhargava *et al.* (3). The difference is more striking in the groups with overall less atherosclerosis. This fact may indicate that the atherosclerotic process starts in the ICA area. Experimentally the ICA area is a site of increased permeability (16), platelet deposition (9, 11) and endothelial cell injury (27, 28, 29). Increased cell replication (32) and the inception of experimental

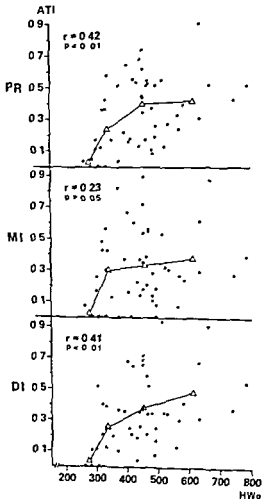


Fig 4 Diagram of the atherosclerotic extent in the cranial, middle and distal thirds of the non ICA area of the DTA plotted against the corresponding heart weights. The triangles represent mean atherosclerotic index within each of the four groups based on heart weights in gram (200–299, 300–399, 400–499, 500 and above). ATI = atherosclerotic index. HWg = heart weight in gram. r = correlation coefficient. PR, MI and DI as in Fig 1.

atherosclerosis are described in the same area (2, 15, 21, 22). According to most authors the particular flow conditions at the ICA area are of importance for the predominance in this area of all the mentioned phenomena.

In the non ICA-area of the DTA we found a higher degree of atherosclerosis in the proximal and distal thirds compared to the middle third. The degree of atherosclerosis in the non ICA area of the proximal and distal parts of the DTA was significantly correlated with the heart weight.

morphometric point-counting procedure in which each dias photograph was projected on a screen with regularly arranged points

The reliability of the morphometric method had been controlled in a study comprising 22 aortas. Intra- and inter observer comparisons showed a high reproducibility by using statistical tests. The correlation coefficient ranged from 0.96 to 0.98 in both inter- and intra observer comparisons. The standard deviation of the random measurements error expressed in per cent of the mean value of the replicate measurements ranged from 8 to 12 per cent, and the slope of the regression coefficient did not differ from unity by more than 0.045 in any of the comparisons (6).

By adjusting the distance from the dias-projector to the screen each DTA of all 49 aortas comprised a standardized number of 21 point-rows from the 1 intercostal artery orifices to the celiac trunk. All points falling upon fatty streaks, plaques and complicated lesions (ulcerations, hemorrhage, calcifications and mural thrombus) were counted as atherosclerotic lesions and mapped on graph paper together with points falling upon normal areas. The DTA was divided into three equal fields each comprising seven point-rows and was also divided into ICA-area and non intercostal artery area (non-ICA-area) as shown in Fig 1. The points falling closest lateral to the intercostal artery orifices and points falling at the dorsal wall in between the intercostal

artery orifices were allotted to the ICA area. All other points falling upon the DTA were allotted to the non ICA-area which represented the lateral and ventral aspects of the DTA. A mean atherosclerotic index for the whole ICA-area and the whole non ICA-area was estimated. Also a mean atherosclerotic index for each of the 3 point-rows in the ICA-area and non ICA area of all 49 aortas was calculated. Furthermore mean atherosclerotic indices of the proximal, middle and caudal third of the non ICA-area of the DTA were estimated. A correlation analysis between the heart weights and atherosclerosis in each of the latter-mentioned areas was made.

RESULTS

In the descending thoracic aorta the ICA area showed consistently relatively more atherosclerosis than the non-ICA area. The difference between the two areas was greatest in the groups with low total atherosclerosis and less in the groups with high total atherosclerosis (Fig 2).

A mean atherosclerotic index based upon all 49 aortas for each of the 21 point-rows in the ICA area and non-ICA-area of the DTA was calculated. In the non-ICA-area more atherosclerotic lesions were found in the proximal and distal thirds compared with the middle third (Fig 3). In the same area caudal increase of atherosclerosis at the very beginning of the DTA and a decrease when approaching the celiac trunk was observed (Fig 3). In the ICA-area, however, the distribution had an opposite pattern (Fig 3).

Fig 4 shows the heart weights plotted against the respective atherosclerotic indices for the proximal, middle and distal thirds of the non-ICA-area of the DTA. In both the proximal and distal thirds there are statistically significant correlations between heart weight and degree of atherosclerosis. In the

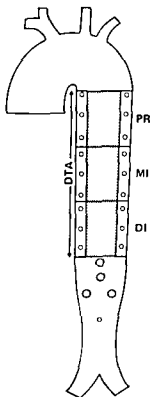


Fig 1 Schematic representation of the opened aorta. DTA = descending thoracic aorta, PR = proximal part of DTA, MI = middle part of DTA, DI = distal part of DTA. The hatched field represents the non ICA-area of the DTA, the unhatched field of the DTA the ICA area.

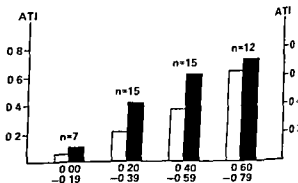


Fig 2 Extent of atherosclerotic lesions in the ICA area (filled bars) versus non ICA-area of the DTA (open bars). Four groups based on increasing overall atherosclerotic index of the DTA are arranged. The bars express mean values. ATI = atherosclerotic index.

- 4 Dalih F and Malko M Calcified plaques in the brachiocephalic arteries A concept of focal atherogenesis J Atheroscler Res 2 416-423 1962
- 5 F... R H Peters R J Cuddy R P Smulyan... and Lyons R H The hemodynamics in labile hypertension Amer Heart J 63 188-195 1962
- 6 ... T J and Svendsen E Unpublished observations
- 7 ... J A and Hugh A E Localization of ... roma A theory based on boundary layer ... of in ... iration Brit Heart J 28 388-399 1966
- 8 ... E D Tara i R C and Dustan H P ... I amination of the hemodynamics of hyperten ... Am J Med Sci 257 9-23 1969
- 9 Geissinger H D Mustard J F and Rowsell H C The occurrence of microthrombi on the aortic endothelium of swine Can Med Assoc J 87 405-408 1962
- 10 Gristein W H and Schneck D J In vitro boundary layer studies of blood flow in branched tubes J Atheroscler Res 7 295-299 1967
- 11 Jorgensen L Packham M A Rowsell H C and Mustard J F Deposition of formed elements of blood on the intima and signs of intimal injury in the aorta of rabbit pig and man Lab Invest 27 341-350 1972
- 12 Kneriem H J and Hueber R Quantitative morphologische Untersuchungen an der Aorta des Menschen Beitr path Anat 140 280-297 1970
- 13 Ledingham J M and Cohen R D Changes in the ...
- 14 Lund Johansen P Hemodynamics in early essential hypertension Acta med scand (Suppl 482) 101 pp 1967
- 15 Murphy E A Rowsell H C Downie H G Robinson G A and Mustard J F Encrustation and atherosclerosis The analogy between early in vivo lesions and deposits which occur in extracorporeal circulations Canad Med Ass J 87 259-274 1962
- 16 Packham M A Rowsell H C Jorgensen L and Mustard J F Localized protein accumulation in the wall of the aorta Exp Mol Path 7 214-232 1967
- 17 Palma E C Arteriosklerose hemodynamique Localisation et traitement chirurgical Chirurgie 102 756-768 1976
- 18 Pinchak A C and Ostrach S Blood flow in branching vessels J Appl Phys 41 646-658 1976
- 19 Ramirez E and Pont P H G Relation of arterial blood pressure to the transverse diameter of the heart in compensated hypertensive heart disease Circulation 31 542-550 1965
- 20 Rebel W Hoer P W Langhoff J and Loewe K R Planimetrische Untersuchung über die Ausbreitung der Atherosklerose Zeitschrift für Kreislaufforschung 61(6) 516-522 1971
- 21 Roach M Fletcher T and Cornhill J F The effect of the duration of cholesterol feeding on the development of sudanophilic lesions in the rabbit aorta Atherosclerosis 25 1-11 1976
- 22 Rowsell H C Downie H G and Mustard J F Comparison of the effect of egg yolk or butter on the development of atherosclerosis in swine Can Med Assoc 7 83 1175-1186 1960
- 23 Schwartz C J Ardlie N G Carter R F and Paterson J C Gross aortic sudanophilia and hemosiderin deposition Arch Path 83 325-332 1967
- 24 Solberg L A and Eggen D A Localization and sequence of development of atherosclerotic lesions in the carotid and vertebral arteries Circulation 43 711-724 1971
- 25 Stephenson Jr S E Mann G V Younger A B R and Scott H W Factors influencing the segmental deposition of atheromatous material Archives of Surgery 84 49-55 1961
- 26 Svendsen E and Jorgensen L Intimal pits of aorta in rabbits Imprints of vortices of blood flow Acta path microbiol scand Sect A 85 25-32 1977
- 27 Svendsen E and Jorgensen L Focal spontaneous alterations and loss of endothelial cells in rabbit aorta Acta path microbiol scand Sect A 86 1-13 1978
- 28 Svendsen E Focal endothelial cell injury in rabbit aorta aggravation of injury by 2 days of cholesterol feeding Acta path microbiol scand Sect. A 87 123-130 1979
- 29 Svendsen E and Jorgensen L Loss of endothelial cells in rabbit aorta following short term cholesterol feeding IV International Symposium on Atherosclerosis Aug 24-28 1976 Tokyo Japan
- 30 Weiss S Haynes F W and Shore R The relation of arterial pulse pressure to the hemodynamic of arterial hypertension Amer Heart J 11 402-415 1936
- 31 Wiggers C J The dynamics of hypertension Amer Heart J 16 515-543 1938
- 32 Wright H P Mitosis pattern in aortic endothelium Atherosclerosis 15 93-100 1972

TABLE 1 *Clinical Parameters, Mean Heart Weights as well as Atherosclerotic Indices of the Non-Intercostal Artery Area of the Descending Thoracic Aorta in Groups with Heart Weight above and below 425 g*

		Heart weight \geq 425 g	Heart weight < 425 g
Number		29	20
Mean age (years)		68.2	64.4
Mean heart weight (g)		518	340
Mean systolic BP (mmHg)		167.6	150.5
Mean PP (mmHg)		66.8	62.3
Mean ATI of non-intercostal artery area of the descending thoracic aorta	Proximal third	0.41	0.22
	Middle third	0.34	0.27
	Distal third	0.40	0.27

BP = blood pressure PP = pulse pressure ATI = atherosclerotic index

Kmeriem & Hueber (12) found a diffuse, in some cases, patchy thickening of the aortic intima, especially of the distal thoracic aorta, with increasing age, and the weight of the aorta increased with increasing heart weight.

The preponderance of atherosclerosis in the proximal third of the non-ICA-area compared to the middle third of the DTA may be explained by the occurrence of boundary layer separation with vortices. This area blends with the lesser curvature of the aortic arch where this type of flow disturbance is supposed to occur (7, 10, 15, 26). Hypertension may leave the cardiac output unaltered (8). Labile hypertension, however, is attended by increased cardiac output (5, 14). Further reduced distensibility of large arteries (19, 31) and increased pulse wave velocity (32) may occur in hypertension. Thus, raised blood pressure may produce a more intensive flow disturbance in the distal area of the lesser curvature of the aortic arch.

The preponderance of atherosclerosis in the distal third compared with the middle third of the non-ICA-area of the DTA may also have a similar explanation. This site, however, has hitherto not been suspected to have more flow disturbance than the middle third. Hydrostatic pressure may play a role. The fact, however, that the atherosclerotic process decreases when approaching the celiac trunk may be an argument against this assumption. If we can take it for granted that the hearts with more than normal weight have a larger than normal size, an alternative explanation may be that the increased presence of atherosclerosis in the non-ICA-area of the distal third of the DTA is a direct effect of the enlarged heart. The enlarged heart is located closer to the ventral aspect of the aorta. It is possible that

the beats of an enlarged heart may pound against the aorta to a greater extent than normal and thus affect the aorta. This explanation is in accordance with Solberg & Eggen (24) as well as Palma (17); Stephanson *et al.* (25) who put forward a hypothesis that atherosclerosis may occur as a result of mechanical influence on the vessel wall from outside.

In conclusion, this work has shown a consistent predominance of atherosclerosis in the ICA as versus the non-ICA-area of the DTA at all degrees of atherosclerosis.

This predominance is more pronounced in patients with a small or moderate overall degree of atherosclerosis of the DTA.

Atherosclerosis is more prevalent in the upper and lower thirds of the non-ICA-area of the DTA compared with the middle third. The two former mentioned areas in contrast with the latter correlate significantly with increasing heart weight.

We owe our gratitude to Prof. L. Jørgensen and Dr. L. Solberg for professional criticism, Dr. Alex Tindall for reading, and Mrs. Dagny Madsen Fauske for typing the manuscript.

REFERENCES

1. Al-Hashimi A S and Williams G. A morphometric method for assessment of atherosclerotic lesions. *Atherosclerosis* 14: 401-409, 1971.
2. Antischlow N. Über die Atherosklerose der Aorta beim Kaninchen und über deren Entstehungsbedingungen. *Beitr. z. Path.* 59: 306-349, 1914.
3. Bhagwat, A. G., and Robertson A. L. Distribution and severity of atherosclerotic lesions in the human thoracic aorta. *Angiology* 24: 181-190, 1973.

IMMUNOCYTOCHEMICAL DEMONSTRATION OF ENKEPHALIN AND β -ENDORPHIN IN ENDOCRINE TUMORS OF THE RECTUM

A Survey of 27 Colo Rectal Carcinoids

J ALUMETS S FALKMER L GRIMELIUS R HÅKANSON O LJUNGBERG
F SUNDLER and E WILANDER

Departments of Histology Pathology (in Malmö) and Pharmacology University of Lund and the
Department of Pathology University of Uppsala Sweden

Alumets J Falkmer S Grimelius L Håkanson R Ljungberg O Sundler F & Wilander E
Immunocytochemical demonstration of enkephalin and β -endorphin in endocrine tumors of the rectum
A survey of 27 colo rectal carcinoids Acta path microbiol scand Sect. A 88 103-109 1980

In a histopathological and immunocytochemical study of biopsy and/or operation specimens from 27 patients with endocrine tumors of the colon and rectum (hind gut carcinoids*) enkephalin immunoreactive tumor cells were observed in two cases. Both patients were obese women about 50 years of age with a history of constipation. The tumors were situated near the anus in the dorsal wall of the rectum. One tumor had metastasized to a lymph node and the other showed vascular invasion. The tumor cells were non-argyrophil, some were argyrophil. One tumor contained only few enkephalin immunoreactive cells but had numerous β -endorphin immunoreactive cells which were distinct from the former. The other contained large numbers of enkephalin immunoreactive cells but no β -endorphin cells. Both tumors also harboured glucagon immunoreactive cells in one there were also cells containing immunoreactive pancreatic polypeptide. These cells were distinct from the enkephalin-storing ones. No 5-hydroxytryptamine could be detected in the two tumors.

Key words: Rectal carcinoid, mixed endocrine tumor, enkephalin, β -endorphin, immunocytochemistry.

Sture Falkmer, Professor and Chairman, Department of Pathology, University of Lund, Malmö General Hospital, S-214 01 Malmö, Sweden.

Accepted as submitted 16 x 79

The pentapeptide enkephalin, first isolated from brain tissue by virtue of its potent opiate receptor agonist activity (1) occurs in two varieties, one having leucine (leu-enkephalin) the other methionine (met-enkephalin) in COOH terminal position (1). By immunocytochemistry, enkephalin-like material has been demonstrated in nerve fibres and nerve cell bodies of the gut wall and in endocrine cells of the antrum and duodenum (2, 3). The endocrine cells demonstrated with antiserum against leu-enkephalin were found to be of the 5-hydroxytryptamine (5-HT)-containing type (3). Enkephalin immunoreactive cells have recently been demonstrated also in the exocrine parenchyma of pig pancreas (4) and in some bronchial endocrine

tumors (5). Another endogenous opioid peptide is β -endorphin, which occurs in high concentrations in the pituitary gland, including pituitary adenomas (6). So far, β -endorphin has not been found in peripheral tumors.

The findings of immunoreactive enkephalin in gut endocrine cells and in bronchial carcinoids prompted a search for enkephalin in endocrine tumors of the digestive tract. We started by examining 27 cases of colo-rectal carcinoids*. In all two cases were found. They form the basis of the present report.

* The term "carcinoid" is used here to mean primary endocrine tumors of the digestive tract, irrespective of the presence or absence of 5-HT (7).



Fig 1 Case No 1 Low and medium power photomicrographs of hematoxylin-erythrosin stained sections of the rectal carcinoid and adjacent mucosal crypts showing nests and trabecules of small regular epithelial tumor cells growing in the basal part of lamina propria invading the submucosa (Fig 1A) and displaying the ribbon growth pattern typical of this kind of tumors (Fig 1B). By the PAP immunocytochemical procedure cells were found displaying β -endorphin immunoreactivity in the normal mucosa overlying the tumor (Fig 1C arrows) as well as in the tumor itself (not shown in the figure) whereas enkephalin immunoreactivity occurred in a few scattered tumor cells only (Fig 1D). X100X (A), X255X (B) and X300X (C and D).

MATERIAL AND METHODS

The material consisted of blocks of paraffin embedded specimens from hind gut carcinoids collected from 27 patients. Twelve of these tumors had previously been analyzed for the presence of cells containing glucagon and substance P like immunoreactivity (8). The specimens were either from extirpated tumors or from biopsy specimens; they were fixed in 10% formalin. For light microscopic analysis 4–6 µm thick sections were stained with haematoxylin eosin, van Gieson's stain, the periodic acid Schiff (PAS) reagent, the Masson Hamperl argentaffin technique (9, 10) as well as with the Grimelius argyrophil procedure (11).

Deparaffinized sections from all tumors were examined for enkephalin and β endorphin immunoreactive cells using the indirect immunofluorescence method (12) or the peroxidase anti peroxidase (PAP) procedure (13). Sections were thoroughly rinsed in buffer over night and incubated with the antiserum for 3 hrs at room temperature (immunofluorescence) or for 24 hrs at +4 °C (PAP procedure). The sections were washed repeatedly with phosphate buffered saline and the site of the antigen antibody reaction was revealed by incubation with fluoresceinated or non fluoresceinated anti rabbit IgG in dilution 1:20. In the PAP procedure the PAP complex was applied in dilution 1:320. Control sections were exposed to antiserum inactivated by the addition of antigen in excess (100 µg/ml). The tumors displaying

opioid peptide immunoreactivity were then analyzed histochemically for various other hormones and hormone candidates. Details of the antisera used are given in Table 1. Sections from these tumors were also examined for 5 HT. This amine condenses with formaldehyde yielding a fluorophore which is detectable upon excitation with UV light (365 nm) (32).

RESULTS

Two out of the 27 examined rectal carcinoids contained enkephalin immunoreactive cells (case 1 and 2 below). In addition one of the two (case 1) contained β endorphin immunoreactive cells.

Case No 1 Previously healthy obese 49 year-old woman was examined by rectoscopy because of pains in the sacral and anal regions. For several months she had suffered from constipation. A slightly protruding nodule about 1 cm in diameter was observed located on the dorsal wall 5–7 cm above the anus. An X-ray examination of the colon showed no other nodules, polyps or tumors. A biopsy specimen was taken. The histopathological examination (Umeå 25932/76) revealed a rectal carcinoid. About a month later an abdominal perineal extirpation of the rectum was made with a sigmoidectomy. About half the tumor remained in the extirpated rectum. It was a firm nodule with an

TABLE 1 Survey of Antisera Used

Antisera raised against	Code No	Working dilution		Source	Refer
		Immuno fluorescence	PAP staining		
Adrenocorticotrophic hormone (ACTH)		1:80	1:640	Own	14
β Endorphin	7763	1:20	1:240	Milab Malmö Sweden	15
Leu Enkephalin	170	1:60	1:240	K. J. Chang Burroughs Wellcome Research Triangle Park NC USA	3, 16
Gastric inhibitory peptide (GIP)	R D 11/19/77	1:80		T. O. Dorisio Ohio State University Columbus Ohio USA	17, 18
Gastrin (2-17)	4562	1:640	1:25000	J. F. Rehfeld Århus Univ Århus DK*)	19
Glucagon	4304 XII	1:80	1:2560	J. J. Holst Bispebjerg Hosp DK	20, 21
Human pancreatic polypeptide (HPP)		1:20		R. E. Chance Eli Lilly Indianapolis Indiana USA	22
Insulin	LA 1	1:80		L. Heding Novo Res Institute DK	
Motilin	MBR 616		1:640	N. Yanaihara Shizuoka Coll Pharm Jap	23
Neurotensin	HC 8	1:40	1:640	R. E. Carraway Harvard Med School USA	24, 25
Secretin	5585	1:80	1:2560	J. Fahrenkrug & O. B. Schaffalitzky de Muckadell Bispebjerg Hosp DK	26, 27
Somatostatin	19578	1:80	1:1280	M. P. Dubois Inst Nat Recherche Agriculture Nouzilly France	28, 29
Substance P	JK1	1:320		P. Emson Cambridge University GB	
Vasoactive intestinal polypeptide (VIP)	89 N		1:320	S. I. Said Dallas Tx USA	30, 31

DK Denmark

apparently intact overlying mucosa. Its cut surface was grey white and it grew mainly in the submucosa and the

constipation and no signs of the carcinoid syndrome when examined three years after the operation (in January 1980).

The tumor appeared well differentiated and was composed of small uniform polyhedral cells with unimorphic nuclei arranged in thin trabeculae which often were only one cell in thickness and which formed a marked whorled ribbon growth pattern (Fig. 1). There were no PAB positive cells. Mitoses were inconspicuous. A few cells displaying leu-enkephalin like immunoreactivity were found scattered in the tumor tissue. Fairly numerous tumor cells contained immunoreactive β -endorphin. Such cells were also found in the mucosa overlying the tumor. Many tumor cells also displayed moderate to intense glucagon immunoreactivity. No tumor cells showed formaldehyde induced fluorescence. The enkephalin immunoreactive cells were weakly argyrophil. No tumor cells were argentaffin. This tumor did not belong to the previously published series (8).

Case No. 2 The patient was a previously healthy obese 53 year-old woman suffering from constipation. Rectal palpation and rectoscopy revealed a large bulging tumor situated in the dorsal wall of the rectum just above the anal sphincter. The overlying mucosa was intact but the tumor appeared rather firmly attached to the coccyx. A biopsy specimen was taken. The microscopic examination suggested a poorly differentiated carcinoid. X ray examination of the colon and rectum revealed an expansive process between the rectum and the sacrum; there were no signs of additional tumors. A pre-operative high voltage X ray therapy of altogether 3000 rad. given for 3 weeks had no effect on the tumor mass. An abdomino-perineal rectum extirpation and colostomy was made. The tumor seemed to have invaded the periosteum of the sacrum but could be radically extirpated. The gross and microscopic examinations (Halmstad 3017/78) showed a large solid tumor just above the anus measuring $5 \times 10 \times 15$ cm with an intact rectal mucosa. The cut surface was pink with necrotic areas in the central parts. The tumor was encapsulated. The postoperative course was complicated by anuria requiring catheterization of the ureters by lateral nephrostomy and haemodialysis. At the latest follow up (Febr. 1980) almost two years after the operation the patient had no constipation and there were no signs of the carcinoid syndrome.

The tumor had a lobular architecture forming nodules of irregularly arranged and closely packed tumor cells surrounded by broad strands of connective tissue stroma. The cells displayed a marked anaplasia with irregular atypical nuclei showing coarse chromatin pattern with clump nucleoli and mitoses were frequent (Fig. 2). In some places there was a gradual transition towards a more differentiated tumor where a distinct ribbon growth pattern could be found which was quite similar

to that seen in the tumor in case No. 1. There were no PAS-positive tumor cells. The tumor had infiltrated through all layers of the bowel wall into the perirectal and perianal tissue and veins were also invaded. Certain areas contained numerous tumor cells displaying moderate to intense leu-enkephalin like immunoreactivity whereas other areas were devoid of such cells. No enkephalin immunoreactive cells were observed in the overlying mucosa. In addition many tumor cells were found to contain immunoreactive glucagon or HPP. Immunocytochemical staining of consecutive sections revealed that the enkephalin storing cells were distinct from these two cell types. No β -endorphin cells could be demonstrated. Most tumor cells were argyrophil none were argentaffin. No cells displayed yellow formaldehyde induced fluorescence indicating absence of 5 HT. Even this tumor was not included in the previously published series (8).

DISCUSSION

The two patients whose rectal carcinoid tumors contained enkephalin immunoreactive cells had the following features in common. They were both obese women about 50 years of age with a history of constipation. Both tumors were located near the anus in the dorsal wall of the rectum. The overlying mucosa was intact, but both tumors were obviously malignant in one case with a lymph node metastasis. Both tumors also contained well differentiated areas with the features of hind-gut carcinoids (7). In case No. 2 the major part of the

in
cells exhibiting
enkephalin like immunoreactivity have to the best of our knowledge not been described in endocrine tumors. Recently we have observed immunoreactive enkephalin in scattered cells of a pancreatic islet-cell tumor. This tumor contained also numerous vasoactive intestinal peptide (VIP) immunoreactive cells and was associated with watery diarrhoea. By personal communication we have been informed that enkephalin immunoreactive cells have been observed in a pancreatic endocrine tumor also by others (33).

Gastro-entero-pancreatic tumors often contain several different peptide hormone producing cell types. Nevertheless many such tumors are clinically »silent» and are often found incidentally at autopsy. Others give rise to clinical symptoms which as a rule reflect overproduction of only one such hormone (34). Although enkephalin inhibits gut neuronal activity and β -endorphin has been associated with overeating (35) we believe that the modest clinical symptoms displayed by the two

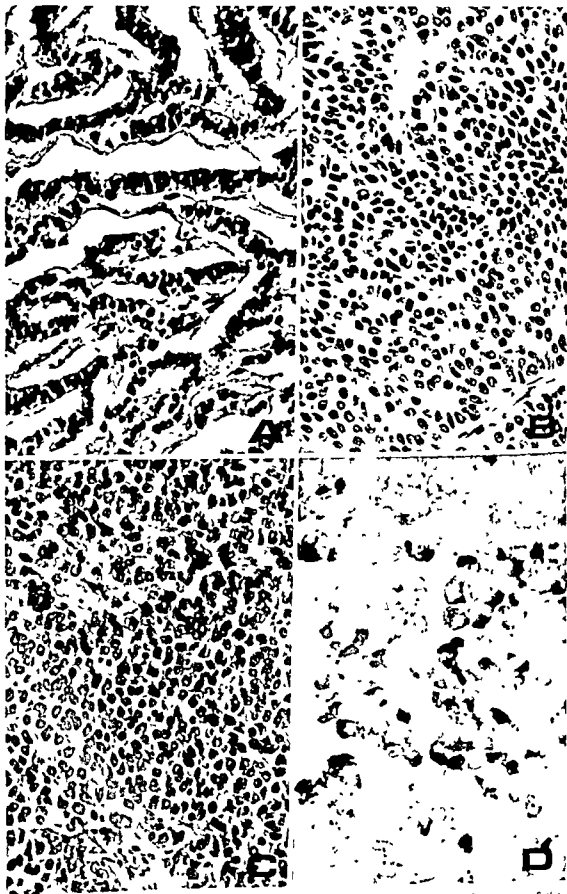


Fig 2 - Case No 2 Medium power photomicrographs of hematoxylin-erythrosin stained sections of the rectal carcinoid showing the wide range of differentiation observed in various parts of the tumor. Areas of the same ribbon growth pattern as in the tumor of Case No 1 occurred (Fig 2A) merging into moderately well differentiated parts with rosette formations and palisading cells in the margin of tumor nodules (Fig 2B). In the most undifferentiated parts only closely packed irregularly distributed tumor cells with marked atypia were found (Fig 2C). By the PAP immunocytochemical procedure fairly numerous tumor cells were displaying enkephalin immunoreactivity of varying intensity (Fig 2D). The cells occurred as single cells or as clusters. X255(2A, B X300(2D)

- tion of neurotensin in endocrine cells of the gut *Cell Tiss Res* 178 313-321 1977
- 26 *Fahrenkrug J Schaffalitzky de Muckadell O B & Rehfeld J F* Production and evaluation of antibodies for radioimmunoassay of secretin *Scand J Clin Lab Invest* 36 281-287 1976
 - 27 *Larsson L I Sundler F Alumets J Håkanson R Schaffalitzky de Muckadell O B & Fahrenkrug J* Distribution, ontogeny and ultrastructure of the mammalian secretin cell *Cell Tiss Res* 181 361-368 1977
 - 28 *Dubois M P* Presence of immunoreactive somatostatin in discrete cells of the endocrine pancreas *Proc Nat Acad Sci* 72 1340-1343 1975
 - 29 *Alumets J Sundler F & Håkanson R* Distribution, ontogeny and ultrastructure of somatostatin immunoreactive cells in the pancreas and gut *Cell Tiss Res* 185 465-479 1977
 - 30 *Said S I & Rosenberg R N* Vasoactive intestinal polypeptide: Abundant immunoreactivity in neural cell lines and normal nervous tissue *Science* 192 907-908 1976
 - 31 *Sundler F Alumets J Fahrenkrug J Håkanson R & Schaffalitzky de Muckadell O B* Cellular localization and ontogeny of immunoreactive vasoactive intestinal polypeptide (VIP) in the chicken gut *Cell Tiss Res* 196 193-201 1979
 - 32 *Bjorklund A Falck B & Owman C* Fluorescence microscopic and microspectrofluorometric techniques for the cellular localization and characterization of biogenic monoamines. In Rall J E & Kopin I J (eds) *Methods of investigative and diagnostic endocrinology Vol 1: The thyroid and biogenic amines* North Holland Publ. Amsterdam 1972 pp 318-368
 - 33 *Gutniak M Rosenqvist U Grimelius L Lundberg J M Hokfelt T Rokaeus A Rosell S Lundqvist G Fahrenkrug J Sundblad R & Gutniak E* Report on a patient with watery diarrhoea syndrome caused by a pancreatic tumour containing neurotensin, enkephalin and calcitonin *Acta Med Scand* (in press)
 - 34 *Larsson L I Grimelius L Håkanson R Rehfeld J F Stadl F Holst J J Angervall L & Sundler F* Mixed endocrine pancreatic tumors producing several peptide hormones *Am J Pathol* 79 271-284 1975
 - 35 *Margules D L Moisset B Lewis M J Shibuya H & Pert C B* β -Endorphin is associated with overeating in genetically obese mice (ob/ob) and rats (fa/fa) *Science* 202 988-991 1978

patients do not necessarily reflect overproduction of endogenous opiates

This work was supported by grants from the *Swedish Cancer Society* (Project No 806 05XA) and the *Swedish Medical Research Council* (projects Nos 12X102 12X718 and 14X4499)

Thanks are due to Dr Görel Östberg, Director of the Department of Pathology at the Central Hospital in Halmstad, Sweden, for providing us with specimens and valuable information about case 2 in the present report

REFERENCES

- Hughes J, Smith T W, Austerlitz H W, Fothergill L A, Morgan B A & Morris H R. Identification of two related pentapeptides from the brain with potent opiate agonist activity. *Nature* 258: 577-579 1975
- Polak J M, Bloom S R, Sullivan S N, Facer P & Pearse A G E. Enkephalin like immunoreactivity in the human gastro intestinal tract. *Lancet* i 972-974 1977
- Alumets J, Håkanson R, Sundler F & Chang A J. Leu enkephalin like material in nerves and enterochromaffin cells in the gut. An immunohistochemical study. *Histochemistry* 56: 187-196 1978
- Sundler F, Alumets J & Håkanson R. Six types of immunohistochemically and ultrastructurally identified endocrine cells in pig pancreas. *Scand J Gastroenterol* 13 (Suppl 49): 179 1978
- Sundler F, Alumets J & Håkanson R. Majority and minority cell populations in GEP and bronchial endocrine tumors. *Scand J Gastroenterol* 14 (Suppl 53): 9-13 1979
- Celik M R. Distribution of β endorphin immunoreactive cells in human fetal and adult pituitaries and in pituitary adenomas. *J Histochem Cytochem* 27: 1215-1216 1979
- Davis I M P. The endocrine cells of the gastro intestinal tract and the neoplasms which arise from them. *Clin Topics Path* 63: 221-259 1976
- Wahlstedt C, Faria Gomes G, Grimelius L, Lundqvist G & Skoog L. Enteroglucagon and substance P like immunoreactivity in argentaffin and argyrophil neural carcinoids. *Virchows Arch B Cell Pathol* 25: 111-124 1977
- Singh I A. Modification of the Masson-Hamperl method for staining of argentaffin cells. *Anat Anz* 115: 81-82 1964
- Håkanson R, Öman C, Spörrens B & Sundler F. Electron microscopic classification of amine producing endocrine cells by selective staining of ultra thin sections. *Histochemistry* 27: 226-242 1971
- Grimelius L. A silver nitrate stain for A2 cells in human pancreatic islets. *Acta Soc Med Upsal* 73: 243-270 1968
- Coons A H, Leduc E H & Conolly J M. Studies on antibody production. I. A method for the histochemical demonstration of specific antibody and its application to a study of the hyperimmune rabbit. *J Exp Med* 102: 49-60 1955
- Sternberger L. *Immunocytochemistry*. Prentice Hall Inc, Englewood Cliffs, New Jersey 1974, p 143-144
- Håkanson R, Sundler F, Larsson L I, Ekman R & Sjöberg N O. Peptides with NII-term in tryptophan in adrenocorticotrophic hormone an melanocyte stimulating hormone granules of adenohypophysis. *J Histochem Cytochem* 23: 65-71 1975
- Alumets J, Håkanson R, Sundler F & Thorell J. Neuronal localization of immunoreactive enkephalin and β -endorphin in the earthworm (*Lumbricus terrestris*). *Nature* 279: 805-806 1979
- Miller R J, Chang A J, Cooper B & Clemmings P. Radioimmunoassay and characterization of enkephalins in rat tissues. *J Biol Chem* 253: 531-538 1978
- O'Dorisio T, Cataland S, Stevenson M J & Mazzaferri E L. Gastric inhibitory polypeptide (GIP). Intestinal distribution and stimulation by amino acids and medium chain triglycerides. *Am J Dig Dis* 21: 761-765 1976
- Alumets J, Håkanson R, O'Dorisio T, Sjölund A & Sundler F. Is GIP a glucagon cell constituent? *Histochemistry* 58: 253-257 1978
- Loren I, Alumets J, Håkanson R & Sundler F. Distribution of gastrin and CCK like peptides in rat brain. An immunocytochemical study. *Histochemistry* 59: 249-257 1979
- Holst J J & Aasted B. Production and evaluation of glucagon antibodies for radioimmunoassay. *Acta Endocr* 77: 715-726 1974
- Larsson L I, Holst J J, Håkanson R & Sundler F. Distribution and properties of glucagon immunoreactivity in the digestive tract of various mammals. An immunohistochemical and immunohistochemical study. *Histochemistry* 44: 181-290 1975
- Larsson L I, Sundler F & Håkanson R. Pancreatic polypeptide - a postulated new hormone. Identification of its cellular storage site by light and electron microscopic immunocytochemistry. *Diabetologia* 17: 211-226 1976
- Yanaihara C, Sato H, Yanaihara N, Naruse S, Förssmann W G, Helmstaedt J, Fujita T, Yamaguchi K & Abe K. Motilin, substance P and somatostatin like immunoreactivities in extracts from dog, *Tupaia* and monkey brain and GI tract. In Grossman M, Speranza V, Bresso N & Lezoché E (eds). *Gastrointestinal hormones and pathology of the digestive system*. Plenum Press, New York 1978, pp 269-283
- Carraway R E & Leeman S E. Radioimmunoassay of neurotensin, a hypothalamic peptide. *J Biol Chem* 251: 7035-7044 1976
- Sundler F, Håkanson R, Hamner R A, Alumets J, Carraway R E, Leeman S E & Zimmerman E A. Immunohistochemical localization

EFFECT OF ESTRADIOL AND PROGESTERONE ON THE ADENYLATE CYCLASE ACTIVITY IN GRAFTS OF 3-METHYLCHOLANTHRENE INDUCED CARCINOMAS IN THE MOUSE UTERINE CERVIX

STENER KVINNSLAND PER EYSTEIN LØNNING and JOHN GUNNAR FORSBERG

Cell Biology Research Group Preclinical Institutes University of Bergen Norway

Kvinnsland S Lønning P E & Forsberg J G Effect of estradiol and progesterone on the adenylate cyclase activity in grafts of 3 methylcholanthrene induced carcinomas in the mouse uterine cervix Acta path microbiol scand Sect A 88 111-118 1980

Grafts from a methylcholanthrene induced mouse uterine cervical carcinoma (NMRI mice) were grown in neonatal female mouse hosts. The hosts were treated for 12 days with estradiol and progesterone alone or in combination. Controls were injected with the solvent (olive oil) only. Pieces from every graft were used for histological study for study of the proliferation rate and for study of the adenylate cyclase activity in homogenate. All the grafts were well differentiated squamous carcinomas and the histological picture was the same irrespective of hormonal treatment. The proliferation rate was the same in control grafts as in those from hosts treated with hormones. Grafts from progesterone and progesterone/estradiol injected hosts had significantly higher levels of adenylate cyclase activity compared with grafts from control hosts. Estradiol alone resulted in a trend towards increased activity but the difference to controls was not statistically significant.

Key words: Cervical carcinoma, mouse, neoplasm transplantation, adenylate cyclase, estradiol, progesterone.

J G Forsberg, Institute of Anatomy, Årstadvollén 19, N-5000 Bergen, Norway.

Received 25 viii 79 Accepted 18 x 79

The effect of exogenous sex steroid hormones on the incidence and latency period of chemically induced uterine cervical carcinomas in mice has been extensively studied, often with highly contradictory results (for a review, see 32). For the present study, it is enough to mention that ovariectomy may be associated with an increased incidence of invasive tumors, while intact females have a higher incidence of *in situ* carcinoma. Estrogen may inhibit invasiveness (26, 27, 30), possibly through an effect at the differentiation level (22, 33). The histological type of tumour may be dependent on hormonal conditions: ovariectomy and progestins promote mucin-secreting or mucoepidermoid tumours, while

estrogen promotes squamous cell carcinomas (17, 36).

Manifest tumours of different types are reported to have an increased basal activity of adenylate cyclase and changed sensitivity to hormones or PGE_1 (4, 19, 20, 24, 28, 34, 37). However, there is a wide variation in tumour adenylate cyclase response to hormones and other factors (12). A decreased intracellular cAMP level has been described for e.g. colon adenocarcinoma and from tumour cells or transformed cells grown *in vitro* (11, 13, 40, 42).

As both cytochemical and biochemical studies indicate an effect of exogenous estradiol on the adenylate cyclase activity in the neonatal normal

Calif) draining into a neutral alumina column (Bio Rad). The eluate (4 ml) from the alumina column was collected into a scintillation vial 16 ml of Instagel (Packard) was added and the radioactivity counted in a Packard 2425 Tri-Carb liquid scintillator with separate channels for ^3H and ^{32}P . The recovery of product was 50-60%. Control incubations containing boiled homogenate or buffer were incubated in each series.

Adenylate cyclase activity in homogenates from 15 tumours (including tumours from olive oil and hormonal treated animals) was estimated from linear parts of curves relating enzyme activity either to incubation time or protein concentration. Adenylate cyclase activity was linear with incubation time for at least 10 min and with protein concentration between 50 and 300 μg per assay in the presence and absence of NaF. Enzyme activity of the other homogenates was measured in triplicate incubation time 10 min and protein concentration 200-250 μg . The results were expressed as pmoles cAMP produced per 10 min and related to mg wet weight, mg protein or mg DNA.

Measurement of DNA and protein in homogenates Part of the homogenate from every tumour was dissolved in 10 volumes of 1 N NaOH and the DNA concentration measured by the method described above using 3 dilutions (each measured in duplicate) from each homogenate.

Protein was measured in the dissolved homogenate using the method of Klungasayr (23) with bovine serum albumin (Sigma) as standard. Protein concentration was measured in 3 dilutions from each homogenate.

Statistical method Provided the error variance between different groups to be compared did not vary significantly.

of va
cases
comp
measurements (41). The T values from the Mann-Whitney test and significance levels are given in Figs 2-5. Significance levels: 0.05 > p > 0.01* (probably significant); 0.01 > p > 0.001** (significant).

RESULTS

Histology Histological sections of biopsy pieces from the same grafts as used for studies of ^3H TdR incorporation and adenylate cyclase activity all showed well growing cancer tissue without any round cell infiltration (Fig. 1). Irrespective of the sections being taken from grafts in control or hormonally treated females (estradiol and/or progesterone) the tumour tissue had the same histological type: well-differentiated squamous carcinoma. The histological study did not reveal any tendency to a mucocutaneous tumor type in grafts exposed to estradiol and progesterone in combination or progesterone alone. The distribution between the stromal and epithelial compartment did not seem to differ between the different grafts studied.

^3H -TdR incorporation The results are demonstrated in Fig. 2. None of the hormonal treatments used (E_2 , $\text{E}_2 + \text{P}$, P) influenced the proliferative activity as measured by the ^3H TdR incorporation per μg DNA. Even though the variances seemed to be larger in the $\text{E}_2 + \text{P}$ and P groups compared with the control and E_2 groups, a Bartlett's test for homogeneity of variances did not demonstrate any significant difference in intragroup error variances.

Adenylate cyclase activity The adenylate cyclase activity, measured as the formation of cAMP during a 10 min period, was related to the wet weight of the preparations studied (Fig. 3) and to their DNA (Fig. 4) and protein (Fig. 5) content. All homogenates were incubated in the absence or presence of NaF. Grafts from E_2 treated hosts had higher mean values for enzyme activity than preparations from olive oil injected hosts but the difference was never statistically significant. However, irrespective of the enzyme activity being related to wet weight, DNA or protein content, grafts from $\text{E}_2 + \text{P}$ and P treated hosts had statistically significant higher enzyme activity than controls, and this both in the absence or presence of NaF in the incubation medium. In no case was there any difference between the $\text{E}_2 + \text{P}$ and P groups.

When the adenylate cyclase activity per mg DNA (Fig. 3) was compared in homogenates without or supplemented with NaF, it was evident that the mean quotient (\pm NaF) was 3.15 for control grafts, 2.85 for grafts from E_2 injected hosts and 2.58 and 2.70 for grafts from $\text{E}_2 + \text{P}$ and P treated hosts respectively. A variance analysis of these quotients demonstrated probably significant higher quotients for the control grafts than for the hormonally treated grafts ($F = 3.127$ for 3 and 25 d.f., $0.05 > p > 0.01$). Similar results were obtained also when the enzyme activity was related to the protein content or wet weight.

No correlation occurred between ^3H TdR incorporation and adenylate cyclase activity neither in control nor in hormonally stimulated grafts.

DISCUSSION

All the tumour grafts included in this study belonged to the 10th transplantation generation of one single methylcholanthrene induced primary cervical carcinoma. Both the primary tumour and the transplantation generation was randomly chosen for this study among all the transplantation generations from different primary tumours available at the laboratory. Moreover, because of the transplantation protocol, all the grafts in this material are descended from one single graft in the

uterine cervical epithelium of mice (25), we found it of interest to study the adenylate cyclase response to exogenous estradiol and progesterone in grafts of methylcholanthrene induced mouse cervical carcinomas

MATERIAL AND METHODS

Animals All the animals used belonged to a non inbred NMRI mouse strain. The animals were fed a standard pellet diet and given water *ad libitum*. A few days before birth pregnant females were put into separate cages (one female in every cage) where they gave birth to their young. On the day of birth the male and female young were separated and every mother allowed to nurse 8–10 females.

Tumour induction Female mice 6–9 weeks old were laparotomized under ether anaesthesia. A cotton thread impregnated with 3-methylcholanthrene (MCA, Sigma) in beeswax was inserted into the uterine cervix as earlier described (15–31). Beginning 3 months after insertion of the MCA thread and thereafter once every other week the females were palpated and when a palpable cervical tumour was identified the female was killed. The tumour was dissected out and put into Parker medium 199. Part of the tumour was placed in Bouin's solution for fixation and later histological study. The remaining part was cut into small pieces and washed twice in Parker medium 199 with added penicillin and streptomycin (penicillin 100 IU/ml, streptomycin 100 µg/ml).

Tumour grafting Neonatal females were used within 24 hours after birth. They were anaesthetized by cooling on ice. A small cutaneous incision was made on the left side of the abdomen and from this incision two subcutaneous 'tunnels' were made with a small forceps. Two small tumour pieces were placed in each tunnel and the skin incision closed with 8/10 thread on an atraumatic needle.

About two weeks (11–18 days) after transplantation the hosts were checked for tumour growth. The size of the transplants varied but on every host it was possible to find one or two tumour grafts showing active growth with a several fold enlargement compared with the inserted tumour pieces.

Those grafts with an active growth were removed and placed in Parker medium 199. Most of the tumour tissue was frozen and stored in liquid nitrogen. Before freezing small parts were removed from different regions of the tumour graft and these pieces were used for biopsy. One of the pieces was cut into smaller pieces and these were used for retransplantation into new hosts according to the same technique as described above. In this way tumour pieces from the same primary tumour were retransplanted at an interval of about two weeks. From some primary tumours we have now transplanted for 15 generations.

Hormonal treatment Nineteen hosts carrying the 10th generation of transplants from a single primary tumour were used. Beginning on day 3 after birth the host females were given subcutaneous injections of 0.05 ml olive oil (controls, 6 females), 1 µg estradiol 17β (E₂, 7

females), 500 µg progesterone (P, 3 females) or combination of E₂ and P (3 females). The hormones were dissolved in olive oil and were both from Sigma. The host females were injected with single daily injections for 12 days and killed 24 hours after the last injection. One or two well growing tumour transplants were removed from every host for further study.

Studies on ³H-thymidine (³H-TdR) incorporation From every tumour transplant removed 9 small pieces were randomly cut out from different regions of the tumour, while the rest of the tumour was preserved in liquid nitrogen for further treatment (see below). The pieces were incubated in Leighton tubes (3 pieces in each tube) in 2 ml medium (90% Parker medium 199, 10% fetal calf serum/Gibco) supplemented with 5 µCi ³H-TdR (sp act 5 Ci/mmol, Radiochemical Centre, Amersham). The incubation took place in an atmosphere of 95% O₂ and 5% CO₂ (non-capable tubes) at 37 °C for 1 hour. After incubation the tumour pieces were washed in 5% trichloroacetic acid (4 °C) for 1 hour (3 shifts) and finally for 15 min in saline. The preparations were solubilized in 1 N NaOH and the DNA content was measured using the indole method (2). Calf thymus DNA (BDH Biochemicals) was used as standard. To 100 µl of the NaOH hydrolysate was added 1 ml Luma Solu (Luma Systems AG, Basel) and 14 ml scintillation liquid (fluorochromes in toluene). Scintillation counting took place in a Packard 2425 Tri-Carb liquid scintillator. The counting efficiency was 36%. The radioactivity was expressed as cpm/µg DNA and this value was taken as a measure of cell proliferation.

Preparation of homogenates The tumours were stored in liquid nitrogen, weighed on a sensitive Mettler balance and homogenized (Thomas type A teflon/glass homogenizer 975 rpm, 5 strokes) in 10 volumes of 2 mM glycylglycine buffer (pH 7.4) containing 20 mM KCl, 20 mM NaCl and 1 mM MgSO₄. The homogenate kept on ice was assayed for adenylate cyclase activity within 30 min.

Adenylate cyclase activity The method described by Salomon *et al.* (39) was used with minor modifications. An aliquot (50 µl) of the homogenate was incubated in a total volume of 100 µl containing 25 mM Tris HCl buffer (pH 7.6), 5 mM MgCl₂, 1 mM adenosine 3',5'-cyclic monophosphoric acid (cAMP, Sigma), 20 mM phosphocreatine (Sigma Chem. Co.), 100 U/ml creatine phosphokinase (Sigma Chem. Co.) and 1 mM ATP (Sigma Chem. Co.) 2–4 × 10⁶ cpm ³²P-ATP (sp act 15–25 Ci/mmol, The Radiochemical Centre, Amersham) and in some experiments 5 mM NaF. The reaction was started with the addition of the homogenate and was

incubated at 37 °C for 5 min. The enzyme sample was heated in a boiling water bath for 4 min. The samples were then centrifuged at 1200 g for 10 min. To 900 µl of the supernatant was added ³H-cAMP (ca. 10 000 cpm sp act 27 Ci/mmol, The Radiochemical Centre, Amersham) in 100 µl Tris HCl buffer and the 1 ml sample was applied to a Dowex column (AG 50W X4, 200–400 mesh, H⁺ form, Bio Rad, Richmond

cpm(^3H TdR)/ μg DNA \pm SE

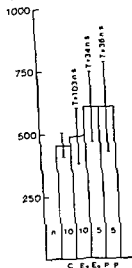
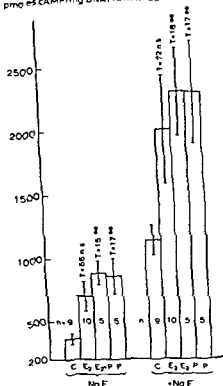
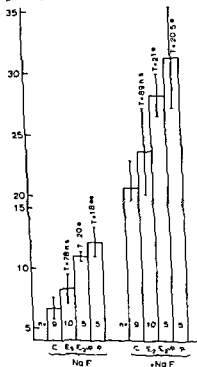


Fig. 2 The cell proliferation (^3H TdR incorporation into DNA) level in grafts from differently treated hosts. C controls E₂ estradiol P progesterone

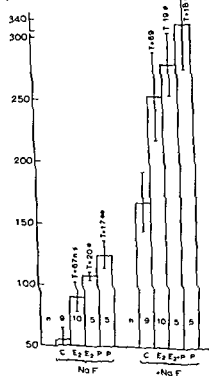
pmoles cAMP/mg DNA/10 min \pm SE



pmoles cAMP/mg wet weight/10 min \pm SE



pmoles cAMP/mg prote n/10 min \pm SE



Figs 3-5 The adenylate cyclase activity in grafts from differently treated hosts (C controls E₂ estradiol P progesterone) and in the absence or presence of NaF. The enzyme activity was related to mg wet weight (Fig. 3) mg DNA (Fig. 4) or mg protein (Fig. 5). For T values and significance levels see Statistical method



Fig 1 A-D Microphotographs of sections of grafts from control (*A*) or hormone treated hosts (*B-D*) *B* estradiol *C* estradiol and progesterone *D* progesterone Magnification 220 \times

- Bontling S L & Jones M Determination of microgram quantities of deoxyribonucleic acid and protein in tissues grown in vitro Arch Biochem Biophys 66 340-353 1957
- Brown H D Chattopadhyay S K Spjut H J Spratt Jr J S & Pennington S N Adenylcyclase activity in dimethylamino biphenyl induced breast carcinoma Biochim Biophys Acta 192 372-375 1969
- Brustad G O Christoffersen T Johansen E J & Oye I Effect of prostaglandins and hormones on cyclic AMP formation in rat hepatomas and liver tissue Br J Cancer 38 737-744 1978
- Coffino P & Gray J W Regulation of S49 lymphoma cells growth by cyclic adenosine 3'5' monophosphate Cancer Res 38 4285-4288 1978
- Coffino P Gray J W & Tomkins G M Cyclic AMP a nonessential regulator of the cell cycle Proc Natl Acad Sci USA 72 878-882 1975
- Cho Chung Y S Interaction of cyclic AMP and estrogen in tumor growth control In Sharma R K & Criss W E Eds Endocrine Control in Neoplasia New York Raven Press 1978 pp 335-346
- Cho Chung Y S Bodwin J S & Clair T Cyclic AMP binding proteins Inverse relationships with estrogen receptors in hormone-dependent mammary tumor regression Eur J Biochem 86 51-60 1978
- Cho Chung Y S & Clair T Altered cyclic AMP binding and db cyclic AMP unresponsiveness in vivo Nature 265 452-454 1977
- Cho Chung Y S & Newcomer S F Adenylate cyclase cyclic adenosine 3'5' monophosphate phosphodiesterase and regression of Walker 256 mammary carcinoma Cancer Res 37 4493-4499 1977
- Cohen L A & Chan P C Intracellular cAMP levels in normal rat mammary gland and adenocarcinoma. In vivo vs in vitro Life Sci 16 107-115 1975
- Criss W E Muganda P Sahai A & Morris H P Cyclic nucleotide metabolism in solid tumor tissue Adv exp Med Biol 92 489-516 1977
- DeRubeis F R Chavoith R & Field J B The content and metabolism of cyclic adenosine 3'5' monophosphate and cyclic guanosine 3'5' monophosphate in adenocarcinoma of the human colon J Clin Invest 57 641-649 1976
- Deskeland S O Kalland T Stray Breistein L Fosberg T M & Ueland P M The isozyme pattern of cyclic AMP-dependent protein kinase and the distribution of a cervicovaginal antigen in experimental carcinoma of the cervix uteri of mice Acta path microbiol scand Sect A 86 121-130 1978
- Forsberg J G & Stray Breistein L Carcinogenesis with 3 methylcholanthrene in uterine cervix of mice treated neonatally with estrogen J Natl Cancer Inst 49 155-172 1972
- Forsberg J G & Stray Breistein L A synergistic effect of oestradiol and prolactin influencing the incidence of 3 methylcholanthrene induced cervical carcinomas in mice Acta path microbiol scand Sect A 84 384-390 1976
- Glucksmann A & Cherry C P The effect of castration and of additional hormonal treatments on the induction of cervical and vulval tumors in mice Br J Cancer 16 634-652 1962
- Heidrich M L & Ryan W L Cyclic nucleotides on cell growth in vitro Cancer Res 30 376-378 1970
- Hickie R A Regulation of cyclic AMP and cyclic GMP in Morris hepatomas and liver Adv exp Med Biol 92 451-488 1977
- Hunt N H Shortland J R Michelangeli V P Hammonds J C Atkins D & Martin T J Adenylate cyclase activity of renal cortical carcinoma and its relation to histology and ultrastructure Cancer Res 38 23-31 1978
- Jost J P & Rickenberg H V Cyclic AMP Ann Rev Biochem 40 741-774 1971
- Klavins J V & Kaufman N Neoplastic changes in cervix uterine following administration of estradiol benzoate and 20 methylcholanthrene Acta cytol 6 267-272 1962
- Klungsoyr L Quantitative estimation of protein Analyt Biochem 27 91-98 1969
- Kung W Bechtel E Geyer E Salokangas Preiss J Huber P Torhorst J Jungmann R A Talmadge K & Eppenberger U Altered levels of cyclic nucleotides cyclic AMP phosphodiesterase and adenyl cyclase activities in normal dysplastic and neoplastic human mammary tissue FEBS letters 82 102-106 1977
- Kilnitsland S Adenylate cyclase activity in the uterine cervix of neonatal and immature mice 1978
- 26
- 27 Mannan A A H M & Zaman H Effect of ovariectomy on the fate of 20 methylcholanthrene induced dysplasia of the mouse uterine cervix Acta cytol 12 243-250 1968
- 28 Martin T J Hunt N H Boyd H Ellison M Michelangeli V P & Atkins D Hormone receptors and cyclic nucleotide metabolism in cancer cells Clin Endocrinol 5 Suppl 373-386 1976
- 29 Marusik R J & Hils R Relationship of adenosine 3'5'-cyclic monophosphate and guanosine 3'5' monophosphate to growth of dimethyl benz[a]anthracene induced mammary tumors in rats J Natl Cancer Inst 56 659-661 1976
- 30 Mueenuddin G & Zaman H Effect of ovariectomy on the induction by 20-methylcholanthrene of carcinoma of the mouse uterine cervix Acta cytol 11 205-210 1967
- 31 Murphy E D Carcinogenesis of the uterine cervix in mice effect of diethylstilbestrol after limited application of 3 methylcholanthrene J Natl Cancer Inst 27 611-653 1961
- 32 Myhre E & Bjørø K Hormones and cervical cancer Universitetsforlaget Oslo 1971

9th transplantation generation. This confers a high degree of cellular homogeneity on the material used, which is also visible from the histological study of biopsy pieces from the grafts. The grafts displayed an active growth in the neonatal hosts, without any evidence of round cell infiltration or necrosis.

All the female hosts were killed on day 15 after birth, after being injected with hormone(s) or olive oil on day 3-14. Day 15 was chosen for sacrifice because all our previous results showed that at this time surviving grafts are in a period of active growth. The duration of the hormonal treatment was rather long because we were more interested in long-term results than in «acute» effects.

It has earlier been pointed out that there is an inconsistency in the results when the level of cyclic nucleotides or activities or related enzymes are expressed relative to protein, RNA, DNA, wet weight or cellularity (24, 29, 37). In this study the adenylate cyclase activity was related to wet weight, mg protein and DNA content, and in all three instances there was a remarkable degree of consistency.

The most important results from this study are the definite evidences for a steroid-induced influence on the adenylate cyclase activity, and this in a tumour type where steroid effects have been debated. So far the results are in agreement with those earlier described (25) from experiments using neonatal mouse cervical preparations. The general opinion in literature is that the adenylate cyclase - cAMP and its effector system are not involved in the mechanism of steroid action (43).

Some reports, however, stress that steroids may have important effects related to the cell membrane (1, 35). The mechanism behind the steroid-induced activation of the adenylate cyclase in neonatal mouse uterine cervix and cervical tumours is not known. Both direct and indirect effects are possible (21, 38). The NaF induced adenylate cyclase activation was less pronounced in grafts from hormonally treated hosts compared with controls.

Treatment of the hosts with estradiol and/or progesterone did not influence the cellular proliferation in the grafts as measured from ^3H -TdR incorporation per mg DNA. However an earlier and transient estradiol induced proliferation wave should not be excluded from these results. Nor in our earlier studies have we obtained evidence for estradiol alone stimulating the growth of primary cervical tumours (16). The failure in this study to find any hormonally induced effects on cell proliferation argues against the possibility that the increased adenylate cyclase activity in the grafts, after injecting the hosts with progesterone, is related to a hormone induced tumour regression (7, 18).

Generally speaking, increased levels of cAMP have a growth-arresting effect on cells *in vitro* (5, 6) and exogenous cAMP can induce regression of responsive Walker 256 mammary carcinoma (11). Rat mammary carcinomas, induced with 1,1-dimethyl-4-amino biphenyl, are reported to have increased activity of adenylate cyclase as compared with the normal, lactating mammary gland (3). The same holds true for the basal adenylate cyclase activity in different other types of tumours (4, 20, 24, 28, 34, 37).

No conclusions should be drawn from increased enzyme activity described in this paper about the actual intracellular level of cAMP. The latter reflects both synthesizing and degrading processes, only the former is reported to be increased. Increased cAMP-phosphodiesterase activity may be concomitant with increased adenylate cyclase activity (8). Moreover, an increased level of cAMP may be combined with mutational changes in the cAMP effector system, leading to a defect protein kinase (12, 19).

All the tumour grafts, irrespective of treatment, the hosts, were well-differentiated squamous carcinomas. Neither progesterone nor progesterone in combination with estradiol resulted in a tendency towards a mucinous or mucocystic tumour type. This is in contrast to results reported earlier both from this (16) and other laboratories (36). As the latter results are based on treatment of animals with primary tumours for longer periods than used in this study, the discrepancy may be explained by both the time factor and specific characteristics of the primary tumour used here.

The consequences of the steroid induced activation of the adenylate cyclase in the grafts can only be a matter of speculation before other links in the cAMP-effector system have been studied. Studies on 12 primary methylcholanthrene-induced cervical carcinomas revealed no differences in protein kinase properties compared to normal vaginal epithelium (4). It should not be excluded that both the neonatal mouse cervix and the tumour grafts studied here may reveal in a more analysable way an aspect of the steroid mechanism of action which is difficult to grasp in normal immature and adult stages.

This investigation was supported by grants from the Norwegian Cancer Society.

REFERENCES

1. Baulieu E-E. Cell membrane a target for steroid hormones. *Mol Cell Endocrinol* 12: 247-251, 1978.

FORMATION OF LARGE VACUOLES IN TUMOUR CELLS GROWN IN SUSPENSION

A. L. JAKOBSEN and J. CHEMNITZ

Winslow Institute of Human Anatomy University of Odense Odense Denmark

Jakobsen A. L. & Chemnitz J. Formation of large vacuoles in tumour cells grown in suspension. Acta path microbiol scand Sect A 88 119-124 1980

In suspension cultures of JB 1 E cells approximately 11% of the cells contained a single large vacuole (balloon cells) or signet ring cells. Such cells were rarely observed in monolayer cultures where the cells were attached to a substrate. Only a few balloon cells were observed in suspension cultures of HeLa S3 cells. Both cell lines were able to phagocytize latex particles of 5.7 µm mean diameter. Nocodazole significantly reduced the formation of balloon cells in suspension cultures of JB 1 E cells. Transmission electron microscopy indicated that various cytoplasmic membrane components probably could contribute to the membrane material of the vacuoles. It is believed that the formation of balloon cells is due to changes in the regulation of the cellular membrane material.

Key words: Vacuoles, suspension culture, tumour cells, TEM, microtubules.

A. L. Jakobsen Winslow Institute of Human Anatomy University of Odense Campusvej 55 DK 5230 Odense N Denmark

Received 19.11.79 Accepted 7.12.79

Several observations on cytoplasmic vacuolization in tumour cells leading to the formation of balloon cells (i.e. cells with a single large vacuole and a flattened eccentric nucleus) have been published (Seeger 1937 Selby et al 1955-56 Wessel & Bernhard 1957 Tolnai 1964 Burns 1967 Chemnitz et al 1974).

Cytoplasmic vacuolization of ascites tumour cells has commonly been regarded as a sign of cell degeneration, a cellular degenerative process preceding cell death (Selby et al 1955-56 Wessel & Bernhard 1957). However, mitotic activity of the balloon cells and uptake of tritiated thymidine in the nucleus indicate that they are living cells (Tolnai 1964 1965 Chemnitz et al 1975).

The aim of the present investigation with two different cell lines grown in suspension and monolayer

in suspension cultures contained balloon cells while they were rarely observed among flattened spindle shaped JB 1 E cells attached to a substrate.

MATERIALS AND METHODS

Cells and Growth Media

In the present

were:

JB 1 E

tumour

JB che

the H

purchased from GIBCO

Stock cultures of both cell lines were maintained at 37 °C in 75 cm² Nunc flasks in Eagle's minimal essential medium (EMEM-F11) (GIBCO) supplemented with 10% foetal calf serum.

In GIBCO the media were aerated with a mixture of 95% air and 5% CO₂ and changed every other day.

Chemicals

Nocodazole (methyl 5 (2-thienylcarbonyl) 1 H

Our results showed that the JB 1 E cells grown

- 33 Negata, I., Sutoh, K., Misnou, Y. & Miura, Y. Effect of estrogen on the uterine cancer induced by 20-methylcholanthrene (From the autoradiographic observation) *Cancer* 57: 403-412, 1966
- 34 Niles, R. M. & Makarski, J. S. Hormonal activation of adenylate cyclase in mouse melanoma variants *J Cell Physiol* 96: 355-360, 1978
- 35 Pietras, R. J. & Szego, C. Surface modifications evoked by estradiol and diethylstilbestrol in isolated endometrial cells: evidence from lectin probes and extracellular release of lysosomal protease *Endocrinology* 97: 1445-1454, 1975
- 36 Reboud, S. & Pageau, G. Co-carcinogenic effect of progesterone on 20-methylcholanthrene induced cervical carcinoma in mice *Nature* 241: 398-399, 1973
- 37 Rillema, J. A., Mulder, J. A. & Anderson, L. D. Cyclic nucleotides and their associated enzymes in 9,10-dimethyl-1,2-benzanthracene-induced mammary tumors of rats *Cancer Res* 38: 741-744, 1978
- 38 Rinard, G. A. & Chew, C. S. Uterine cyclic AMP formation: Biphasic effect of estrogen on catecholamine sensitivity *Life Sci* 22: 2043-2050, 1978
- 39 Salomon, J., Londos, C. & Rodbell, M. A highly sensitive adenylate cyclase assay *Analyt. Biochem* 58: 541-548, 1974
- 40 Sheppard, J. R. Difference in the cyclic adenosine 3',5'-monophosphate levels in normal and transformed cells *Nature New Biol* 236: 14-16, 1972
- 41 Snedecor, G. W. & Cochran, W. G. *Statistical methods* 6th ed. Iowa State University Press Ames, Iowa, 1969
- 42 Stevens, R. H., Laven, D. P., Osborne, J. W., Prall, J. P. & Lawson, A. J. Cyclic nucleotide concentrations in 1,2-dimethylhydrazine induced rat colon adenocarcinoma *Cancer Letters* 4: 27-33, 1977
- 43 Yamamoto, K. R. & Alberts, B. M. Steroid receptors: elements for modulation of eukaryotic transcription *Ann Rev Biochem* 45: 721-746, 1976

lets of untreated JB 1 E cells cultivated for 24 h in suspension cultures were obtained by centrifugation were fixed in 4% formaldehyde pH 6.8 for approximately 24 h embedded in paraffin and sections were stained with one of the following dyes

periodic acid Schiff (PAS) without nuclear staining (McManus and Mowry 1964)

alcian blue (pH 3 and pH 1) (McManus and Mowry 1964)

After 24 h of growth the cultures were fixed using 6% glutaraldehyde buffered with PM buffer (polyzation mix) introduced by Lufg *et al* (1977). One portion was made concerning some of the spinner is containing 20×10^6 cells of the JB 1 E cell line. The cells were fixed with 2.5% glutaraldehyde buffered with 0.1 M Na-cacodylate buffer 4% sucrose 7.2 (fixative vehicle 300 mOsm). Ruthenium red (1%) was added to the fixative using the method of *et al* as described by Behnke (1968). The cells were fixed at 37 °C for 2 h and postfixed in 1% OsO_4 for 3 h and the further procedure is the same as described for other spinner cultures.

Spinner Cultures. The cells were fixed at 37 °C for 2–3 h, centrifuged for 10 min and the cell pellets were suspended in agar dissolved in warm PBS. After cooling ice-water small cubes of agar were washed in 0.1 M cacodylate buffer (300 mOsm) pH 7.2 and postfixed in 1% OsO_4 in cacodylate buffer pH 7.2 for 1 h at 4 °C. After staining with 1% uranyl in re-distilled water for 1 h the cells were dehydrated in increasing conc of acetone and embedded in Araldite.

Monolayer Cultures. After fixation in 2.5% glutaraldehyde in PM buffer for 2–4 h the cells were postfixed in 1% OsO_4 in 0.2 M cacodylate buffer (300 mOsm) pH 7.2 for 1 h and pre stained with 1% uranyl acetate in re-distilled water for 1 h then dehydrated in series of alcohols and embedded in Araldite. After polymerization selected areas were cut out of the bottom of the tissue flasks for sectioning.

Ultra thin sections from cultures pre stained with uranyl acetate were contrasted with 0.4% lead citrate at room temperature for 5 min. Ultra thin sections from cultures fixed with RR were contrasted with 1% uranyl acetate at 60 °C for 10 min and 0.4% lead citrate at room temp for 5 min.

Semi thin sections were cut and stained with 1% toluidine blue and prepared for light microscopy.

RESULTS

Light Microscopy

Spinner and Monolayer Cultures of the JB 1 E Cells. Tumour cells with a large vacuole and a flattened excentric nucleus were observed in suspension cultures of the JB 1 E cells (Fig. 1a). The percentage of 'balloon cells' was approximately

11% (500 cells studied). The vacuoles were not stained by PAS and alcian blue. The spindle-shaped cells attached to a solid surface did not contain any large vacuoles (Fig. 1b).

Spinner and Monolayer Cultures of Hela S3 Cells. Only a few 'balloon cells' were observed in suspension cultures of Hela S3 cells (Fig. 1c) and none in cells of monolayer cultures (Fig. 1d).

Phagocytosis of Latex Particles. Approximately 6–8% of the cells of both cell lines were able to phagocytize latex particles of 5.7 µm mean diameter. Only few latex particles were found in the large vacuoles in JB 1 E balloon cells.

JB 1 E Cells Treated with Nocodazole. The number of 'balloon cells' was significantly reduced in suspension cultures of JB 1 E cells treated with nocodazole. Only 1–2% of the cells developed large vacuoles.

TEM of 'Balloon Cells' in vitro. 'Balloon cells' formed in vitro resembled those observed in the ascites tumour. Golgi complex and vesicles were often observed in the vicinity of the vacuole membrane and vesicles often appeared to fuse with the vacuole membrane. Microfilaments and microtubules were located around the vacuole. Microfilaments often radiating out from the vacuole membrane. Vesicles and endoplasmic reticulum were found dispersed in the cytoplasm around the vacuole (Fig. 2a–b). The content of the vacuoles was structureless and no remnants of hetero- or autophagocytotic matter were observed. The content had a fluid character. In specimens stained during the fixation with ruthenium red the cell surface membranes were stained while the membranes of the cellular vacuoles remained unstained (Fig. 3).

DISCUSSION

Vacuolization of tumour cells is a general phenomenon and it has been observed in a variety of tumour cells (Weasel & Bernhard 1957; Tolnai 1964; Burns 1967; Chemnit *et al* 1974; Bader & Bader 1976).

Intracellular cysts of breast and gastric carcinoma cells often contain mucous material (Nevalainen & Järvi 1976). The Krukenberg tumour consists of metastatic carcinoma cells which are mucous producing. The distended cytoplasm and flattened nuclei of individual cells produce a signet ring appearance.

However the vacuole membrane was

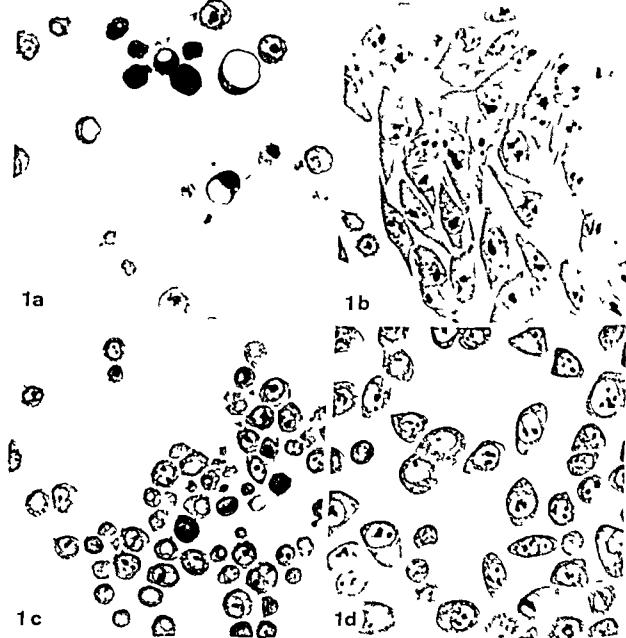


Fig 1a-d a) JB 1 E cells grown in spinner cultures. Typical balloon cells are present $\times 400$ b) JB 1 E cells grown as a monolayer. No balloon cells are seen among the attached spindle shaped cells $\times 400$ c + d) Hela S3 cells grown in suspension (c) and as monolayer (d). No balloon cells are present in either case $\times 400$

benzimidazol 2-yl) carbonyl R 17934) was obtained from Aldrich Chemical Company. IC Nocodazole is a new synthetic anticancer drug which interferes with the structure and function of microtubules both in interphase and mitosis (DeBrabander *et al* 1976). Before use nocodazole was dissolved in dimethylsulphoxide (DMSO). The usual concentration used in the experimental studies was $1 \mu\text{g/ml}$ culture medium.

Experimental Cultures

After centrifugation 8×10^6 cells of the JB 1 E and Hela S3 cell lines were inoculated separately into Bellco Spinner flasks containing 20 ml culture medium. The spinner flasks were aerated and incubated at 37°C for

24 h. stirring speed was set to 200–300 rpm. Simultaneously with the start of the spinner cultures cells from the respective stock cultures were inoculated into Nunc flasks (25 cm²) containing 5 ml culture medium. The flasks were aerated with a mixture of 5% CO₂ and 95% air and incubated at 37°C for 24 h. Spinner and monolayer cultures had a cell density of 400 000 cells/ml medium. To some of the spinner cultures nocodazole added ($1 \mu\text{g/ml}$ medium). The tumour cells were treated for 24 h.

Phagocytosis of Latex Particles 60×10^6 latex particles of $5.7 \mu\text{m}$ mean diameter were added to the suspension cultures with 20×10^6 JB 1 E or Hela S3 cells.

Light Microscopy

Pellets of untreated JB 1 E cells cultivated for 24 h in suspension cultures were obtained by centrifugation and were fixed in 4% formaldehyde, pH 6.8 for approximately 14 h, embedded in paraffin and sections of pellets were stained with one of the following dyes

Periodic acid Schiff (PAS) without nuclear staining (McManus and Mowry 1964)

Alcian blue (pH 3 and pH 1) (McManus and Mowry 1964)

TEM

After 24 h of growth the cultures were fixed using 5% glutaraldehyde buffered with P.M. buffer (polymerization mix) introduced by Lufsig *et al.* (1977). One exception was made concerning some of the spinner flasks containing 20×10^6 cells of the JB 1 E cell line: these cells were fixed with 2.5% glutaraldehyde buffered with 0.1 M Na cacodylate buffer 4% sucrose H 7.2 (fixative vehicle 300 mOsm) Ruthenium red (RR) was added to the fixative using the method of Luft as described by Behnke (1968). The cells were refixed at 37 °C for 2 h and postfixed in 1% OsO_4 for 3 h, and the further procedure is the same as described for the other spinner cultures.

Spinner Cultures The cells were fixed at 37 °C for 2–4 h, centrifuged for 10 min and the cell pellets were suspended in agar dissolved in warm PBS. After cooling in ice-water small cubes of agar were washed in 0.1 M cacodylate buffer (300 mOsm) pH 7.2 and postfixed in 1% OsO_4 in cacodylate buffer pH 7.2 for 1 h at 4 °C. After staining with 1% uranyl in re-distilled water for 1 h the cells were dehydrated in increasing conc. of acetone and embedded in Araldite.

Monolayer Cultures After fixation in 2.5% glutaraldehyde

selected areas were cut out of the bottom of the flask for sectioning.

Ultra thin sections from cultures pre stained with uranyl acetate were contrasted with 0.4% lead citrate at room temperature for 5 min. Ultra thin sections from cultures fixed with RR were contrasted with 1% zinc uranyl acetate at 60 °C for 10 min and 0.4% lead citrate at room temp for 5 min.

Semi thin sections were cut and stained with 1% toluidine blue and prepared for light microscopy.

RESULTS

Light Microscopy

Spinner and Monolayer Cultures of the JB 1-E Cells Tumour cells with a large vacuole and a flattened eccentric nucleus were observed in suspension cultures of the JB 1 E cells (Fig. 1a). The percentage of 'balloon cells' was approximately

11% (500 cells studied). The vacuoles were not stained by PAS and alcian blue. The spindle-shaped cells attached to a solid surface did not contain any large vacuoles (Fig. 1b).

Spinner and Monolayer Cultures of Hela S3 Cells Only a few 'balloon cells' were observed in suspension cultures of Hela S3 cells (Fig. 1c) and none in cells of monolayer cultures (Fig. 1d).

Phagocytosis of Latex Particles Approximately 6–8% of the cells of both cell lines were able to phagocytose latex particles of 5.7 μm mean diameter. Only few latex particles were found in the large vacuoles in JB 1-E balloon cells.

JB 1-E Cells Treated with Nocodazole The number of 'balloon cells' was significantly reduced in suspension cultures of JB 1-E cells treated with nocodazole. Only 1–2% of the cells developed large vacuoles.

TEM of 'Balloon Cells' in vitro 'Balloon cells' formed *in vitro* resembled those observed in the ascites tumour. Golgi complex and vesicles were often observed in the vicinity of the vacuole membrane, and vesicles often appeared to fuse with the vacuole membrane. Microfilaments and microtubules were located around the vacuole, microfilaments often radiating out from the vacuole membrane. Vesicles and endoplasmic reticulum were found dispersed in the cytoplasm around the vacuole (Fig. 2a–b). The content of the vacuoles was structureless, and no remnants of hetero- or autophagocytotic matter were observed. The content had a fluid character. In specimens stained during the fixation with ruthenium red the cell surface membranes were stained, while the membranes of the cellular vacuoles remained unstained (Fig. 3).

DISCUSSION

Vacuolization of tumour cells is a general phenomenon and it has been observed in a variety of tumour cells (Wessel & Bernhard 1957; Tolnai 1964; Burns 1967; Chemnitz *et al.* 1974; Bader & Bader 1976).

Intracellular cysts of breast and gastric carcinoma cells often contain mucous material (Nevalainen & Järvi 1976). The Krukenberg tumour consists of metastatic carcinoma cells which are mucous-producing. The distended cytoplasm and flattened nuclei of individual cells produce a signet ring appearance.

Histochemical methods have failed to give a positive reaction for mucous substances of 'balloon cells' in ascites tumours (Tolnai 1964; Chemnitz *et al.* 1974). However, the vacuole membrane was

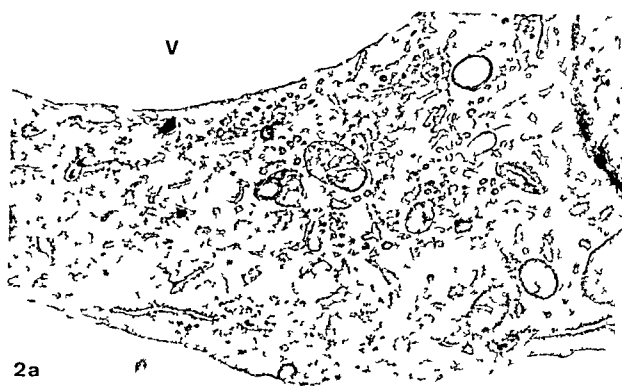


Fig 2 a-b a) A section through part of the cytoplasm around the large vacuole (V) in a balloon cell. The Golgi complex (G) and some vesicles are seen together with strands of smooth endoplasmic reticulum. Note the several small vesicles in relation to the Golgi complex and the vacuole membrane. $\times 6000$ b) A similar section showing that microfilaments are present beneath the vacuole and that some apparently are in association with the vacuole membrane. Mitochondria and vesicles (arrowheads) are seen among the filaments. $\times 78000$

stained with PAS and alcian blue (pH 2.5) indicating the presence of glycoproteins (Chemnitz *et al* 1974)

The morphology of JB1E cells grown in a suspension culture resembles the JB1 ascites

tumour *in vivo* (Chemnitz *et al* 1974). The balloon cells develop from regular JB1E cells indicating that some of the JB1E cells are able to develop large vacuoles when grown in suspension contrary to cells attached to a substrate



Fig 3 This micrograph demonstrates staining of the «balloon cells» with ruthenium red added to the fixative. Note the heavy staining of the surface membrane of the cell and the complete absence of staining of the membrane of the vacuole (V) $\times 99\ 000$

The large vacuoles are partly formed by membrane material accumulated in the cytoplasm. Morphological observations indicate the function of the Golgi complex in this process. Other elements of the vacuolar system also seem to contribute.

Besides the role of the Golgi complex in the anabolic functioning of the cell, the organelle also plays a substantial role in the catabolic functioning of the cell. The large vacuoles could be formed by the supplement of membrane material to hetero- and autophagocytotic processes in the cytoplasm. However, preliminary results have failed to show any cytochemical reaction for acid phosphatases in or near the large vacuoles (unpublished observations). RR staining indicates that at the time of fixation the large vacuoles are intracellular vacuoles having no communication with the extracellular environment.

Phagocytosis of large solid particles (latex beads) does not seem to be coupled with the formation of the large vacuoles.

vacuolization could also be a consequence of changes in membrane functions, especially in the regulation of membrane transport and/or membrane turnover.

Nevertheless, our results have shown a conspicuous difference in tumour cell behaviour due to culture conditions. The JB 1 E cell line showed a higher degree of heterogeneity than the Hela S3 cell line. It is indicated that the cytoplasmic microtubule complex is of importance in the process of vacuole formation, although the exact mechanism remains to be elucidated.

This study was supported by grants from Ingemann O. Buck's Fund and Carla Cornel's Stichting Møller's Legat. It is a pleasure to acknowledge the technical assistance of Mrs E. Berg, Mrs I. Holst, Mrs R. Lønstrup and Mr E. Pantou.

REFERENCES

- Bader A. V. & Bader J. P. Transformation of cells by Rous sarcoma virus. Cytoplasmic vacuolization. *J. Cell Physiol.* 87: 33-46, 1976.
- Behnke O. An electron microscope study of the megakaryocyte of the rat bone marrow. I. The development of the demarcation membrane system and the platelet surface coat. *J. Ultrastruct. Res.* 24: 412-433, 1968.
- Bichel P., Barfod N. M. & Jakobsen A. Employment of synchronized cells and flow microfluorometry in investigations on the JB 1 ascites tumour clones. *Vitrochows Arch. B Cell Pathol.* 19: 127-133, 1975.
- Burns E. R. Tumour cell - tumour cell emperipolesis. *Exp. Cell Res.* 48: 229-231, 1967.
- Chemnitz J., Skaaring P. & Bichel P. Light and electron microscopy of the JB 1 ascites tumour at different stages of growth. *Z. Krebsforsch.* 82: 111-131, 1974.
- Chemnitz J., Skaaring P. & Bichel P. Increasing occurrence of tumour cell - tumour cell emperipolesis in the regenerating JB 1 ascites tumour. *Z. Krebsforsch.* 84: 98-96, 1975.
- DeBrabander M. J., Van de Veire R. M. L., Aerts F. E. M., Borgers M. & Janssen P. A. J. The effects of methyl (5-(2-thienylcarbonyl)-1H-benzimidazol-2-yl) carbonate (R 17934, NSC 238159), a new synthetic antitumoral drug interfering with microtubules, on mammalian cells cultured in vitro. *Cancer Res.* 36: 905-916, 1976.

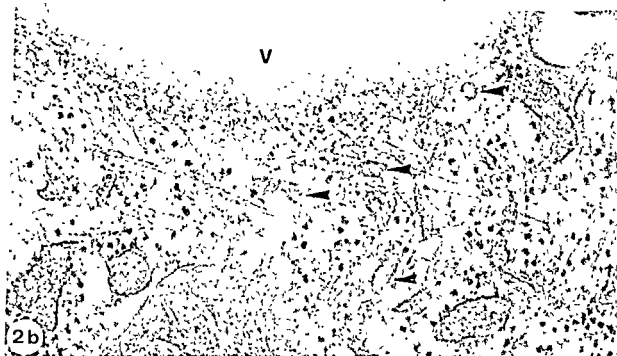
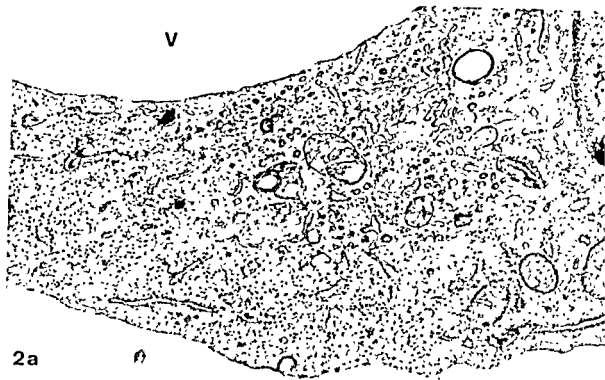


Fig. 2 a-b a) A section through part of the cytoplasm around the large vacuole (V) in a «balloon cell». The Golgi complex (G) and some vesicles are seen together with strands of smooth endoplasmic reticulum. Note the several small vesicles in relation to the Golgi complex and the vacuole membrane $\times 26,000$ b) A similar section showing that microfilaments are present beneath the vacuole and that some apparently are in association with the vacuole membrane. Microtubules and vesicles (arrowheads) are seen among the filaments $\times 78,000$

stained with PAS and alcian blue (pH 2.5), indicating the presence of glycoproteins (Chemnitz *et al* 1974)

The morphology of JB-1-E cells grown in a suspension culture resembles the JB-1 ascites

tumour *in vivo* (Chemnitz *et al* 1974). «The balloon cells» develop from regular JB-1-E cells, indicating that some of the JB-1-E cells are able to develop large vacuoles when grown in suspension, contrary to cells attached to a substrate.

A SILVER-GOLD IMPREGNATION TECHNIQUE FOR DEMONSTRATION OF STRIATED MUSCLE ELEMENTS

LARS GRIMELIUS and YNGVE OLSSON

Neuropathological Laboratory Institute of Pathology University of Uppsala Uppsala, Sweden

Grimelius L. & Olsson Y. A silver gold impregnation technique for demonstration of striated muscle elements. Acta path microbiol scand Sect. A 88 125-127 1980

A silver gold impregnation technique for demonstration of cross striations in skeletal muscles is presented. It is easily performed and all ingredients are chemically well characterized and easily available. The method has been successfully applied to formalin fixed paraffin-embedded material from human muscles and can be of value in the histopathological diagnosis of rhabdomyosarcomas and other tumors of muscular origin.

Key words: Silver gold histochemical technique muscle soft tissue tumors

L. Grmelius Institute of Pathology Uppsala University Box 553 S 751 22 Uppsala Sweden

Accepted as submitted 24 x 79

For certain diagnostic purposes demonstration of cross-striations in muscles is of crucial importance and optimal staining methods are then required. One example is the diagnosis of rhabdomyosarcomas.

We have previously described a silver gold impregnation technique for axons and neurofibrillary changes (Grimelius & Olsson 1978) and have noted that it could also be used for demonstration of cross-striations in muscles. We have now found that the staining is improved by initial oxidation of the sections and would therefore like to present one procedure which in our experience gives optimal results for human muscles.

MATERIAL AND METHODS

The cross striations were studied in small samples obtained from autopsies within 24 h after the death of the patient (in m. vastus lateralis gastrocnemius biceps brachii). In addition we have used mouse diaphragm and gastrocnemius muscle and gained some experience with human soft tissue tumors of muscular origin.

The samples measuring about 2 x 4 x 8 mm were fixed in 10% aqueous formalin for 24-78 h at room

temperature. After dehydration clearing in xylene and embedding in paraffin 5 µm thick longitudinal sections were cut. They were treated for 1 min in 0.025% potassium permanganate solved in re-distilled water. The sections were then bleached in 20% sodium bisulphite in re-distilled water for 15 sec, rinsed in 3 baths of re-distilled water each for 3 min and finally impregnated in silver gold according to Grmelius & Olsson (1978). Control sections were stained without preoxidization. All sections were mounted in Canada balsam.

RESULTS

In human muscles cross striations could easily be visualized with the original method but oxidation in potassium permanganate followed by bleaching resulted in the most distinct pictures (Fig. 1). This variation is therefore our method of choice and can also be applied to mouse muscles and biopsies from human rhabdomyosarcomas (Fig. 2).

Under low magnification the cross-striations in skeletal muscles appear as alternating dark and light bands. Higher magnification reveals that silver staining is most intense in the periphery of the A bands and in the Z line.

- Gez, G O, Coffman, W D & Kubicek, M T Tissue culture studies of the proliferative capacity of cervical carcinoma and normal epithelium *Cancer Res* 12 264-265, 1952
- Lufing, R B, McMillan, P N, Weatherbee, J A & Weihung, R R Increased visualization of microtubules by an improved fixation procedure *J Histochem Cytochem* 25 175-187, 1977
- McManus, J F A & Mowry, R W Staining Methods Histologic and Histochemical Harper and Row, New York, 1964
- Nesäläinen T J & Järvi, O H Intracellular cysts in gastric carcinoma *Acta path microbiol scand Sect A*, 84 517-522, 1976
- Seeger, P G Untersuchungen am Tumoraszites der Maus I Mitteilung Vitalfärbbarkeit der Asciteszellen *Arch exp Zellforsch* 20 280-335, 1937
- Selby, C C, Bieseke, J J & Grey, C E Electron microscopy studies of ascites tumor cells *Ann Acad Sci* 63 748-773, 1955-56
- Tolnai, S Cytological studies of »balloon cells« occurring in the Ehrlich ascites carcinoma *Canad J of Biochem* 42 1375-1381, 1964
- Tolnai, S An analysis of the life cycle of Ehrlich ascites tumor cells *Lab Invest* 14 No 6, Part 1, 701-710 1965
- Wessel, W und Bernhard, W Vergleichende elektron mikroskopische Untersuchung von Ehrlich - und Yoshida - Ascitestumorzellen *Z Krebsforsch* 62 140-162, 1957

REFERENCES

- Adams R D* Diseases of muscle 3rd ed Harper and Row New York 1975
- Bodian D* A new method of staining nerve fibres and nerve endings in mounted paraffin sections *Anat. Rec.* 65 89-97 1936
- Dempsey E W W* *Wislocke G B & Singer M* Some observations on the chemical cytology of striated muscle *Anat. Rec.* 96 221-248 1946
- Grimelius L & Olsson Y* A silver gold impregnation technique for routine neuropathological use *Acta neuropath. (Berl.)* 41 161-164 1978
- Van de Velde R L & Brown B A* A modified Bodian protargol stain for identification of striated muscle elements *Amer. J. Clin. Path.* 54 768-771 1970

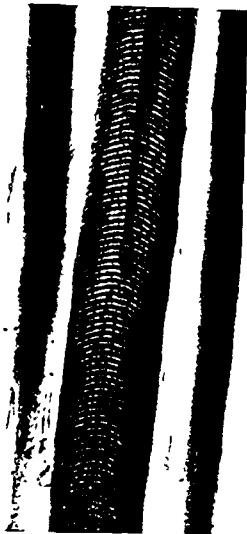


Fig 1 Longitudinal section from human skeletal muscle. Cross striations are distinctly visualized. Tissue treated according to our proposed method.

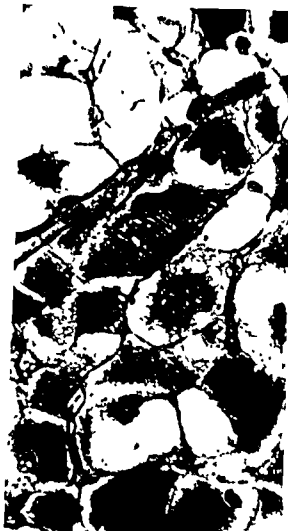


Fig 2 Tissue from a case of rhabdomyoma of adult type. The diagnosis of this rare tumor relies *inter alia* on the demonstration of cross striations in tumor cells which in this particular tumor type may be difficult to observe. Silver-gold staining according to our proposed method reveals easily visible striations in the cytoplasm of a tumor cell (arrow).

DISCUSSION

The most commonly used staining methods for demonstration of cross striations in skeletal muscle employ iron hematoxylin or phosphotungstic acid hematoxylin (Adams 1975). On the basis of our own data and on some other observations in the literature we would suggest metallic impregnation with silver-gold as an alternative when demonstration of cross-striations is required for diagnostic purposes.

There are only a few earlier reports on silver methods for visualization of cross-striations in muscle. Dempsey *et al* (1946) in a study on the histochemical properties of mammalian striated muscle noted that the Z disc is silver positive when using an ammonical silver nitrate method and the entire isotropic segment was stained by the Bodian procedure. Van de Velde and Brown (1970) also

described a modified version of the Bodian protargol method for the identification of striated muscle elements.

The method described by Bodian (1936) relies on silver proteinate (protargol), a chemical substance not fully chemically characterized. The quality of silver proteinate varies, therefore, often from one batch to another. As was pointed out by van de Velde and Brown (1970) the type of protargol determines whether or not staining of muscle will be successful. For routine use it must therefore be of value to apply a method like ours in which easily obtained, well characterized chemicals are used.

MICROFILAMENTS IN CELLS ASSOCIATED WITH INDUCED HETEROTOPIC BONE FORMATION IN GUINEA PIGS

An Immunofluorescence and Ultrastructural Study

RUNE NILSEN

Department of Oral Pathology and Forensic Odontology School of Dentistry University of Bergen
5016 Haukeland Hospital Norway

Nilsen R Microfilaments in Cells associated with induced heterotopic bone formation in guinea pigs
An immunofluorescence and ultrastructural study Acta path microbiol scand Sect A 88 129-134
1980

Sera from patients with active chronic hepatitis were used to demonstrate actin microfilaments in cells of a bone induced model. Demineralized and freeze dried allogenic dentine was implanted in the abdominal muscles of Guinea pigs. After 21 and 28 days the tissue was excised and showed a) resorption areas of the dentine contained dentinoclasts and macrophages b) osteoid and bone and c) areas of fibroblastic proliferation. Osteoblasts and young osteocytes showed the strongest fluorescent staining. Electron microscopy of these cells demonstrated abundant 5-7 nm microfilaments interpreted as actin in the outer parts and cell projections in which some microtubules also were observed. Fewer microfilaments were present in mature osteocytes although the cell projections in mineralized bone also showed microfilaments. Microfilaments were also found in some dentinoclasts where the actin was located in projections from the ruffled border protruding into the dentine. The localization in the ruffled border corresponded to the distribution of the fluorescent staining of actin. The high amount of actin in osteoblasts and osteocytes may be correlated to the synthesis and transport of the new matrix components. The microfilaments in the clear sealing zone of dentinoclasts were considered to have a function in the sealing of the ruffled border.

Key words: Actin, bone, immunofluorescence, transmission electron microscopy.

Rune Nilsen, Department of Oral Pathology and Forensic Odontology, School of Dentistry, University of Bergen, 5016 Haukeland Hospital, Norway.

Received 10 II 79 Accepted 1 XI 79

Microfilaments with a diameter of 5-7 nm are found beneath the plasma membrane of many non muscle cells and it has been shown ultrastructurally that these microfilaments interact with heavy meromyosin (Ushikawa *et al* 1969, Wessells *et al* 1971, Pollard & Weihing 1974). The actin-containing microfilaments are suggested to be contractile in cell motility, streaming, and contraction. Schreiner *et al* (1974) demonstrated binding of heavy meromyosin to

microfilaments in osteoblasts, osteocytes and osteoclasts.

Smooth muscle antibodies (SMA) appear in serum from ...

... and this SMA is directed against actin. This feature has been used to demonstrate actin by indirect immunofluorescence in smooth muscle (Johnson *et al* 1965) and other cell types (Groschel Stuart & Groschel 1974, Lazarides 1975).

MICROFILAMENTS IN CELLS ASSOCIATED WITH INDUCED HETEROTOPIC BONE FORMATION IN GUINEA PIGS

An Immunofluorescence and Ultrastructural Study

RUNE NILSEN

Department of Oral Pathology and Forensic Odontology School of Dentistry University of Bergen
5016 Haukeland Hospital Norway

Nilsen P. Microfilaments in cells associated with induced heterotopic bone formation in guinea pigs. An immunofluorescence and ultrastructural study. Acta path microbiol scand Sect A 88 129-134 1980

Sera from patients with active chronic hepatitis were used to demonstrate actin microfilaments in cells of a bone induced model. Demineralized and freeze dried allogenic dentine was implanted in the abdominal muscles of Guinea pigs. After 21 and 28 days the tissue was excised and showed a) resorption areas of the dentine contained dentinoclasts and macrophages, b) osteoid and bone and c) areas of fibrous tissue. Fewer actin microfilaments were found in the dentinoclasts and macrophages. Fewer actin microfilaments were found in the osteoblasts and osteocytes although the cell projections in mineralized bone also showed microfilaments. Microfilaments were also found in some dentinoclasts where the actin was located in projections from the ruffled border protruding into the dentine. The localization in the ruffled border corresponded to the distribution of the fluorescent staining of actin. The high amount of actin in osteoblasts and osteocytes may be correlated to the synthesis and transport of the new matrix components. The microfilaments in the clear sealing zone of dentinoclasts were considered to have a function in the sealing of the ruffled border.

Key words: Actin, bone, immunofluorescence, transmission electron microscopy.

Rune Nilsen, Department of Oral Pathology and Forensic Odontology, School of Dentistry, University of Bergen, 5016 Haukeland Hospital, Norway.

Received 10 ii 79 Accepted 1 xi 79

Microfilaments with a diameter of 5-7 nm are found beneath the plasma membrane of many non muscle cells and it has been shown ultrastructurally that these microfilaments interact with heavy meromyosin (Ushikawa *et al* 1969, Bessells *et al* 1971, Pollard & Wehling 1974). The actin-containing microfilaments are suggested to be involved in cell mobility (Pollard & Wehling 1974), cytoplasmic streaming (Palewitz *et al* 1974) and cytokinesis (Schroeder 1970). King & Hollop (1975) have demonstrated binding of heavy meromyosin to

microfilaments in osteoblasts, osteocytes and osteoclasts.

Smooth muscle antibodies (SMA) appear in serum from patients with active chronic hepatitis (Johnson *et al* 1965, Calkins *et al* 1971, & Ryan 1971). It has been shown that this SMA is directed against actin. This feature has been used to demonstrate actin by indirect immunofluorescence in smooth muscle (Johnson *et al* 1965) and other cell types (Groschel Stewart & Groschel 1974, Lazarides 1975).

Induction of heterotopic bone formation has been shown to occur after implantation of demineralized allogenic dentine in the abdominal muscles of rats and guinea pigs (Urist *et al* 1967, Bang 1973). Previous electron microscopic investigations using this experimental model demonstrated microfilaments peripherally in osteoblasts (Nilsen 1977).

In this study the presence and distribution of microfilaments have been studied ultrastructurally and correlated with the actin distribution as demonstrated by indirect immunofluorescence.

MATERIALS AND METHODS

Ten young male guinea pigs randomly bred were used. Each animal received 4 implants of allogenic demineralized and freeze dried dentine in the pouches of the abdominal muscles (Bang 1973). The animals were fed a standard diet (Norwegian standard for guinea pigs and rabbits Statens Institutt for Folkehelse Oslo Norway) supplemented with swedes and hay.

After 21 and 28 days respectively the animals 5 in each group were anesthetized with Nembutal® and the implants were excised with some surrounding tissue.

Electron Microscopy

One part of each implant was divided into small pieces (1 mm³) (altogether 80 specimens) and subsequently immersed in 2% glutaraldehyde in 0.1 M cacodylate buffer (pH 7.2) containing 7.5% sucrose (some at room temperature and some at +4 °C) and then postfixed in 2% OsO₄ in the same buffer. The specimens were then dehydrated and embedded in Epon 812. One µm thick sections were cut and stained with toluidine blue and the actual cellular zones were chosen, prepared and cut at 50–60 nm with a diamond knife on a Reichert Om U 3 ultramicrotome. The sections were collected on uncoated grids and double stained with uranyl acetate and lead citrate and examined in a Philips EM 300 electron microscope.

Immunofluorescence

The other part of each implant was directly frozen in isopentane precooled to -140 °C in liquid nitrogen and stored at -80 °C. Serum was taken from a patient with chronic active hepatitis containing specific antibodies against muscles (SMA serum). The titre was 1/128. The serum was also tested for mitochondrial and anti-DNA antibodies and showed negative reactions. In order to test the reproducibility of the results serum with smooth muscle antibodies from three other patients with chronic active hepatitis was used on all specimens in the same manner. Cryostat sections (7 µm) were obtained and washed twice with phosphate buffered saline (PBS) before immersion in cold acetone at +4 °C for 5 minutes. The sections were incubated with SMA serum diluted 1:8 to 1:20 in PBS and incubated in a moist chamber for 60 minutes. The preparations were then washed 3 times in PBS for 30 minutes and incubated for

another hour in a 1:20 dilution of rabbit antihuman IgG coupled to fluorescein isothiocyanate (FITC) (DAK immunoglobulin C ratio 2:3 antibody then washed 3 times immediately by incident light fluorescence microscopy (Leitz Ploem opaque illuminator filters 3.5 mm BG 1 and K 510).

Control sections were treated with 1. PBS or normal human serum 2. SMA serum neutralized by absorbent with homogenates of smooth muscle from rat stomach.

RESULTS

Transmission Electron Microscopy

The light and electron microscopical study demonstrated three main types of cellular reactions appearing consistently in all animals: a) resorption zones with dentinoclasts (multinucleated dentine resorbing giant cells morphologically identical to osteoclasts) and macrophages b) matrix production zones with osteoblasts osteocytes and a few chondroblasts and chondrocytes c) areas consisting of fibroblasts. All three zones were found after 21 days as well as 28 days. At 28 days however more mineralized bone was observed. For a detailed description of these cells see Nilsen (1977). Large amounts of new matrix were found to be produced in all animals.

A young connective tissue which surrounded the three zones exhibited only scattered granulocytes and lymphocytes. Skeletal muscle fibres occupied the outer parts of the specimens representing the abdominal muscles.

Osteoblasts and osteoid osteocytes regularly showed a distinct accumulation of microfilaments along and parallel to the cell membrane facing the newly formed osteoid (Fig. 1). These microfilaments had a diameter of 5–7 nm and seemed to be attached to the cell membrane and extended also into cell projections (Fig. 2). Quite a few of the cell projections of adjacent cells showed tight junctions. Scattered microtubules were observed in both cell projections and the cortical part of the osteoblasts and osteocytes when the specimens were fixed at room temperature. Tissue fixed at +4 °C showed fewer microtubules.

Both osteoid and mineralized bone showed abundant microfilaments in the cell projections. These microfilaments were longitudinally oriented. The mature osteocytes however lacked the distinct accumulation of microfilaments just beneath the cell membrane which was evident in osteoblasts and young osteocytes. Deeper parts of the cytoplasm of young matrix producing cells showed smaller bundles of microfilaments often



Fig 1 Peripheral microfilaments in an osteoid osteocyte. M microtubule (Arrow) Collagen (C) $\times 50\,000$

Fig 2 Longitudinal section of an extension from an osteoid osteocyte containing parallel microfilaments $\times 80\,000$

arranged parallel to the endoplasmatic reticulum.

The distribution of microfilaments was less evident in the resorbing cells than in the matrix producing cells. Areas of the ruffled border in some of the dentinoclasts however contained bundles of microfilaments. These microfilaments were found especially in cellular extensions from the clear sealing zone of the ruffled border (Fig 3). Microtubules however were not found in this area. Accumulation of microfilaments was also found in some macrophages. Fewer microfilaments were found in undifferentiated cells. In a few mature fibroblasts however a subcortical accumulation of microfilaments was demonstrated.

Immunofluorescence

In the young undifferentiated connective tissue surrounding the implants a bright green fluorescence was only found in vessels walls. A few fibroblasts however exhibited a moderate staining and the skeletal muscles had a strong positive immunofluorescence in the I bands.

All the osteoblasts and osteoid osteocytes showed strong cytoplasmic staining for actin (Fig 4). The staining appeared mainly in the periphery of the

osteoid osteocytes. The osteoblast region exhibited also strong cytoplasmic fluorescence. This staining was more diffusely outlined than in osteoid osteocytes. Osteocytes in the mineralized bone had just a weak fluorescent staining.

In some dentinoclasts a strong intracellular fluorescence was observed in the ruffled border area (Fig 4). Other dentinoclasts however had no evident fluorescence. Some macrophages in areas of resorption also showed cytoplasmic fluorescence. The cytoplasmic fluorescence staining in the matrix producing cells as well as the positive staining in dentinoclasts was diffusely outlined.

All the control preparations were negative and gave only low background fluorescence.

DISCUSSION

The cellular reactions to the implanted allogenic dentine including both osteoid and bone formation as well as resorption of dentine confirmed the previous reports of a specific induction of bone (Urist *et al.* 1967, Bang & Urist 1967, Bang 1973, Nilsen 1977). The close relationship between the



Fig 3 Microfilaments (arrow) in a cell extension ruffled border region of a dentinoclast $\times 36\ 900$



Fig 4 Indirect immunofluorescence showing an staining produced by SNA positive serum. N peripheral localization in osteoid osteocytes (A). Strong fluorescence was seen in the ruffled border of a dentinoclast (open arrow) lying in a resorptive lacuna in the dentine (D) $\times 400$

different reaction zones permitted comparison between the reaction zones within each section.

Large amounts of actin were found in the periphery of the osteoblasts and young osteocytes as well as in cell projections of these cells. Since muscle antibodies have not previously been used to show actin in bone cells, actin-containing microfilaments, however, have previously been demonstrated in cultured bone cells with heavy meromyosin, a specific ultrastructural marker (King & Heine, 1975). They suggested that the actin played a role in the intracellular transport of small molecules.

Microtubules were also found in the actin-containing areas in matrix-producing cells. Microfilaments and microtubules are proposed to constitute the contractile part of the cytoskeleton (Wessely *et al.* 1971).

The present study showed the greatest amount of actin in young osteocytes which are actin matrix-producing cells with only a low motility. The accumulation in these cells may then indicate a function of the microfilaments in the synthesis and transport of collagen precursors or other macromolecules. Active microfilaments in myofibroblasts in granulation tissue were recently proposed to be involved in synthesis and transport of type I collagen (Gabbiani *et al.* 1976). Microfilaments recently (Drenckhahn *et al.* 1977) suggested to be involved in transport and exocytosis in acinar cells of salivary glands.

The microfilaments and microtubules were observed in the cellular processes which also show tight junctions to other cellular processes from osteocytes. These findings may indicate a possible function of the microfilaments in the transport between the osteocytes. Other electronmicroscopic studies have proposed a possible transport function of the microfilaments (Stanka, 1975) and microtubules (Furseth, 1973) in the cell extensions.

The localization and amounts of actin in young osteoid osteocytes in the present report suggest a contribution to movements of the osteocytes within the lacunae. These amoeboid movements may have a role in movements of the extracellular fluid.

transport function on account of amoeboid movements of the osteocytes has been proposed previously by Bassett (1967)

The microfilaments may then be involved in both extracellular and intracellular transport of new matrix components

The ruffled border of some dentinoclasts in the present study showed a strong fluorescent reaction and ultrastructurally microfilaments were found to protrude into cell projections of the clear sealing zone. The observed arrangement of microfilaments in the ruffled border of dentinoclasts corresponded with ultrastructural findings in osteoclasts as reported by King & Holtrop (1975). In keeping with King & Holtrop (1975) microtubules were not observed in the ruffled border region. The ruffled border of dentinoclasts and osteoclasts is highly mobile and involved in active phagocytosis (Gothlin & Ericsson 1976). The actin distribution observed in the dentinoclasts of the present study could reflect the mobility of these cells.

The ruffled border with its clear zone is the active site of resorption of mineralized tissues. The clear sealing zone may have a function in making closed environments around the ruffled border in the active resorbing giant cells. This would make a reduction of pH possible which would explain the crystal-dissolving function of these giant cells (Schenk 1974).

The present study shows that the microfilaments could constitute a contractile part of this sealing area of the ruffled border.

The actin microfilaments seem to be involved in a variety of biological processes and this study suggests that they are involved in matrix production of bone as well as resorption of hard tissues.

I thank Mrs Turid Davidson for expert technical assistance. I am also greatly indebted to Dr philos Åge Flaugen for valuable advice and discussion.

REFERENCES

Andersen P, Thesrup Pedersen K & Ladefoged K. Studies of smooth muscle antibodies in active hepatitis. *Acta path microbiol Scand Sect C* 84: 365-371 1976.

Bang G. Induction of heterotopic bone formation by demineralized dentin in guinea pigs: relationship to time. *Acta path microbiol scand Sect A suppl* 236: 60-70 1973.

Bang G & Lriss M R. Bone induction in excavation chambers in matrix of decalcified dentin. *Arch Surg* 94: 781-789 1967.

Bassett C A L. Bone body fluid continuum as influenced by prolonged activity. In: *Human ecology*

in space flight. (Calloway D H ed) vol 11 p 132-135. New York: New York Academy of Science 1967.

Drenckhahn D, Gröchel Stewart U & Unsicker K. Immunofluorescence Microscopic Demonstration of Myosin and Actin in Salivary Glands and Exocrine Pancreas of the rat. *Cell Tiss Res* 183: 273-279 1977.

Furseith R. Tight junctions between osteocyte processes. *Scand J Dent Res* 81: 339-341 1973.

Gabbiani G, Ryan G B, Badonnel M C & Majno G. Smooth muscle antigens in platelets. Immunofluorescence detection using human a-smooth muscle serum. *Pathol Biol* 20: 6-8 1972.

Gabbiani G, Ryan G B, Lamelin P, Vassalli P, Manjor C, Bounier C A, Crushand A & Luscher E F. Human smooth muscle antibody: its identification as antiactin antibody and a study of its binding to non-muscular cells. *Am J Pathol* 72: 473-484 1973.

Gabbiani G & Ryan G. Development of a contractile apparatus in epithelial cells during epidermal and liver regeneration. *J Submicro Cytol* 6: 143-157 1974.

Gabbiani G, Le Lous M, Bailey A J, Barin S & Delaunay A. Collagen and myofibroblasts of granulation tissue: A chemical ultrastructural and immunological study. *Virchows Arch B Cell Path* 21: 133-145 1976.

Groschel Stewart U & Groschel D. Immunological evidence for the presence of smooth muscle type contractile fibres in mouse macrophages. *Experientia* 30: 1152-1153 1974.

Gothlin G & Ericsson J L E. The osteoclast. *Clin Orthop* 120: 201-231 1976.

Ishikawa H, Bischoff R & Holtzer H. Formation of arrowhead complexes with heavy meromyosin in a variety of cell types. *J Cell Biol* 43: 312-328 1969.

Johnson G D, Holbrook E J & Ghann L E. Antibody to smooth muscle in patients with liver disease. *Lancet* ii: 878-879 1965.

King G J & Holtrop M E. Actin like filaments in bone cells of cultured mouse calvaria as demonstrated by binding to heavy meromyosin. *J Cell Biol* 66: 445-451 1975.

La-arides E. Immunofluorescence studies on the structure of actin filaments in tissue culture cells. *J Histochem Cytochem* 23: 507-528 1975.

Lidman K, Biberfeld G, Fagraeus A, Norberg R, Torstenson R, Utter G, Carlsson Luca J & Lindberg U. Antiacin specificity of human smooth muscle antibodies in chronic active hepatitis. *Clin exp Immunol* 24: 266-272 1976.

Nilsen R. Electron microscopic studies on heterotopic bone formation in guinea pigs. *Arch Oral Biol* 22: 485-493 1977.

Palevitz B, Ash J & Hepler P K. Actin in green algae. *Natl Acad Sci USA* 71: 363-366 1974.

Pollard T D & Hethcote R R. Actin and myosin and

- cell movement *CRC Crit Rev Biochem* 2 1-65 1974
- Schenck R K* Ultrastruktur des Knochens *Verh Dtsch Ges Pathol* 58 72-83 1974
- Schroeder T E* The contractile ring 1 Fine structure of dividing mammalian (Hela) cells and the effect of cytochalasin B *Z Zellforsch* 109 431-449 1970
- Stanka P* Occurrence of cell junction and microfilaments in osteoblasts *Cell Tissue Res* 159 413-422 1975
- Urist M R Silverman B F Buring A Dubuc F L & Rosenberg J M* The bone induction principle *Clin Orthop Rel Res* 53 243-283 1967
- Wessells N A Spooner B S Ash J F Bradley M O Luduena M A Taylor E L A Wrenn J T & Yamada K M* Microfilaments in cellular and development processes *Science* 171 135 143 1971

STEREOMICROSCOPIC AND HISTOLOGIC CHANGES IN THE COLON OF GUINEA PIGS FED DEGRADED CARRAGEENAN

P SKOV OLSEN and S SEIER POULSEN

Anatomy Department B University of Copenhagen Denmark

Olsen Skov P & Poulsen Seier S Stereomicroscopic and histologic changes in the colon of guinea pigs fed degraded carrageenan Acta path microbiol scand Sect A 88 135-141 1980

A colitis like state was induced in Guinea Pigs fed degraded carrageenan orally By means of a combined semimacroscopic and histologic technique the course of the disease was followed during 28 days The changes were primarily seen and became most prominent in the caecum The first lesions were observed following 24 hours of treatment as small rounded foci initially with degenerative changes and inflammation in the surface epithelium later forming superficial focal ulcerations Ulcerative changes gradually progressed during the experiment forming linear and later large geographical ulcerations Topographically the ulcerative process was strongly related to the larger submucosal vessels Nonulcerated parts of the mucosa were not changed until following 7-14 days of treatment The mucosa became bulging granulated and finally villus like Accumulation of macrophages was found under the surface epithelium after 7-14 days Possible pathogenetic mechanisms are discussed especially the development of the early lesions and the significance of the macrophages

Key words Colon carrageenan stereomicroscopy histology

Stein Seier Poulsen Anatomy Department B University of Copenhagen the Panum Institute Blegdamsvej 3 DK 2200 Copenhagen N

Received 13 vi 79 Accepted 2 xi 79

Carrageenan is a sulphated polysaccharide derived from the red seaweed *Euchema Spinosum* It is widely used in the food industry as a stabilizer and emulgator (5)

In 1969 Marcus and Watt (11 20) reported that a colitis like disease can be induced in laboratory animals by oral administration of degraded carrageenan in the drinking water Undegraded (native) carrageenan was found to have the same effect but was less effective than the degraded form (20)

The colitis inducing effect of degraded carrageenan has been confirmed by other authors (3 8 12 16 19) Guinea pigs and rabbits are the most susceptible species (11 22 23) but colonic changes have been provoked also in rats and mice (11 23)

(13)

Several reports (2 3 8 12 19 20 22) have dealt with the histopathology of the colonic lesions induced by degraded carrageenan but the results have been varying and in some cases conflicting both as regards the development of the lesions and their localization Watt and Marcus (22) found the changes most pronounced in the caecum but also severe in the rectum and moderate in the rest of the colon Sharratt *et al* (16 17) found the disease almost confined to the caecum whereas van der Waaij *et al* (19) observed the most severe changes in the distal colon In the same way some reports (2 8 16) have considered the well-documented macrophage cytotoxic effect of carrageenan (4) to be the most important factor in the pathogenesis of the ulcerations while other reports (12 19) hardly mention the macrophages

The histopathological technique of investigating gastrointestinal specimens is improved and facilitated by the application of surface staining (9, 13, 14, 15). Following surface staining the structure of the mucosal surface is visualized in the stereomicroscope. Changed areas can be localized and subsequently examined histologically.

The aim of the present study has been by means of the combined stereomicroscopic and histologic technique to investigate the development of the colonic changes induced by degraded carrageenan and to describe the early lesions and the localization of the disease related to the duration of the treatment.

MATERIAL AND METHODS

42 smooth haired Guinea pigs average weight 560 g were given degraded carrageenan 5% in the drinking water. They were sacrificed in groups of six after 1, 2, 4, 7, 14, 21 and 28 days. During the experiment the animals received Purina Lab Chow *ad libitum*. The control material consisted of six untreated Guinea pigs.

For preparation of the colonic specimens the Guinea pigs were anaesthetized with Nembutal 50g/100g i.p. The abdomen was opened and after ligation at the distal end of ileum and rectum the entire colon was fixed *in situ* by direct intraluminal injection of 10% formalin. The colon was then removed and placed in formalin. After fixation for 10 minutes it was cut open antimesenterically and suspended on a polyethylene plate with fine needles. After further fixation for 24 hours the specimens were washed in water and stained with Alcian green 3BX 0.5% in 1% acetic acid for five minutes (9).

The entire specimens were studied under the stereomicroscope. Appropriate areas were photographed and subsequently taken out for histological examination. The section lines were indicated on stereomicroscopic photographs to permit an exact correlation between the stereomicroscopic and the histologic findings. The histological specimens were stained with PAS Hematoxylin Aurenthia and also with Alcian blue 1% in 0.1N HCl (pH 1) for identification of macrophages containing carrageenan (7).

RESULTS

In the surface stained specimens the crypt openings and the goblet cells clearly stand out dark green on a bright green background. In the controls the pattern of crypt openings was regular (Fig. 1). The goblet cells were mainly concentrated in and just around the crypt openings and were only occasionally seen in the surface epithelium. The mucosal surface was even.

Early Lesions

In the caecum and ascending colon delicate changes were observed already after 24 hours of treatment. In the stereomicroscope they were seen as small rounded dark foci 0.5–1 mm in diameter (Fig. 2a). The luminal parts of the crypt tubules were seen in the areas as white rings while the interjacent surface was stained dark green by the Alcian. In the caecum the small foci were regularly arranged in longitudinal rows closely related to the course of the larger submucosal vessels overlying the three tenia coli. In the ascending colon they were observed along the attachment of the mesentery.

Histological examination of the small foci (Fig. 2b) primarily showed a pronounced flattening of the surface epithelium with disorganization of the epithelial cells, lack of nuclear polarity and infiltration with a few leucocytes. In areas with changes a little more advanced the crypt epithelium was also affected. The crypt tubules seemed to degenerate, being narrow and shortened, leaving a gap between the base of the crypt and the muscularis mucosae. In some areas the crypt tubules had disappeared completely. In the lamina propria a moderate infiltration with leucocytes was observed.

Ulcerative Changes

After 2 and 4 days epithelial defects were seen in the small foci, forming punctuate ulcerations with well-defined edges (Fig. 3). The number of foci had increased and they had extended also along the transverse ramifications of the longitudinal vessels (Fig. 4).

After 7 days many of these small punctuate erosions had become confluent, forming shallow linear ulcerations (Fig. 4) mainly oriented longitudinally yet following the course of the larger vascular structures.

The ulcerative changes gradually progressed and in the fully developed stages as seen after 21 and 28 days of treatment the ulcerations were large, irregular and confluent, involving large parts of the mucosal surface (Fig. 5).

Histologically all the ulcerations were superficial. Penetration of the lamina muscularis mucosae was not observed. In the bottom of the ulcerations acute inflammatory exudate and granulation tissue was found.

The Appearance of the Non Ulcerated Mucosa

Within the first week of treatment the mucosal surface was flat as in the controls. After 7 days a local bulging was observed in the mucosa surrounding the ulcerations. The remaining surface was normal.

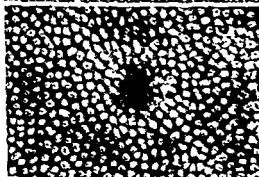
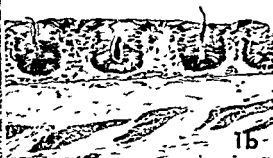
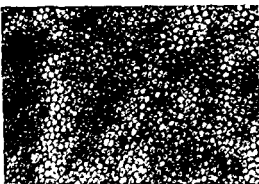


Fig 1a Stereomicroscopic appearance of the normal Guinea pig colon. The crypt tubules are seen as white rings with the dark crypt opening in the center (Alcian $\times 20$)

Fig 1b Corresponding histological section showing the appearance of the normal mucosa (PAS-Aurentia $\times 200$)

Fig 2a An early focal lesion observed as a rounded heavily stained area with blurred outlines of crypt openings (Alcian $\times 20$)

Fig 2b Corresponding histological section showing affection of the surface and crypt epithelium. The epithelium is infiltrated by inflammatory cells and the epithelial cells are disarranged and flattened (PAS Aurentia $\times 200$)

Fig 3a Punctate ulceration. A well defined superficial lesion surrounded by a mucosa with increased number of goblet cells in the surface epithelium (Alcian $\times 20$)

Fig 3b Corresponding histological section showing superficial ulceration. Lamina muscularis mucosa is unaffected (PAS Aurentia $\times 200$)

Diffuse changes in the mucosal surface structure were observed in the caecum and ascending colon after 14 and 21 days. They were most pronounced

in the caecum where the entire surface was bulging and granulated. After 28 days the bulging had progressed giving the surface a villus like appearance.



Fig 4 Several punctate and linear ulcerations following the course of the submucosal vascular structures. The mucosa surrounding the ulcerations is granulated (Alcian $\times 6.3$)

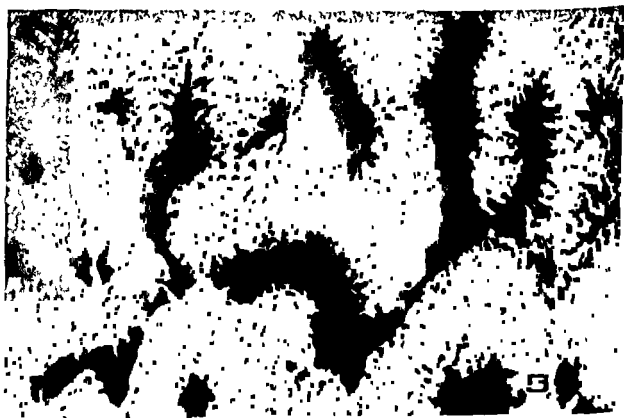


Fig 5 Several large ulcerations surrounded by a villus like mucosa (Alcian $\times 6.3$)



Fig 6a Villus like mucosa. Crypt openings may be seen between the villus like structures. Plenty of goblet cells are seen in the surface epithelium (Alcian $\times 10$)



Fig 6b Corresponding histological section showing villus like structures. Large numbers of PAS-positive macrophages are accumulated in the stroma beneath the surface epithelium (PAS-Aurentia $\times 200$)

rance (Fig 6a). In the ascending colon the changes were less pronounced. The surface was swollen slightly granulated, often of a gyriform appearance. In the distal colon changes were observed only around the ulcerations.

Histologically the stroma in non ulcerated areas was normal within the first week. In the bulging and villus like mucosa observed in the later stages plenty of large PAS positive macrophages were observed mostly located just beneath the surface epithelium (Fig 6b). The accumulation of macrophages was evident after 7–14 days of treatment. Besides there was edema and a moderate infiltration with acute and chronic inflammatory cells. The space between the crypt tubules was increased, but the epithelial cells in the crypt and surface epithelium appeared normal.

Localization of Disease

Changes can be classified as focal (ulcerative) and diffuse (surface contours, macrophage infiltration and edema). Focal changes developed considerably earlier than the diffuse changes and in less affected areas they were still the only changes.

The caecum was always the most affected part of the colon. Small punctuate lesions were observed in the caecum already after 24 hours, quickly progressing to form superficial erosions. The ulcerative changes gradually progressed during the 4 weeks of treatment from punctuate to linear and later large confluent ulcerations. Diffuse changes in non ulcerated parts of the mucosa were not observed until 14 days after initiation of treatment.

In the rest of the colon all changes appeared later and they never became as advanced as in the caecum. In this they had the same

morphology. Punctuate ulcerations were seen in the proximal colon after 4 days. They gradually spread distally and were found in the distal colon and rectum after 21 days. In these parts of the colon they remained small, never exceeding 2–3 mm in diameter. Changes in non ulcerated areas were only moderately developed and were not observed in the distal colon. The disease involves the proximal colon in the first place and subsequently spreads distally in continuity to the distal colon.

In the rectum however diffuse mucosal inflammation increased space between the crypt tubules and degeneration of the epithelium might be observed in the later stages.

DISCUSSION

When investigating the development of the colonic changes induced by degraded carrageenan it is essential to define the early lesions. Applying similar doses of carrageenan the early lesions previously have been described after 5–7 days (2, 8, 12). A sequence of events preceding ulceration has been proposed (2):

- 1) Penetration of carrageenan into the lamina propria
- 2) Accumulation of macrophages containing carrageenan under the surface epithelium
- 3) Release of lysosomal enzymes from the macrophages inducing inflammation and edema in the stroma followed by
- 4) degenerative changes and inflammation in the surface epithelium finally leading to
- 5) ulceration

In the present investigation early lesions were identified already after 24 hours. The first changes observed were

- 1) Focal affection of the surface epithelium
- 2) Affection of the crypt epithelium and acute inflammation in the mucosal stroma and finally
- 3) focal ulceration

Accumulation of macrophages was not observed at this early stage. A macrophage reaction was not evident until 7-14 days after initiation of treatment and was mostly observed in the bulging or villus-like mucosa. Considering that lesions developed within the first 24 hours of treatment the macrophage accumulation is hardly a part of the primary ulcerative process but rather a secondary foreign body reaction. This is moreover supported by the fact that even following direct s.c. injection of carrageenan accumulation of macrophages is only demonstrated after 5 days (24). Carrageenan is cytotoxic to macrophages (4). It is taken up and stored in the macrophages which are unable to sequester the compound (2, 10). Accumulation of macrophages and release of lysosomal enzymes may be involved in the development of the generalized - non ulcerative changes - as the heavy bulging of the mucosa as seen in the fully developed stages. This is in agreement with the observation in other studies that the aggregations of macrophages are connected with the bulging and villus like mucosa (2).

It has been discussed how the large carrageenan molecules (MW 30 000) are able to penetrate the intact surface epithelium (2, 8) which is necessary if the macrophage reaction is initiating the ulcerative process. The explanation may be that the permeability of the epithelium is increased secondarily to the acute affection of the surface epithelium.

This may also be the reason why the focal early changes are detected in the stereomicroscope as areas with increased stainability. The large Alcian molecules are probably able to penetrate the damaged epithelium in the focal areas and are retained in the lamina propria staining these areas dark green contrasting to the rest of the mucosal surface where the goblet cells are stained selectively.

In the present study strong topographical relationships have been observed between the larger submucosal vascular structures and the initial ulcerative process. This relationship has not been noticed in previous studies and we have no explanation for it. Further investigation will be needed to evaluate its pathogenetic significance.

The reason why the disease is most pronounced in the caecum of the Guinea pig might be that Guinea pigs like other ruminants have a large caecum in which the intestinal contents have a long transit time (18). The mucosal surface in the caecum

therefore is exposed earlier and for a longer time to the carrageenan than is the rest of the colon. Moreover, some of the carrageenan may be absorbed or decomposed in the caecum resulting in reduced contents of carrageenan in the rest of the colon.

It has been well documented that carrageenan is a biologically very active compound (6) with several possible side-effects. The important question is only whether it is absorbed or not. It has been discussed whether carrageenan might be an etiological factor in human ulcerative colitis (8, 11, 16, 17, 21, 22). This has been rejected since there are several pathological differences between experimental and human ulcerative colitis (8, 16, 17). Moreover only Guinea pigs and rabbits are sensitive to the undegraded form of carrageenan; the large molecules of which do not seem to be absorbed for instance by rats and monkeys (3, 8, 10). On the other hand it is possible that carrageenan is harmful to patients who already suffer from ulcerative colitis. In the present paper it has been proposed that carrageenan penetrates the surface epithelium only when this has been damaged primarily. In ulcerative colitis atrophy and necrosis are frequently observed in the surface epithelium. This may increase the risk of penetration of carrageenan. If the widespread application of carrageenan in the food industry should be questioned at all it would be reasonable initially to concentrate on this group of patients in order to find out whether carrageenan is absorbed by them or not and if it is whether it has any harmful effects.

REFERENCES

1. Abraham R, Goldberg L & Coulston F. Uptake and storage of degraded carrageenan in lysosomes of reticuloendothelial cells of the rhesus monkey. *Macaca Mulatta* Exp. Mol. Pathol. 17: 77-93, 1972.
2. Abraham R, Fabian R, J. Goldberg M, B. & Coulston F. Role of lysosomes in carrageenan induced cecal ulceration. *Gastroenterology* 67: 1169-1181, 1974.
3. Benni N, F. Goldberg L & Coulston F. Intestinal effects of carrageenan in the rhesus monkey. *Macaca Mulatta* Fed. Cosmet. Toxicol. vol. 11. Pergamon Press pp. 565-575, 1973.
4. Calanaro P, J. Schwartz H, J. & Graham R. C. Spectrum and possible mechanism of carrageenan cytotoxicity. *Amer. J. Path.* 64: 387-404, 1971.
5. Christensen O. Carrageenan a useful food additive. *Manuf.* 39: 49, 1964.
6. Di Rosa M. Biological properties of carrageenan. review. *J. Pharm. Pharmacol.* 24: 99-107, 1972.

- 7 Gangoli S D Wright M G & Grasso P Identification of carrageenan in mammalian tissues. An analytical and histochemical study. *Histochemical Journal* 5 37-48 1973
- 8 Grasso P Sharrat M Carpanini F M B & Gangoli S D Studies on carrageenan and large bowel ulceration in mammals. *Fd Cosmet Toxicol* vol 11 Pergamon Press pp 555-561 1973
- 9 Landboe Christensen E & Parapat S Staining of the mucosal surface of the human digestive tract. *IRCS* 2 1034 1974
- 10 Mankes R & Abraham R Lysosomal dysfunction in colonic submucosal macrophages of rhesus monkeys caused by degraded Iota carrageenan. *Proc Soc Exp Biol Med* 150 166-170 1975
- 11 Marcus R & Wall J Seaweeds and ulcerative colitis in laboratory animals. *Lancet* 2 489-490 1969
- 12 Onderdonk A B Hermos J A Dink J L & Bartlett J G Protective effect of Metronidazole in experimental ulcerative colitis. *Gastroenterology* 74 521-526 1978
- 13 Poulsen S S & Sabo S Mucosal surface morphology and histologic changes in the duodenum of the rat following administration of cysteamine. *Br J exp Path* 58 1-8 1977
- 14 Poulsen S S & Petri M Surface staining of small intestinal biopsies. *Scand J Gastroenterol* 12 235-240 1977
- 15 Poulsen S S Christensen N C Petri M & Jarnum S Stereomicroscopic examination of stained rectal biopsies. *Scand J Gastroenterol* 13 605-608 1978
- 16 Sharrat M Grasso P Carpanini F M B & Gangoli S D Carrageenan ulceration as a model for human ulcerative colitis. *Lancet* 2 932 1970
- 17 Sharrat M Grasso P Carpanini F M B & Gangoli S D Carrageenan ulceration as a model for human ulcerative colitis. *Lancet* 1 192-193 1971
- 18 Varga F Transit time changes with age in the gastrointestinal tract of the rat. *Digestion* 14 319-324 1976
- 19 Waay D van der Cohen B J & Amer D V M Mitigation of experimental inflammatory bowel disease in guinea pigs by selective elimination of the aerobic gram negative intestinal microflora. *Gastroenterology* 67 460-472 1974
- 20 Wall J & Marcus R Ulcerative colitis in the guinea pig caused by seaweed extract. *J Pharm Pharmacol* 21 suppl 1875-1885 1969
- 21 Wall J & Marcus R Hyperplastic mucosal changes in the rabbit colon produced by degraded carrageenan. *Gastroenterology* 59 760-768 1970
- 22 Wall J & Marcus R Carrageenan induced ulceration of the large intestine in the guinea pig. *Gut* 12 164-171 1971
- 23 Wall J & Marcus R Experimental ulcerative disease of the colon in animals. *Gut* 14 506-510 1973
- 24 Williams G Histological study of the connective tissue reaction to carrageenan. *J Path Bact* 73 557-563 1957

PROTEOGLYCANS, DNA, AND RNA IN RAT GRANULATION TISSUE, SKIN, AND AORTA BIOCHEMICAL AND HISTOLOGICAL STUDIES

T MØRK HANSEN C GARBARSCHE G HELIN P HELIN B HÖLUND
B KOFOD and I LORENZEN

Medical Department C Gentofte Hospital and Laboratory of Histochemistry and Cytochemistry
Anatomy Department A University of Copenhagen Department of Pathological Anatomy and
Department of Medicine Section of Rheumatology Hvidovre Hospital University of Copenhagen

Hansen T M Garbarsch C Helin G Helin P Hölund B Kofod B & Lorenzen I
Proteoglycans DNA and RNA in rat granulation tissue skin and aorta Biochemical and histological
studies Acta path microbiol scand Sect A 88 143-150 1980

Proteoglycans in skin and aorta and nucleic acids in skin were studied in rats with subcutaneous sponge implants and in unoperated rats and compared with the sponge induced granulation tissue during a 42 day period. In rat aorta there was a predominance of the sulphated glycosaminoglycans in particular heparan sulphate while in skin there was a predominance of hyaluronic acid and dermatan sulphate. The subcutaneous sponge implantation caused a decrease in the dry weights of skin and aorta but did not influence the concentrations of the measured variables. In aorta the concentrations of chondroitin sulphate and dermatan sulphate decreased with age while in skin there was a slight fall in the concentrations of hyaluronic acid and heparan sulphate with age. The rate of biosynthesis of proteoglycans as estimated from the ^{35}S sulphate uptake was higher in skin than in aorta. A sequential development was noticed in granulation tissue with an initial high content of hyaluronic acid followed by increasing amounts of chondroitin sulphate and dermatan sulphate in older granulation tissue. The RNA/DNA ratio reached a maximum in 14 day old granulation tissue but was unchanged in skin throughout the 42 day period. It is concluded that the distribution of proteoglycans and nucleic acids differs from tissue to tissue. This may be of relevance for tissue differences in susceptibility to diseases and to the effects - and side-effects - of drugs. The morphological and biochemical development of sponge induced granulation tissue from rats was similar to other types of granulation tissue during the first 4 weeks.

Key words: Proteoglycans, nucleic acids, granulation tissue, rats.

T Mørk Hansen, Medical Department, Section of Rheumatology, Hvidovre Hospital, Høstegaardsvej 30, DK-2650 Hvidovre, Denmark.

Received 17 v 79 Accepted 9 xi 79

The inflammatory process and the production of granulation tissue is part of the normal biological defence mechanism. The production of chronic granulation tissue, however, may also be one of the pathogenic alterations in diseases such as the rheumatic diseases. Information on the composition of connective tissue and granulation tissue may promote the understanding of the connective tissue diseases and be a guidance to appropriate medical

treatment. In a previous study (Hansen 1975) the collagen development in granulation tissue in subcutaneously implanted viscose cellulose sponges was compared with collagen of skin and aorta from rats implanted with sponges and from unoperated rats.

The purpose of the present investigation was to compare the proteoglycans and nucleic acids in granulation tissue, skin, and aorta of rats during a 42 day period after the induction of granulation

TABLE 1 Dry Defatted Weight (DDW) of Aorta (A) Skin Samples (S) and Granulation tissue (G) and the Concentration of Glycosaminoglycans (μg Hexosamine per mg DDW) and of RNA and DNA (μg Ribose and Deoxyribose per mg DDW) and $^{35}\text{SO}_4$ Incorporation in Glycosaminoglycans

		Days after sponge implantation							SD	P value
		0	4	8	14	22	33	42		
DDW	A	-O 12.1 +O	15.0 13.8	17.6 16.2	21.7 19.1	24.0 23.5	27.2 24.2	28.2 27.5	3.7	<0.01
	S	-O 185 +O	195 180	215 170	217 197	239 246	318 302	339 313	34	<0.01
	G		71	137	127	135	183	181	28	<0.01
	HA	A 0.26 S 0.44 G	0.43 0.45 0.54	0.21 0.48 0.45	0.22 0.45 0.40	0.20 0.39 0.31	0.26 0.37 0.21	0.17 0.40 0.24	0.24 0.08 0.12	ns <0.05 <0.01
	ChS	A 0.70 S 0.14 G	0.60 0.12 0.22	0.62 0.13 0.34	0.57 0.12 0.63	0.46 0.13 0.48	0.45 0.13 0.32	0.44 0.13 0.35	0.11 0.02 0.13	<0.01 ns <0.01
	DS	A 0.66 S 0.33 G	0.66 0.34 0.05	0.57 0.33 0.16	0.62 0.40 0.40	0.54 0.41 0.48	0.53 0.35 0.65	0.45 0.40 0.58	0.10 0.06 0.14	<0.01 ns <0.01
RNA	HS	A 0.76 S 0.11 G	0.78 0.12 0.07	0.77 0.09 0.08	0.79 0.10 0.08	0.89 0.09 0.10	0.84 0.08 0.12	0.87 0.09 0.13	0.19 0.02 0.05	ns <0.01 <0.05
	RNA	S 3.82 G	2.99 2.86	2.61 4.95	1.81 6.86	1.86 7.10	1.57 6.92	1.16 7.22	0.26 1.34	<0.01 <0.01
	DNA	S 2.15 G	1.82 4.23	1.54 3.33	1.01 3.56	1.05 4.14	0.92 4.46	0.63 4.65	0.20 0.82	<0.01 <0.01
	RNA/DNA	S 1.84 G	1.65 0.70	1.70 1.47	1.80 1.92	1.81 1.72	1.72 1.56	1.86 1.56	0.21 0.12	ns <0.01
	ChS	A 11.4 S 6.3			5.3 4.8			3.8 4.8	1.3 1.2	<0.01 <0.01
	DS + HS	A 12.6 S 19.3			6.1 18.0			4.2 15.5	1.4 3.8	<0.01 <0.05
^{35}S cpm mg ADW	ChS + DS + HS	G			9.1			10.0	2.4	ns

HA hyaluronic acid ChS chondroitin 4/6 sulphate DS dermatan sulphate HS heparan sulphate -/+ O -/+ operation with subcutaneous sponge implantation SD standard deviation within the groups P values derived by an analysis of variance ns not statistically significant ($P > 0.05$) (4-24 animals per group)

0.05 $P_{\text{HA}} < 0.01$) There was no detectable effect of the operation on the concentrations or total amounts of glycosaminoglycans or on the $^{35}\text{SO}_4$ uptake in aorta. In skin the concentrations of the glycosaminoglycans, the $^{35}\text{SO}_4$ uptake and RNA

and DNA were unaffected by the sponge implantation, whereas the total content per skin sample of hyaluronic acid, dermatan sulphate and heparan sulphate was decreased in accordance with the decrease in the total dry weight of the skin.

tissue. Skin and aorta from operated and unoperated rats were compared. Furthermore histological studies of the connective tissue development in subcutaneously implanted viscose cellulose sponges in rats were performed. Sponge granulation tissue from rats was compared with granulation tissue from rabbit aorta previously described (Helin *et al* 1971).

MATERIALS AND METHODS

108 male Sprague Dawley rats weighing 140–150 g were used. At the beginning of the experiment each of 48 rats had 2 viscose cellulose sponges of $1 \times 1 \times 2$ cm implanted subcutaneously symmetrically in the infrascapular region (Viljanio 1964). On the same day 12 unoperated animals were killed by decapitation. On the 4th, 8th, 22nd and 33rd day after the operation 6 operated and 6 unoperated animals were decapitated. On the 14th and 42nd day 12 operated and 12 unoperated animals were decapitated. The rats killed at the beginning of the experiment and on the 14th and 42nd day received 48 hours before decapitation $100 \mu\text{Ci } ^{35}\text{S}$ sulphate in 1 ml of physiological saline containing $120 \mu\text{g}$ unlabelled sodium sulphate.

Biochemical Analyses

The subcutaneously implanted sponges with their contents of granulation tissue were removed and freed from adherent connective tissue. Circular pieces of skin of 2.1 cm in diameter were taken from the lumbar regions 1–2 cm away from the skin wound in the sponge bearing rats. The hair of the skin was cut with an electrical hair cutter and the subcutaneous fat removed with a scalpel. The entire aorta from the aortic valve to the bifurcation was removed and the adventitia stripped off. All the samples were freeze dried ground with a Wiley mill defatted with chloroform/methanol (1/3) and dried *in vacuo*.

The glycosaminoglycans were isolated and determined as described by Thunell (1967). Samples were digested with papain for 6 hours at 67° and centrifuged to remove undigested material. Cetylpyridinium chloride was added to the supernatant. The precipitate was redissolved in *n*-propanol and again precipitated with ethanol as sodium salts. This precipitate was digested with hyaluronidase (testicular Leo Halsborg activity 15 000–20 000 IU/mg) overnight after which the glycosaminoglycans were fractionated on cellulose columns into depolymerized and nondepolymerized fractions. In samples from granulation tissue the salt precipitates were digested with nucleases before the hyaluronidase digestion because of the high content of nucleic acids.

The hexosamines were liberated by hydrolysis and the content of glucosamine and galactosamine in skin and aorta was determined by the use of a gas chromatograph (90 cm column 0.3 cm diameter SR 2300 100/120 Mesh 205°C) after transformation of the hexosamines to their alditolacetates dissolved in dimethylformamide. From granulation tissue the glucosamine and galactosamine were separated on a Dowex 50 microcolumn (An

tonopoulos 1966) and determined as hexosamines (E & Morgan 1933).

The total activity of ^{35}S sulphate in glycosaminoglycans in granulation tissue was determined after papain digestion and precipitation of the glycosaminoglycans with cetylpyridinium chloride. In skin and aorta the sulphate activities were determined separately in depolymerized and non-depolymerized glycosaminoglycans after the hyaluronidase digestion. All counts were performed in a liquid scintillation spectrometer (Packard model 3385).

The determinations of DNA and RNA were also performed in skin and granulation tissue owing to shortage of aortic tissue. The samples were boiled for minutes to inactivate nucleases before digestion with papain. After papain digestion the nucleic acids were precipitated with cadmium and the content of DNA and RNA determined according to the method of Hatcher & Goldstein (1969).

Histological Preparations

A 2 mm thick slice was cut from the middle of one of the implanted sponges from each animal. The tissue was fixed in 0.5% cetylpyridinium chloride in 4% formal (Williams & Jackson 1956) and the specimens were orientated in the paraffin so as to allow distinction between the superficial and the profound surfaces of the granulation tissue in the sponges.

The 6–8 μ thick sections were stained using the following staining methods:

- 1 Haematoxylin and eosin
 - 2 Van Gieson stain for collagen fibers (Lill *et al* 1965)
 - 3 Orcein staining for elastic fibers (Lillie 1965)
 - 4 Acid glycosaminoglycans were stained with
 - a 0.3% Alcian Blue 8GX (G.T. Gurr) at pH 1 and pH 2.5 (Pearse 1968) in order to distinguish between weakly and strongly sulphated mucosubstances
 - b 0.1% toluidine blue O (Merck) in 30% ethanol (Kramer & Windrum 1955)
 - c 0.1% toluidine blue in McIlvaine buffers at pH 1 and pH 3 and in Walpole buffers at pH 2 and pH 1 (modified after Kröger & Kasprzyk 1961)
 - 5 A combined method for acid glycosaminoglycans, elastic fibers, collagen fibers and nuclei (Garbarsch 1973)
 - 6 The Calcium red method of McGee & Russell as described by Pearse (1972) for calcium deposits
- The ingrowth of tissue into the sponges was measured on the cross sections with a Leitz ASM Image Analysis System at a magnification of $40\times$. The ingrowth was determined as the mean of the maximum ingrowth in 2 dimensions.

RESULTS

Biochemical Observations

The biochemical results are given in Table 1 and Fig. 1 and 2. The defatted dry weight of the aorta and skin samples was slightly smaller in sponge bearing rats than in unoperated animals ($P_{\text{aorta}} <$

TABLE 1 Dry Defatted Weight (DDW) of Aorta (A) Skin Samples (S), and Granulation tissue (G) and the concentration of Glycosaminoglycans (μg Hexosamine per mg DDW) and of RNA and DNA (μg Ribose and Deoxyribose per mg DDW) and $^{35}\text{SO}_4$ Incorporation in Glycosaminoglycans

		Days after sponge implantation							SD	P _{tme}
		0	4	8	14	22	33	42		
DDW	A	-O 12.1	15.0	17.6	21.7	24.0	27.2	28.2	3.7	<0.01
		+O	13.8	16.2	19.1	23.5	24.2	27.5		
	S	-O 185	195	215	217	239	318	339	34	<0.01
		+O	180	170	197	246	302	313		
	G		71	137	127	135	183	181	28	<0.01
HA	A	0.26	0.43	0.21	0.22	0.20	0.26	0.17	0.24	ns
	S	0.44	0.45	0.48	0.45	0.39	0.37	0.40	0.08	<0.05
	G		0.54	0.45	0.40	0.31	0.21	0.24	0.12	<0.01
ChS	A	0.70	0.60	0.62	0.57	0.46	0.45	0.44	0.11	<0.01
	S	0.14	0.12	0.13	0.12	0.13	0.13	0.13	0.02	ns
	G		0.22	0.34	0.63	0.48	0.32	0.35	0.13	<0.01
DS	A	0.66	0.66	0.57	0.62	0.54	0.53	0.45	0.10	<0.01
	S	0.33	0.34	0.33	0.40	0.41	0.35	0.40	0.06	ns
	G		0.05	0.16	0.40	0.48	0.65	0.58	0.14	<0.01
HS	A	0.76	0.78	0.77	0.79	0.89	0.84	0.87	0.19	ns
	S	0.11	0.12	0.09	0.10	0.09	0.08	0.09	0.02	<0.01
	G		0.07	0.08	0.08	0.10	0.12	0.13	0.05	<0.05
RNA	S	3.82	2.99	2.61	1.81	1.86	1.57	1.16	0.26	<0.01
	G		2.86	4.95	6.86	7.10	6.92	7.22	1.34	<0.01
DNA	S	2.15	1.82	1.54	1.01	1.05	0.92	0.63	0.20	<0.01
	G		4.23	3.33	3.56	4.14	4.46	4.65	0.82	<0.01
RNA/DNA	S	1.84	1.65	1.70	1.80	1.81	1.72	1.86	0.21	ns
	G		0.70	1.47	1.92	1.72	1.56	1.56	0.12	<0.01
ChS	A	11.4			5.3			3.8	1.3	<0.01
	S	6.3			4.8			4.8	1.2	<0.01
DS + HS	A	12.6			6.1			4.2	1.4	<0.01
	S	19.3			18.0			15.5	3.8	<0.05
ChS + DS + HS	G				9.1			10.0	2.4	ns

HA hyaluronic acid ChS chondroitin 4/6 sulphate DS dermatan sulphate HS heparan sulphate -/+O -/+ operation with subcutaneous sponge implantation SD standard deviation within the groups P values derived by an analysis of variance ns not statistically significant ($P > 0.05$) (4-24 animals per group)

0.05 $P < 0.01$) There was no detectable effect of the operation on the concentrations or total amounts of glycosaminoglycans or on the $^{35}\text{SO}_4$ uptake in aorta. In skin the concentrations of the glycosaminoglycans the $^{35}\text{SO}_4$ uptake and RNA

and DNA were unaffected by the sponge implantation whereas the total content per skin sample of hyaluronic acid dermatan sulphate and heparan sulphate was decreased in accordance with the decrease in the total dry weight of the skin.

tissue. Skin and aorta from operated and unoperated rats were compared. Furthermore, histological studies of the connective tissue development in subcutaneously implanted viscose cellulose sponges in rats were performed. Sponge granulation tissue from rats was compared with granulation tissue from rabbit aorta previously described (Helin *et al* 1971).

MATERIALS AND METHODS

108 male Sprague-Dawley rats weighing 140–150 g were used. At the beginning of the experiment each of 48 rats had 2 viscose cellulose sponges of $1 \times 1 \times 2$ cm implanted subcutaneously symmetrically in the infrascapular region (Viljanto 1964). On the same day 12 unoperated animals were killed by decapitation. On the 4th, 8th, 22nd and 33rd day after the operation 6 operated and 6 unoperated animals were decapitated. On the 14th and 42nd day 12 operated and 12 unoperated animals were decapitated. The rats killed at the beginning of the experiment and on the 14th and 42nd day received 48 hours before decapitation 100 μ Ci 35 S sulphate in 1 ml of physiological saline containing 120 μ g un-labelled sodium sulphate.

Biochemical Analyses

The subcutaneously implanted sponges with their contents of granulation tissue were removed and freed from adherent connective tissue. Circular pieces of skin of 2.1 cm in diameter were taken from the lumbar regions 1–2 cm away from the skin wound in the sponge bearing rats. The hair of the skin was cut with an electrical hair cutter and the subcutaneous fat removed with a scalpel. The entire aorta from the aortic valve to the bifurcation was removed and the adventitia stripped off. All the samples were freeze-dried ground with a Wiley mill defatted with chloroform/methanol (1/3) and dried *in vacuo*.

The glycosaminoglycans were isolated and determined as described by Thunell (1967). Samples were digested with papain for 6 hours at 67° and centrifuged to remove undigested material. Cetylpyridinium chloride was added to the supernatant. The precipitate was redissolved in *n*-propanol and again precipitated with ethanol as sodium salts. This precipitate was digested with hyaluronidase (testicular Leo Helsingborg activity 15 000–20 000 IU/mg) overnight after which the glycosaminoglycans were fractionated on cellulose columns into depolymerized and non depolymerized fractions. In samples from granulation tissue the salt-precipitates were digested with nucleases before the hyaluronidase digestion, because of the high content of nucleic acids.

The hexosamines were liberated by hydrolysis and the content of glucosamine and galactosamine in skin and aorta was determined by the use of a gas chromatograph (90 cm column, 0.3 cm diameter, SR 2300 100/120 Mesh, 205 °C) after transformation of the hexosamines to their alditolacetates dissolved in dimethylformamide. From granulation tissue the glucosamine and galactosamine were separated on a Dowex-50 microcolumn (An-

tonopoulos 1966) and determined as hexosamines (Elsa & Morgan 1933).

The total activity of 35 S sulphate in glycosaminoglycans in granulation tissue was determined after papain digestion and precipitation of the glycosaminoglycan with cetylpyridinium chloride. In skin and aorta the 35 S sulphate activities were determined separately in depolymerized and non depolymerized glycosaminoglycans after the hyaluronidase digestion. All counts were performed in a liquid scintillation spectrometer (Packard model 3385).

The determinations of DNA and RNA were only performed in skin and granulation tissue owing to a shortage of aortic tissue. The samples were boiled for 15 minutes to inactivate nucleases before digestion with papain. After papain digestion the nucleic acids were precipitated with cadmium and the content of DNA and RNA determined according to the method of Hatcher & Goldstein (1969).

Histological Preparations

A 2 mm thick slice was cut from the middle of one of the implanted sponges from each animal. The tissue was fixed in 0.5% cetylpyridinium chloride in 4% formalin (Williams & Jackson 1956) and the specimens were orientated in the paraffin so as to allow distinction between the superficial and the profound surfaces of the granulation tissue in the sponges.

The 6–8 μ thick sections were stained using the following staining methods:

- 1 Haematoxylin and eosin
- 2 Van Gieson stain for collagen fibers (Lillie 1965)
- 3 Orcein staining for elastic fibers (Lillie 1965)
- 4 Acid glycosaminoglycans were stained with a 0.3% Alcian Blue 8GX (G.T. Gurr) at pH 1 and pH 2.5 (Pearse 1968) in order to distinguish between weakly and strongly sulphated mucosubstances.
 - a 0.1% toluidine blue O (Merck) in 30% ethanol (Kramer & Windrum 1955)
 - c 0.1% toluidine blue in McIlvaine buffers at pH 5 and pH 3, and in Walpole buffers at pH 2 and pH 1 (modified after Krygier & Kasprzyk 1961)
- 5 A combined method for acid glycosaminoglycans, elastic fibers, collagen fibers and nuclei (Garbarsch 1973)
- 6 The Calcium red method of McGee Russell as described by Pearse (1972) for calcium deposits.

The ingrowth of tissue into the sponges was measured on the cross sections with a Leitz ASM Image Analysis System at a magnification of 40 \times . The ingrowth was determined as the mean of the maximum ingrowth in 2 dimensions.

RESULTS

Biochemical Observations

The biochemical results are given in Table 1 and Fig. 1 and 2. The defatted, dry weight of the aorta and skin samples was slightly smaller in sponge-bearing rats than in unoperated animals ($P_{\text{aorta}} <$

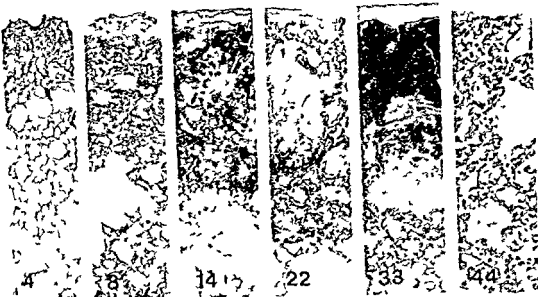


Fig 4 Ingrowth of granulation tissue into subcutaneously implanted viscose cellulose sponges in rats during a 42 day period (Toluidine blue $\times 18$). Numbers refer to days after the sponge implantation

that 50% of the total granulation tissue had been produced already 8 days after the sponge implantation and 90% after 22 days

A detailed description of the development of granulation tissue in the viscose cellulose sponge has been given by Holund *et al* (1979)

The sponge consisted of irregular outlined cellulose trabeculas unreactive to the stains employed

Four days after the implantation the interior of the sponge contained PAS positive amorphous material and numerous leucocytes. Capillaries and fibroblasts proliferated into the sponge behind a front of macrophages and a vanishing PTAH positive fibrinous network. A collagen capsule surrounded the sponge containing dispersed mast cells stained with orcein. PTAH Alcian blue at pH 1 and 2.5 and metachromatically with toluidine blue at all pH levels. In the capsule and the proliferating zone of fibroblasts spots of amorphous intercellular substance alcinophilic at pH 1 and 2.5 and metachromatic below pH 5 accumulated. Some foreign body giant cells were lodged on the peripheral trabeculas

On day 8 the capsule was more prominent with coarser collagen fibers and numerous arterioles. Among the proliferating fibroblasts dispersed granulocytes and mononuclear cells were noticed. The polymorphous leucocytes in the sponge exhibited karyorrhexis and karyolysis. Foreign body giant cells appeared

originally as fusing macrophages. Areas with metachromasia at pH 7 and pH 5 and alcinophilic were observed between the proliferating



Fig 5 Macrophages in the front of the proliferation of granulation tissue after 14 days of sponge implantation. The macrophages contain integrated material from the interior of the sponge (Toluidine blue $\times 320$)

A marked tissue difference was noticed in the glycosaminoglycan pattern (Table 1) In aorta, there was a predominance of the sulphated glycosaminoglycans, in particular heparan sulphate, while the concentration of hyaluronic acid was lower in aorta than in skin and granulation tissue In skin, there was a predominance of hyaluronic acid and dermatan sulphate In granulation tissue, the glycosaminoglycan pattern changed distinctly with age A high concentration of hyaluronic acid was noticed during the first week of granulation tissue production and fell thereafter The concentration of chondroitin 4/6 sulphate reached a maximum at 2 weeks while the concentration of dermatan sulphate reached a maximum after 4 weeks The concentration of heparan sulphate was small in granulation tissue in comparison with the other glycosaminoglycans The total contents of the glycosaminoglycans in granulation tissue showed the same maxima as the concentrations (Fig. 1) In aorta there was a fall in the concentrations of chondroitin 4/6 sulphate and dermatan sulphate, while in skin there was a fall in the concentrations of hyaluronic acid and heparan sulphate with time The total contents of the different glycosaminoglycans, however increased with time in both aorta and skin

The incorporation of ^{35}S sulphate in the glycosaminoglycans per mg dry defatted weight decreased with time in aorta and skin while there was no difference in granulation tissue between 14 and 42 days The incorporation of ^{35}S sulphate was higher in dermatan sulphate + heparan sulphate than in chondroitin 4/6 sulphate in skin but not in aorta The total incorporation of $^{35}\text{SO}_4$ per mg dry defatted weight was higher in skin than in aorta and

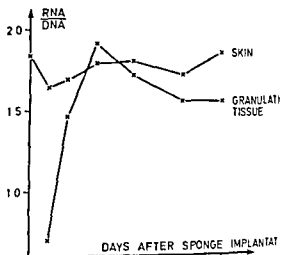


Fig. 2 RNA/DNA ratio in skin and sponge induced granulation tissue in rats

granulation tissue The total $^{35}\text{SO}_4$ uptake in glycosaminoglycans per sample decreased in aorta with time but increased in skin and granulation tissue

The concentrations and total amounts of DNA and RNA decreased with time in skin and increased in granulation tissue There was no change with time in RNA/DNA ratio in the skin while in granulation tissue the ratio increased to a maximum at 14 days (Fig. 2)

Histological Observations

The one-dimensional ingrowth of granulation tissue into the sponge reached a maximum after 42 days of implantation (Fig. 3 and 4) A calculation of the three dimensional ingrowth however shows

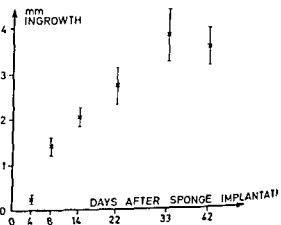
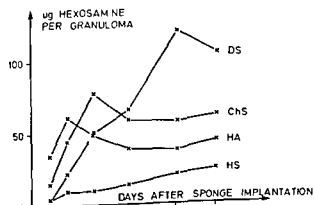


Fig. 3 Ingrowth of granulation tissue into subcutaneously implanted viscose cellulose sponges in rats during 42 day period The bars indicate the standard deviation of the means

The morphological development of granulation tissue in viscose cellulose sponges in the present investigation accords with that of previous investigations (Thomasson *et al* 1973, Pallin *et al* 1975) but in these studies giant cells are not mentioned. This lack of giant cells may be due to differences in sizes of pores (Sahatore *et al* 1961) or other physical characteristics of the sponges (Bing 1955) since the sponge material itself was the same. The histology of the granulation tissue in viscose sponge and in different plastic sponge materials (Bing 1955, Edwards *et al* 1957, Kelly 1962, Bole *et al* 1962, Wiener *et al* 1975) also corresponds mutually although there are a few differences (Holund *et al* 1979).

The glycosaminoglycans in the sponge are histochemically reflected by the metachromasia and the alcianophilia (Bole *et al* 1962, Kelly 1962). In the present investigation however the metachromasia did not correspond well with the content of sulphated glycosaminoglycans in the intercellular substance in contradistinction to the alcianophilia. This may be due to the competitive protein effect on the anions at low pH levels (Kelly 1955, Andersen and Ehlers 1967) and to binding of the sulphated glycosaminoglycans to the collagen (Sugiyama 1972).

In conclusion the content and distribution of glycosaminoglycans and nucleic acids differs from tissue to tissue. The sequential development of glycosaminoglycans and the histological observations are similar in granulation tissue from different sources although the duration of the production of granulation tissue may depend on the tissue and the type of induction of inflammation.

This work was supported by grants from the Danish Medical Research Council and The Association Against Rheumatism.

REFERENCES

- Andersen H & Ehlers N. Deamination to prevent the competitive effect of proteins in the metachromatic staining of sections at low pH values. *Histochemie* 8: 252-263, 1967.
- Antonopoulos C A. Separation of glucosamine and galactosamine on the microgram scale and their quantitative determination. *Ark. kem.* 25: 243-247, 1966.
- Bales A J & Robins S P. Development and maturation of the crosslinks in the collagen fibres of skin. In Robert L & Robert B (Eds) *Frontiers of matrix biology* vol 1. Karger Basel 1973 p 130-156.
- Bentley J P. Mucopolysaccharide synthesis in healing wounds. In Dunphy J E & van Winkle Jr W (Eds) *Repair and regeneration*. Mc Graw Hill Book Company New York Toronto Sydney London 1968 p 151-160.
- Berenson G S & Dofferer E R. Identification of acid mucopolysaccharides from granulation tissue in rat. *Brit J exp Path* 41: 422-429, 1960.
- Bing J. The tissue reaction to implanted plasucs. *Acta pathol microbiol scand* 105: 16-26, 1955.
- Bole G G & Robinson W D. Histochemical and biochemical variations in the connective tissue in polyvinyl alcohol sponge implants. *J Lab clin Med* 59: 713-729, 1962.
- Edwards L C, Pernokas L N & Dunphy J E. The use of a plastic sponge to sample regenerating tissue in healing wounds. *Surg Gynec Obstet* 105: 303-309, 1957.
- Elson L A & Morgan W T J. A colorimetric method for the determination of glucosamine and chondrosamine. *Biochem J* 27: 1824-1828, 1933.
- Garbarsch C II. Enzyme histochemistry of rabbit thoracic aorta following a single mechanical dilation injury. *Acta histochem* 46: 300-313, 1973.
- Hansen T M. Collagen development in granulation tissue as compared with collagen of skin and aorta from injured and non injured rats. *Acta pathol microbiol scand Sect A* 83: 721-732, 1975.
- Hatcher D W & Goldstein G. Improved methods for determination of RNA and DNA. *Anal Biochem* 31: 42-50, 1969.
- Helin P, Lorenzen I, Garbarsch C & Matthiessen M E. Repair in arterial tissue. Morphological and biochemical changes in rabbit aorta after a single dilatation injury. *Circul Res* 29: 542-554, 1971.
- Holund B, Junker P, Garbarsch C, Christoffersen P & Lorenzen I. Formation of granulation tissue in subcutaneously implanted sponges in rats. A comparison between granulation tissue developed in viscose cellulose sponges (V isella®) and in polyvinyl alcohol sponges (Ivalon®). *Acta pathol microbiol scand Sect A* 87: 367-374, 1979.
- Kelly J W. Suppression of metachromasy by basic proteins. *Acta biochem* 55: 130-137, 1955.
- Kelly Jr E W. Histology of sponge implant in the albino rat. *Arch Pathol* 74: 72-80, 1962.
- Kirckheiner B. C vitamin mangels indflydelse på binde væv. Munksgaard København 1968 p 1-131.
- Kramer H & Windrum G M. The metachromatic staining reaction. *J Histochem Cytochem* 3: 227-237, 1955.
- Krygier A & Kasprzyk K. The influence of hydrogen ion concentrations and some other ions on metachromasia in staining mucopolysaccharides with toluidine blue. *Acta Med Pol* 2: 123-145, 1961.
- Lampiaho K & Kulonen E. Metabolic phases during the development of granulation tissue. *Biochem J* 105: 333-341, 1967.
- Lehtonen A. The mucopolysaccharides in ageing experimental granulation tissue. *Acta physiol scand suppl* 310, 1968.
- Lille R D. Histopathologic technique and practical histochemistry. 3ed. Mc Graw Hill Book Co. New York Toronto-Sydney London, 1965.



Fig 6 Fibrinoid substance in 33 day old granulation tissue (PTAH $\times 100$)

ting centrally located cells besides a general weak alcianophilia at pH 1 and pH 2.5

On day 14 peripheral giant cells filled with pyknotic nuclei seemed to disintegrate in some places and mononuclear cells accumulated around the trabeculas in these areas. The macrophages at the front of the proliferating fibroblasts contained nuclear material from the leucocytes in the interior of the sponge (Fig. 5).

On day 22 lymphocytes and plasma cells were observed; the fibroblasts had propagated further centrally and the number of leucocytes in the sponge interior was diminished. Accumulation of alcianophilic amorphous intercellular substance was observed, but no metachromasia was seen below pH 2.

On days 33 and 42 most of the sponges were filled with connective tissue and the central accumulation of leucocytes vanished. Fat cells extended from the capsule into the outer part of the loose connective tissue in the sponge. In some sponges »fibrinoid« substances characterized by eosinophilia, PTAH-positivity and a weak PAS-positivity were observed (Fig. 6).

DISCUSSION

As for collagen (Bailey & Robins 1973) differences in glycosaminoglycan pattern between tissues are greater than the differences between the same

tissues from different species (Stefanovich & Akijama 1970, Utto et al 1971, Helin et al 1971).

The relatively higher rate of synthesis of dermatan sulphate and heparan sulphate in skin than in aorta as estimated from the $^{35}\text{SO}_4$ incorporations of these proteoglycans is consistent with a high turnover in skin than in aorta. The decrease in the concentrations of hyaluronic acid, heparan sulphate in skin and of chondroitin sulphate and dermatan sulphate in aorta is in due to a dilution effect caused by increased amounts of for example, collagen and elastin (Hansen 1975) as the total content of glycosaminoglycans in skin and aorta increased with time. Although the cell content per skin area as estimated from the DNA and RNA content decreased with time, the ability of proteoglycan synthesis (^{35}S uptake) was increased. This indicates either that decrease in cell content is confined to other cell types than those synthesizing proteoglycans or that capacity of the individual cells to synthesize proteoglycans increases with time.

In granulation tissue the initial high level DNA and low RNA/DNA ratio may be explained by a high content of leucocytes which do not synthesize protein. This is in accordance with experiments by Pallin et al (1975) who aspirated leucocytes from sponge granulation tissue and determined the DNA and RNA content. The maximum RNA/DNA ratio in granulation tissue was achieved after 14 days at the time of maximum collagen synthesis (Lampiaho & Kulonen 1967).

The variation with time of glycosaminoglycans in granulation tissue (Fig. 1) is in agreement with other studies of granulation tissue (Berenson et al 1960, Dalferes 1960, White et al 1961, Kirckheiner 1966, Bentley 1968, Reid & Flint 1974), but differs from the observations by Lehtonen (1968). This difference may be explained by interference from nucleic acids (Thunell 1967) which in the present study was overcome by digestion with nucleases.

The production of granulation tissue in the subcutaneously implanted viscose cellulose sponge seemed to cease after 33 days (Fig. 1, 3 and 4). This is in contrast to the injured rabbit aorta where the production of granulation tissue and proteoglycan continued beyond 60 days (Helin et al 1971). The difference may be due either to the continuous haemodynamic stimulus of the vascular wall or to the different reactivity of the smooth muscle cells in a bradytrophic tissue. The production of proteoglycans with time in sponge granulation tissue was similar to that of granulation tissue of aorta. Morphological studies also showed the same phases in the inflammatory reaction and fibroproductive processes (Helin et al 1971, Garbarsch 1973).

PULMONARY BLASTOMA

A Clinico-Pathological Study of Eleven Cases

MARIANNE JACOBSEN* and DORTHE FRANCIS**

The Department of Pathology Bispebjerg Hospital 2400 Copenhagen NV Denmark

Jacobsen M & Francis D Pulmonary blastoma A clinico pathological study of eleven cases Acta path microbiol scand Sect A 88 151-160 1980

Eleven cases of pulmonary blastoma are presented the largest series reported from one department to date The frequency of pulmonary blastoma was found to be 0.5 per cent of all primary lung cancers The variegated histologic appearance of the tumour and the diverging metastatic pattern are described in detail In light of the complex histological picture and the biological behaviour a suggestion of the histogenesis of pulmonary blastoma is attempted

Key words Pulmonary blastoma frequency

Marianne Jacobsen Emiliekløvedej 54 2930 Klampenborg Denmark

Accepted as submitted 27 xi 79

Pulmonary Blastoma (PB) is a very rare primary lung tumour consisting of a mixture of immature epithelial and mesenchymal components The tumour was first reported in 1945 by Barrett and Barnard (2) and was again reported by Barnard in 1952 (1) In 1961 Spencer (25) added three further cases and defined the tumour entity He drew attention to the similarities to nephroblastoma and suggested the commonly used term pulmonary blastoma Indeed based on the number of cases previously reported it would seem to be rare however between 1971 and 1978 11 cases were diagnosed from amongst the lung tumour cases at the Department of Pathology at Bispebjerg Hospital In view of this unprecedented number of cases we are prompted to describe their clinico pathological findings

MATERIAL AND METHODS

During the period 1971-1978 nine cases of PB were diagnosed at Bispebjerg Hospital and another two

typical cases were revealed by a survey of the microscopic material from all malignant primary lung tumours diagnosed during the same period as sarcomas or mixed tumours The criterion for the diagnosis PB was a tumour consisting of both an immature mesenchymal and an epithelial component in accordance with the description given by Spencer (26) Monotypic or doubtful cases of PB were not included in this material For comparison all malignant primary lung tumours diagnosed at Bispebjerg Hospital from 1973 to 1975 were registered and recorded as to histological type (17)

RESULTS

In Table 1 the 11 cases are presented Two were women and nine men and the mean age was 67 years

Ten patients had a brief duration of symptoms One patient (case 2) had had a known atelectasis for seven years before severe expectoration led to resection despite an impaired lung function In one patient (case 8) a lung infiltrate was found at

*Department of Pathology Herlev Hospital University of Copenhagen 2730 Herlev

**Department of Pathology Frederiksborg County Hospital 3400 Hillerød

autopsy two weeks later In two patients (cases 10

- Pallin B Ahonen J Rank F & Zederfeldt B Granulation tissue formation in viscose cellulose sponges of different design *Acta chir scand* 141 697-701 1975
- Pearse A G E Histochemistry theoretical and applied Churchill Livingstone Edinburgh and London vol 1 1968
- Pearse A G E Histochemistry theoretical and applied Churchill Livingstone Edinburgh and London vol 2 1972
- Reid T & Flint M Changes in glycosaminoglycan content of healing rabbit tendon *J Embryol exp Morph* 2 489-495 1974
- Savatore J E Gilmer W S Kashgarian M & Barbee W R An experimental study of the influence of pore size of implanted polyurethane sponges upon subsequent tissue formation *Surg Gynec Obstet* 112 463-468 1961
- Stefanovich I & Akiyama A Comparative studies of aortic acid mucopolysaccharides in fifteen species *Comp biochem physiol* 34 125-130 1970
- Sugihama T Histochemical demonstration of collagen masked mucopolysaccharides In Takeuchi T Ogawa A & Fujita S (Eds) Histochemistry and cytochemistry Proceedings of the international congress of histochemistry and cytochemistry august 21st to 26th Kyoto Japan 1972 p 81-82
- Thomasson B Vilyanto J Jaaskola A & Raekallio J Enzyme histochemical observation on the formation of granulation tissue in rabbit fetuses and does *Acta Chir Scand* 139 327-333 1973
- Thunell S Procedures for the micro scale investigation of vessel wall glycosaminoglycans *Acta Univ Lund Sec 2* 1967 91
- Uitto J Helin G Helin P & Lorenzen I Connective tissue in scleroderma *Acta Dermatovenereol* 51 401-406 1971
- Vilyanto J Biochemical basis of tensile strength in wound healing An experimental study with viscose cellulose sponges in rats *Acta chir scand Suppl* 333 25-27 1964
- White B N Shetlar M R & Schilling J A Tissue glycoproteins and their relationship to the healing of wounds *Ann NY acad Sci* 94 297-307 1961
- Wiener S L Wiener R Platt N Urvelsky M & Mellman E The need for modification of the polyvinyl sponge model of connective tissue growth Histologic and biochemical studies in rabbit Connective tissue res 3 213-225 1975
- Williams G & Jackson D C Two organic fixatives for acid mucopolysaccharides *Stain Technol* 31 189-191 1956

and 11) lung infiltrates were diagnosed during invagation of arteriosclerotic heart disease which made them inoperable

The tumours were right sided in seven cases and left-sided in four. In eight cases the tumour was confined to one lobe, in one case to two neighbouring lobes and in two cases the tumour involved parts of all three lobes of the right lung.

Gross Pathology

The tumours were rounded, rather well demarcated and surrounded by a pseudocapsule of compressed lung tissue or bronchial wall which further investigation showed to be invaded by tumour growth. The tumour size ranged from 2.5 cm to 10 cm in diameter. In five cases (cases 2, 3, 5, 8, 9) the tumours showed partly intrabronchial growth, part of which appeared as smooth polypoid grape-like processes free of the bronchial mucosa. In one case (case 10) a similar smooth finger-like process was seen in a branch of a pulmonary vein extending into the left auricle of the heart. The cut surface of the tumours was smooth and bulging and on inspection was greyish white to pink with scattered haemorrhages and necroses. The consistency was rather soft. In two cases (cases 2 and 4) a central part of the tumour matched the above description, the surrounding tumour tissue being greyish to yellow and rather dry with a plane cut surface.

Microscopic Findings

Some histologic features of the tumours are listed in Table 1. All tumours showed a blastomatous or undifferentiated mesenchymal component and an epithelial component. The components were mixed and present in varying amounts in different sections of the tumours and showed several types of differentiation and varying degrees of maturation. Besides the typical blastomatous component myxoid areas were seen in ten cases and chondroid differentiation in two, one of which also revealed extensive bone formation. Maturation in the epithelial component appeared as tubular formations in ten of the cases and signs of epidermoid differentiation were seen in seven cases.

The variegated histologic spectrum shown by these tumours is illustrated in Fig. 1-22. The blastomatous areas consisted of small cells with dark nuclei and a sparse undemarcated light cytoplasm. The cells were arranged without orientation and often appeared as cuffs around thin walled endothelial lined vessels (Fig. 1) the intermediate

clearly blastomatous areas now appeared epithelial and in some instances were oriented around a central defect or a lumen (Fig. 3). Reticulin positive fibers surrounded these small rounded areas but were not seen within (Fig. 4). The epithelial component consisted of small cubic to box shaped cells with small dark nuclei and a light rather well demarcated cytoplasm. The cells were arranged in branching tubular formations or in solid cords (Fig. 2 and 5). In one case there were areas in which the solid cords showed numerous keratin pearl formations (Fig. 6). Signs of differentiation in the mesenchymal component were seen as cellular elongation and arrangement in fascicles (Fig. 7) or as stellate cells placed in a more abundant alcian positive intercellular ground substance which seemed to point towards myxoid differentiation (Fig. 8). Collagenous fibers were sparse as were islands of immature cartilage (Fig. 9) and areas with bone formation (Fig. 10). Evidence of myofibrils or crossstriation was not found. From areas of the above described appearance there were transitions to areas with a marked pleomorphism of the cells.

In five cases the tumours had areas of varying size dominated by a single tumour component which looked like a monotypic carcinoma (cases 1, 2 and 4) (Fig. 11) or a monotypic sarcoma (cases 7 and 10) (Fig. 12). A constant feature of the tumours was an abundance of vessels. Infiltrative tumour growth within and outside the tumour pseudocapsule appeared as islands of either mesenchymal or epithelial tumour components. In only one case (case 1) were such islands of mixed type (Fig. 21). In two cases (cases 2 and 4) the infiltrative tumour growth outside the blastoma was particularly pronounced according to the macroscopic findings. In both cases the rounded blastomas were laterally and caudally surrounded by an adenocarcinoma of mixed monomorphic (Fig. 13) and pleomorphic appearance (Fig. 14) while medially and cranially there were epidermoid carcinomas (Fig. 15) of several types and grades of differentiation, some areas of which appeared as solid islands (Fig. 16) with transitions into a 'basaloid' (Fig. 17) or cribriform pattern and in others of which the tumour cells were box shaped with a light and well demarcated cytoplasm. In both cases there were zones of collision consisting of a mixture of infiltrating adenocarcinoma and epidermoid carcinoma.

The local recurrences appeared microscopically less differentiated (Fig. 18) than the corresponding surgical specimens (Fig. 12) and they were mainly monotypic either mesenchymal or epithelial.

The metastases were also mainly monotypic. Within the thoracic cavity they were either epithelial

TABLE 1 *Pulmonary Blastoma: Summary of Clinical and Pathological Findings in 11 Patients, Bixbyburg Hospital, 1971-1978*

Age No. Sex	Symptoms Duration	Primaries			Secondaries			Follow up	Au- (months) topsy
		Treatment	Size	Loca- tion	Epithelial maturation	Mesenchymal maturation	Location	(components)	
1 59	Pain 1 month	Pneumonectomy Chemotherapy	6 x 5 x 5	RML RLL	Tubular	Myxoid	Hilar nodes Lung, pleura Suprarenal g	(tubular) (limited) (mesenchymal)	1 Yes
2 64	Unproductive 8-14 months	Pneumonectomy	5 x 4 x 3 Polypoid	RL	Tubular Epidermoid	Myxoid	Hilar nodes	(tubular)	1/2 Yes
3 58	Hemoptysis Cough 2 months	Pneumonectomy Chemotherapy	8 x 4 x 4 Polypoid	RL	Tubular	Myxoid Cartilage	Chest wall	(mesenchymal)	15 Alive
4 66	Hemoptysis 1 month	Pneumonectomy	10 x 8 x 5	RUL	Tubular Epidermoid	Myxoid	Hilar nodes and recurrence	(tubular)	12 Yes
5 73	Cough 1 month	Pneumonectomy	2 x 3 x 3 Polypoid	RUL	Tubular Epidermoid	Myxoid bone Cartilage	Hilar nodes and recurrence	(epidermoid)	24 Yes
6 67	Hemoptysis 4 months	Lobectomy	2 x 2 1/2 x 2 1/2	LLL	Tubular Epidermoid	Myxoid	Recurrence	(epidermoid)	82 Yes
7 69	Lung infiltrate 1 month	Lobectomy	4 x 5 x 6	RUL	Tubular Epidermoid	Myxoid	Hilar nodes and recurrence	(mesenchymal)	6 Yes
8 66	Neurologic 1 month	Cranotomy Chemotherapy Radiation	10 x 8 x 4 Polypoid	LUL	Tubular	Myxoid	Hilar nodes Lung, brain Kidney	(tubular) (mesenchymal) (mixed)	9 Yes
9 68	Cough 1 month	None	3 x 5 x 5 Polypoid	LLL	Tubular		Hilar nodes and lung	(tubular)	1/2 Yes
10 69	Lung infiltrate Incidentally	None	10 x 10 x 10	LLL	Tubular Epidermoid	Myxoid	Hilar nodes Lung, liver and intestine	(mesenchymal) epidermoid	6 Yes
11 77	Lung infiltrate Incidentally	None	10 x 10 x 10	RLL	Epidermoid	Myxoid	Hilar nodes	(epidermoid)	0 Yes

and 11) lung infiltrates were diagnosed during investigation of arteriosclerotic heart disease which made them inoperable.

The tumours were right sided in seven cases and left-sided in four. In eight cases the tumour was confined to one lobe, in one case to two neighbouring lobes and in two cases the tumour involved parts of all three lobes of the right lung.

Gross Pathology

The tumours were rounded, rather well demarcated and surrounded by a pseudocapsule of compressed lung tissue or bronchial wall which further investigation showed to be invaded by tumour growth. The tumour size ranged from 2.5 cm to 10 cm in diameter. In five cases (cases 2, 3, 5, 8, 9) the tumours showed partly intrabronchial growth, part of which appeared as smooth polypoid grape-like processes free of the bronchial mucosa. In one case (case 10) a similar smooth finger-like process was seen in a branch of a pulmonary vein extending into the left auricle of the heart. The cut surface of the tumours was smooth and bulging and on inspection was greyish white to pink with scattered haemorrhages and necroses. The consistency was rather soft. In two cases (cases 2 and 4) a central part of the tumour matched the above description, the surrounding tumour tissue being greyish to yellow and rather dry with a plane cut surface.

Microscopic Findings

Some histologic features of the tumours are listed in Table 1. All tumours showed a blastomatous or undifferentiated mesenchymal component and an epithelial component. The components were mixed and present in varying amounts in different sections of the tumours and showed several types of differentiation and varying degrees of maturation. Besides the typical blastomatous component myxoid areas were seen in ten cases and chondroid differentiation in two, one of which also revealed extensive bone formation. Maturation in the epithelial component appeared as tubular formations in ten of the cases and signs of epidermoid differentiation were seen in seven cases.

The variegated histologic spectrum shown by these tumours is illustrated in Fig. 1-22. The blastomatous areas consisted of small cells with dark nuclei and a sparse undemarcated light cytoplasm. The cells were arranged without orientation and often appeared as cuffs around thin walled endothelial lined vessels (Fig. 1); the intermediate areas often showing necroses. The reticulin pattern was delicate and indistinct. A slight change in this picture was seen as small rounded areas consisting of tumour cells which though of the same size as the

clearly blastomatous areas now appeared epithelial and in some instances were oriented around a central defect or a lumen (Fig. 3). Reticulin positive fibers surrounded these small rounded areas but were not seen within (Fig. 4). The epithelial component consisted of small cubic to box shaped cells with small dark nuclei and a light rather well demarcated cytoplasm. The cells were arranged in branching tubular formations or in solid cords (Fig. 2 and 5). In one case there were areas in which the solid cords showed numerous keratin pearl formations (Fig. 6). Signs of differentiation in the mesenchymal component were seen as cellular elongation and arrangement in fascicles (Fig. 7) or as stellate cells placed in a more abundant alcian positive intercellular ground substance which seemed to point towards myxoid differentiation (Fig. 8). Collagenous fibers were sparse as were islands of immature cartilage (Fig. 9) and areas with bone formation (Fig. 10). Evidence of myofibrils or crossstriation was not found. From areas of the above described appearance there were transitions to areas with a marked pleomorphism of the cells.

In five cases the tumours had areas of varying size dominated by a single tumour component which looked like a monotypic carcinoma (cases 1, 2 and 4) (Fig. 11) or a monotypic sarcoma (cases 7 and 10) (Fig. 12). A constant feature of the tumours was an abundance of vessels. Infiltrative tumour growth within and outside the tumour pseudocapsule appeared as islands of either mesenchymal or epithelial tumour components. In only one case (case 1) were such islands of mixed type (Fig. 21). In two cases (cases 2 and 4) the infiltrative tumour growth outside the blastoma was particularly pronounced according to the macroscopic findings. In both cases the rounded blastomas were laterally and caudally surrounded by an adenocarcinoma of mixed monomorphic (Fig. 13) and pleomorphic appearance (Fig. 14) while medially and cranially there were epidermoid carcinomas (Fig. 15) of several types and grades of differentiation, some areas of which appeared as solid islands (Fig. 16) with transitions into a «basaloid» (Fig. 17) or cribriform pattern and in others of which the tumour cells were box shaped with a light and well demarcated cytoplasm. In both cases there were zones of collision consisting of a mixture of infiltrating adenocarcinoma and epidermoid carcinoma.

The local recurrences appeared microscopically less differentiated (Fig. 18) than the corresponding surgical specimens (Fig. 12) and they were mainly monotypic either mesenchymal or epithelial.

The metastases were also mainly monotypic. Within the thoracic cavity they were either epithelial

TABLE 1 *Pulmonary Blastoma: Summary of Clinical and Pathological Findings in 11 Patients, Bispebjerg Hospital 1971-1978*

Age No. Sex	Symptoms Duration	Treatment	Primaries			Secondaries			Follow up	Au (months) topsy
			Loca tion	Size	Epithelial maturation	Mesenchymal maturation	Location	(components)		
1 59 ♀	Pain 3 months	Pneumonectomy Chemotherapy	RHL RLL	6 × 5 × 5	Tubular	Myxoid	Hilar nodes Lung pleura Suprarenal gl	(tubular) (mixed) (mesenchymal)	Dead	1 Yes
2 64 ♀	Dyspnoea 84 months	Pneumonectomy	RL	5 × 4 × 3 Polypoid	Tubular Epidermoid	Myxoid	Hilar nodes	(tubular)	Dead of postoperative respiratory failure	½ Yes
3 58 ♂	Hemoptysis Cough 2 months	Pneumonectomy Chemotherapy	RL	8 × 4 × 4 Polypoid	Tubular	Myxoid Cartilage	Chest wall	(mesenchymal)	Alive with recurrence	15 Alive
4 66 ♂	Hemoptysis 1 month	Pneumonectomy	RUL	10 × 8 × 5	Tubular Epidermoid	Myxoid	Hilar nodes and recurrence	(tubular)	Dead	12 Yes
5 73 ♂	Cough 1 month	Pneumonectomy	RUL	2 × 3 × 3 Polypoid	Tubular Epidermoid	Myxoid bone Cartilage	Hilar nodes and recurrence	(epidermoid)	Dead	24 Yes
6 67 ♂	Hemoptysis 4 months	Lobectomy	LLL	2 ½ × 2 × 2 ½	Tubular Epidermoid	Myxoid	Recurrence	(epidermoid)	Dead	82 Yes
7 69 ♂	Lung infiltrate 1 month	Lobectomy	RUL	4 × 5 × 6	Tubular Epidermoid	Myxoid	Hilar nodes and recurrence	(mesenchymal)	Dead	6 Yes
8 66 ♂	Neurologic 1 month	Cranotomy Chemotherapy Radiation	LUL	10 × 8 × 4 Polypoid	Tubular	Myxoid	Hilar nodes Lung brain Kidney	(tubular) (mesenchymal) (mixed)	Dead 9 months after craniotomy	9 Yes
9 68 ♂	Cough 1 month	None	LLL	5 × 5 × 5 Polypoid	Tubular		Hilar nodes and lung	(tubular)	Dead	½ Yes
10 69 ♂	Lung infiltrate Incidentally	None	LLL	10 × 10 × 10	Tubular Epidermoid	Myxoid	Hilar nodes Lung liver and intestine	(mesenchymal)	Dead 6 months after biopsy	6 Yes
11 77 ♂	Lung infiltrate Incidentally	None	RLL	10 × 10 × 10	Epidermoid	Myxoid	Hilar nodes	(epidermoid)	Autopsy diagnosis	0 Yes

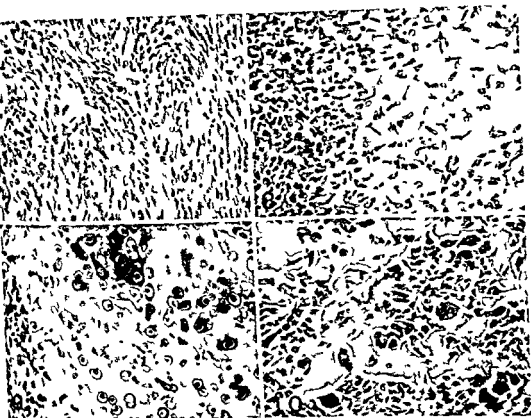


Fig 7 10 Pulmonary Blastoma proper mesenchymal differentiation

- 7 Fascicles of elongated mesenchymal tumour cells a few showing mitotic activity (Case 9 autopsy specimen)
- 8 Myxoid differentiation Stellate cells in an abundant myxomatous ground substance (Case 3 surgical specimen)
- 9 Chondromatous differentiation Edge of island of fetal type cartilage (Case 5 surgical specimen)
- 10 Osteoid differentiation Osteoclasts and osteoblasts lining bony trabeculae (Case 5 surgical specimen)

ial (Fig 19) or mesenchymal while extrathoracic metastases were mesenchymal of appearance (Fig 20). In only two cases (cases 1 and 8) were solitary metastases of mixed type found (Fig 21 and 22).

Treatment and Follow up

In seven patients a resection was performed of these six had a radical resection while in one (case 1) tumour tissue in the chest wall and diaphragm remained. In three cases (cases 1, 2 and 4) lymph node metastases were resected as well.

Of these seven patients two died shortly after the operation, one because of rapid tumour dissemination (case 1) and one because of an impaired lung function. Four survived respectively 6, 12, 24 and 82 months and at autopsy all four showed recurrent tumour tissue and/or metastases. One patient (case 3) was still alive 15 months postoperatively with a histologic recurrent tumour in the chest wall.

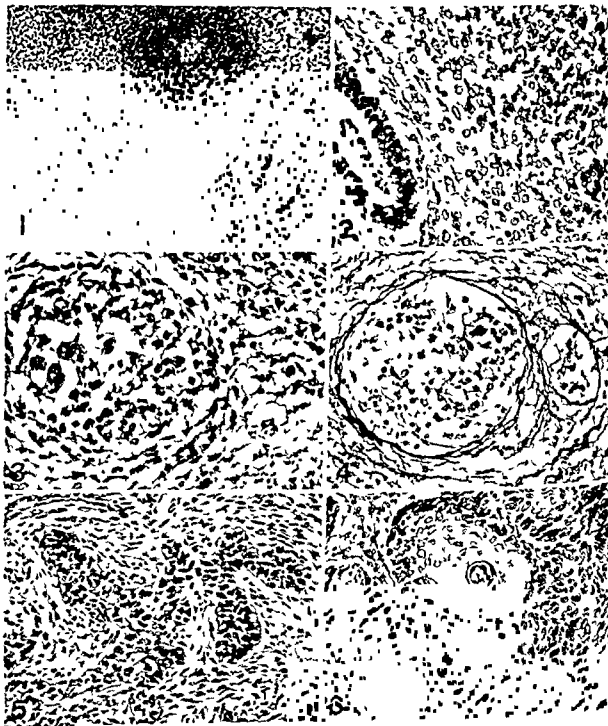
Without surgical treatment or

resection of the lung tumour and in each case autopsy showed lung tumour with metastases.

In the three year period 1973 through 1975 1185 cases of malignant primary lung tumours were histologically diagnosed at the department of pathology Bispebjerg Hospital. In Table 2 these cases are shown according to the histologic type. Six of our cases of PB were diagnosed in the same period. The frequency of PB thus was 0.5 per cent of all primary malignant lung tumours.

DISCUSSION

The diagnosis of the 11 cases of PB presented here was based on the characteristic and widely accepted microscopic appearance, a mixture of immature mesenchymal and epithelial components. The differential diagnosis would involve distinguishing other lung tumours of mixed type. Tumours as epider-



Original magnification 160 and hematoxylin eosin stain unless otherwise noted

Figs 1-6 Pulmonary Blastoma (PB) proper epithelial differentiation

1 Most immature and most characteristic feature of a PB as registered in all the presented cases. Undifferentiated tumour cells seen as cuffs around small vessels. The cuff in the lower right corner reveals the earliest possible epithelial like differentiation (Case 11 autopsy specimen $\times 63$)

2 Classic PB. An undifferentiated immature stroma and part of tubular formation resembling fetal lung tissue were seen (Case 8 autopsy specimen)

3 Two islands of tumor cells (Case 8 autopsy specimen Silver)

4 Immature box shaped epithelial cells arranged in branching cords

5 Tubular formations of tubular formations (Case 6 surgical specimen)

6 Cords of small immature epithelial cells. In one cord abrupt differentiation into a keratin pearl is seen (Case 5 surgical specimen)

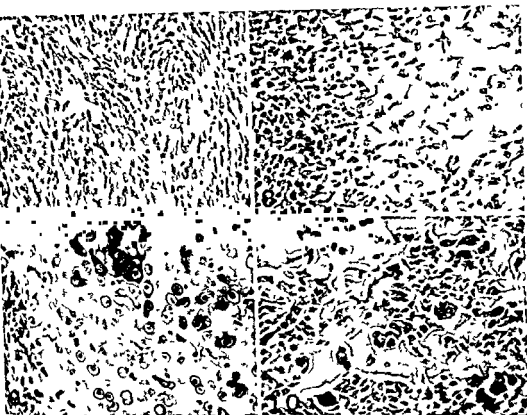


Fig 7-10 Pulmonary Blastoma proper mesenchymal differentiation

- 7 Fascicles of elongated mesenchymal tumour cells a few showing mitotic activity (Case 9 autopsy specimen)
 8 Myxoid differentiation Stellate cells in an abundant myxomatous groundsubstance (Case 3 surgical specimen)
 9 Chondromatous differentiation Edge of island of fetal type cartilage (Case 5 surgical specimen)
 10 Osteoid differentiation Osteoclasts and osteoblasts lining bony trabeculae (Case 5 surgical specimen)

hal (Fig 19) or mesenchymal while extrathoracic metastases were mesenchymal of appearance (Fig 20). In only two cases (cases 1 and 8) were solitary metastases of mixed type found (Fig 21 and 22).

Treatment and Follow up

In seven patients a resection was performed of these, six had a radical resection while in one (case 1) tumour tissue in the chest wall and diaphragm remained. In three cases (cases 1, 2 and 4) lymph node metastases were resected as well.

Of these seven patients two died shortly after the operation, one because of rapid tumour dissemination (case 1) and one because of an impaired lung function. Four survived respectively 6, 12, 24 and 82 months and at autopsy all four showed recurrent tumour tissue and/or metastases. One patient (case 3) was still alive 15 months postoperatively with a histologic recurrent tumour in the chest wall.

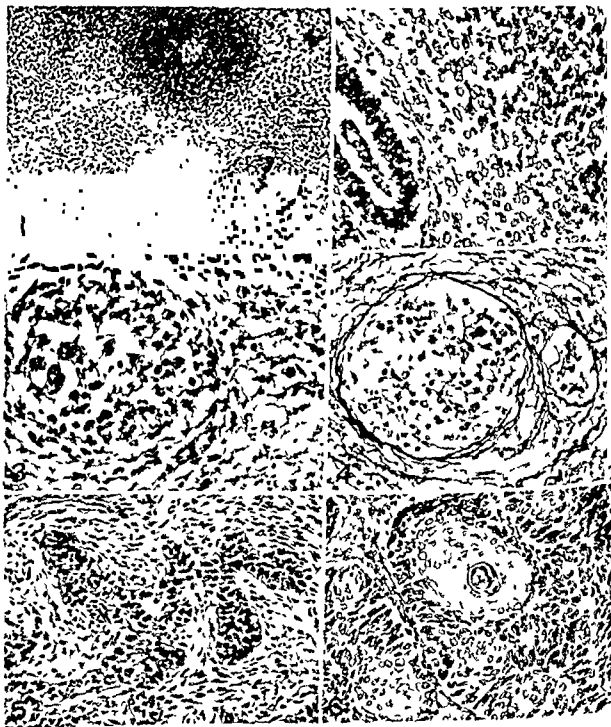
Four patients died without surgical treatment or

resection of the lung tumour and in each case autopsy showed lung tumour with metastases.

In the three year period 1973 through 1975 1185 cases of malignant primary lung tumours were histologically diagnosed at the department of pathology Bispebjerg Hospital. In Table 2 these cases are shown according to the histologic type. Six of our cases of PB were diagnosed in the same period. The frequency of PB thus was 0.5 per cent of all primary malignant lung tumours.

DISCUSSION

The diagnosis of the 11 cases of PB presented here was based on the characteristic and widely accepted microscopic appearance, a mixture of immature mesenchymal and epithelial components. The differential diagnosis would involve distinguishing other lung tumours of mixed type. Tumours as epider-



Original magnification 160 and hematoxylin eosin stain unless otherwise noted

Figs 1-6 Pulmonary Blastoma (PB) proper epithelial differentiation

- 1 Most immature and most characteristic feature of a PB as registered in all the presented cases. Undifferentiated tumour cells seen as cuffs around small vessels. The cuff in the lower right corner reveals the earliest possible epithelial like differentiation (Case 11 autopsy specimen $\times 63$)
- 2 Classic PB. An undifferentiated immature stroma and part of tubular formation resembling fetal lung tissue (2 weeks gestational age) (Case 2 surgical specimen)
- 3 Two islands of small tumour cells of epithelial like appearance (Case 8 autopsy specimen)
- 4 Same area as Fig 3. Reticulin positive fibers surround the two islands (Case 8 autopsy specimen Silver impregnation)
- 5 Obvious epithelial differentiation. Small immature box shaped epithelial cells arranged in branching cords two of which show necrotic centers as to beginning of tubular formations (Case 6 surgical specimen)
- 6 Epidermoid differentiation. Well demarcated cords of small immature epithelial cells. In one cord abrupt differentiation into a keratin pearl is seen (Case 5 surgical specimen)

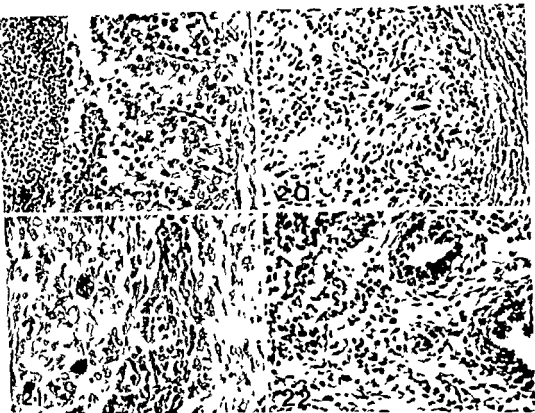


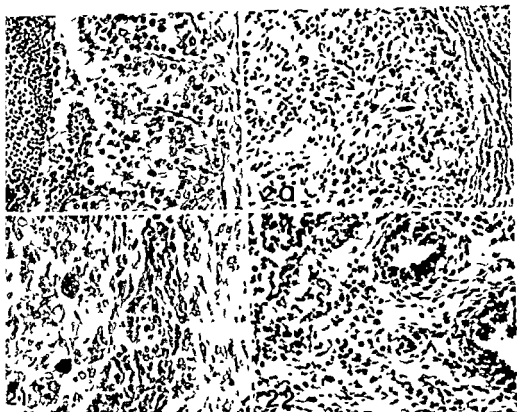
Fig 19-22 Pulmonary Blastoma different types of appearance in the metastases

- 19** Lymph node metastasis. Box shaped tumour cells with light cytoplasm. The tumour cells arranged in adenomatous formations appearing in the marginal sinus of a hilar lymph node. Other types of epithelial differentiation in this case are shown in Fig 14 and 15 (Case 4 surgical specimen)
- 20** Liver metastasis. Elongated tumour cells of monotypic mesenchymal appearance (Case 10 autopsy specimen)
- 21** Satellit tumour of the lung. Island of epithelial tumour cells surrounded by a very pleomorphic mesenchymal tumour component. Same case as Fig 11 (Case 1 surgical specimen)
- 22** Biphasic differentiation in metastatic lesion of the kidney. Several tubular formations in an undifferentiated stromal component (Case 8 autopsy specimen)

Fig 11-18 Pulmonary Blastoma different types of monotypic differentiation

- 11** Monomorphic adenocarcinoma. Small box shaped cells with dark nuclei and a light well demarcated cytoplasm (Case 1 surgical specimen)
- 12** Monomorphic sarcoma. Fascicular arrangement of spindle cells. The nuclei are enlarged and there are several mitoses (Case 7 surgical specimen)
- 13** Monomorphic adenocarcinoma. Small undemarcated cylindrical cells with vesicular nuclei. Crowding of cells (Case 2 surgical specimen)
- 14** Polymorphic adenocarcinoma (Mature type) (Case 4 surgical specimen)
- 15** Epidermoid carcinoma. Same case as Fig 14. Typical epidermoid differentiation of tumour showing keratinisation and cellular pleomorphism (Case 4 surgical specimen)
- 16** Undifferentiated carcinoma. Well demarcated islands of undifferentiated monomorphic epithelial tumour cells (Case 2 surgical specimen)
- 17** «Basaloma» like area. Same case as Fig 2 13 and 16 (Case 2 surgical specimen)
- 18** Recurrence. No organisation or differentiation of tumour cells visible. To be compared with the primary tumour in Fig 12 (Case 7 surgical biopsy from chest wall)





19-22 Pulmonary Blastoma: different types of appearance in the metastases

Lymph node metastasis: Box shaped tumour cells with light cytoplasm. The tumour cells arranged in anomalous formations appearing in the marginal sinus of a hilar lymph node. Other types of epithelial differentiation in this case are shown in Fig. 14 and 15 (Case 4: surgical specimen).

Liver metastasis: Elongated tumour cells of monotypic mesenchymal appearance (Case 10: autopsy specimen).

Satellitumour of the lung: Island of epithelial tumour cells surrounded by a very pleomorphic mesenchymal tumour component. Same case as Fig. 11 (Case 1: surgical specimen).

Biphasic differentiation in metastatic lesion of the kidney: Several tubular formations in an undifferentiated (romal) component (Case 8: autopsy specimen).

Fig. 11-18 Pulmonary Blastoma: different types of monotypic differentiation

1 Monomorphic adenocarcinoma: Small box shaped cells with dark nuclei and a light well demarcated cytoplasm (Case 1: surgical specimen).

2 Monomorphic sarcoma: Fascicular arrangement of spindle cells. The nuclei are enlarged and there are several mitoses (Case 7: surgical specimen).

3 Monomorphic adenocarcinoma: Small undemarcated cylindrical cells with vesicular nuclei. Crowding of cells (Case 2: surgical specimen).

4 Polymorphic adenocarcinoma (Mature type) (Case 4: surgical specimen).

5 Epidermoid carcinoma: Same case as Fig. 14. Typical epidermoid differentiation of tumour showing keratinisation and cellular pleomorphism (Case 4: surgical specimen).

6 Undifferentiated carcinoma: Well demarcated islands of undifferentiated monomorphic epithelial tumour cells (Case 2: surgical specimen).

17 «Basalioma» like area: Same case as Fig. 2, 13 and 16 (Case 2: surgical specimen).

18 Recurrence: No organisation or differentiation of tumour cells visible. To be compared with the primary tumour in Fig. 12 (Case 7: surgical biopsy from chest wall).

TABLE 2 *Histologic Type Distribution (WHO classification) in 1185 Cases of Primary Lung Cancer Diagnosed at Bispebjerg Hospital 1972-1975*

Sex	Number of cases	Epidermoid carcinoma Per cent	Small cell carcinoma Per cent	Adeno carcinoma Per cent	Large cell carcinoma Per cent	Others Per cent	Pulmonary blastoma Per cent
♀	240	32.9	20.4	27.5	12.5	6.3	0.4
♂	945	48.9	23.5	11.4	13.3	2.4	0.5
Total	1185	45.7	22.7	14.7	13.2	3.1	0.5

moid carcinoma with a spindle cell component, mixed mucosa gland tumours and teratomas should be reasonably easy to distinguish. Difficulties, however, may arise in separating PB from certain cases of mesothelioma, hamartoma and carcinosarcoma. Transitions between these latter mentioned tumour types and PB have been described (7, 16, 23).

To our knowledge as of 1978, 65 cases of PB had been reported (10). The mean age in the series presented was rather high (11). One of our patients had had symptoms of long duration before treatment. Similar long duration of symptoms were reported in the cases of *Bauermeister et al* (1966) and *Parker et al* (1966). Except for a rather high mean age, a high frequency of intrabronchial tumour growth and a high frequency of metastases, our cases did not differ from reported cases with regard to size, location or frequency of local recurrences of the tumour or duration of survival (11). Microscopically we found a high frequency of cases with signs of epidermoid differentiation a component which has only recently begun to be accepted in PB (6, 7, 13, 22, 23, 29).

Extensive growth of an adenocarcinoma and an epidermoid carcinoma in close contact with a PB as seen in two of our cases have not been previously described. Collision of different types of malignant tumours in these cases could be a possible explanation for this. The variegated microscopical appearance of the carcinomas being different from ordinary primary bronchogenic carcinomas, however, points towards all the tumour tissue components originating from the blastomas.

In all the cases presented here monotypic secondaries were found, metastases of mixed type having been recorded in only two cases. This is in contrast to reported cases where most of the histologically described metastases were of mixed type.

The prognosis in our cases was poor, within two years nine patients died as a result of their tumour, and one died seven years after resection with a large

recurrent tumour. A similar case of long term survival ending with death of recurrent tumour was reported by *Kern et al* (1976). Cases of tumour free long-term survival were reported by *Barnard* (1952), *Kennedy & Prior* (1976) and *Iverson & Strachley* (1973).

Some authors regard the PB as a subgroup of carcinosarcoma (18, 23, 27) while others regard the PB as a separate entity (14, 19, 20, 21, 24) developed from a pluripotent cell of a single germ layer, here the pulmonary blastema of the mesoderm (25, 26). Mesodermal mixed tumours however, are widely accepted in several other organ systems. They all consist of a mixture of mesenchymal and epithelial tumour components showing varying differentiation and maturation although monotypic cases have been recorded (4, 5, 9). Unlike in teratomas, heterotopic components are not found in PB.

The etiology of neoplastic growth from the pluripotent cells is unknown. Some of the differences in structural appearance and biological behaviour of these mixed tumours might be explained by the primary cellular change, the location of the cell and the induction from the surrounding tissue.

The secondaries in our material only occasionally were of the mixed type. The usually monotypic sarcomatous or carcinomatous appearance of the secondaries lent support to the hypothesis that in the blastoma one or several transformations had taken place resulting in a local dominance or metastatic growth of the transformed tumour components which in some instances were more anaplastic in appearance.

Supported by the reports of transitions between blastoma and carcinosarcoma (7, 23) and by the reports of morphological similarities between fetal lung tissue hamartoma and blastoma (11, 16, 26, 28) our opinion is that these three tumours are mixed mesodermal tumours originating from the same cell type. Differences in morphology and biological behaviour may be explained by the type of cellular defect produced by the initiating factors.

The 11 cases presented here constitute the largest material of PB diagnosed in a single department. To date Davis *et al* (1972) reported five cases and in the 50 year period 1915-1965 Stackhouse *et al* (1969) found only four from the Mayo Clinic. Six of our cases were diagnosed in a three year period during which 1185 cases of primary malignant lung tumour were diagnosed at our department. The frequency of PB thus was 0.5 per cent of all malignant lung tumours.

A possible explanation for the high number of cases diagnosed at our department might be related to our particular interest in this type of tumour and the search that we therefore directed specifically towards it combined with the fact that the Danish autopsy regulations, data registry, health service system and health service contact pattern help to facilitate the follow up in a single department of a patient's course through biopsy, treatment and ultimately autopsy.

A preoperative diagnosis of PB is very difficult to establish. The presence of both mesenchymal and epithelial tumour cells or tumour tissue in the preoperative microscopic specimens are highly suggestive of a mixed tumour, hence PB (8). Further examples of this tumour might be disclosed among cases of lung cancer with secondaries of divergent microscopic appearance. PB is considered a very rare tumour but the results of this survey would indicate that it is remarkably more common than previously believed.

We wish to thank Mrs. Bodil Tjellesen for carefully typing the manuscript and Mr. Aksel Ankerstjerne for his technical assistance.

REFERENCES

- Barnard W G Embryoma of lung Thorax 7 299-301 1952
- Barrett N R & Barnard W G Some unusual thoracic tumours Brit J Surg 32 447-457 1944-45
- Bauermeister D E Jennings E R Beland A H & Judson H A Pulmonary blastoma a form of carcinosarcoma Am J Clin Pathol 46 322-329 1966
- Bennington J L & Beckwith J B Tumors of the kidney renal pelvis and ureter Armed Forces Institute of Pathology Washington DC 1975 p 31
- Chakrabarti A Gujral J S & Ailal B A Embryonal sarcoma of the lung A case report with a discussion regarding its morphogenesis J Thorac Cardiovasc Surg 57 657-662 1969
- Danziger H Pulmonary blastoma Can Med Assoc J 102 146-147 1970
- Davis P W Briggs J C Seal R M E & Storting F K Benign and malignant mixed tumours of the lung Thorax 27 657-673 1972
- Francis D & Jacobsen M Pulmonary blastoma preoperative cytologic and histologic findings Acta Cytol 23 437-442 1979
- Francis D & Olsen N J Adult nephroblastoma Scand J Urol Nephrol 11 305-308 1977
- Francis D & Jacobsen M Pulmonary blastoma To be published in Curr Top Pathol
- Fung C H Lo J W Yonon T N Millon F J Hakami M M & Changus G W Pulmonary blastoma An ultrastructural study with a brief review of literature and a discussion of pathogenesis Cancer 39 153-163 1977
- Iverson R E & Straehley C J Pulmonary blastoma longterm survival of juvenile patient Chest 63 436-440 1973
- Jayel A Bosc C & Saegesser F Pneumoblastomes A propos de deux observations Schweiz med Wschr 107 349-352 1977
- Karcioglu Z A & Someren A O Pulmonary blastoma A case report and review of the literature Am J Clin Pathol 61 287-295 1974
- Kennedy A & Prior A L Pulmonary blastoma a report of two cases and a review of the literature Thorax 31 776-781 1976
- Kern H H & Siles Q R Pulmonary blastoma J Thorac Cardiovasc Surg 72 801-808 1976
- Kreyberg L International histological classification of tumours No 1 Histological typing of lung tumours WHO Geneva 1967
- McCann M P Fu Y S & Kay S Pulmonary blastoma A light and electron microscopic study Cancer 38 789-797 1976
- Nazari A Amir Mokri E Sarraf A & Yaghmai I Pulmonary blastoma Chest 60 187-189 1971
- Parker J C Payne W S & Woolner L B Pulmonary blastoma (embryoma) Report of two cases J Thorac Cardiovasc Surg 51 694-699 1966
- RajChaudhuri M Eastham W N & Fredricks P A Pulmonary blastoma with diverse mesenchymal proliferation Thorax 27 487-491 1972
- RajChaudhuri M & Winstanley D P Pulmonary blastoma with diverse metastases J Pathol 98 81-82 1969
- Roth J A & Elgueabal A Pulmonary blastoma evolving into carcinosarcoma Am J Surg Pathol 2 407-413 1978
- Saura R C Peasley E D & Takano T Pulmonary blastomas A distinctive group of carcinosarcomas of the lung Ann Thorac Surg 1 259-268 1965
- Spencer H Pulmonary blastomas J Pathol Bacteriol 81 161-165 1961
- Spencer H Pathology of the lung 3rd ed Pergamon Press Oxford 1977 pp 973-997

TABLE 2 *Histologic Type Distribution (WHO classification) in 1185 Cases of Primary Lung Cancer Diagnosed Bispebjerg Hospital 1972-1975*

Sex	Number of cases	Epidermoid carcinoma Per cent	Small cell carcinoma Per cent	Adeno carcinoma Per cent	Large cell carcinoma Per cent	Others Per cent	Pulmonary blastoma Per cent
♀	240	32.9	20.4	27.5	12.5	6.3	0.4
♂	945	48.9	23.5	11.4	13.3	2.4	0.5
Total	1185	45.7	22.7	14.7	13.2	3.1	0.5

moid carcinoma with a spindle cell component mixed mucosa gland tumours and teratomas should be reasonably easy to distinguish. Difficulties however may arise in separating PB from certain cases of mesothelioma, hamartoma and carcinosarcoma. Transitions between these latter mentioned tumour types and PB have been described (7, 16, 23).

To our knowledge as of 1978, 65 cases of PB had been reported (10). The mean age in the series presented was rather high (11). One of our patients had had symptoms of long duration before treatment. Similar long duration of symptoms were reported in the cases of *Bauermeister et al* (1966) and *Parker et al* (1966). Except for a rather high mean age, a high frequency of intrabronchial tumour growth and a high frequency of metastases, our cases did not differ from reported cases with regard to size, location or frequency of local recurrences of the tumour or duration of survival (11). Microscopically we found a high frequency of cases with signs of epidermoid differentiation, a component which has only recently begun to be accepted in PB (6, 7, 13, 22, 23, 29).

Extensive growth of an adenocarcinoma and an epidermoid carcinoma in close contact with a PB as seen in two of our cases have not been previously described. Collision of different types of malignant tumours in these cases could be a possible explanation for this. The variegated microscopical appearance of the carcinomas being different from ordinary primary bronchogenic carcinomas however points towards all the tumour tissue components originating from the blastomas.

In all the cases presented here monotypic secondaries were found, metastases of mixed type having been recorded in only two cases. This is in contrast to reported cases where most of the histologically described metastases were of mixed type.

The prognosis in our cases was poor, within two years nine patients died as a result of their tumour and one died seven years after resection with a large

recurrent tumour. A similar case of long survival ending with death of recurrent tumour was reported by *Kern et al* (1976). Cases of tumour of long term survival were reported by *Barni* (1952), *Kennedy & Prior* (1976) and *Iverson Strachley* (1973).

Some authors regard the PB as a subgroup carcinosarcoma (18, 23, 27) while others regard PB as a separate entity (14, 19, 20, 21, 22) developed from a pluripotent cell of a single germ layer, here the pulmonary blastema of the mesoderm (25, 26). Mesodermal mixed tumours however are widely accepted in several other organ systems. They all consist of a mixture of mesenchymal and epithelial tumour components showing varying differentiation and maturation although monotypic cases have been recorded (4, 5, 6). Unlike in teratomas heterotopic components are not found in PB.

The etiology of neoplastic growth from pluripotent cells is unknown. Some of the differences in structural appearance and biological behaviour of these mixed tumours might be explained by the primary cellular change, the location of the cell and the induction from the surrounding tissue.

The secondaries in our material only occasionally were of the mixed type. The usually monotypic sarcomatous or carcinomatous appearance of the secondaries lent support to the hypothesis that in the blastoma one or several transformations had taken place resulting in a local dominance or metastatic growth of the transformed tumour component which in some instances were more anaplastic in appearance.

Supported by the reports of transitions between blastoma and carcinosarcoma (7, 23) and by the reports of morphological similarities between fetal lung tissue, hamartoma and blastoma (11, 16, 26, 28) our opinion is that these three tumours are mixed mesodermal tumours originating from the same cell type. Differences in morphology and biological behaviour may be explained by the type of cellular defect produced by the initiating factors.

1. The 11 cases presented here constitute the largest material of PB diagnosed in a single department. To date Davis *et al* (1972) reported five cases and in the 50 year period 1915-1965 Stackhouse *et al* (1969) found only four from the Mayo Clinic. Six of our cases were diagnosed in a three year period during which 1185 cases of primary malignant lung tumour were diagnosed at our department. The frequency of PB thus was 0.5 per cent of all malignant lung tumours.

A possible explanation for the high number of cases diagnosed at our department might be related to our particular interest in this type of tumour and the search that we therefore directed specifically towards it combined with the fact that the Danish autopsy regulations, data registry, health service system and health service contact pattern help to facilitate the follow up in a single department of a patient's course through biopsy, treatment and ultimately autopsy.

A preoperative diagnosis of PB is very difficult to establish. The presence of both mesenchymal and epithelial tumour cells or tumour tissue in the preoperative microscopic specimens are highly suggestive of a mixed tumour, hence PB (8). Further examples of this tumour might be disclosed among cases of lung cancer with secondaries of divergent microscopic appearance. PB is considered a very rare tumour but the results of this survey would indicate that it is remarkably more common than previously believed.

We wish to thank Mrs. Bodil Tjellesen for carefully typing the manuscript and Mr. Aksel Ankersjerne for his technical assistance.

REFERENCES

- Barnard W G Embryoma of lung Thorax 7 299-301 1952
- Barrett A R & Barnard W G Some unusual thoracic tumours Brit J Surg 32 447-457 1944-45
- Bauermeister D E Jennings E R Beland A H & Judson H A Pulmonary blastoma, a form of carcinosarcoma Am J Clin Pathol 46 322-329 1966
- Bennington J L & Beckwith J B Tumors of the kidney, renal pelvis and ureter Armed Forces Institute of Pathology Washington D C 1975 p 31
- Chitambar J A Gujral J S & Aikat B K Embryonal sarcoma of the lung. A case report with a discussion regarding its morphogenesis J Thorac Cardiovasc Surg 57 657-662 1969
- Danziger H Pulmonary blastoma Can Med Assoc J 102 146-147 1970
- Davis P B Briggs J C Seal R M E & Storrer F A Benign and malignant mixed tumours of the lung Thorax 27 657-673 1972
- Francis D & Jacobsen M Pulmonary blastoma: preoperative cytologic and histologic findings Acta Cytol 23 437-442 1979
- Francis D & Olsen N J Adult nephroblastoma Scand J Urol Nephrol 11 305-308 1977
- Francis D & Jacobsen M Pulmonary blastoma To be published in Curr Top Pathol
- Fung C H Lo J W Yonan T N Millov F J Hakami M M & Changus G B Pulmonary blastoma: An ultrastructural study with a brief review of literature and a discussion of pathogenesis Cancer 39 153-163 1977
- Iverson R E & Straehler C J Pulmonary blastoma: longterm survival of juvenile patient Chest 63 436-440 1973
- Juret A Bissic C & Saegesser F Pneumoblastomes A propos de deux observations Schweiz med Wschr 107 349-352 1977
- Karcoglu Z A & Someren A O Pulmonary blastoma: A case report and review of the literature Am J Clin Pathol 61 287-295 1974
- Kennedy A & Prior A L Pulmonary blastoma: a report of two cases and a review of the literature Thorax 31 776-781 1976
- Kern W H & Siles Q R Pulmonary blastoma J Thorac Cardiovasc Surg 72 801-808 1976
- Kreyberg L International histological classification of tumours No 1 Histological typing of lung tumours WHO Geneva 1967
- McCann M P Fu Y S & Aai S Pulmonary blastoma: A light and electron microscopic study Cancer 38 789-797 1976
- Nazari A Amir-Mokri E Sarraf A & Yaghmai I Pulmonary blastoma Chest 60 187-189 1971
- Parker J C Payne W S & Woolner L B Pulmonary blastoma (embryoma): Report of two cases J Thorac Cardiovasc Surg 51 694-699 1966
- RajChaudhuri M Eastham W N & Fredricks P A Pulmonary blastoma with diverse mesenchymal proliferation Thorax 27 487-491 1972
- RajChaudhuri M & Winstanley D P Pulmonary blastoma with diverse metastases J Pathol 98 81-82 1969
- Roth J A & Elgue-abat A Pulmonary blastoma evolving into carcinosarcoma Am J Surg Pathol 2 407-413 1978
- Souza R C Peasley E D & Takaro T Pulmonary blastomas: A distinctive group of carcinosarcomas of the lung Ann Thorac Surg 1 259-268 1965
- Spencer H Pulmonary blastomas J Pathol Bacteriol 82 161-165 1961
- Spencer H Pathology of the lung 3rd ed Pergamon Press Oxford 1977 pp 973-997

- 27 *Stackhouse E M Harrison E G & Ellis F H* Primary mixed malignancies of lung Carcinosarcoma and blastoma *J Thorac Cardiovasc Surg* 57 385-399 1969
- 28 *Stone F J & Churg A M* The ultrastructure of pulmonary hamartoma *Cancer* 39 1064-1070 1977
- 29 *Valderrama E Saluja G Shende A Lan kowsky P & Berkman J* Pulmonary blastoma Report of two cases in children *Am J Surg Pathol* 1 415-422 1978

OSTEOGENIC SARCOMA OF THE BREAST

Report of a Case

KRISTRÚN BENEDIKTSÐÓTTIR FREDRIK LAGERBERG LARS LUNDELL and ANDERS THULIN

Departments of Pathology Oncology and Surgery Centrallasarettet Jonkoping Sweden

Benediktsson K Lagerberg F Lundell L & Thulin A Osteogenic sarcoma of the breast Report of a case Acta path microbiol scand Sect A 88 161-165 1980

The clinical, mammographical, cytological and histological features of a mammary osteogenic sarcoma are reported. The tumor, which was removed by only local excision, had suddenly appeared in the same breast from which previously an intraductal papilloma had been removed. Nearly three years after the operation there is no indication of recurrence.

Key words Breast osteogenic sarcoma

Lars Lundell Department of Surgery Centrallasarettet S 551 85 Jonkoping Sweden

Received 14 ix 79 Accepted 28 xi 79

Extra skeletal bone formation may be formed under a variety of different conditions. The occurrence of true osteogenic sarcoma outside the skeleton is however rare. Extra skeletal osteogenic sarcomas have been described for instance in the kidney the thyroid gland the urinary bladder the soft tissue of the extremities and in the breast (Fine & Stout 1956 Jernstrom *et al* 1963 Rao *et al* 1978). Bonet (1700) may have been the first to observe a bony tumor in the female breast. However Lancereaux (1860) gave the first description of the histological picture of a breast tumor consisting of osteoid tissue.

Sarcoma of the breast may constitute between 0.2-3% of all breast malignancies. These neoplasms are a heterogenous group of mesenchymal tumors and may to different extents contain bone cartilage fibrous and osteoid tissue. Breast sarcomas with osteoid components have been presented as teratoid mixed tumors (Mc Huer 1923) osteoid sarcoma (Rattino & Howley 1945) osteochondroma (1943) or 1963 Sun. These discrepancies regarding the nomenclature may to some

degree account for the difficulties encountered in the estimation of the true incidence of osteogenic sarcoma in the mammary gland. Furthermore, *Rottino and Howley* (1945) pointed out that the osteoid component could easily be overlooked and be found first in a secondary tumor. Still *Jernstrom et al* (1963) reported the incidence of osteogenic sarcoma to be about 10% of all sarcoma of the breast.

In this report we present the clinical mammo-graphical cytological and histological features of a true mammary osteogenic sarcoma

CASE HISTORY

A previously healthy 72 year-old woman attended the out patient clinic in November 1968 with a tumour in the upper lateral quadrant of the left breast. She had been aware of a lump for 2 months. No clinical sign of malignancy was found. A fineneedle aspiration biopsy revealed an intraductal papilloma a diagnosis later confirmed by local excision. The lesion was however interpreted to be of a pre-cancerous nature but had been radically removed. The patient was followed up at the

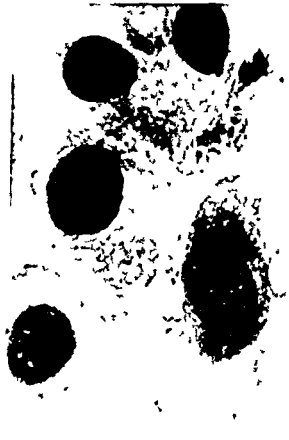


Fig 1 Mammography demonstrating a b cyclic calcified tumor in the upper part of the breast

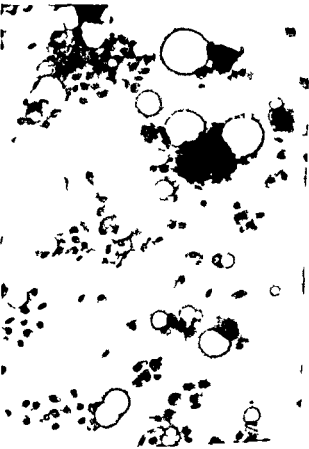


Fig 2 The cytological appearance of the tumor (a) The two cell types: epithelial like spindle cells and multinucleated giant cells (MGG $\times 25$) (b) Spindle cells one showing mitotic figure (MGG high power field) (c) Multinucleated giant cell (MGG high power field)

out patient clinic until 1971 with no indication of recurrence

In december 1976 she returned to the Department of Oncology with a tumor in about the same place as the one previously excised. The lump measured about 3 cm in diameter and was not fixed to the surrounding structures. The tumor was irregular in shape but well circumscribed. She had noticed this tumor for a couple of weeks and she presented no concomitant breast complaint. There was no history of nipple discharge and no discoloration of the skin. Mammographic investigation (Fig 1) revealed a bi-cyclic tumor with calcifications particularly in the walls of the cystic formations. The tumor was not considered malignant. Fine needle aspiration was performed. The smears were difficult to interpret (see below) but the picture could be consistent with a malignant tumor. Owing to the discrepancy between the two pre-operative investigations a frozen section procedure was carried out with the patient under general anesthesia. The pathologist reported a mesenchymal tumor with osteoid but no further classification could be made. The wound was closed and the post-operative course was uneventful. The patient refused any further operation and she has since then been followed up at the out patient clinic. Two subsequent ^{99m}Tc diphosphonate skeletal scintigraphies have not revealed any primary tumor in the skeleton or a dissemination of the disease. Repeated X ray surveys of the skeleton and the lungs have also been normal. In September 1979 the patient is free from any symptom indicating recurrence and/or metastases from the sarcoma.

Pathology

The fine needle aspiration biopsy from the lesion revealed a very cellular material with two cell types mostly dissociated (Fig 2). The more common type was moderately large and epithelial like with abundant cytoplasm and rather big nucleus with enlarged and prominent nucleolus. Furthermore many mitotic figures were seen. The nucleus often lay eccentric in the cell. The other type was a giant cell with granulated cytoplasm containing small round nuclei. This unusual cytological picture suggested malignancy.

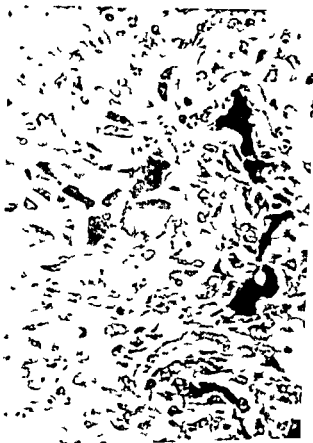
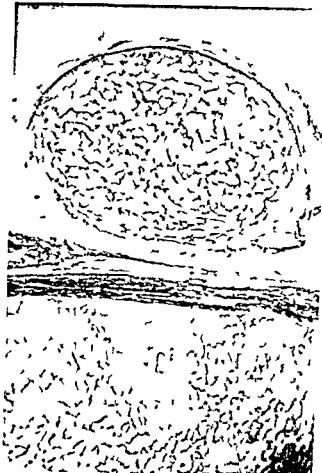
The specimen obtained by local excision consisted of breast tissue with a globular tumor that measured $4 \times 5 \times 3.5$ cm and was well circumscribed but unencapsulated (Fig 3). At the margins small knobs were seen protruding and pushing their way into the surrounding fat. The cut surface was grey homogenous firm and gave a gritty sensation suggesting the presence of bone. Frozen sections showed a mesenchymal tumor with areas of osteoid which could not be properly classified. Paraffin sections showed a very cellular tumor uniform in appearance (Fig 4). The tumor was characterized by



Fig 3 The cut surface of the tumor with a sharp contour at the periphery and whitish calcified areas

types of cells. The cells forming the bulk of the tumor were large spindle cells displaying a varying degree of pleomorphism with rectorial type of nuclei mostly eccentric. The cells were grouped in intertwining whorling bundles. Many cells were undergoing mitotic division. In high power field (HPF) one could find in the most cellular areas four mitotic figures at the most. Interspersed among these cells often in close contact with the osteoid were giant cells containing many small deeply-staining nuclei. In some areas there was much osteoid substance partly mineralized but other areas were purely cellular. Between the cells there was a delicate fibrous stroma and scattered blood vessels. Accordingly the tumor had the character of a pure osteogenic sarcoma indistinguishable from osteogenic sarcoma of skeletal origin. Surrounding the tumor mass there was fat with strands of breast tissue with small ducts. No evidence of intraductal papilloma or fibroadenoma was found in the sections. Furthermore no cartilage was seen. In the tumor tissue there was free marrow.

Fig 4 (a) Knobbing at the margins of the tumor. A of dark stained osteoid separated by cellular sheets. Cellular area with closely packed pleomorphic spindle cells, multinucleated giant cells and osteoid tissue (H. $\times 25$)



DISCUSSION

Osteogenic sarcoma of the breast is a disease of adult and old age and has only once been described in a male breast (Sun 1952). The time between discovery of the tumor and the medical attention varies between a month in our case up to 30 years (Rottino & Howley 1945; Sun 1952). There seem to be no characteristic features of osteogenic sarcoma that clinically distinguish them from other malignant breast tumors.

It is difficult to gain an insight into the clinical behaviour of specific histological types of breast sarcomas owing to their uncommon occurrence and the confusion in terminology. There are, however, indications that malignant bone and/or cartilage in a breast sarcoma is a sign of poor prognosis (Smith & Taylor 1969; Barnes & Pietruszka 1977). Accordingly, osteogenic sarcoma of the breast are considered highly malignant, often rapidly growing, giving early local recurrence and metastases by the hematogenous route to primarily the lungs, but metastases in the brain and kidney are also known (Rottino & Howley 1945; Rottino & Willson 1945; Sun 1952; Wester & Finlay Jones 1960; Jernstrom et al 1963; Smith & Taylor 1969). Lymphatogenous spread is rare and axillary metastases have only occasionally been described. An adequate surgical treatment would thus be a simple mastectomy. There is no information available that describes any positive effect of adjuvant therapy such as radiotherapy and/or cytotoxic drugs.

There are certain microscopic features of the tumor that have been discussed in relation to the prognosis of the patients. Although Allan and Soule (1971) found no histological difference between tumors with rapid and prolonged courses, others have claimed that the prognosis rests upon the number of mitotic figures per HPF and how the tumor behaves towards the surrounding breast tissue, as well as the cellular atypia and tumor size (Norris & Taylor 1968; Barnes & Pietruszka 1977). Tumors that had less than 5 mitoses per HPF and pushed their margins were suggested to have better prognosis than those with 8–10 mitoses per HPF and infiltration into the breast tissue. According to these criteria the sarcoma of our patient would have

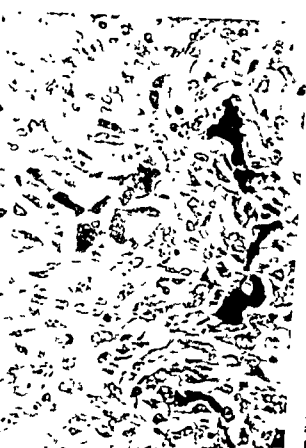
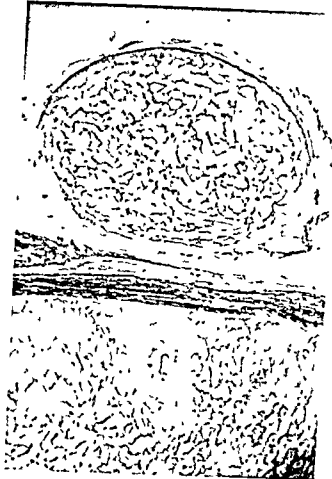
a favourable prognosis which the clinical course hitherto would also suggest

Efforts to explain the ethiology of breast sarcoma in general and osteogenic sarcoma in particular have given rise to a number of different theories through the years. The histogenesis is however still not settled. The concept most generally held is that these tumors arise through metaplasia and malignant change in stromal cells (mesenchymal connective tissue cells) considered to be totipotential, being able to differentiate into various directions under the proper environmental stimulus (Das Gupta *et al* 1968). Another theory is misplacement of pluripotential embryonic cells during development much like a teratomatous growth (Mc Iver 1923). Others have observed an intimate association between osteogenic sarcoma and fibroadenoma (Rottino & Howley 1945, Curran & Dodge 1962, Jernstrom *et al* 1963). Smith and Taylor (1969) described two patients with mixed mesenchymal tumors who had previously been operated for intraductal papilloma in the same area and five other cases having intraductal papillomas within ducts adjacent to the tumor. In the present case there was no evidence of fibroadenoma in either the first or the second specimen and no residue of intraductal papilloma could be found in the tissue around the sarcoma. It should however be pointed out that previously an intraductal papilloma had been removed from almost the same place in which the osteogenic sarcoma later occurred.

REFERENCES

- Allan C J & Soule E H Osteogenic sarcoma of the somatic soft tissues - Clinicopathologic study of 26 cases and review of literature *Cancer* 27 1121-1133 1971
- Barnes L & Pietruszka M Sarcomas of the breast. A clinicopathologic analysis of ten cases *Cancer* 40 1577-1585 1977
- Bonet T *Mammæ osseæ in virgine cum pectoris hydropse in sepulchretum sine anatomia practica ex cadaveribus morbo denatis* Vol 2 Geneva Cramer and Perachon 1700 p 522
- Carlucci G A & Wagner R F Osteochondrofibrosarcoma of the breast case report. *Am J Surg* 61 271-276 1943
- Curran R C & Dodge O G Sarcoma of the breast, with particular reference to its origin from fibroadenoma *J Clin Path* 15 1-16 1962
- Das Gupta T K Hajdu S I & Foote F W Extrasosseous osteogenic sarcoma *Ann Surg* 168 1011-1022 1968
- Fine G & Stout A P Osteogenic sarcoma of the extraskelatal soft tissues *Cancer* 9 1027-1043 1956
- Jernstrom P, Lindberg A L & Meland O N Osteogenic sarcoma of the mammary gland *Am J Clin Pathol* 40 521-526 1963
- Lancereaux E *Bull Soc Anat de Paris* 35 293 1860
- Mc Iver M A Teratoid mixed tumors of the breast. report of case *Ann Surg* 354-357 1923
- Norris H J & Taylor H B Sarcomas and related mesenchymal tumors of the breast *Cancer* 22 22-28 1968
- Rao U, Cheng A & Didolkar M S Extrasosseous osteogenic sarcoma - Clinicopathological study of eight cases and review of literature *Cancer* 41 1488-1496 1978
- Rottino A & Howley C P Osteoid sarcoma of the breast a complication of fibroadenoma *Arch Pathol* 40 44-50 1945
- Rottino A & Willson K Osseous cartilaginous and mixed tumors of the human breast *Arch Surg* 50 184-193 1945
- Smith B H & Taylor H B The occurrence of bone and cartilage in mammary tumors *Am J Clin Pathol* 51 610-618 1969
- Sun P Y Osteogenic sarcoma of the breast - review of literature and report of a case *Chinese Med J* 70 46-53 1952
- Wester J G & Finlay-Jones L R Osteogenic sarcoma of the breast. Tropical and Geographical Med 12 222-223 1960

Fig 4 (a) Knobbing at the margins of the tumor of dark-stained osteoid separated by cellular shee Cellular area with closely packed pleomorphic si cells, multinucleated giant cells and osteoid tissue (l $\times 25$)



DISCUSSION

Osteogenic sarcoma of the breast is a disease adult and old age and has only once been descri in a male breast (Sun 1952) The time betw discovery of the tumor and the medical attent varies between a month in our case up to 30-years (Rottino & Howley 1945 Sun 1952) Th seem to be no characteristic features of osteoge sarcoma that clinically distinguish them from ot malignant breast tumors

It is difficult to gain an insight into the clin behaviour of specific histological types of brea sarcomas owing to their uncommon occurren and the confusion in terminology There ar however indications that malignant bone and/c cartilage in a breast sarcoma is a sign of po prognosis (Smith & Taylor 1969, Barnes & Pietruszka 1977) Accordingly osteogenic sarcoma c the breast are considered highly malignant oft rapidly growing giving early local recurrence and metastases by the hematogenous route to primaril the lungs, but metastases in the brain and kidney are also known (Rottino & Howley 1945 Rottino & Willson 1945 Sun 1952 Wester & Finlay Jones 1960 Jernstrom et al 1963, Smith & Taylor 1969) Lymphatogenous spread is rare and axillary metastases have only occasionally been described An adequate surgical treatment would thus be a simple mastectomy There is no information available that describes any positive effect of adjuvant therapy such as radiotherapy and/or cytotoxic drugs

There are certain microscopic features of the tumor that have been discussed in relation to the prognosis of the patients Although Allan and Souk (1971) found no histological difference between tumors with rapid and prolonged courses others have claimed that the prognosis rests upon the number of mitotic figures per HPF and how the tumor behaves towards the surrounding breast tissue as well as the cellular atypia and tumor size (Norris & Taylor 1968 Barnes & Pietruszka 1977) Tumors that had less than 5 mitoses per HPF and pushed their margins were suggested to have better prognosis than those with 8-10 mitoses per HPF and infiltration into the breast tissue According to these criteria the sarcoma of our patient would have

CORONARY ATHEROSCLEROSIS IN MIDDLE-AGED AND ELDERLY FINNISH MEN PATHOLOGICAL STUDY OF CORONARY ARTERIES IN VIOLENT AND SUDDEN CORONARY DEATHS

VILJO RISSANEN

Department of Forensic Medicine University of Helsinki and University Central Hospital Kuopio
Finland

Rissanen Viljo Coronary atherosclerosis in middle aged and elderly Finnish men Pathological study of
coronary arteries in violent and sudden coronary deaths Acta path microbiol scand Sect A 88 167-
173 1980

The occurrence of coronary atherosclerosis was studied in 271 Finnish men aged 40 years or more of whom 143 had met a violent death and 128 had died suddenly of coronary heart disease (CHD). A coronary stenosis was found in half of the men who had met a violent death and were over 50 years old. The occurrence of the stenosis was closely related to the extent of the raised atherosclerotic lesions (RL) and to the degree of the plaque calcification. In 60 % of the sudden deaths (SD) the extent of RL did not differ from that in violent deaths. The stenosis patterns in these SD were similar to those in living CHD patients. The remaining SD had an extreme stage of coronary artery involvement, i.e. extensive plaques with severe obstructive changes. The men in this study series of violent deaths born in various parts of the country did not differ with regard to the extent of RL. Within the upper half of the RL area range men born in the east were consistently shown to have a stenosis while the occurrence in men from the western counties was more random. Severe stages of coronary artery involvement tended to be more frequent in SD patients born in the east than in those born in the west. It was concluded that there are probably two background factors concerning the difference in CHD mortality between men in western and eastern Finland: 1) the tendency to form a stenosis by the advancement of RL extent is stronger and 2) the progressive development of coronary artery disease in CHD patients is more frequent in the east than the west.

Key words: Atherosclerosis, coronary artery, coronary heart disease, Finnish men.

Viljo Rissanen, University Central Hospital SF 70210 Kuopio 21, Finland.

Received 24 ix 79 Accepted 30 xi 79

Patho-anatomic studies on coronary atherosclerosis have not revealed a clear explanation for the regional difference in the mortality from coronary heart disease (CHD) in Finland. The extent of coronary plaques seems to be similar in men from eastern and western Finland (Rissanen 1974) although the mortality rate of coronary heart disease is clearly higher in the former than the latter (Valkonen & Niemi 1978). Calcific degeneration of the plaques does, however, seem to occur earlier and be more extensive in men from eastern Finland (Mottonen 1969, Rissanen 1974).

In the present study coronary atherosclerosis was studied in a Finnish autopsy series of violent deaths and in a series of sudden coronary deaths. The risk population with regard to coronary artery involvement was determined on the basis of the comparison of these two series. Particular interest was focused on coronary lesions causing stenosis. Men born in various regions of the country were compared in order to formulate a theory for atherosclerosis which could explain the regional differences in CHD mortality.

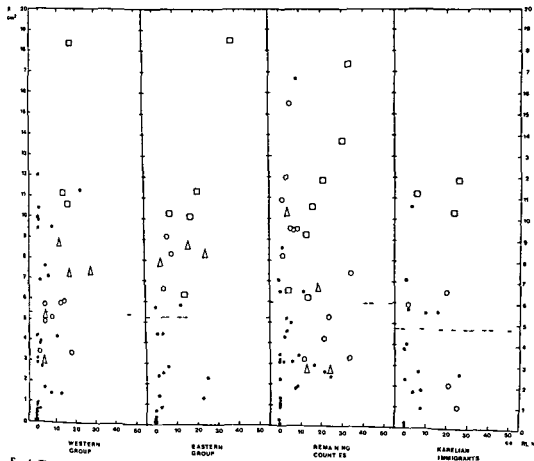


Fig 1 The area of raised lesion (cm^2) in relation to the degree of calcification ($\text{cal/RL} \%$) and the occurrence of different stenosis patterns in birthplace groups of violent deaths. The dotted line indicates the mean of the RL.
 □—triple vessel disease stenosis in 3 coronaries
 △—double vessel disease stenosis in 2 coronaries
 ○—single vessel disease stenosis in 1 coronary artery
 ●—no stenosis

and 55% of the violent deaths the extent of RL exceeded 4 cm^2 . The prevalence of single vessel disease was the same (27%) in SD with a normal extent of RL i.e. below 12 cm^2 as in violent deaths (26%) with an RL of $4\text{--}12 \text{ cm}^2$ (Table 1). Double and triple vessel diseases were twice as common in the former (22% and 42%) as in the latter (12.5% and 19.5%). Taking into account the extent of RL and the type of the stenosis pattern it was estimated that about 40% of the sudden deaths could be used to form a random sample of men with a stenosis from the population. The remaining SD victims had a severe stage of coronary artery involvement i.e. extensive plaques and/or severe obstructive changes.

Calcifications were found in all violent deaths with a coronary stenosis (Fig 1) in 90% of men

with no stenosis but with an RL over 4 cm^2 and in 54% of men with no stenosis and an RL below 4 cm^2 . The degree of calcific degeneration of the plaques was most advanced in men with triple vessel disease ($\text{cal/RL } 15.2 \pm 6.6\%$) or double ($\text{cal/RL } 14.3 \pm 8.9\%$) vessel disease (Fig 1). Also the degree of calcification was more advanced in

cases without stenosis ($\text{cal/RL } 4.6 \pm 5.6\%$) even if the area of the RL was similar ($4\text{--}12 \text{ cm}^2$) (t test $p < 0.05$).

Regional Differences

In the study series of violent deaths the mean extent and range of the RL were the same in men from all the regions (Fig 1). The area of the RL in

MATERIAL AND METHODS

Violent deaths The series consists of 143 men aged 40 to 78 years who met a violent death i.e. accident, suicide or homicide. The autopsies were performed during a period of 12 months at the Department of Forensic Medicine of the University of Helsinki.

Coronary deaths The series comprises 128 men aged 40 to 77 years who died suddenly within 24 hours after the onset of the fatal attack. The original series included 140 men collected from among victims classified as coronary deaths at routine medico-legal autopsies performed during a ten-month period at the Department of Forensic Medicine of the University of Helsinki. The autopsy rate of prehospital sudden deaths (SD) is about 80% in Helsinki. All such autopsies are carried out at the Department of Forensic Medicine. In the analysis twelve cases were excluded from the original series for the following reasons: five men were younger than 40 years, two men were born abroad and were not Finns, the birthplace of one man was unknown and in four men whose death was unwitnessed definite proof of a CHD death was missing and other causes of death were possible. An acute myocardial infarction (AMI) was revealed in 49% of the 128 men accepted in the series. In the remaining cases the diagnosis of a CHD death was based on the disease history, history of the fatal attack, autopsy findings of the heart and exclusion of other causes of death.

Place of birth

On the basis of birthplace the individuals of the two series were divided into four groups.

Western group Men born in the present four western counties of Finland (Åland, Turku and Pori, Häme, Vaasa) where the mortality rate of CHD is the lowest (Pöyälä 1974). The group included 43 violent and 28 sudden deaths. The mean age in the former case was 56.0 and in the latter 57.3 years.

Eastern group men born in the present five counties in the eastern and central parts of the country (North Karelia, Kuopio, Mikkeli, Oulu, Central Finland) where the mortality rate of CHD in men is the highest (Pöyälä 1974). There were 27 men in both series born in these counties: the mean age in cases of violent death being 53.2 and of sudden death 55.9 years.

Remaining provinces Men born in the three remaining counties (Uusimaa, Kymi, Lapland) where the rate of CHD mortality lies between that of the western and eastern counties (Pöyälä 1974). The group included 51 cases of both violent and sudden deaths. The mean age of the former was 56.0 and of the latter 56.4 years.

Carelian immigrant group Men born in areas ceded to the Soviet Union in 1944. There were 22 men in both series born in these areas: the mean age in cases of violent death being 53.8 and of sudden death 53.4 years. The immigrants have become integrated with the rest of the population and no reliable data specifically concerning their rate of CHD mortality are available.

Estimation of the Severity of Coronary Atherosclerosis

The principles developed and used in international studies on atherosclerosis (Gu-man *et al.* 1968) were followed in the present study. The methodological details have been described in previous papers (Rissanen 1972, Rissanen & Pöyälä 1972). Arterial specimens were prepared from the longitudinally opened right coronary artery and left anterior descending and left circumflex coronary arteries. The arterial specimens were fixed in 10% formalin. The specimens were radiographed for the exact determination of calcification.

The specifications set down by the study group of the International Atherosclerosis Project (Gu-man *et al.* 1968) were followed in the definition of atherosclerotic lesions. *Raised lesion* was a firm elevated intimal lesion with or without other changes covering it or underlying it.

The areas of the atherosclerotic lesions measured in square centimetres were assessed from the arterial specimens by the point counting technique (Rissanen 1972, Rissanen & Pöyälä 1972). The degree of coronary calcification was measured from the radiographs of the specimens by applying the point counting technique. As shown in the previous papers (Rissanen 1972, Rissanen & Pöyälä 1972) the reproducibility of the result obtained by the point counting technique was good and the accuracy comparable to that obtained by planimetry.

The degree of the coronary stenosis was estimated visually in the arterial specimens (Rissanen 1972). Stenosis of 50% or more was regarded as significant. The sites of occlusions or near occlusions were also recorded. The reproducibility of the estimation of stenosis was rather good (Rissanen 1972). The prevalences of coronary stenosis obtained by this visual estimation in the SD series were very similar to those obtained in another SD series studied by postmortem coronary angiography (Rissanen *et al.* 1978) as well as in an autopsy series of AMI hospital deaths studied in cross sections of the coronary arteries (Rissanen 1972) (Table 1).

RESULTS

Coronary atherosclerosis in the total series of violent and sudden deaths

A 50% stenosis of a coronary artery was found in half of the violent deaths over the age of 50 years. A stenosis was rare (14%) if the extent of RL was below 4 cm² (Table 2) but it was found in nearly half of the men with an RL of 4–8 cm² and in the three out of four men with a larger lesion. The upper limit of the range of the RL area seemed to be constant at about 12 cm² (Fig. 1). There were only few cases above this level.

Although the mean extent of the raised lesion was twice as large in sudden deaths (SD) as in violent deaths (Fig. 2), marked overlapping between two series was found. In 95% of the sudden deaths

TABLE 1 The Percentages of Different Stenosis Patterns in Violent and Sudden Deaths According to the Extent of Raised Lesion (RL) Compared with the Corresponding Prevalences in Two Postmortem and Two Clinical Series

Series	Triple vessel disease* (%)	Double vessel disease* (%)	Single vessel disease* (%)	No stenosis (%)
Present series				
Violent deaths (RL 4-12 cm ²)	19.5	12.5	26	42
Sudden deaths (RL > 12 cm ²)	69	25	6	-
Sudden deaths (RL < 12 cm ²)	42	22	27	9
Other postmortem series				
Sudden deaths studied by coronary angiography (Rissanen et al. 1978)				
with an old MI	69	28	2	1
without an old MI	37	37	23	3
AMI deaths at hospital (Rissanen 1979)	50.5	35	11.5	3
Clinical series of coronary arteriography				
CHD patients in Helsinki (Hekali 1976)	31	41	28	
CHD patients in the USA (Fuster et al. 1975)				
angina pectoris	31	37	24	
subendocardial MI	42	40	13	
transmural MI	38	30	27	

*1 \geq 50 per cent stenosis

TABLE 2 The Occurrence of Different Stenosis Patterns in Violent and Sudden Deaths in Relation to the Extent of Raised Lesion (RL)

Series	Number of cases	Triple vessel disease		Double vessel disease		Single vessel disease		No stenosis	
		cases	%	cases	%	cases	%	cases	%
Violent deaths									
RL > 12 cm ²	6	4	66	-	-	1	17	1	17
RL 8-12 cm ²	32	11	34.5	4	12.5	8	25	9	28
RL 4-8 cm ²	40	3	7.5	5	12.5	11	27.5	20	52.5
RL < 4 cm ²	65	-	-	3	5	6	9	56	86
Total	143	18	13	12	8	26	18	87	61
Sudden deaths									
RL 16-20 cm ²	17	8	67	3	25	1	8	-	-
RL 12-16 cm ²	39	77	69	10	26	2	5	-	-
RL 8-12 cm ²	39	20	51	9	23	7	18	3	8
RL < 8 cm ²	38	12	32	8	21	14	37	4	10
Total	128	67	52	30	23	24	19	7	6

numbers of sudden and violent deaths was 2.3 in the present western group but 1.1 in the eastern group. The numbers of violent deaths probably reflect the ratio of men in Helsinki born in the west and east of the country. On the other hand the appearance of sudden deaths in the series reflects the

CHD mortality rates in these sub-populations. The ratio of the mortality rates of CHD in the sub-populations in Helsinki originating from the west and east was 1.1.

†

5

* 1 \geq 50 per cent stenosis

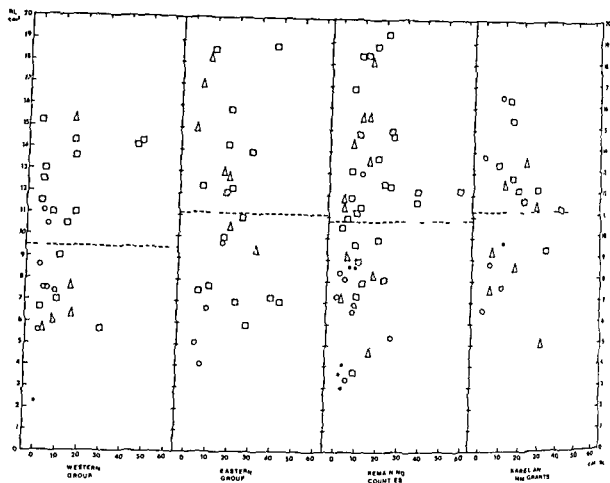


Fig 2 The area of raised lesion (cm^2) in relation to the degree of calcification (cal/RL %) and the occurrence of different stenosis patterns (symbols similar to those in Figure 1) in birthplace groups of sudden deaths. The dotted line indicates the mean of the RL.

the upper range ($6-12 \text{ cm}^2$) was consistently associated with a stenosis in men born in eastern Finland. In the other groups a stenosis was more randomly related to the extent of RL, particularly in men from the western counties (Fig. 1). The difference between the eastern and western groups was statistically significant (hypergeometric distribution test $p < 0.1$). As mentioned above, a portion of the series of sudden deaths overlapped with violent deaths with an RL of $4-12 \text{ cm}^2$. In these violent deaths the prevalence of a 50% stenosis was lower in the western group (48%) and immigrants (45%) than in the eastern (71%) and remaining (67%) groups (Fig. 1). The geographical groups of violent deaths did not differ significantly with regard to the degree of calcification (cal/RL: western men $8.4 \pm 7.6\%$, eastern men $10.1 \pm 7.7\%$).

Severe coronary atherosclerosis exceeding the degree which commonly seemed to occur in the population (RL over 12 cm^2) was less frequent in the western group of sudden deaths (29%) than the other groups (eastern 48%, remaining 39%

immigrants 45%) (Fig. 2). There were no significant differences in the prevalences of different stenosis patterns, i.e. triple, double or single vessel disease, between SD victims born in various geographic regions. A severe triple vessel disease, i.e. an occlusion or multiple 50% stenosis in all three coronaries, was however most frequent in the eastern SD group (41%), least frequent in the western SD group (18%) and of intermediate frequency in the remaining (24%) and immigrant (27%) groups.

DISCUSSION

It has been shown that people moving to Helsinki from various counties retain the same rate of mortality from CHD as those staying in their home counties (Karpela 1960). At the time of this study the ratio of the rate of CHD mortality between western and eastern men living in the counties was 2.3 (400/617/100 000) in the 35-64 year age group (Pyörälä 1974). The ratio between the

- Piorala K Aromaa A Karvonen M J & Rissanen V* On going research in cardiovascular diseases in Finland in 1979 (in Finnish) The National Research Council for Medical Sciences the Finnish Academy Helsinki 1979
- Rissanen V* Aortic and coronary atherosclerosis in a Finnish autopsy series of violent deaths. *Ann Acad Sci Fenn A V Medica* 155 1972
- Rissanen V & Piorala K* Application of point counting technique to quantitative assessment of coronary and aortic atherosclerosis. *Acta path microbiol scand Sect A* 80 412-420 1972
- Rissanen V* Coronary and aortic atherosclerosis in Finnish men born in various regions of the country. *Atherosclerosis* 20 495-506 1974
- Rissanen V Romo M & Silanen P* Prehospital sudden death from ischemic heart disease. A postmortem study. *Brit Heart J* 40 1025-1033 1978
- Rissanen V* Sudden coronary death and coronary artery disease. A clinicopathologic appraisal. *Cardiol* 64 289-302 1979
- Rose G* Detection of high coronary risk. *Postgrad med J* 52 452-456 1976
- Valkonen Y & Niemi M L* Regional differences in death rates from coronary heart disease in Finland (in Finnish) *Suom laak* 1 33 1968-1973 1978
- Varpela E* Cardiovascular mortality rate in Helsinki (in Swedish) *Nord Med* 63 127-129 1960

expected to be comparable with that in men living in the counties

The risk of CHD is determined by the development of a stenosis in the coronary arteries. This seems to be related to both the extent of the plaques and their degree of degeneration. The risk of a stenosis and at the same time the risk of a coronary death begins to increase when the area of raised atherosclerotic lesions exceeds about 4 cm² in the coronary artery tree. On the other hand there may be a critical upper level in the extent of coronary raised lesions (about 12 cm²) related to vitality (Rissanen 1979) persons with a more extensive coronary artery involvement tend to disappear from the population. For instance in the present series of violent deaths which represented a sample of the population the RL exceeded 12 cm² in only 4 % of cases.

In about 60% of the SD victims the area of raised lesion did not differ from that in the violent deaths. The occurrence of different stenosis patterns in these SD seems to correspond to figures reported in living CHD patients studied by clinical coronary arteriography (Fuster *et al* 1975 Hickali 1976 Table 1). This portion of the coronary deaths thus seems to form a sample of clinical patients or in part (40%) a sample from among the large number of men with a stenosis in the population. Epidemiological studies have shown that most cases of CHD of the community occur among the majority of individuals at moderate risk and only a minor proportion among the few clearly high risk people (Rose 1976). Correspondingly it is obvious that a great proportion of coronary deaths occur among the majority of individuals with moderate coronary lesions. On the basis of the vital statistics (Pyörälä 1974) it can be calculated that about half of those with a stenosis in the population will eventually die of CHD. In the occurrence of the fatal cases individuals prone to an exceptionally progressive development of coronary artery disease play a considerable role. This portion of the coronary deaths probably originates from a small fraction of the population.

Although there was no difference in the areas of raised lesions between men born in the west and the east the men did differ with regard to the tendency to develop a coronary stenosis. Within the upper half of the RL area range men born in the east were consistently shown to have a stenosis while the occurrence in men from the western counties was more random. The ratio of the prevalence of a stenosis was 2.3 in the western and eastern men with an RL area of 4–12 cm² which is a similar ratio to that found in the CHD mortality rate between the western and eastern male populations

(Pyörälä 1974). The CHD mortality in men from these regions is probably closely related to this tendency to develop a coronary stenosis in association with an advancement of the coronary artery involvement due to RL. This is supported by previous studies which have demonstrated more severe coronary calcification in men from eastern Finland (Mottonen 1969 Rissanen 1974). An increased tendency to calcification clearly increases the risk of a stenosis. Present findings in men from the remaining counties are also in accordance with the hypothesis.

CHD runs a short course and has a poor prognosis among men living in eastern Finland (Punsar 1972). A probable explanation is progressive development of coronary artery disease in many eastern CHD patients. Severe stages of coronary artery involvement tended to be less frequent in SD patients born in the west. Hence there are probably two background factors concerning the regional difference in the CHD mortality in Finland: 1) the tendency to form a stenosis by the advancement of the RL extent is stronger and 2) the progressive development of coronary artery disease in CHD patients is more prevalent in the east than in the west. It is possible that response of the coronary arteries to the risk factors is different in these populations. Recent epidemiological studies have shown that correlation of hypercholesterolemia, hypertension and smoking with a risk of CHD death is stronger in men living in eastern and central parts of Finland than in their western compatriots (Pyörälä *et al* 1979).

REFERENCES

- Fuster V, Frye R L, Connolly D C, Danielson M A, Elveback L R & Kurland L T. Arteriographic patterns early in the onset of the coronary syndrome. *Brit Heart J* 37: 1250–1255 1975.
- Gurman M A, McMahon C A, McGill H C Jr, Stronk J P, Tejada C, Rissipio C, Eggen D A, Robertson W B & Solberg L A. Selected methodologic aspects of the International Atherosclerosis Project. *Lab Invest* 18: 479–497 1968.
- Hickali P. Coronary angiography and clinical symptomatology. *Acta Radiol. suppl* 354 p. 80 1976.
- Mottonen M. Myocardial infarction and coronary atherosclerosis in Finland. An autopsy study covering 12 months in 1964–1965. *Acta path. microbiol. Scand. Sect. A* 75 suppl. 205 1969.
- Punsar S. Prognosis of CHD in East and West Finland. *Scand J clin. lab. invest.* 29 suppl. 122 19 1972.
- Pyörälä K. Epidemiology of coronary heart disease in Finland (in Finnish). *Duodecim* 90: 1605–1622 1974.

IMMUNOHISTOCHEMICAL DEMONSTRATION OF A HITHERTO UNDESCRIBED LOCALIZATION OF HEMOGLOBIN A AND F IN ENDODERMAL CELLS OF NORMAL HUMAN YOLK SAC AND ENDODERMAL SINUS TUMOR

R ALBRECHTSEN* U WEWER* and P D WIMBERLEY**

*University Institute of Pathological Anatomy and **Department of Neonatology Rigshospitalet
University of Copenhagen

Albrechtsen R, Wewer U & Wimberley P D Immunohistochemical demonstration of a hitherto
undescribed localization of hemoglobin A and F in endodermal cells of normal human yolk sac and
endodermal sinus tumor Acta path microbiol scand Sect A 88 175-178 1980

In this study of 4 human yolk sacs the presence of hemoglobin A and F (HbA and HbF) is
demonstrated for the first time in epithelial cells (type 1) and erythroid like cells (type 2) in the
endodermal layer by immunoperoxidase technique. Our findings strongly support the hypothesis
previously proposed that the red blood cells formed in the yolk sac are of endodermal origin. Tumor
with yolk sac differentiation (8 endodermal sinus tumors and 1 embryonal carcinoma with vitelline
areas) similarly showed HbA and HbF localisation in endodermal cells. None of 59 germ cell tumors
of other types contained these hemoglobins in the neoplastic cells.

Key words: Hemoglobin A and F, human yolk sac, endodermal sinus tumor, immunohistochemistry.

R Albrechtsen, University Institute of Pathological Anatomy, Frederik V's Vej 11, DK 2100 Copenhagen
Denmark.

Accepted as submitted 7 XII 79

The earliest erythropoiesis in human fetal life is
generally accepted to arise from mesenchymal cells
lying close to the yolk sac and allantois (9).
However, origin from the endoderm of the yolk sac
has been suggested by several authors based on their
findings of primitive erythroblasts in this layer (3,
5, 10). During investigations of the localization of a
series of oncofetal antigens in the normal human
yolk sac and in endodermal sinus (yolk sac) tumors,
we have observed the presence of focal endogenous
peroxidase activity confined to both normal and
neoplastic yolk sac cells. The purpose of the present
study was to investigate whether this peroxidase
activity was due to the presence of hemoglobin.

MATERIAL AND METHODS

The material includes 4 human yolk sacs obtained from
operated tubal pregnancies and 68 cases of testicular and
ovarian mone...

... according to Terlum's histogenetic
classification (1966) ...
... against AFP, HbA and IgG from
Dako Denmark and HbF (γ-chain) from Behringwerke
Hoechst Denmark. In this method 10% H₂O₂ in
methanol is used for total inhibition of endogenous

Fig 1 Wall of the yolk sac of a 6 week human embryo showing the presence of HbA in type 1 and 2 cells of the endodermal layer (EL) M indicates the mesenchyme (IP technique $\times 105$)

Fig 2 Same case as in Fig 1 HbA demonstrated in typical endodermal cells (type 1) (IP technique $\times 730$)

Fig 3 Same case as in Fig 1 HbA demonstrated in type 2 cells (erythroid like cells) of the endodermal layer. Note the cell (X) with an epithelial like upper contour (as type 1) and a rounded lower margin (as type 2) (IP technique $\times 730$)

Fig 4 HbF demonstrated in an endodermal sinus tumor. Several of the endodermal cells (E) show positivity (IP technique $\times 180$)

Fig 5 Embryonal carcinoma with vitelline areas. HbF is seen in several of the tumor cells. The insert shows a vessel close to the demonstrated area with erythroblasts (B) staining positive for HbF (IP technique $\times 204$)

peroxidase activity in the tissue sections. The sections were counterstained with haematoxylin. The visualisation of the peroxidase activity was made optimal with an interference filter fitted to the microscope which changed the reaction product from brown to red (4). Absorption of the specific antisera with corresponding antigens (AFP, HbA and HbF from hemolysed adult and fetal blood) and using non immunized rabbit serum in place of the specific antisera served as negative controls.

RESULTS

In all 4 yolk sacs variable intensity of AFP was localized only to the endodermal cells. HbA and HbF were both demonstrated in all 4 yolk sacs in 2 different cell types of the endodermal layer. Type 1 cells were columnar epithelial cells lying singly at some distance from each other and mainly localized to the middle and deeper portions of the endodermal layer (Fig 1, 2). Type 2 cells were round erythroid like cells with same localization as type 1 (Fig 3). Transformation from type 1 to type 2 was often indicated as the contour of some cells on one side was characteristic for an epithelial cell (type 1) and round on the other side as an erythroid like cell (type 2) (Fig 3).

Clusters of mainly type 2 cells intermingled with a few type 1 cells were found predominantly in the part of the endodermal layer which spread to the mesenchyme having the appearance of blood islands. Some mesenchymal cells including the pericytes also showed positive reaction but in all 4 cases this positivity was significantly less marked than in the endodermal cells. Attempts at demonstration of IgG in the endodermal cells were constantly negative in all 4 cases.

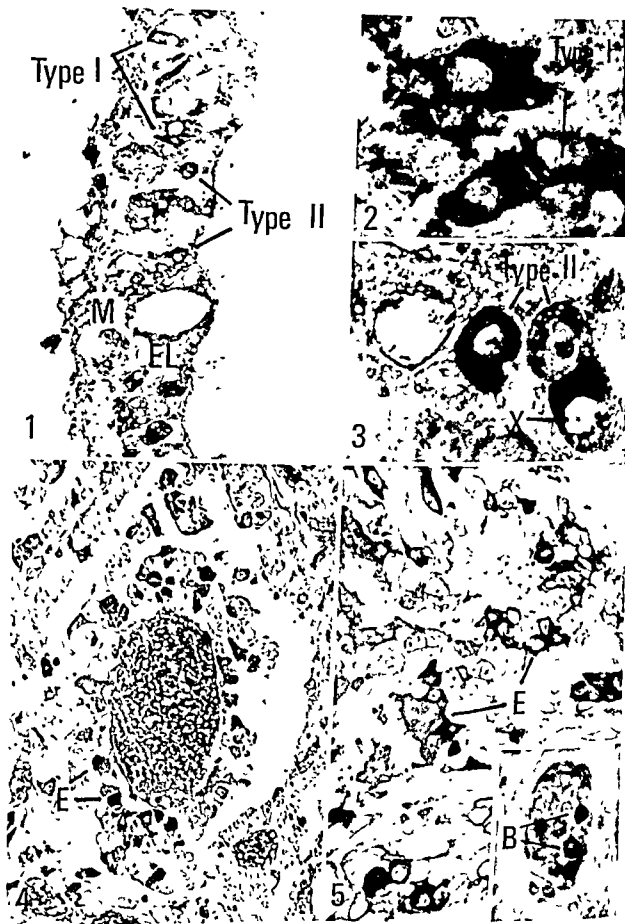
Demonstration of HbF (Fig 4). HbA and AFP in the tumors showed positive reaction only in areas with endodermal sinus tumor differentiation (8 out of 15 cases) and only in the endodermal cells. We were not able to discriminate the characteristic type

1 and type 2 cells in the tumors as in the normal yolk sac. Only one of the other germ cell tumors, an embryonal carcinoma, also showed positive reaction for HbF (Fig 5). HbA and AFP IgG could not be demonstrated in the tumor cells. The remaining germ cell tumors which included seminomas, embryonal carcinomas and mature teratomas were negative for HbF. HbA and AFP in tumor cells in successive sections. The specificity of the immunohistochemical staining technique for HbA and HbF was confirmed by the constantly positive reaction of the erythrocytes in the normal human fetus and tumors.

COMMENTS

The present study shows for the first time the localization of HbA and HbF in the human yolk sac endoderm. The absence of IgG in this layer excludes passive indiffusion of hemoglobin (1). Also phagocytosis of hemoglobin material by the endodermal cells is unlikely as the intracellular distribution was not localized focally but diffusely in each cell cytoplasm. It may thus be concluded that the endodermal cells in the human yolk sac are able to synthesize hemoglobins thereby supporting the hypothesis previously proposed that the primitive erythroblasts formed in the yolk sac are of endodermal origin. Furthermore we have demonstrated that HbA and HbF are present in human yolk sac as early as 6 weeks of age. The expected presence of embryonic hemoglobins (6) could not be confirmed immunohistochemically in this study as no antisera are yet available. However the isolation and purification of the embryonic hemoglobins (2, 11) have recently opened the possibility of the production of such antisera.

Of the germ cell tumors investigated, it was only in those with endodermal sinus tumor differentiation that localization of HbA and HbF was found and confined to the endodermal cells as in the



HEART PATHOLOGY IN RATS FED PARTIALLY HYDROGENATED FISH OIL, RAPESEED OIL OR PEANUT OIL FOR 30 WEEKS

H SVAAR and F T LANGMARK

Department of Pathology Ullevål Hospital and Department of Pathology The Norwegian Radium
Hospital Montebello Oslo Norway

Svaar H & Langmark F T Heart pathology in rats fed partially hydrogenated fish oil rapeseed oil
or peanut oil for 30 weeks Acta path microbiol scand Sect A 88 179-187 1980

132 male *Sprague Dawley* rats were given diets for 30 weeks including rapeseed oil with 41.4% erucic acid partially hydrogenated fish oil with 15.1% docosenoic acids or peanut oil with no docosenoic acids. Four diets were isocaloric and contained respectively 21% rapeseed oil (8.7% w/w erucic acid), 10.5% rapeseed oil and 10.5% peanut oil (4.4% w/w erucic acid), 21% partially hydrogenated fish oil (3.2% w/w docosenoic acids) and 21% peanut oil. The fifth diet contained 4.3% peanut oil. The relative heart weights increased in rats fed rapeseed oil and partially hydrogenated fish oil and abnormally enlarged hearts were found in 32% of the rats fed 21% rapeseed oil and in 5% of those fed 10.5% rapeseed oil. Heart lesions consisting of focal or confluent destruction of muscle cells were seen in all groups. The incidence was 96% and the average severity grade 2.5 when 21% rapeseed oil was given and 61% and 1.3 respectively when 10.5% rapeseed oil was given. Minor heart lesions were found in 14% of the rats fed 21% partially hydrogenated fish oil, in 39% of those fed 21% peanut oil and in 12% when 4.3% peanut oil was given. It is concluded that partially hydrogenated fish oil is markedly less cardiopathogenic than high erucic rapeseed oil. The heart lesions that were found do not differ in incidence, severity or morphology from those found when peanut oil was given or from those reported when other control fats and oils are given to rats for prolonged feeding periods.

Key words: Fish oil, rapeseed oil, heart lesions, rats.

Helge Svaar, Patologisk anatomisk afdeling, Sentralsykehuset i Akershus, 1474 Nordbyhagen, Norge.

Received 1 v 79 Accepted 15 xii 79

Long term feeding of rats with diets containing rapeseed oil rich in erucic acid (C22:1 cis-omega 9) is accompanied by heart muscle destruction, histiocytic infiltration and scar tissue formation (2, 3, 5, 6, 8, 15). Male rats of the *Sprague Dawley* and *Wistar* strains are particularly sensitive to these diets (3, 12, 18). The erucic acid has been considered to be the main cardiotoxic factor since shortly after intake heart muscle lipidosis occurs to a degree that is directly related to the dietary concentration of the erucic acid. There is no known explanation for the heart muscle destruction, however, since the lipidosis is transient and the heart muscle lesions are seen after prolonged feeding periods (12).

The transient lipidosis phenomenon at . . .

... in which a small proportion is erucic acid while the balance is made up of other positional and geometrical isomers of erucic acid (13). We have previously examined the heart morphology in rats fed partially hydrogenated fish oils for 16 weeks and we were unable to find cardiac lesions that could be ascribed to these oils since similar changes of the same incidence and severity were found in the rats fed lard and tallow oil mixtures as control fats (16).

The present study was therefore undertaken to observe the cardiac changes after prolonged feeding

normal human yolk sac. This is expected from the finding that this tumor type is well characterized by a selective overgrowth of yolk sac endoderm and that hematopoiesis can often be found in this tumor in contrast to other germ cell tumors (13). Kellen & Malkin (1979) have shown significant elevation of HbF in the blood of some patients with ovarian and testicular cancers compared to other cases of malignant tumors. Our results suggest that this finding could be due to the tumors' own production of HbF. Further studies are required to elucidate whether fetal and embryonic hemoglobins could be useful markers for endodermal sinus tumors.

Our thanks are due to the Department of Pathological Anatomy, Aalborg Sygehus, Århus Nord and Department of Obstetric and Gynecology, Frederiksborg Amts Centralsygehus, Hillerød, who made the embryonal material available to us.

REFERENCES

- Engelhardt N V, Goussev A I, Shipova L Ya & Abelev G I. Immunofluorescent study of alpha fetoprotein (afp) in liver and liver tumours. I. Technique of afp localization in tissue sections. *Int J Cancer* 7: 198-206 1971.
- Gale R E, Clegg J B & Huehns E R. Human embryonic haemoglobins Gower 1 and Gower 2. *Nature (Lond)* 280: 162-164 1979.
- Gladstone R J & Hamilton W J. A presomite human embryo (Shaw) with primitive streak and chorda canal with special reference to the development of the vascular system. *J Anat* 76: 9-44 1941.
- Heyderman E. Personal communication 1977.
- Hoyes A D. The human foetal yolk sac. An ultrastructural study of four specimens. *Z Zellforsch* 99: 469-490 1969.
- Huehns E R, Flynn F J, Butler E A & Beaven G H. Two new haemoglobin variants in a very young human embryo. *Nature (Lond)* 189: 496-497 1961.
- Kellen J A & Malkin A. Alkali resistant hemoglobin in cancer patients. In: Lehmann F G (Ed). *Carcino-embryonic proteins*. Vol 2. Elsevier North Holland Press, Amsterdam 1979. pp 593-597.
- Langman J. *Medical embryology*. 3rd ed. The Williams & Wilkins Company, Baltimore 1973. p 75.
- Maximow A A. Relation of blood cells to connective tissues and endothelium. *Physiol Rev* 4: 533-563 1924.
- Piney A. Recent advances in haematology. J & A Churchill, London 1931. pp 17-39.
- Rutherford T R, Clegg J B & Weatherall D J. H562 human leukaemic cells synthesise embryonic haemoglobin in response to haemin. *Nature (Lond)* 280: 164-165 1979.
- Taylor C R & Burns J. The demonstration of plasma cells and other immunoglobulin-containing cells in formalin fixed paraffinembedded tissues using peroxidase labelled antibody. *J Clin Pathol* 27: 14-20 1974.
- Teilum G. Classification of endodermal sinus tumour (Mesoblastoma vitellinum) and so-called «embryonal carcinoma» of the ovary. *Acta path microbiol scand* 64: 407-429 1965.

HEART PATHOLOGY IN RATS FED PARTIALLY HYDROGENATED FISH OIL, RAPESEED OIL OR PEANUT OIL FOR 30 WEEKS

H SVAAR and F T LANGMARK

Department of Pathology Ullevål Hospital and Department of Pathology The Norwegian Radium
Hospital Montebello Oslo Norway

Svaar H & Langmark F T Heart pathology in rats fed partially hydrogenated fish oil rapeseed oil
or peanut oil for 30 weeks Acta path microbiol scand Sect A 88 179-187 1980

132 male *Sprague Dawley* rats were given diets for 30 weeks including rapeseed oil with 41.4% erucic acid and partially hydrogenated fish oil with 15.1% docosenoic acids or peanut oil with no docosenoic acids. Four diets were isocaloric and contained respectively 21% rapeseed oil (8.7% w/w erucic acid), 10.5% rapeseed oil and 10.5% peanut oil (4.4% w/w erucic acid), 21% partially hydrogenated fish oil (3.2% w/w docosenoic acids) and 21% peanut oil. The fifth diet contained 4.3% peanut oil. The relative heart weights increased in rats fed rapeseed oil and partially hydrogenated fish oil and abnormally enlarged hearts were found in 32% of the rats fed 21% rapeseed oil and in 5% of those fed 10.5% rapeseed oil. Heart lesions consisting of focal or confluent destruction of muscle cells were seen in all groups. The incidence was 96% and the average severity grade 2.5 when 21% rapeseed oil was given and 61% and 1.3 respectively when 10.5% rapeseed oil was given. Minor heart lesions were found in 14% of the rats fed 21% partially hydrogenated fish oil, in 39% of those fed 21% peanut oil and in 12% when 4.3% peanut oil was given. It is concluded that partially hydrogenated fish oil is markedly less cardiopathogenic than high erucic rapeseed oil. The heart lesions that were found do not differ in incidence, severity or morphology from those found when peanut oil was given or from those reported when other control fats and oils are given to rats for prolonged feeding periods.

Key words: Fish oil, rapeseed oil, heart lesions, rats.

Helge Svaar, Patologisk anatomisk avdeling, Sentralsykehuset i Akershus, 1474 Nordbyhagen, Norge.

Received 1 v 79 Accepted 15 xii 79

Long term feeding of rats with diets containing rapeseed oil rich in erucic acid (C22:1 cis omega 9) is accompanied by heart muscle destruction, histiocytic infiltration and scar tissue formation (2, 3, 5, 6, 8, 15). Male rats of the *Sprague Dawley* and *Wistar* strains are particularly sensitive to these diets (3, 12, 18). The erucic acid has been considered to be the main cardiotoxic factor since shortly after intake heart muscle lipidosis occurs to a degree that is directly related to the dietary concentration of erucic acid. There is no known explanation for the

The transient lipidosis phenomenon also occurs when partially hydrogenated fish oils are given (17). The latter oils contain 10-30% C22:1 fatty acids of which only a small proportion is erucic acid while the balance is made up of other positional and geometrical isomers of erucic acid (13). We have previously examined the heart morphology in rats fed partially hydrogenated fish oils for 16 weeks and we were unable to find cardiac lesions that could be ascribed to these oils since similar changes of the same incidence and severity were found in the rats fed lard and corn oil mixtures as control fats (16).

The present study was therefore undertaken to observe the cardiac changes after prolonged feeding

normal human yolk sac. This is expected from the finding that this tumor type is well characterized by a selective overgrowth of yolk sac endoderm and that hematopoiesis can often be found in this tumor in contrast to other germ cell tumors (13). *Kellen & Malkin* (1979) have shown significant elevation of HbF in the blood of some patients with ovarian and testicular cancers compared to other cases of malignant tumors. Our results suggest that this finding could be due to the tumors' own production of HbF. Further studies are required to elucidate whether fetal and embryonic hemoglobins could be useful markers for endodermal sinus tumors.

Our thanks are due to the Department of Pathological Anatomy Aalborg Sygehus afsnit Nord and Department of Obstetric and Gynecology Frederiksborg Amts Centralsygehus Hillerød who made the embryonal material available to us.

REFERENCES

1. Engelhardt N V, Goussev A I, Shipova L Ya & Abelev G I. Immunofluorescent study of alpha fetoprotein (afp) in liver and liver tumours. I. Technique of afp localization in tissue sections. *Int J Cancer* 7: 198-206 1971.
2. Gale R E, Clegg J B & Huehns E R. Human embryonic haemoglobins. *Gower 1 and Gower 2 Nature (Lond)* 280: 162-164 1979.
3. Gladstone R J & Hamilton W J. A presumptive human embryo (Shaw) with primitive streak and chorda canal with special reference to the development of the vascular system. *J Anat* 76: 9-44 1941.
4. Heyderman E. Personal communication 1977.
5. Hoyer A D. The human foetal yolk sac. An ultrastructural study of four specimens. *Z Zellforsch* 99: 469-490 1969.
6. Huehns E R, Flynn F V, Butler E A & Beaton G H. Two new haemoglobin variants in a very young human embryo. *Nature (Lond)* 189: 496-497 1961.
7. Kellen J A & Malkin A. Alkali resistant hemoglobin in cancer patients. In Lehmann F G (Ed). *Carcino embryonic proteins Vol 2*. Elsevier North Holland Press, Amsterdam 1979. pp 593-597.
8. Langman J. *Medical embryology* 3rd ed. The Williams & Wilkins Company, Baltimore 1975. p 75.
9. Maximow A A. Relation of blood cells to connective tissues and endothelium. *Physiol Rev* 4: 533-563 1924.
10. Pinney A. *Recent advances in haematology* J & A Churchill, London 1931. pp 17-39.
11. Rutherford T R, Clegg J B & Weatherall D J. K562 human leukaemic cells synthesise embryonic haemoglobin in response to haemin. *Nature (Lond)* 280: 164-165 1979.
12. Taylor C R & Burns J. The demonstration of plasma cells and other immunoglobulin-containing cells in formalin fixed paraffin embedded tissues using peroxidase labelled antibody. *J Clin Pathol* 27: 14-20 1974.
13. Teilum G. Classification of endodermal sinus tumour (Mesoblastoma vitellinum) and so called embryonal carcinoma of the ovary. *Acta path microbiol scand* 64: 407-429 1965.

TABLE 2 Fatty Acid Composition of Dietary Oils (w/w %)

Fatty acid	PO	PHFO	RSO
12:0	—	0.1	—
14:0	0.1	8.2	0.1
15:0	—	0.4	—
16:0	10.9	13.7	2.7
16:1	0.2	8.9	0.2
17:0	—	0.6	—
17:1	0.1	—	—
18:0	3.0	3.4	1.1
18:1	37.3	15.9	16.8
18:2	40.6	2.5	14.9
18:3	—	—	9.0
19:0	—	0.3	—
20:0	1.2	1.9	0.6
20:1	1.8	16.2	9.4
20:2	—	—	0.7
20:3 poly	—	5.0	—
21:0	—	0.5	—
21:1	3.2	2.1	0.6
22:1	—	15.1	41.6
22:2	—	—	0.6
22:3 poly	—	4.1	—
24:0	1.6	—	0.2
24:1	—	1.1	—
Others	—	1.1	—

Diets Five diets were prepared with the composition shown in Table 1. All the oils were commercial samples obtained from DeNoFa/Lilleborg Fabrikker, Fredrikstad, Norway. The fatty acid composition of the oils used is shown in Table 2. The partially hydrogenated fish oil was produced from capelin oil and had a melting point of 31–33°C. The diet contained 3.2% w/w C22:1 and 3.4% w/w C20:1. The rapeseed oil diets contained 8.7% w/w and 4.4% w/w C22:1 (erucic acid) and 2.0% w/w and 1.1% w/w C20:1 respectively. The peanut oil diets had no C22:1 fatty acids and 0.4% w/w C20:1. The low fat peanut oil diet had a fat amount similar to the commercial pellets used as standard rat food.

RESULTS

All diets were well tolerated and the rats had a steady weight increase up to the 24th week. At this time an increasing number of rats fed 21% rapeseed oil or 21% peanut oil began to eat less and to lose weight. These rats appeared irritable but no other signs of sickness could be detected. All the diets were analyzed to verify composition but no faults were detected. The weight loss continued in the two groups even with newly prepared diets including

fresh salt and vitamin mixtures. The other three groups had a weight increase even after week 24 but their growth curves levelled off and from week 27 a weight loss was found also in these groups (Fig. 1). The growth rate for the first 24 weeks was highest in the group fed 21% peanut oil and significantly lower in the group fed partially hydrogenated fish oil. The lag in weight increase was most pronounced during the first 8 weeks afterwards the weight increase stabilized at a level of 71–76% of the peanut oil group.

Five rats fed partially hydrogenated fish oil died in the early stages of the experiment (after 2, 8, 9, 10 and 11 weeks). They had all appeared healthy and their weight increases were similar to the other rats in the group up to the time of death. One of these rats had severe degeneration and inflammation of the epididymis and all of them had dilatation of the kidney tubules and calcification of some tubular cells. The other organs had normal morphology at autopsy and no evidence of cardiac lesions was found. One rat fed 10.5% rapeseed oil + 10.5% peanut oil appeared to be sick for one week. A malignant tumor was then discovered and

pneumonia was found at autopsy.

Symptoms of essential fatty acid (EFA) deficiency were sought with particular care but during the experimental period no signs of scaliness of the tails or feet were found in any of the rats, no hairloss was observed and all the rats developed a brown yellow colour of the fur on their backs.

At autopsy the relative organ weights in the rats fed 4.3% and 21% peanut oil were similar while the mean weights of the lung, the heart and the kidney were increased in the rats fed 21% rapeseed oil and the heart, the liver and the kidney were enlarged in the rats fed 21% partially hydrogenated fish oil ($p < 0.01$, Wilcoxon rank sum test). Microscopical changes in the lungs, the livers and the kidneys are summarized in Table 3. Focal interstitial pneumonia was found in 13% of the rats. Accumulation of lipid-containing foam cells in the lung tissue was more frequent in rats fed the fat rich diets. Steatosis in the livers was moderate and involved individual liver cells. Calcification of individual kidney tubular cells was seen in all groups but most frequently in the rats fed 21% rapeseed oil.

The body weight and the hearts were considered to be abnormally enlarged when they weighed more than 0.43 g/100g body weight.

of partially hydrogenated fish oil. Two diets containing peanut oil were chosen as »negative« controls and two diets containing rapeseed oil rich in erucic acid served as »positive« controls.

MATERIAL AND METHODS

Feeding 132 male *Sprague Dawley* rats were obtained from *Anticimex Sollentuna* Sweden when 3 weeks old. They were fed commercial pellets for one week in individual cages before being randomly distributed to one of five experimental diets. The rats were kept in one room at 21–22 °C at a relative humidity of 40–50%, in wire mesh cages with elevated floor. They had access to tap water *ad libitum*. The diets were given in plastic cups at 10g per day the first 4 weeks, 15g per day the next 4 weeks and 20g per day during the rest of the experiment. Food consumption appeared to be similar in all the groups as judged from leftovers in the cups and spills in the cages, but these amounts were not weighed. The rats were handled once a week for weighing and inspection.

Pathology The animals were killed with an overdose of ether. A complete autopsy was performed and after weighing on a *Mettler 2000C* electric balance the organs were fixed in 4% neutral formaldehyde. Ten hearts selected by random numbers from each group were examined for evidence of cardiac hypertrophy: the right ventricle wall was carefully dissected from the interventricular septum and the left ventricle wall and both parts

weighed separately. All the hearts were divided in 5–6 transverse slices that were embedded in paraffin. Two sections were made from each block. One was stained with hematoxylin and eosin and the other with *von Gieson* for demonstration of connective tissue. Sections from all organs were stained with hematoxylin and eosin and in addition the kidney sections were stained with *von Kossa* for demonstration of calcium salt.

Five hearts selected at random from each group were perfused for 3–4 minutes with 2% glutaraldehyde in *Sørensen's* phosphate buffer via a canula in the aorta at a pressure of 75 cm water. The hearts were cut in transverse sections and small pieces from the left and right papillary muscles and the left and right ventricle walls were postfixed in osmium tetroxide and embedded in *Epon 812*. Ultrathin sections were cut with glass knives on *LAB Ultratomes*, stained with uranyl acetate and lead citrate and studied with a *Zeiss EM10* electron microscope. The remainder of the transverse heart sections were processed for light microscopy as above. All the rats and the histological sections were examined without knowledge of the dietary groups until the study was completed.

The heart lesions were scored according to the following grading system: grade 1 = 1–3 small focal areas with muscle cell destruction; grade 2 = more than 3 small lesions or 1–3 large lesions; grade 3 = more than 3 large lesions; grade 4 = transmural lesions. A small lesion covers an area less than the microscope field at magnification 40 × 1.25 × 10 using a *Reichert* hepar microscope. A large lesion covers an area larger than one

TABLE 1. Composition of the Diets in Grams per 10 000 Grams

	PO 4.3	PO 21	PHFO 21	RSO 10.5	RSO 21
Sucrose	2 000	2 000	2 000	2 000	2 000
Corn starch	4 820	3 150	3 150	3 150	3 150
Casein*	2 000	2 000	2 000	2 000	2 000
Cellulose	100	100	100	100	100
Salt mixture**	500	500	500	500	500
Vitamin mixture**	150	150	150	150	150
Peanut oil (PO)	430	2 100		1 050	
Partially hydrogenated capelin oil (PHFO)	–	–	2 100	–	–
Rapeseed oil (RSO)	–	–	–	1 050	2 100
% C22:1	0	0	3.2	4.4	8.7

*Casein supplemented with 40 g methionin per 2 000 g

**AOAC Methods XIth edition 1970 p 800

***AOAC Methods XIth edition 1970 p 885

PO 4.3 = 4.3% w/w peanut oil in diet

enated fish oil in diet

nd 10.5% w/w peanut oil in diet

et

TABLE 4 *Distribution of Heart Lesions in Groups*

Number of rats in group	PO 43 26	PO 21 26	PHFO 21 22	RSO 10.5 26	RSO 21 25
Macroscopical lesions				27%	48%
Microscopical lesions					
Grade 1	12%	27%	9%	19%	8%
Grade 2		8%	5%	19%	20%
Grade 3		4%	—	23%	68%
Hearts with lesions	12%	39%	14%	61%	96%
Average grade per heart	0.1	0.5	0.2	1.3	2.5
% C221 index	0	0	3.2	4.4	8.7

(the heart weight in control groups + 4 standard deviations). Abnormally enlarged hearts were found in 32% of the rats fed 21% rapeseed oil and one rat fed 10.5% rapeseed oil had a heart weight of 0.63. The hearts were symmetrically enlarged and the ratio of the interventricular septum + left free wall weight/right ventricle wall weight was 3.9 ± 0.4 in all groups.

By macroscopical examination patchy fibrosis was found on the epicardial surface of 19 hearts all from rats fed rapeseed oil. The distribution of the microscopical heart lesions is shown in Table 4. The lesions were in general located in the outer 1/3 of the left and right ventricle walls (the subepicardial zone) but in the rats fed rapeseed oil lesions were also found in other parts of the walls fairly

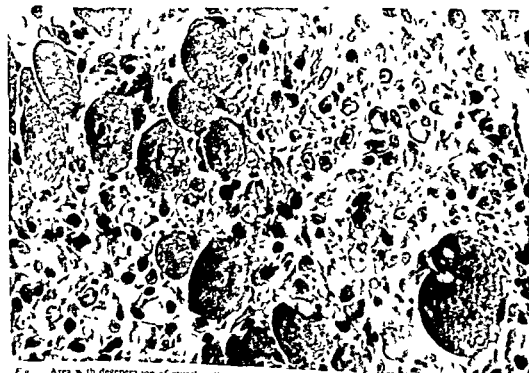


Fig. Area with degeneration of muscle cells, necrosis and infiltration of leukocytes, rat fed RSO 21, 500x.

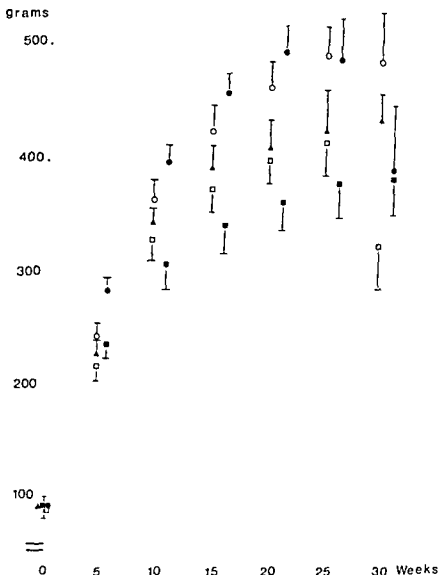


Fig 1 Average growth of male Sprague-Dawley rats fed the test diets for 30 weeks (with SD)

- ▲ 4.3% peanut oil PO 4.3
 ● 21% peanut oil PO 21
 ■ 21% partially hydrogenated fish oil PHFO 21
 □ 21% rapeseed oil RSO 21
 ○ 10.5% rapeseed oil + 10.5% peanut oil RSO 10.5

TABLE 3 Morphological Changes in Lungs Livers and Kidneys

Number of rats in group	PO 4.3 26	PO 21 26	PHFO 21 22	RSO 10.5 26	RSO 21 25
Lungs					
Pneumonia	15%	12%	0	12%	20%
Granuloma	4%	12%	23%	15%	16%
Foam cells	12%	58%	41%	50%	64%
Livers					
Steatosis	0	0	4%	0	20%
Kidneys					
Calcified tubules	12%	4%	50%	15%	20%

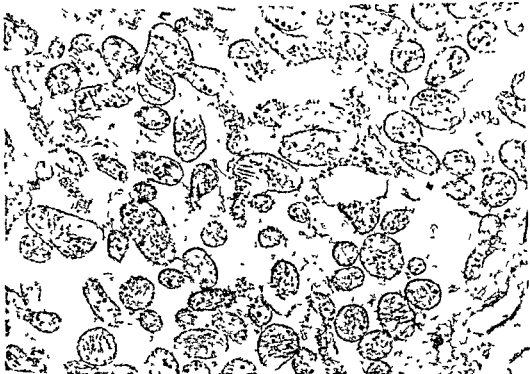


Fig 4 Increase of mitochondria and loss of myofibrils in heart muscle Same heart as fig 3 15 000 x

96% when the rapeseed oil amount was increased to give 1.6% w/w erucic acid. In these studies there seems to be a good correlation between the incidence and severity of the heart lesions and the amount of rapeseed oil in the diet but the erucic acid concentrations in the diets causing 50–60% incidence varies considerably (4.4%, 1.1% and 0.6%).

There has been some speculation as to other factors in rapeseed oil that contribute to the cardiopathogenic effects. Partial hydrogenation of rapeseed oil rich in erucic acid was accompanied by a reduction in the cardiopathogenic effects in male Sprague Dawley rats fed for 16 weeks (5). Partial hydrogenation reduced the content of linoleic acid and linolenic acid and increased the proportion of saturated fatty acids. McCutcheon *et al* (14) fed semipurified diets with fat from different vegetable sources to male Wistar rats for 25 weeks. The most severe heart lesions were found in rats given 5–6% w/w erucic acid irrespective of the vegetable source (two rapeseed oils *Brassica napus* and *Brassica campestris* and oil from nasturtium *Trapaetolum majus*) and the incidence was 100%. Similar heart lesions were found in 50% of the rats fed a low-erucic rapeseed oil (*Brassica napus*) with 0.15% erucic acid while one diet containing 5.5% w/w erucic acid and no linolenic acid resulted

in a marked reduction in the incidence/severity rating of the heart lesions. The authors therefore postulated that linolenic acid plays a role in the cardiopathogenicity of rapeseed oil. Hulan *et al* (10) obtained rendered pig fat containing 5.6% erucic acid after having fed rapeseed oil to pigs for 16 weeks. When the pig fat was given to Sprague Dawley rats for 16 weeks minor heart lesions were found with the same incidence as in rats fed the control fat (lard). A similar incidence and severity was found when lard supplemented with 5.6% free erucic acid was given while Span rapeseed oil (*Brassica campestris*) containing 4.8% erucic acid caused a significant increase in the incidence and severity of the heart lesions. These results suggest that erucic acid is not alone responsible for the heart lesions.

In the present study peanut oil was given as control fat at two levels 4.3% and 21%. Heart lesions with the same morphological appearance as found after rapeseed oil feeding were seen in both groups but more pronounced changes were found

unexplained weight loss during the last 6 weeks of the experiment and this may be of importance. Most

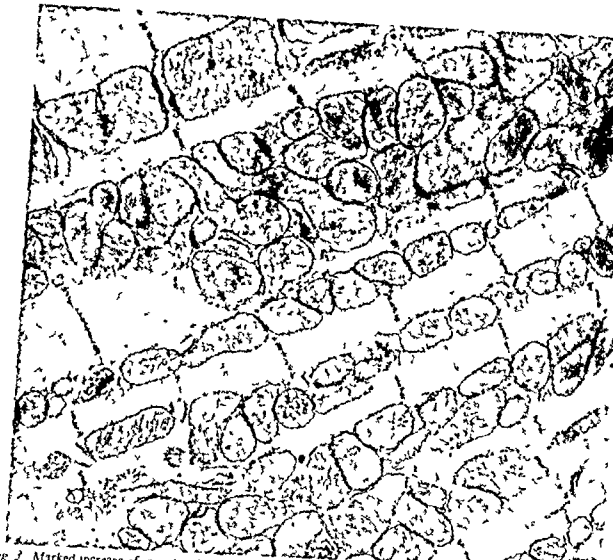


Fig 3 Marked increase of mitochondria in heart muscle from rat fed RSO 10.5 The heart was markedly enlarged 15 000 ×

frequently in the subendocardial zone in the left ventricle wall. Degenerating or necrotic muscle cells were seen in all hearts scored as positive. In addition infiltrations of histiocytes were found together with areas of fibrotic scar tissue (Fig 2). Electron microscopical examination of the largest heart showed a marked increase of mitochondria (Fig 3) and focal areas with loss of myofibrils in the heart muscle cells (Fig 4). The partially hydrogenated fish oil had produced minor lesions in 3 out of 22 hearts (14%) and the changes appeared similar to those found in the other groups.

DISCUSSION

In this study the pathological effect of rapeseed oil rich in erucic acid given to male Sprague Dawley rats is clearly demonstrated. The main changes in

the heart are muscle cell necrosis and scar tissue formation. More pronounced changes appear when the dietary concentration is increased from 50% to 100% of the fat (erucic acid content from 4.4% w/w to 8.7% w/w) the incidence increased from 61% to 96% and the severity grade from 1.3 to 2.5. These results confirm other studies with long term feeding of this type of oil to rats. Thus Abdellatif & Klee (13) found heart lesions in 50% of male Sprague Dawley rats fed 2.5% rapeseed oil (1.1% w/w erucic acid) for 32 weeks and the incidence increased to 88–100% when the rapeseed oil constituted 62%–75% of the dietary fat (5.5%–6.5% w/w erucic acid). They found similar changes when 30% w/w rapeseed oil or 15% w/w trierucin was given to Wistar rats for 24 weeks (each diet contained 12.5% w/w erucic acid). Ziemiński *et al.* (19) found an incidence of 61% when a 5% rapeseed oil diet with 0.6% w/w erucic acid was given for 28 weeks.

The excellent facilities and good help supplied by Dr med vet. L. Scherven and the Animal Unit, Rikshospitalet, Oslo are acknowledged. The technical assistance of Mrs G. Berg Pedersen is greatly appreciated. DeNoFa og Lilleborg Fabrikker, Fredrikstad supplied the oils and Mr T. Grimsvang and Mr B. Bauge were responsible for the fatty acid analysis. This work was supported by the Royal Norwegian Council for Scientific and Industrial Research and the Norwegian Research Association for Edible Fats.

REFERENCES

- 1 Aas Jørgensen E. Essential fatty acids. *Physiological Reviews* 41: 1-51 1961.
- 2 Abdellatif A M M & Vles R O. Pathological effects of dietary rapeseed oil in rats. *Nutr. Metabol.* 12: 285-295 1970.
- 3 Abdellatif A M M & Vles R O. Short term and long term pathological effects of glyceryl trierucate and of increasing levels of rapeseed oil in rats. *Nutr. Metabol.* 15: 219-231 1973.
- 4 Ackman R G. Myocardial alterations from feeding partially hydrogenated marine oils and peanut oil to rats. *Lipids* 9: 1032-1035 1974.
- 5 Beare Rogers J L, Nera E A & Heggveit H A. Myocardial alteration in rats fed rapeseed oils containing high or low levels of erucic acid. *Nutr. Metabol.* 17: 213-222 1974.
- 6 Charlton K M, Corner A H, Daves K, Kramer J K G, Mahadevan D & Sauer F D. Cardiac lesions in rats fed rapeseed oil. *Can. J. Comp. Med.* 39: 262-269 1975.
- 7 Clark S B, Ekkers T E, Singh A, Balni J A, Holt P R & Rodgers J B. Fat absorption in essential fatty acid deficiency: a model experimental approach to studies of the mechanism of fat malabsorption of unknown etiology. *J. Lipid Res.* 14: 581-588 1973.
- 8 Engfeldt B & Brunus E. Morphological effects of rapeseed oil in rats. II. Long term studies. *Acta Med. Scand. Suppl.* 585: 27-46 1975.
- 9 Holman R T. Essential fatty acid deficiency in animals. In: Rechcigl M (Ed). *Handbook of nutrition and foods*. C. R. C. Press, Ohio, Cleveland 1977. pp. 491-515.
- 10 Hulan H W, Kramer J K G, Mahadevan S, Sauer F D & Corner A H. Relationship between erucic acid and myocardial changes in male rats. *Lipids* 11: 9-15 1976.
- 11 Kaunni H & Johnson R E. Exacerbation of heart and liver lesions in rats by feeding of various mildly oxidized fats. *Lipids* 8: 329-336 1973.
- 12 Kramer J K G, Hulan H W, Trenholm H L & Corner A H. Growth, lipid metabolism and pathology of two strains of rats fed high fat diets. *J. Nutr.* 109: 202-213 1979.
- 13 Lambertsen G, Mykkestad H & Braekkan O R. Studies on monoene fatty acid isomers in hydrogenated marine fat. *J. Amer. Oil Chem. Soc.* 48: 389-391 1971.
- 14 McCutcheon J S, Umermura T, Bhattacharya M K & Walker B L. Cardiopathology of rapeseed oils and oil blends differing in erucic, linoleic and linolenic acid content. *Lipids* 11: 545-555 1976.
- 15 Rocquelin G, Cluzan R, Levillain R & Causseret J. Aspects biochimiques et anatomo-pathologiques du myocarde chez différentes espèces animales ingérant de l'huile de colza. *Arch. Mal. Coeur.* 66: 1085-1100 1973.
- 16 Svaar H & Langmark F T. Morphological studies on the cardiac effects of dietary long chain fatty acids in the rat, the domestic pig and the gerbil. In: «Effects physiopathologiques des acides gras à chaîne très longue 1971-1973. Action Thématique INSERM. Paris 1975. 329-335.
- 17 Teige B & Beare Rogers J L. Cardiac fatty acids in rats fed marine oils. *Lipids* 8: 584-587 1973.
- 18 Voglmann H, Christian R, Hardin R T & Clandinin D R. The effects of high and low erucic acid rapeseed oils in the diets for rats. *Internat. J. Vit. Nutr. Res.* 45: 221-229 1975.
- 19 Ziemińska S, Opuszyńska-Freyer T, Bulhak Jachymczyk B, Olszewska I, Woźniak E, Krus S & Ziemińska S. Pathomorphology of myocardium in experimental animals fed a rapeseed oil containing diet. *Pol. Med. Sci. Hist. Bull.* 15(1): 3-10 1974.

investigators studying the cardiac effects of fats and oils include reports on cardiac lesions in the experimental animals receiving the control diets. The incidence varies considerably from experiment to experiment but the average incidence seems to be about 20% with a range from 0 to 40% Kaunitz &

experiment with male *Charles River* rats. Unspecific degenerative changes consisting of focal muscle cell destruction, histiocytic infiltrations and focal fibrosis were frequent. The incidence increased with age from 26% of those dying between 400 and 500 days to 80% of those dying over 900 days of age. The most severe degenerative changes were brought about by the relatively unsaturated vegetable oils (corn oil, soyabean oil and olive oil) while the relatively more saturated animal fats (beef fat, butter, chicken fat and lard) induced fewer cardiac changes than expected after age correlated analysis.

In this study the partially hydrogenated fish oil was given without supplement of essential fatty acids and this may be a serious objection to the experimental design. The oil contained 2.3% C18:2 and this corresponds to 1 cal% of the diet, a level that has been considered the minimal daily requirement for rats (9). But most likely only a fraction of C18:2 in this oil is the essential fatty acid C18:2omega6 (linoleic acid). Aaes Jørgensen (1) induced EFA deficiency after 7-8 weeks with partially hydrogenated fish oils free of EFA and this suggests that the fatty acid composition in such oils increases the requirement for EFA since 24-26 weeks on a fat free diet and 16-17 weeks on partially hydrogenated peanut oil were needed to induce similar evidence of EFA deficiency in the rats. Unfortunately the most sensitive indicator of EFA deficiency, the ratio between C20:3 and C20:4 in the serum, was not determined in our study. Other indicators of EFA deficiency such as weight curves, appearance of the skin and tail histology of the testicles, the kidneys and the livers have been closely examined. The testicles were normal with mature spermatozoa in the tubules. The kidney weight was increased (+22% of controls) and focal calcification of tubular cells was found in 50% of the rats. The liver weight was increased (+37% of controls) and 4% had moderate steatosis. Thus some findings may indicate that the rats fed partially hydrogenated fish oil were deficient in EFA but these indicators are not specific since similar changes were found in other groups, particularly in the group fed 21% rapeseed oil (Table 3).

The groups fed 21% partially hydrogenated fish oil and 21% rapeseed oil had very similar weight

increases during the first 4 weeks; the next 4 weeks the weight increase was 10% less in the group fed partially hydrogenated fish oil and in the following 16 weeks the two groups developed at the same rate. This suggests that the absorption rates were fairly similar for the two diets since no difference was observed in the food consumption. Most likely the rats fed partially hydrogenated fish oil had borderline EFA deficiency but corn starch as used in all the diets probably contained enough essential fatty acids to prevent manifest symptoms. EFA deficiency appears to affect the synthesis or release of chylomicrons while the intestinal absorption appears unchanged (7). To our knowledge there are no data to indicate that the dietary essential fatty acids influence the utilization of C22:1 fatty acids to a higher degree than other fatty acids. We therefore think it unlikely that the low incidence and severity of the cardiac lesions found in rats fed partially hydrogenated fish oils are due to a reduced utilization of C22:1 fatty acids. The results of the histopathological examination of the hearts are in agreement with those found after giving similar partially hydrogenated fish oils to male *Charles River* and *Sprague Dawley* rats for 16 weeks (4, 16).

Judging from long term feeding experiments with partially hydrogenated fish oil one can not exclude the possibility that their content of C22:1 fatty acids may have cardiopathogenic effects similar to rapeseed oils containing erucic acid. Some recent observations from the studies cited above point to features of partially hydrogenated fish oil that may modify possible cardiac effects in the rats in a favourable direction: they originate from an animal source and the oils contain more saturated fatty acids than most vegetable oils; they have no linolenic acid content and the C22:1 fatty acids consist of a variety of geometrical and positional isomers of which erucic acid constitutes very little and trans isomers at least 50% (13).

At the present time it is not possible to know whether and to what degree these features are important in determining any pathological effects of partially hydrogenated fish oils. Our experiment suggests that diets including partially hydrogenated fish oil containing 3% C22:1 fatty acids do not cause cardiac lesions to a greater extent than do vegetable oils commonly accepted as healthful or mixtures of fats and oils of animal and vegetable origin. The few lesions observed are probably unspecific or related to the conditions of the experimental situation and a fat rich diet may be one of the conditioning factors.

The excellent facilities and good help supplied by Dr med vet. L. Scherren and the Animal Unit, Rikshospitalet, Oslo are acknowledged. The technical assistance of Mrs G. Berg Pedersen is greatly appreciated. DeNoFa og Lilleborg Fabrikker, Fredrikstad supplied the oils and Mr T. Grimsvang and Mr B. Baugø were responsible for the fatty acid analysis. This work was supported by the Royal Norwegian Council for Scientific and Industrial Research and the Norwegian Research Association for Edible Fats.

REFERENCES

- 1 Aas Jørgensen E. Essential fatty acids. *Physiological Reviews* 41: 1-51 1961
- 2 Abdellatif A M M & Vles R O. Pathological effects of dietary rapeseed oil in rats. *Nutr. Metabol* 12: 285-295 1970
- 3 Abdellatif A M M & Vles R O. Short term and long term pathological effects of glyceryl trierucate and of increasing levels of rapeseed oil in rats. *Nutr. Metabol* 15: 219-231 1973
- 4 Ackman R G. Myocardial alterations from feeding partially hydrogenated marine oils and peanut oil to rats. *Lipids* 9: 1032-1035 1974
- 5 Beare Rogers J L, Nera E A & Hegghoven H A. Myocardial alteration in rats fed rapeseed oils containing high or low levels of erucic acid. *Nutr. Metabol* 17: 213-222 1974
- 6 Charlton K M, Corner A H, Davey K, Kramer J K G, Mahadevan D & Sauer F D. Cardiac lesions in rats fed rapeseed oil. *Can J Comp Med* 39: 262-269 1975
- 7 Clark S B, Ekkers T E, Singh A, Balint J A, Holt P R & Rodgers J B. Fat absorption in essential fatty acid deficiency: a model experimental approach to studies of the mechanism of fat malabsorption of unknown etiology. *J Lipid Res* 14: 581-588 1973
- 8 Engfeldt B & Brunius E. Morphological effects of rapeseed oil in rats. II Long term studies. *Acta Med Scand Suppl* 585: 27-46 1975
- 9 Holman R T. Essential fatty acid deficiency in animals. In Rechcigl M (Ed) *Handbook of nutrition and foods*. C R C Press, Ohio, Cleveland 1977 pp 491-515
- 10 Hulan H W, Kramer J K G, Mahadevan S, Sauer F D & Corner A H. Relationship between erucic acid and myocardial changes in male rats. *Lipids* 11: 9-15 1976
- 11 Kaunitz H & Johnson R E. Exacerbation of heart and liver lesions in rats by feeding of various mildly oxidized fats. *Lipids* 8: 329-336 1973
- 12 Kramer J K G, Hulan H W, Trenholm H L & Corner A H. Growth, lipid metabolism and pathology of two strains of rats fed high fat diets. *J Nutr* 109: 202-213 1979
- 13 Lambertsen G, Myklestad H & Braekkan O R. Studies on monoene fatty acid isomers in hydrogenated marine fat. *J Amer Oil Chem Soc* 48: 389-391 1971
- 14 McCutcheon J S, Uemura T, Bhatnagar M A & Walker B L. Cardiopathology of rapeseed oils and oil blends differing in erucic, linoleic and linolenic acid content. *Lipids* 11: 545-555 1976
- 15 Rocquelin G, Cluettan R, Levillain R & Causseret J. Aspects biochimiques et anatomo-pathologiques du myocarde chez différentes espèces animales ingérant de l'huile de colza. *Arch Mal Coeur* 66: 1085-1100 1973
- 16 Sjaar H & Langmark F T. Morphological studies on the cardiac effects of dietary long chain fatty acids in the rat, the domestic pig and the gerbil. In «Effects physiopathologiques des acides gras à chaîne très longue 1971-1973. Action Thématique INSERM Paris 1975: 329-335
- 17 Teige B & Beare Rogers J L. Cardiac fatty acids in rats fed marine oils. *Lipids* 8: 584-587 1973
- 18 Voglmann H, Christian R, Hardin R T & Clandinin D R. The effects of high and low erucic acid rapeseed oils in the diets for rats. *Internat J Vit Nutr Res* 45: 221-229 1975
- 19 Ziemlanski S, Opuszynska-Freyer T, Bulhak Jachymczyk B, Olszewska I, Worniak E, Krus S & Szymanska S. Pathomorphology of myocardium in experimental animals fed a rapeseed oil containing diet. *Pol Med Sci Hist Bull* 15(1): 3-10 1974

AN ESTABLISHED HUMAN CELL LINE DERIVED FROM A MALIGNANT MEDIASTINAL TERATOMA¹

C SUNDSTRÖM J MARK and B WESTERMARK

The Department of Pathology and the Wallenberg Laboratory University of Uppsala Sweden and
Department of Pathology Central Hospital of Skövde Skövde Sweden

Sundström C Mark J & Westermarck B An established human cell line derived from a malignant mediastinal teratoma Acta path microbiol scand Sect A 88 189 194 1980

An established cell line derived from a human malignant mediastinal teratoma is described The cell line was characterized by histological and cytological examination and by chromosome analysis. The cell line grew in primary culture and in serial passage in vitro. The cell line was characterized by histological and cytological examination and by chromosome analysis. The cell line grew in primary culture and in serial passage in vitro. The cell line was characterized by histological and cytological examination and by chromosome analysis. The cell line grew in primary culture and in serial passage in vitro.

Chromosome banding showed a hypertriploid stemline number S-78 Almost all of the analysed karyotypes had seven markers in common Eleven other markers occurring at low frequency were also detected The origin of all markers except one could be deduced

Key words Teratoma malignant established cell line

C Sundström Department of Pathology University of Uppsala P O Box 553 S 751 22 Uppsala Sweden

Accepted as submitted 17 XII 79

Numerous efforts have been made to establish permanent cell lines from human malignancies With a few exceptions such as melanoma

establishment is very low and only in the order of a few per cent (5) We have recently managed to establish a cell line from a malignant teratoma The present communication describes some of the features of this cell line designated U 1161

MATERIALS AND METHODS

Case report The patient was a 26 years old Caucasian male who had suffered from thoracal pains for four months prior to operation At surgery a mediastinal grapefruit-sized tumor weighing about 1000 g was removed The histological picture revealed a tumor with major parts consisting of mesenchymal fibrous tissue

of the tumor seminomatous areas were seen partly intermingled with a lymphoid component Within the mesenchymal and epithelial components a strong atypia was observed No thymic tissue could be found The histological appearance of the tumor was consistent with malignant teratoma partly with admixture of seminoma Embryonal carcinoma or teratocarcinoma was not present (7) Renewed histological examination of a pleural metastasis 3 months after the primary operation showed that all components of the original tumor were present although the atypia within the fibrous tissue part was more pronounced and the growth here was more sarcomatous

The tumor mass could not be radically excised and the patient died eight months after operation No autopsy was performed

Cell culture Pieces of fresh tumor obtained at primary surgery were immediately transported to the laboratory and cut into small pieces

The tumor mass was cut into small pieces containing 5% CO₂ Medium was changed twice weekly Dense cultures were subcultivated 1:2 after a brief treatment with 0.25% trypsin solution

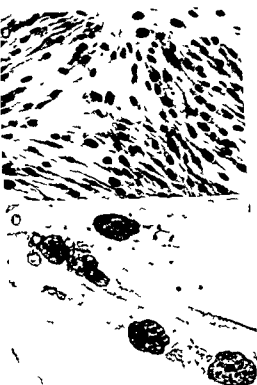


Fig 2 Micrographs of cultures of cell line U 1161 (a) Low power view showing fibroblastic appearance of cultures with cells often lying in bundles (b) High power view showing nuclear shape of individual tumor cells

Characteristics of the established cell line The cell line was uniformly composed of elongated spindle shaped cells with a notable fibroblastic appearance (Fig 2a) Most of the nuclei were oval but more irregularly shaped nuclei were commonly seen (Fig 2b) The chromatin pattern was coarse Most nuclei contained 1-3 heavily stained nucleoli A fraction of multinucleated cells was always present The growth pattern was also fibroblastic with cells growing in bundles (Fig 2a) although the growth

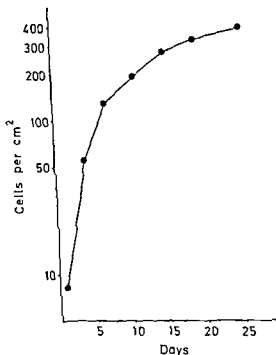


Fig 3 Growth curve of U 1161 Population doubling time during exponential growth was 24 h

pattern was more irregular than is usually seen in cultures of normal fibroblasts

Sparsely seeded cells multiplied rather rapidly and the population-doubling time during the phase of exponential growth was 24 h (cf Fig 3) As the cultures became denser growth rate progressively decreased until it became very slow at a cell density of 350 000 cells/cm² At this stage the cultures were very crowded and piling up of cells could be observed

The cultures could be subcultivated twice a week The cell line has now been grown for more than 100 passages

Table I shows the chromosome counts in the 155

TABLE I Chromosome Counts in U 1161

Chromosome numbers

50-60	70	71	72	73	74	75	76	77	78	79	80	81	82	83	84	85	86	87	88	89	94	± 160
1	1	1	-	73	42	52	114	193	4110	237	93	2	31	1	1	2	3	2	51	1	1	102

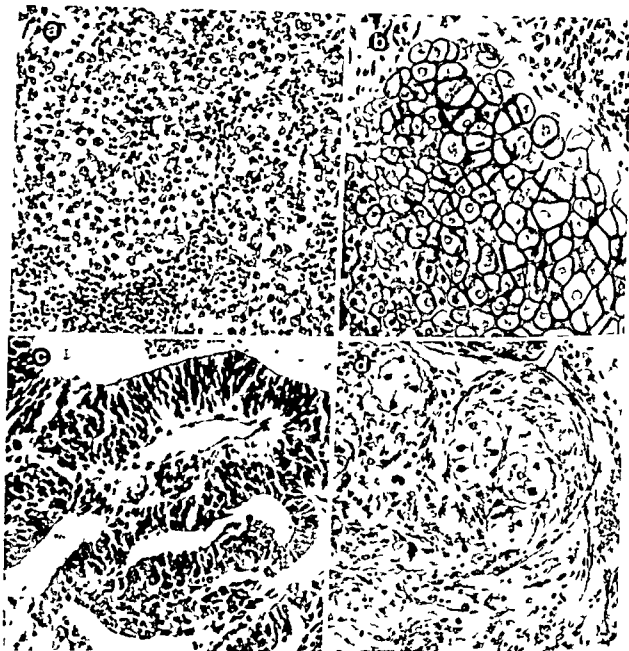


Fig 1 Micrographs showing different parts of the malignant teratoma from which cell line U 1161 was derived. The tumor contained a mixture of different tissue elements for example as shown here parts with seminoma like appearance containing anaplastic tumor cells and surrounded by a stroma with lymphocytic infiltrate (a) with cartilage (b) with cystic spaces lined by irregular palisaded neural epithelium (c) and areas built up of irregular connective tissue containing notochordal cells (d). In mesenchymal and epithelial components atypia was noted ($\times 260$)

Cell counts Cells were detached with trypsin and the cell number was determined on duplicates by the aid of an electronic particle counter (AB Lars Ljungberg, Stockholm, Sweden).

Cytogenetical methods The chromosomes were studied in preparations of 4 different subcultures viz passages 34, 37, 70 and 75. The cytogenetical findings were similar in the different passages and therefore the results are combined below. The methods for the chromosome preparations, the G and C banding techniques and the nomenclature have been described in detail earlier (3).

RESULTS

Early cell culture characteristics The early outgrowth of cells was composed of a mixture of different cell types, mainly epithelial cells, fibroblast like cells and some large polygonal cells. The mitotic activity of the epithelial and polygonal elements was low, whereas the fibroblast like cells proliferated more rapidly, leading to an increase in the proportion of these cells. After approximately 20 subcultivations only fibroblast like cells were detected.

TABLE 2 *The Representation of Normal Chromosome Types in 41 Karyotyped Modal Near-Modal Cells*

Chromosome No	Number of each chr type						The predominating number of each chromosome type
	0	1	2	3	4	5	
1	-	32	4	3	2	-	1
2	-	-	6	35	-	-	3
3	-	3	33	4	1	-	2
4	-	-	7	29	5	-	3
5	-	-	4	5	32	-	4
6	-	-	-	7	34	-	4
7	-	-	2	36	3	-	3
8	-	-	-	11	29	1	4
9	-	-	38	2	1	-	2
10	-	-	6	35	-	-	3
11	-	-	-	18	23	-	3-4
12	-	-	3	37	1	-	3
13	-	34	7	-	-	-	1
14	-	-	-	-	39	2	3
15	-	1	11	29	-	-	4
16	-	-	-	39	1	1	3
17	-	-	2	39	-	-	3
18	-	-	1	3	35	2	4
19	-	-	2	28	11	-	3
20	-	-	2	4	35	-	4
21	-	3	4	23	11	-	3
22	-	-	-	14	27	-	4
Y	2	6	33	-	-	-	2
X	-	4	37	-	-	-	2

TABLE 3 *The Derivation and Frequency of the Marker Chromosome in 41 Karyotyped Modal-Near Modal Cells*

Marker no	Number of cells with the marker	Mode of origin
I = 1q-	36	t(11 10)(1pter - 1q21 10q11 - 10qter)
II = 1q-	33	t(1q)
III = 1q-	36	t(1p 7q)
IV = 3q-	36	del(3)(q11)
V = 3p-	34	t(3q 7p)
VI = 10q+	34	t(11 10)(1qter - 1q21 10q11 - 10pter)
VII = 13p+	35	t(9q 13q)
VIII = 1p+	5	t(1 ?)(1qter - 1p36 ?)
IX = 1q-	4	del(1)(q11)
X = 2q+	1	t(2 ?)(2pter - 2q37 ?)
XI = 3q+	1	t(3 ?)(3pter - 3q29 ?)
XII = 5p+	1	t(5 ?)(5qter - 5p15 ?)
XIII = 10q+	1	t(10 ?)(10pter - 10q26 ?)
XIV = 11p-	5	del(11)(p12)
XV = 12q-	1	del(12)(q23)
XVI = 21p+	1	t(21q)
XVII = Xq+	1	t(X ?)(Xpter - Xq28 ?)
XVIII - minute	2	very small banded marker with unknown derivation

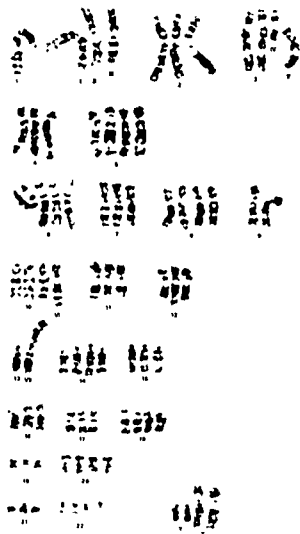


Fig. 4. Karyotype of U 1161 showing a hypertriploid stemline ($S = 78$)

cells studied from the four different passages. The distribution of the 41 karyotyped cells on the various chromosome numbers is indicated by the upper figures in the Table.

The established cell line U 1161 had a hypertriploid stemline (S) number $S = 78$. There was a considerable spread around the modal number and a fairly low frequency of doubling products of modal-near-modal cells.

Five of the analysed cells with the S number had the same karyotype. This is illustrated in Fig. 4, and it can be written as follows: $78, XXYY, 1 +2, +4, +5, +5, +6, +6, +7, +8, +8, +10, +11, +12, +13, +14, +14, +15, +16, +17, +18, +18, +19, +20, +20, +21, +22, +22, +7$ markers (= mar I-VII). The origin of all the seven different marker types could be completely elucidated (Table 3). The results by C-banding corroborated the interpretations presented in Table 3, and the observations by

this technique were especially valuable for characterizing the mar I, II, III and VII. A striking feature as regards the formation of mar I-VII was the preferential involvement of the centromeric and near-centromeric regions.

The 34 analysed variant cells with chromosome numbers in the modal region were all closely related to the S -cells. This feature is very clear from the data given in Tables 2 and 3. In these 34 variant cells 11 new marker types were observed (mar VIII-XVIII, Table 3). Their derivation could be wholly or partly deduced, except for mar XVIII.

Two octaploid cells were analysed. The representation of normal chromosome types and markers accorded well with their origin from doubling products of cells of the modal group. No new marker types were seen in these high polyploid cells.

DISCUSSION

Teratomas are characterized by their content of all three germ layers. They are most often benign tumors but occasionally malignant variants appear. When occurring, malignancies are most often adenocarcinomas although other types of malignant tumors have been described (for a recent review, see ref. no. 1). In the present mediastinal tumor both the epithelial and mesenchymal components showed atypia. However, the recurring tumor was more sarcomatous. Also, the cell line that was established from the primary tumor specimen was mesenchymal with cells resembling normal fibroblasts except for a certain cellular atypia and a somewhat more irregular growth pattern than is usually seen in normal fibroblast cultures. The possibility that the cell line was composed of normal fibroblasts could be excluded by the fact that it has been subcultivated for over 100 passages. Also the markedly abnormal karyotype is consistent only with neoplasia.

The original tumor contained mesenchymal elements of different lineages. Of all cell types fibroblasts are those most prone to grow in tissue culture. It is conceivable that this is the reason why cells committed to the «fibroblastic lineage» overgrew the other cell types that were present in the early cultures. Thus, the emerging permanent cell line although derived from a teratoma, was probably a differentiated one and not composed of pluripotent, uncommitted cells. In this respect U-1161 differs from mouse teratocarcinoma lines which are either pluripotent or undifferentiated multipotent (4). Consequently, all our efforts to induce differen-

SOMATOPETAL TRANSPORT OF HORSERADISH PEROXIDASE FOLLOWING INCORPORATION INTO AXONAL SPROUTS AND AXONS IN NEUROMAS AFTER NERVE TRANSECTION

TOMAS OLSSON

Department of Pathology II University of Linköping Linköping Sweden

Olsson T Somatopetal transport of horseradish peroxidase following incorporation into axonal sprouts and axons in neuromas after nerve transection *Acta path microbiol scand Sect A 88 195-199 1980*

Horseradish peroxidase (HRP) applied to the proximal stump of the facial nerve of the mouse 5 h after section diffused into the endoneurium and was incorporated by endocytosis into axons densely packed with organelles. By 24 h to 16 days after the section uptake of the tracer into profiles of outgrowing axonal sprouts rich in vesicles and vacuoles was registered. Subsequently HRP accumulated in corresponding perikarya. Tracer transport from neuromas was demonstrated 32 and 64 days after section. In this way influences from outgrowing nerve sprouts and axons in neuromas may reach nerve cell bodies.

Key words: Horseradish peroxidase, axons, nerve transection.

T Olsson, Department of Pathology II, University of Linköping, S-581 85 Linköping, Sweden.

Received 14 XI 79 Accepted 20 XII 79

It has been shown that somatopetal transport of macromolecules to nerve cell bodies occurs after leakage into damaged axons immediately after an axotomy (16) and later during reinnervation of the target organ after incorporation into nerve terminals (8, 15, 21). The biological significance of this phenomenon is unclear but it may be of importance for the nerve cell body's interaction with its periphery after axon injury (14) for further evaluation of these phenomena the present study was undertaken to obtain information about axonal uptake and somatopetal transport of macromolecules also during the period after axotomy when the axolemma is reconstituted and outgrowth of regenerating axonal sprouts starts. In addition transport of macromolecules from axons in neuroma formation developed after impeded reinnervation was studied. In order to obtain outgrowing sprouts in restricted areas which are easy to localize axotomy was performed by transection in the present study.

MATERIALS AND METHODS

The left facial nerve of 60 to 70-day-old male Swiss albino mice was transected below its exit from the stylomastoid foramen and a strip of parafilm placed around the proximal nerve stump. In groups of mice 2 mg HRP (Type II Sigma St. Louis) was applied on the proximal nerve stump various time intervals after the transection (number of mice and time intervals see Table 1). The mice were then perfused after 30 min with 2.5% glutaraldehyde in Sørensen's phosphate buffer pH 7.4 with 0.01% CaCl_2 added. The distal parts of the

For estimation of the HRP accumulation in these neurons the contralateral ones were used as reference by section of the right nerve followed by immediate application of 2 mg of the tracer. After 9 or 24 h the

Chromosome banding data on human teratomas are scanty. Sonta *et al* (8) have published data on three testicular tumors viz one hyperdiploid ($S \approx 53$) seminoma, one hypotriploid ($S = 67$) teratoma and one metastatic diploid ($S = 46$) embryonal carcinoma. It is surprising that no marker chromosomes were included in any of these $S =$ karyotypes. In the present cell line, the $S =$ karyotypes contained seven markers, the exact origin of which could be deduced.

Supported by grants from the Swedish Cancer Society (S5 B75 11A).

REFERENCES

1. Canty C & Simons R. Malignant Mediastinal Teratoma in a 15 Year Old Girl. *Cancer* 41: 1623-1626 1978.
2. Cornain S, de Vries J E, Collard J, van Wingerden I & Rümke P. Antibodies and Antigen Expression in Human Melanoma Detected by the Immuno Adherence test. *Int J Cancer* 16: 981-997 1975.
3. Mark J, Westermarck B, Ponten J & Hugosson R. Banding Patterns in Human Glioma Cell Lines. *Hereditas* 87: 243-260 1977.
4. Martin G R. Teratocarcinomas as a Model System for the Study of Embryogenesis and Neoplasia. *Cell* 5: 229-243 1975.
5. Moore G E & Koike A. Growth of Human Tumor Cells in Vitro and in Vivo. *Cancer* 17: 11-20 1964.
6. Nadkarni J S, Nadkarni J J, Clifford P, Manolos G, Finvo E M & Klein E. Characteristics of New Cell Lines Derived from Burkitt Lymphomas. *Cancer* 23: 64-79 1969.
7. Oberman H A & Libcke J H. Malignant germinal neoplasms of the mediastinum. *Cancer* 17: 498-507 1964.
8. Sonta S I, Oshimura M, Evans J T & Sandberg A A. Chromosomes and Causation of Human Cancer and Leukemia. XX. Banding Patterns of Primary Tumors. *J Nat Cancer Inst* 58: 49-59 1977.
9. Westermarck B, Ponten J & Hugosson R. Determinants for the Establishment of Permanent Tissue Culture Lines from Human Gliomas. *Acta path microbiol scand sect A* 81: 791-805 1971.

SOMATOPETAL TRANSPORT OF HORSE RADISH PEROXIDASE FOLLOWING INCORPORATION INTO AXONAL SPROUTS AND AXONS IN NEUROMAS AFTER NERVE TRANSECTION

TOMAS OLSSON

Department of Pathology II University of Linköping Linköping Sweden

Olsson T Somatopetal transport of horseradish peroxidase following incorporation into axonal sprouts and axons in neuromas after nerve transection Acta path microbiol scand Sect A 88 195-199 1980

Horseradish peroxidase (HRP) applied to the proximal stump of the facial nerve of the mouse 5 h after section diffused into the endoneurium and was incorporated by endocytosis into axons densely packed with organelles. By 24 h to 16 days after the section uptake of the tracer into profiles of outgrowing axonal sprouts rich in vesicles and vacuoles was registered. Subsequently HRP accumulated in corresponding perikarya. Tracer transport from neuromas was demonstrated 32 and 64 days after section. In this way influences from outgrowing nerve sprouts and axons in neuromas may reach nerve cell bodies.

Key words: Horseradish peroxidase; axons; nerve transection.

T Olsson Department of Pathology II University of Linköping S-581 85 Linköping Sweden

Received 14 xi 79 Accepted 20 xii 79

It has been shown that somatopetal transport of macromolecules to nerve cell bodies occurs after leakage into damaged axons immediately after an axotomy (16) and later during reinnervation of the target organ after incorporation into nerve terminals (8, 15, 21). The biological significance of this phenomenon is unclear but it may be of importance for the nerve cell body's interaction with its periphery after axon injury (14) for further evaluation of these phenomena the present study was undertaken to obtain information about axonal uptake and somatopetal transport of macromolecules also during the period after axotomy when the axolemma is reconstituted and outgrowth of regenerating axonal sprouts starts. In addition transport of macromolecules from axons in neuroma formation developed after impeded reinnervation was studied. In order to obtain outgrowing sprouts in restricted areas which are easy to localize axotomy was performed by transection in the present study.

MATERIALS AND METHODS

The left facial nerve of 60 to 70 day-old male Swiss albino mice was transected below its exit from the stylomastoid foramen and a strip of parafilm placed around the proximal nerve stump. In groups of mice 2 mg HRP (Type II Sigma St. Louis) was applied on the proximal nerve stump various time intervals after the transection (number of mice and time intervals see Table 1). The mice were then perfused after 30 min with 2.5% glutaraldehyde in Sørensen's phosphate buffer pH 7.4 with 0.01% CaCl_2 added. The distal parts of the proximal nerve stumps were dissected out, reacted for HRP and prepared for electron microscopy (21).

For studies of HRP transport to neuronal perikarya 2 mg of the tracer was applied on the left proximal nerve stump in groups of mice various time intervals after section (number of mice and time intervals see Table 1). For estimation of the HRP accumulation in these neurons the contralateral ones were used as reference by section of the right nerve followed by immediate application of 2 mg of the tracer. After 9 or 24 h the

TABLE 1 *Survey of the Material in Which HRP Was Applied on Proximal Stumps of Facial Nerves at Various Time Intervals after Transection. Subsequently Incorporation of HRP into Axons and Accumulation of the Tracer in Perikarya Was Studied*

Time intervals		1 h	5 h	24 h	48 h	5 days	16 days	32 days	64 days
No. mice for studies of	HRP uptake in axons	2	2	4	2	3	2	2	2
	HRP accumulation in perikarya	7	6	4	3	4	3	2	3

mice were perfused as described above the brain stems dissected out and postfixed for 30 min. Frozen section 40 μ m thick were cut and reacted for HRP (18). The intensity of the HRP reaction product in the left facial nucleus was then evaluated with a scoring procedure (21).

The morphological response of facial nerve cell bodies to a nerve transection was also studied. Groups of 2-3 mice were perfused with 4% formalin 6, 8, 12, 18, 20, 24, 32, 34 and 38 days after the axotomy and paraffin embedded sections stained with cresyl violet acetic acid.

RESULTS

1.5 h after the section the distal parts of the axons in the proximal nerve stump showed a finely granular axoplasm. HRP had diffused into the endoneurium and in between the axolemma and the myelin sheath but only occasionally intra axonal HRP labelling occurred. By 5.5 h distal parts of many axons were densely packed with vesicles, occasional dense core vesicles, vacuoles and mitochondria. HRP outlined these axons beneath the myelin sheath and many vesicles and vacuoles contained HRP (Fig. 1). Clusters of outgrowing nerve sprouts had appeared by 24.5 h. A basal lamina surrounded the clusters of sprouts which were partly embedded in a sparse Schwann cell cytoplasm. In many cases sprouts were also seen associated with a Schwann cell belonging to a myelinated axon (Fig. 2). Sprouts

appearing in these two types of clusters have previously been shown to represent collateral and/or terminal sprouts of single myelinated axons (19). Organelles such as vesicles, vacuoles, elongate tubular structures, multivesicular bodies, mitochondria and dense lamellar bodies were seen in some of the nerve sprouts profiles. In these many HRP labelled vesicles and vacuoles occurred (Figs 3 and 4). The majority of HRP labelled and non labelled vesicles had a size between 40 and 80 μ m but vacuoles up to 260 μ m were also registered. Other profiles of sprouts showed very few vesicles and vacuoles and HRP labelling was infrequent in these areas. Clusters of sprouts with a similar morphology were seen after 48 h and 5 days. In mice used after 16 days each section showed fewer profiles of sprouts with large amounts of vesicles and vacuoles. Such structures and intra axonal HRP labelling occurred only occasionally by 32 and 64 days. At these time intervals neuromas built up of myelinated and unmyelinated axons had developed (Fig. 5). No or only a faint blue black reaction product appeared in left sided perikarya when the tracer was applied 1 h after section whereas most nerve cell bodies showed a weak reaction product in mice used after 5 h. The left sided perikarya contained a strong, clearly visible HRP reaction product at all later time intervals and neurons used 48 h after section appeared to possess more reaction product than the right sided ones (Fig. 6).

Fig. 1 Axon densely packed with organelles 5.5 h after transection. Note black HRP reaction product outlining the axolemma and HRP labelling of intra axonal vesicles and vacuoles. $\times 11\,000$.

Fig. 2 Clusters of nerve sprouts 24.5 h after transection. In the cluster to the right the sprouts are embedded in a Schwann cell belonging to a myelinated axon. Note black HRP reaction product in the endoneurium. $\times 11\,000$.

Fig. 3 Profile of sprout from a cluster similar to the one to the left in Fig. 2, 24.5 h after transection. The profile contains vesicles, dense core vesicles and vacuoles. HRP reaction product outlines the sprout and occurs in membrane limited organelles. $\times 26\,400$.

Fig. 4 Profile of sprout embedded in a Schwann cell belonging to a myelinated axon. Note HRP reaction product in membrane limited organelles. $\times 49\,600$.





Fig 5 Myelinated and unmyelinated axons in a neuroma 64 days after section. Note HRP reaction product in the endoneurium surrounding unmyelinated axons $\times 4\ 800$



Fig 6 Granular HRP reaction product in facial nerve cell bodies in a mouse where HRP was applied 48 h after transection $\times 490$

The morphological response of the facial nerve cell bodies consisted of dispersion of the Nissl substance, an increase in cytoplasmic basophilia, in the size of cells and nucleoli. This was followed by a decrease in basophilia and still later a loss of neurons was registered. These results are in accordance with those by Torvik and Skjorten (26).

DISCUSSION

Previously it has been shown that HRP leaks through injured axolemma and distributes diffusely in axons immediately after an axotomy (16). The present study showed that 1 h after axotomy HRP outlined an intact axolemma with no or only a slight axonal HRP uptake and transfer to perikarya. Later, 5 h after axotomy, distal parts of axons in the proximal nerve stump were densely packed with organelles. At this time intra-axonal vesicles and vacuoles of endocytotic origin were formed. Other

vesicles and vacuoles in these axons may represent lysosomes (13) or budded parts of smooth endoplasmic reticulum (6).

By 24 h after axotomy profiles of axonal sprouts containing vesicles and vacuoles were observed. Such structures have been interpreted as growth in tips of sprouts (2, 10, 11, 17). The present observed endocytosis in *in vivo* sprouts shows that they are in this respect similar to growth cones *in vitro* whose endocytotic activity is well known (1, 4, 22, 25). However, they differ from growth cones in the developing cerebellum of the rat which are an organelle poor and have a low uptake of HRP (5). An increase in HRP reaction product in perikarya similar to that observed in the present study in mice used after 48 h has previously been observed in the chick visual system 6.75 to 18 h after axon injury (12). It may reflect an increased peripheral uptake of the tracer which can be due to larger amounts of nerve sprouts and/or higher endocytotic activity in individual sprouts. Not only exogenous tracers but also endogenous proteins and glycoproteins are retrogradely transported in higher amounts outgrowth of axons after an axotomy (9). After somatopetal transport to perikarya HRP is localised to lysosomes (3). Nevertheless, macromolecules may after endocytosis and intracellular transport affect the metabolism of the cell (7, 23). It is therefore conceivable that the mechanism of incorporation and subsequent somatopetal axonal transport of macromolecules during outgrowth of axons may be important for the understanding of how the nerve cell body's metabolism may be influenced by the periphery as proposed by Griffin and Price (11).

Tracer transport from the neuromas was observed in the present study indicating a pathway for introduction of substances which could reduce the neuron's regenerative capacity as proposed by Spencer (24). As discussed above, HRP uptake occurs most extensively in axonal structures which are rich in vesicles and vacuoles. In accordance with a previous study (20), such structures were observed infrequently at late times after nerve section. The discrepancy between the conspicuous accumulation of tracer in perikarya and the infrequent observation of HRP uptake by axons in the neuromas may be explained by a difficulty to localize the vesicle-rich axonal structure which may be spread over larger areas caused by an indefinite growth of axons after nerve section (24).

I thank professor Arster Kristensson for kind support during the completion of this work. The study was supported by grants from the Swedish Medical Research Council project No B80 12\ 04480 06C and Östergötlands Läns Landstings Medicinska Forskningsnämnd.

REFERENCES

- Birks R I, Mackey M C & Weldon P R. Organelle formation from pinocytotic elements in neurites of cultured sympathetic ganglia. *J Neurocytol* 1: 311-340 1972
- Blumcke S & Niedorf H R. Elektronenmikroskopische untersuchungen an wachstumsendkolben regenerierender peripherer nervenfaser. *Virch Arch Path Anat* 340: 93-104 1965
- Broadwell R D & Brightman M W. Cytochemistry of undamaged neurons transporting exogenous proteins *in vivo*. *J Comp Neurol* 185: 31-73 1979
- Bunge M B. Initial endocytosis of peroxidase or ferritin by growth cones of cultured nerve cells. *J Neurocytol* 6: 407-439 1977
- Del Cerro M. Uptake of tracer proteins in the developing cerebellum particularly by the growth cones and blood vessels. *J Comp Neurol* 157: 245-279 1974
- Dro B, Rankbourg A & Koenig H L. The smooth endoplasmic reticulum: structure and role in renewal of axonal membrane and synaptic vesicles by fast axonal transport. *Brain Res* 93: 1-14 1975
- Edels R P J & Cohn Z A. Endocytosis: regulation of membrane interactions. In Poste G and Nicolson G L (Eds) *Membrane fusions*. Elsevier/North Holland Biomedical press Amsterdam pp 387-405 1978
- Enerback L, Kristensson K & Olsson T. Cytophotometric quantification of retrograde axonal transport of a fluorescent tracer (Primuline) in mouse facial neurons. *Brain Res* in press
- Friell M, McLean W G & Sjostrand J. Retrograde axonal transport of rapidly migrating labelled proteins and glycoproteins in regenerating peripheral nerves. *J Neurochem* 27: 191-196 1976
- Griffin J W, Drachman D B & Price D L. Fast axonal transport in motor nerve regeneration. *J Neurobiol* 7: 355-370 1976
- Griffin J W & Price D L. Axonal transport in motor neuron pathology. In Andrews J M et al (Eds) *Almyotrophic lateral sclerosis: recent research trends*. UCLA forum in medical diseases Volume 19. Academic Press New York pp 33-67 1977
- Halperin J J & La Vail J H. A study of the dynamics of retrograde transport and accumulation of horseradish peroxidase in injured neurons. *Brain Res* 100: 253-269 1975
- Holtzman E & Novikoff A B. Lysosomes in the rat sciatic nerve following crush. *J Cell Biol* 27: 651-669 1965
- Kristensson K. Retrograde transport of macromolecules in axons. *Ann Rev Pharmacol Toxicol* 18: 97-110 1978
- Kristensson K & Sjostrand J. Retrograde transport of protein tracer in the rabbit hypoglossal nerve during regeneration. *Brain Res* 45: 175-181 1972
- Kristensson K & Olsson Y. Retrograde transport of horseradish peroxidase in transected axons. 3. Entry into injured axons and subsequent localization in perikaryon. *Brain Res* 115: 201-213 1976
- Lampert P W. A comparative electron microscopic study of reactive degenerating regenerating and dystrophic axons. *J Neuropathol Exp Neurol* 26: 345-368 1967
- Mesulam M M. Tetramethyl benzidine for horseradish peroxidase neurochemistry. A non-carcinogenic blue reaction product with superior sensivity for visualizing neural afferents and efferents. *J Histochem Cytochem* 2: 106-117 1978
- Morris J H, Hudson A R & Weddel G. A study of degeneration and regeneration in the divided rat sciatic nerve based on electron microscopy. II. The development of the regenerating unit. *Z Zellforsch* 124: 103-130 1972
- Morris J H, Hudson A R & Weddel G. A study of degeneration and regeneration in the divided rat sciatic nerve based on electron microscopy. III. Changes in the axons of the proximal stump. *Z Zellforsch* 124: 131-164 1972
- Olsson T, Forsberg I & Kristensson K. Uptake and retrograde axonal transport of horseradish peroxidase in regenerating facial motor neurons of the mouse. *J Neurocytol* 7: 323-336 1978
- Pomeroy C M, Hendelman W J, Raiborn C W & Massey J F. Dynamic activities of nervous tissue *in vitro*. In Hyden H (Ed) *The Neuron*. Elsevier Amsterdam pp 119-178 1967
- Schwab M E, Suda K & Thoenen H. Selective retrograde transsynaptic transfer of a protein tetanus toxin subsequent to its retrograde axonal transport. *J Cell Biol* 82: 798-810 1979
- Spencer S P. The traumatic neuroma and the proximal stump. *The Bulletin of the hospital for joint diseases* 35: 82-102 1974
- Tischner K. Uptake of horseradish peroxidase by sensory nerve fibres *in vitro*. *J Anat* 124: 83-97 1977
- Torvik A & Skjorten F. Electron microscopic observations on nerve cell regeneration and degeneration after axon lesions. I. Changes in the nerve cell cytoplasm. *Acta Neuropathol* 17: 248-169 1971

A NEW HYPOTHESIS FOR ALLOXAN DIABETES

LENNART BOQUIST

Institute of Pathology University of Umeå Umeå Sweden

Boquist L. A new hypothesis for alloxan diabetes *Acta path microbiol scand Sect A* 88 201-209 1980

A new hypothesis (' P_i pH hypothesis') for alloxan diabetes is presented. It is based upon data from our own studies and from the literature. The following data and interpretations are assumed to be of special importance for the B-cytotoxicity of alloxan: Inhibition of a mitochondrial sulphydryl dependent transport system for inorganic phosphate (P_i) leading to increased concentration of P_i and decreased pH in the cytosol and to inhibition of NAD-dependent oxidations and oxidative phosphorylation; mitochondrial lesion because of altered localization and concentration of P_i ; inhibited synthesis and glucose induced release of insulin at least partly due to a fall in intracellular pH and finally necrosis because of absent mitochondrial function. An inverse relationship between P_i and pH may exist in the B-cells, alloxan sensitivity being associated with high P_i and low pH. Alloxan antagonism may be due to induction of low P_i and high pH in the cytosol. The selectivity of the B cell for alloxan is believed to be associated with its free permeability for glucose.

Key words: Alloxan diabetes, alloxan antagonism, pathogenesis, inorganic phosphate, intracellular pH, mitochondrial lesion.

L. Boquist, Institute of Pathology, University of Umeå, S 901 87 Umeå, Sweden.

Received 10 ix 79 Accepted 20 xii 79

Although the diabetogenic action of alloxan has been known for more than 35 years and in spite of intense research during this period, the pathogenesis of alloxan diabetes is still unknown. Several hypotheses for the development of this kind of experimental diabetes have been presented, but none has so far been proved. Since data from our own studies in this field have not been compatible with any of these hypotheses, we have tried to find a new hypothesis that agrees with our own results and with data from the literature. As preliminarily reported (Boquist 1978 a, d and e; Boquist & Hagström 1979; Lorenzon & Boquist 1979), this search has resulted in a working hypothesis tentatively called the ' P_i pH hypothesis', which here is presented in more details with the addition of some new data.

Mitochondrial Lesion and Inorganic Phosphate

Selective necrosis of the pancreatic islet B-cells represents the ultimate effect of alloxan B-cytotoxicity and forms the basis of manifest diabetes. Hence it is obvious that alterations in these cells play a central role in the development of this kind of diabetes. Since it is generally considered that alloxan is toxic for the B-cells only during a short period of time, probably within the first five to ten minutes after its administration into the circulation, the earliest structural and biochemical changes in the B-cells are most important for the study of the pathogenesis of alloxan diabetes. Alterations recorded in these cells when hyperglycemia is manifest may well be of interest.

...

are all found to be localized to the mitochondria and the pattern of pyroantimonate precipitation (Boquist 1977 a). The mitochondrial changes have been verified by ultrastructural stereological methods (Lorenzon & Boquist 1979). The observations were started 10 min following alloxan administration and already at this time many mitochondria

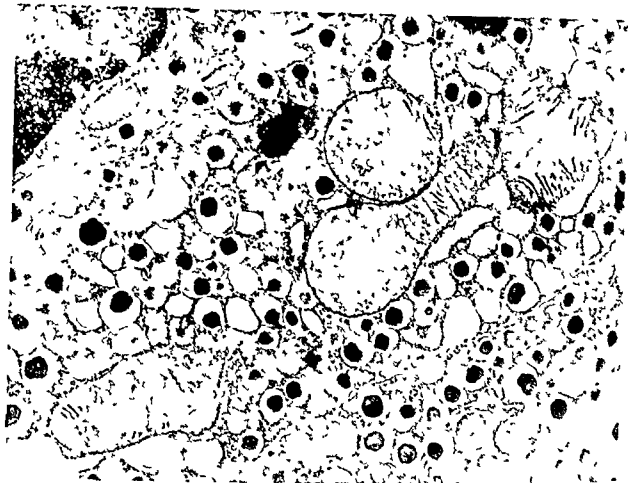


Fig 1 Electron micrograph of mouse B-cells 10 min after alloxan injection. Swollen mitochondria with partly disrupted cristae are seen $\times 11\,000$

exhibited swelling and occasionally rupture of inner membranes (Fig 1). At the following observation times the mitochondrial changes were more advanced and subsequently the mitochondria were disintegrated.

Since mitochondrial changes of the kind observed in the B-cells were not found in the other endocrine cells or in the exocrine cells of the pancreas these changes obviously do not represent an artifact or unspecific reaction but seem to be a structural manifestation of a rapidly appearing specific lesion directly or indirectly caused by alloxan.

The other alteration observed already at the 10 min observation time is a pattern of pyroantimonate precipitation in the B-cells of alloxan treated mice different from that of control mice. Thus animals injected with alloxan exhibit precipitates mainly localized to the cytoplasmic ground substance (Fig 2) whereas most precipitates are seen in mitochondria and secretory granules in the controls (Boquist 1977a). This may be consistent with an increased occurrence of Ca^{2+} and inorganic phosphate (Pi) in the cytosol and the finding thus supports the Pi pH hypothesis (see below).

The endoplasmic reticulum, Golgi complex and nucleus are structurally altered first at late observation times and the secretory granules are usually preserved even in severely damaged but non necrotic B-cells (Fig 3) indicating an inhibition of the release of insulin stored in granules in alloxan treated mice. This agrees with the observation that alloxan inhibits glucose induced insulin secretion (Gunnarsson & Hellerstrom 1973, Henquin *et al* 1979). This inhibition is abolished by glucose *in vitro* (Tomita & Lacy 1972). Alloxan also blocks insulin synthesis in isolated mouse islets (Gunnarsson 1975). Both qualitative and quantitative electron microscopic data support the view of an inhibition of the synthesis and release of insulin in alloxan treated mice (Boquist 1977a, Boquist & Lorenzon 1979).

What is the mechanism underlying the mitochondrial lesion in alloxan treated mice? So far it has not been clarified whether alloxan passes the plasma membrane of the B-cell or not. Therefore one possibility is that alloxan passes into the B-cell and acts directly on the mitochondria. Another possibility is that alloxan through an action on

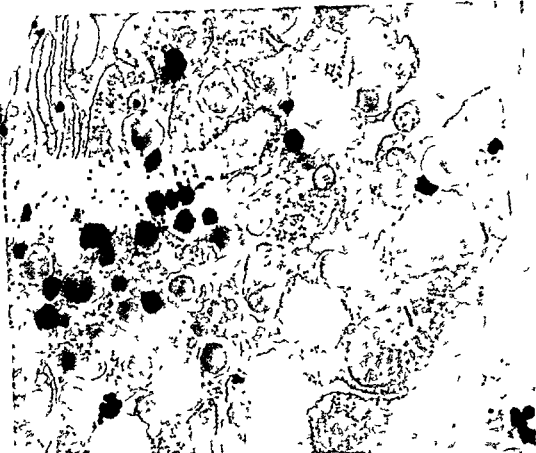


Fig. 2. Portion of mouse B-cell 10 min after alloxan administration. The precipitates are present in the cytoplasm. Also found a technique

te precipitates are
Some precipitate
Pyroantimonate

other organelles or cellular constituents or through a direct action on the plasma membrane alters the intracellular milieu in such a way that the mitochondria are secondarily damaged.

The data from our own studies do not permit any definite interpretation of whether alloxan passes the B-cell membrane or not. However, the absence of early-appearing structural changes in organelles other than mitochondria argues against the possibility of an action of alloxan on such organelles and although many authors advocate this

1978) or for an intracellular action besides plasma membrane effects (Henquin *et al.* 1979). Autoradiography has revealed that mouse islets accumulate alloxan (Hammarstrom *et al.* 1967). Moreover, *in vitro* experiments have disclosed an action of alloxan on mitochondria from rat liver and kidney (Younathan 1962). Therefore it is believed that alloxan passes the plasma membrane of the B-cells supposedly through a hexose transport system and acts intracellularly. In addition, alloxan may directly or indirectly act on the plasma membrane.

If alloxan really passes through a hexose transport system, the entry into the B-cells may not only be associated with that of glucose but also with that of sodium and P_i since glucose and P_i entry e.g. in the proximal tubule cells (which also are alloxan sensitive) of rabbit kidney is sodium-dependent (Dennis & Brady 1978). Therefore the transport of

about damaging the plasma membrane (McDaniel *et al.* 1975; Weaver *et al.*

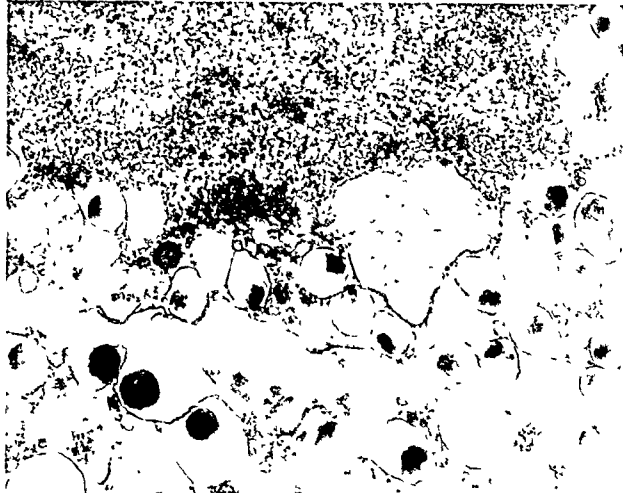


Fig 3 Portion of severely damaged B cell 6 hours after alloxan injection. Note that some of the secretory granules exhibit an altered configuration of the core and/or rupture of the membrane. $\times 19\,000$

sodium and P_i into the B-cells may affect the development of alloxan diabetes. Inhibition of a univalent-cation pump in the B-cell membrane has been suggested to play a role in alloxan diabetes although it need not be the most basic action of alloxan (Dahl *et al* 1977).

Assuming a direct intracellular action of alloxan it is important to note that certain sulfhydryl reagents specifically inhibit the phosphate carrier of rat liver mitochondria without affecting a number of other mitochondrial functions (*cf* Chappell 1970, Lehninger 1975), and that one of the most well-known properties of alloxan is its role as sulfhydryl reagent. The B-cell mitochondria like those of liver, are supposed to possess a sulfhydryl dependent phosphate transport system which is inhibited by alloxan (Lorenzon & Boquist 1979). This inhibition may result in a decreased mitochondrial content of P_i and an increased concentration of P_i in the cytosol which in turn may be consistent with the increased concentration of P_i in whole islets

(Boquist 1978 e), and with the altered pattern of pyroantimonate precipitation in the B-cells of alloxan treated mice (Boquist 1977a). The alterations in the localization and concentration of P_i may be associated with similar alterations of Ca^{2+} .

Since starvation is well known to increase the B-cell sensitivity to alloxan, it should be noted that starvation has been reported to alter the activation site for the «phosphate flush» in rat islets (Asplund & Freinkel 1978) although this is not directly applicable to the supposed mitochondrial transport mechanism for phosphate.

Mitochondrial lesion, and alterations in the localization and concentration of P_i may affect the release of insulin. P_i plays a so far, not fully clarified role in insulin secretion. Islet stimulation reduces the islet pool of phosphate, the total islet content of phosphate declines as much as 40–50% following glucose stimulation (Bukowiecki *et al* 1979), and P_i may inhibit glucose induced insulin release *in vitro* (Andersson 1978). Thus high

cytosolic concentration of P_i in the B-cells may contribute to inhibited glucose induced insulin secretion in alloxan treated mice

In vitro studies of mitochondria from some kinds of cells have demonstrated swelling and loss of

changes and inactivates the oxidative and phosphorylative systems (Hunter & Ford 1955) The NAD dependent oxidations of the tricarboxylic acid cycle

oxidative phosphorylation by some organic mercury compounds of the phosphate

of 1978)

Alloxan inhibits the oxidative phosphorylation of glucose in various tissues (Bhattacharya 1955) and abolishes the respiratory stimulation with glucose and decreases the oxidation of glucose in isolated mouse islets (Gunnarsson & Hellerstrom 1973) The notion that alloxan inhibits the NAD linked steps of the tricarboxylic acid cycle (Younathan 1962) is of interest since a deficient oxidation of oxaloacetate and citrate but an unaffected oxidation of succinate has been reported in isolated mouse islets exposed to alloxan (Gunnarsson & Hellerstrom 1973) and since phosphate transport is an obligatory requirement for the net transport of malate α -oxoglutarate and citrate (cf Barritt et al 1978) It should also be noted that a protection against alloxan toxicity has been found by NAD *in vitro* (Younathan 1962) and by nicotinamide *in vivo* (Lazarow et al 1950)

Against this background the supposed block by alloxan of a transport system for phosphate in the B-cell mitochondria is believed primarily to give rise to an inhibition of the NAD linked oxidations and oxidative phosphorylation and to an increased cytosolic concentration of P_i which secondarily causes swelling and further functional impairment and finally disintegration of the mitochondria. Intact mitochondrial function is necessary for the energy production and survival of all cells and hence the mitochondrial lesion may be the cause of β -cell necrosis in alloxan treated animals (Boquist 1977 a, Lorenzon & Boquist 1979)

Because of the finding of mitochondrial lesions in alloxan treated mice the effects on the endocrine pancreas of *p* hydroxymercuribenzoate (PHB) were investigated (Boquist 1978 c and 1979 a) since this compound is a relatively specific sulfhydryl reagent with an established inhibitory effect on mitochondrial function *in vitro* suggested to be due to

interaction with mitochondrial permeation of phosphate (Fortoy & Bessmann 1968) PHB admini-
-ed in a second round induced transient hyperglycemia

1979 a) and inhibited insulin release *in vivo* (Boquist 1979 d) and *in vitro* (our unpublished
-ed in a second round induced no B

and B-cell morphology in starved mice. Thus
-ed in a second round induced no B
support

indirectly the contribution that the PHB-data make to the P_i pH hypothesis

Hydrogen Ion Concentration

In contrast to the increased concentration of P_i recorded in whole islets of alloxan treated mice (Boquist 1978 e) a decrease was observed in islet pH (Boquist 1978 a) Since the islets of the mice used mainly are composed of B-cells data for whole islets can be regarded as representative for these cells. Although these data give no information about the localization of ions inside the B-cells they are probably most representative for the cytosol. As may be the case in serum there may be an inverse relationship between P_i and pH in the B cells and as in lower organisms (Harold 1972) mitochondrial uptake of P_i may result in alkalization of the exterior milieu whereas efflux of P_i may give rise to alkalization of the mitochondrial interior. Therefore the P_i pH hypothesis includes a supposition of an inverse relationship between P_i and pH in the B cells although pH alterations are not necessary to explain the development of mitochondrial lesions and necrosis of B-cells

Changes in hydrogen ion concentration obviously affect B-cell function *in vitro*. The net release of H^+ is markedly increased by glucose (Malaisse et al 1979) and modifications in extracellular pH may interfere with emiocytosis (Rebolledo et al 1978) Reduced pH has been reported to inhibit glucose induced insulin release (Lernmark 1971) whereas a rise in pH enhances insulin secretion possibly through a dissolution of secretory granules (Hellman 1975) Isolated secretory granules exhibit an optimal stability at pH 6.0 (Coore et al 1969)

Carbonic anhydrase (CAH) activity has been demonstrated in mouse B-cells by light and electron microscopic histochemistry (Boquist & Hagstrom 1979) (our unpublished data)

transient hyperglycemia and markedly decreased

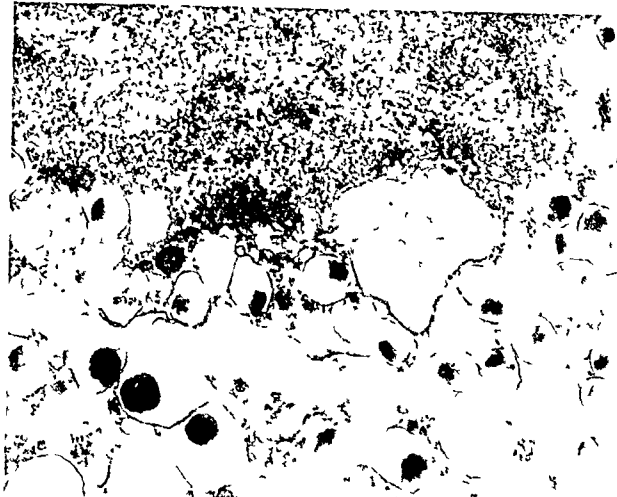


Fig 3 Portion of severely damaged B cell 6 hours after alloxan injection. Note that some of the secretory granules exhibit an altered configuration of the core and/or rupture of the membrane. $\times 19,000$

sodium and P_i into the B-cells may affect the development of alloxan diabetes. Inhibition of a univalent-cation pump in the B cell membrane has been suggested to play a role in alloxan diabetes although it need not be the most basic action of alloxan (Jdahl *et al* 1977).

Assuming a direct intracellular action of alloxan it is important to note that certain sulfhydryl reagents specifically inhibit the phosphate carrier of rat liver mitochondria without affecting a number of other mitochondrial functions (*cf* Chappell 1970, Lehninger 1975) and that one of the most well known properties of alloxan is its role as sulfhydryl reagent. The B-cell mitochondria like those of liver are supposed to possess a sulfhydryl dependent phosphate transport system which is inhibited by alloxan (Lorentzen & Boquist 1979). This inhibition may result in a decreased mitochondrial content of P_i and an increased concentration of P_i in the cytosol which in turn may be consistent with the increased concentration of P_i in whole islets

(Boquist 1978c) and with the altered pattern of pyroantimonate precipitation in the B-cells of alloxan treated mice (Boquist 1977a). The alterations in the localization and concentration of P_i may be associated with similar alterations of Ca^{2+} .

Since starvation is well known to increase the B cell sensitivity to alloxan it should be noted that starvation has been reported to alter the activation site for the γ -phosphate flush in rat islets (Asplund & Freinkel 1978) although this is not directly applicable to the supposed mitochondrial transport mechanism for phosphate.

Mitochondrial lesion and alterations in the localization and concentration of P_i may affect the release of insulin. P_i plays a so far not fully clarified role in insulin secretion. Islet stimulation reduces the islet pool of phosphate, the total islet content of phosphate declines as much as 40–50% following glucose stimulation (Bukowiecki *et al* 1979) and P_i may inhibit glucose induced insulin release *in vitro* (Andersson 1978). Thus high

cytosolic concentration of P_i in the B-cells may contribute to inhibited glucose induced insulin secretion in alloxan treated mice

In vitro studies of mitochondria from some kinds of cells have demonstrated swelling and loss of function in the presence of P_i . Thus exposure of rat liver mitochondria to P_i has been reported to be the mildest treatment which causes marked structural changes and inactivates the oxidative and phosphorylative systems (Hunter & Ford 1955). The NAD dependent oxidations of the tricarboxylic acid cycle are both inhibited by this kind of treatment (Hunter & Ford 1955) and in rat kidney homogenates by exposure to alloxan (Younathan 1962). Inhibition of oxidative phosphorylation by some organic mercurial compounds is due to inhibition of the phosphate entry into the mitochondria (cf Fonyo 1968) which may regulate oxidative phosphorylation (Barritt *et al* 1978).

Alloxan inhibits the oxidative phosphorylation of glucose in various tissues (Bhattacharya 1955) and abolishes the respiratory stimulation with glucose and decreases the oxidation of glucose in isolated mouse islets (Gunnarsson & Hellerstrom 1973). The notion that alloxan inhibits the NAD linked steps of the tricarboxylic acid cycle (Younathan 1962) is of interest since a deficient oxidation of oxaloacetate and citrate but an unaffected oxidation of succinate has been reported in isolated mouse islets exposed to alloxan (Gunnarsson & Hellerstrom 1973) and since phosphate transport is an obligatory requirement for the net transport of malate, α -oxoglutarate and citrate (cf Barritt *et al* 1978). It should also be noted that a protection against alloxan toxicity has been found by NAD *in vitro* (Younathan 1962) and *y* nicotinamide *in vivo* (Lararow *et al* 1950).

Against this background the supposed block by alloxan of a transport system for phosphate in the B-cell mitochondria is believed primarily to give rise to an inhibition of the NAD linked oxidations and oxidative phosphorylation and to an increased cytosolic concentration of P_i which secondarily causes swelling and further functional impairment and finally disintegration of the mitochondria. Intact mitochondrial function is necessary for the energy production and survival of all cells and hence the mitochondrial lesion may be the cause of B-cell necrosis in alloxan treated animals (Boquist 1977a, Lorentson & Boquist 1979).

Because of the finding of mitochondrial lesions in alloxan treated mice the effects on the endocrine pancreas of *p* hydroxymercuribenzoate (PMB) were

interaction with mitochondrial permeation of phosphate (Fonyo & Bessmann 1968). PMB administration to fed mice induced transient hyperglycemia and structural B-cell changes similar to those found early after alloxan treatment (Boquist 1978c and 1979a) and inhibited insulin release *in vivo* (Boquist 1979d) and *in vitro* (our unpublished observation). However, PMB injection caused no B-cell necrosis or any permanent diabetes and was without effect on the blood glucose concentration and B-cell morphology in starved mice. Thus although the effects on the endocrine pancreas of alloxan and PMB are not identical the similarities in these effects are sufficiently great to support indirectly the contribution that the PMB-data make to the P_i pH hypothesis.

Hydrogen Ion Concentration

In contrast to the increased concentration of P_i recorded in whole islets of alloxan treated mice (Boquist 1978c) a decrease was observed in islet pH (Boquist 1978a). Since the islets of the mice used mainly are composed of B-cells data for whole islets can be regarded as representative for these cells. Although these data give no information about the localization of ions inside the B-cells they are probably most representative for the cytosol. As

... stimulation of the exterior milieu whereas efflux of P_i may give rise to alkalinization of the mitochondrial interior. Therefore the P_i pH hypothesis includes a supposition of an inverse relationship between P_i and pH in the B-cells although pH alterations are not necessary to explain the development of mitochondrial lesions and necrosis of B-cells.

Changes in hydrogen ion concentration obviously affect B-cell function *in vitro*. The net release of H^+ is markedly increased by glucose (Malaisse *et al* 1979) and modifications in extracellular pH may interfere with emiocytosis (Rebolledo *et al* 1978). Reduced pH has been reported to inhibit glucose induced insulin release (Lernmark 1971) whereas a rise in pH enhances insulin secretion possibly through a dissolution of secretory granules (Hellman 1975). Isolated secretory granules exhibit an optimal stability at pH 6.0 (Coore *et al* 1969).

Carbonic anhydrase (CAH) activity has been demonstrated in mouse B-cells by light and electron microscopic histochemistry (Boquist & Hargstrom 1979). CAH is the B-cell which is transient

... *in vitro* suggested to be due to

glucose tolerance (Boquist 1979 b) This emphasizes that pH alterations may play a prominent role in B-cell function

It is also of interest that glycolysis in various tissues is influenced by the hydrogen ion concentration Glycolysis in erythrocytes, which may be alloxan sensitive since hemolysis occurs in alloxan diabetes, is inhibited both by high concentrations of P_i (cf Schrier 1970) and by acidification (Tulin et al 1947), whereas low concentration of P_i and alkalization have an opposite effect

Against this background it seems that an increased pH in the B-cell cytosol may facilitate, or be necessary, for insulin release, at least for secretion of insulin stored in granules If so, the inhibited insulin secretion after exposure to alloxan may at least in part be due to decreased pH Moreover, reduced pH is believed to potentiate the action of alloxan in the B-cells, since it is known that alloxan *in vitro* is highly unstable in neutral and alkaline solutions, whereas acidity increases its stability, and since *in vivo* studies have disclosed that the alloxan effect is potentiated in rats by acidosis (Klebanoff & Greenbaum 1954), but antagonized in mice by metabolic alkalosis (Boquist 1979 c) Acidity may even be a prerequisite for alloxan toxicity in the B-cells

HYPOTHESIS

Summing up (Fig 4), alloxan is believed to pass the plasma membrane of the B-cells, probably through a glucose transport channel, which may be associated also with transport of sodium and phosphate In addition there is possibly a direct or indirect action on the plasma membrane Inside the B-cell alloxan is believed to inhibit a sulfhydryl-dependent transport system for phosphate in the (inner membrane of?) mitochondria leading to increased concentration of P_i in the cytosol and, since an inverse relationship is supposed to exist between P_i and pH secondarily to a fall in pH in the cytosol Secondly, the localization and concentration of Ca^{2+} in the B-cell may also be affected The block of mitochondrial phosphate transport also gives rise to inhibition of the NAD-dependent oxidations of the tricarboxylic acid cycle and oxidative phosphorylation The increase in cytosolic concentration of P_i causes mitochondrial swelling, which possibly further impairs mitochondrial function The fall in pH in the cytosol increases the stability of alloxan and therefore potentiates and prolongs the action of alloxan Acidity may even be a prerequisite for alloxan toxicity Moreover, the fall in pH inhibits the synthesis and the glucose induced release of

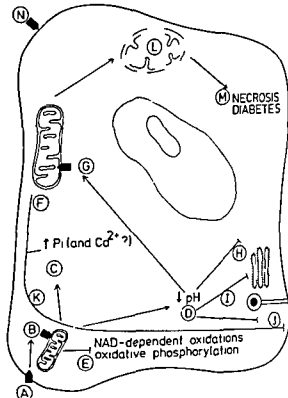


Fig 4 Schematic representation of the P_i pH hypothesis for alloxan diabetes Alloxan (■) passes the B-cell membrane through a channel (A) which probably is associated with transport of glucose and possibly also with that of sodium and phosphate and inhibits a mitochondrial sulfhydryl dependent transport system for P_i (B) This results in an increased concentration of P_i (C) and a fall in pH (D) in the

cytosol The increase in cytosolic P_i concentration causes a swelling of the mitochondria (F) The lowering of the pH increases the stability of alloxan (G) and possibly causes a decreased glycolysis (H) and an inhibition of insulin synthesis (I) and the glucose induced release of insulin (J) The mitochondrial changes and the increased concentration of P_i in the cytosol may also contribute to the inhibition of glucose induced secretion of insulin (K) The swollen mitochondria are subsequently disintegrated (L) the energy production ceases and B-cell necrosis and diabetes develop (M) In addition to the effect on the mitochondria there may be a direct or indirect action of alloxan on the plasma membrane (N) The selectivity of alloxan for the B-cell is believed to be associated with the permeability of this cell for glucose

insulin, and causes possibly decreased glycolysis Mitochondrial lesion, and increased concentration of P_i in the cytosol may contribute to inhibition of glucose induced insulin secretion The swollen mitochondria are subsequently disintegrated, which results in absence of energy production, necrosis of B-cells, and development

In order to test the hypothesis studies have been carried out of factors affecting the B-cell sensitivity to alloxan. These studies disclosed an inhibition of the development of alloxan diabetes in starved and/or fed mice pretreated with D glucose, D mannose, D fructose, sodium lactate, NaHCO_3 , D mannose, PMB and acetazolamide and in mice given L-leucine before or within 3 min after alloxan injection, whereas no effect on the B-cell sensitivity to alloxan was observed after administration of D galactose, L arginine, NaH_2PO_4 or Ca^{2+} (Boquist 1977 a, 1978 a, b, c, d, e, 1979 b, c, d and e). A potentiation of alloxan toxicity on the other hand was induced by starvation or pretreatment with 1,25 dihydroxycholecalciferol or parathormone (Boquist et al 1977).

A rise in islet pH was observed after administration of those substances which are antagonistic to alloxan, whereas a fall in islet pH was found after starvation and as described above after alloxan administration (Boquist 1978 a). The islet concentration of P_i on the other hand was assayed after exposure to D glucose, L-leucine and as described above after administration of alloxan; the P_i concentration in the islets was decreased after D glucose and L-leucine but increased after alloxan (Boquist 1978 e). Thus it appears that alloxan sensitivity is associated with high P_i and low pH and that alloxan protection is associated with low P_i and high pH. These findings support the P_i pH hypothesis.

A high pH may act antagonistically by decreasing the stability of alloxan and a low P_i may make the mitochondria more resistant to alloxan. Conversely a low pH increases the stability of alloxan and a high P_i increases the size of the mitochondria thereby possibly making these organelles vulnerable. Mitochondrial hypertrophy and enhanced succinate dehydrogenase activity have been observed in isolated islets exposed to low glucose (Boquist 1977 b) which might be associated with high P_i and low pH.

Glucose, mannose and fructose are the only sugars which can be glycolyzed by most cells (Villar Palasi et al 1957). Therefore the reason why pretreatment with these hexoses protect against alloxan may be that they through glycolysis affect P_i and pH in the B-cells. This could explain why these hexoses protect against alloxan.

More

efflu

rat

(Freinkel et al 1976)

Also L-leucine causes a transitory heightened efflux of P_i from isolated rat islets (Freinkel et al 1976) which conceivably decreases the B-cell

concentration of P_i thereby antagonizing alloxan toxicity according to the P_i pH hypothesis. It should be noted that the effect of L-leucine on P_i efflux is not inhibited by D-mannoheptulose (Freinkel et al 1976) since pretreatment with L-leucine does not affect the hyperglycemic response of fed mice to D-mannoheptulose (Boquist 1979 e). In contrast to the other compounds tested, L-leucine protected also when given a few minutes after alloxan, possibly indicating another protective mechanism than for the other compounds tested (Boquist 1979 b). One may speculate whether L-leucine passes into the B-cells and causes P_i efflux also after these cells have been exposed to alloxan, whereas e.g. glucose does not.

The metabolic alkalosis induced in mice pretreated with sodium lactate or NaHCO_3 (Boquist 1979 c) might have decreased the stability of alloxan already when it is present in the circulation. Another possibility is that the increase in blood pH was associated with a rise in B-cell pH which inhibited alloxan toxicity intracellularly.

The selectivity of the B-cells for alloxan toxicity is believed to be due to the fact that these cells are freely permeable to glucose. Also the few other kinds of cells which are sensitive to alloxan are freely permeable to glucose, e.g. the kidney tubule epithelial cells. Still other cells which are not freely permeable to glucose are resistant to alloxan toxicity. The free permeability to glucose may directly or indirectly be associated with a free permeability also for alloxan. An alternative explanation is that alloxan induces inhibited insulin release, and that in the absence of sufficient amounts of insulin, glucose and P_i (which are supposed to enter the cell in association) pass into those cells.

Sucrose accumulation is deleterious to the cell according to the P_i pH hypothesis.

Supported by grants from the Swedish Medical Research Council (Project No. B78 12X-00718 13).

REFERENCES

- Andersson T. Phosphate induced modifications of ^{45}Ca fluxes and secretory activity in pancreatic B-cells. *Diabetologia* 15: 215, 1978.
- Asplund K & Freinkel N. Effect of fasting on ^{32}P translocation in pre-labelled pancreatic islets. *Acta Endocrinol* 88: 545-555, 1978.
- Barrist G J, Thorne R F W & Hughes B P. Effects of hormones and $\text{N}^{6,0^2}$ -dibutryl adenosine 3,5

- cyclic monophosphate administered *in vivo* on phosphate transport and metabolism in isolated rat liver mitochondria *Biochem J* 172 577-585 1978
- Bhattacharya G Studies on the mechanism of the diabetogenic action of alloxan *Proc Nat Inst Sci India (New Delhi)* 21 210-221 1955
- Boquist L The endocrine pancreas in early alloxan diabetes *Acta path microbiol scand Sect A* 85 219-229 1977 a
- Boquist L Pancreatic islets subjected to different concentration of glucose *in vitro* A study with special regard to mitochondrial changes *Virch Arch B Cell Path* 23 219-226 1977 b
- Boquist L Further studies of factors affecting the β -cell sensitivity to alloxan *Acta Endocrinol* 88 12 Suppl 219 1978 a
- Boquist L Factors affecting the β cell sensitivity to alloxan *in vivo* Influence of pre and posttreatment with protective substances *Acta Endocrinol* 88 556-561 1978 b
- Boquist L *p* hydroxymmercuribenzoate induced hyperglycemia in mice *in vivo* *Acta Endocrinol* 88 13 Suppl 219 1978 c
- Boquist L Pancreatic B-cell sensitivity to alloxan *in vivo* A study of antagonizing compounds serum inorganic phosphate and acid base balance *Acta path microbiol scand Sect A* 86 313-318 1978 d
- Boquist L Alloxan diabetes in mice Study of factors affecting the B cell sensitivity to alloxan *Diabetologia* 15 220-221 1978 e
- Boquist L Hyperglycemia following *p* hydroxymmercuribenzoate administration to mice *Acta Diabetol Lat* 16 35-44 1979 a
- Boquist L Carbonic anhydrase activity in the endocrine pancreas and effect of acetazolamide on serum glucose and insulin and alloxan sensitivity of mice *Acta Endocrinol* In press 1979 b
- Boquist L Effect of metabolic alkalosis on the B-cell sensitivity to alloxan *in vivo* *Horm Metab Res* 10 477-481 1979 c
- Boquist L *p* hydroxymmercuribenzoate induced hyperglycemia Influence of pre and posttreatment with L leucine tolbutamide D mannoheptulose insulin and alloxan *J Endocrinol Invest* In press 1979 d
- Boquist L Effect of D mannoheptulose on blood glucose and alloxan sensitivity in mice *Acta Endocrinol* In press 1979 e
- Boquist L & Hagstrom S Carbonic anhydrase activity in mouse endocrine pancreas *Acta path microbiol scand Sect A* 87 157-164 1979
- Boquist L & Lorentzon R Stereological study of
- Bukowiecki L Trus M Matschinsky F M & Frenkel N Alterations in pancreatic islet phosphate content during secretory stimulation with glucose *Biochim Biophys Acta* 583 370-377 1979
- Chappel J B Mitochondrial and microbial anion transporting systems *Biochem J* 116 3p-4p 1970
- Coore H G Hellman B Pihl E & Taljedal I B Physicochemical characteristics of insulin secretion granules *Biochem J* 111 107-113 1969
- Dennis V B & Bray P C Sodium phosphate glucose bicarbonate and alanine interactions in the isolated proximal convoluted tubule of the rabbit kidney *J Clin Invest* 61 387-397 1978
- Fonyo A Phosphate carrier of rat liver mitochondria Its role in phosphate outflow *Biochem Biophys Res Commun* 32 624-628 1968
- Fonyo A & Bessman S P Inhibition of inorganic phosphate penetration into liver mitochondria by *p*-mercuribenzoate *Biochem Med* 2 145-163 1968
- Freinkel N El Youssef C & Dawson R M C Insulin release and phosphate ion efflux from rat pancreatic islets induced by L leucine and its nonmetabolizable analogue 2 aminobicyclo (2 2 1) heptane 2 carboxylic acid *Proc Natl Acad Sci USA* 73 3403-3407 1976
- Gunnarsson R Inhibition of insulin biosynthesis by alloxan streptozotocin and N nitrosomethylurea *Molecul Pharmacol* 11 759-765 1975
- Gunnarsson R & Hellerstrom C Acute effects of alloxan on the metabolism and insulin secretion of the pancreatic B cell *Horm Metab Res* 5 404-409 1973
- Hammarstrom L Hellman B & Ullberg S On the accumulation of alloxan in the pancreatic β -cells *Diabetologia* 3 340-345 1967
- Harold F M Conservation and transformation of energy by bacterial membranes *Bact Rev* 36 172-230 1972
- Hellman B The significance of calcium for glucose stimulation of insulin release *Endocrinology* 97 392-398 1975
- Henquin J C Mahaux P & Lamber A E Alloxan induced alteration of insulin release rubidium efflux and glucose metabolism in rat islets stimulated by various secretagogues *Diabetologia* 16 253-260 1979
- Hunter F E & Ford L Inactivation of oxidative and phosphorylative systems in mitochondria by preincubation with phosphate and other ions *J Biol Chem* 216 357-369 1955
- Idahl L A Lernmark A Sehlin J & Taljedal I B Alloxan cytotoxicity *in vitro* Inhibition of rubidium pumping in pancreatic β cells *Biochem J* 162 9-18 1977
- Klebanoff S J & Greenbaum A L The effect of pH on the diabetogenic action of alloxan *J Endocrinol* 11 314-322 1954
- Laarow A Liambies J & Tausch A J Protection against diabetes with nicotinamide *J Lab Clin Med* 36 249-258 1950

- Lehninger A L (ed) *Biochemistry* Sec ed Worth Publ Inc 1975 p 530
- Lernmark Å Isolated mouse islets as a model for studying insulin release *Acta Diabetol Lat* 8 649-697 1971
- Lorentson R & Boquist L Stereological study of B-cell mitochondria in alloxan treated mice *Virch Arch B Cell Path* 31 227-233 1979
- Malaisse W J Hutton J C Kawan S Herchuel A Valverde I & Sener A The stimulus secretion coupling of glucose induced insulin release *Diabetologia* 16 331-341 1979
- McDaniel M Roth C Fink J Fyfe G & Lacy P Effects of cytochalasins B and D on alloxan inhibition of insulin release *Biochem Biophys Res Commun* 66 1089-1096 1975
- Rebolledo O R Hernandez R E Zanetta A C & Gagliardino J J Insulin secretion during acid base alterations *Am J Physiol* 234 E426-E429 1978
- Schrier S L Transfer of inorganic phosphate across erythrocyte membranes *J Lab Clin Med* 75 422-434 1970
- Tomita T & Lacy P E Interaction of alloxan and glucose on glucose induced insulin secretion of isolated rat islets perfused in vitro *Diabetes* 21 (Suppl 1) 326 1972
- Tulin M Danowski T S Hald P M & Peters J P The distribution and movements of inorganic phosphate between cells and serum of human blood *Am J Physiol* 149 678-687 1947
- Villar Palasi C Carballido A Sols A & Arieta J L Sensitivity of pancreas hexokinase towards alloxan and its modification by glucose *Nature* 180 387-388 1957
- Weaver D C McDaniel M L & Lacy P E Alloxan uptake by isolated rat islets of Langerhans *Endocrinology* 102 1847-1855 1978
- Younathan E S Inhibition of the citric acid cycle by alloxan *J Biol Chem* 237 608-611 1962

- cyclic monophosphate, administered *in vivo* on phosphate transport and metabolism in isolated rat liver mitochondria *Biochem J* 172 577-585 1978
- Bhattacharya G Studies on the mechanism of the diabetogenic action of alloxan *Proc Nat Inst Sci India (New Delhi)* 21 210-221, 1955
- Boquist L The endocrine pancreas in early alloxan diabetes *Acta path microbiol scand Sect A* 85 219-229, 1977 a
- Boquist L Pancreatic islets subjected to different concentration of glucose *in vitro* A study with special regard to mitochondrial changes *Virch Arch B Cell Path* 23 219-226 1977 b
- Boquist L Further studies of factors affecting the β -cell sensitivity to alloxan *Acta Endocrinol* 88 12 Suppl 219, 1978 a
- Boquist L Factors affecting the β cell sensitivity to alloxan *in vivo* Influence of pre and posttreatment with protective substances *Acta Endocrinol* 88 556-561, 1978 b
- Boquist L *p* hydroxymercuribenzoate induced hyperglycemia in mice *in vivo* *Acta Endocrinol* 88 13 Suppl 219 1978 c
- Boquist L Pancreatic B-cell sensitivity to alloxan *in vivo* A study of antagonizing compounds serum inorganic phosphate and acid base balance *Acta path microbiol scand Sect A* 86 313-318 1978 d
- Boquist L Alloxan diabetes in mice Study of factors affecting the B cell sensitivity to alloxan *Diabetologia* 15 220-221 1978 e
- Boquist L Hyperglycemia following *p* hydroxymercuribenzoate administration to mice *Acta Diabetol Lat* 16 35-44 1979 a
- Boquist L Carbonic anhydrase activity in the endocrine pancreas and effect of acetazolamide on serum glucose and insulin and alloxan sensitivity of mice *Acta Endocrinol* In press 1979 b
- Boquist L Effect of metabolic alkalosis on the B cell sensitivity to alloxan *in vivo* *Horm Metab Res* 10 477-481 1979 c
- Boquist L *p* hydroxymercuribenzoate induced hyperglycemia Influence of pre and posttreatment with L leucine tolbutamide D mannoheptulose insulin and alloxan *J Endocrinol Invest* In press 1979 d
- Boquist L Effect of D mannoheptulose on blood glucose and alloxan sensitivity in mice *Acta Endocrinol* In press 1979 e
- Boquist L & Hagstrom S Carbonic anhydrase activity in mouse endocrine pancreas *Acta path microbiol scand Sect A* 87 157-164 1979
- Boquist L & Lorenzon R Stereological study of
- Bukowiecki L Trus M Matschinsky F M & Freink N Alterations in pancreatic islet phosphate content during secretory stimulation with glucose *Biochim Biophys Acta* 583 370-377 1979
- Chappel J B Mitochondrial and microbial amino transporting systems *Biochem J* 116 3p-4p 197
- Coore H G, Hellman B Pohl E & Taljedal I L Physicochemical characteristics of insulin secretory granules *Biochem J* 111 107-113 1969
- Dennis V W & Brazy P C Sodium phosphate, glucose, bicarbonate and alanine interactions in the isolated proximal convoluted tubule of the rabbit kidney *J Clin Invest* 61 387-397 1978
- Fonyo A Phosphate carrier of rat liver mitochondria: Its role in phosphate outflow *Biochem Biophys Res Commun* 32 624-628 1968
- Fonyo A & Bessman S P Inhibition of inorganic phosphate penetration into liver mitochondria by *p* mercuribenzoate *Biochem Med* 2 145-163 1968
- Freinkel N El Yousfi C & Dawson R M C Insulin release and phosphate ion efflux from rat pancreatic islets induced by L leucine and its nonmetabolizable analogue 2 aminobicyclo (2 2 1) heptane 2-carboxylic acid *Proc Natl Acad Sci USA* 73 3403-3407 1976
- Gunnarsson R Inhibition of insulin biosynthesis by alloxan streptozotocin and N nitrosomethylurea *Molec Pharmacol* 11 759-765 1975
- Gunnarsson R & Hellersstrom C Acute effects of alloxan on the metabolism and insulin secretion of the pancreatic B cell *Horm Metab Res* 5 404-409 1973
- Hammarstrom L Hellman B & Ullberg S On the accumulation of alloxan in the pancreatic β -cells *Diabetologia* 3 340-345 1967
- Harold F M Conservation and transformation of energy by bacterial membranes *Bact Rev* 36 172-230 1972
- Hellman B The significance of calcium for glucose stimulation of insulin release *Endocrinology* 97 392-398 1975
- Henquin J C Mahaux P & Lambert A E Alloxan induced alteration of insulin release rubidium efflux and glucose metabolism in rat islets stimulated by various secretagogues *Diabetologia* 16 253-260 1979
- Hunter F E & Ford L Inactivation of oxidative and phosphorylative systems in mitochondria by preincubation with phosphate and other ions *J Biol Chem* 216 357-369 1955
- Idahl L Å Lernmark Å Schlin J & Taljedal I B Alloxan cytotoxicity *in vitro* Inhibition of rubidium ion pumping in pancreatic β cells *Biochem J* 162 9-18 1977
- Kiebanoff S J & Greenbaum A L The effect of pH on the diabetogenic action of alloxan *J Endocrinol* 11 314-322 1954
- Lazarow A Liambres J & Tausch A J Protection against diabetes with nicotinamide *J Lab Clin Med* 36 249-258 1950

THE DIAGNOSIS OF CARCINOMA IN TRANSURETHRAL RESECTATES OF THE PROSTATE

A Study of the Probability of Overlooking Malignant Tissue when only Part of the Material Is Embedded for Histological Examination

BJØRN RISMYHR TOR J EIDE and HELGE STALSBERG

The Institute of Medical Biology University of Tromsø Tromsø Norway

Rismyhr B Eide T J & Stalsberg H The diagnosis of carcinoma in transurethral resectates of the prostate A study of the probability of overlooking malignant tissue when only part of the material is embedded for histological examination *Acta path microbiol scand Sect A 88 211-215 1980*

The purpose of this retrospective study based on the findings in routinely processed material from fifty two consecutive cases of prostatic carcinomas is a mathematical calculation of the probability of including a carcinoma in the histological sections from tissue obtained by transurethral resection of the prostate when different embedding practices are followed The analysis shows that if a material of a composition similar to ours were examined the calculated probability to include at least one prostatic chip with malignant tissue in the histological sections would be about 91% if one paraffin block is made The probability increases to about 96% when two blocks are used and comes close to 99% with four blocks

Key words Prostate carcinoma transurethral resectates histology overlooking

Tor J Eide Department of Pathology University Hospital 9012 Tromsø Norway

Received 25 vii 79 Accepted 3 i 80

The amount of tissue obtained by transurethral resection of the prostate varies considerably from case to case It is common practice in most laboratories not to embed more material for microscopic examination than can be placed in a few paraffin blocks of standard size However in a small proportion of cases malignant tissue is present only in very few tissue chips and the diagnosis of carcinoma will be missed if all of these happen to be in the unembedded part of the material

The present study was incited by the report of Lefer & Rosier (1976) who found a significant increase in the prevalence of prostatic cancer by embedding about twice as much material for microscopic examination as they did previously

The purpose of this study is a mathematical calculation of the probability of including a carci-

noma in the histological sections when different embedding practices are followed The calculations are based on the findings in routinely processed material from 52 consecutive cases of prostatic carcinoma diagnosed histologically in transurethral resectates

MATERIAL AND METHODS

This retrospective study was performed at the Depart-

ment of Pathology at the University Hospital in Tromsø. The weight of the prostatic material received and the proportion of the material embedded were taken from the reports. No fixed embedding rules had been followed during the period, but at least 2 or 3

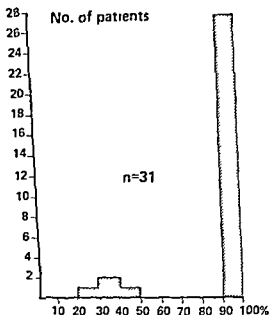
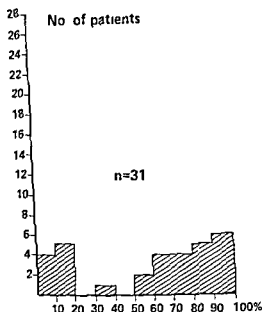
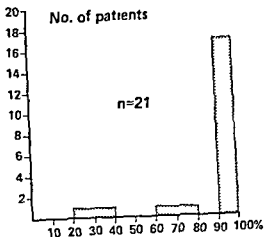
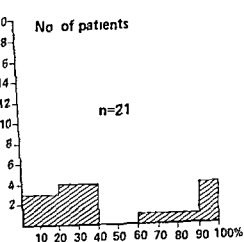


Fig 1 Distribution of patients with clinically benign prostatic disease (upper diagrams) and with clinically malignant prostatic disease (lower diagrams) in 10 per cent intervals according to the proportion of prostatic chips (both left diagrams) and the proportion of paraffin blocks (both right diagrams) containing malignant tissue

malignant diagnosis. In the two clinical groups taken together the proportion of malignant to benign chips was less than 1.5 in fifteen cases (29%), less than 1.0 in seven cases (13%) and less than 1.20 in four cases (8%). As seen from the diagrams the distribution of the proportion of malignant chips appears to be biphasic in both clinical groups with one peak frequency at 100% malignant chips and another peak at about 20% malignant chips.

Table 2 shows the calculated probability in per cent to include at least one prostatic chip with malignant tissue in the histological sections if a material of a composition similar to ours were examined under different embedding practices. It is assumed that the maximum number of blocks is always used except when the total material can be embedded in a smaller number of blocks and that fourteen chips are contained in each block except the last which may have a smaller number. If the

plastic cassettes (Ames Company No 4187) were filled for embedding when sufficient material was available. The tissue was embedded in paraffin and sections were cut at 5 μ m and stained with hematoxylin and eosin.

One section from each block was used for microscopic examination in the present study. Each prostatic chip was marked on the slide with coloured ink for having either malignant or only benign tissue. The evaluation was performed by two observers using a discussion microscope. The presence of malignancy was based on standard histological and cytological criteria (Evans 1978) and each chip was evaluated individually regardless of the presence of malignancy in other chips on the same slide. The numbers of chips with and without malignant tissue were counted including only chips with a maximum diameter ≥ 0.5 mm. The measurement was performed with an ocular micrometer.

The total number of chips present in the material received in the laboratory was estimated from the observed number of chips sectioned and the information on the proportion of the material embedded given in the pathology reports. The number of blocks required for embedding of the total material from each patient was calculated from the observed mean number of chips per block in the total material.

The probability finding at least one prostatic chip with malignant tissue among a given number of chips (q_n) was calculated by the following formula

$$q_n = 1 - p_1 p_2 \dots p_i \dots p_n$$

where

n is the number of chips examined and p_1 is the probability that one randomly selected chip does not contain malignant tissue.

p_i is the probability that the i th randomly selected chip does not contain malignant tissue when all of the $i-1$ randomly selected chips also do not contain malignant tissue.

p_1 is calculated by

$$p_1 = \frac{B}{T}$$

B is the total number of chips without malignant tissue.

T is the total number of chips.

p_i is calculated by

$$p_i = \frac{B - (i-1)}{T - (i-1)}$$

RESULTS

The fifty-two patients in whom primary adenocarcinoma of the prostate was microscopically confirmed constituted 19.1% of all patients from whom transurethral resectates of the prostate were received in the department during the period under study. The clinical diagnosis was benign enlargement of the prostate (CBP) in twenty-one patients

TABLE 1 Age-Distribution of Fifty-Two Patients with Prostatic Carcinoma in Transurethral Resectates

Age-groups	Clinical diagnosis		Total
	Benign	Malignant	
50-59	3	1	4
60-69	3	8	11
70-79	8	13	21
80+	7	9	16
All ages	21	31	52

and suspected malignant disease of the prostate (CMP) in the remaining thirty-one patients. Table 1 shows the age-distribution of the two categories of patients. The mean age of the patients with CBP and CMP was 74 and 73 years respectively.

The weight of the material received was known in twenty-five cases and ranged from 1 to 30 g with a mean of 11.9 g. From the frequently rather rough estimates regarding the proportion of the material that had been embedded for microscopic examination it was estimated that an average of 69% of the material had been embedded in cases of CBP and 81% in cases of CMP. The mean number of paraffin-blocks prepared was 3.4 in cases of CBP and 2.6 in cases of CMP. The mean number of prostatic chips counted in one section from a block was 14.2 and was similar in both categories of patients.

Fig. 1 shows the distribution of patients according to the proportion of prostatic chips and the proportion of paraffin blocks that contained malignant tissue. The results are given separately for patients with clinically benign (upper diagrams) and clinically malignant (lower diagrams) prostatic disease.

In forty-four of the fifty-two cases, all blocks contained malignant tissue. Of the remaining cases malignant tissue was present only in half of the blocks or less in six. There was no significant difference between the two clinical groups in this respect.

The proportion of individual chips that contained malignant tissue was on the average 42% among patients with a clinically benign diagnosis and 59% among patients with a clinically malignant diagnosis. As might have been expected it was relatively more common to find only a small proportion of chips with malignant tissue in cases with a clinically benign diagnosis, but such findings also occurred in a substantial number of cases with clinically

of latent microcarcinomas. A follow-up study is planned to answer this question.

In any case, one would wish to have a reasonably high probability of diagnosing a carcinoma when this is present in the material received in the laboratory, and we would recommend that at least 4 blocks of tissue are embedded when such amounts of tissue are received. Further studies will show whether the proportion of malignant tissue present is of sufficient clinical importance to recommend that it should be stated in the pathology report.

REFERENCES

- Evans R W. Histological appearances of tumours. 3rd ed. Churchill Livingstone. Edinburgh, London and New York 1978, pp 783-796.
- Härbitz T B & Haugen O A. Histology of the prostate in elderly men. A study in an autopsy series. Acta path microbiol scand Section A 80: 756-768, 1972.
- Lefer L G & Rosier R P. Increased prevalence of prostatic carcinoma due to more thorough microscopic examination. New Engl J Med 295: 1432, 1976.
- Medart W S. »Prevalence« of prostatic cancer. New Engl J Med 296: 759, 1977.

TABLE 2 *Calculated Probability in per cent to Include at Least One Prostatic Chip with Malignant Tissue when This Is Present in the Resected Material According to the Maximum Number of Blocks Embedded and According to Clinical Diagnosis*

No of blocks	Clinical diagnosis		Total
	Benign	Malignant	
1	91.5	91.3	91.4
2	95.8	95.9	95.9
3	97.2	98.4	97.8
4	98.0	99.5	98.9
5	98.5	99.9	99.3
6	98.9	99.9	99.5
7	99.2	99.9	99.6
8	99.5	99.9	99.7

practice is that only one paraffin block is made the average probability including at least one prostatic chip with malignant tissue would be about 91% regardless of clinical diagnosis. The probability increased to about 96% when two blocks are used and comes close to 99% with four blocks.

DISCUSSION

Macroscopic assessment of transurethral resected prostatic material for malignancy is time-consuming and unreliable (Lefer & Rosier 1976, Medari 1977) and in most cases the prostatic chips embedded for microscopic examination are taken by chance. When the presence of malignant tissue is limited to a small proportion of the chips received in the laboratory the probability of including a carcinoma is therefore dependent on how much of the resected material that is embedded. Lefer & Rosier (1976) in two series over two periods found an increase in prevalence of carcinoma in transurethral resected prostatic material from 8% in the first series to 14% in the second series. The average number of blocks per patient in the two series was 2.8 and 5.4 respectively and they concluded that the difference in prevalence of carcinoma was due to a more thorough examination of the specimen in the second series. Also Medari (1977) found a higher frequency of prostatic carcinomas as he changed from the processing of only two or three blocks to the processing of the entire specimen.

Most patients in our study did not have malignant tissue in all prostatic chips and 17% of the patients did not have malignant tissue in all blocks. If a material of resectates similar to ours had

been examined by embedding one block containing fourteen chips from each patient malignant tissue would be expected to be present in the histological section in 91% of the cases. This would increase 96% of the cases if two blocks were made and 99% if four blocks were made. There is little difference in this respect between patients with clinically benign diagnosis and those with clinically malignant diagnosis in our material.

The validity of these figures has certain limitations. The number of chips in each block has been counted from the routine histological section which may not have included chips lying deep in the block. On the other hand both ends of curved chips may have been cut and appeared as two separate pieces of tissue on the slide. The calculation of probability is based on the cases in which the histological diagnosis of carcinoma was made in the current routine of the department and a few cases in which malignant tissue has been present in only a few chips may well have been missed. This number cannot be calculated from the present data and a prospective study in which all chips are embedded and sectioned will be needed to give reliable data on this point. The presence of such cases however means that our estimates of the average probability of including a carcinoma when present in the received material are too high and that more blocks will be needed to reach a given level of probability. Also cutting each block at several levels might be expected to reveal more cases with sparse amounts of malignant tissue and this would further change the probability estimates in the same direction.

However the clinical significance of the presence of small amounts of carcinomatous tissue in transurethral resectates is not known. Theoretically the presence of a few malignant chips may be due to a clinically important carcinoma that is located in the peripheral part of the prostate and mostly outside the part of the gland removed by operation or it may be due to a latent micro-carcinoma. Autopsy studies have shown latent micro-carcinomas of the prostate to be present in about 40% of all men over 60 years of age (Harbitz & Hauken 1972) and although most of these were located peripherally some were in a more central position. It must be assumed therefore that these clinically insignificant lesions which cannot be distinguished from other prostatic carcinomas by histological criteria appear in a certain number of transurethral resectates that are removed because of symptoms produced by benign prostatic hyperplasia. The biphasic distribution of the frequency of malignant chips in resectates in our material is striking and it may be questioned whether the low frequency peak could be largely produced by the incidental inclusion

INTESTINAL METAPLASIA WITH COLONIC-TYPE SULPHOMUCINS IN THE GASTRIC MUCOSA; ITS ASSOCIATION WITH GASTRIC CARCINOMA

P SIPPONEN K SEPPALA K VARIS L HJELT T IHAMAKI M KEKKI and M SIURALA

Department of Pathology and Medicine Jorvi Hospital Espoo and Second Department of Medicine
University of Helsinki Helsinki Finland

Sipponen P Seppala K Varis K Hjelt L Ihmaki T Kekki M & Siurala M Intestinal metaplasia with colonic type sulphomucins in the gastric mucosa its association with gastric carcinoma
Acta path microbiol scand Sect. A 88 217-224 1980

The occurrence of intestinal metaplasia with colonic type sulphomucins (abbreviated s IM or s positive IM) in the gastric mucosa was studied in 125 patients with gastric carcinoma (GCA) 62 patients with pernicious anemia (PA) 301 and 183 first-degree relatives of GCA and PA patients 406 outpatients and in 358 controls matched from a large population sample The sulphomucins (s mucins) were demonstrated histochemically in endoscopic biopsy specimens by using high iron diamine and Alcian blue (pH 1) methods The prevalence of s IM especially the strongly s positive IM was significantly higher in GCA patients than in other series or controls of the same age group Further s IM was significantly more common in PA patients and its prevalence higher in GCA relatives and outpatients than in other series or controls The occurrence of s IM was also age dependent and dependent on the extent of IM It was suggested that the occurrence of s IM can be used as a sign of lesions that are more closely associated with GCA than IM is in general

Key words: Gastric carcinoma intestinal metaplasia premalignant lesions carcinogenesis histochemistry

Pentti Sipponen Department of Pathology Jorvi Hospital SF 02740 Espoo 74 Finland

Received 8 xi 79 Accepted 6 i 80

Several studies tentatively indicate a causal interrelationship between intestinal metaplasia (IM) and gastric carcinoma (GCA) (2 6 10 13-16 18) The prevalence of IM is higher in GCA than in benign gastroduodenal diseases (3 6 10) and there exist all transitional forms between IM and GCA (16 19-22 24) In addition the cancerous epithelium itself displays morphological and histochemical characteristics of intestinal epithelium (1 4 5 8 12 23 25 28)

Some IMs seem to contain mucins with sulphated residues characteristic of the colonic epithelium while some of the IMs share only the characteristics of the small bowel epithelium (4 8 12 29) According to a few recent studies the »colonic type

IM« is more closely related to GCA than IM is in general (6 7 29) These studies however are based upon examination of surgical specimens obtained at operations for GCA and benign gastroduodenal ulcer but no data are available on the occurrence of the »colonic type IM« in less selected and more representative materials and in conditions commonly considered precancerous We have studied in this investigation the occurrence of IM with colon-like sulphomucins in antral and body mucosa of the stomach in endoscopic biopsies from patients with GCA or pernicious anemia (PA) from first-degree relatives of GCA or PA patients and from a consecutive series of patients gastroscopized in the out patient department of a hospital A large sample

INTESTINAL METAPLASIA WITH COLONIC-TYPE SULPHOMUCINS IN THE GASTRIC MUCOSA, ITS ASSOCIATION WITH GASTRIC CARCINOMA

P SIPPONEN K SEPPALA, K VARIS L HJELT T IHAMAKI M KEKKI and M SIURALA

Department of Pathology and Medicine Jorvi Hospital Espoo and Second Department of Medicine
University of Helsinki Helsinki Finland

Sipponen P Seppala K Varis K Hjelt L Ihmaki T Kekki M & Siurala M Intestinal metaplasia with colonic type sulphomucins in the gastric mucosa its association with gastric carcinoma
Acta path microbiol scand Sect. A 88 217-224 1980

The occurrence of intestinal metaplasia with colonic type sulphomucins (abbreviated s IM or s positive IM) in the gastric mucosa was studied in 125 patients with gastric carcinoma (GCA) 62 patients with pernicious anemia (PA) 301 and 183 first-degree relatives of GCA and PA patients 406 outpatients and in 358 controls matched from a large population sample The sulphomucins (s mucins) were demonstrated histochemically in endoscopic biopsy specimens by using high iron diamine and Alcian blue (pH 1) methods The prevalence of s IM especially the strongly s positive IM was significantly higher in GCA patients than in other series or controls of the same age group Further s IM was significantly more common in PA patients and its prevalence higher in GCA relatives and outpatients than in other series or controls The occurrence of s IM was also age-dependent and dependent on the extent of IM It was suggested that the occurrence of s IM can be used as a sign of lesions that are more closely associated with GCA than IM is in general

Key words Gastric carcinoma intestinal metaplasia premalignant lesions carcinogenesis histochemistry

Pentti Sipponen Department of Pathology Jorvi Hospital SF 02740 Espoo 74 Finland

Received 8 xi 79 Accepted 6 i 80

Several studies tentatively indicate a causal interrelationship between intestinal metaplasia (IM) and gastric carcinoma (GCA) (2 6 10 13-16 18) The prevalence of IM is higher in GCA than in benign gastroduodenal diseases (3 6 10) and there exist all transitional forms between IM and GCA (16 19-22 24) In addition the cancerous epithelium itself displays morphological and histochemical characteristics of intestinal epithelium (1 4 5 8 12 23 25 28)

Some IMs seem to contain mucins with sulphated residues characteristic of the colonic epithelium while some of the IMs share only the characteristics of the small bowel epithelium (4 8 12 29) According to a few recent studies the »colonic type

IM« is more closely related to GCA than IM is in general (6 7 29) These studies however are based upon examination of surgical specimens obtained at operations for GCA and benign gastroduodenal ulcer but no data are available on the occurrence of the »colonic type IM« in less selected and more representative materials and in conditions commonly considered precancerous We have studied in

consecutive series of patients gastroscopized in the out patient department of a hospital A large sample

of the general adult population of Finland has been used as reference material. The study was aimed to clarify whether IM with colon like sulphomucins is significantly associated with GCA and whether its prevalence is higher in precancerous conditions such as pernicious anemia and in first-degree relatives of GCA or PA patients.

MATERIALS AND METHODS

Materials

The following materials were studied

– *Series 1* consists of 125 consecutive gastric carcinoma patients diagnosed at the gastroenterological units of Jorvi and Meilahti hospitals

– *Series II* consists of 62 consecutive pernicious anemia patients treated at the Outpatient Department of Meilahti hospital

- *Series III* consists of 301 first-degree relatives of 73 consecutive patients with gastric carcinoma diagnosed at the Gastroenterological Unit of Meilahti Hospital

– *Series II* consists of 183 first degree relatives of 68 consecutive pernicious anemia patients.

— *Series 1* consists of 406 consecutive patients without gastric carcinoma studied by direct vision gastric biopsy at Jorvi hospital. The series includes 17 patients with active gastric ulcer and 19 patients with active duodenal ulcer and approximately 200 patients with other circumscribed endoscopic lesions such as polyps erosions atrophy etc.

– **Control series** consists of 358 first degree relatives of subjects computer matched from general population according to age and sex for 73 carcinoma patients of series III

The mean age and sex distribution of the series is given in Table 1. More data on the series and controls are given elsewhere (9-30).

B opsy Procedure

Using the direct vision gastroscopic biopsy method 2-4 specimens were obtained from the antrum mucosa and 6-10 from the body mucosa in series II-IV and in controls. In series I and V approximately 2 specimens were obtained from both antrum and body by employing a similar method. In series I 2 additional specimens were obtained from the cancerous area.

Histochemical Methods and Interpretation of Staining Results

Biopsy specimens were fixed overnight in neutral buffered 10 per cent formalin and were embedded in paraffin. All tissue sections were stained by the haematoxylin-eosin and Alcian blue (pH 2.5)-PAS methods. The occurrence of sulphomucins in IM cases was determined by the Alcian blue (pH 1) (AB1) (17) method. The results of the Alcian blue (pH 1) reaction which was easily distinguished from the background were graded +

and those with an intense staining reaction corresponding the staining intensity of normal colonic mucous substances were graded ++. Examples for the grading are presented in Figs. 1 and 2. The patients and subjects were grouped according to the highest grade in any of the specimens studied.

When the sections were cut for the histochemical studies it sometimes appeared however that the metaplastic foci were not present in the new sections, and accordingly their identification was therefore, not possible. These cases were excluded from the IV group.

The extent of IM in tissue sections was graded arbitrarily as +, ++ or +++ The cases with a single metaplastic gland were graded + and those with extensive IM corresponding the extent in total atrophy were graded +++

Statistics

Statistical significances were calculated by using Student's *t* or χ^2 tests.

RESULTS

Examples of foci with intestinal metaplasia (IM) with or without sulphomucins (abbreviated s IM - s IM + or s IM ++ or s negative IM or s positive IM respectively) are presented in Figs 1 and 2. Sulphomucins were seen in goblet cells and occasionally in the brush border of the metaplastic glands (Fig. 1). The staining intensity of the goblet cells showed a large variability even within the same gland. This variability was most remarkable in cases with an intense staining reaction (s IM ++), in which even non goblet cells were occasionally stained (Fig. 2).

The total prevalences of IM in series and controls are presented in Table 1. The total prevalence of IM is higher in patients with gastric carcinoma (GCA) and pernicious anemia (PA) than in other groups. It also appears however that the mean ages in series III V and in controls are similar but differ from those in series I and II. This necessitates a comparison of series I and II with an age and sex matched sample of the controls. These calculations revealed the total prevalence of IM was significantly higher ($p < 0.01$) in GCA and PA patients than in their matched controls. In addition the corresponding prevalences in GCA relatives and in outpatients were also significantly ($p < 0.05$ and 0.01 respectively) higher than those in controls.

Table 2 shows the occurrence of IM with sulphomucins (s IM) in series and controls. The prevalence of s positive IM is significantly ($p < 0.01$) higher in GCA patients than in matched controls. Also the prevalence of s positive PA patients is significantly ($p < 0.01$) higher than that in matched controls. However no such significant

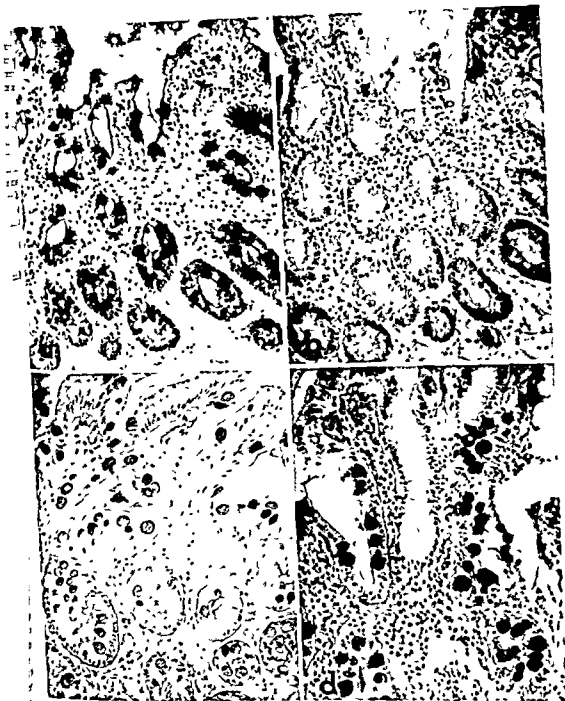


Fig 1 Examples of intestinal metaplasia with and without sulphated colonic type mucosubstances. A IM foci stained with Alcian blue (pH 2.5)-PAS. B same area as in Fig. A stained with high iron diamine (HID). Note the absence of stainable mucosubstances (s IM -). C IM foci stained with HID. Note the staining of goblet cells and a slight staining in the brush border (s IM +). D IM foci with intense staining of mucosubstances with HID (s IM ++). $\times 300$



Fig. 2 Intense staining of mucosubstances with HID (s IM + +) A dysplastic glands stained with Alcian blue (2.5)-PAS B same area stained with HID Note the intense staining of mucosubstances also in non goblet epithelial cells $\times 300$

TABLE 1 Mean Age, Male/Female Ratio and Prevalence of Intestinal Metaplasia (IM) in the Patient Series Studied

Series	Total Number of subjects	Mean Age yrs \pm S.D.	Male/Female Ratio	Subjects with IM	
				Number	Per cent
(I) GCA Patients	125	65 \pm 12	1.8	61	49
(II) PA Patients	62	65 \pm 14	0.4	41	66
(III) GCA Relatives	301	47 \pm 13	0.9	60	20
(IV) PA Relatives	183	47 \pm 16	0.8	24	13
(V) Outpatients	406	52 \pm 15	0.9	141	34
Controls	358	46 \pm 14	0.9	50	14

TABLE 2 Prevalence of Intestinal Metaplasia with Sulphated Colonic Type Mucosubstances (s IM) in the Patient Series Studied

Series	Total Number of Subjects	Subjects with s IM					
		s IM + No	s	s IM + + No	s	s IM Total No	s
(I) GCA Patients	125	24	19	19	15	43	34
(II) PA Patients	62	10	16	1	2	11	18
(III) GCA Relatives	301	25	8	5	2	30	10
(IV) PA Relatives	183	6	3	0	-	6	3
(V) Outpatients	406	36	9	4	1	40	10
Controls	358	19	5	3	1	22	6

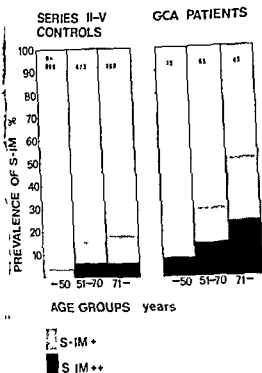


Fig 3 Prevalence of intestinal metaplasia with sulphated colon like mucosubstances (s IM) in patient series in relation to age Controls and patient series without malignancy are treated as one group

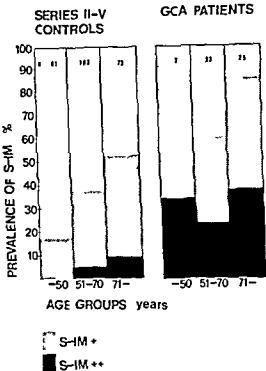


Fig 4 Prevalence of intestinal metaplasia with colon like sulphated mucosubstances (s IM) in patients with intestinal metaplasia Controls and patient series without malignancy are treated as one group

differences are seen between PA relatives and controls. On the other hand the prevalence of s IM is higher in GCA relatives and in outpatients than in controls although this difference is not statistically significant ($0.1 > p > 0.05$).

The age relation of s IM is shown in Figs 3 and 4. Because of the small number of s positive cases all series without carcinoma are treated as one group and are compared with the carcinoma series. It appears that in both groups the prevalence of s positive IM increases with age. The data further reveals that the proportion of s positive IM of all metaplasias increases also with age (Fig 4). However in all age groups the prevalence and proportion of s positive IM was higher in GCA patients than in the non-cancer group.

In agreement with the above results the mean age in subjects without carcinoma tends to be higher in

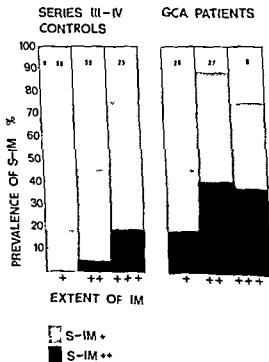


Fig 5 Prevalence of intestinal metaplasia with colon like sulphated mucosubstances (s IM) in relation to extent of IM. The comparison is made between series in which the number of biopsy specimens is the same (controls and series III-IV are compared with carcinoma patients)

relation to the occurrence of s-positive IM. If series II-V and controls are treated as one group, the mean age of strongly s-positive subjects (s-IM++) is significantly higher ($p < 0.01$) than those in slightly s-positive IM (s-IM+) and s-negative IM (s-IM-) cases (mean ages 68 ± 5 , 62 ± 14 and 59 ± 13 years, respectively).

The relationship of s-positive IM with the extent of IM is presented in Fig. 5. The prevalence of s-positive IM tends to increase with increasing extent of IM in subjects without carcinoma. In carcinoma patients, however, this relationship is less pronounced, and carcinoma cases were seen in which even some single metaplastic glands could show an intense staining reaction for sulphomucins.

DISCUSSION

Intestinal metaplasia (IM) is a common finding in biopsy specimens from the stomach. We have found IM in about 20 per cent of subjects matched from a population sample representative of the general adult population of Finland (26). Although IM has been suggested to be a premalignant condition, its common occurrence inhibits its use as a marker of threatening malignancy. The heterogeneity of IM has been known for a long time (1, 12, 23, 35). Some reports have been published in recent years which suggest that IM with colon-like characteristics is more closely associated with gastric carcinoma than IM without these characteristics (6, 7, 29). In this study, we have used histochemical mucin stains in order to differentiate metaplasia into those containing colon-like sulphated mucosubstances (here abbreviated s-positive IM or s-IM) and those which do not have these characteristics (abbreviated s-negative IM or s-IM-). We studied the association of s-positive IM with gastric carcinoma and tried to clarify the relationship of s-positive IM to factors that could indicate its premalignant nature.

We were able to demonstrate transitional forms between s-negative IM and strongly s-positive IM (s-IM++). In addition, the present data showed that s-positive IM is clearly age dependent and is related to the extent of IM. In agreement with these results it was found that the mean age of subjects with strongly s-positive IM was significantly higher than that of s-negative subjects. These results seem to indicate that with respect to s-negative and s-positive IM we are dealing with different stages of the same process rather than with two qualitatively different phenomena. Whether the end stage of this process is gastric carcinoma cannot, however, be proven by the present study.

In gastric carcinoma s-positive IM (especially s-IM++ cases) was found significantly more often than in any other series studied also when comparison was made with age- and sex-matched controls. The results are well in line with those obtained by other investigators (6, 7, 29) and suggest some relationship between s-positive IM and gastric carcinoma. The results are also in line with the initial observation of Järvi and Lauren (10) that a major part of gastric carcinomas show morphogenesis through s-c intestinalization. It is therefore, understandable that colon-like characteristics are also seen in benign lesions that possibly are precancerous, such as IM.

There appeared also some association between s-positive IM and overt pernicious anemia (PA) or first-degree relatives of gastric carcinoma (GCA) which are often considered to be premalignant states (2, 9, 26, 30). The prevalence of s-positive IM was significantly higher in patients with PA and higher in GCA relatives than in controls age and sex matched from a population sample. S-IM could therefore, be a factor which links PA and GCA relatives with GCA. On the other hand, there are many morphological and functional similarities between these states other than s-IM which might also explain the higher risk of patients to develop GCA (26, 30). It should be also noted that we could not find differences in the occurrence of s-IM between controls and PA relatives, who also have been considered gastric carcinoma risk subjects (16, 30). However, according to Lehtola (11) the risk of gastric carcinoma among first-degree relatives of GCA patients is only less than twofold higher than in the population at large. Accordingly, even if we assume that s-IM is responsible for the increased risk among GCA relatives, the expected difference between GCA relatives and controls cannot be very great. Indeed, there was a difference in this respect: the prevalence of s-IM in GCA relatives was nearly twofold that in the controls although this difference was not statistically significant.

In spite of the association of s-IM with GCA and some precancerous states, the present investigation can give only tentative hints as to relationships between s-IM and GCA. The results do not exclude either the possibility that GCA is a primary lesion in relation to s-IM or the possibility of mere coincidence. It is hardly possible to solve this problem by a simple cross-sectional study. A adequate long-term follow-up is necessary, and such a study has already been started by our team.

The limitations of the present study lie also in the methodology employed. Although in most series 10 or more biopsies were obtained from each subject, the specimens still represent only a small fraction of

the whole gastric mucosa. This means that IM and IM could have been overlooked in some cases. In addition when new sections were cut the IM finally present could no longer be found in some specimens. It is therefore probable that the represented data on the prevalence of IM and s IM do not express the actual values but are considerably

We acknowledge the financial support received from the Sgrd Juselius Foundation and from the Paulo Foundation Helsinki Finland

REFERENCES

- Abe M, Ohuchi N & Sokano H. Enzyme histo and biochemistry of intestinalized gastric mucosa. *J Histochem Cytochem* 7: 282-289 1974
- Correa P & Cuelllo C. Pathogenese des Magenkarzinoms. *Epidemiologische Pathologie vorangehen der Läsionen. Leber Magen Darm* 6: 72-79 1976
- Elster K, Reiss S & Heinkel K. Histotopographische Untersuchungen ueber die Intestinale Metaplasie in Carcinom und Ulcusmagen. *Z ges inn Med* 15: 1053-1061 1960
- Goldman H & Ming S C. Mucins in normal and neoplastic gastrointestinal epithelium. *Histochemical distribution. Arch Pathol* 85: 580-586 1968
- Goldman H & Ming S C. Fine structure of intestinal metaplasia and adenocarcinoma of the human stomach. *Lab Invest* 18: 203-210 1968
- Heilmann K. *Gastritis. Intestinale Metaplasie. Carcinom*. Thieme Verlag Stuttgart 1978
- Heilmann K & Hopker W W. Loss of differentiation in intestinal metaplasia in cancerous stomach. A comparative morphologic study. *Path Res Pract* 164: 249-258 1979
- Hakkinen I, Grootenroos J & Kunnas R. Sulphoglycoproteins in normal metaplastic and cancerous gastric mucosa as detected by immunofluorescence. *Ann Med exp Biol Fenn* 45: 206-212 1967
- Ihamaki T, Varis K & Siurala M. Morphological functional and immunological state of the gastric mucosa in gastric carcinoma families. Comparison with a random family sample. *Scand J Gastroent* in press
- Jarvi O & Lauren P. On the role of heterotopias of the intestinal epithelium in the pathogenesis of gastric cancer. *Acta path microbiol scand* 29: 26-48 1951
- Lehtola J. Family study of gastric carcinoma with special reference to histological types. *Scand J Gastroent Suppl* 50: 1978
- Lev R. The mucin histochemistry of normal and neoplastic gastric mucosa. *Lab Invest* 14: 2080-2100 1965
- Magnus H A. Observations on the presence of intestinal epithelium in the gastric mucosa. *J Path Bact* 44: 389-398 1937
- Ming S C, Goldman H & Freeman D G. Intestinal metaplasia and histogenesis of carcinoma in human stomach. Light and electron microscopic study. *Cancer* 20: 1418-1429 1967
- Morson B C. Intestinal metaplasia of the gastric mucosa. *Br J Cancer* 9: 365-376 1955
- Morson B C. Carcinoma arising from areas of intestinal metaplasia in the gastric mucosa. *Br J Cancer* 9: 337-385 1955
- Mowry R W. The special value of methods that color both acidic and vicinal hydroxyl groups in the histochemical study of mucins. With revised directions for colloidal iron stain, the use of Alcian blue 8GX, and their combinations with periodic acid Schiff reaction. *Ann NY Acad Sci* 106: 402-432 1963
- Mulligan R M. Histogenesis and biological behaviour of gastric carcinoma. *Ann Path* 7: 349-415 1972
- Nagayo T, Ito M & Yokoyama H. Early phases of human gastric cancer. Morphological study. *Gann* 56: 101-120 1965
- Nagayo T. Histological diagnosis of biopsied gastric mucosa with special reference to that of borderline lesions. *Gann Monogr Cancer Res* 11: 245-256 1972
- Nagayo T & Komagoe T. Histological studies of gastric mucosal cancer with special reference to relationship of histological pictures between the mucosal cancer and the cancer bearing mucosa. *Gann* 52: 109-119 1961
- Nakamura K, Sugano H & Takagi K. Carcinoma of the stomach in incipient phase. Its histogenesis and histological appearances. *Gann* 59: 251-258 1968
- Planteydt H T & Willighagen R G J. Enzyme histochemistry of gastric carcinoma. *J Path Bact* 90: 393-398 1965
- Schade R O K. The borderline between benign and malignant lesions in the stomach. In: *Grundmann E, Grunze H & Witte S (Eds) Early Gastric Cancer*. Springer Verlag Berlin Heidelberg New York 1974 pp 45-53
- Sheahan D G & Jervis H R. Comparative histochemistry of gastrointestinal mucosubstances. *Am J Anat* 146: 103-132 1976
- Siurala M, Villako K, Ihamaki T, Kekki M, Lehtola J, Sipponen P & Varis K. Atrophic gastritis. Its genetic and dynamic behaviour and its relations to gastric carcinoma and pernicious anemia. *E Farber (Ed) Pathophysiology and Carcinogenesis in Digestive Organs*. Univ of Tokyo/Univ Park Press Baltimore 1977 pp 135-150
- Spicer S S. Diamine methods for differentiating mucosubstances histochemically. *J Histochem Cytochem* 13: 211-234 1965
- Stoffels G L, Desneux J J & Gepts W. Gastroscopic and histochemical study of normal atrophic and hypertrophic mucosa. *Digestion* 6: 23-24 1972

- 29 *Teglbjaerg, P & Nielsen, H O* »Small intestinal type« and »colonic type« intestinal metaplasia of the stomach, and their relationship to the histogenetic types of gastric adenocarcinoma. *Acta path microbiol scand Sect A* 86 351-355, 1978
- 30 *Varis K, Ihamäki T, Härkönen M, Samloff I M & Siurala M* Gastric morphology, function and immunology in first-degree relatives of proband with pernicious anemia and controls. *Scand J Gastroent* 14 129-139, 1979

ALPHA-1-ANTITRYPSIN GLOBULES IN LIVER BIOPSIES

PER PRÆTORIUS CLAUSEN

Department of Pathology Hvidovre Hospital and Department of Pathology Herlev Hospital
University of Copenhagen

Clausen Per Prætorius Alpha 1 antitrypsin globules in liver biopsies Acta path microbiol scand
Sect A 88 225 230 1980

In order to examine the frequency of alpha 1 antitrypsin (AAT) deficiency of phenotype Pi Z in a consecutive liver biopsy material PAS/diastase resistant globules with positive immunohistochemical reaction for AAT (AAT globules) were used as a marker of the Pi Z gene. 34 (4%) of 850 liver biopsies contained AAT globules. More than half of the biopsies with globules had chief histological diagnoses within the groups fibrosis, suspicion of cirrhosis and cirrhosis. Micronodular cirrhosis was significantly more frequent in biopsies with AAT globules. The results support the assumption that AAT deficiency of phenotype Pi Z, as well in homozygous as heterozygous form, is associated with development of liver cirrhosis.

Key words: Alpha 1 antitrypsin deficiency, alpha 1 antitrypsin globules, cirrhosis, liver biopsies.

Per P. Clausen, Department of Pathology, Hvidovre Hospital, University of Copenhagen, DK 2650 Hvidovre.

Accepted as submitted 7.1.80

The association between liver disease and α_1 antitrypsin (AAT) deficiency of phenotype ZZ was first described by Sharp *et al.* in 1969 (21). An increased frequency of juvenile cirrhosis was found among children with phenotype ZZ, and further, more the presence of intracytoplasmic diastase resistant PAS positive globules (PAS/DIA globules) was described in liver tissue from these patients. The PAS/DIA globules have subsequently been shown by immunohistochemical and biochemical methods to contain AAT (12, 19). The globules always seem to be present in patients with phenotype ZZ, but occur in varying amounts and are sometimes lacking in biopsies from patients with the heterozygous phenotype.

A few papers based on consecutive autopsy materials have used the occurrence of PAS/DIA globules with positive immunohistochemical reactions for AAT (AAT globules) as a morphological marker for the Pi Z gene (2, 10, 16, 18). The occurrence of AAT globules in a consecutive liver biopsy material has, however, not previously been described.

The aims of the present study have been to examine the frequency of AAT globules in a consecutive liver biopsy material and to compare morphological changes in biopsies with and without globules.

MATERIALS AND METHODS

The investigation is based on 919 consecutive liver biopsies received in the period 01.01.-30.11.1977 at the Department of Pathology, Hvidovre Hospital in Copenhagen. 55 rebiopsies and 14 unsuitable biopsies were excluded from the material. The material described below thus consists of 850 biopsies from 850 patients.

Since it is still uncertain to what extent the phenotype MZ predisposes to development of liver disease (2, 11, 15).

The biopsies were fixed in 10% buffered formalin for 1-4 hours and following routine processing at room temperature embedded in Paraplast® at 59 °C. 5 µm serial sections were cut and for the morphological evaluation stained by the following methods: hematoxylin-eosin, van Gieson, Masson trichrome, reticulin staining, a.m. Gordon and Sweets, staining for iron pigment a.m. Perl's, PAS staining with and without pretreatment with diastase and orcein supplemented by immunoperoxidase staining for HBsAg (6).

Furthermore, the biopsies were stained by immunohistochemical technique in order to demonstrate AAT in the tissue. Indirect peroxidase labelled antibody technique described elsewhere was used (5).

The following antisera were used: 1) Rabbit anti-human AAT (DAKO, Denmark, code no. 10 012, lot 017 (titer SRI 0.7 g/l, immunoglobulin concentration 11 g/l)) used in dilution 1:40. 2) Peroxidase labelled swine-antirabbit IgG (DAKO, code no. P 2190, lot 057, (immunoglobulin concentration 1.3 g/l, molar peroxidase/antibody ratio 0.8)) used in dilution 1:20.

For control stainings anti-AAT antiserum absorbed with AAT was used in dilution 1:40. Furthermore, the immunoglobulin fraction of serum from non immunized rabbits (DAKO code no. X 903, immunoglobulin concentration 20 g/l) was used in dilution 1:80. In addition the primary antiserum was replaced by phosphate buffered saline.

All biopsies in which PAS/DIA globules of at least 1 µm could be demonstrated in the cytoplasm of hepatocytes and where in the same cells positive immunoperoxidase staining for AAT could be demonstrated corresponding to the globular rim as well as in granular form were recorded as biopsies with AAT globules.

The size of globules in the individual biopsy was estimated and according to the maximum size of the globules in the biopsies the positive biopsies were classified in two groups. One with globules up to 3 µm and one with globules larger than 3 µm.

Phenotyping of the serum from the patients was not available during the period of investigation.

For the statistical evaluation the χ^2 test was used. The limit for type I error was set at 0.05.

RESULTS

Of the 850 patients 486 were male and 364 female. In 34 of the 850 biopsies or 4% AAT globules were found. The distribution of sex and age of patients with and without AAT globules is shown in Table 1. No significant difference was observed in the distribution neither of sex nor age in the two groups ($p > 0.1$).

The chief histological diagnoses of biopsies with and without globules are shown in Table 2.

76 biopsies were morphologically normal. In 5 of these or 6.6% AAT globules were present. The frequency of biopsies with normal morphology showed no significant difference in the groups of biopsies with and without globules ($0.8 > p > 0.7$).

Neither did the frequency of biopsies with non-specific changes and granulomas in the two groups show any difference ($0.7 > p > 0.5$), while a significantly increased frequency of acute viral hepatitis was found in biopsies without globules ($0.05 > p > 0.02$).

More than half of the biopsies with AAT globules had morphological changes according to the diagnosis fibrosis, suspicion of cirrhosis and cirrhosis hepatis. Comparing the groups of biopsies with and without globules no significant difference was found in the frequency of fibrosis and morphological changes suspicious of cirrhosis.

In contrast significantly more biopsies with cirrhosis were found in biopsies with than without globules ($0.02 > p > 0.01$). 8% of all biopsies with cirrhosis contained AAT globules. The increased frequency of cirrhosis in biopsies with globules was due to a highly significant increase in micronodular cirrhosis ($0.01 > p > 0.001$), as no difference in frequency was found as regards macronodular cirrhosis ($0.99 > p > 0.98$).

In order to investigate to what extent supplementary aetiological factors could be demonstrated with

TABLE 1. Distribution of Sex and Age in Patients with and without AAT Globules

Age (years)	15-20	21-30	31-40	41-50	51-60	61-70	71-80	≥ 81	Total
Sex	♂ ♀	♂ ♀	♂ ♀	♂ ♀	♂ ♀	♂ ♀	♂ ♀	♂ ♀	
No. of patients without AAT-globules	14 16	82 43	78 32	69 50	100 69	84 64	30 63	7 15	816
No. of patients with AAT-globules	1 0	1 2	2 1	4 1	7 0	5 7	2 1	0 0	34

TABLE 2 *Chief Histological Diagnosis of Biopsies with and without AAT Globules*

Chief histological diagnosis	Biopsies without AAT globules		Biopsies with AAT globules	
Liver without pathological changes	71	(8.7 %)	5	(14.7 %)
Liver with non specific changes	101	(12.3 %)	3	(8.8 %)
Liver with granuloma	6	(0.7 %)	0	
Acute viral hepatitis	120	(14.7 %)	0	
Chronic aggressive hepatitis	5	(0.6 %)	0	
Chronic persistent hepatitis	17	(2.1 %)	0	
Hepatitis sequelae	7	(0.9 %)	0	
Primary biliary cirrhosis	3	(0.4 %)	0	
Alcoholic hepatitis	6	(0.7 %)	0	
Cholestatic hepatitis (incl. drug lesion)	19	(2.3 %)	0	
Liver with fibrosis	59	(7.2 %)	4	(11.8 %)
Obs. cirrhosis	38	(4.7 %)	3	(8.8 %)
Cirrhosis (micronodular)	83	(10.2 %)	10	(29.4 %)
Cirrhosis (macronodular)	37	(4.5 %)	1	(2.9 %)
Fatty liver	122	(15.0 %)	3	(8.8 %)
Large duct obstruction	55	(6.7 %)	4	(11.8 %)
Malignant tumour primary	7	(0.9 %)	1	(2.9 %)
Malignant tumour secondary	37	(4.5 %)	0	
Haemosiderosis	9	(1.1 %)	0	
Amyloidosis Dubin Johnson	3	(0.4 %)	0	
Sinusoidal dilatation	11	(1.3 %)	0	
Total	816	(100 %)	34	(100 %)

different frequency in biopsies with cirrhosis with and without globules a semiquantitative morphological evaluation has been performed as regards the presence of the following morphological features: Fat iron pigment bile pigment alcoholic hepatitis parenchymal activity centrilobular fibrosis bile duct proliferation chronic aggressive hepatitis and Hb,Ag in liver tissue.

The most essential results of this investigation are

shown in Table 3. None of the mentioned features showed any difference in frequency in biopsies with and without globules ($p > 0.05$).

The relation between the maximum size of the globules and the chief histological diagnosis is shown in Table 4. Biopsies containing globules larger than $3 \mu\text{m}$ were mainly found in the diagnostic groups: Fibrosis, suspicion of cirrhosis, cirrhosis and hepatocellular carcinoma.

TABLE 3 *Morphological Features in Biopsies with Cirrhosis with and without AAT Globules*

	Fat		Iron		Parenchymal activity		Alcoholic hepatitis		Hb,Ag in liver tissue		Chronic aggressive hepatitis	
	0	+	0	+	0	+	0	+	0	+	0	+
No. of biopsies with AAT globules	11	0	11	0	7	4	8	3	11	0	10	1
No. of biopsies without AAT globules	94	26	113	7	98	22	101	19	117	3	119	1

TABLE 4 *Relation between Chief Histological Diagnosis and Maximum Size of AAT-Globules*

Chief histological diagnosis	No. of biopsies with AAT-globules	
	≤ 3 µm	> 3 µm
Liver without pathological changes	4	1
Liver with non-specific changes	3	0
Liver with fibrosis	2	2
Suspicion of cirrhosis	2	1
Cirrhosis (micronodular)	6	4
Cirrhosis (macronodular)	0	1
Fatty liver	2	1
Large duct obstruction	4	0
Hepatocellular carcinoma	0	1

DISCUSSION

Since the first description of presence of AAT globules in liver tissue from patients with phenotype ZZ several papers have described the presence of globules in liver tissue from patients carrying the Pi-Z gene as well in homozygous as heterozygous form (review see 20)

The need of supplementary immunohistochemical staining for AAT in the characterization of PAS/DIA globules is emphasized by the fact that PAS/DIA globules without immunohistochemical reaction for AAT have been demonstrated in patients with normal phenotype (MM) (23) and are not rarely found in autopsy materials (17, 18)

The specificity of AAT globules as a morphological marker of the Pi-Z allele has been questioned in a few recent papers (4-13) describing the presence of AAT globules in liver tissue from patients carrying the alleles Pi-M and Pi-S. A more detailed investigation correlating the serum phenotypes with the histochemical and immunohistochemical staining patterns is thus needed in order to state the specificity of AAT globules as a marker of Pi-Z gene. The above mentioned cases are however few in comparison to the great number of cases describing AAT globules in Pi-Z patients. For all practical purposes the presence of AAT globules thus seems to be rather specific as a morphological expression of the presence of the Pi-Z gene. The size of the globules has previously only been specified to a limited extent. In one paper only globules up to at least 3 µm were recorded (2). A previous investigation (14) has, however, shown that at least 1 µm globules were compatible with the presence of Pi-Z gene, for which reason 1 µm was chosen as the lower limit in the present investigation.

The frequency of AAT-globules in liver tissue has until now only been investigated to a limited extent in unselected materials and only in autopsy material. Eriksson *et al* (10) examining 760 consecutive autopsies found AAT globules in 3.7% of the patients. Reintoft (16) and Blenkinsopp & Haffenden (2) demonstrated AAT globules in respectively 6.3% and 3.6% of the autopsies. These frequencies are in accordance with the distribution of phenotypes in populations in Scandinavia (8) and England (7) where the frequency of the phenotype MZ is 3-4% and ZZ less than 1/1000. The frequency of AAT globules in liver biopsies does not seem to have been systematically investigated previously. Eriksson *et al* (10) mentioned that the frequency in an unpublished investigation was found to be 1%, while Blenkinsopp & Haffenden (2) stated that the frequency in biopsies was lower than found in autopsy material without indicating any figures.

I have in the present investigation found a frequency of AAT globules in liver biopsies of 4%. This frequency is thus in accordance with the above mentioned figures in autopsy material but larger than recorded previously in biopsy materials. The difference is probably to a large extent due to the fact that globules in biopsies often are smaller and more sparse for which reason they often are overlooked unless supplementary immunohistochemical staining for AAT is used.

While rather widespread agreement exists concerning the correlation of phenotype ZZ to liver cirrhosis and probably hepatocellular carcinoma it is still not clarified whether phenotype MZ is connected to the development of liver disease to a greater extent than other phenotypes. Morin *et al* (15) using phenotyping of 132 patients with alcoholic cirrhosis and 37 patients with cryptogenic cirrhosis did not find an increased frequency of phenotype MZ in comparison to a control group of healthy blood-donors. Fisher *et al* (11) measuring the AAT serum concentration and using selected phenotyping of patients with decreased serum concentration could not demonstrate an increased frequency of Pi-Z heterozygous with cirrhosis in comparison to the controls.

In contrast Eriksson *et al* (10) with significantly increased frequency found cirrhosis and liver fibrosis in patients with AAT globules. Blenkinsopp & Haffenden (2) found in 64 autopsies with cirrhosis 10 patients with AAT globules while only 4 of 110 control patients had globules. Seven patients with cirrhosis and globules had macronodular cirrhosis.

In accordance with the two last mentioned investigations I have in the present investigation

found a significantly increased frequency of cirrhosis in patients with AAT globules in the biopsies. In contrast to previous descriptions (2-3) I have found a predominance of micronodular cirrhosis (all nodules smaller than 1 mm) in cirrhosis with AAT globules. Macronodular cirrhosis was not found more frequently in biopsies with than without globules.

The discrepancies between the above mentioned results are probably to some extent due to differences in the methods used to examine the frequency of Pi Z gene. In one paper (11) the serum concentration of AAT was used as a primary screening method. As the serum concentration of AAT is normal in many heterozygous (MZ) patients (22) the stated frequency of heterozygous was

AAT globules cannot be interpreted until the specificity of AAT globules as a marker of the Pi Z gene has been investigated.

Previous papers (2-3-23) have investigated to what extent other aetiological factors could be demonstrated to be of importance for the development of liver disease in patients with AAT deficiency. *Triger et al* (23) did not find any morphological indications of an increase in alcoholic hepatitis or hepatitis B infection. *Blenkinsopp & Haffenden* (2-3) demonstrated Hb_sAg in 4 out of 15 cases of cirrhosis with globules. In the present investigation no increase in alcoholic hepatitis or Hb_sAg was found when comparing biopsies with cirrhosis with and without globules.

The higher frequency of acute viral hepatitis in patients without globules could be due to a greater resistance of Pi Z patients to viral hepatitis. It is however more likely that liver cells with globules are more sensitive to viral induced tissue damage. In this way globules could be more difficult to demonstrate.

It is noteworthy that the major part of biopsies without primary parenchymal changes contained globules smaller than 3 µm while globules larger than 3 µm mainly were seen in biopsies with fibrosis and cirrhosis.

The results of the present investigation lend support to the previously mentioned assumption that both homozygous and heterozygous Pi Z patients are predisposed to the development of liver cirrhosis. Further studies are however needed in order to determine the specificity of AAT globules as a morphological marker of AAT deficiency.

I wish to thank *Annelise Petersen* and *Niels Johansen* for technical assistance.

REFERENCES

1. *Berg N O & Eriksson S* Liver disease in adults with alpha₁ antitrypsin deficiency. *New Engl J Med* 287 1264-1267 1972
2. *Blenkinsopp W K & Haffenden G P* Alpha 1 antitrypsin bodies in the liver. *J clin Path* 30 132-137 1977
3. *Blenkinsopp W K & Haffenden G P* Aetiology of cirrhosis, hepatic fibrosis and hepatocellular carcinoma. *J clin Path* 30 579-584 1977
4. *Bradfield J W B & Blenkinsopp W K* Alpha 1 antitrypsin globules in the liver and Pi M phenotype. *J clin Path* 30 464-466 1977
5. *Clausen P P* Immunohistochemical demonstration of α₁ antitrypsin in liver tissue. To be published
6. *Clausen P P & Thomsen P* Demonstration of hepatitis B surface antigen in liver biopsies. *Acta path microbiol scand Sect. A* 86 383-388 1978
7. *Cook P J L* Genetic aspects of the Pi system. *Postgrad Med J* 50 362-364 1974
8. *Eriksson S* Studies in α₁ antitrypsin deficiency. *Acta med scand Suppl* 432 177 1-85 1965
9. *Eriksson S & Hagerstrand I* Cirrhosis and malignant hepatoma in α₁ antitrypsin deficiency. *Acta med scand* 195 451-458 1974
10. *Eriksson S, Moestrup T & Hagerstrand I* Liver lung and malignant disease in heterozygous (Pi MZ) α₁ antitrypsin deficiency. *Acta med scand* 198 243-247 1975
11. *Fisher R L, Taylor L & Sherlock S* α₁ antitrypsin deficiency in liver disease. The extent of the problem. *Gastroenterology* 71 646-651 1976
12. *Jeppsson J O, Larsson C & Eriksson S* Characterization of α₁ antitrypsin in the inclusion bodies from the liver in α₁ antitrypsin deficiency. *New Engl J Med* 293 576-579 1975
13. *Kelly J K, Taylor T V & Milford Ward A* Alpha 1 antitrypsin Pi S phenotype and liver cell inclusion bodies in alcoholic hepatitis. *J clin Path* 32 706-709 1979
14. *Lindskov J, Reinicke V & Clausen P P* Pulmonary emphysema and hepatic changes in alpha 1 antitrypsin deficiency. Investigation of a family. *Ugeskr læg* 140 1551-1555 1978
15. *Morin T, Feldman G, Benhamou J P, Martin J P, Rueff B & Ropart C* Heterozygous alpha₁ antitrypsin deficiency and cirrhosis in adults: a fortuitous association. *Lancet* i 250-251 1975
16. *Reintoft I* Alpha 1 antitrypsin deficiency. *Acta path microbiol scand Sect. A* 85 649-655 1977
17. *Reintoft I* Periodic acid Schiff positive non glycolytic globules in hepatocytes. *Acta path microbiol scand Sect. A* 86 325-329 1978
18. *Reintoft I* Alpha 1 antitrypsin globules in livers from a medicolegal autopsy material. *Acta path microbiol scand Sect. A* 87 447-450 1979
19. *Sharp H L* Alpha 1 antitrypsin deficiency. *Hosp Pract* 6 83-96 1971

- 20 *Sharp, H L*. The current status of α -1-antitrypsin a protease inhibitor, in gastrointestinal disease *Gastroenterology* 70 611-621, 1976
- 21 *Sharp H L, Bridges R A, Krivit W & Freier, E F* Cirrhosis associated with alpha-1-antitrypsin deficiency A previously unrecognized inherited disorder *J Lab clin Med* 73 934-939, 1969
- 22 *Talamo R C, Langley, C E, Levine B H, Kazemi, H* Geneuc vs quantitative analysis of serum alpha₁-antitrypsin *New Engl J Med* 28 1067-1069, 1972
- 23 *Triger, D R, Milward Sadler G H, Czarkowski A A, Trowell, J & Wright R* Alpha 1 antitrypsin deficiency and liver disease in adults *Quart J Med* 45 351-372 1976

CYTOPLASMIC EFFECTS OF X-IRRADIATION ON CULTURED CELLS IN A NON-DIVIDING STAGE

4 Studies of Sparsely Grown Serum-Deprived Cells

HANS HAMBERG ULF T BRUNK JAN L E ERICSSON and BO JUNG

Departments of Pathology Radiophysics and Oncology at the University of Uppsala Uppsala Sweden

Hamberg H Brunk U T Ericsson J L E & Jung B Cytoplasmic effects of X irradiation on cultured cells in a non-dividing stage 4 Studies of sparsely grown serum-deprived cells Acta path microbiol scand Sect A 88 231-239 1980

Cultured human glial cells were blocked in interphase (G₁) by 24 h of serum starvation and subsequently subjected to 200 Gy 8 MV X radiation Immediately following irradiation the cultures were transferred to serum-containing medium Time lapse cinemicrography performed during the next 48 h showed a profuse redistribution of microtubules and microfilaments

cytoplasmic reorganization of the irradiated cells but otherwise no detectable alterations in structure or distribution of either microtubules or microfilaments It is suggested that the alteration in the arrangement of filament bundles is of importance to the impaired locomotion of the irradiated cells

Key words X-irradiation cultured human cells transmission electron microscopy cell motility microtubules microfilaments

H Hamberg Department of Pathology University of Uppsala Box 553 S 751 22 Uppsala Sweden

Received 5 x 79 Accepted 11 ii 80

Heavy X irradiation of cultured human non cycling glial cells blocked in G₁ by density dependent inhibition of cell division results within 24 h in (a) Alterations in cell shape (b) increased and structurally abnormal plasma membrane motility associated with macropinocytosis (rarely found in dense cultures) and (c) enhanced autophagocytosis with accumulation of autophagic vacuoles containing cell sap and cytoplasmic organelles in various stages of degradation (Hamberg *et al* 1976 1977 1978) The possible relation between these alterations is not clear Increased plasma membrane motility with associated internalization of the plasma membrane may serve to eliminate damaged parts of the membrane or provide membrane material for the formation of autophagic vacuoles within the cytoplasm It may also signify damage to

the motility apparatus of the cell or to the regulatory mechanisms thereof

Cell motility

(J J Langer 1970) The microtubules seem to be part of a «cytoskeletal» system responsible for the maintenance of the normal shape and polarity of cells (Porter 1966 Gail & Boone 1971) The microfilaments are believed to participate in many motile processes for example membrane ruffling pinocytosis and cell locomotion (Wessels *et al* 1973)

It appeared interesting to investigate if there were any alterations in the filamentous structures associated with the derangements of cell shape and plasma membrane motility of the irradiated cells We also wished to know if the pattern of locomotion was

disturbed in the irradiated cells since locomotion seems to be closely connected with plasma membrane motility and cell shape.

In order to study the alterations of cellular motility and locomotion in some detail it is necessary to use cultures where the cells are sparsely grown and thus not in a state of density-dependent inhibition of growth and locomotion. In order to obtain sparse cultures of cells in interphase we subjected the cultures to serum depletion which is known to result in ceased DNA synthesis and arrest in G₁ within 24 h (Lindgren *et al.* 1975, 1976).

A rewarding method for ultrastructural evaluation of the three-dimensional organization of cultured cells is the «whole cell technique» where cells are cultured on carbon/formvar-coated grids and studied by TEM after fixation and critical point drying. Another approach uses fluorescein-labelled antibodies to tubulin and actin.

MATERIAL AND METHODS

Culture Conditions and Irradiation Procedure

The experiments were performed on *in vitro* cultured human glial cells of the U 787 CG line established in culture by B. Westermarck. The Wallenberg Laboratory, Uppsala, according to the methods described by Pontén and MacIntyre (1968). Only phase II cells in early passages were utilized and culture conditions were as described earlier (Hamberg *et al.* 1976).

A cell suspension consisting of 20 000 cells/ml in Eagle's MEM (EMEM) fortified with 10% calf serum was seeded in 36 mm plastic Petri dishes, 2.5 ml in each dish. For time lapse cinematography and immunofluorescence microscopy the dishes contained round (25 mm) or square (18 mm) glass coverslips, respectively. For SEM the cells were grown on 12 × 6 × 1 mm glass slides and for TEM on carbon/formvar coated gold grids (Gershenbaum *et al.* 1974; Holoszewich and Porter 1976; Collins *et al.* 1978).

Twenty four hours after seeding, the EMEM was replaced by Ham's F10 medium with 0.1% human serum albumin (Brunk *et al.* 1977). After another 24 h the cells were exposed to 8 MV X irradiation 200 Gy at a dose rate of 17 Gy/min (Hamberg *et al.* 1976). Immediately following irradiation the serum deficient medium was replaced by F10 medium supplemented with 10% calf serum.

Time Lapse Cinematography and Phase Contrast Light Microscopy

Time lapse cinematography covered the interval between 1 and 48 h after irradiation. The filming was performed in essentially the same way as described earlier (Hamberg *et al.* 1978) although the film speed was kept low (3–10 exposures/min in the various experiments) in order to facilitate surveillance of cell movements during prolonged uninterrupted periods.

For phase contrast microscopy cells were fixed in glutaraldehyde in 0.1 M Na-cacodylate HCl buffer + 0.1 M sucrose (pH 7.2, total osmolality ~ 510 mOsm, vehicle osmolality ~ 300 mOsmol) (Collins *et al.* 1978) at 6, 12, 18, 24 and 48 h after irradiation and prepared as described earlier (Hamberg *et al.* 1978).

Electron Microscopy

For scanning electron microscopy cells were fixed in the glutaraldehyde fixative mentioned above possibly 1% OsO₄ in 0.15 M Na-cacodylate buffer for 90 min and critical point dried from CO₂ as previously described (Hamberg *et al.* 1978). For transmission electron microscopy cells growing on gold grids were harvested 24 and 48 h after irradiation, glutaraldehyde-OsO₄ fixed and critical point dried as for SEM (Collins *et al.* 1978). The grids with cells were studied in a Jeol 100 microscope with a side entrance goniometer at 100°. Stereo pair micrographs were taken at various angles to 20° depending on the magnification.

Immunofluorescence Microscopy

The cultures were fixed at the same intervals as TEM, i.e. 24 and 48 h after irradiation. The immunofluorescent technique for the staining of cytoplasmic microtubules is well established (Hamberg *et al.* 1975, 1978). The cells were fixed in prewarmed (37°C) 2% formaldehyde in PBS. The plasma membranes were made permeable to macromolecules by incubation 5 min in 0.1% Triton X 100 at room temperature. Cells were then incubated with affinity purified rabbit antibodies to tubulin and later with fluorescein isothiocyanate conjugated swine anti rabbit IgG. Between aforementioned steps the coverslips were washed in PBS and finally mounted cell side down in Elvar.

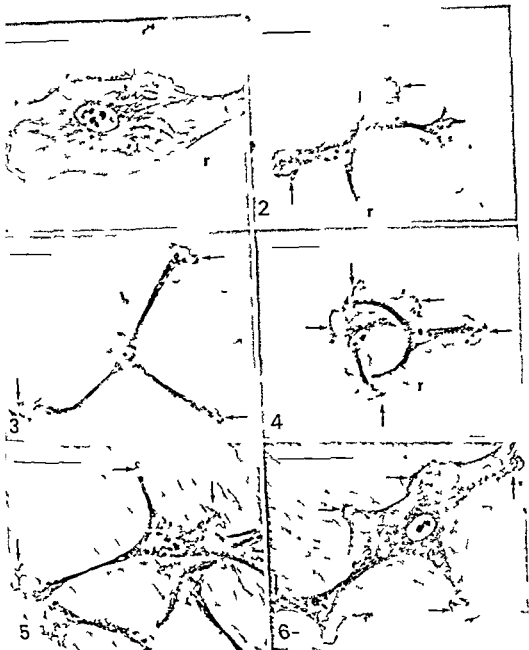
A technique taking advantage of the affinity of DAPI for actin was utilized for the visualization of filaments (Hwang and Goldberg 1976; Lindberg *et al.* 1979; Carlsson 1979). Following fixation and treatment with Triton X 100 the cells were incubated in a solution of electrophoretically purified DNase I and rabbit antibodies to DNase I and finally FITC conjugated anti rabbit IgG.

RESULTS

Phase Contrast Microscopy, Time Lapse Cinematography and SEM

Control cells. After 24 h in serum free medium the cultures consisted mainly of elongated bipolar stellate cells often with a perinuclear cluster of vacuoles. Ruffles were few and small in size. The picture was consistent with earlier reports on response of this glia cell line to serum deprivation (Schellens *et al.* 1976; Brunk *et al.* 1977).

Following the change to a medium containing 10% calf serum the perinuclear vacuoles gradually disappeared during the first 12 hours concomitant with the appearance of more numerous and larger



Figs 1-6 Sparsely growing cells fixed in glutaraldehyde 24 h after return from serum free to serum-containing growth medium. Phase contrast light microscopy. Magnification indicated by bars representing 50 μ m.

Fig 1 A control cell with a typical leading edge with ruffling lamellae (a row). Note regular cell shape and retraction (b) at the trailing end of the cell (r).

Figs 2-6 Irradiated cells with various regular configurations and multiple lamellae with ruffles (a rows). Most ruffling areas are smaller than normal and sometimes tuft-like (Fig 6). Macropinocytotic vacuoles are sometimes formed as best seen in Fig 5. Retraction fibrils are indicated (r).

disturbed in the irradiated cells, since locomotion seems to be closely connected with plasma membrane motility and cell shape

In order to study the alterations of cellular motility and locomotion in some detail, it is necessary to use cultures where the cells are sparsely grown and thus not in a state of density-dependent inhibition of growth and locomotion. In order to obtain sparse cultures of cells in interphase we subjected the cultures to serum depletion, which is known to result in ceased DNA synthesis and arrest in G_1 within 24 h (Lindgren et al 1975, 1976)

A rewarding method for ultrastructural evaluation of the three dimensional organization of cultured cells is the «whole cell technique», where cells are cultured on carbon/formvar-coated grids and studied by TEM after fixation and critical point drying. Another approach uses fluoresceinlabelled antibodies to tubulin and actin

MATERIAL AND METHODS

Culture Conditions and Irradiation Procedure

The experiments were performed on *in vitro* cultured human glial cells of the U 87 CG line established in culture by B. Westermark. The Wallenberg Laboratory Uppsala according to the methods described by Ponten and MacIntyre (1968). Only phase II cells in early passages were utilized and culture conditions were as described earlier (Hamberg et al 1976)

A cell suspension consisting of 20 000 cells/ml in Eagle's MEM (EMEM) fortified with 10% calf serum was seeded in 36 mm plastic Petri dishes, 2.5 ml in each dish. For time lapse cinemicrography and immunofluorescence microscopy the dishes contained round (25 mm) or square (18 mm) glass coverslips respectively. For SEM the cells were grown on 12 × 6 × 1 mm glass slides and for TEM on carbon/formvar coated gold grids (Gershenbaum et al 1974, Woloszewicz and Porter 1976, Collins et al 1978)

Twenty four hours after seeding the EMEM was replaced by Ham's F10 medium with 0.1% human serum albumin (Brunk et al 1977). After another 24 h the cells were exposed to 8 MV X irradiation 200 Gy at a dose rate of 17 Gy/min (Hamberg et al 1976). Immediately following irradiation the serum deficient medium was replaced by F10 medium supplemented with 10% calf serum

Time Lapse Cinemicrography and Phase Contrast Light Microscopy

Time lapse cinemicrography covered the interval between 1 and 48 h after irradiation. The filming was performed in essentially the same way as described earlier (Hamberg et al 1978) although the film speed was kept low (3–10 exposures/min in the various experiments) in order to facilitate surveillance of cell movements during prolonged uninterrupted periods

For phase contrast microscopy cells were fixed in glutaraldehyde in 0.1 M Na-cacodylate HCl buffer, 0.1 M sucrose (pH 7.2, total osmolality ~ 510 mOsm; vehicle osmolality ~ 300 mOsm) (Collins et al 1978) at 6, 12, 18, 24 and 48 h after irradiation and prep as described earlier (Hamberg et al 1978)

Electron Microscopy

For scanning electron microscopy cells were fixed in the glutaraldehyde fixative mentioned above postfixed in 1% OsO_4 in 0.15 M Na-cacodylate buffer for 90 min and critical point dried in CO_2 as previously described (Hamberg et al 1978). For transmission electron microscopy cells growing on gold grids were harvested 24 and 48 h after irradiation, glutaraldehyde fixed, postfixed in 1% OsO_4 and critical point dried as for SEM (Collins et al 1978). The grids with cells were studied in a Jeol 10 microscope with a side entrance goniometer at 100 kV. Stereo pair micrographs were taken at various angles to 20°, depending on the magnification

Immunofluorescence Microscopy

The cultures were fixed at the same intervals as for TEM, i.e. 24 and 48 h after irradiation. The immunofluorescent technique for the staining of intracellular plasmic microtubules is well established (Westermark et al 1975, 1978). The cells were fixed in prewarmed (37°C) formaldehyde in PBS. The plasma membranes were made permeable to macromolecules by incubation for 10 min in 0.1% Triton X 100 at room temperature. Cells were then incubated with affinity purified anti-rabbit IgG

PBS and finally mounted cell side down in Elvanol

A technique taking advantage of the affinity of DAPI for actin was utilized for the visualization of filaments (Wang and Goldberg 1976, Lindberg et al 1979, Carlsson 1979). Following fixation and treatment with PBS, cells were incubated in a solution of DAPI

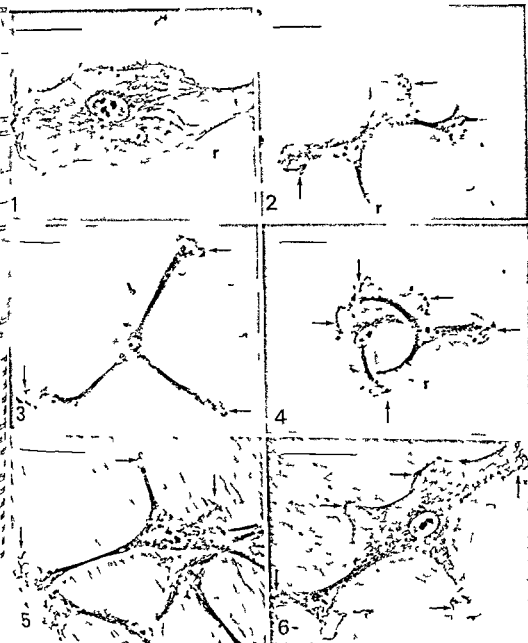
anti rabbit IgG

RESULTS

Phase Contrast Microscopy, Time Lapse Cinemicrography and SEM

Control cells. After 24 h in serum free medium the cultures consisted mainly of elongated bipolar stellate cells often with a perinuclear cluster of vacuoles. Ruffles were few and small in size. The picture was consistent with earlier reports on response of this glia cell line to serum deprivation (Schellens et al 1976, Brunk et al 1977)

Following the change to a medium containing 10% calf serum the perinuclear vacuoles gradually disappeared during the first 12 hours concomitant with the appearance of more numerous and larger



Figs 1-6 Sparsely growing cells fixed in glutaraldehyde 24 h after return from serum free to serum-containing growth medium. Phase contrast light microscopy. Magnification indicated by bars representing 50 μ m.

Fig 1 A control cell with a typical leading edge with ruffling lamellae (arrow). Note regular cell shape and retraction fibers at the trailing end of the cell (r).

Figs 2-6 Irradiated cells with variable irregular configurations and multiple lamellae with ruffles (arrows). Most ruffling areas are smaller than normal and sometimes tuft-like (Fig 6). Macropinocytotic vacuoles are sometimes formed, as best seen in Fig 5. Retraction fibers are indicated (r).

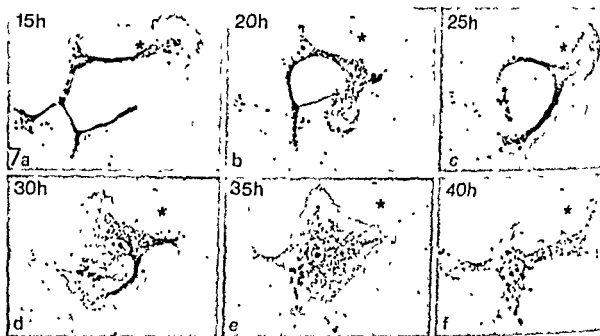


Fig 7 Time-lapse sequence (a-f) showing an irradiated cell changing shape without the formation of a definite leading edge. The cell shows almost no net locomotion as seen by comparing the position of the nucleus in relation to indicated fixed point (*) on the coverslip. Time in hours after irradiation is indicated in the top left hand corner.

ruffles at the cell borders and with diminution of the slender cytoplasmic extrusions. At 24 h, and even more so at 48 h, most of the control cells had regained an almost normal cell shape with a well defined leading lamella and a broad, fan-shaped ruffling area with associated intermittent macropinocytosis, and often with retraction fibrils at the end of the cell opposite the leading lamella (Fig 1). Cell locomotion followed a normal pattern with considerable net movement during the observation period (Pontén *et al* 1969).

Irradiated cells During the first 12 h after irradiation and return to a serum-containing medium, the irradiated cells appeared to resume ruffling activity in a manner similar to control cells. From that time on, however, it became evident that the irradiated cells failed to regain the orderly cell polarization and movement characteristic of controls. Instead they became increasingly ramified with broad or slender extrusions and multiple, small, often tuft-like ruffles occurring simultaneously at different parts of the cell border (Figs 2-6).

Best revealed by time-lapse cinematography, the

irradiated cells sometimes formed one dominant broad lamella with a ruffling area, on a par with controls regaining normal polarity and locomotion. However, this orderly orientation did not persist in the irradiated cells, and the morphology showed

of the central cell body with its nucleus (Fig 11).

Whole Cell TEM

Control cells The fine structure of the control cells 24 and 48 hours after return to serum-containing medium did not differ from early findings regarding proliferating cells of this cell line (Collins *et al* 1978, 1979). Thus the cells often displayed a wide leading lamella with a thin lamellopodium forming a broad ruffling area with occasional associated macropinocytotic vacuoles (Fig 8). The leading lamella contained microfilaments some of which were arranged in bundles oriented in the direction of movement of the cell (Fig 10). Microfilament bundles were also seen

Fig 8 Peripheral area of control cell growing on carbon/formvar coated gold grid and studied at 100 kV by TEM after fixation and CPD 48 h after return to serum-containing medium. A ruffling area is depicted. No macropinocytotic vacuoles emerging behind the ruffle (v). Many slender, sometimes branched mitochondria (m) are revealed. Bar = 5 µm.

Fig 9 Electron micrograph of a peripheral part of a cell 48 h after irradiation and change to serum-containing medium. Many large lysosomes (ly) surround the nucleus (outside the depicted area). Small, tuft-like, rudimentary ruffles with associated long microspikes are indicated by arrows. Bar = 3 µm.



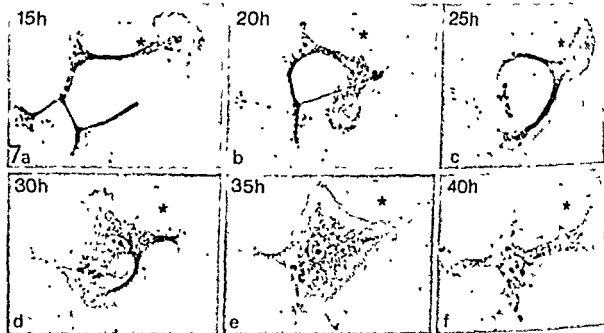


Fig 7 Time-lapse sequence (a-f) showing an irradiated cell changing shape without the formation of a definite leading edge. The cell shows almost no net locomotion as seen by comparing the position of the nucleus in relation to the indicated fixed point (*) on the coverslip. Time in hours after irradiation is indicated in the top left hand corner.

ruffles at the cell borders and with diminution of the slender cytoplasmic extrusions. At 24 h, and even more so at 48 h, most of the control cells had regained an almost normal cell shape with a well defined leading lamella and a broad, fan-shaped ruffling area with associated intermittent macropinocytosis, and often with retraction fibrils at the end of the cell opposite the leading lamella (Fig 1). Cell locomotion followed a normal pattern with considerable net movement during the observation period (Pontén *et al* 1969).

Irradiated cells During the first 12 h after irradiation and return to a serum-containing medium, the irradiated cells appeared to resume ruffling activity in a manner similar to control cells. From that time on, however, it became evident that the irradiated cells failed to regain the orderly cell polarization and movement characteristic of controls. Instead they became increasingly ramified with broad or slender extrusions and multiple, small, often tuft-like, ruffles occurring simultaneously at different parts of the cell border (Figs 2-6).

Best revealed by time-lapse cinematography, the

irradiated cells sometimes formed one dominant broad lamella with a ruffling area, on a par with controls regaining normal polarity and locomotion. However, this orderly orientation did not persist in the irradiated cells, and the morphology showed continuing gross alterations. Thus the ruffling area tended to occur at different parts of the cell border and there was usually no significant net movement of the central cell body with its nucleus (Fig 7).

Whole Cell TEM

Control cells The fine structure of the control cells 24 and 48 hours after return to serum-containing medium did not differ from earlier findings regarding proliferating cells of this cell line (Collins *et al* 1978, 1979). Thus the cells often displayed a wide leading lamella with a thin lamellopodium forming a broad ruffling area with occasional associated macropinocytotic vacuoles (Fig 8). The leading lamella contained microfilaments some of which were arranged in bundles oriented in the direction of movement of the cell (Fig 10). Microfilament bundles were also seen

Fig 8 Peripheral area of control cell growing on carbon/formvar-coated gold grid and studied at 100 kV by TEM after fixation and CPD 48 h after return to serum containing medium. A ruffling area is depicted. Not macropinocytotic vacuoles emerging behind the ruffle (v). Many slender sometimes branched mitochondria (m) are revealed. Bar = 5 μ m.

Fig 9 Electron micrograph of a peripheral part of a cell 48 h after irradiation and change to serum-containing medium. Small, tuft-like rudimentary





Fig 10 Control cell 48 h after reversal of serum starvation. Part of leading lamella with bundles of microfilaments (large arrows) and numerous microtubules (small arrows) but no other organelles. Bar = 2 μ m.

Fig 11 Peripheral part of a cell 48 h after irradiation. Microfilament bundles (large arrows) and microtubules (small arrows) are well preserved and show no detectable alterations as compared with the controls. There are several membrane veils or small ruffles along the cell border. Note the presence of numerous coated vesicles (cv). Bar = 3 μ m.

adjacent and parallel to the cell borders except at the foremost end of the leading lamella and were numerous in the retraction fibrils found at the trailing end of the cell. A great number of microtubules with no discernible pattern of organization were also present in the leading lamella (Fig 110). The lamellipodia contained no organelles or

more numerous in the perinuclear area (not accessible to detailed studies by reason of its thickness) (Fig 8).

Irradiated cells The fine structure of the irradiated cells was difficult to study in the central parts of the cells and the slender extrusions where the cell body seemed to be condensed and impenetrable. However the thin flattened lamellar areas at the end of the extrusions or elsewhere on the cell periphery were seen to contain microtubules and microfilaments which in structure and arrangement resembled the observations in the control cells (Figs 9 and 11). The light and scanning electron microscopy findings of small undeveloped and irregular ruffles were confirmed

rot.
ruffles of some malignant glioma cell lines (Collins *et al* 1979). Many small vesicles were demonstrated (Fig 11) and at 48 h after irradiation large vacuolated lysosomes abounded in the central parts of the cells (Fig 9).

Immunofluorescence Microscopy

The pattern of fluorescent antibody stained microtubules in the non irradiated glial cells showed no major divergences from other interphase cells (Weber 1976, Brinkley *et al* 1976). The cells contained an elaborate array of abundant straight or curved microtubules which were often arranged in a radiating fashion around the nucleus and terminating close to the cell border.

Furthermore the fluorescence pattern obtained with the DNase antibody system resembled that

resulting from the use of actin antibodies on other tissue culture cells (Lazarides 1975, Goldman *et al* 1975). The fluorescence in the glial cells was largely diffuse and most intense in the perinuclear region with a few thin elongated filaments arranged mainly along the line of movement of the cell. A speckled rather intense fluorescence was also observed immediately associated with the ruffling membranes. A detailed report on the microfilamentous system in the glial cells will be published elsewhere (Hoglund *et al*).

While the control cells contained filament bundles arranged mainly along the direction of movement of the cells the irradiated ones displayed stainable filaments and microtubules along the longitudinal axes of practically all the asymmetric cellular processes. In the flattened lamellar parts of

the cell - such as -
compared with controls

DISCUSSION

The effects of irradiation on the serum deprived sparsely grown glial cells may not be directly comparable with the results of our previous studies utilizing density-dependent growth inhibited cells because the radiosensitivity may differ. However serum depletion appears to be the best method available to block a sparse culture of cells in G₁ during irradiation. By so doing the sensitive replication phase is avoided and yet the block can be reverted after irradiation allowing study on any induced disturbance in cell movement and locomotion. Furthermore the whole cell TEM and the immunofluorescent techniques do not lend themselves to observation of densely grown and partly overlapping cells.

Following stimulation with calf serum the irradiated cells started ruffling of the peripheral parts of the plasma membrane in much the same way as the controls. No definite polarization and coordinated locomotion ensued however. Instead ruffling was distributed in small areas all round the cell periphery and peripheral lamellar areas at



- Lindgren A, Westermarck B & Ponten J Serum stimulation of stationary human glia and glioma cells in culture. *Exptl Cell Res* 95 311-319 1975
- Lindgren A & Westermarck B Subdivision of the G₁ phase of human glia cells in culture. *Exptl Cell Res* 99 357-362 1976
- Monen J & MacIntyre E H Long term culture of normal and neoplastic human glia. *Acta path microbiol scand* 74 465-486 1968
- Ponten J, Westermarck B & Hugosson R Regulation of proliferation and movement of human glia like cells in culture. *Exptl Cell Res* 58 393-400 1969
- Porter K R Cytoplasmic microtubules and their functions. In Wolstenholme G E W & O'Connor M (Eds) *Principles of biomolecular organization*. Ciba Foundation Symposium 308-345 Churchill London 1966
- Porter K R Motility in cells. In Goldman R, Pollard T & Rosenbaum J (Eds) *Cell motility*. Cold Spring Harbor Conferences on cell proliferation vol 3 1-23 1976
- Schellens J P M, Brunk U T & Lindgren A Influence of serum on ruffling activity, pinocytosis and proliferation of in vitro cultivated human glia cells. *Cytobiologie* 13 93-106 1976
- Wang E & Goldberg A R Changes in microfilament organization and surface topography upon transfection of chick embryo fibroblasts with Rous sarcoma virus. *Proc Natl Acad Sci USA* 73 4065-4069 1976
- Weber K, Bibring T & Osborn M Specific visualization of tubulin containing structures in tissue culture cells by immunofluorescence. *Exptl Cell Res* 95 111-120 1975
- Weber K Visualization of tubulin containing structures by immunofluorescence microscopy. Cytoplasmic microtubules, mitotic figures and Vinblastine induced paracrystals. In Goldman R, Pollard T & Rosenbaum J (Eds) *Cell Motility*. Cold Spring Harbor Conferences on cell proliferation vol 3 403-417 1976
- Weber K, Rathke P C & Osborn M Cytoplasmic microtubular images in glutaraldehyde fixed tissue culture cells by electron microscopy and by immunofluorescence microscopy. *Proc Natl Acad Sci USA* 75 1820-1824 1978
- Wessels N K, Spooner B S & Luduena M A Surface movements, microfilaments and cell locomotion. In *Locomotion of Tissue Cells*. Ciba Foundation Symposium vol 14 53-77 Associated Scientific Publishers Amsterdam 1973

different ends of the cells became dominant one after the other, but only briefly and without resultant significant net movement of the cells. This disturbed locomotor activity resembles the effects of colchicine/colcemid on cultured cells (Goldman 1971, Gail and Boone 1971) but in contrast to colchicine treated cells the irradiated glial cells retained their asymmetry. The studies on phagokinetic tracks of 3T3 cells by Albrecht-Buehler (1977) has revealed that the main actin-containing bundles parallel the direction of migration of cultured cells on their substratum. In the irradiated glial cells filament bundles projected into several cytoplasmic extrusions mostly without any dominating direction. It seems possible that this alteration in the arrangement of filament bundles is of importance to the impaired locomotion of the irradiated cells. The peripheral lamellar parts of the irradiated cells displayed no obvious alterations in the structure or distribution of neither microtubules nor microfilaments. However, the possibility of damage to microtubules and/or microfilaments at a level not perceptible by the methods used remains. Furthermore, irradiation may have an adverse effect on the regulatory systems of cell movement and locomotion. The possible implications of the altered cell motility on plasma membrane turnover remain obscure.

Immunofluorescence stainings were performed by R. Karlsson, the CEMO group, the Wallenberg Laboratory, University of Uppsala, Uppsala, Sweden.

Supported by grants from the Swedish Medical Research Council.

REFERENCES

- Albrecht-Buehler G. Phagokinetic tracks of 3T3 cells. Parallels between the orientation of track segments and of cellular structures which contain actin or tubulin. *Cell* 12 333-339 1977.
- Allison A C. The role of microfilaments and microtubules in cell movement: endocytosis and exocytosis. In *Locomotion of Tissue Cells*. Ciba Foundation Symposium vol 14 109-143. Associated Scientific Publishers, Amsterdam 1973.
- Brinkley B R, Fuller G M & Highfield D P. Tubulin antibodies as probes for microtubules in dividing and nondividing mammalian cells. In *Goldman R, Pollard T & Rosenbaum J* (Eds.) *Cell Motility*. Cold Spring Harbor conferences on cell proliferation vol 3 435-456 1976.
- Brunk U T, Schellens J P M, Westermark B & Collins V P. Effect of serum deprivation on Carlsson L. Thesis. Acta Universitatis Upsalensis (Abstracts of Uppsala dissertations from the Faculty of Science) 1979.
- Collins V P, Arborgh B & Brunk U. A comparison of the effects of three widely used glutaraldehyde fixatives on cellular volume and structure. *Acta path microbiol scand Sect A* 85 157-168 1977.
- Collins V P, Brunk U T, Fredriksson B & Westermark B. The fine structure of growing and non growing whole glia cell preparations. *Cytobiologie* 18 327-338 1978.
- Collins V P, Brunk U T, Fredriksson B & Westermark B. The fine structure of growing human glia and glioma cells. *Acta path microbiol scand Sect A* 87 29-36 1979.
- Gail M H & Boone C W. Effect of colchicine on fibroblast motility. *Exptl Cell Res* 65 221-227 1971.
- Gershenbaum M R, Shay J W & Porter K R. Effects of cytochalasin B on BALB/3T3 mammalian cells cultured *in vitro* as observed by scanning high voltage electron microscopy. In *O Johari* (Ed) *Scanning electron microscopy* vol 3 589-596. Research Institute, Chicago 1974.
- Goldman R D. The role of three cytoplasmic fibers: BHK-21 cell motility. I. Microtubules and effects of colchicine. *J Cell Biol* 51 752-762 1974.
- Goldman R D, Laarides E, Pollard R & Weber. The use of actin antibody in the localization of actin within the microfilament bundles of mouse cells. *Exptl Cell Res* 90 333-344 1975.
- Hamberg H, Brunk U T, Ericsson J L E & Jung. Cytoplasmic effects of X irradiation on cultured cells in a nondividing stage. I. Establishment of experimental model. *Acta path microbiol scand Sect A* 84 201-214 1976.
- Hamberg H, Brunk U T, Ericsson J L E & Jung. Cytoplasmic effects of X irradiation on cultured cells in a nondividing stage. II. Alterations in lysosomal plasma membrane, Golgi apparatus and related structures. *Acta path microbiol scand Sect A* 625-639 1977.
- Hamberg H, Brunk U T, Ericsson J L E & Jung. Cytoplasmic effects of X irradiation on cultured cells in a nondividing stage. III. Alterations in plasma membrane motility. *Acta path microbiol scand Sect A* 86 487-494 1978.
- Hoglund A S, Karlsson R, Arvo E, Fredriksson A & Lindberg U. Visualization of the peripheral weave of microfilaments in glia cells. Submitted to *Muscle Research and Cell Motility*.
- Laarides E. Immunofluorescence studies on the structure of actin filaments in tissue culture cells. *Histochem J* 23 507-528 1975.
- Lindberg U, Carlsson L, Markey F & Nyström L. The unpolymerized form of actin in non muscle cells. In *G Gabbiani* (Ed) *Methods and Achievements in Experimental Pathology* vol 8. Cytoskeleton in normal and pathologic processes. Karger, Basel 1976.

AUTOLOGOUS IMMUNE COMPLEX NEPHRITIS AND DOCA- NaCl LOAD A NEW MODEL OF HYPERTENSION

ILKKA TIKKANEN FREJ FYHRQUIST AARO MIETTINEN and TOM TÖRNROTH

The Minerva Institute for Medical Research Department of Bacteriology and Immunology University of Helsinki and IVth Department of Medicine Helsinki University Central Hospital Helsinki Finland

Tikkanen I Fyhrquist F Miettinen A & Tornroth T Autologous immune complex nephritis and DOCA NaCl load a new model of hypertension Acta path microbiol scand Sect. A 88 241-250 1980

In order to explore immunological features of hypertension we studied autologous immune complex nephritis (Heymann nephritis) combined with DOCA NaCl treatment This combination resulted in hypertension and increased heart weight whereas DOCA NaCl treatment alone induced only a slight elevation of blood pressure and a moderate increase in heart weight Nephritic rats without DOCA NaCl load remained normotensive their heart weights being comparable to those of controls This new model of hypertension was neither characterized by azotemia nor by reduced renal excretory capacity Hypertension was not renin angiotensin-dependent DOCA NaCl treatment accelerated the development of proteinuria In the hypertensive rats systolic blood pressure correlated to daily urinary protein excretion Renal histopathology revealed changes resembling those of malignant nephrosclerosis Immunohistology and electron microscopy showed a typical membranous glomerulonephritis in all immunized animals It was concluded that immune complex disease of the Heymann nephritis type may interfere with normal hemodynamic adaptation to hypervolemic sodium load resulting in hypertension

Key words Hypertension nephritis DOCA NaCl immune complexes rat

Ilkka Tikkanen Minerva Institute for Medical Research P O Box 819 SF-00101 Helsinki 10 Finland

Received 3 xii 79 Accepted 15 ii 80

The involvement of immunological mechanisms in hypertension has been suggested by several authors (for references see 22-25) In experimental animals gamma globulin deposits have been found in vascular lesions caused by deoxycorticosterone NaCl (DOCA NaCl) hypertension (30) and hypertension following partial renal infarction (Loomis type) in which autoantibodies against arterial wall and kidney tissue were detected as well (37) Hypertensive arterial damage is accompanied by an inflammatory cellular reaction regardless of the experimental model used (7-33) This reaction seems to be thymus-dependent in DOCA NaCl and mice (33) The thymus was

not however important for the development and early phases of hypertension

The severity of lesions in serum sickness is increased by hypertension (38) Hypertension may be associated with the development of arteritis (7, 28) On the other hand NZB mice with spontaneous immune complex disease get hypertension which can be ameliorated by immunosuppression (32) We therefore studied the effect of a chronic immune complex disease on the development of hypertension Autologous immune complex glomerulonephritis

treatment in female Wistar rats

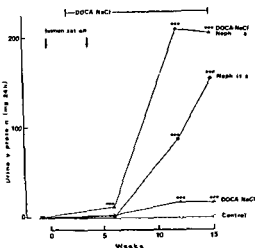


Fig 2 Onset and severity of proteinuria in different experimental groups * $p < 0.05$ ** $p < 0.01$ *** $p < 0.001$ compared with controls

proteinuria in the DOCA NaCl nephritis group at the end of the experiment ($r = 0.82$, $p < 0.01$). Serum protein was slightly decreased in the DOCA-NaCl nephritis group (Table 1). α -Globulins increased slightly while β - and γ globulins decreased in both nephritic groups. Serum albumin concentration did not decrease. Ascites or edema were not observed.

Creatinine clearance and renal handling of electrolytes None of the immunized rats became azotemic, whether treated with DOCA NaCl or not (Table 1). No differences were observed in weight gain, urine volumes, urinary sodium and potassium excretion and the sodium/potassium ratio (Table 2) and serum sodium and potassium concentrations (Table 1) between the hypertensive DOCA NaCl-nephritis and the non hypertensive DOCA NaCl groups. Both increased their urine output 6 fold, urinary sodium/potassium ratio 10 fold and sodium excretion up to 20 fold compared with the control animals.

Plasma renin activity and serum osmolality (Table 1). PRA was clearly suppressed in both groups treated with DOCA NaCl. Serum osmolality values did not differ.

Histological findings All immunized animals had membranous glomerulonephritis visible in PASM-stained paraffin sections, as either/ both a diffuse vacuolization (36) or/and diffuse projections of the glomerular basement membrane (Table 3). Proliferative sclerotic glomerular changes were present in the DOCA NaCl nephritis group, resembling the picture of malignant nephrosclerosis (Fig. 3).

TABLE 1 Heart Weight and Analytical Findings at the End of Experiment (Mean \pm SD)

	Control (n = 11)	Nephritis (n = 11)	DOCA NaCl (n = 11)	DOCA NaCl nephritis (n = 10)
Heart weight/body weight (mg/g)	3.03 \pm 0.23	3.15 \pm 0.23	3.65 \pm 0.22**	3.98 \pm 0.29* ⁺
Hematocrit (%)	47.4 \pm 2.4	46.1 \pm 2.7	46.1 \pm 2.9	44.7 \pm 3.8*
Serum proteins (g/l)	70.5 \pm 1.7	68.8 \pm 3.9	68.4 \pm 3.0	63.5 \pm 10.3*
albumin	44.2 \pm 1.9	48.3 \pm 3.9**	45.1 \pm 2.7	44.9 \pm 7.0
α globulin	5.1 \pm 1.0	6.8 \pm 1.7**	5.7 \pm 1.2	7.6 \pm 2.8*
β globulin	12.6 \pm 2.8	9.1 \pm 2.7**	11.3 \pm 1.9	7.7 \pm 3.1* ⁺
γ globulin	7.6 \pm 1.1	4.1 \pm 1.9***	6.0 \pm 1.6	3.6 \pm 2.4**
Serum sodium (mmol/l)	143 \pm 2.9	141 \pm 3.9	145 \pm 0.9*	144 \pm 5.1
Serum potassium (mmol/l)	5.0 \pm 0.4	5.2 \pm 0.6	4.0 \pm 0.5***	4.2 \pm 0.3***
Creatinine clearance (ml/min)	0.95 \pm 0.30	1.17 \pm 0.24	1.69 \pm 0.30***	1.49 \pm 0.26***
Plasma renin activity (ng/ml/h)	14.2 \pm 6.9	11.2 \pm 8.6	0.04 \pm 0.12***	0***†
Serum osmolality (mosmol/kg)	297 \pm 11	294 \pm 14	291 \pm 15	285 \pm 16

* $p < 0.05$ ** $p < 0.01$ *** $p < 0.001$ compared with controls

† $p < 0.05$ + $p < 0.01$ DOCA NaCl nephritis compared with DOCA NaCl

‡ below limit of assay sensitivity

MATERIAL AND METHODS

General design 44 female Wistar rats (Animark Helsinki, Finland) weighing about 180 g were divided into 4 equal groups. 1) Control animals received only sham injections and immunizations. 2) Nephritis group immunized (see below) to induce autologous immune complex nephritis. 3) DOCA-NaCl group received weekly DOCA (Percorten M Ciba 30 mg/kg s.c.) injections and 0.9% NaCl solution as the only drink. 4) DOCA-NaCl nephritis group with a combination of DOCA-NaCl treatment and nephritis.

DOCA-NaCl regimen was started 2 weeks after the first immunization. At 16 weeks blood was collected from abdominal aorta under ether anesthesia. Hematocrit was determined. EDTA plasma 6 g of Na₂EDTA/liter of blood and serum were separated by centrifugation and stored at -20 °C until assayed.

Induction of autologous immune complex nephritis A brush border (BB) membrane fraction was isolated from kidney cortices of Sprague Dawley rats as described (26). Each rat received 2 injections of BB antigen mixed with equal amounts of Freund's complete adjuvant (Difco Laboratories, Detroit, USA) containing 5 mg of Mycobacterium tuberculosis H 37 Ra (Difco) per ml. At the first immunization 0.4 ml of antigen emulsion with 200 µg of BB protein was given into foot pads and 25 µl of pertussis vaccine (Per Vaccin Orion Pharmaceuticals, Helsinki, Finland) containing 22 × 10⁶ killed Hemophilus pertussis bacteria/ml was injected into the dorsum of each foot (21). 4 weeks later BB antigen emulsion was given subcutaneously without pertussis vaccine. This immunization schedule results in the development of autologous immune complex nephritis within 2 months (27).

Blood pressure recordings Systolic blood pressure was measured at regular intervals in conscious animals by a tail cuff (Harvard Apparatus Co, Massachusetts, USA) method using a Doppler ultrasonic flowmeter (Parks Electronics Lab, Beaverton, USA) to detect the pulse (6). The tail was first warmed for 10 min at 37 °C.

Analytical methods Urinary protein output was measured from 18 h samples collected individually by the method of Lowry *et al.* (24) after trichloroacetic acid precipitation. Total serum proteins were determined by the Biuret method, analyzed electrophoretically on cellulose acetate membranes and the concentrations of albumin, α, β and γ globulins were calculated densitometrically (Hefena autoscanner, Helena Lab, Beaumont, TX).

concentrations were measured by a modification (19) of the kinetic creatinine assay (Merckotest 3384, Merck). Serum osmolality was determined by a vapor pressure osmometer (Wescor Inc, Logan, USA). Plasma renin activity (PRA) was determined by radioimmunoassay (11) modified for rat plasma using 50 mM hydroxyquinoline as enzyme inhibitor and pH 6.5 during the

paraffin. Sections 2-3 µ thick were stained with hematoxylin and eosin (H&E), periodic acid Schiff (PAS), periodic acid silver methenamine (PASM) and Masson's trichrome.

Immunofluorescence (IFL) studies 5 µ cryostat sections of the snap frozen kidney and heart samples were fixed for 10 min in -20 °C acetone and washed in phosphate buffered saline (PBS) pH 7.2. For direct IFL cryostat sections were reacted with fluorescein isothiocyanate (FITC)-conjugated antisera for 30 min, washed in PBS for 10 min and mounted in buffered glycerol. Serum BB autoantibodies were determined by an indirect IFL technique. For this 5 µ cryostat sections of normal rat kidney were reacted with rat sera diluted 1/2 and 1/4 in PBS for 30 min, washed in PBS for 10 min, reacted with FITC conjugated anti rat IgG for 30 min and after a final wash mounted in glycerol. The stained sections were studied with a Zeiss standard microscope (23). The F/p ratios of the FITC conjugated rabbit anti rat IgG β₂C/C₃, fibrinogen and albumin (Nordic Immunological Lab, Tilburg, The Netherlands) were 2.3, 1.7, 1.1 and 1.5 and the protein contents of the dilutions used were 0.5 mg/ml, 2.3 mg/ml, 0.7 mg/ml and 0.4 mg/ml respectively.

Electron microscopy Specimens from 5 rats (one from group 2 and 2 from groups 2 and 4) were processed for electron microscopic study (35). Two glomeruli from each of the 5 rats were examined.

Statistics The significance of the differences between mean values was evaluated by Student's t test preceded by logarithmic transformation when values showed skewed distribution.

RESULTS

Blood pressure Only rats with both nephritis and DOCA-NaCl treatment became hypertensive (Fig. 1). DOCA-NaCl alone induced only a slight increase in blood pressure. Nephritic rats without DOCA

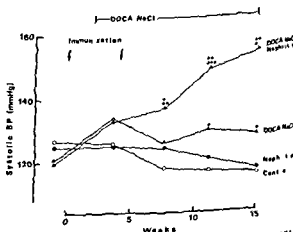


Fig. 1 Systolic blood pressure during the experiment. * $p < 0.05$, ** $p < 0.01$, *** $p < 0.001$ compared with control; + $p < 0.05$, ++ $p < 0.01$ DOCA-NaCl nephritis compared with DOCA-NaCl.

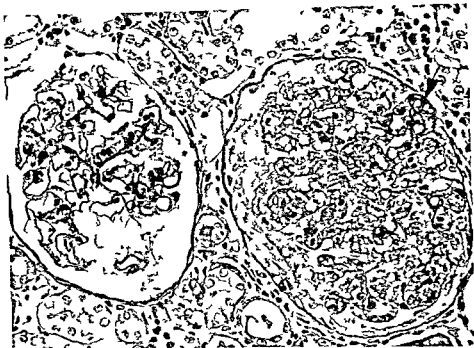


Fig 3 An almost normal glomerulus and a glomerulus with extensive proliferative sclerotic changes including hyaline subendothelial or intraluminal deposits (arrow). From DOCA NaCl nephritis group. PAS stain, $\times 310$.

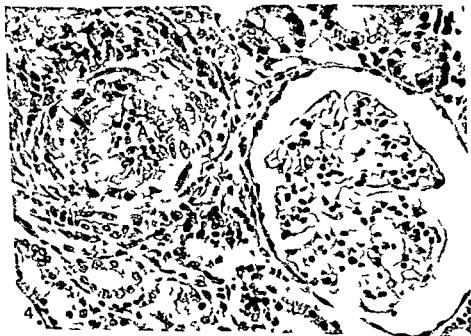


Fig 4 An intralobular artery (A) with marked thickening of the wall, fibrinoid necrosis (arrow), and inflammatory cell infiltration of the wall. The glomerulus appears normal at this magnification. From DOCA NaCl nephritis group. H&E stain, $\times 320$.

TABLE 2 *Body Weight and Urine Electrolytes during the Experiment (Mean \pm SD)*

	Time (weeks)	Control (n = 11)	Nephritis (n = 11)	DOCA-NaCl (n = 11)	DOCA-NaCl nephritis (n = 11)
Body weight (g)	0	236 \pm 8.2	237 \pm 13	241 \pm 7.8	238 \pm 11
	6	289 \pm 11	276 \pm 14*	287 \pm 17	288 \pm 18
	12	293 \pm 8.7	293 \pm 14	303 \pm 16	302 \pm 18
	15	303 \pm 12	298 \pm 18	308 \pm 18	307 \pm 21
Urine volumes (ml/24 h)	0	6.6 \pm 2.6	5.2 \pm 2.9	7.4 \pm 4.2	6.3 \pm 3.6
	6	10.1 \pm 4.8	10.8 \pm 5.7	27.5 \pm 13***	27.9 \pm 7.8***
	12	9.3 \pm 4.8	10.4 \pm 4.4	50.9 \pm 28***	45.3 \pm 13***
	15	10.5 \pm 9.0	14.3 \pm 10	63.9 \pm 28***	64.8 \pm 22***†
Sodium excretion (mmol/24 h)	0	0.34 \pm 0.10	0.30 \pm 0.14	0.43 \pm 0.19	0.46 \pm 0.21
	6	0.47 \pm 0.17	0.43 \pm 0.21	3.69 \pm 2.0***	3.75 \pm 1.1***
	12	0.36 \pm 0.15	0.39 \pm 0.12	8.56 \pm 5.0***	6.91 \pm 1.9***
	15	0.42 \pm 0.20	0.27 \pm 0.10*	8.63 \pm 3.4***	9.27 \pm 3.9***†
Potassium excretion (mmol/24 h)	0	0.89 \pm 0.24	0.75 \pm 0.22	0.79 \pm 0.27	0.91 \pm 0.21
	6	0.79 \pm 0.16	0.82 \pm 0.19	0.77 \pm 0.20	0.72 \pm 0.20
	12	0.63 \pm 0.21	0.72 \pm 0.24	1.21 \pm 0.50**	1.28 \pm 0.42**
	15	0.57 \pm 0.31	0.61 \pm 0.16	0.98 \pm 0.29**	1.28 \pm 0.59***†
Urine sodium/potassium	0	0.38 \pm 0.18	0.45 \pm 0.24	0.59 \pm 0.25	0.49 \pm 0.13
	6	0.58 \pm 0.14	0.55 \pm 0.30	4.63 \pm 1.7***	5.29 \pm 1.9***
	12	0.63 \pm 0.32	0.57 \pm 0.22	6.76 \pm 1.7***	5.73 \pm 1.8***
	15	0.83 \pm 0.32	0.47 \pm 0.17**	8.75 \pm 2.8***	7.82 \pm 3.0***†

* $p < 0.05$, ** $p < 0.01$, *** $p < 0.001$ compared with controls, † $n = 10$

DOCA-NaCl-nephritis compared with DOCA-NaCl; all differences non significant

However, only 2 rats had vascular changes, which also affected arteries larger than arterioles (Fig. 4). One rat in the DOCA-NaCl group had similar but milder glomerulosclerotic changes. It is noteworthy that all rats with these proliferative-sclerotic lesions had both heavy proteinuria and high blood pressure. Tubulo-interstitial changes, mostly degenerative and inflammatory, seemed to reflect the severity of the glomerular disease.

(Fig. 5) C_3 deposited in a similar way was seen in 20% of the rats. Granular, often focal and segmental glomerular deposits of albumin were frequently seen. Tubular cytoplasmic and luminal albumin, IgG and C_3 were seen in most immunized animals. No systematic differences were seen.

TABLE 3 *Histopathological Changes in the Kidneys*

	Control (n = 11)	Nephritis (n = 11)	DOCA-NaCl (n = 11)	DOCA-NaCl nephritis (n = 11)
Membranous glomerulonephritis	—	11	—	11
Proliferative sclerotic glomerular changes	—	—	1	5
Tubulo-interstitial changes	—	2	1	6
Vascular changes	—	—	—	2



Fig 3 An almost normal glomerulus and a glomerulus with extensive proliferative sclerotic changes including hyaline subendothelial or intraluminal deposits (arrow) From DOCA NaCl nephritis group PAS stain $\times 310$

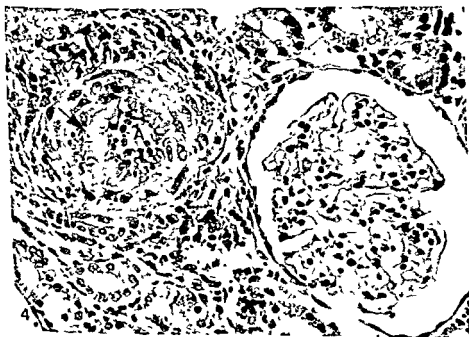


Fig 4 An intralobular artery (A) with marked thickening fibrinoid necrosis (arrow) and inflammatory cell infiltration of the wall The glomerulus appears normal at this magnification From DOCA NaCl nephritis group H&E stain, $\times 320$

5

Fig 5 Immunofluorescence micrograph showing granular deposits of IgG along glomerular capillary walls of kidney of a rat immunized with the brush border antigen and treated with DOCA NaCl. Staining with conjugated anti rat IgG $\times 1300$

TABLE 4 Immunohistological Findings in the Kidneys and Serum Brush Border (BB) Autoantibodies at the Experiment

		Control (n = 11)	Nephritis (n = 11)	DOCA NaCl (n = 11)	DOCA NaCl nephritis (n = 10)
<i>Glomeruli</i>					
Granular deposits of IgG along the capillary walls		—	11	—	10
Granular deposits of C ₃ along the capillary walls		—	2	—	2
<i>Tubuli</i>					
IgG	Lumen/BB	—	7	—	6
	Cytoplasm	—	6	—	5
C ₃	Lumen/BB	—	8	1	6
	Cytoplasm	—	4	—	2
Fibrinogen	Lumen/BB	—	5	—	7
	Cytoplasm	—	2	—	2
Albumin	Lumen/BB	—	4	—	3
	Cytoplasm	—	7	2	6
<i>Serum</i>					
Brush border antibodies		—	10	—	8



Fig. 6. Electron micrograph of glomerular capillary showing multiple subepithelial electron-dense deposits (arrows) characteristic of membranous glomerulonephritis. The DOCA NaCl nephritis group. V: epithelial vesicles; LU: capillary lumen; US: urinary space. $\times 6000$.

between nephritic rats treated or untreated with DOCA NaCl. In non-immunized rats only irregular mainly mesangial deposits of IgG were seen. We found no deposits of IgG or C₃ in the arterioles of the kidneys of any rat. At the end of the experiment brush border autoantibodies were present in the sera of 18 of the 21 immunized rats (Table 4).

Electron microscopic studies. The four rats from groups 2 and 4 showed multiple subepithelial or intramembranous electron dense deposits corresponding to phase B and phase C membranous glomerulonephritis (36) (Fig. 6). No ultrastructural differences were noted between the two groups. In addition these rats showed huge blebs or vesicles within the cytoplasm of glomerular visceral epithelial cells (Fig. 6). The significance of these vesicles which have been described previously in NN-diacetyl benzidine induced nephrosis (9) is as yet unknown.

DISCUSSION

Hypertension developed only in rats with both immune complex nephritis and DOCA NaCl load in the present study. This type of hypertension was

shown to be due to reduced sodium excretory capacity of kidneys.

Heymann nephritis is considered a model of autoimmune immune complex nephritis (1, 15, 29). During its development antibodies are formed against renal tubular brush border antigens. Circulating immune complexes are then deposited in the glomeruli. A local formation of immune complexes has been suggested in the heterologous type of immune complex nephritis (31) which may also apply to Heymann nephritis. Our findings of serum antibodies against renal tubular brush border granular pattern of IgG deposits along basement membranes of glomerular capillaries and subepithelial localization of electron-dense deposits confirm the observations of others (3, 16).

DOCA NaCl treatment results in sodium and water retention, increased extracellular and plasma volumes, increased cardiac output and hypertension (8, 13) which may later predominantly be due to elevated peripheral resistance but show normalized cardiac output (8). Susceptibility to DOCA NaCl hypertension varies genetically and in some rat strains sensitization through the removal of one kidney is required in order for hypertension to develop (18, 34). With both kidneys left the Wistar rats used in our study were able to adapt to DOCA NaCl treatment without any marked increase in blood pressure (Fig. 1).

Hypertension in the DOCA-NaCl-nephritis group would not appear to be renin-angiotensin dependent (Table 1). The hypertensive mechanisms are probably related either to DOCA-induced sodium retention, mechanisms associated with immune complex nephritis or both.

According to *Guyton* (17), a given filtration pressure is required in order for a sodium load to be excreted, in hypertension the higher blood pressure actually reflects — for unknown reasons — a resetting of this relationship. This 'pressure diuresis' hypothesis as a cause of hypertension is, however, based on work with isolated kidneys and has not been unequivocally demonstrated in the whole organism. On the other hand, the capacity of single nephrons to increase their fractional electrolyte excretion compensatorily to nephron loss has been pointed out (5) and also demonstrated in Heymann nephritis (2). In our study, hypertensive DOCA-NaCl-nephritis rats were able to excrete the same amount of sodium and water as non-hypertensive DOCA-NaCl rats throughout the experiment.

In nephrotic syndrome associated with Heymann nephritis, inability of sodium excretion has been reported (4). However, such nephrotic syndrome did not develop in the present hypertensive model, since ascites, edema and hypoalbuminemia were lacking.

Salt-resistant rat strains are able to adapt to increased cardiac output by compensatory peripheral vasodilation (34). On the other hand salt-sensitive rats react by autoregulatory vasoconstriction resulting in elevated peripheral resistance and hypertension. The non-hypertensive DOCA NaCl group in our study probably adapted to increased cardiac output by lowering the peripheral resistance. In the DOCA NaCl nephritis group elevated blood pressure thus means that peripheral resistance has either remained normal or else been increased further.

DOCA-NaCl treatment accelerated protein leakage from glomerular capillaries (Fig. 2). Arterial wall permeability to plasma macromolecules has been shown to be increased in hypertension (14). Gamma globulin deposits have been found in vascular lesions of DOCA NaCl-induced hypertension (30). Hypervolemia may thus promote vascular insudation of immune complexes which may make the peripheral resistance rise and render nephritic rats sensitive to DOCA-NaCl treatment.

It is unclear whether proliferative sclerotic glomerular changes in the hypertensive rats are a cause or effect of hypertension. Primary and secondary nephroscleroses are usually histologically similar (7). High blood pressure as such may cause nephrosclerosis and, on the other hand sclerotic

lesions may be primary, later followed by hypertension. *Byrom* (7) has suggested that a weakened vascular wall is susceptible to the mechanical stress of even normal blood pressure, whereas high blood pressure may damage intact vasculature as well. Thus the immunological model studied may have accelerated the development of the sclerotic lesions.

Giese (14) has shown that during experimentally induced angiotensin hypertension the vascular lesions appear in the areas of dilated arterioles and that increased permeability to plasma components and possibly ischemia of the vascular wall are important in this context. The lesions of experimental serum sickness are aggravated by high blood pressure (38). This may explain why immune complex nephritis together with DOCA NaCl load exceeds the glomerular and vascular tolerance resulting in irreversible injury. Perturbation of vascular wall metabolism and function takes place in DOCA-NaCl hypertension even prior to the appearance of lesions visible in a light microscope (12).

The data on the new experimental rat model presented here accord with and extend previous data that immunological factors may be involved in the pathogenesis of hypertension (30, 32, 33, 37). This may have important bearings on immunological features in human hypertension as well (22, 25).

Supported by the Finnish National Research Council for Medical Research, the Sigrid Jusélius Foundation, the Minerva Foundation, the Finnish Medical Foundation (Helsinki) and Nordisk Insulinfond (Copenhagen). Percorten M was kindly supplied by Ciba Geigy.

REFERENCES

1. Abrass C A, Border W A & Glasscock R J. Demonstration of circulating immune complexes (CIC) in autologous immune complex nephritis (AICN) of rats. *Kidney Int* 12: 508, 1977.
2. Allison M E M, Wilson C B & Goitschalk C H. Pathophysiology of experimental glomerulonephritis in rats. *J clin Invest* 53: 1402-1423, 1974.
3. Alousi M A, Post R S & Heymann H. Experimental autoimmune nephrosis in rats. Morphogenesis of the glomerular lesions: immunohistochemical and electron microscopic studies. *Amer J Path* 54: 47-57, 1969.
4. Bernard D B, Alexander E A, Couser W G & Lewinsky N G. Renal sodium retention during volume expansion in experimental nephrotic syndrome. *Kidney Int* 14: 478-485, 1978.
5. Bricker N S, Bourgoignie J J & Weber H. The renal response to progressive nephron loss. In Brenner B M & Rector F C (eds) *The kidney*

- vol 1 W B Saunders Company Philadelphia
1976 pp 703-736
- 3 Bunag R D Validation in awake rats of a tail-cuff
method for measuring systolic pressure J appl
Physiol 34 279-282 1973
- 7 Byrom F B Tension and the artery: the experimen-
tal elucidation of pseudo uraemia and malignant
nephrosclerosis Clin Sci Molec Med 51 3s-11s
1976
- 8 Carretero O A & Romero J C Production and
characteristics of experimental hypertension in
animals In Genest J Korw E & Kuchel O
(eds) Hypertension McGraw Hill Inc New York
1977 pp 485-507
- 9 Carroll N Crock G W Funder C C Green C
R Ham K N & Tange J D Glomerular
epithelial cell lesions induced by N^N-diacetylbenz-
idine Lab Invest 31 239-245 1974
- 10 Edgington T S Glasscock R J & Dixon F J
Autologous immune complex nephritis induced with
renal tubular antigen I Identification and isolation
of the pathogenetic antigen J exp Med 127 555-
572 1968
- 11 Fjhrquist F Sverri P Puutula L & Stenman U
H Radioimmunoassay of plasma renin activity
Cln Chem 22 250-256 1976
- 12 Gardner D L & Matthews M A Ultrastructure of
the wall of small arteries in early experimental rat
hypertension J Path 97 51-62 1968
- 13 Gavras H Brunner H R Laragh J H Vaughan
E D Jr Koss M Cole L C & Gavras I
Malignant hypertension resulting from deoxy-
corticosterone acetate and salt excess Role of renin
and sodium in vascular changes Circulat Res 36
300-309 1975
- 14 Giese J Renin, angiotensin and hypertensive
vascular damage: a review Amer J Med 55 315-
332 1973
- 15 Glasscock R J Edgington T S Watson J I &
Dixon F J Autologous immune complex nephritis
induced with renal tubular antigen II The pathoge-
netic mechanism J exp Med 177 573-587 1968
- 16 Grupe W E & Kaplan M H Demonstration of an
antibody to proximal tubular antigen in the pathoge-
nesis of experimental autoimmune nephrosis in rats
J Lab clin Med 71 400-409 1969
- 17 Guston A C Coleman T G Conley A W Jr
Scherl K W Manning R D Jr & Norman R A
Arterial pressure regulation: Overriding domi-
nance of the kidneys in long term regulation and in
hypertension Amer J Med 57 584-594 1972
- 18 Hall C E & Hall O Resistance of Fischer 344
rats to deoxycorticosterone hypertension Life Sci
20 1239-1247 1977
- 19 Harjanne A Korhola T Pitkanen E & Rauta-
Aro L Serum creatinine determination by an
automatic kinetic method Scand J clin Lab
Invest suppl 147 103 1977
- 20 Heymann W Hackel D B Harwood S Wilson
S G F & Hunier J L P Production of nephrotic
syndrome in rats by Freund's adjuvants and rat
kidney suspensions Proc Soc exp Biol (NY)
100 660-664 1959
- 21 Klassen J Sugisaki T Milgrom F & McCluskey
R T Studies on multiple renal lesions in Heymann
nephritis Lab Invest 25 577-585 1971
- 22 Lancet Immunogenetics and essential hypertension
Lancet 2 409-410 1978
- 23 Linder E Miettinen A & Tornroth T Fibronectin
as a marker for the glomerular mesangium in
immunohistology of kidney biopsies Lab Invest
42 70-75 1980
- 24 Lowry D H Rosenbrough N J Farr A L &
Randall R J Protein measurement with the Folin
phenol reagent J biol Chem 193 265-275 1951
- 25 Mathews J D Whittingham S & Mackay I R
Autoimmune mechanisms in human vascular dis-
ease Lancet 2 1423-1427 1974
- 26 Miettinen A & Linder E Membrane antigens
.
27 Miettinen A Tornroth T & Virtanen I Lectin
affinity chromatography in the purification of the
nephritogenic autoantigen(s) (Nag) of rats Protides
of the Biological Fluids 27 627-630 1979
- 28 Mullink J W M A Polyarteritis in mice due to
spontaneous hypertension J comp Path 80 99-
106 1979
- 29 Naruse T Fukasawa T Kirokawa N Oike S &
Miyakawa Y The pathogenesis of experimental
glomerular glomerulonephritis induced with ho-
mologous nephritogenic tubular antigen J exp
Med 144 1347-1362 1976
- 30 Ohta G Cohen S Singer E J Rosenfield R &
Strauss L Demonstration of gamma globulin in
vascular lesions of experimental necrotizing arteritis
in the rat Proc Soc exp Biol (NY) 107 187-
189 1959
- 31 Salant D J Belok S Stilmant M M Darby C
& Couser W G Determinants of glomerular
localization of subepithelial immune deposits Ef-
fects of altered antigen to antibody ratio, steroids,
vasoactive amine antagonists, and aminonucleoside
of puromycin on passive Heymann nephritis in rats
Lab Invest 41 89-99 1979
- 32 Svendsen U G Spontaneous hypertension and
hypertensive vascular disease in the NZB strain of
mice Acta path microbiol scand Sect A 85 548-
554 1977
- 33 Svendsen U G The importance of the thymus for
hypertension and hypertensive vascular disease in
rats and mice Acta path microbiol scand Sect A
suppl 267 1-15 1978
- 34 Tobian L Salt and hypertension In Genest J
Korw E & Kuchel O (eds) Hypertension
McGraw Hill Inc New York 1977 pp 423-433
- 35 Tornroth T The fate of subepithelial deposits in
acute post-streptococcal glomerulonephritis Lab
Invest 35 461-474 1976
- 36 Tornroth T Tallqvist G Pasternack A & Linder
E Nonprogressive histologically mild membra

- nous glomerulonephritis appearing in all evolutionary phases as histologically «early» membranous glomerulonephritis *Kidney Int* 14 511-521, 1978
- 37 *White, F N & Grollman, A* Experimental periarteritis nodosa in the rat *Arch Path* 78 31-36 19
- 38 *Wilens, S L & Henderson D* Glomerulonephritis in pressor drug enhanced serum sickness of rabbit *Proc Soc exp Biol (N Y)* 120 866-868 196

THE RELIABILITY OF MALIGNANT THYROID TUMOR DIAGNOSIS IN THE SWEDISH CANCER REGISTRY

Review of 200 Cases

LARS ERIK HOLM TORSTEN LÖWHAGEN and CLAES SILFVERSWARD

Department of General Oncology Radiumhemmet and Institute of Tumor Pathology Karolinska
Hospital Stockholm Sweden

Holm L E Lowhagen T & Silfversward C The reliability of malignant thyroid tumor diagnosis in
the Swedish Cancer Registry Review of 200 cases. Acta path microbiol scand Sect A 88 251-254
1980

Two age stratified periodical samples of 100 cases of malignant thyroid tumors from the Stockholm
region and 100 such cases from other parts of Sweden reported to the Swedish Cancer Registry
between 1958 and 1972 were studied The cytologic and/or histologic slides were re-examined by two
pathologists independently In 85 per cent of the cases reported from Stockholm and in 94 per cent of
the cases from other parts of Sweden the pathologists agreed on the original diagnosis of malignant
tumor The remaining cases (weighted mean 8%) were at re-examination considered to be benign
thyroid lesions

Key words Malignant thyroid tumor diagnosis Swedish Cancer Registry

Lars Erik Holm Dept of General Oncology Radiumhemmet Karolinska Hospital S-104 01 Stockholm
Sweden

Accepted as submitted 15 II 80

The histopathologic classification of thyroid
tumors has progressed considerably during recent
years The most significant publication in this
respect is the World Health Organization (WHO)
classification (1974) partly based on earlier com-
prehensive efforts to standardize the diagnostic
criteria of these tumors (Woolner *et al* 1961)

Uniformity in the classification of malignant
tumors is a prerequisite for epidemiologic studies
and for comparison between different medical
centers The absence of specific diagnostic criteria
prior to the introduction of the WHO classification
implies possible variations in the incidence of
malignant thyroid tumors reported to different
tumor registries In one study 696 cases of such
tumors reported in the course of a few years to the
national cancer registries of Finland Iceland
Norway and Sweden the review showed 12.5 per
cent to be benign (Saxén *et al* 1978) It was

therefore considered of value to review a representa-
tive material of malignant thyroid tumors reported
to the Swedish Cancer Registry over a longer period
of time and to apply the criteria proposed by WHO
to ascertain the reliability of the diagnosis of such
tumors in that registry

MATERIALS AND METHODS

Two age stratified periodical samples of 100 cases of malignant thyroid tumors from the Stockholm
region and 100 from other parts of
Sweden The distribution of the cases by the original
histologic classification is shown in Table 1 Of the
reported tumors 100 were originally classified as
papillary carcinomas 58 as follicular 16 as anaplastic
and 26 as other types of malignant thyroid tumors In

TABLE 1 *Tumor Classification of the Statistical Samples of Malignant Thyroid Tumors Reported to the Swedish Cancer Registry*

Original histologic classification	No of reported carcinomas		
	Stockholm region	Rest of Sweden	Total
Papillary carcinoma	49	51	100
Follicular carcinoma	30	28	58
Anaplastic carcinoma	11	5	16
Other malignant thyroid tumors	10	16	26
Total	100	100	200

this last group were included 4 medullary carcinomas and also cases with unspecific diagnoses, such as adenocarcinoma and carcinoma

Information on the name and date of birth of the patients was obtained from the Swedish Cancer Registry. The histologic and/or cytologic slides, on which the diagnoses were based, and relevant patient record data from the time of the tumor diagnosis were obtained from the reporting hospitals. Available slides were re-examined and reclassified on the basis of the WHO classification (1974) by two pathologists (*T. Lowhagen* and *C. Silfversward*) independently and without knowledge of the original tumor classification. The diagnosis was based on histologic slides in 184 cases and on cytologic slides in 16 cases. The size of the tumors was estimated from the histologic sections as being less than 15 mm in diameter, 15 mm or more or not known.

The tumors were first evaluated as benign or malignant. If considered malignant they were further classified into papillary, follicular or anaplastic carcinomas or other types of malignant thyroid tumors. In cases ($n = 21$) where the pathologists disagreed the slides were re-examined and reclassified by them simultaneously through a double headed microscope. A common decision on the diagnosis and of the classification was reached in all but 2 cases. In one of these 2 cases the pathologists disagreed on the diagnosis of malignant tumor and in the other case they differed in the classification. In both cases one of them agreed on the original diagnosis and classification, these being taken as final.

RESULTS

The original diagnosis of malignant thyroid tumor was at re-examination confirmed in 85 per cent of the cases from the Stockholm region and in 94 per cent of the cases from the other parts of Sweden.

The remaining 21 cases were at review considered to be benign lesions, 16 were originally classified as follicular, 3 as papillary and 2 unclassified carcinomas. Five of these follicular carcinomas and 1 of the papillary carcinomas were reported from outside Stockholm, the remainder of the benign lesions being reported from the Stockholm region.

The size of the thyroid tumors is shown in Table 2. There was no difference in the tumor size distribution between the two samples. The majority of the 200 cases (64 per cent) had a tumor size of 15 mm or more. Nine of the confirmed papillary carcinomas were less than 5 mm in diameter. The size of the lesions considered to be benign at re-examination was in 10 cases less than 15 mm, in 11 cases 15 mm or more and in 1 case the size was not known.

The correlation between the original histologic diagnoses and those obtained at re-examination is presented in Table 3. Agreement was obtained in 93 per cent of the cases of papillary

TABLE 2 *Estimated Tumor Size Distributed by the Original Tumor Classification*

Original tumor classification	Tumor size		
	<15 mm No	≥15 mm No	Not known No
Papillary carcinoma	31	61	8
Follicular carcinoma	8	44	6
Anaplastic carcinoma	0	11	5
Other malignant thyroid tumors	3	12	11
Total	42	128	30

TABLE 3 Statistical Samples of Malignant Thyroid Tumors Distributed by the Original Tumor Classifications and Those Obtained at Re examination

Original tumor classification	In agreement with original diagnosis No	Other malignant thyroid tumor No	Benign thyroid lesion No
Papillary carcinoma	93	4	3
Follicular carcinoma	36	6	16
Anaplastic carcinoma	12	4	0
Other malignant thyroid tumors	12	12	2
Total	153	26	21

62 per cent of the follicular and in 75 per cent of the anaplastic carcinomas and in 46 per cent of the cases of other types of malignant thyroid tumors

In 9 cases the malignant tumor was diagnosed at autopsy. In 2 of the cases considered to be benign at re-examination the original diagnosis of malignant thyroid tumor had already been revised to benign lesions. The reports to the Swedish Cancer Registry had not been withdrawn, however.

DISCUSSION

The present study disclosed, when using the WHO classification, benign thyroid lesions in 15 per cent (95 per cent confidence limits 8.7-23.5) of the cases reported as malignant from the Stockholm region and in 6 per cent (2.2-12.6) of the cases from the rest of Sweden, with a weighted mean of 8 per cent (3.5-15.2). These figures are consistent with those found by *Saxen et al* (1978).

The tumours most often erroneously reported as carcinomas were the follicular adenomas. A possible explanation for this discrepancy may be that in some of these cases cellular atypia was considered the basis for the diagnosis and in others that areas of hyperplasia in nodular goiter or thyroiditis were misinterpreted as follicular carcinomas. At the re-examination, however, the presence of vascular or capsular invasion was the main distinguishing factor between adenomas and carcinomas of the follicular type. In a study by *Franssila & Saxen* (1972) the overdiagnosis of atypical nodules and adenomas was considered to be a possible explanation for the high incidence of follicular carcinomas in areas of endemic goiter.

It must be emphasized that this review was based on available slides and the divergence between the diagnoses of the reviewers and the original diagnoses might to some extent be explained by the possibility that all histologic slides, without our knowledge, were not present at the re-examination.

Furthermore, we do not know the proportion of malignant thyroid tumors wrongly registered in the Swedish Cancer Registry as other types of malignant tumors. Two of the 200 malignant thyroid tumors of the present study had at an earlier re-examination been revised to benign thyroid lesion but apparently neither of the two reports were withdrawn from the registry.

In the samples studied there were 9 carcinomas with a size of less than 5 mm in diameter. It is well known that the larger the number of histologic sections of the thyroid gland examined, the higher has been the figure obtained for the prevalence of occult carcinoma (*Sampson et al* 1969). Serial sectioning of thyroid glands at autopsy has disclosed carcinomas in 3-28 per cent of the glands examined (*Mortensen et al* 1955, *Sampson et al* 1969, *Fukunaga and Yatani* 1975, *Sasaki et al* 1976, *Sobrinho-Santos et al* 1979).

That genetic and possibly social and cultural factors can be of etiologic importance in explaining this difference. It has been suggested too that the majority of occult thyroid carcinomas - which are generally of the papillary type - remain occult and that only a few are detected clinically. The fact that the incidence of clinical thyroid carcinoma in the Japanese does not differ significantly from that in many other countries supports this assumption (*Fukunaga and Yatani* 1975).

The regions of Stockholm, Malmö and Gothenburg (the three largest cities in Sweden) have an incidence of malignant tumors that is higher than that of the rest of Sweden (*Ringert* 1971). For malignant thyroid tumors the ratio is 1.41. Differences in diagnostic criteria of such tumors can be one factor that partly explains the higher incidence in these regions. Whether there is a higher proportion of benign thyroid lesions reported from the regions of Malmö and Gothenburg as was

indicated to be the case for the Stockholm region than for other parts of Sweden is not known. There is also a possibility that a higher frequency of thyroid surgery and a higher autopsy rate in these regions might contribute to their higher incidence of malignant thyroid tumors.

We wish to thank Mrs Elisabeth Bjurstedt and Mrs Karin Sten for their excellent secretarial assistance, Mrs Kerstin Wannerstrom for helping us find the histologic and cytologic slides of this study and Professor Gunnar Eklund for advice in connection with epidemiologic problems.

This work was supported by grants from the National Institute of Radiation Protection (Project SSI/P133-79) Stockholm, Sweden.

REFERENCES

- Bondeson L & Ljungberg O. Personal communication 1980.
- Franssila A & Saxen E. Histologic classification as a problem in the epidemiology of thyroid cancer. Recent Results Cancer Res 39: 47-55, 1972.
- Fukunaga F H & Yajani R. Geographic pathology of occult thyroid carcinomas. Cancer 36: 1095-1099, 1975.
- Mortensen J D, Woolner L B & Bennett W A. Gross and microscopic findings in clinically normal thyroid glands. J Clin Endocrinol Metab 15: 1270-1280, 1955.
- Ringertz N. ed. Cancer Incidence in Sweden 1959-1965. National Board of Health and Welfare. The Cancer Registry, Stockholm, 1971.
- Sampson R J, Key C R, Buncher C R & Ijima S. Thyroid carcinoma in Hiroshima and Nagasaki. I. Prevalence of thyroid carcinoma at autopsy. JAMA 209: 65-70, 1969.
- Sasaki J, Seta A, Takahashi S, Murata T, Saio K & Yagawa A. Clinicopathological studies on latent and occult carcinoma of the thyroid. In J Robbins, L E Braverman, F J G Ebling & I W Henderson. Thyroid Research. Proceedings of the Seventh International Thyroid Conference, Boston, Massachusetts, 1976: 565-576. Excerpta Medica, Amsterdam, Oxford, 1976.
- Saxen E, Franssila A, Bjarnason O, Normann T & Ringertz N. Observer variation in histologic classification of thyroid cancer. Acta path. microbiol. scand. Sect. A 86: 483-486, 1978.
- Sobrinho Simoes M A, Sambade M C & Gonçalves I. Latent thyroid carcinoma at autopsy. A study from Oporto. Portugal. Cancer 43: 1702-1706, 1979.
- WHO. International Histological Classification of Tumours. No. 11. Histological Typing of Thyroid Tumours. Eds Chr Hedinger & Sobin L H. World Health Organization, Geneva, 1974.
- Woolner L B, Beahrs O H, Black B M, McConahan W M & Keating F R Jr. Classification and prognosis of thyroid carcinoma. A study of 885 cases observed in a thirty year period. Am J Surg 102: 354-387, 1961.

QUANTITATIVE STUDIES OF THE GASTRIN-PRODUCING CELLS OF THE HUMAN ANTRUM

A Methodological Study

H OVERGAARD NIELSEN S HALKEN and M LORENTZEN

The Institute of Pathology Odense University Denmark

Nielsen H O Halken S & Lorentzen M Quantitative studies of the gastrin producing cells of the human antrum A methodological study Acta path. microbiol. scand. Sect. A 88 255-261 1980

The antral gastrin producing cells (G-cells) have been identified by the indirect immunoperoxidase technique in two antrum preparations removed due to a recurrent duodenal and gastric ulcer. Morphometric principles were applied to the G-cells with determination of their volume density, numerical density and mean cell volume. The study showed that within-observer variation between observer variation and within patient variation were negligible provided at least 200 G-cells were counted. A biopsy material can be used as well as larger tissue blocks when this minimum sample size is respected. A method for estimating the total G-cell population and the total G-cell volume in the antrum was developed. In the antrum removed due to a gastric ulcer the number of G-cells was 190×10^6 and their total volume 176 mm^3 .

Key words: Antral gastrin producing cells immunohistochemistry quantitation

H Overgaard Nielsen Institute of Pathology Odense University Hospital DK 5000 Odense C Denmark

Received 26 x 79 Accepted 19 ii 80

A quantitative estimate of the gastrin producing cells (G-cells) has acquired new interest following the development of selective vagotomy techniques for duodenal and gastric ulcer surgery. Unexplained deviations from the expected clinical and physiological responses to this treatment predominantly directed against parietal cell function have raised the question of the role of the G-cell population with regard to the postoperative results. This is especially true with regard to the striking difference in recurrence rates after proximal gastric vagotomy for duodenal and gastric ulcer (2).

Different kinds of G-cell abnormality may exist. The possibility of a G-cell hyperplasia in some duodenal ulcer patients (15) or a G-cell hypertrophy (7) has been suggested. Differences in G-cell distribution between patients with duodenal and gastric ulcer were found by Stave & Brandtzaeg (21) but they observed no relation between the total

G-cell population and certain gastro-duodenal diseases. At the present time no definite answer can be given to the questions regarding the influence of G-cell population or function on the clinical outcome of ulcer disease and especially the response to medical or surgical therapy.

Earlier work in this field (3, 4, 6, 9, 12, 14, 18, 20) has largely been concentrated on numerical density of G-cells per area in larger tissue blocks. This technique seems inadequate for repeated studies in sizable patient materials which necessitate measurement using endoscopic biopsies. The reliability of small biopsies has however been questioned (21) while others find them satisfactory (13).

In this work a method for determination of volume density, numerical density and mean volume of G-cells will be evaluated in respect of within and between-observer variation as well as within patient variation. The minimum sample size

indicated to be the case for the Stockholm region than for other parts of Sweden is not known. There is also a possibility that a higher frequency of thyroid surgery and a higher autopsy rate in these regions might contribute to their higher incidence of malignant thyroid tumors.

We wish to thank Mrs Elisabeth Bjurstedt and Mrs Karin Sjöen for their excellent secretarial assistance, Mrs Kerstin Wennerström for helping us find the histologic and cytologic slides of this study and Professor Gunnar Eklund for advice in connection with epidemiologic problems.

This work was supported by grants from the National Institute of Radiation Protection (Project SSI/P133-79) Stockholm, Sweden.

REFERENCES

- Bondeson L & Ijungberg O. Personal communication 1980.
- Franssila A & Saxen E. Histologic classification as a problem in the epidemiology of thyroid cancer. Recent Results Cancer Res 39: 47-55, 1972.
- Fukunaga F H & Yatani R. Geographic pathology of occult thyroid carcinomas. Cancer 36: 1095-1099, 1975.
- Mortensen J D, Woolner L B & Bennett W A. Gross and microscopic findings in clinically normal thyroid glands. J Clin Endocrinol Metab 15: 1270-1280, 1955.
- Ringertz N. ed. Cancer Incidence in Sweden 1959-1965. National Board of Health and Welfare, The Cancer Registry, Stockholm 1971.
- Sampson R J, Key C R, Buncher C R & Ijima S. Thyroid carcinoma in Hiroshima and Nagasaki. I. Prevalence of thyroid carcinoma at autopsy. JAMA 209: 65-70, 1969.
- Sasaki J, Seta A, Takahashi S, Murata T, Saito K & Yagawa A. Clinopathological studies on latent and occult carcinoma of the thyroid. In J Robbins, L E Braverman, F J G Ebling & I D Henderson. Thyroid Research. Proceedings of the Seventh International Thyroid Conference, Boston, Massachusetts 1976: 565-576. Excerpta Medica, Amsterdam, Oxford 1976.
- Scand Sect A 86: 483-486, 1978.
- Sobrinho Simoes M A, Sambade M C & Gonçalves J. Latent thyroid carcinoma at autopsy. A study from Oporto, Portugal. Cancer 43: 1702-1706, 1979.
- WHO. International Histological Classification of Tumours No. 11. Histological Typing of Thyroid Tumours. Eds Chr Hedinger & Sobin L H. World Health Organization, Geneva 1974.
- Woolner L B, Beahrs O H, Black B M, McConahay W M & Keatinge F R Jr. Classification and prognosis of thyroid carcinoma. A study of 383 cases observed in a thirty year period. Am J Surg 102: 354-387, 1961.

the smallest and the three with the largest counts
between the figures from

popular on and total G cell volume First the junction of the mucosa of the antrum and that of the body of the stomach was determined by means of multiple sections examined by freeze microscopy. After the site of this junction had been ascertained the antral mucosa was stripped from the underlying tissue and the volume determined by submersion into water and measurement of the amount of water thus displaced. As this volume includes mucosa and submucosa the fraction of the two components was determined by point counting in the same manner as described for V_v of the G cells.

Section thickness was controlled by a Tesatronic Elektronstester (TESA S.A. Renens Switzerland).

Statistical methods The chi square test was used for all comparisons. The figures were placed in a 2 X K table (19) when comparing the values of P_G and the corresponding values of $P_M - P_G$ the values of N and corresponding values of P_M . The test for expected values

RESULTS

Small diffuse areas of intestinal metaplasia devoid of G-cells were observed in slides from both antrum preparations but apart from these areas the distribution of the G-cells was found to be uniform corresponding to the middle part of the mucosa (11). No G-cells were seen in control sections. Tissue block No. 4 from antrum No. 2 was unsuccessful as the mucosa was lost during preparation.

Figures 1, 2, 3 and 4 are based on data from antrum No. 1 and it can be seen that the minimum sample size determined as the minimum number of P_G giving the accepted levels of the relative standard error is about one hundred corresponding to a G

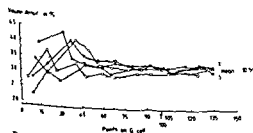


Fig 1 Relationship between volume density and points falling on G-cells (1 100 points - dispersion between curves are < 10% of the mean value of volume density)

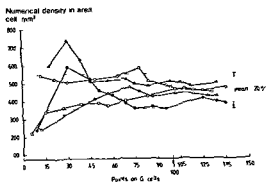


Fig 2 Relationship between numerical density in area and points falling on G-cells (1 100 points - dispersion between the curves are < 20% of the mean value of numerical density in area)

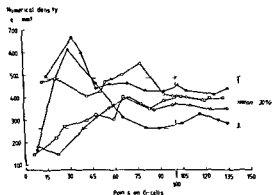


Fig 3 Relationship between numerical density and points falling on G-cells (1 100 points - dispersion between the curves is < 30% of the mean value of numerical density)

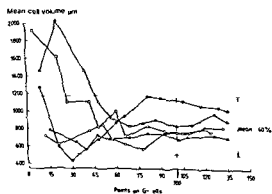


Fig 4 Relationship between mean cell volume and points falling on G-cells (1 100 points - dispersion between the curves < 40% of the mean value of mean cell volume)

necessary for reproducible results will be estimated, and the comparability of results obtained from biopsy material to results obtained from larger tissue blocks will be evaluated. Furthermore estimation of the population of G-cells and their total volume from resected antrum preparations will be attempted.

MATERIAL AND METHODS

The material comprises 2 preparations from 2 antra. No 1 was removed due to recurring duodenal ulcer, and used as it was expected to show a relatively high number and even distribution of the G cells (18). No 2 was removed owing to a gastric ulcer, and chosen because it was reasonable to expect a non uniform distribution of the G cells (22).

Preparation and immunohistochemistry. Five tissue blocks of approximately 10 mm in length and 5 mm in width were taken from No 1. Eight tissue blocks of the same size were removed from No 2 and in addition 5 biopsies taken approximately 2 cm from the pylorus using a gastroscopic forceps.

The tissue removed was fixed in 4% methanol free paraformaldehyde and embedded in paraffin. The G cells were identified on 5 µm thick sections by means of the indirect immunoperoxidase technique (11) using anti gastrin (2717) raised in rabbits against synthetic human gastrin I (17) in radioimmunoassay. This anti serum will determine all four main gastrin components (gastrin 14 17 34 and component I) (16). The method was modified so that the diaminobenzidine was replaced by 3-amino-9-ethyl carbazole (Sigma Chemical Comp. St. Louis U.S.A.) during the development. The same procedure was employed on control sections with the exception of a) the exclusion of anti gastrin serum and b) letting the anti gastrin serum react with gastrin (synthetic human gastrin I, Calbiochem Behring Corp. U.S.A.) 10 µg per ml diluted anti serum before application to the sections.

Morphometry. Using a square grid in the ocular of the microscope having 400 points with a mutual distance between them of 0.5 mm (d) and a magnification of 400 a systematic count of points falling on the G cells (P_G), the number falling on the mucosa (P_M) as well as the total number of G cells (N) was carried out on the entire histological slide from each preparation. The counting was started at the upper left point falling on the preparation, the point being made of horizontal and vertical lines with a distance between them of 1 mm. The following variables were then determined:

$$\text{Volume density (Vv) in \%} = \frac{P_G}{P_M} \times 100 \quad (23)$$

$$\text{Numerical density per unit area (N}_A\text{) stated as cells/mm}^2 = \frac{N \times \text{magnification}^2}{P_M \times d^2}$$

$$\text{Numerical density (N}_V\text{) stated as cells/mm}^3 = \frac{h \times N_A^{3/2}}{\beta \times V_v^{1/2}} \quad (24)$$

The factor h depends on the relative size distribution of the G-cells. We used the value 1.07 as the standard deviation in preliminary studies was found to be below 25% of the mean diameter of the G-cells (23). The coefficient β depends on the shape. We found the cells ellipsoid with the largest diameter 22.3 ± 2.2 (SD) µm and the smallest 14.3 ± 1.1 (SD) µm. Using the diagram of Weibel (23) and the values for G-cell diameters we found a value for β of about 1.5.

$$\text{Mean particle volume (V) in } \mu\text{m}^3 = \frac{V_v}{N_v}$$

The minimum sample size sufficient for giving an acceptably small variation of the results for the different variables was determined by the cumulative mean plots (10). For this we used the tissue blocks from No 1. We determined the cumulative means of V_v , N_A , N_v and V by analyzing an increasing number of microscopic fields from each histological slide. Acceptable levels of variation expressed as the relative standard error were arbitrarily fixed at $\pm 10\%$ for V_v , $\pm 20\%$ for N_A , $\pm 30\%$ for N_v and $\pm 40\%$ for V . To ensure that the minimum sample size would give acceptable levels for the coefficient of error (CE), this coefficient was determined for the variables with the greatest variation, V . It can be seen from the formula that V only depends on the proportion between P_G and N . CE for minimum sample size was calculated from preparation No 1. The formula $CE^2 (\Sigma P_G / \Sigma N) = CE^2 (P_G) + CE^2 (N) - 2r \times CE(P_G) \times CE(N)$ was used where r = the coefficient of correlation between P_G and the corresponding values of N . CE for P_G was calculated from the formula:

$$\frac{\text{standard deviation of } P_G}{\text{mean value of } P_G \times \text{number of fields} /}$$

CE for N was calculated likewise. A value of CE below 10% was accepted as satisfactory.

Figures for within observer variation were obtained by letting the same observer (A) count P_G and P_M twice in the preparation from No 1. The values of P_G and the corresponding values of $P_M - P_G$ from the two counts were compared for calculating the variation. In order to

preparation
) The homogeneity of the preparations was evaluated by comparing the different tissue blocks in respect of the values of P_G and the corresponding values of $P_M - P_G$ as well as the values of N and the corresponding values of P_M . The figures for V_v , N_A , N_v and V from each tissue block from both antra were also compared. The samples from No 2 were used to find the minimum number of biopsies to be counted in order to obtain a sample size for P_G sufficient for an acceptably small variation in the estimated variables. To test whether this minimum sample size was actually valid for antrum No 2 the values of P_G and the corresponding values of $P_M - P_G$ were compared for the biopsy with the smallest and the one with the largest count. For the two with the smallest and the two with the largest counts and the three with

TABLE 3 *Morphometric Data from No. 2*

ser	Tissue block No	P _G	P _M	P _M -P _G	N	V _V in %	N _A cells/mm ²	N _V cells/mm ³ × 10	\bar{V} μm ³
	1	106	6390	6284	216	1.66	216	175	949
	2	116	7086	6970	241	1.64	218	178	919
	3	117	6452	6335	223	1.73	214	169	1024
	4	unsuccessful							
	5	63	5013	4950	126				
	6	128	7798	7671	276	1.64	226	188	871
	7	98	5364	5266	209	1.83	249	206	827
	8	105	5303	5198	215	1.98	259	210	941
Mean ± SD						1.75 ± 0.14 NS	230 ± 19 NS	188 ± 17 NS	922 ± 68 NS
	1	86	5920	5834	189	1.45	204	172	844
	2	106	6787	6681	215	1.56	202	163	956
	3	98	6013	5915	206	1.63	219	180	904
	4	unsuccessful							
	5	60	6764	6704	116				
	6	115	6707	6592	209	1.71	200	154	1113
	7	87	4628	4541	189	1.89	241	193	978
	8	153	8156	8003	308	1.88	242	195	964
Mean ± SD						1.69 ± 0.18 NS	218 ± 19 NS	176 ± 16 NS	960 ± 90 NS

ing a reasonable homogeneity. When the data for V_V , N_A , N_V and \bar{V} were compared, a statistically significant difference was seen between the values of \bar{V} for the tissue blocks of No. 1 (which can be explained by the considerable dispersion tolerated in the estimation of the value of \bar{V}) while no differences were seen in the other variables.

It can be seen from Table 4 that a minimum of three biopsies are required in order to give values of P_G of approximately one hundred. By comparing the values of P_G and the corresponding values of $P_M - P_G$ from the biopsy with the lowest (C) and that with the highest (E) count, as well as the two biopsies with the lowest (A + C) and the two with the highest (B + E) counts, statistically significant differences were found. When however the biopsies with the lowest (A + C + D) and the three with the highest (B + D + E) counts were compared,

no difference was seen. Neither was any difference found between the figures from the tissue blocks and the figures from the three biopsies with the lowest or the three with the highest counts (Tables 2 and 4). Thus three biopsies were the minimum number giving a reproducible count.

The volume of the stripped antrum mucosa was found to be 11.5 ml. The fraction of the mucosa was 91.6% and of the submucosa 8.4% of the total volume. This gave a mucosal volume of 10.5 ml which, using the average value of N_V from the eight tissue blocks (188×10^2 cells/mm³, Table 3, observer A) gave a G-cell population of 197×10^6 . When the values of N_V from the biopsies A + C + D and B + D + E (Table 4) were used, the population was estimated to be 173×10^6 and 200×10^6 respectively, the mean value being 190×10^6 cells. When the corresponding figures for

TABLE 4 *Morphometric Data for the Biopsies from Preparation No. 2*

Biopsy No	P _G	P _M	P _M -P _G	N	V _V in %	N _A cells/mm ²	N _V cells/mm ³ × 10 ²	\bar{V} μm ³
A								
B	37	2172	2135	76	1.70	224	186	931
C	43	2200	2157	101	1.95	294	256	762
D	25	2143	2118	40	1.17	119	85	1365
E	38	2034	1996	86	1.86	271	232	801
A + C + D	43	3003	2960	74	1.43	158	118	1213
B + D + E	100	6349	6249	202	1.58	204	165	958
	124	7237	7113	261	1.71	231	191	895

TABLE 1 *The Coefficient of Error of $\Sigma P_G/\Sigma N$ (Preparation No. 1 First Count of A)*

Tissue block No	ΣP_G	ΣN	$\Sigma P_G/\Sigma N$	r	n	CE
1	104	242	0.43	0.898	10	6.4
2	108	261	0.41	0.839	10	7.3
3	109	264	0.41	0.893	10	7.2
4	100	217	0.46	0.651	9	9.9
5	91	171	0.53	0.819	8	7.8

ΣP_G = the summation of P_G values

ΣN = the summation of N values

r = coefficient of correlation between the value of P_G and corresponding value of N

n = number of fields counted

CE = coefficient of error in per cent

cell count of approximately two-hundred (Table 1). The value of CE for $\Sigma P_G/\Sigma N$ was in all five tissue blocks below 10% with this number of P_G .

The data from antrum No. 1 are seen in Table 2, and from No. 2 in Tables 3 and 4.

No difference was found, indicating a negligible within-observer variation (coefficient of variation 2%) by comparing the values of P_G and the corresponding values of $P_M - P_G$ for the two counts of observer (A) (Table 2).

In the same manner no differences were found when the values of P_G and the corresponding values of $P_M - P_G$ were compared for observers A and B

(Table 3), or the values for A and C (Table 2) indicating a negligible between-observer variation (coefficient of variation 5%).

No difference was found in No. 1 when comparing the values of P_G and the corresponding values of $P_M - P_G$, as well as the values of N and the corresponding values of P_M from the tissue blocks of both antra, this indicated a high degree of homogeneity. In No. 2, a statistically significant difference was seen when the figures from tissue block No. 5 were included (in this block the P_G count was less than optimal, 60 and 63). With block No. 5 excluded, no difference was found, confirm

TABLE 2 *Morphometric Data from No. 1*

Observer	Tissue block No	P_G	P_M	$P_M - P_G$	N	N in μ^2	N_A cells/mm ²	N_A cells/mm ² $\times 10$	\bar{N} μm^2
(count)	1	127	4147	4020	294	1.06	454	393	779
	2	133	4766	4113	109	1.15	463	199	789
	3	115	4199	4264	335	1.11	494	442	704
	4	136	4755	4119	284	1.20	428	151	897
	5	135	4367	4232	261	1.09	382	302	1021
	Mean \pm SD					3.17 ± 0.05 NS	444 ± 42 NS	377 ± 51 NS	838 ± 124 P<0
(double count)	1	126	3987	3861		3.16			
	2	135	4141	4006		3.26			
	3	129	4031	3902		3.20			
	4	119	3684	3565		3.23			
	5	138	4409	4271		3.13			
	Mean \pm SD					3.20 ± 0.05 NS			
	1	108	3334	3226		3.24			
	2	143	4206	4063		3.40			
	3	154	4464	4310		3.45			
	4	106	3072	2966		3.45			
	5	128	3951	3823		3.24			
	Mean \pm SD					3.36 ± 0.11 NS			

- 3 *Creutzfeldt W, Arnold R, Creutzfeldt C & Track N S* Mucosal gastrin concentration molecular forms of gastrin number and ultrastructure of G cells in patients with duodenal ulcer *Gut* 17 745-754 1976
- 4 *Crvell D, Pera A, Ferrari A, Rizzetto M, Lombardo L, Babando G & Verme G* G-cell count in antral endoscopic biopsies by immunofluorescence *Scand J Gastroent.* 12 721-726 1977
- 5 *Eisenberg R B, Kuda M A & Peter B J* Stereological analysis of mammalian skeletal muscle *J Cell Biol* 60 732-754 1974
- 6 *Ganguli P C, Polak J M, Pearse A G E & Elder J B* Antral gastrin-cell hyperplasia in peptic-ulcer disease *Lancet* i 583-586 1974
- 7 *Heir Ph U, Oberholzer M, Kayasseh L, Gyr K, Stalder G A & Rohr H P* Duodenal ulcer Hyperplasia or hypertrophy of G-cells? *Scand J Gastroent.* 49 86 1978
- 8 *Hobbs S E & Polak J M* Quantitative immunohistochemistry pp 87-91 In *S R Bloom* Ed Gut hormones Churchill Livingstone Edinburgh London and New York 1977
- 9 *Keuppens F, Willems G, Vansteenkiste Y, Woussen Colle M C* Estimation of the antral and duodenal gastrin cell population removed by gastrectomy from patients with peptic ulcer *Surg Gynecol Obstet* 146 400-406 1978
- 10 *Mayhew T M, Cope G H, Williams M A, Hahn M & Cruz Orive L M* Stereology A demonstration of some
- 11 *Nelsen H O, Teglbjaerg P S & Hage E* Gastrin cells and enteroglucagon cells in human antra With special reference to intestinal metaplasia *Scand J Gastroent. Suppl* 54 101-103 1979
- 12 *Piris J & Whitehead R* Quantitation of G-cells in fibroptic biopsy specimens and serum gastrin levels in healthy normal subjects *J Clin Path* 28 636-638 1975
- 13 *Polak J M, Bloom S R, Pearse A G E & Welbourn R B* Endocrine quantitation of clinical gastrin biopsies *Gut* 16 406-407 1975
- 14 *Polak J M, Stagg B & Pearse A G E* Two types of Zollinger Ellison syndrome Immunofluorescent cytochemical and ultrastructural studies of the antral and pancreatic gastrin cells in different clinical states *Gut* 13 501-512 1972
- 15 *Polak J M & Bloom S R* Quadriennial Reviews 6 world congress of gastroenterology Madrid 1978
- 16 *Rehfeld J F* Personal communication 1980
- 17 *Rehfeld J F, Stadil F & Rubin B* Production and evaluation of antibodies for the radioimmunoassay of gastrin *Scand J clin Lab Invest.* 30 221-232 1972
- 18 *Roystone C M S, Polak J M, Bloom S R, Cooke W M, Russel R C G, Pearse A G E, Spencer J, Welbourn R B & Baron J H* G cell population of gastric antrum plasma gastrin and gastric acid secretion in patients with and without duodenal ulcer *Gut* 19 689-698 1978
- 19 *Snedecor G W & Cochran W G* Statistical methods pp 232-233 and 240-242 6th edition Iowa State University Ames USA 1969
- 20 *Stave R & Brandt aeg P* Immunochemical investigation of gastrin producing cells (G-cells) The distribution of G-cells in resected human stomach *Scand J Gastroent* 11 705-712 1976
- 21 *Stave R & Brandt aeg P* Immunohistochemical investigation of gastrin producing cells (G-cells) Estimation of antral density mucosal distribution and total mass of G-cells in resected stomachs from patients with peptic ulcer disease *Scand J Gastroent* 13 199-203 1978
- 22 *Stave R, Elton K A, B, J, P, C, C*
- 23 *Weibel E R* Stereological techniques for electron microscopic morphometry pp 244-246 and 248-251 In *Principles and Techniques of electron microscopy* 2nd edn J. Teichgraber, ed. New York/London 1968
- 24 *Weibel E R* Stereological techniques for electron microscopic morphometry pp 244-246 and 248-251 In *Principles and Techniques of electron microscopy* 2nd edn J. Teichgraber, ed. New York/London 1968
- 25 *Weibel E R, Staubli W, Gnani H R & Hess F A* Correlated morphometric and biochemical studies on the liver cell *J Cell Biol* 42 68-91 1969

mean cell volume $922 \mu\text{m}^3$ (Table 3 observer A) 958 and $895 \mu\text{m}^3$ (Table 4) were used the total G cell volume was found to be 182 mm^3 166 mm^3 and 179 mm^3 respectively the mean value being 176 mm^3

DISCUSSION

General use of quantitative methods for an investigation of the antral gastrin producing cells depends on the availability of a satisfactory technique

An acceptable constant examination result is essential for a suitable method and the method should not be too time-consuming

In the present investigation we found using direct microscopy and point counting that the reproducibility was good in respect of within and between observer variation. This reproducibility was obtained with a minimum number of G-cells of about two hundred. When the figures for this minimum sample size were used we also found good agreement between the counted numbers from single tissue blocks from the same preparation. The same was true for figures obtained from biopsy material and tissue blocks

Some dispersion between the figures for mean cell volume was seen. We had to accept this from a practical point of view because a smaller relative standard error for the values of the mean cell volume would necessitate an unpractically high value of the gastrin-cell count. The coefficient of error for mean cell volume was below 10% which means that only differences between values for the mean cell volume of more than 10% can be considered as statistically significant in comparative investigations. In order to employ the formula of Weibel & Gome (24) for the determination of the numerical density it was necessary to assume that the G cells were of uniform size and shape. Further no correction was made for the over estimation caused by the Holmes effect nor for the under estimation due to the inability to recognize and count very small particles (image loss) as we assumed as others that these two effects may cancel out (5, 25)

Stave *et al* (21, 22) in contrast to our results found in an investigation based on a resection material that the G cells had a very non uniform distribution within the same antrum. Their method gave the number of G-cell profiles per mucosa unit defined as specimens of $6 \mu\text{m}$ in thickness and 1 mm in width and $6 \mu\text{m}$ in thickness and $720 \mu\text{m}$ in width. The great variation within the units can be explained by the fact that these individual units may contain too few G-cells for a reliable and reproducible estimate (Fig. 2)

Our results in respect of the use of biopsy material for quantitation of G-cells are in agreement with Hobbs & Polak (8) as well as Polak *et al* (13). However their method cannot be employed in daily routine work as the results were obtained by means of analysis in a specially constructed television Image Analyzer which gives the results as the number of cells per measuring unit. They cannot measure the volume density, numerical density nor the mean cell volume by this method.

Biopsy material permits the data of N_V and N_V to be expressed as density. Determination of the total G-cell population or the total G-cell volume will however require a resection material comprising the whole antrum. The method described by Keuppens *et al* (9) and Roystone *et al* (18) in which the area of the antrum is determined by planimetry necessitates complete and uniform stretching of the preparation which we found difficult to achieve. The formula of Abercrombie (1) for the determination of the number of G-cells has the limitation that it is truly applicable for spherical particles only (23). Our method with the determination of the volume is simple but gives over-estimated values as we do not correct for tissue shrinkage.

CONCLUSIONS

This investigation demonstrates that density studies of the human antral gastrin producing cells are possible and that biopsy material can be used when simple precautions are taken in respect of the sample size. A simple method is described for the estimation of the G-cell population and the total G cell volume in resected antra.

The anti gastrin serum was kindly donated by Professor J F Relfeld Aarhus. The authors wish to thank Professor D Andersen Odense for permission to use the antrum preparations and for help in preparation of the manuscript. The work was supported by the Danish Medical Research Council (Journal number 552/944).

REFERENCE

1. Abercrombie M. Estimation of nuclear population from microtome sections. *Anat Rec* 94: 239-274 1946.
2. Andersen D, Hastrup H & Amdrup E. The Aarhus County Vagotomy Trial II. An interim report on reduction in acid secretion and ulcer recurrence rate following parietal cell vagotomy and selective gastric vagotomy. *World J Surg* 2: 91-100 1978.

EFFECTS OF A CHEMOTACTIC FACTOR AND *BACTEROIDES FRAGILIS* LIPOPOLYSACCHARIDE ON BONE RESORPTION IN TISSUE CULTURE

KJELL SVEEN

The Gade Institute Department of Microbiology Laboratory of Oral Microbiology University of
Bergen Bergen Norway

Sveen, K. Effects of a chemotactic factor and *Bacteroides fragilis* lipopolysaccharide on bone resorption in tissue culture Acta path microbiol scand Sect A 88 263-268 1980

Release of previously incorporated ^{45}Ca from fetal rat bone in tissue culture was stimulated by preparations of the polymorphonuclear leukocyte chemotactic factor isolated from lipopolysaccharide (LPS)-induced inflammatory exudate in rabbits as well as by *Bacteroides fragilis* LPS. High concentrations of released hydroxyproline and lactate seemed to correlate well with a high percentage of ^{45}Ca liberated into the culture medium. An active bone resorption was stimulated by a concentration of $1\text{ }\mu\text{g/ml}$ of the chemotactic factor. The peak in amount of released ^{45}Ca was at a concentration of $5\text{ }\mu\text{g/ml}$ of the chemotactic factor (LPS-CF) as well as of the LPS preparation, whereas the parathyroid hormone was most active at 1 IU/ml . Their effect was connected with the formation of osteoclasts. Neither LPS-CF nor LPS stimulated a release of ^{45}Ca or hydroxyproline from heat-deactivated bones. Heparin added to LPS-CF did not enhance its resorptive potential, whereas when added to LPS it had a synergistic effect. It is suggested that the bone resorptive effect exerted by LPS may be caused by chemotactic factors elaborated by activation of the complement system, and that these factors may be of importance in the pathophysiology of periodontal disease.

Key words: Bone resorption, chemotactic factor, *Bacteroides fragilis* lipopolysaccharide.

K. Sveen, Mikrobiologisk avdeling, MFH bygget, N-5016 Haukeland sykehus, Norway.

Received 25.1.80 Accepted 15.11.80

Gradually increasing mobility of teeth is caused by the loss of bone supporting tooth roots. Epidemiological studies clearly demonstrate a positive correlation between the severity of periodontal disease and the amount of bacterial and microbial products in the gingival region (1). However, the pathways connecting these microorganisms with the characteristic tissue-destructive mechanisms of periodontal disease are not well understood. Microbial products and components originating from degraded cells enter the soft and hard tissues. These either directly activate mechanisms destructive to the tissue or indirectly trigger defence mechanisms which in turn might generate mediators destructive to the same tissue.

Bacterial lipopolysaccharides (LPS) have been found to stimulate bone resorption in *in vitro* tissue cultures (7, 8). Also, the supernatant after centrifugation of immune complexes has been reported to induce bone resorption, and this was suggested to be due to some activated complement components (3).

This report is concerned with studies utilizing a previously characterized complement-derived chemotactic factor (16, 17). The aim of the study was to find out whether the chemotactic factor induced bone resorption, and if so, to what extent this activity was comparable to that of LPS isolated from *Bacteroides fragilis* ss *fragilis* strain Lille 323 and of parathyroid hormone.

EFFECTS OF A CHEMOTACTIC FACTOR AND *BACTEROIDES FRAGILIS* LIPOPOLYSACCHARIDE ON BONE RESORPTION IN TISSUE CULTURE

KJELL SVEEN

The Gade Institute Department of Microbiology Laboratory of Oral Microbiology University of
Bergen Bergen Norway

Sveen K Effects of a chemotactic factor and *Bacteroides fragilis* lipopolysaccharide on bone resorption
in tissue culture Acta path microbiol scand Sect A 88 263-268 1980

Release of previously incorporated ^{45}Ca from fetal rat bone in tissue culture was stimulated by
preparations of the polymorphonuclear leukocyte chemotactic factor isolated from lipopolysaccharide
(LPS)-induced inflammatory exudate in rabbits as well as by *Bacteroides fragilis* LPS High
concentrations of released hydroxyproline and lactate seemed to correlate well with a high percentage of

hormone was most active at 1 IU/ml Their effect was connected with the formation of osteoclasts
Neither LPS CF nor LPS stimulated a release of ^{45}Ca or hydroxyproline from heat-deactivated bones
The results had a
importance in the pathophysiology of periodontal disease

Key words Bone resorption chemotactic factor *Bacteroides fragilis* lipopolysaccharide

K Sveen Mikrobiologisk aveling MFH bygget N 5016 Haukeland sykehus Norway

Received 25 i 80 Accepted 15 iii 80

Gradually increasing mobility of teeth is caused
by the loss of bone supporting tooth roots
Epidemiological studies clearly demonstrate a posi
tive correlation between the severity of periodontal
disease and the amount of bacterial and microbial
products in the gingival region (1) However the
pathways connecting these microorganisms with
the characteristic tissue-destructive mechanisms of
periodontal disease are not well understood Micro
bial products and components originating from
degraded cells enter the soft and hard tissues These
either directly activate mechanisms destructive to
the tissue or indirectly trigger defence mechanisms
which in turn might generate mediators destructive
in the tissue

Bacterial lipopolysaccharides (LPS) have been
found to stimulate bone resorption in *in vitro* tissue
cultures (7-8) Also the supernatant after centrifuga
tion of immune complexes has been reported to
induce bone resorption and this was suggested to be
due to some activated complement components (3)

This report is concerned with studies utilizing a
previously characterized complement-derived che
motactic factor (16-17) The aim of the study was
to find out whether the chemotactic factor induced
bone resorption and if so to what extent this
activity was comparable to that of LPS isolated
from *Bacteroides fragilis* ss *fragilis* strain Lille 323
and of parathyroid hormone

lactate (mmol/l)

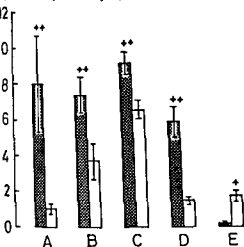


Fig 2 Effect of optimal doses of LPS CF LPS and of heparin added to LPS on the release of lactate from fetal rat bones cultured for 48 h in Biggers modified medium. Each column represents the mean amount (mmol) of lactate per litre culture medium \pm standard deviation (vertical bar) from six test bones. Closed columns illustrate culture medium + test substance open columns culture medium alone. Test cultures contain per ml of medium A) 5 µg LPS CF B) 5 µg LPS C) 5 µg LPS + 10 IU heparin and the control medium 5 µg of LPS D) 1 IU PTH E) 10 IU heparin. + $P > 0.05$ = not statistically significant. ** $P \leq 0.025$

giving optimal response at a specific dose (Fig. 1)

most active at a concentration of 1 IU per ml of the medium. The activity of LPS-CF was considerably

Hydroxyproline (µg/ml)

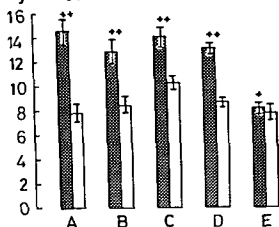


Fig 3 Effect of optimal doses of LPS CF LPS PTH and of heparin alone and added to LPS on the release of hydroxyproline from fetal rat bones cultured for 48 h in Biggers modified medium. Each column represents the mean amount (µg) of hydroxyproline per ml of culture medium \pm standard deviation (vertical bar) from six test bones. Closed columns illustrate culture medium + test substance open columns culture medium alone. Test cultures

higher than that of LPS on a weight basis and showed values of ^{45}Ca liberated significantly above that of the controls at all dilution steps tested.

Heparin alone induced no release of ^{45}Ca but when heparin was added to LPS there was a pronounced increase in the release ($p = 0.025$) (Ta

TABLE 1 Effect of Adding Heparin to Biggers Modified Medium Containing LPS on the Release of ^{45}Ca Lactate and Hydroxyproline from Living Fetal Rat Bone and the Effect of LPS on Devitalized Fetal Rat Bone in Tissue Culture

Treatment of bone	^{45}Ca (%) (mean \pm s.d.)	P ^a	Hydroxyproline (µg/ml) (mean \pm s.d.)	P	Lactate (mmol/l) (mean \pm s.d.)	P
Heparin 10 IU/ml	4.46 \pm 2.96 ^b		8.33 \pm 0.18		0.14 \pm 0.19	
LPS 5 µg/ml	9.56 \pm 1.74	0.025	10.17 \pm 1.65	0.025	6.51 \pm 1.07	0.025
Heparin 10 IU/ml + LPS 5 µg/ml	13.43 \pm 3.86	0.025	13.82 \pm 2.03	0.025	9.15 \pm 1.49	N.S.
70 °C for 8 min	3.20 \pm 0.87	N.S. ^c	4.99 \pm 1.19		N.D. ^d	
70 °C for 8 min + LPS 5 µg/ml	4.17 \pm 0.85		4.97 \pm 1.30	N.S.	N.D.	

^a Values of $P \leq 0.05$ were accepted as statistically significant, mean calculated from 4-6 samples

^b Difference statistically significant to control

^c N.S. = not significant

^d N.D. = not detected

MATERIALS AND METHODS

Test Materials

LPS (endotoxin) was isolated from *Bacteroides fragilis* ss. *fragilis* strain Lille E 323 by phenol-water extraction (20) and purified by ultracentrifugation and treatment with ribonuclease and deoxyribonuclease as described before (12). The complement-derived chemotactic factor was elaborated *in vivo* by the injection of LPS-E 323 suspensions into wound chambers implanted subcutaneously in rabbits as described earlier (18), and the inflammatory exudate sampled 3 h later. The fractionation procedure of the LPS-induced inflammatory exudate and the isolation of the chemotactic factor (LPS-CF) has been reported in detail (16). Heparin was purchased from A/S Apothekernes Laboratorium for Specialpræparater, Oslo, and parathyroid hormone used as a positive control, was supplied by Lilly, Indianapolis, Ind., USA.

Animals

Female rats from an inbred Wistar strain were used. On the eighteenth or nineteenth day of pregnancy they were injected subcutaneously with 100 μ Ci of 45 Ca. One day later the rats were killed, the abdomen washed with 0.05 per cent Pyricept® followed by 5 per cent iodine in ethanol. The fetal ulnae and radii were removed and explanted as pairs for organ culture.

Culture Medium

Bigger's modified medium (Flow Laboratories, Irvine, Scotland) containing 0.1 per cent of bovine serum albumin (Armour Pharmaceutical Company Ltd., England) was used throughout. No antibiotics were employed.

Culture Method

Two bones from the fetus were used as controls and the two others as experimental bone. The explanted bones were precultured for 24 h in 0.5 ml of the culture medium. Thereafter experimental radii and ulnae were cultured for 48 h in the same volume of the culture medium containing test materials. In one experiment one ulna and one radius from the same fetus were used as experimental bone and the contralateral ulna and radius were used as controls (Table 2). Cultures were maintained at 37 °C in an atmosphere of 5 per cent CO₂, 20 per cent O₂ and 75 per cent N₂.

Quantification of Released 45 Ca

After cultivation of the bones for 48 h, 0.1 ml of the culture medium was prepared for liquid scintillation counting of 45 Ca. The bones were then demineralized in 0.5 ml of 1 N HCl for 24 h, and 0.1 ml of the HCl extract was prepared for liquid scintillation. The amount of 45 Ca released from the bones during culture was expressed as the percentage of the total radioactivity initially present, calculated from the total counts per minute (cpm) in the bone. In one experiment, the amount of 45 Ca released was expressed as the ratio between the 45 Ca released (cpm) from the treated bones and from the comparable control bones (Table 2).

Quantification of Lactate and Hydroxyproline

The lactate concentration of the test culture and the control medium was determined by the reduction of nicotinamide adenine dinucleotide with lactate dehydrogenase (Boehringer, GmbH Mannheim, West-Germany) and measured spectrophotometrically. Free hydroxyproline (OH-proline) was estimated in both media according to the method of Dabek & Struck (2).

Histological Examination

Bones were fixed in 10 per cent formalin in phosphate buffered saline, pH 7.2. The bones were then demineralized in 0.1 M EDTA overnight and embedded in paraffin. Longitudinally cut sections of 5 μ m thickness were stained with hematoxylin and eosin.

Statistical Methods

For evaluation of the difference between the test and control groups, the *t*-test was used. The amount of 45 Ca release was performed according to the *t*-test (4).

RESULTS

The release of 45 Ca from prelabelled embryonic rat bones into the culture medium was effected by the materials tested over a certain concentration range.

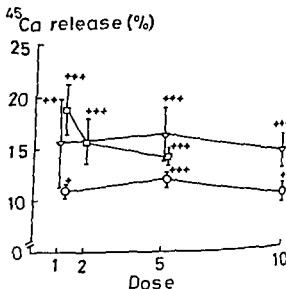


Fig. 1 Effect of different concentrations (μ g/ml Bigger's modified medium) of chemotactic factor (LPS CF) and lipopolysaccharide (LPS) and of parathyroid hormone (PTH) (IU/ml) on the release of previously incorporated 45 Ca from fetal rat bones cultured for 48 h. Each point represents the mean percentage \pm one standard error of the mean (vertical bar) from six test bones. For calculation of bone resorption, see Materials and methods. ∇ —LPS CF, \circ —LPS, \square —PTH. Values of $P > 0.05$ = statistically not significant to control; $+ P \leq 0.05$, $++ P \leq 0.025$.

percentage of ^{45}Ca mobilized from the same fetal bone by the stimulant used. Also, high concentrations of lactate in the culture medium seemed to correlate well with a high percentage of ^{45}Ca liberated as well as with the amount of OH proline released. Each of the parameters used thus could reflect the magnitude of the osteoclastic activity induced by the special stimulant used.

Morphologically, LPS-CF and LPS caused a proliferation of osteoclasts and a removal of the matrix as shown by others using LPS isolated from *Bacteroides melaninogenicus* (7) and from *Escherichia coli* (8). These stimulated osteoclasts also contain a greater number of nuclei than those seen in the controls using LPS (5) and PTH (11) as stimulants.

Large doses of LPS-CF in the culture medium resulted in a decreased release of ^{45}Ca . This was also demonstrated with high doses of LPS and PTH which would suggest the occurrence of either an inhibitory mechanism or a toxic effect. Neither LPS-CF nor LPS stimulated ^{45}Ca release beyond that of PTH when tested on the peak of their bell-shaped dose response curves. It is likely that the inductive mechanism of LPS-CF also is quite different.

LPS have a lipid A quite different from that of *Fusobacterium* LPS. It has been put forward that this part of the endotoxin molecule is responsible for the biological activities exerted by LPS (6). Also, lipid A has been suggested to be responsible for the active ^{45}Ca release from bone (9). It is known that lipid A activates the classical complement pathway and that the polysaccharide portion initiates the activation of the alternative pathway. *B. fragilis* LPS has been shown to activate the alternative pathway (15) resulting in the elaboration of the complement-derived chemotactic factor C5a (16).

There is no proof that embryonic bone does or does not contain endogenous complement factors. It may be suggested therefore that complement factors are available inside as well as outside the bone and are activated by LPS resulting in the elaboration of chemotactic factors. It is not likely that LPS-CF and LPS, which are each unique molecular entities, should react with the same receptor in the cell membrane of the osteoclast and initiate the biochemical events resulting in bone resorption. It is more likely that these events are mediated by the elaboration of the chemotactic factor C5a binding to receptors in the cell membrane. However, LPS molecules via the lipid part

may also bind to the membrane by the opening of the lipid bilayer which would allow interaction of the fatty acids. Results (unpublished) indicate however that the main part of the bone resorptive activity after the splitting of the *Fusobacterium* LPS with 1 per cent acetic acid was retained in the supernatant and not in the pellet. This may indicate that lipid A is not the only portion of the LPS molecule in which the potential for biological activities are integrated. This is in keeping with other studies (12, 13, 14, 16, 19).

The addition of heparin to the culture medium significantly increased the resorptive activity of LPS as has also been shown by others (8) whereas no such effect was found when heparin was added to the culture medium containing LPS-CF. The mechanism of this synergistic effect is unknown although heparin is known to activate the classical complement pathway and thus induce the elaboration of complement-derived factors which may be active in stimulation of bone resorption. Why heparin did not enhance the bone resorptive effect induced by LPS-CF is also unknown.

number of osteoclasts whereas the effect of LPS causes changes in cell calcium as well as an increase in the number of nuclei of the osteoclasts. The dynamics behind the inductive mechanism of calcium release by LPS as well as by LPS-CF are uncertain. However, neither calcium nor cAMP needs to be the final mediator of bone resorption.

The potentiating effect of heparin on LPS from *B. fragilis* is interesting in that no correlation between the number of mast cells and heparin content of inflamed gingival tissues has been found (21) which indicates that mast cells have degranulated. This also is supported by the finding that severe inflamed gingiva contain fewer mast cells than healthy gingiva do. Furthermore, a stimulation of the synthesis of mast cells in the connective tissue adjacent to the gingival microbial plaque has been indicated (22). It may thus be concluded from the results presented that the synergistic effect of heparin on endotoxin as well as the activity of the LPS-induced complement-derived chemotactic factor on bone resorption could be significant factors in the pathophysiology of periodontal disease.

REFERENCES

1. Burnet G W & Scherp H W. Oral microbiology and infectious disease. A textbook for students and practitioners of dentistry. 3rd ed. The Williams and Wilkins Co. Baltimore 1968. pp 409-466.

TABLE 2 Effect of Adding Heparin to Bigger's Modified Medium Containing Chemotactic Factor (LPS CF) on Release of ^{45}Ca and Hydroxyproline from Fetal Rat Bone in Tissue Culture

Treatment of bone	Ratio treated to control ^a			
	^{45}Ca (mean \pm s.e.)	p ^b	Hydroxyproline (mean \pm s.e.)	p
LPS CF 5 $\mu\text{g}/\text{ml}$	1.13 \pm 0.05	< 0.05	1.52 \pm 0.16	< 0.05
LPS CF 5 $\mu\text{g}/\text{ml}$ + 10 IU/ml heparin	1.14 \pm 0.08	< 0.05	1.52 \pm 0.15	< 0.05

^a Release ratios of ^{45}Ca and hydroxyproline are calculated from four pairs of cultures in each experiment

^b P values based on a difference of a ^{45}Ca and hydroxyproline release ratio from 1.0

ble 1) The difference in the release of ^{45}Ca from prelabelled experimental bones and control bones was not statistically significant

Except for heparin (Table 1) all the test materials examined in doses giving optimal ^{45}Ca release into the culture medium also induced the liberation of lactate, which was significantly higher than in the medium of their respective controls (Fig. 2)



giant cells (arrows) in A and B. Both sections are oriented with the periosteum at the upper edge. Hematoxylin and eosin $\times 488$

However, the concentration of lactate in medium containing heparin only was insignificant although it seemed to potentiate the release of lactate into the medium containing LPS ($p = 0.025$) (Table 1)

A significant release of OH proline into the culture medium containing LPS CF, LPS and PTH in optimal concentrations was demonstrated (Fig. 3). Ten units of heparin did not affect the release of OH proline (Table 1) but the same concentration of heparin enhanced the effect of LPS significantly above that induced by LPS alone ($p = 0.025$)

The activity of LPS CF to induce the liberation of ^{45}Ca and OH proline into the culture medium with or without heparin added, gave values significantly above that of the controls ($p < 0.05$) (Table 2). However, heparin did not potentiate the capacity of LPS CF to induce either the release of ^{45}Ca or OH proline into the culture medium ($p > 0.05$)

Fetal bones cultured for 48 h with LPS-CF or LPS showed an increase in cell density with the finding of multinuclear cells close to the bone as well as a scarcity of bone matrix as compared to control bones (Fig. 4)

DISCUSSION

Preculture of fetal rat bone under strictly defined conditions in culture medium only for 24 h contributes to an exchange of loosely completed ^{45}Ca with the stable calcium. Both metabolic and passive exchange mechanisms are primarily responsible for the release of ^{45}Ca from prelabelled rat bone in *in vitro* cultures (9). The magnitude of the passive exchange component may be estimated from prelabelled heat-devitalized bone in the culture medium. Neither LPS-CF nor endotoxin had any effect on the exchange mechanism of devitalized bone.

A large amount of OH proline liberated from the bone matrix was found to be related to a high

THE INTRA-LESIONAL VARIATION OF TYPE, LEVEL OF INVASION, AND TUMOUR THICKNESS OF PRIMARY CUTANEOUS MALIGNANT MELANOMA

55 Malignant Melanomas Studied by Serial Block Technique

KNUD SONDERGAARD

Department of Pathology the Finsen Institute Copenhagen Denmark

Sondergaard K The Intralesional variation of type level of invasion and tumour thickness of primary malignant melanoma 55 malignant melanomas studied by serial block technique Acta path microbiol scand Sect A 88 269-274 1980

In order to evaluate the prognostic importance of type of melanoma, level of invasion and tumour thickness in a retrospective study of cutaneous melanomas it is prerequisite that the available histological material be representative To investigate this condition 55 primary cutaneous melanomas were studied randomly by serial block technique The histological classification of each tissue block as to 1) type of melanoma 2) level of invasion and 3) tumour thickness was correlated with the overall classification of the corresponding whole melanoma lentigo maligna melanoma

and arranged in 6 mm and more than 600 mm) The study revealed a consistency of 95% (52/55) between the type of the central cross section and the type of the whole tumour In 96% (53/55) of the central cross sections the level of invasion was equal to that of the whole tumour In 95% (52/55) of the central cross sections the tumour thickness was situated in the same group as that of the whole tumour It is concluded that type level and thickness of malignant melanomas can be evaluated in retrospective studies if central cross sections of the melanomas are available for histological examination

Key words Malignant melanoma cutaneous classification

Knud Sondergaard Department of Pathology the Finsen Institute Strandboulevarden 49 2100 Copenhagen Denmark

Accepted as submitted 3 III 80

The most widely used histological parameters in the prognostic evaluation of primary cutaneous malignant melanoma are the types of melanoma and the level of invasion

evaluate the frequency of incorrect histological grouping when only selected parts of the lesions are examined microscopically as may be the case in retrospective studies

MATERIAL AND METHODS

The material consisted of 55 cutaneous melanomas operated at the Finsen Institute during the period July 1976 to June 1977 The size of the lesions was 3 mm

bl...
pa...
2

- 2 Dabew D & Struck H Microliter determination of free hydroxyproline in blood serum Biochem Med 5 17-21 1971
- 3 Dingle J T Fell H B & Coombs R R A The breakdown of embryonic cartilage and bone cultured in the presence of complement sufficient antiserum 2 Biochemical changes and the role of lysosomal system Int Arch Allergy 31 283-303 1967
- 4 Documenta Geigy Scientific Tables Diem K (Ed) 7th ed J R Geigy SA Basel 1975 pp 164-165 and p 192
- 5 Dziak R Hausmann E & Chang Y W Effects of lipopolysaccharides and prostaglandins on rat bone cell calcium and cyclic AMP Arch oral Biol 24 347-353 1979
- 6 Galanos C Physical state and biological activity of lipopolysaccharides Toxicity and immunogenicity of the lipid A component Z Immun Forsch 149 214-229 1975
- 7 Hausmann E Raisz L G & Miller W A Endotoxin stimulation of bone resorption in tissue culture Science 168 862-864 1970
- 8 Hausmann E Weinfeld N & Miller W A Effects of lipopolysaccharides on bone resorption in tissue culture Calc Tiss Res 9 272-282 1972
- 9 Hausmann E Luderitz O Knox K & Weinfeld N Structural requirements for bone resorption by endotoxin and lipoteichoic acid J dent Res 54B 94-99 1975
- 10 Hofstad T The distribution of heptose and 2 keto 3 deoxy octonate in Bacteroides J gen Microbiol 85 314-320 1974
- 11 Rowe D J & Hausmann E Quantitative analyses of osteoclast changes in resorbing bone organ cultures Calc Tiss Res 23 283-289 1977
- 12 Sveen A The capacity of lipopolysaccharides from Bacteroides Fusobacterium and Veillonella to produce skin inflammation and the local and generalized Schwartzman reaction in rabbits J periodont Res 12 340-350 1977
- 13 Sveen K Rabbit polymorphonuclear leukocyte migration in vitro in response to lipopolysaccharides from Bacteroides Fusobacterium and Veillonella Acta path microbiol scand Sect B 85 374-380 1977
- 14 Sveen K Rabbit polymorphonuclear leukocyte 1977
- 15 Sveen K The importance of C5 and the role of the alternative complement pathway in leukocyte chemotaxis induced in vivo and in vitro by Bacteroides fragilis lipopolysaccharide Acta path microbiol scand Sect B 85 93-100 1978
- 16 Sveen K Rabbit polymorphonuclear leukocyte chemotactic factor generated in vivo by Bacteroides fragilis lipopolysaccharide I Isolation and physicochemical characterization Acta path microbiol scand Sect B 86 226-236 1978
- 17 Sveen K Rabbit polymorphonuclear leukocyte chemotactic factor generated in vivo by Bacteroides fragilis lipopolysaccharide II Antigenic and biologic properties Acta path microbiol scand Sect B 86 237-245 1978
- 18 Sveen K & Hofstad T Use of preformed cavity in rabbits for the quantitation of leukocyte chemotaxis caused by bacterial lipopolysaccharides Acta path microbiol scand Sect B 84 252-258 1977
- 19 Sveen K Hofstad T & Milner K C Lethality to mice and chick embryos pyrogenicity in rabbits and ability to gelate lysate from amoebocytes of Limulus polyphemus by lipopolysaccharides from Bacteroides Fusobacterium and Veillonella Acta path microbiol scand Sect B 85 388-396 1977
- 20 Westphal O Luderitz O & Bister F Über die Extraktion von Bakterien mit Phenol/Wasser Z Naturforsch 7B 148-155 1952
- 21 ..
- 22 Zachrisson B U Mast cells of the gingiva IV Experimental gingivitis J periodont Res 4 46-55 1968

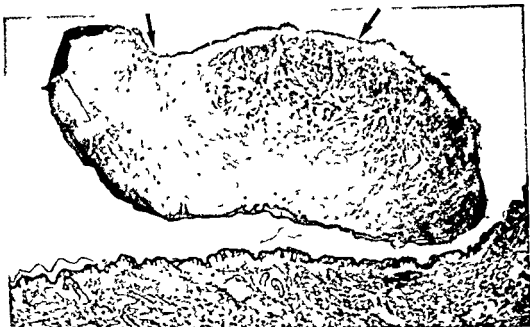


Fig 2 A section from the peripheral part of a polypoidal malignant melanoma graded as NM level II. The polypoidal part of the tumour is massively infiltrated by melanoma cells and the upper surface is ulcerated (arrows). Haematoxylin and eosin $\times 14$.

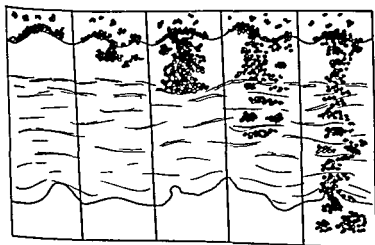
tumour cells were present there the block was typed NM.

2) *Level of invasion* was graded according to the description by Clark *et al* (5) as shown in Fig 3. Level I indicated that the tumour cells were confined to the epidermis. Level II indicated tumour cells which extended into the papillary dermis but did not reach the reticular dermis. The level III tumour cells impinged

upon the interface between the papillary and the reticular dermis but did not invade the reticular dermis. Level IV designated tumour cells clearly extending between the collagen bundles of the reticular dermis and the level V tumour invasion progressed into the subcutaneous fat.

3) *Tumour thickness* was measured on the histologic sections by means of an ocular micrometer as the maximal distance in mm from the top of the epidermal

LEVEL I LEVEL II LEVEL III LEVEL IV LEVEL V



EPIDERMIS

PAPILLARY DERMIS

RETICULAR DERMIS

SUBCUTANEOUS TISSUE

Fig 3 The levels of invasion used in this study.

the macroscopic photos of each lesion. The blocks were embedded in paraffin and 4 to 6 haematoxylin and eosin stained sections were prepared from each block.

The histological sections were mixed and randomly studied by light microscopy. Without the help of any clinical or other informations, each block was classified as to 1) type of melanoma, 2) level of invasion and 3) tumour thickness.

Criteria and Definitions

1) *Type of melanoma*. The following groups were used in the typing of the blocks.

Superficial spreading melanoma (SSM) characterized by an intra epidermal Pagetoid extension of atypical melanocytes. When dermal invasion was present the intra epidermal spread of tumour cells extended more than 3 rete ridges from areas of clear dermal invasion (5).

Lentigo maligna melanoma (LMM) characterized by a continuous proliferation of pleomorphic melanocytes in the basal layer of the epidermis. Epidermal atrophy and solar dermal elastosis were present (5). The group

included non invasive lesions (lentigo maligna) as well as invasive melanomas.

Acral lentiginous melanoma (ALM) characterized by lentiginous intra-epithelial proliferation of pleomorphic tumour cells extending more than 3 rete ridges from areas of dermal invasion. Marked acanthosis and elongation of rete ridges was present (9).

Nodular melanoma (NM) being an invasive melanoma with peripheral intra epidermal spread of tumour cells extending less than 4 rete ridges from areas of dermal invasion (5).

Melanomas of unclassifiable type designating melanomas not included in the above mentioned groups.

Nevoid lesions designating blocks containing too little tumour tissue for the diagnosis of invasive or non invasive melanoma to be made.

The serial blocking of polypoidal melanomas (Fig. 1) resulted in a number of blocks without visible connection between the polypoidal part of the melanoma and the skin (Fig. 2). The typing of such blocks was based on the growth pattern of tumour in the underlying skin. If

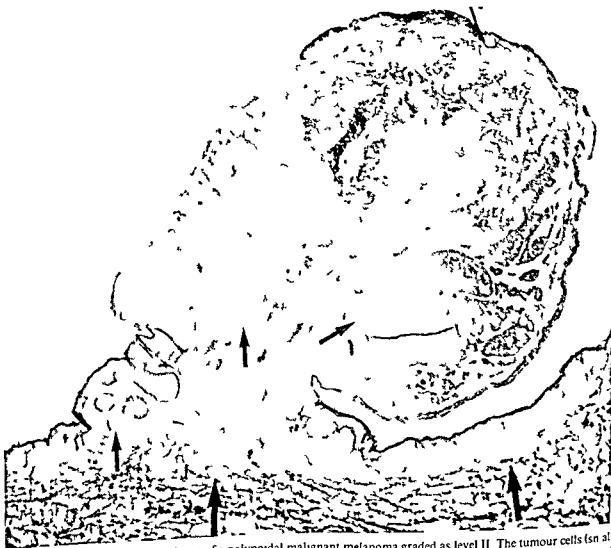


Fig. 1. A section from the central part of a polypoidal malignant melanoma graded as level II. The tumour cells (small arrows) do not reach the interface between the papillary and the reticular dermis (large arrows). Haematoxylin and eosin $\times 14$.

TABLE 3 The Tumour Thickness of 55 Melanomas and the Rate of Consistency between Tumour Thickness of the Central Block and that of the Whole Tumour Correlated to the Type of Melanoma

The overall type of 55 melanomas		The overall thickness of 55 melanomas (mm)						Central blocks with thickness consistent with that of the whole tumour		
Type	Number	0-0.75	0.76-1.50	1.51-2.25	2.26-3.00	3.01-6.00	>6.00	Number	%	95% confidence limits
SSM	44	6	6	9	7	11	5	42	95	85-99
LMM	4	1	0	0	0	1	2	4	100	40-100
ALM	1	0	0	0	0	1	0	1		
NM	6	0	0	0	1	2	3	5	83	36-100
Total	55	7	6	9	8	15	10	52	95	85-99

vel of invasion was consistent with that of the whole tumour (Table 2) whereas the level in 2 blocks diverged from that of the whole tumour. In 5% (170/261) of all blocks the level agreed with that of the whole tumour. In 91 blocks coming predominantly from the peripheral parts of the lesions the level diverged from that of the whole tumour.

Tumour thickness. Table 3 shows the distribution of the 55 melanomas according to the thickness of the whole tumour (7 lesions 0-0.75 mm, 6 lesions 0.76-1.50 mm, 9 lesions 1.51-2.25 mm, 8 lesions 2.26-3.00 mm, 15 lesions 3.01-6.00 mm and 10 lesions more than 6.00 mm). In 95% (52/55) of the central blocks the tumour thickness was in the same group as that of the whole tumour (Table 3). In 2 central blocks the thickness diverged from that of the whole tumour. In 65% (169/261) of all the blocks the thickness corresponded with that of the whole tumour. In 92 blocks coming predominantly from the peripheral parts of the melanomas the thickness diverged from that of the whole tumour.

DISCUSSION

Type of melanoma. In 1969 Clark *et al.* (5) demonstrated the prognostic significance of a histologic classification of primary cutaneous melanomas into 3 types (SSM, LMM and NM). Recently Reed (9) found that melanomas on the palm of the hand and on the sole of the foot diverged histologically from Clark's 3 types of melanoma and he proposed the new subtype named ALM. SSM, LMM and ALM are characterized by different patterns of intra-epithelial proliferation of tumour cells in the periphery of the lesions in contrast to NM. However the type of melanoma is

unclassifiable in a number of cases. The more tissue blocks available from each tumour the fewer unclassifiable lesions (6). In the present study 95% (52/55) of the central blocks showed a type

of the central cross section and that of the whole tumour.

Level of invasion. In 1969 the prognostic importance of the grading of the depth of invasion of cutaneous melanomas on 5 levels (Fig. 3) was demonstrated by Clark *et al.* (5). However this method involves some problems. Suffin *et al.* (10) tested the comparability of grading of the depth of invasion done by a number of pathologists using Clark's levels. An initial disagreement was found regarding the classification of level II and level III and agreement was reached only after instruction by Dr W. H. Clark. In the present study the level of invasion of 96% (53/55) of the central blocks was consistent with that of the whole tumour. This corresponds reasonably with the impression of Hermanek *et al.* (7) that a few sections from the most prominent part of a melanoma are sufficient to classify the level of invasion.

Tumour thickness. In 1970 Breslow (1) showed that the prognosis of cutaneous melanomas depended on their thickness defined as the greatest distance in mm from the epidermal granular cell layer to the deepest invasion of tumour. 5 groups were used (0-0.75 mm, 0.76-1.50 mm, 1.51-2.25 mm, 2.26-3.00 mm and more than 3.00 mm) (1) and the greater the thickness the poorer the prognosis (1, 2). A problem of this method is that an artificial increase in tumour thickness will be measured if the tumour is not cut at 90 degrees to the surface of the skin. A gross error of 22.5

granular cell layer to the deepest point of tumour invasion, as described by Breslow (1, 2). The thickness was measured at 90 degrees to the skin surface (4). In ulcerated lesions the thickness was measured from the most superficially placed tumour cells in the ulcer base to the deepest tumour invasion (2, 4).

In blocks without visible connection between the polypoidal part of a melanoma and the skin (Fig. 2) the thickness was measured from the granular cell layer of the upper epidermal lining of the polypoidal part to the deepest invasive tumour cells in the polypoidal part. If a greater distance was found from the epidermal granular cell layer of the underlying skin to tumour cells invading the corium or the subcutis, this distance was used.

In melanomas without dermal invasion the thickness was designated as 0 mm. In the evaluation of the results 6 groups were used: 0-0.75 mm, 0.76-1.50 mm, 1.51-2.25 mm, 2.26-3.00 mm, 3.01-6.00 mm, and more than 6.00 mm.

Finally the overall type of melanoma, level of invasion and tumour thickness were designated. The overall type of each of the 55 melanomas was found by reviewing all the sections of each melanoma. The overall level of invasion and the overall tumour thickness of the whole tumour were indicated as the deepest level and the greatest thickness found in one or more sections of the tumour.

In the present study the classification of the melanomas was based on the principles demonstrated and discussed by Dr W. H. Clark and Dr A. Breslow (11).

RESULTS

The material consisted of 10 polypoidal melanomas (Fig. 1) and 45 non-polypoidal melanomas. The serial blocking resulted in 261 tissue blocks. In 10 tissue blocks no connection was seen between the polypoidal part of the melanoma and the skin (Fig. 2).

Type of melanoma. Based on all the blocks the material included 44 SSM, 4 LMM, 1 ALM and 6

TARIF 1 The Overall Type of 55 Melanomas

The overall type of each melanoma		Central blocks with type consistent with that of the whole tumour		
Type	Number	Number	%	95% confidence limits
SSM	44	42	95	85-95
LMM	4	3	75	19-95
ALM	1	1		
NM	6	6	100	54-100
Total	55	52	95	85-95

NM (Table 1). In 95% (52/55) of the lesions the type of melanoma based on the central block was consistent with that of the whole tumour.

In 26 blocks the type was in agreement with that of the whole tumour. In 26 blocks the type was different from that of the whole tumour: 11 blocks from the peripheral parts of the melanomas were graded as nevus lesions, 8 blocks showed melanomas of unclassifiable type, whereas 7 blocks showed melanomas without lateral intra-epidermal tumour invasion although they originated from melanomas classified as SSM and LMM.

Level of invasion. By using all the blocks the following distribution of the 55 melanomas was found: 1 lesion level I, 4 lesions level II, 21 lesions level III, 21 lesions level IV, and 8 lesions level V (Table 2). In 96% (53/55) of the central blocks the

TABLE 2 The Level of Invasion of 55 Melanomas and the Rate of Consistency between the Level of Invasion of the Central Block and that of the Whole Tumour

The overall type of 55 melanomas		The overall level of 55 melanomas					Central blocks with levels consistent with that of the whole tumour		
Type	Number	I	II	III	IV	V	Number	%	95% confidence limits
SSM	44	0	4	19	17	4	43	98	88-100
LMM	4	1	0	0	1	2	4	100	40-100
ALM	1	0	0	0	1	0	1		
NM	6	0	0	2	2	2	5	83	36-100
Total	55	1	4	21	21	8	53	96	87-100

MALIGNANT MELANOMA OF THE FOOT

A Clinicopathological Study of 125 Primary Cutaneous Malignant Melanomas

KNUD SØNDERGAARD and GRETE OLSEN

Department of Pathology and Department of Plastic Surgery, the Finsen Institute, Copenhagen, Denmark

Søndergaard K. & Olsen G. Malignant melanoma of the foot. A clinicopathological study of 125 primary cutaneous malignant melanomas. Acta path. microbiol. scand. Sect. A 88: 275-283, 1980.

In a retrospective study of 125 primary cutaneous malignant melanomas of the foot treated from 1949 to 1977 the prognostic importance of various histological and clinical factors was observed. Clinical stage, location of tumour on the foot, level of invasion, tumour thickness, mitotic rate and presence of ulceration correlated well with survival, while sex and histological type did not. A histological transition was found between the superficial spreading type and the acral lentiginous type, indicating a close biological relationship between the two types of melanoma.

Key words: Malignant melanoma, cutaneous, foot, classification.

Knud Søndergaard, Department of Pathology, the Finsen Institute, Strandboulevarden 49, 2100 Copenhagen, Denmark.

Accepted as submitted 3 III 80

Various studies have found primary malignant melanoma of the foot to account for 3-15% of the total number of primary skin melanomas (11, 15, 16, 19, 21). In 1969 Clark *et al.* (5) demonstrated the prognostic significance of a histological classification of primary cutaneous melanoma into 3 types (superficial spreading melanoma, nodular melanoma, and lentigo maligna melanoma). Recently Reed (24) described a new type of melanoma, acral lentiginous melanoma, on plantar and palmar surfaces.

A clinicopathologic study of 125 patients with malignant melanoma of the foot was undertaken in order both to investigate the frequency and prognostic importance of the new type of melanoma described by Reed and to estimate the prognostic significance of the following clinical and histological variables: Clinical stage, sex, site of tumour on the foot, type of melanoma according to Clark, level of invasion according to Clark, tumour thickness according to Breslow, mitotic rate and presence of ulceration.

MATERIAL AND METHODS

From 1949 to 1977 149 patients were operated on at the Finsen Institute for primary cutaneous malignant melanoma of the foot. In 126 patients the tumour was primarily excised, whereas 23 patients were admitted for extended excision after primary excision elsewhere. Inguinal lymph nodes were dissected where clinically enlarged. Postoperatively the patients received frequent follow-up examinations at the Finsen Institute (the Radium Centre and the Department of Plastic Surgery) for up to 10 years or more.

In 125 patients the histological material from the primary lesion was suitable for the microscopic classification, which was made by one of the authors (K.S.). The histological sections were stained by haematoxylin and eosin.

The Clinical Reporting of Patients with Melanoma of the Foot Included

1) *Site of tumour*: a) sub-/parungual region, b) planta pedis, and c) dorsum pedis, comprising the rest of the foot.

2) *Sex*

3) *Clinical Stage* as described by Olsen (19, 20)

degrees increases the apparent thickness by 9% (3). In the present study a 6th group was used (more than 6.00 mm) in order to separate very thick melanomas. By using these 6 groups 95% (52/55) of the central blocks showed a tumour thickness consistent with that of the whole tumour.

Conclusion The present study demonstrates a 4–5% inconsistency between the central block and the whole tumour with regard to the classification of type level and thickness. This means that it is possible to evaluate the prognostic significance of type level and thickness in retrospective studies provided that central cross sections are available for the histological examination. It can also be concluded that selected parts of a cutaneous melanoma may be removed for electron microscopic examination or other tissue analyses with only a minimal risk of interference with the histological classification if the most elevated part of the lesion is reserved for the microscopic evaluation.

Supported by grants from the *Danish Cancer Society* (Project No. 59/77).

REFERENCES

- 1 Breslow A. Thickness, cross sectional areas and depth of invasion in the prognosis of cutaneous melanoma. *Ann Surg* 172: 902–908 1970.
- 2 Breslow A. Tumour thickness, level of invasion, node dissection in stage I cutaneous melanoma. *Ann Surg* 182: 572–575 1975.
- 3 Breslow A. Problems in the measurement of tumour thickness and level of invasion in cutaneous melanoma. *Hum Path* 8: 1–2 1977.
- 4 Breslow A. Personal communication 1977.
- 5 Clark W H, From L, Bernardino E A & M, M C. The histogenesis and biologic behaviour of primary human malignant melanomas of the skin. *Cancer Res* 29: 705–727 1969.
- 6 Clark W H, Ainsworth A M, Bernardino E, Yang C H, Mihm M C & Reed R J. The developmental biology of primary human malignant melanomas. *Seminars in Oncology* 2: 83 1975.
- 7 Hermanek P, Hornstein O P, Tonak J, Weidner F. Malignes Melanom: Invasionstiefe, Melanomtyp. *Beitrage Pathol* 157: 269–282 1975.
- 8 Larsen T E. The Classification of primary cutaneous malignant melanoma. *Acta Path Microbiol Scand Sect A* 86: 451–459 1978.
- 9 Reed R J. New concepts in surgical pathology of the skin. 1st ed. John Wiley & Sons, New York 1976, pp. 89–90.
- 10 Suffin S C, Waisman J & Clark W. Congruence of diagnosis of malignant melanoma. *Lab Invest* 32: 436 1975.
- 11 Workshop supported by the International Cancer Research Workshop of the Union International Contre le Cancer. The histologic classification, morphologic characterization and clinicopathologic evaluation of malignant melanomas. *Melanoma* November 21–25 1977.

MALIGNANT MELANOMA OF THE FOOT

A Clinicopathological Study of 125 Primary Cutaneous Malignant Melanomas

KNUD SØNDERGAARD and GRETE OLSEN

Department of Pathology and Department of Plastic Surgery the Finsen Institute Copenhagen Denmark

Søndergaard K & Olsen G Malignant melanoma of the foot. A clinicopathological study of 125 primary cutaneous malignant melanomas Acta path microbiol scand Sect. A 88 275-283 1980

In a retrospective study of 125 primary cutaneous malignant melanomas of the foot treated from 1949 to 1977 the prognostic importance of various histological and clinical factors was observed. Clinical stage, location of tumour on the foot, level of invasion, tumour thickness, mitotic rate and presence of ulceration correlated well with survival while sex and histological type did not. A histological transition was found between the superficial spreading type and the acral lentiginous type indicating a close biological relationship between the two types of melanoma.

Key words: Malignant melanoma, cutaneous, foot, classification.

Knud Søndergaard, Department of Pathology, the Finsen Institute, Strandboulevarden 49, 2100 Copenhagen, Denmark.

Accepted as submitted 3 III 80

Various studies have found primary malignant melanoma of the foot to account for 3-15% of the total number of primary skin melanomas (11, 15, 16, 19, 21). In 1969 Clark *et al* (5) demonstrated the prognostic significance of a histological classification of primary cutaneous melanoma into 3 types (superficial spreading melanoma, nodular melanoma and lentigo maligna melanoma). Recently Reed (24) described a new type of melanoma, acral lentiginous melanoma, on plantar and palmar surfaces.

A clinicopathologic study of 125 patients with malignant melanoma of the foot was undertaken in order both to investigate the frequency and prognostic importance of the new type of melanoma described by Reed and to estimate the prognostic significance of the following clinical and histological variables: Clinical stage, sex, site of tumour on the foot, type of melanoma according to Clark, level of invasion according to Clark, tumour thickness according to Breslow, mitotic rate and presence of ulceration.

MATERIAL AND METHODS

From 1949 to 1977 149 patients were operated on at the Finsen Institute for primary cutaneous malignant melanoma of the foot. In 126 patients the tumour was primarily excised, whereas 23 patients were admitted for extended excision after primary excision elsewhere. Inguinal lymph nodes were dissected where clinically enlarged. Postoperatively the patients received frequent follow up examinations at the Finsen Institute (the Radium Centre and the Department of Plastic Surgery) for up to 10 years or more.

In 125 patients the histological material from the primary lesion was suitable for the microscopic classification, which was made by one of the authors (K.S.). The histological sections were stained by haematoxylin and eosin.

The Clinical Reporting of Patients with Melanoma of the Foot Included

1) *Site of tumour*: a) sub-/parungual region, b) plantar pedis and c) dorsum pedis, comprising the rest of the foot.

2) *Sex*

3) *Clinical Stage* as described by Olsen (19, 20)

degrees increases the apparent thickness by 9% (3). In the present study a 6th group was used (more than 6.00 mm) in order to separate very thick melanomas. By using these 6 groups 95% (52/55) of the central blocks showed a tumour thickness consistent with that of the whole tumour.

Conclusion The present study demonstrates a 4–5% inconsistency between the central block and the whole tumour with regard to the classification of type, level and thickness. This means that it is possible to evaluate the prognostic significance of type, level and thickness in retrospective studies provided that central cross sections are available for the histological examination. It can also be concluded that selected parts of a cutaneous melanoma may be removed for electron microscopic examination or other tissue analyses with only a minimal risk of interference with the histological classification if the most elevated part of the lesion is reserved for the microscopic evaluation.

Supported by grants from the *Danish Cancer Society* (Project No. 59/77).

REFERENCES

- 1 Breslow A. Thickness, cross sectional areas and depth of invasion in the prognosis of cutaneous melanoma. *Ann Surg* 172: 902–908 1970.
- 2 Breslow A. Tumour thickness, level of invasion and node dissection in stage I cutaneous melanoma. *Ann Surg* 182: 572–575 1975.
- 3 Breslow A. Problems in the measurement of tumour thickness and level of invasion in cutaneous melanoma. *Hum Path* 8: 1–2 1977.
- 4 Breslow A. Personal communication 1977.
- 5 Clark W H, From L, Bernardino E A & Mihm M C. The histogenesis and biologic behaviour of primary human malignant melanomas of the skin. *Cancer Res* 29: 705–727 1969.
- 6 Clark W H, Ainsworth A M, Bernardino E A, Yang C-H, Mihm M C & Reed R J. The developmental biology of primary human malignant melanomas. *Seminars in Oncology* 2: 83–111 1975.
- 7 Hermanek P, Hornstein O P, Tonak J. The histogenesis and biologic behaviour of primary human malignant melanomas of the skin. *Cancer Res* 29: 705–727 1969.
- 8 ---. The histogenesis and biologic behaviour of primary human malignant melanomas of the skin. *Cancer Res* 29: 705–727 1969.
- 9 Reed R J. New concepts in surgical pathology of the skin. 1st ed. John Wiley & Sons, New York 1976. pp. 89–90.
- 10 Suffin S C, Waisman J & Clark W H. Congruence of diagnosis of malignant melanoma. *Lab Invest* 32: 436 1975.
- 11 Workshop supported by the International Cancer Research Workshop of the Union Internationale Contre le Cancer. The histologic classification, morphologic characterization and clinicopathologic evaluation of malignant melanomas. *Mil Med* November 21–25 1977.

MALIGNANT MELANOMA OF THE FOOT

A Clinicopathological Study of 125 Primary Cutaneous Malignant Melanomas

KNUD SØNDERGAARD and GRETE OLSEN

Department of Pathology and Department of Plastic Surgery the Finsen Institute Copenhagen Denmark

Søndergaard K & Olsen G Malignant melanoma of the foot. A clinicopathological study of 125 primary cutaneous malignant melanomas. Acta path. microbiol. scand. Sect. A 88 275-283 1980

In a retrospective study of 125 primary cutaneous malignant melanomas of the foot treated from 1949 to 1977 the prognostic importance of various histological and clinical factors was observed. Clinical stage, location of tumour on the foot, level of invasion, tumour thickness, mitotic rate and presence of ulceration correlated well with survival, while sex and histological type did not. A histological transition was found between the superficial spreading type and the acral lentiginous type, indicating a close biological relationship between the two types of melanoma.

Key words: Malignant melanoma, cutaneous, foot, classification.

Knud Søndergaard, Department of Pathology, the Finsen Institute, Strandboulevarden 49, 2100 Copenhagen, Denmark.

Accepted as submitted 3 III 80

Various studies have found primary malignant melanoma of the foot to account for 3-15% of the total number of primary skin melanomas (11, 15, 16, 19, 21). In 1969 Clark *et al.* (5) demonstrated the prognostic significance of a histological classification of primary cutaneous melanoma into 3 types (superficial spreading melanoma, nodular melanoma and lentigo maligna melanoma). Recently Reed (24) described a new type of melanoma, acral lentiginous melanoma, on plantar and palmar surfaces.

A clinicopathologic study of 125 patients with malignant melanoma of the foot was undertaken in order both to investigate the frequency and prognostic importance of the new type of melanoma described by Reed and to estimate the prognostic significance of the following clinical and histological variables: Clinical stage, sex, site of tumour on the foot, type of melanoma according to Clark, level of invasion according to Clark, tumour thickness according to Clark, and presence of

MATERIAL AND METHODS

From 1949 to 1977 149 patients were operated on at the Finsen Institute for primary cutaneous malignant melanoma of the foot. In 126 patients the tumour was primarily excised, whereas 23 patients were admitted for extended excision after primary excision elsewhere. Inguinal lymph nodes were dissected where clinically enlarged. Postoperatively the patients received frequent follow-up examinations at the Finsen Institute (the Radium Centre and the Department of Plastic Surgery) for up to 10 years or more.

In 125 patients the histological material from the primary lesion was suitable for the microscopic classification, which was made by one of the authors (K.S.). The histological sections were stained by haematoxylin and eosin.

The Clinical Reporting of Patients with Melanoma of the Foot Included

1) *Site of tumour:* a) sub-/parungual region, b) planta pedis, and c) dorsum pedis, comprising the rest of the foot.

2) *Sex*

3) *Clinical Stage* as described by Olsen (19, 20)

degrees increases the apparent thickness by 9% (3). In the present study a 6th group was used (more than 6.00 mm) in order to separate very thick melanomas. By using these 6 groups 95% (52/55) of the central blocks showed a tumour thickness consistent with that of the whole tumour.

Conclusion The present study demonstrates a 4–5% inconsistency between the central block and the whole tumour with regard to the classification of type, level and thickness. This means that it is possible to evaluate the prognostic significance of type, level and thickness in retrospective studies provided that central cross sections are available for the histological examination. It can also be concluded that selected parts of a cutaneous melanoma may be removed for electron microscopic examination or other tissue analyses with only a minimal risk of interference with the histological classification if the most elevated part of the lesion is reserved for the microscopic evaluation.

Supported by grants from the Danish Cancer Society (Project No. 59/77).

REFERENCES

- 1 Breslow A. Thickness, cross sectional areas and depth of invasion in the prognosis of cutaneous melanoma. *Ann Surg* 172: 902–908, 1970.

- 2 Breslow A. Tumour thickness, level of invasion & node dissection in stage I cutaneous melanoma. *Ann Surg* 182: 572–575, 1975.
- 3 Breslow A. Problems in the measurement of tumour thickness and level of invasion in cutaneous melanoma. *Hum Path* 8: 1–2, 1977.
- 4 Breslow A. Personal communication, 1977.
- 5 Clark W H, From L, Bernardino E A & Mihm M C. The histogenesis and biologic behaviour of primary human malignant melanomas of the skin. *Cancer Res* 29: 705–727, 1969.
- 6 Clark W H, Ainsworth A M, Bernardino E A, Yang C-H, Mihm M C & Reed R J. The developmental biology of primary human malignant melanomas. *Seminars in Oncology* 2: 83–10, 1975.
- 7 Hermanek P, Hornstein O P, Tonak J.
- 8 cutaneous malignant melanoma. *Acta Pathol Microbiol Scand Sect A* 86: 451–459, 1978.
- 9 Reed R J. New concepts in surgical pathology of the skin. 1st ed. John Wiley & Sons, New York, 1976, pp. 89–90.
- 10 Suffin S C, Waisman J & Clark W H. Congruence of diagnosis of malignant melanoma. *Lab Invest* 32: 436, 1975.
- 11 Workshop supported by the International Cancer Research Workshop of the Union Internationale Contre le Cancer. The histologic classification, morphologic characterization and clinicopathological evaluation of malignant melanomas. *Mila* November 21–25, 1977.

Fig 1 Malignant melanoma, superficial spreading type (SSM) Planta. Marked Pagetoid extension of tumour cells into the hyperplastic epidermis is seen. No dermal invasion is found in this area. Haematoxylin and eosin. X 130

Fig 2 Malignant melanoma, acral lentiginous type (ALM) Sub-/parungual region. A lentiginous pattern of tumour cells is seen in the hyperplastic epidermis. No dermal invasion is found in this area. Haematoxylin and eosin. X 130

Fig 3 Malignant melanoma, histologically intermediate between superficial spreading melanoma and acral lentiginous melanoma (SSM ALM) Planta. In this area of tumour moderate Pagetoid extension of tumour cells is present as well as lentiginous growth pattern and epidermal hyperplasia. Haematoxylin and eosin. X 130

Fig 4 Malignant melanoma, nodular type (NM) Dorsum. No adjacent intra-epidermal extension of tumour cells is present. Haematoxylin and eosin. X 130

Stage I No clinical signs of metastases

Stage II Clinically enlarged and suspicious inguinal lymph nodes and/or a few cutaneous metastases close to the primary lesion

Stage III Other signs of metastases, i.e. further groups of lymph nodes, cutaneous metastases along the lymphatic trunks, remote cutaneous metastases and visceral and cerebral metastases

The Histological Evaluation of the Melanomas Included

1) The histological type of melanoma according to Clark *et al* (5) and Reed (24) as previously described by Sundergaard (26):

Superficial spreading melanoma (SSM) (Fig 1)

Lentigo maligna melanoma (LM) (Fig 2)

Acral lentiginous melanoma (ALM) (Fig 2)

Nodular melanoma (NM) (Fig 4)

Melanoma of unclassifiable type

2. Level of invasion was graded according to Clark *et al* (5) as described by Sundergaard (26): Level I ~ epidermis, level II ~ papillary dermis, level III ~ papillary-reticular interface, level IV ~ reticular dermis and level V ~ subcutis. Polypoidal melanomas

in which tumour cells did not reach the papillary-reticular interface were named level PM II

3. Tumour thickness was measured in mm from the top of the epidermal granular cell layer to the deepest point of tumour invasion as described by Breslow (3, 4)

4. Mitotic rate: In at least 1 mm² (using high power fields X 400) the mitoses were counted and converted to 1.0 mm² by πr^2 . In our microscope the area of 10 high power fields (diameter 0.35 mm) was 0.96 mm², i.e. very close to 1 mm²

5. Ulceration: Size of ulceration if any was measured in mm by an ocular micrometer on the histological cross section of the tumour

Statistical Analysis

The cumulative survival rates were calculated by the life table method and compared by the Logrank test (2, 23). Where appropriate Chi² test was used. Significance was assessed at P less than 0.05

RESULTS

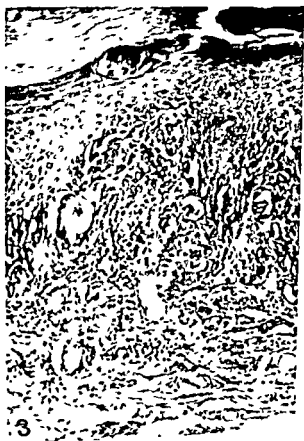
In 125 patients the histological material from the primary lesion was available and suitable for microscopic classification. From each tumour 1-5 cross sectional tissue blocks including the central part of the tumour were preserved.

The age of the patients varied from 22 to 94 years (mean value 60 years). 45 patients (36%) were under and 80 (64%) over 55 years of age.

Site of melanoma: 14 melanomas (11%) were localized sub-/parungually, 50 (40%) at planta and 61 (49%) at dorsum. The 10 year survival rates were: Sub-/parungual 21%, planta 40%, and dorsum 55% (Fig 5a). In patients with sub-/parungual melanoma the survival rate was significantly lower than in patients with lesions of the rest of the foot ($X^2 = 4.073$, df 1, $P < 0.05$). In patients with melanoma at planta the survival rate was lower than in patients with melanoma at dorsum but the difference was not significant ($X^2 = 1.552$, df 1, $P > 0.2$).

TABLE 1 Sex of 125 Patients with Melanomas of the Foot Correlated to the Site of Tumour

Sex	Sub-/parung		Planta		Dorsum		Total	
	No	%	No	%	No	%	No	%
Male	5	36	17	34	19	31	41	33
Female	9	64	33	66	42	69	84	67
Total	14	100	50	100	61	100	125	100



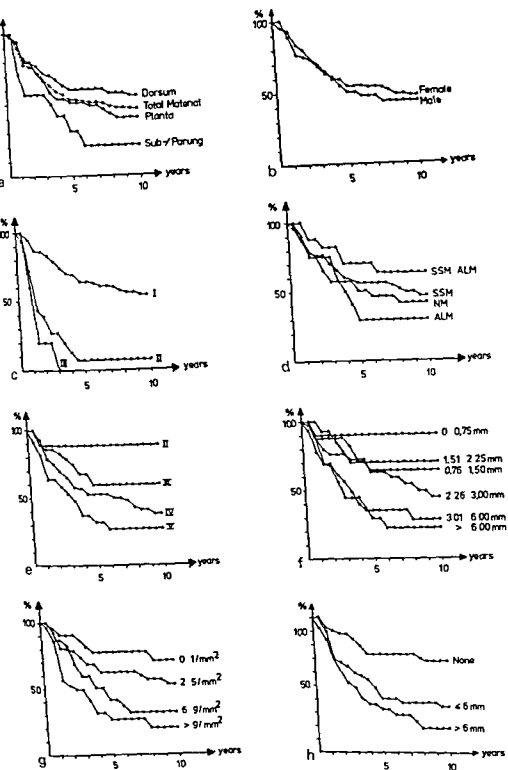


Fig 5 Cumulative survival rates for patients with malignant melanoma of the foot according to (a) site of the foot (125 patients); (b) sex (125 patients); (c) clinical stage (125 patients); (d) type (120 patients); (e) level of invasion (121 patients); (f) tumour thickness (124 patients); (g) mitotic rate (118 patients); and (h) ulceration (125 patients)

TABLE 2 *Clinical Stage of 125 Melanomas of the Foot Correlated to the Site of Tumour*

Clinical Stage	Sub /parung		Planta		Dorsum		Total	
	No	%	No	%	No	%	No	%
I	9	64	39	78	54	88	102	82
II	2	14	10	20	6	10	18	14
III	3	22	1	2	1	2	5	4
Total	14	100	50	100	61	100	125	100

Sex Of the 125 patients 84 were female and 41 male Table 1 demonstrates that the proportion of melanomas in each of the various regions of the foot was 21 women to men

The 10 year survival rates for women and men showed no significant difference ($X^2 = 0.094$ df 1 $P > 0.7$) (Fig 5b)

Clinical stage 102 patients were in stage I 18 in stage II and 5 in stage III Table 2 shows the regional distribution of lesions The 10 year survival was significantly higher for stage I patients (54%) than for stage II (7%) or III (0%) patients ($X^2 = 42.047$ df = 1 $P < 0.0005$) (Fig 5c)

Histological type Of 125 melanomas 55 were SSM 28 NM 20 ALM none LMM and 22 unclassifiable 17 of the unclassifiable melanomas histologically took up a position intermediate between SSM and ALM and were named SSM ALM A lentiginous proliferation of tumour cells was found as well as areas with moderate Pagetoid extension of tumour cells (Fig 3) In the remaining 5 melanomas of unclassifiable type it was uncertain whether or not the lateral intra-epidermal prolifera-

tion of tumour cells extended more than 3 rete ridges beyond areas of clear dermal invasion i.e. whether the melanomas were NM or melanomas with adjacent intra-epidermal component (ACM) (17) The 5 melanomas were designated NM ACM

As shown in Table 3 ALM and SSM ALM predominantly were localized sub /parungually and at planta The different types (SSM NM ALM and SSM ALM) did not influence the 10 year survival rate significantly ($X^2 = 3.061$ df 3 $P > 0.3$) (Fig 5d)

Level of invasion Of 121 melanomas 9 showed level II 29 level III 61 level IV and 22 level V In 2 patients polypoidal lesions level PM II were found One of these patients died of metastases 1/ years after operation while the other was still alive 7/ years after operation Further 2 melanomas were unclassifiable because of a very illdefined papillary reticular interface

Only one patient with a sub /parungual melanoma level II (and tumour thickness 0.64 mm) died of metastases half a year after operation Histologically total regression of the central part of the tumour was noted which was in agreement with

TABLE 3 *Histological Type of 125 Melanomas of the Foot Correlated to the Site of Tumour*

Histological Type	Sub /parung		Planta		Dorsum		Total	
	No	%	No	%	No	%	No	%
SSM	3	21	17	34	35	57	55	44
NM	4	29	7	14	17	28	28	22
ALM	5	36	12	24	3	5	20	16
SSM ALM	2	14	11	22	4	7	17	14
NM ACM	0	0	3	6	2	3	5	4
Total	14	100	50	100	61	100	125	100

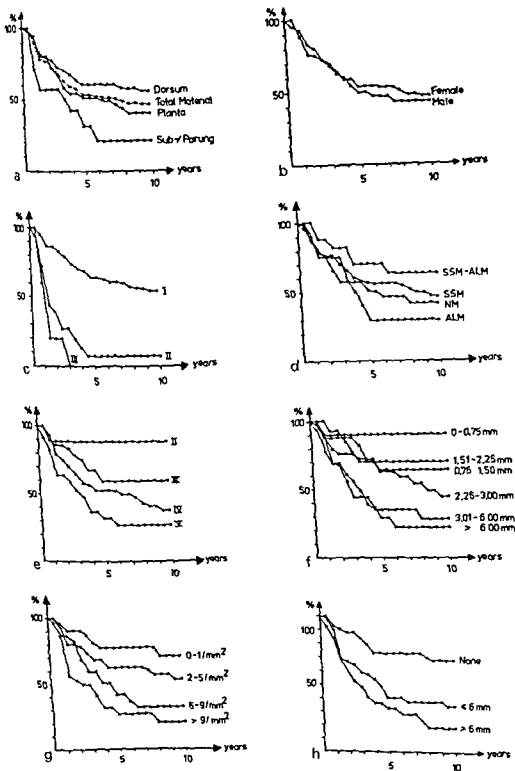


Fig 5 Cumulative survival rates for patients with malignant melanoma of the foot according to (a) site of the foot (125 patients) (b) sex (125 patients) (c) clinical stage (125 patients) (d) type (120 patients) (e) level of invasion (121 : 118 patients) and (h) ulceration (125 patients)

TABLE 4 *Level of Invasion of 125 Melanomas of the Foot Correlated to the Site of Tumour*

Level of Invasion	Sub /parung		Planta		Dorsum		Total	
	No	%	No	%	No	%	No	%
II	2	14	2	4	5	8	9	7
PM II	0	0	0	0	2	3	2	2
III	5	36	10	20	14	23	29	23
IV	3	21	29	58	29	48	61	48
V	4	29	9	18	9	15	22	18
Unclass	0	0	0	0	2	3	2	2
Total	14	100	50	100	61	100	125	100

TABLE 5 *Tumour Thickness of 125 Melanomas of the Foot Correlated to the Site of Tumour*

Tumour Thickness (mm)	Sub /parung		Planta		Dorsum		Total	
	No	%	No	%	No	%	No	%
0 -0.75	2	14	1	2	7	11	10	8
0.76-1.50	4	29	4	8	9	15	17	13
1.51-2.25	1	7	9	18	4	7	14	11
2.26-3.00	2	14	12	24	11	18	25	20
3.01-6.00	2	14	19	38	21	34	42	34
>6.00	3	22	5	10	8	13	16	13
Unclass	0	0	0	0	1	2	1	1
Total	14	100	50	100	61	100	125	100

TABLE 6 *Mitotic Rate of 125 Melanomas of the Foot Correlated to the Site of Tumour*

Mitoses/mm ²	Sub /parung		Planta		Dorsum		Total	
	No	%	No	%	No	%	No	%
0-1	1	7	9	18	13	21	23	18
2-5	4	29	13	26	25	41	42	34
6-9	2	14	11	22	10	16	23	18
>9	3	21	15	30	12	20	30	24
Unclass	4	29	2	4	1	2	7	6
Total	14	100	50	100	61	100	125	100

TABLE 7 *Ulceration of 125 Melanomas of the Foot Correlated to the Site of Tumour*

Ulceration (mm)	Sub /parung		Planta		Dorsum		Total	
	No	%	No	%	No	%	No	%
0	3	21	20	40	35	58	58	46
≤ 6	6	43	20	40	16	26	42	34
> 6	5	36	10	20	10	16	25	20
Total	14	100	50	100	61	100	125	100

information from the patient that the flat lesion originally had been elevated

10 year survival decreased significantly by deeper invasion Level II 89% level III 60% level IV 38% and level V 27% ($T=10.515$ df 1 $P<0.005$) (Fig 5c)

Table 4 shows that the frequency of lesions level II and III was greater in sub-/parungual region (7/14 50%) than in the rest of the foot (31/107 29%), but the difference was not significant ($X^2 2.541$ df 1 $P>0.1$)

Tumour thickness Of 124 melanomas 10 showed a thickness of 0-0.75 mm 17 of 0.76-1.50 mm 14 of 1.51-2.25 mm 25 of 2.26-3.00 mm 42 of 3.01-6.00 mm and 16 of >6.00 mm One melanoma was unclassifiable as it obviously had not been cut perpendicular to the original skin surface As described above only one melanoma less than 0.76 mm thick (and level II) with severe regression of the central part of the tumour metastasized causing the patient's death

The 10 year survival diminished significantly with increasing thickness 0-0.75 mm 90% 0.76-1.50 mm 64% 1.51-2.25 mm 70% 2.26-3.00 mm 44% 3.01-6.00 mm 28% and >6.00 mm 22% ($T 16.109$ df 1 $P<0.0005$) (Fig 5d)

Table 5 shows that tumours measuring less than 1.51 mm constituted a significantly greater proportion of sub-/parungual melanomas (6/14 43%) than of melanomas of the rest of the foot (21/110 19%) ($X^2 4.118$ df 1 $P<0.05$)

Mitotic rate Of 118 lesions 23 showed 0-1 mitoses/mm² 42 2-5 mitoses/mm² 23 6-9 mitoses/mm² and 30 >9 mitoses/mm² 7 melanomas were too small to permit examination of 1 mm² tumour tissue

The 10 year survival decreased significantly with increasing mitotic rate 0-1 mitoses/mm² 71% 2-5 mitoses/mm² 53% 6-9 mitoses/mm² 32% and more than 9 mitoses/mm² 20% ($T=15.982$ df 1 $P<0.0005$) (Fig 5g)

Table 6 shows an equal mitotic activity in the various regions

Ulceration Of 125 melanomas 67 were ulcerated. Ulceration was 6 mm or less in 42 lesions and deeper in 25

of 118 df 1 $P<0.0005$) (Fig 5h)

Table 7 shows that 79% (11/14) of sub-/parungual melanomas were ulcerated as opposed to

60% (30/50) of planta and 42% (26/61) of dorsum

DISCUSSION

The present study comprised all patients operated on at the Finsen Institute for primary malignant melanoma of the foot in the period from 1949 to 1977 where the histological material was available and suitable for microscopic classification

Part of the material has previously been published (19, 20). As shown by Søndergaard (26) it is possible to evaluate the prognostic significance of histological type, level of invasion and tumour thickness without serial blocking of the melanomas provided that at least one cross section through the most elevated part of the lesion is preserved for the histological examination. As far as we know this requirement is fulfilled in the present material.

Though the age of the patients varied from 22 to 94 years 64% (80/125) were older than 54 which is in accordance with the findings of Petersen (22) and Magnus (15).

11% (14/125) of the melanomas were located sub-/parungually 40% (50/125) were of planta and 49% (61/125) of dorsum.

The survival rate was significantly lower for patients with sub-/parungual melanomas than for patients with melanomas of the rest of the foot despite the fact that the sub-/parungual melanomas were not as thick or as deeply invading as the tumours of the planta and dorsum. Melanoma in planta indicated a poorer prognosis than melanoma of the dorsum but the difference was not significant ($P=0.12$).

It ought to be particularly high in toes and planta which may explain the very high mortality from melanomas of sub-/parungual region and planta.

As was the case in other studies (9, 11, 15, 16, 19, 22, 27) we found more women than men in the material. The proportion of men was 55%.

Of the 125 patients 82% were noted

82% of the patients were in clinical stage I which is more than expected. This is explained by the greater frequency of insufficient histological material in patients stage II and III than in patients stage I. At time of operation patients with sub-/parungual lesions presented metastases more often.

Of the 125 patients

TABLE 4 *Level of Invasion of 125 Melanomas of the Foot Correlated to the Site of Tumour*

Level of Invasion	Sub /parung		Planta		Dorsum		Total	
	No	%	No	%	No	%	No	%
II	2	14	2	4	5	8	9	7
PM II	0	0	0	0	2	3	2	2
III	5	36	10	20	14	23	29	23
IV	3	21	29	58	29	48	61	48
V	4	29	9	18	9	15	22	18
Unclass	0	0	0	0	2	3	2	2
Total	14	100	50	100	61	100	125	100

TABLE 5 *Tumour Thickness of 125 Melanomas of the Foot Correlated to the Site of Tumour*

Tumour Thickness (mm)	Sub /parung		Planta		Dorsum		Total	
	No	%	No	%	No	%	No	%
0-0.75	2	14	1	2	7	11	10	8
0.76-1.50	4	29	4	8	9	15	17	13
1.51-2.25	1	7	9	18	4	7	14	11
2.26-3.00	2	14	12	24	11	18	25	20
3.01-6.00	2	14	19	38	21	34	42	34
>6.00	3	22	5	10	8	13	16	13
Unclass	0	0	0	0	1	2	1	1
Total	14	100	50	100	61	100	125	100

TABLE 6 *Mitotic Rate of 125 Melanomas of the Foot Correlated to the Site of Tumour*

Mitoses/mm ²	Sub /parung		Planta		Dorsum		Total	
	No	%	No	%	No	%	No	%
0-1	1	7	9	18	13	21	23	18
2-5	4	29	13	26	25	41	42	34
6-9	2	14	11	22	10	16	23	18
>9	3	21	15	30	12	20	30	24
Unclass	4	29	2	4	1	2	7	6
Total	14	100	50	100	61	100	125	100

TABLE 7 *Ulceration of 125 Melanomas of the Foot Correlated to the Site of Tumour*

Ulceration (mm)	Sub /parung		Planta		Dorsum		Total	
	No	%	No	%	No	%	No	%
0	3	21	20	40	35	58	58	46
≤6	6	43	20	40	16	26	42	34
>6	5	36	10	20	10	16	25	20
Total	14	100	50	100	61	100	125	100

- 1 Bonnerie O Juhl E Andersen B & Winkel P Overlevelsesmodeller i klinisk forskning Ugeskr Læg 133 1859-1864 1971
- 2 Breslow A Thickness cross sectional areas and depth of invasion in the prognosis of cutaneous melanoma Ann Surg 172 902-908 1970
- 3 Breslow A Tumour thickness level of invasion and node dissection in stage I cutaneous melanoma Ann Surg 182 572-575 1975
- 4 Clark W H From L Bernardino E A & Mihm M C The histogenesis and biologic behaviour of primary human malignant melanomas of the skin Cancer Res 29 705-727 1969
- 5 Clark W H Bernardino E A Reed R J & Kopf A W Acral lentiginous melanomas including melanomas of mucous membranes Human malignant melanoma Clinical oncology monographs Grune & Stratton New York 1979 pp 109-124
- 6 Cochran A J Histology and prognosis in malignant melanoma J Path 97 459-468 1969
- 7 Donnellan M J Seemayer T Huvos A G Mike V & Strong E W Clinicopathologic study of cutaneous melanoma of the head and neck Am J Surg 124 450-455 1972
- 8 Eldh J Boeryd B & Peterson L E Prognostic factors in cutaneous malignant melanoma in stage I A clinical morphological and multivariate analysis Scand J Plast Reconstr Surg 12 243-255 1978
- 9 Gromet M A Epstein W L & Blois M S The regression thin malignant melanoma A distinctive lesion with metastatic potential Cancer 42 2282-2292 1978
- 10 Larsen T E & Grude T H A retrospective histological study of 669 cases of primary cutaneous malignant melanoma in clinical stage I 1 Histological classification sex age of patients localization of tumour and prognosis Acta Path Microbiol Scand Sect A 86 437-450 1978
- 11 Larsen T E & Grude T H A retrospective histological study of 669 cases of primary cutaneous malignant melanoma in clinical stage I 3 The relation between the tumour associated lymphocyte infiltration and age and sex tumour cell type pigmentation cellular atypia mitotic count depth of invasion ulceration tumour type and prognosis Acta Path Microbiol Scand Sect A 86 523-530 1978
- 12 Larsen T E & Grude T H A retrospective histological study of 669 cases of primary cutaneous malignant melanoma in clinical stage I 5 The consequences of a reclassification of the original group of lentigo maligna melanomas Acta Path et Microbiol Scand Sect A 87 255-260 1979
- 13 Little J H Histology and prognosis in cutaneous malignant melanoma In McCarthy W H (Ed) International cancer conference Sydney 1972 Melanoma and skin cancer Proceedings 1st ed Blight V C N Government Printer Sydney 1972 pp 107-119
- 14 Magnus A Prognosis in malignant melanoma of the skin Significance of stage of disease anatomical site sex age and period of diagnosis Cancer 40 389-397 1977
- 15 McGovern V J The classification of melanoma and its relationship with prognosis Pathology 2 85-98 1970
- 16 McGovern V J Mihm M C Bailly C Booth J C Clark W H Cochran A J Hardy E G Hicks J D Levene A Lewis M G Little J G & Milton G W The classification of malignant melanoma and its histologic reporting Cancer 32 1446-1457 1973
- 17 McGovern V J Shaw H M Milton G W & Farago G A Prognostic significance of the histological features of malignant melanoma Histopathology 3 385-393 1979
- 18 Olsen G The malignant melanoma of the skin New theories based on a study of 500 cases Thesis Acta Chir Scand Suppl 365 1966
- 19 Olsen G The malignant melanoma of the skin New theories based on a study of 500 cases Danish Medical Bulletin 14 229-238 1967
- 20 Petersen N C Bodenham D C & Lind O C Malignant melanomas of the skin A study of the origin development aetiology spread treatment and prognosis Brit J Plast Surg 15 49-94 1962
- 21 Petersen N C Malignant melanoma of the foot Scand J Plast Reconstr Surg 2 144-153 1968
- 22 Peio R Pike M C Armitage P Breslow N E Cox D R Howard S V Mantel N McPherson K Peio J & Smith P G Design and analysis of randomized clinical trials requiring prolonged observation of each patient II Analysis and examples Br J Cancer 35 1-39 1977
- 23 Reed R J New concepts in surgical pathology of the skin 1st ed John Wiley & Sons New York 1976 pp 89-90
- 24 Søndergaard K & Hou Jensen K Histologi og prognose ved kutant malignt melanom Ugeskr Læg 139 2993-2996 1977
- 25 Søndergaard K The intralesional variation of type level of invasion and tumour thickness of primary cutaneous malignant melanoma 55 malignant melanomas studied by serial block technique Acta Path Microbiol Scand Sect A 88 269-274 1980
- 26 Wanebo H J Woodruff J & Forner J G Malignant melanoma of the extremities A clinicopathologic study using levels of invasion (micro stage) Cancer 35 666-676 1975

SSM was the most prevalent type of melanoma (44%) of the foot followed by NM (22%) Both types were evenly distributed In accordance with other studies we found no LMM (6 13 27)

16% (20/125) of the tumours were readily classifiable as ALM according to the description of Reed (24) ALM was predominantly seen in planta and sub /parungually as reported by Reed (24) and Clark *et al* (6) According to Clark *et al* (6) ALM represents a clinicopathological entity However we found histologically a transition between SSM and ALM in that as many as 14% (17/125) of the melanomas (SSM ALM) showed characteristic features from both SSM and ALM This indicates that ALM is a subgroup of SSM rather than a specific entity which is further supported by the findings that prognosis is the same for patients with SSM as for patients with ALM

Difficulty in differentiating between SSM and ALM probably explains why Clark *et al* (6) state that the majority of volar subungual melanomas are ALM while Wanebo *et al* (27) found that AIM (called »melanoma of squamous mucosa«) account for only 10% (2/20) of melanomas of the sole heel and instep

Generally Clark's and Reed's types did not influence prognosis significantly in patients with melanomas of the foot

On the other hand both Clark's levels of invasion and Breslow's tumour thickness were of significant prognostic importance as deeper invasion and greater thickness indicated a significantly poorer outcome This is in accordance with studies of other anatomical regions (1 3 4 5 8 9 12 16 18 25 27)

We found Clark's and Breslow's methods to be of equal value in determination of prognosis

When using Breslow's method in melanomas of the foot the following intervals were prognostically relevant 0-0.75 mm 0.76-2.25 mm 2.26-3.00 mm and >3.00 mm as shown in Fig 5f

The prognosis is especially good for patients with melanomas level II and thickness less than 0.76 mm Many authors state a 100% survival rate for such patients (1 9 12 27) In our study one woman from this group died of metastases less than one year after operation Clinically marked tumour regression had taken place which histologically was demonstrated by fibrotic stroma devoid of tumour cells in the center of the lesion This supports the findings of Gromet *et al* (10) that the prognostic value of level and thickness is not valid in cases with pronounced regression

Polypoidal melanomas represent a special problem in Clark's grading of level if the tumour cells do not reach the papillary reticular interface In this

study they were designated as level PM II because of their poor prognosis (14) contrary to the good prognosis of non polypoidal melanomas level II

As did others (7 9 12 14 16 18 25) we found that the survival rate diminished with increasing mitotic rate Although the presence of few mitoses is of importance for the diagnosis of malignant melanoma the prognosis was seriously aggravated only if more than 5 mitoses/mm² were noticed

Ulceration was seen in 54% of the tumours and was especially frequent in sub /parungual lesions 79% of which were ulcerated In accordance with other studies (1 7 9 12 14 25) we found that ulceration was correlated with a poor prognosis The greater the ulceration the lower the survival rate

CONCLUSIONS

1) Melanoma of the foot was predominantly seen in elderly patients as 80/125 patients were more than 54 years of age

2) The most prevalent type was SSM which occurred twice as often as NM No LMM of the foot was found One quarter of the melanomas of sub /parungual region and of planta were ALM but an equal number of melanomas histologically were intermediate between ALM and SSM indicating a close biological relationship between ALM and SSM The type of melanoma did not influence the survival rate significantly

3) The survival rate for patients with sub /parungual melanomas was significantly lower than for patients with melanomas of planta and dorsum

4) The proportion was 2:1 between women and men Sex did not influence the prognosis

5) As is the case with melanomas in other anatomical regions melanomas of the foot in clinical stage I were correlated with a better prognosis than melanomas in stages II and III

6) The following histological features indicated a bad prognosis Clark's level IV and V tumour thickness more than 2.25 mm more than 5 mitoses/mm² and presence of ulceration

Supported by grants from the Dan sh Cancer Society (Project No 59/77)

REFERENCES

- 1 Balch C M Murad T M Soong S J Ingalls A L Halpern N B & Maddox W A A multifactorial analysis of melanoma Prognostic histopathological features comparing Clark's and Breslow's staging methods *Ann Surg* 188 732-742 1978

- 2 Bonnevise O Juhl E Andersen B & Winkel P Overlevelsmodeller i klinisk forskning Ugeskr Læg 133 1859-1864 1971
- 3 Breslow A Thickness cross sectional areas and depth of invasion in the prognosis of cutaneous melanoma. Ann Surg 172 902-908 1970
- 4 Breslow A Tumour thickness level of invasion and node dissection in stage I cutaneous melanoma. Ann Surg 182 572-575 1975
- 5 Clark W H From L Bernardino E A & Mihm M C The histogenesis and biologic behaviour of primary human malignant melanomas of the skin. Cancer Res 29 705-727 1969
- 6 Clark W H Bernardino E A Reed R J & Kopf A W Acral lentiginous melanomas including melanomas of mucous membranes Human malignant melanoma. Clinical oncology monographs Grune & Stratton New York 1979 pp 109-124
- 7 Cochran A J Histology and prognosis in malignant melanoma J Path 97 459-468 1969
- 8 Donnellan M J Seemayer T Huvois A G Mike V & Strong E W Clinicopathologic study of cutaneous melanoma of the head and neck. Am J Surg 124 450-455 1972
- 9 Eldh J Boerjeld B & Peterson L E Prognostic factors in cutaneous malignant melanoma in stage I. A clinical morphological and multivariate analysis. Scand J Plast. Reconstr Surg 12 243-255 1978
- 10 Gromet M A Epstein W L & Blois M S The regressing thin malignant melanoma. A distinctive lesion with metastatic potential. Cancer 42 2282-2292 1978
- 11 Larsen T E & Grude T H A retrospective histological study of 669 cases of primary cutaneous malignant melanoma in clinical stage I. I. Histological classification sex age of patients localization of tumour and prognosis. Acta Path Microbiol Scand Sect A 86 437-450 1978
- 12 Larsen T E & Grude T H A retrospective histological study of 669 cases of primary cutaneous malignant melanoma in clinical stage I. 3. The relation between the tumour associated lymphocyte infiltration and age and sex tumour cell type pigmentation cellular atypia mitotic count depth of invasion ulceration tumour type and prognosis. Acta Path Microbiol Scand Sect A 86 523-530 1978
- 13 Larsen T E & Grude T H A retrospective histological study of 669 cases of primary cutaneous malignant melanoma in clinical stage I. 5. The consequences of a reclassification of the original group of lentigo maligna melanomas. Acta Path et Microbiol Scand sect A 87 255-260 1979
- 14 Little J H Histology and prognosis in cutaneous malignant melanoma. In McCaig W H (Ed) International cancer conference Sydney 1972 Melanoma and skin cancer Proceedings 1st ed Blight A C N Government Printer Sydney 1972 pp 107-119
- 15 Magnus K Prognosis in malignant melanoma of the skin Significance of stage of disease anatomical site sex age and period of diagnosis. Cancer 40 389-397 1977
- 16 McGovern V J The classification of melanoma and its relationship with prognosis. Pathology 2 85-98 1970
- 17 McGovern V J Mihm M C Baillie C Booth J C Clark W H Cochran A J Hardy E G Hicks J D Levene A Lewis M G Little J G & Milton G W The classification of malignant melanoma and its histologic reporting. Cancer 32 1446-1457 1973
- 18 McGovern V J Shaw H M Milton G W & Farago G A Prognostic significance of the histological features of malignant melanoma. Histopathology 3 385-393 1979
- 19 Olsen G The malignant melanoma of the skin. New theories based on a study of 500 cases. Thesis. Acta Chir Scand Suppl 365 1966
- 20 Olsen G The malignant melanoma of the skin. New theories based on a study of 500 cases. Danish Medical Bulletin 14 229-238 1967
- 21 Petersen N C Bodenham D C & Lloyd O C Malignant melanomas of the skin. A study of the origin development aetiology spread treatment and prognosis. Brit J Plast Surg 15 49-94 1962
- 22 Petersen N C Malignant melanoma of the foot. Scand J Plast Reconstr Surg 2 144-153 1968
- 23 Peo R Pike M C Armitage P Breslow N E Cox D R Howard S V Mani N McPherson K Peto J & Smith P G Design and analysis of randomized clinical trials requiring prolonged observation of each patient. II. Analysis and examples. Br J Cancer 35 1-39 1977
- 24 Reed R J New concepts in surgical pathology of the skin. 1st ed John Wiley & Sons New York 1976 pp 89-90
- 25 Søndergaard K & Hou Jensen K Histologi og prognose ved kutant malignt melanom. Ugeskr Læg 139 2993-2996 1977
- 26 Søndergaard K The intralesional variation of type level of invasion and tumour thickness of
- 27 Wanebo H J Woodruff J & Fortner J G Malignant melanoma of the extremities. A clinicopathologic study using levels of invasion (micro stage). Cancer 35 666-676 1975

SSM was the most prevalent type of melanoma (44%) of the foot, followed by NM (22%). Both types were evenly distributed. In accordance with other studies we found no LMM (6, 13, 27).

16% (20/125) of the tumours were readily classifiable as ALM according to the description of Reed (24). ALM was predominantly seen in planta and sub-/parungually, as reported by Reed (24) and Clark *et al* (6). According to Clark *et al* (6) ALM represents a clinicopathological entity. However, we found histologically a transition between SSM and ALM, in that as many as 14% (17/125) of the melanomas (SSM-ALM) showed characteristic features from both SSM and ALM. This indicates that ALM is a subgroup of SSM rather than a specific entity, which is further supported by the findings that prognosis is the same for patients with SSM as for patients with ALM.

Difficulty in differentiating between SSM and ALM probably explains why Clark *et al* (6) state that the majority of volar-subungual melanomas are ALM, while Wanebo *et al* (27) found, that ALM (called «melanoma of squamous mucosa») account for only 10% (2/20) of melanomas of the sole heel and instep.

Generally Clark's and Reed's types did not influence prognosis significantly in patients with melanomas of the foot.

On the other hand both Clark's levels of invasion and Breslow's tumour thickness were of significant prognostic importance, as deeper invasion and greater thickness indicated a significantly poorer outcome. This is in accordance with studies of other anatomical regions (1, 3, 4, 5, 8, 9, 12, 16, 18, 25, 27).

We found Clark's and Breslow's methods to be of equal value in determination of prognosis.

When using Breslow's method in melanomas of the foot the following intervals were prognostically relevant: 0–0.75 mm, 0.76–2.25 mm, 2.26–3.00 mm and > 3.00 mm, as shown in Fig. 5f.

The prognosis is especially good for patients with melanomas level II and thickness less than 0.76 mm. Many authors state a 100% survival rate for such patients (1, 9, 12, 27). In our study one woman from this group died of metastases less than one year after operation. Clinically marked tumour regression had taken place, which histologically was demonstrated by fibrotic stroma devoid of tumour cells in the center of the lesion. This supports the findings of Gromet *et al* (10) that the prognostic value of level and thickness is not valid in cases with pronounced regression.

Polypoidal melanomas represent a special problem in Clark's grading of level if the tumour cells do not reach the papillary reticular interface. In this

study they were designated as level PM II because of their poor prognosis (14), contrary to the good prognosis of non-polypoidal melanomas level II.

As did others (7, 9, 12, 14, 16, 18, 25) we found that the survival rate diminished with increasing mitotic rate. Although the presence of few mitoses is of importance for the diagnosis of malignant melanoma, the prognosis was seriously aggravated only if more than 5 mitoses/mm² were noticed.

Ulceration was seen in 54% of the tumours and was especially frequent in sub-/parungual lesions, 79% of which were ulcerated. In accordance with other studies (1, 7, 9, 12, 14, 25) we found that ulceration was correlated with a poor prognosis. The greater the ulceration, the lower the survival rate.

CONCLUSIONS

1) Melanoma of the foot was predominantly seen in elderly patients, as 80/125 patients were more than 54 years of age.

2) The most prevalent type was SSM, which occurred twice as often as NM. No LMM of the foot was found. One quarter of the melanomas of sub-/parungual region and of planta were ALM, but an equal number of melanomas histologically were intermediate between ALM and SSM, indicating a close biological relationship between ALM and SSM. The type of melanoma did not influence the survival rate significantly.

3) The survival rate for patients with sub-/parungual melanomas was significantly lower than for patients with melanomas of planta and dorsum.

4) The proportion was 2:1 between women and men. Sex did not influence the prognosis.

5) As is the case with melanomas in other anatomical regions, melanomas of the foot in clinical stage I were correlated with a better prognosis than melanomas in stages II and III.

6) The following histological features indicated a bad prognosis: Clark's level IV and V, tumour thickness more than 2.25 mm, more than 5 mitoses/mm² and presence of ulceration.

Supported by grants from the Danish Cancer Society (Project No. 59/77).

REFERENCES

1. Balch C M, Murad T M, Soong S J, Ingalls A L, Halpern N B & Maddox W A. A multifactorial analysis of melanoma. Prognostic histopathological features comparing Clark's and Breslow's staging methods. *Ann Surg* 188: 732–742, 1978.

TERATOGENIC EFFECT OF MATERNAL ALCOHOL CONSUMPTION ON THE MOUSE FETUS

A Histopathological Study

B BRUUN RASMUSSEN and N CHRISTENSEN

Department of Pathology Frederiksberg Hospital Copenhagen and Eye Pathology Institute Copenhagen Denmark

Rasmussen B Bruun & Christensen N Teratogenic effect of maternal alcohol consumption on the mouse fetus A Histopathological study Acta path microbiol scand Sect A 88 285-289 1980

During pregnancy C₃H mice were solely kept on a 10 or 20% liquid supply. They had free access to solids. All animals including a group of controls were chloroformed on the 19th day of pregnancy and the fetuses were examined for growth retardation, intrauterine death and microscopic malformations. Among the animals given alcohol we found a significantly raised incidence of malformations as well as a raised number of intrauterine deaths and significant growth retardation as compared to the control animals. At the same time we found a clear dose-effect relation. The malformations were localized to the facial skeleton, the CNS, the eyes and lungs.

Key words: Alcohol consumption, maternal, fetal death, growth retardation, microscopic malformations.

B Bruun Rasmussen, Dept of Pathology, The Finsen Institute, Strandboulevarden 49, DK 2100 Copenhagen Ø, Denmark.

Accepted as submitted 8 ix 79

The fetal alcohol syndrome (FAS) was described as a well-defined syndrome by Jones *et al* (3-6) in children born by mothers with a history of heavy alcohol consumption before and during pregnancy. The syndrome consists of general growth retardation, defects in the facial skeleton and CNS and as a less constant phenomenon heart malformations and joint deformities. Several reports have later confirmed the teratogenic effect of alcohol in man (2, 7, 8, 9, 13, 15).

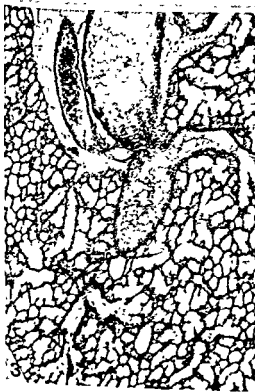
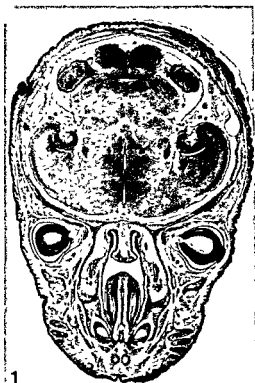
A lot of experimental work has been published especially on rodents (1, 10, 11, 12, 16). In the

and in Chernoff's work (1) one finds changes in mice comparable to those found in humans.

Up till now all the reports have confined themselves to a macroscopic and stereomicroscopic examination of the animal fetuses. In our study we have used a microscopic screening technique and at the same time looked for a dose-effect relation by giving the animals different alcohol concentrations.

MATERIAL AND METHODS

The mice were kept in cages with one mouse in each cage. One group of mice - the control group - had free access to food and



water. In two experimental groups the only liquid offered throughout pregnancy was in one group 10% alcohol in the other 20% while they had free access to solids. The amount of consumed water and alcohol solution was determined by daily weight control of the bottles.

The control group consisted of 131 fetuses the group given 10% alcohol 72 fetuses and the group given a 20% solution 66 fetuses. On day 19 of pregnancy all mice were chloroformed and the fetuses removed by section. The number of intrauterine deaths were registered as well as the weight of the fetuses. A stereomicroscopic examination was then performed. For the histological screening the fetuses were decapitated and the heads fixed in Bouin's solution for 4 days, mounted in paraffin and cut in serial sections. The bodies too were fixed in Bouin's solution and after 4 days of fixation by a horizontal transverse section separated in two at the level

hematoxylin eosin and ad modum Van Gieson - Hansen combined with alcian blue. All the slides were then screened for microscopic malformations.

The Kruskal Wallis one way analysis of variance was used to evaluate differences in weight and concerning fetal death and number of malformed fetuses the chi square test was employed.

RESULTS

During the experiment none of the animals showed signs of disease and the behavior of the animals drinking alcohol did not differ from that of control group.

Measurements of the daily alcohol consumption showed in both experimental groups rising values throughout pregnancy and the initial minimal liquid intake was always higher than the minimal daily requirement of the animals. The average amount of consumed alcohol throughout pregnancy was for animals given a 10% solution 83.5 (range 73.2-90.6) and for the animals given a 20% solution 56.7 ml (range 52.0-78.0). The total amount of alcohol was thus larger in the group given 20% (11.3 gr) than in the group given 10% (8.3 gr). The reproductive data are given in Table which shows the number of pregnant and non pregnant mice, the number of living fetuses and the resorption incidence given as the number of intrauterine deaths as a percentage of the total number of implantations. Furthermore the table shows the mean birth weight of the fetuses.

Of the 46 expected pregnant mice in the maternal group 9 were shown not to be pregnant at day 19 in spite

TABLE 1 Pregnant and Non Pregnant Mothers, Live Fetuses, Resorption Incidence and Mean Birth Weight

	Pregnant	Non pregnant	Live fetuses	Res. %	Weight (mean gms)
Control	17	0	131	7.1	10.1 (8.7-12.0)
10%	10	1	72	8.9	9.3 (8.3-10.0)
20%	10	8	66	21.4	7.7 (5.7-9.6)

TABLE 2 Number of Live Fetuses, Number of Malformed Fetuses and Number of Defects in the Face, Cerebrum, Eyes and Lungs

	Live	Malformed	Face	Cerebrum	Eyes	Lungs
Control	131	4	1	3	2	0
10%	72	11	0	9	3	5
20%	66	48	26	27	19	28

Fig 1 Horizontal section through the normal mouse head on the 19 day of gestation (13x)

Fig 2 Horizontal section through the head of treated fetus on day 19 of gestation showing microcephaly and open eyelids (13x)

Fig 3 Section showing normal lung of fetus on the 19 day of gestation (100x)

Fig 4 Section of lung from treated animal on day 19 of gestation showing severe hypoplasia. Same magnification as Fig 3 (100x)

REFERENCES

- 1 Chernoff G F The fetal alcohol syndrome in mice an animal model *Teratology* 15 223-229 1977
- 2 Hanson J W *et al* The effect of moderate alcohol consumption during pregnancy on fetal growth and morphogenesis *J Pediatr* 92 457-460 1978
- 3 Jones K L & Smith D W Recognition of the fetal alcohol syndrome in early infancy *Lancet* II 999-1001 1973
- 4 Jones K L *et al* Pattern of malformation in offspring of chronic alcoholic mothers *Lancet* I 1967-1971 1973
- 5 Jones K L *et al* Outcome in offspring chronic alcoholic women *Lancet* I 1076-1078 1974
- 6 Jones K L & Smith D W The fetal alcohol syndrome *Teratology* 12 1 10 1975
- 7 Little Ruth E Moderate alcohol use during pregnancy and decreased infant birth weight *Am J Public Health* 67 1154-1156 1977
- 8 Mulvihill J J & Yeager A M The fetal alcohol syndrome *Teratology* 13 345-348 1976
- 9 Palmer R H *et al* Congenital malformations in offspring of a chronic alcoholic mother *Pediatrics* 53 490-494 1974
- 10 Papara Nicholson D & Telford I R Effect of alcohol on reproduction and fetal development in the guinea pig *Anat. Rec.* 127 438 1957
- 11 Sandor S & Amels D The action of ethanol on the prenatal development of albino rats *Rev Roum Embryol Cytol Ser Embryol* 8 105-118 1971
- 12 Sandor S & Elias S The influence of ethylalcohol on the development of the chick embryo *Rev Roum Embryol Cytol Ser Embryol* 5 51-76 1968
- 13 Streissguth A P Fetal alcohol syndrome An epidemiologic perspective *Am J Epidemiol* 107 467-478 1978
- 14 Streissguth A P Personal communication 1977
- 15 Tenbrinck M S & Buchin S Y Fetal alcohol syndrome Report of a case *J Am Med Ass* 232 1144 1975
- 16 Tre W J & Lee M Adverse effects of maternal alcohol consumption on pregnancy and fetal growth in rats *Nature* 257 479-480 1975

of an obvious vaginal plug 8 of these were found in the group given 20% alcohol and 1 in the group with 10%. None of the non pregnant uteri showed any histologic sign of implantation

The resorption incidence in the experimental groups was significantly raised as compared to that of the control group ($p < 0.05$ and 0.01) and it was greater in the group given a 20% solution than in the 10% group ($p < 0.05$). The growth retardation expressed as the mean birth weight was significant in both experimental groups compared to the control group and again there was a significant difference between the two experimental groups ($p < 0.0005$). Table 2 gives the number of living fetuses, the number of malformed fetuses and the number of the malformations most frequently shown.

The frequency of malformed fetuses was significantly raised in the experimental groups compared to the control group ($p < 0.01$ and 0.001) and there was a significant number of malformed fetuses in the group given 20% as compared to the group given a 10% solution ($p < 0.001$). As shown in the figures representing the different types of malformations, several of the fetuses had more than one malformation.

Pathology

At the stereomicroscopic examination a certain pattern of malformations was found, all located to the head. In the group given a 20% solution there were certain characteristics: a shortening of the nose, sometimes in combination with low set ears and open eyes. The eye defect also occurred isolated in a few animals in the control group. There were no malformations of extremities, no abdominal wall defects and no defects of the neural tube. The microscopic defects, as the stereomicroscopic examination had suggested, were mostly localized to the head.

Fig. 1 shows a horizontal cut through the head of an animal from the control group. In fetuses with shortened nose a uniform hypoplasia of all structures in the splanchnocranium and its soft parts was found, often combined with a moderate microcephalia and dilated ventricles of the brain. Severe forms of microcephalia were often combined with open eyes (Fig. 2). The only consistent change in the body was varying degrees of isolated hypoplasia of the lungs, a change that especially occurred among animals given a 20% solution. Fig. 3 shows a horizontal cut of the lung from an animal in the control group, while Fig. 4 – same magnification – shows lung tissue from an animal in the experimental group. In the lungs most heavily affected, narrow bronchioles with a folded mucosa and only

here and there a few small alveolae like structures covered by columnar epithelium were found.

DISCUSSION AND CONCLUSION

The amount of consumed alcohol was decided by daily weighing of the bottles, and all bottles were before use controlled for spontaneous loss of content. The amount of consumed food was not registered, since the amount of alcohol here used does not influence the calorie intake from other food sources (1, 16).

The occurrence of 8 non pregnant mother animals in the group given a 20% solution cannot be explained by the unreliability of the method of confirming pregnancy. As microscopy of these uteri revealed no histologic sign of earlier or present pregnancy, it is likely that the alcohol has interfered with implantation in these animals. We have not seen this phenomenon described in other experimental models.

Although several experimental reports on the teratogenic effect of alcohol are available, a combination of malformations that are comparable to FAS in man was first described by Chernoff (1977). He found, apart from perinatal growth reduction and incomplete ossification, malformations in the CNS, the skeleton and the heart. Like Chernoff, we also found dilated ventricles of the brain and eyelid defects, but we did not find aplasia of the corpora callosa. We did not find heart malformations, e.g. septal defects. The reason for this is probably that our method of cutting horizontal sections of the body would not disclose small defects, but only bigger ones. The difference in results concerning malformations of the skeletal system can be explained by Chernoff making special preparations regarding this part of the body. We have not in earlier experimental studies seen descriptions of the pulmonary changes, neither have they been described in children with FAS (14).

Even though only two alcohol concentrations have been examined, there was a clear dose-effect relation. This was seen not only in regard to growth reduction, resorption incidence, and the frequency of malformations, but also in the fact that the high alcohol concentration apparently can interfere with nidation. On the other hand, there is no morphological difference between malformations induced by the various alcohol concentrations.

The authors wish to acknowledge the assistance of Aart Jensen and Eggert Hansen, laboratory technicians, P. Ul Schlichting, M.D., and S. Olesen Larsen, Statistician, Statens Lægevidenskabelige Forskningsråd.

REFERENCES

- 1 Chernoff G F The fetal alcohol syndrome in mice an animal model *Teratology* 15 223-229 1977
- 2 Hanson J W *et al* The effect of moderate alcohol consumption during pregnancy on fetal growth and morphogenesis *J Pediatr* 92 457-460 1978
- 3 Jones K L & Smith D W Recognition of the fetal alcohol syndrome in early infancy *Lancet* II 999-1001 1973
- 4 Jones K L *et al* Pattern of malformation in offspring of chronic alcoholic mothers *Lancet* I 1967-1971 1973
- 5 Jones K L *et al* Outcome in offspring chronic alcoholic women *Lancet* I 1076-1078 1974
- 6 Jones K L & Smith D W The fetal alcohol syndrome *Teratology* 12 1-10 1975
- 7 Little Ruth E Moderate alcohol use during pregnancy and decreased infant birth weight *Am J Public Health* 67 1154-1156 1977
- 8 Mulvihill J J & Yeager A M The fetal alcohol syndrome *Teratology* 13 345-348 1976
- 9 Palmer R H *et al* Congenital malformations in offspring of a chronic alcoholic mother *Pediatrics* 53 490-494 1974
- 10 Papara Nicholson D & Telford I R Effect of alcohol on reproduction and fetal development in the guinea pig *Anat Rec* 127 438 1957
- 11 Sandor S & Amels D The action of aethanol on the prenatal development of albino rats *Rev Roum Embryol Cytol Ser Embryol* 8 105-118 1971
- 12 Sandor S & Elias S The influence of aethylalcohol on the development of the chick embryo *Rev Roum Embryol Cytol Ser Embryol* 5 51-76 1968
- 13 Streissguth A P Fetal alcohol syndrome An epidemiologic perspective *Am J Epidemiol* 107 467-478 1978
- 14 Streissguth A P Personal communication 1977
- 15 Tenbrunck M S & Buchin S Y Fetal alcohol syndrome Report of a case *J Am Med Ass* 232 1144 1975
- 16 Tze W J & Lee M Adverse effects of maternal alcohol consumption on pregnancy and fetal growth in rats *Nature* 257 479-480 1975

SURFACE CHANGES IN THE ARTICULAR CARTILAGE OF RABBIT KNEE DURING IMMOBILIZATION. A SCANNING ELECTRON MICROSCOPIC STUDY OF EXPERIMENTAL OSTEOARTHRITIS

T CANDOLIN and T VIDEMAN

Research Laboratory of the Invalid Foundation and Institute of Occupational Health Helsinki Finland

Candolin T & Videman T Surface changes in the articular cartilage of rabbit knee during immobilization. A scanning electron microscopic study of experimental osteoarthritis Acta path microbiol scand Sect A 88 291-297 1980

Osteoarthritis was produced by the immobilization of rabbit knees in extension for 1-8 weeks (with a subsequent mobilization period of 0 or 8 weeks). The development of articular surface changes in the tibia, the femur and the patella was examined with scanning electron microscopy (SEM). During the development of osteoarthritis the normal undulations and fine regular fibre network disappeared, the number of fibres and the variation in the thickness of the fibre bundles increased and scalloped irregularities appeared. Some degenerative changes in the contralateral non-immobilized knee were also observed. The normal femoral condyles showed a different pattern of earlier studies but the histological changes were similar. The SEM method seems to be useful for the study of articular surfaces, however the area studied must be defined.

Key words: Cartilage, immobilization, osteoarthritis, scanning electron microscopy.

Tapio Videman, Haartmaninkatu 1, SF-00290 Helsinki 29, Finland.

Received 22 x 79 Accepted 7 iii 80

Scanning electron microscopy (SEM) presents a unique method for studying joint surfaces (Redler & Zimny 1970). Generally the methods used for examining normal and osteoarthritic joints provide a limited view of the condition of joints. Studies on

with histological sections. The characteristics of osteoarthritis are revealed best by macroscopic and/or SEM examinations. However the results of SEM studies of normal articular cartilage are somewhat contradictory and there is doubt as to whether or not some of the changes noted are artefacts (Ghadially et al 1977).

The surface of normal human articular cartilage is gently undulated and consists of an arrangement of regular ridges (1-100 µm) and bowl shaped depressions, sometimes forming »figure eights«. The articular surface is composed of a dense random network of fine collagen fibrils (0.1 µm) (Clarke 1971, Cotta 1973, Redler 1974, 1976, 1969). Age, articular cartilage, depressions, increasing and the number of ridges decreasing with age (Inoue 1972).

Osteoarthritic articular surfaces are disrupted and exhibit irregular nodular fibres and microcraters (Redler 1974, Refior 1974). The degeneration of the surface of articular cartilage has been classified primarily on the basis of surface roughness into six

stages by Kotani *et al* (1975). In transmission electron microscopy osteoarthritic cartilage shows increasing forms of surface folding and splitting with debris and collagen fibres of diminished size and an altered structure (Weiss 1973).

On the other hand the SEM features of an arthrotic joint vary greatly from one kind of joint to another and from one site to another, and it is difficult to distinguish different stages of the arthrotic process when specimens are taken from a big human joint (Weiss 1973, Kotani *et al* 1975, Inoue 1972).

If the changes are compared with those of a non-immobilized leg and the legs of control rabbits the possible methodological errors should be accounted for.

In the present study we have examined articular surface changes of experimental osteoarthritis produced by immobilization using SEM. The development of this condition has been studied earlier radiographically, histologically and biochemically as a function of immobilization time (Langenskiöld *et al* 1979). The aim of the present study was to correlate the changes found with SEM with the results of earlier experiments on the development of osteoarthritis.

MATERIAL AND METHODS

In a pilot study we used 8 rabbits to determine suitable and easily definable regions for examination.

In the present study we used 24 9-month-old rabbits of both sexes. Six were immobilized for 1 to 2 weeks (Group II) and 6 from 6 to 8 weeks (Group III) without a subsequent mobilization period. Six rabbits immobilized for 3 to 5 weeks were mobilized for more than 8 weeks after the immobilization (Group IV); the last 6 rabbits were controls living normally in their coops (Group I).

Osteoarthritis was produced in one knee of the rabbits with an earlier published immobilization method (right knee held in extension with a PVC plastic splint and a Tensoplast® bandage) (Langenskiöld *et al* 1979).

Immediately after the rabbits were killed the following samples were carefully prepared: the patella, the femoral condyles and the lateral tibial condyles including the whole thickness of cartilage with a 5 mm thick piece of subcondral bone. The samples were washed in physiological saline and fixed in a 2.5% glutaraldehyde solution buffered by 0.1 M cacodylate for 2–7 days at +4 °C. The samples were thereafter washed in a solution of 0.1 M cacodylate and 0.2 M sucrose and dehydrated by a graded series of increasing ethanol concentrations for 3 days. Most of the samples were dried in air, i.e. all except the patellae of the 6 control rabbits which were dried according to the critical point method (Cameron *et al* 1976). The samples were



- Group I control rabbits living normally in their coops
 Group II the right leg immobilized (IZ) for 1–2 weeks and followed (F) for 0 weeks
 Group III IZ = 6–8 weeks F = 0 weeks
 Group IV IZ = 3–5 weeks F = 12 weeks

Fig. 1 Articular cartilage of medial femoral condyle. The picture represents a control rabbit (Group I) and shows regular undulations and no fibre bundles (700×).

Fig. 2 Articular cartilage from the medial femoral condyle of a rabbit from Group II. The picture represents changes in the immobilized knee: the articular surface shows fibre bundles of varying thicknesses (arrows) but the undulations are clearly visible (700×).

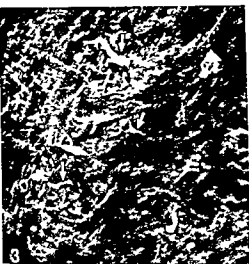
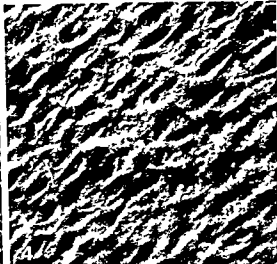


Fig 3 Medial femoral condyle of a rabbit from Group III. The picture shows the appearance of the immobilized knee there is variation in the fibre bundles, scaly irregularities (arrows) and a disappearance of regular undulations (700 \times)

Fig 4 The picture shows the corresponding region from the contralateral femur of the same rabbit as in figure 3, the appearance is normal (700 \times)



thereafter attached to a specimen holder and coated with a layer of carbon and gold in a vacuum evaporator. The JEOL JSM U scanning electron microscope of the Department of Electron Microscopy of the University of Tokyo was used for the examination. The area of the femoral condyle against the tibia (in extension)

In the SEM examination the specimens were tilted at an angle of 30–40°. All samples were photographed at a magnification of 50 \times and the central point was photographed with magnifications of 500 and 1500 \times . Two workers assessed the photographs independently and they evaluated every specimen separately with respect to fibre appearance and scaly irregularities (sharp folds) using the following scale: 0 = no degenerative changes; 2 = slight changes; 4 = moderate changes; and 6 = severe degenerative changes (Kotani *et al.* 1975).

RESULTS

The appearance of articular surfaces varies in different joints and also in the different regions of the same joint and therefore only corresponding areas were compared.

The normal appearance of the central region of the articular surface of the medial femoral condyle showed regular ridges and undulations (Fig. 1). These features disappeared during immobilization. In addition the fibre bundles became thicker and

varied in thickness, and some scaly irregularities also appeared (Figs. 2–6). There was considerable normal variation but statistically the degenerative changes increased clearly with increasing immobilization time, and the contralateral surface remained normal (Fig. 7).

The normal weight bearing area of the articular surface of the lateral tibial condyle showed smooth undulations with or without a fine regular network (Fig. 9). During immobilization the undulations became shallower and irregular fibre bundles appeared. The surface also became scaly (Fig. 8). The aforementioned degenerative changes increased as the immobilization period increased and the appearance on the contralateral surface remained normal (Fig. 10).

The normal view of the central region of the articular surface of the patella consisted of weak undulations and a fine fibre network, and the general appearance was regular (Fig. 11–12). An increase in the number of

irregularities in the articular surface of the non-immobilized knees in correlation to the length of the immobilization period was not statistically significant (Fig. 13–14). It was also obvious that degenerative changes progressed after the immobilization period. The degenerative changes were »slight to moderate« after the shortest immobilization time used (= 1 week).



Fig 5 Medial femoral condyle of a rabbit from group IV The picture shows the surface changes from immobilized knee ridges vary and the surface is irregular (700 \times)

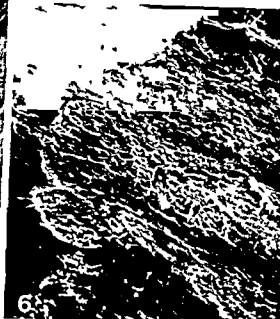


Fig 6 Medial femoral condyle The picture (200 \times) shows severe osteoarthritic changes in the central part (A) of picture almost all of the articular cartilage has disappeared The knee was immobilized for 8 weeks before the rabbit was killed (Group III)

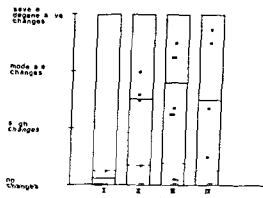


Fig 7 Assessments of the degenerative changes found with SEM of the articular cartilage surfaces of the medial femoral condyles ■ assessments of the SEM photographs of the immobilized leg — median for the leg assessments □ assessments of the SEM photographs of the nonimmobilized leg — median for the nonimmobilized leg assessments

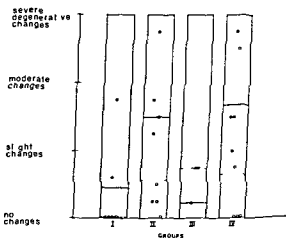


Fig 10 Assessment of degenerative changes found with SEM of the articular cartilage surfaces of the lateral tibial condyles

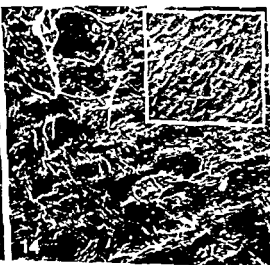
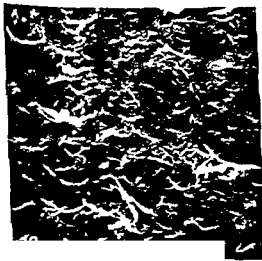
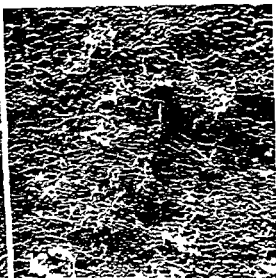
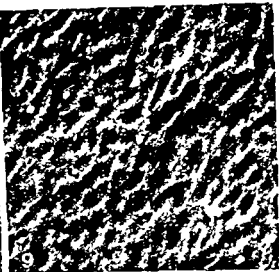
Fig 8 Lateral tibial condyle of a rabbit from Group IV The picture shows the arthrotic changes from the immobilized knee there are fibre bundles of varying thicknesses scaly irregularities and a partial disappearance of the undulations (700 \times)

Fig 9 The photograph is of the corresponding region of the contralateral non immobilized knee of the same rabbit as in figure 8 the appearance is normal (700 \times)

Fig 11-12 Articular cartilage of the patella The pictures represent Group I and show normal variations Fig 11 reveals weak undulations and in fig 12 the fine fibre network is dominant (700 \times)

Fig 13 Articular cartilage of the patella The picture represents changes in Group III Irregular fibre bundles are the predominant feature in this stage of osteoarthritis development (700 \times)

Fig 14 Articular cartilage of the patella from group IV The picture represents severe osteoarthritic changes (700 \times) The inset shows the appearance from the non immobilized knee of the same rabbit and there are also some degeneration changes in this picture (200 \times)



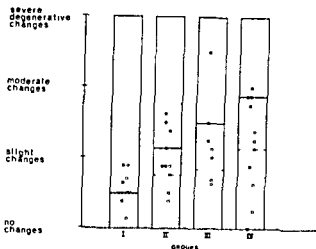


Fig. 15 Comparison of the assessments of the degenerative changes found with SEM of the articular cartilage of the patella

The irregularities were more marked in the rabbits immobilized 3–4 weeks and followed for 8 weeks than in rabbits with only an immobilization period of 6–8 weeks (Fig. 15)

DISCUSSION

There is some reason to believe that compression against a joint surface increases during immobilization causing arthrotic changes in the joint (Videman & Michelsson 1977). If this assumption is correct, the degenerative changes in the central region of the articular cartilage occur first and the marked changes in the marginal part of the joint (e.g. osteophytes) follow. Therefore we examined the load bearing area of articular cartilage in the present study.

There was no general difference between the surfaces of the samples dried with either the critical point technique or air. Both methods gave an appearance of weak undulations and a fine fibrillar network. In the specimens from tibial condyles there were often fissures which were thought to be artefacts. The fissures were caused in our opinion by the different contractile forces in the bone and cartilage during the drying and it can be assumed that the loading resistance in tibial condyles is good against compressive forces and weak in the tangential direction. Neither is a fibre network a general feature of tibial condyle surfaces.

The earliest osteoarthrotic changes in the radiographs of rabbit knees are visible after 2 weeks of immobilization, and these changes are definite after 3–4 weeks. The first histological arthrotic cartilage changes are seen after 10 days of immobilization and with biochemical methods it is noted that the glycosaminoglycan synthesis rate increases after 6

days of immobilization. After 5–6 weeks of immobilization rabbit knees show moderate or severe osteoarthrotic changes, including a disappearance of articular cartilage (Langenskiöld *et al* 1979, Eronen *et al* 1978).

The SEM changes that occurred during immobilization correlated well with corresponding histological changes. After 1 week of immobilization the degenerative SEM changes were relatively more marked than those found in a histological examination. This difference can be easily understood if it is remembered that osteoarthrotic changes start in cartilage as fibrillation of the surface (Sokoloff 1969, Weiss 1973).

Typical features of the articular surface from tibial and femoral condyles with developing osteoarthritis are the increasing number of fibres and the varying thicknesses of the fibre bundles. However, on the articular surface of the patella a fibre network is a normal characteristic.

In earlier studies with experimental immobilization osteoarthritis the contralateral non immobilized knee has been identical when compared with the knees of rabbits living normally in their coops (Eronen *et al* 1978, Langenskiöld *et al* 1979). In the present study the articular surface of the patella on the non immobilized side showed some degenerative changes after the immobilization. The changes were slight but the variation was relatively great. Not many animals were examined and the difference was not evaluated statistically (Fig. 15). It is possible that the immobilization of one knee strains the other or that there are some general factors in the development of osteoarthritis which affect all joints.

This study was supported by grants from the Sigrid Juselius Foundation and Juho Vainio Foundation.

REFERENCES

- Cameron C H S, Gardner D L & Longmore R B. The preparation of human articular cartilage for scanning electron microscopy. *J Microsc* 108: 1–12 1976.
- Clark I C. Surface characteristics of human articular cartilage – a scanning electron microscope study. *J Anat* 108: 23–30 1971.
- Cotta H. Die Pathogenese der gonarthrose. *Z Orthop* 111: 490–494 1973.
- Eronen I, Videman T, Friman C & Michelsson J-F. Glycosaminoglycan metabolism in experimental osteoarthritis caused by immobilization. *Acta orthop scand* 49: 329–334 1978.
- Ghadiali F N, Moshurhak E M & Thomas I. Humps on young human and rabbit articular cartilage. *J Anat* 124: 425–435 1977.

- noue H Kodama T & Fujita T Scanning electron microscopy of normal and rheumatoid articular cartilages Arch Histol Jap 30 425-435 1969
- onue H Orthopaedic Surgery and Traumatology In Delchef J de Marneffe R & Vander Elst E Proceedings of the 12th Congress of SICOT Tel Aviv October 9-12 1972 Excerpta Medica Amsterdam 1972 pp 33-43
- otani P T Oonishi H Shikita T & Hamaguchi T Study on the surface shape and contours of the femoral head and acetabulum of the human joint Bull Hosp Jt Dis (N Y) 36 81-108 1975
- ogenskuold A Michelsson J E & Videman T Osteoarthritis of the knee in the rabbit produced by immobilization Acta orthop scand 50 1-14 1979
- Redler I A scanning electron microscopic study of human normal and osteoarthritic articular cartilage Clin Orthop 103 262-268 1974
- Redler I & Zimny M L Scanning electron microscopy of normal and abnormal articular cartilage and synovium J Bone Jt Surg 52 A 1395-1404 1970
- Sokoloff L The biology of degenerative joint disease The University of Chicago Press Chicago and London 1969 pp 6-10
- Videman T & Michelsson J E Inhibition of development of experimental osteoarthritis by distraction during immobilization Int res comm syst 5 139 1977
- Weiss C Ultrastructural characteristics of osteoarthritis Fed Proc 32 1459-1466 1973

IMMUNOHISTOCHEMICAL DEMONSTRATION OF ALPHA-1-ANTITRYPSIN IN LIVER TISSUE

A Methodological Investigation

PER PRÆTORIUS CLAUSEN

Department of Pathology Herlev Hospital and Department of Pathology Hvidovre Hospital
University of Copenhagen

Clausen Per Prætorius Immunohistochemical demonstration of alpha 1 antitrypsin in liver tissue A
methodological investigation Acta path microbiol scand Sect A 88 299-306 1980

The influence of the tissue preparation on the immunohistochemical demonstration of alpha 1 antitrypsin (AAT) in liver tissue was evaluated using autopsy and biopsy material with and without AAT globules. On comparing frozen sections of unfixed material with paraffin sections of formalin fixed material a slightly better preservation of the immunoreactivity of AAT was observed in frozen sections. On comparing different fixatives fixation in 10% neutral buffered formalin Lillies AAF or 96% ethanol/1% acetic acid caused a clearly better preservation of demonstrable AAT than fixation in Clarke's or Bouin's fixatives. The fixation time had only minor influence when using fixation times within a week. Extremely long fixation for several months caused however a clear reduction in demonstrable AAT. Pre-examination of tissue caused an increase in fixation time. On comparing peroxidase/anti peroxidase staining with indirect immunoperoxidase staining sensitivity was observed between the three techniques. It is concluded that for the immunohistochemical demonstration of AAT in liver tissue the employment of indirect immunoperoxidase staining on formalin fixed paraffin embedded material is recommendable as it combines a sensitive staining technique with a satisfactory preservation of immunoreactivity and tissue morphology.

Key words: Alpha 1 antitrypsin liver tissue immunohistochemistry fixation

Per P Clausen Department of Pathology Hvidovre Hospital University of Copenhagen DK 2650 Hvidovre

Accepted as submitted 26 III 80

In 1971 Sharp described the presence of PAS positive diastase resistant globules in liver tissue from patients with alpha 1 antitrypsin (AAT) deficiency of Pi phenotype ZZ (24). Using immunohistochemical techniques it was shown that these globules contained AAT and the globules are therefore usually named AAT globules.

In a number of papers AAT globules have later on been described in as well ZZ as MZ individuals in both children and adults with and without liver disease (1 4 5 6 8 12 16 17).

The employment of immunohistochemical staining for AAT in liver tissue as a supplement to the PAS/diastase staining is important among others because PAS positive diastase resistant globules with negative reaction for AAT have been described in individuals with the phenotype MM (20 25). In addition heterozygous (MZ) individuals in some cases lack PAS positive diastase resistant globules while AAT deposits still can be demonstrated in the liver tissue (14).

The possibility of identifying an individual as a carrier of the Z gene by using immunohistochemical staining for AAT of the liver tissue has special importance in connection with retrospective investigation.

gations made on autopsy and biopsy material where analysis of the serum cannot be performed. Furthermore the immunohistochemical staining technique is valuable because AAT phenotyping of serum until now only has been performed in a few specialized laboratories while immunohistochemical investigations on routine processed material in increasing degree are used in histopathological diagnostics.

A prerequisite for using immunohistochemical investigation for AAT is however that the staining results are reproducible and that the preparation of the tissue does not significantly affect the staining result. In previous papers discrepancies as regards the suitability of different forms of tissue preparation and immunological techniques for demonstration of AAT in liver tissue have been described (3, 15, 18, 25).

The present investigation aims at examining the influence of the tissue preparation on the immunohistochemical demonstration of AAT in liver tissue and to compare results obtained by using three different immunohistochemical techniques.

MATERIAL AND METHODS

Tissue and Tissue Preparation

The material consists of liver tissue from 16 different patients. In six cases (A-F) the tissue was obtained in connection with autopsy performed within 12 hours after death. In one case (G) obtained peroperatively as a surgical knife biopsy and in the remaining 9 cases (H-N) as percutaneous needle biopsies. A survey of the tissue materials, chief histological diagnoses, fixatives and fixation times used is shown in Table 1.

Autopsy material was divided in pieces measuring $20 \times 20 \times 5$ mm. Liver tissue from A-C contained intracytoplasmic PAS positive diastase resistant globules with positive reaction for AAT and measuring up to at least $3 \mu\text{m}$. Liver tissue from D-F did not contain PAS positive globules.

The autopsy material was immediately after removal fixed at 20°C in the following fixatives: 10% phosphate buffered formalin, pH 7, Lillie's AAF, Clarke's fixative and Bouin's fixative (13 a). In each fixative the tissue was incubated for 1, 4, 8 and 24 hours and 7 days. In a few cases tissue was in addition fixed in 10% buffered formalin for 18 months. Following fixation the tissue was dehydrated in ethanol and xylene and embedded in

TABLE 1. Source of Tissue, Diagnosis and Fixation

Tissue		Chief histological diagnosis	Fixatives					Fixation time						
			Buffered formalin	AAF	Clarke	Bouin	EA (4 °C)	1 hour	4 hours	8 hours	24 hours	7 days	24 days	18 months
Autopsy with AAT globules	A	Chronic congestion	+	+	+	+	+	+	+	+	+	+	+	+
	B	Portal fibrosis	+	+	+	+	+	+	+	+	+	+	+	+
	C	Macronodular cirrhosis	+									+	+	
Autopsy without AAT globules	D	Chronic congestion	+	+	+	+	+		+		+	+		
	E	Normal	+	+	+	+	+		+		+	+		
	F	Normal	+	+	+	+	+		+		+	+		
Biopsy with AAT globules	G	Macronodular cirrhosis	+						+					
	H	Non specific changes	+						+					
	I	Large duct obstruction	+						+					
	K	Hepatocellular carcinoma	+						+					
	L	Micronodular cirrhosis	+						+					
Biopsy without AAT globules	M	Macronodular cirrhosis	+						+					
	N	Normal	+						+					
	O	Micronodular cirrhosis	+						+					
	P	Non specific changes	+						+					
	Q	Large duct obstruction	+						+					

EA: 96% ethanol + 1% acetic acid



1 Test of the monospecificity of anti alpha 1 antitrypsin by crossed immunoelectrophoresis. 2 μ l of 25 % pooled normal human serum has been run against anti alpha 1 antitrypsin at a concentration of 2 μ l/cm² gel.



2 Test of the purity of alpha 1 antitrypsin by crossed immunoelectrophoresis. 2 μ l alpha 1 antitrypsin (1 mg/ml) has been run against anti human serum at a concentration of 8 μ l/cm² gel.

iraplast at 59 °C. In addition to the fixatives mentioned tissue from A and B was fixed at 4 °C in 96% ethanol and 1% acetic acid (EA) for 4, 8 and 24 hours and 24 days. In these cases the tissue was dehydrated in ethanol and xylene at 4 °C increasing to room temperature and embedded in Paraplast at 56 °C (22).

Additional tissue from A and B fixed in buffered formalin for 18 months was washed for 48 hours in 0.1 M phosphate buffer pH 7.5 at 4 °C, frozen with CO₂ ice and stored at -20 °C. Some tissue from C-F was frozen unfixed at -20 °C.

The biopsies with AAT globules (G-L) and without AAT globules (N-Q) were fixed at room temperature for 4 hours in 10% phosphate buffered formalin pH 7, dehydrated in ethanol and xylene and embedded at 59 °C. Following embedding or freezing serial sections at 5 μ m were cut and placed on gelatinized slides.

Pretreatment of Sections with Proteolytic Enzymes

Deparaffinized sections from some of the formalin fixed material (B) were before the staining incubated at 37 °C in 0.1% trypsin (SIGMA type no. III) or 0.1% protease (SIGMA type no. V) for 15 min in 0.0045 M calcium chloride adjusted to pH 7.8 with 0.1 M sodium hydroxide (10, 11).

Antibodies and Control Reagents

Antibody no. 1 Anti human AAT (immunoglobulin IgG) fraction of rabbit antiserum (DAKO Denmark code no. 10 012 lot 017 118 and 029 A protein concentration respectively 11.1, 10.6 and 10.6 g/l. Titre 200 (expressed as the amount (microgram) of antigen which has to be added to 1 ml antibody in liquid phase in order to obtain a supernatant without demonstrable amounts of antigen or antibody (23)). Anti AAT was used in various dilutions (see below).

The monospecificity of anti AAT was tested in crossed immunoelectrophoresis against normal human plasma. Only one precipitation line appeared (Fig. 1). The proof of the reaction with AAT and not with other serum proteins was demonstrated in crossed immunoelectrophoresis against human AAT.

Antibody no. 2 Anti rabbit immunoglobulin (IgG fraction of swine antiserum) DAKO code no. 21 090 lot 078 E protein concentration 21 g/l titre 400. The antibody was used in dilution 1:10 determined by titration.

Antibody no. 3 Anti rabbit peroxidase (PAP) (immunoglobulin molecule in average 0.8 peroxidase molecule is conjugated) titre 19. The conjugate is produced using the two step glutaraldehyde method (2). Working dilution 1:20 was determined by chess board titration.

Antibody no. 4 Completes of horseradish peroxidase/rabbit anti horseradish peroxidase (PAP) DAKO code no. 2 113 lot 049 antibody concentration 1.98 g/l peroxidase concentration 0.75 g/l molar peroxidase/antibody ratio in average 1:5. Working dilution 1:50 determined by chess board titration.

Antibody no. 5 Anti rabbit anti human AAT (immunoglobulin IgG) fraction of rabbit antiserum (DAKO Denmark code no. 10 012 lot 017 118 and 029 A protein concentration respectively 11.1, 10.6 and 10.6 g/l. Titre 200 (expressed as the amount (microgram) of antigen which has to be added to 1 ml antibody in liquid phase in order to obtain a supernatant without demonstrable amounts of antigen or antibody (23)). Anti AAT was used in various dilutions (see below).

anti human serum. One strong and one much weaker precipitation line appeared and AAT was therefore based on this criterion almost completely pure (Fig. 2). The amount of AAT necessary for the absorption of anti AAT was determined by Sewell titration (23). The antibody was subsequently absorbed with AAT used in 25% excess. The mixture was stored for 1 hour at 25 °C and 48 hours at 4 °C (interrupted by regular shaking for 5 min every second hour) and at last the mixture was centrifuged. The supernatant – the absorbed antiserum – did not react with human serum in crossed immunoelectrophoresis. The absorbed antiserum was used in the same dilutions as used with non absorbed antiserum.

Control no 2 Ig fraction of serum from non immunized rabbits DAKO code no X 903 lot 076. Protein concentration 20 g/l. Used in dilution 1:80.

Control no 3 Swine serum from non immunized swine. Used undiluted.

Immunohistochemical Techniques

All staining reactions were performed at room temperature and the following techniques were used.

I Indirect immunoperoxidase technique (IP) The staining procedure comprises the following steps:

- 1) Methanol 0.5% H₂O₂ 30 min (only when using fixed material)
- 2) 10% swine serum in phosphate buffered saline (PBS) pH 7.2 15 min
- 3) Rabbit anti human AAT variable dilution 30 min
- 4) Peroxidase conjugated swine anti rabbit immunoglobulin 1:20 30 min
- 5) 0.04% 3-amino-9-ethylcarbazole (SIGMA) in dimethylformamide (9) 0.01% H₂O₂ in 0.5 M sodium acetate/acetic acid buffer pH 5 (15 min)
- 6) Mounting in Apathy gum syrup (13 b)

Control stainings were performed by replacing the reagents one at a time in the following manner: a) step 3 incubation with PBS b) step 3 incubation with control no. 1 c) step 3 incubation with control no. 2 and d) step 3 + 4 incubation with PBS.

II Peroxidase anti peroxidase technique (PAP technique) Step 1, 2 and 3 performed as described for IP technique.

- 4) Swine anti rabbit immunoglobulin 1:10 30 min
 - 5) PAP 1:50 30 min
- Step 6 and 7)

Staining and mounting as described in IP technique step 5 and 6.

Control stainings were performed as described in method I. In addition the following controls were performed: a) step 4 incubation with control no. 3 b) Step 3–5 incubation with PBS.

In technique I and II all antisera were diluted in 10% swine serum in PBS. Between each step sections were washed in PBS for 3 × 5 min.

III Indirect immunofluorescence technique (IF)

- 1) PBS 5 min
- 2) Rabbit anti human AAT variable dilution 30 min
- 3) FITC-conjugated swine anti rabbit immunoglobulin 1:20 30 min
- 4) Mounting in glycerol tris buffer pH 8.5

Control stainings were performed by replacing the reagents one at a time in the following manner: a) step 2 incubation with PBS b) step 2 incubation with control no. 1 and c) step 2 incubation with control no. 2. All antisera were diluted in PBS. Wash between each step with PBS for 3 × 5 min.

Evaluation

The staining results of IP and PAP techniques were evaluated using a DIA LUX light microscope Leitz eye piece 10× objective 40× N.A. 0.65. IF technique was evaluated using Leitz universal fluorescent microscope with transmitted light and Dark Field Ultra Condenser N.A. 1.2 and objective 40× 0.75 N.A. eye piece 10×. Light source HBO 200 W/4 pressure mercury lamp. Filters: Primary interference filter and secondary 3 mm glass filter matched with the primary filter (21).

All tissue was incubated in two fold serial dilutions of anti AAT serum. The evaluation of the influence of fixative fixation time, paraffin embedding, pretreatment with proteolytic enzymes and immunohistochemical technique used on the staining results was based on a comparison of the highest dilution of anti AAT which still gave a clear positive reaction (end point titre). For each parameter examined all sections were stained on the same day and double staining series were performed independently. The variation between end point titres of two comparable staining series was at most one dilution step. The proportion between end point titres within each staining series was constant.

TABLE 3. Influence of Fixative and Fixation on the Immunology

TISSUE	10% buffered formalin			Lillie's AAF			
	4 h	24 h	7 days	4 h	24 h	7 days	4 h
A	1:12800	1:12800	1:12800	1:12800	1:6400	1:6400	1:161
B	1:25600	1:12800	1:12800	1:51200	1:12800	1:12800	1:641
C		1:25600	1:25600				

The table shows the highest dilution of anti alpha 1 antitrypsin which s

TABLE 2 Influence of Tissue Preparation on the Immunological Reactivity of Alpha 1 antitrypsin in Liver Tissue

Tissue	Frozen tissue		Paraffin embedded tissue			
	Without fixation	Prefixation for 18 months in buffered formalin	Fixation in buffered formalin for			
			4 h	24 h	7 days	18 months
A		1:600	1:12800	1:12800	1:12800	1:600
B		1:3200	1:25600	1:12800	1:12800	1:3200
C	1:51200			1:25600	1:25600	

The table shows the highest dilution of anti alpha 1 antitrypsin which still gives a clear positive staining using indirect immunoperoxidase staining technique

RESULTS

The influence of fixative, fixation time and paraffin embedding was examined using IP technique on tissue A-F.

Results of investigations on tissue A-C are shown in Table 2 and 3. Table 2 shows that AAT was demonstrable in unfixed frozen sections using antiserum in a lower concentration than in paraffin embedded formalin fixed sections. No difference was observed between frozen sections of prefixed tissue and paraffin sections.

The influence of the examined fixatives on the immunological reactivity of AAT is shown in Table 3. EA fixation at 4 °C caused the best preservation of AAT, but the staining results were sometimes difficult to evaluate due to rather pronounced background staining - even when using extremely high dilutions of the primary antiserum. Furthermore, the tissue morphology was less satisfactory. End point titres for 10% buffered formalin and AAF were lower than for EA, while titres for Bouin's and Clarke's fixatives were clearly lower than for the afore mentioned. In Table 3 it is furthermore seen that the fixation time did not have

any essential influence on the preservation of the immunoreactivity when using fixation times between 4 hours and 7 days. Extremely long fixation up to 18 months caused a clear decrease in the amount of demonstrable AAT (compare Table 2).

The effect of pretreatment of sections from formalin fixed paraffin embedded material with proteolytic enzymes before the immunoperoxidase staining is shown in Table 4. Treatment with trypsin had no effect on tissue fixed up to 24 hours, while treatment with protease increased the amount of demonstrable AAT. Even more pronounced was the effect on tissue which had been fixed for extremely long time in formalin, as it was in this case possible by using trypsin and especially using protease to unmask antigens in such a degree that the amount of demonstrable AAT was the same as demonstrated after 4 hours fixation.

The same

was also more sensitive than the PAP technique. In general more background staining was found when using PAP technique than with IP technique. The

TABLE 3 Influence of Fixative and Fixation Time on the Immunological Reactivity of Alpha 1 antitrypsin in Liver Tissue

Tissue	Bouin's fixative				96% ethanol + 1% acetic acid (4 °C)		
	7 days	4 h	24 h	7 days	4 h	24 h	24 days
A	1:800	1:3200	1:3200	1:3200	1:51200	1:51200	1:51200
B	1:3200	1:6400	1:3200	1:3200	1:102400	1:51200	1:51200

A clear positive staining using indirect immunoperoxidase technique

TABLE 4 Influence of Pretreatment with Proteolytic Enzymes on the Immunological Reactivity in Formalin Fixed Liver Tissue

Fixation time	Without pretreatment	Pretreatment with trypsin	Pretreatment with protease
4 h	1:25600	1:25600	1:51200
24 h	1:12800	1:12800	1:51200
18 months	1:3200	1:12800	1:51200

The table shows the highest dilution of anti alpha 1 antitrypsin which still gives a clear positive staining using indirect immunoperoxidase staining

background staining was especially annoying in tissue fixed in EA. IF technique showed in a few cases a slightly weaker staining than the two peroxidase techniques. Autofluorescence did not cause trouble and the yellow autofluorescence from lipofuscin was clearly discernible from specific yellow green fluorescence in relation to AAT.

Comparing the results obtained on tissue with and without globules it was found that a much higher concentration of anti AAT was needed for demonstration of AAT in tissue without globules than for AAT in tissue with globules.

Comparing the staining results obtained by using IP technique on autopsy and biopsy material more AAT was found in autopsy material than in biopsy material both as more stained cells and as increased staining intensity of the individual cell. In other respects the staining patterns were however concordant in the two materials.

Control stainings by using absorbed anti AAT

TABLE 5 Comparison of the Sensitivity of Different Immunohistochemical Techniques for Demonstration of Alpha 1 antitrypsin in Liver Tissue

Immunohistochemical technique	Buffered formalin	Bouin's fixative	96% ethanol + 1% acetic acid (4 °C)
IP	1:25600	1:3200	1:51200
PAP	1:12800	1:1600	1:25600
IF	1:12800	1:800	1:25600

The table shows the highest dilution of anti alpha 1 antitrypsin which still gives a clear positive staining. IP Indirect immunoperoxidase technique. PAP Peroxidase antiperoxidase technique. IF Indirect immunofluorescence technique.

(control no. 1) were negative in all biopsy material and in autopsy material without globules. In autopsy material with globules positive reaction could be demonstrated by using high concentration of the absorbed antiserum. The reaction was always weaker by a factor ten than that obtained by using non absorbed antiserum. Using immunoglobulin from non immunized animals and by replacing the primary antiserum with PBS negative staining was obtained in all cases.

DISCUSSION

Following the first description of AAT deposits in liver tissue from patients with AAT deficiency of phenotype ZZ (24) this observation has been confirmed in a number of investigations using direct and indirect IF techniques on cryostat sections of fresh frozen or formalin fixed material (1, 5, 8).

Palmer (17) showed deposits of AAT in liver tissue from patients with phenotype MZ using direct immunofluorescence technique on formalin fixed paraffin embedded tissue. Later on performed a comparative investigation of staining on cryostat and paraffin sections of formalin fixed tissue with and without globules using IP, PAP and IF techniques (18). AAT was demonstrated in cryostat sections of formalin fixed tissue with globules using all three techniques. Using IP and PAP techniques positive AAT staining was found in formalin fixed paraffin embedded material without globules but no staining with IF technique.

Ray & Desmer (19) did not find any difference between AAT staining in unfixed frozen section and sections of Bouin fixed paraffin embedded material using IF technique.

None of the above mentioned investigators were able to demonstrate AAT in liver tissue without globules. In contrast Feldman & al (7) using IF technique on cryostat sections of paraformaldehyde fixed material demonstrated AAT deposits in liver tissue both with and without globules.

A quantitative comparison of the influence of tissue preparation on the immunoreactivity of AAT does not seem to have been described previously. In

... it has been demonstrated that AAT is more stable in unfixed tissue than in paraffin sections of formalin fixed tissue. A slightly better preservation of the immunoreactivity of AAT was found in frozen sections of unfixed tissue than in paraffin sections of formalin fixed tissue.

A comparative investigation of the influence of different fixatives on the preservation of the

immunoreactivity of AAT has not previously been performed. In this investigation a number of factors has been compared by using the same staining technique and the same tissue. EA fixation at 4 °C and fixation in 10% phosphate buffered formalin or Lillie's AAF gave better results than the employment of Bouin's and Clarke's fixatives. EA fixation however caused high background staining and less satisfactory tissue morphology.

The fixation time had only a slight influence when using a fixation period less than a week while fixation for an extremely long period caused a clear reduction of demonstrable AAT. Thus fixation for up to 24 hours in 10% phosphate buffered formalin is recommendable for the immunohistochemical demonstration of AAT in liver tissue as it combines preservation of AAT immunoreactivity and tissue morphology with low background staining in a satisfactory way.

The employment of proteolytic enzymes for unmasking antigen determinants was originally introduced in connection with immunofluorescence staining of formalin fixed paraffin embedded tissue (10). The enzymes have recently also been used in connection with immunoperoxidase staining. In accordance with previous investigations (10-11) I found that pretreatment with trypsin and protease especially of tissue which have been fixed for extremely long time is able to increase the amount of demonstrable AAT in paraffin sections. Unmasking with proteolytic enzymes may be used with advantage in cases where only small amounts of AAT are accumulated in the liver tissue as e.g. in biopsies from heterozygous MZ patients without PAS/diastase resistant globules.

Opinions have previously differed as regards the suitability of the three different immunohistochemical techniques for demonstration of AAT in liver tissue. Palmer (18) found that the two immunoperoxidase staining techniques were better than IF technique and that PAP technique was better than IP technique. Triger & al (25) likewise found that immunoperoxidase technique was more suitable than immunofluorescence technique when using paraffin sections. In contrast Blenkinsopp (3) found that IP technique was inferior to both IF technique and PAP technique.

In this investigation the comparison of IP, PAP and IF technique has been performed using the same primary antiserum and the same tissue and in this case no convincing difference between the techniques has been demonstrated. The sensitivity of IP, PAP and IF techniques was for practical purposes equal.

The different opinions as regards sensitivity and suitability of the three techniques are probably due

to difference in quality of the used immunological reagents as for example differences in conjugation degree and antibody titre.

In conclusion the employment of IP staining on formalin fixed paraffin embedded material for demonstration of AAT in liver tissue has been shown to give satisfactory results as it combines a sensitive staining technique with good preservation of immunoreactivity and morphology of the tissue.

I am grateful to Susanne Smidh and Jytte Limborg for excellent technical assistance to Agnete Ingild for providing absorbed antiserum and for her valuable critical review of the manuscript and to Per Just Svendsen for providing human alpha 1 antitrypsin.

REFERENCES

- 1 Aagenæs O, Matlar A, Elgjo K, Munthe E & Fagerhol M. Neonatal cholestasis in alpha 1 antitrypsin deficient children. *Acta Paediatr Scand* 61: 632-642 1972.
- 2 Avrameas S & Ternyck T. Peroxidase labelled antibody and Fab conjugates with enhanced intracellular penetration. *Immunohistochemistry* 8: 1175-1179 1971.
- 3 Blenkinsopp W K & Haffenden G P. Alpha 1 antitrypsin bodies in the liver. *J Clin Path* 30: 132-137 1977.
- 4 Campra J L, Craig J R, Peters R L & Reynolds T B. Cirrhosis associated with partial deficiency of alpha 1 antitrypsin in an adult. *Ann Intern Med* 78: 233-238 1973.
- 5 De Lell S R A, Balogh K, Merk F B & Chirife A M. Distinctive hepatic cell globules in adult alpha 1 antitrypsin deficiency. *Arch Path* 94: 308-316 1972.
- 6 Feldman G. *Roman's Cytochemistry*. 1970.
- 7 Feldman G, Guillouzo A, Maurice M & Guesnon J. Depressed secretion of plasma proteins synthesized by the liver. An ultrastructural investigation based on immunoperoxidase. In Feldman G, Druet J, Bignon J & Avrameas S (Eds). *Immunoenzymatic techniques*. North Holland Publishing Company Amsterdam 1976. p 379-394.
- 8 Gordon H W, Dixon J, Rogers J C, Mittman C & Lieberman J. Alpha₁ antitrypsin (A₁AT) accumulation in livers of emphysematous patients with A₁AT deficiency. *Hum Pathol* 3: 361-370 1972.
- 9 Graham R C, Lundholm U & Karnovsky M J. Cytochemical demonstration of peroxidase activity with 3-amino-9-ethylcarbazole. *J Histochem Cytochem* 13: 150-152 1965.
- 10 Huang S N. Immunohistochemical demonstration of hepatitis B core and surface antigens in paraffin sections. *Lab Invest* 33: 88-95 1975.

- 11 Huang S-N, Minassian H & More, J D Application of immunofluorescent staining on paraffin sections improved by trypsin digestion *Lab Invest* 35 383-390, 1976
- 12 Ishak K G, Jemis E H & Marshall M L Cirrhosis of the liver association with α_1 -antitrypsin deficiency *Arch Pathol* 94 445-455, 1972
- 13 Lillie, R D & Fullmer, H M Histopathological technic and practical histochemistry (4 ed) McGraw-Hill New York 1976 a) p 25-68, b) p 119
- 14 Lindskov, J, Reinicke, V & Clausen, P P Pulmonary emphysema and hepatic changes in alpha-1-antitrypsin deficiency Investigation of a family *Ugeskr Læg* 140 1551-1555, 1978
- 15 McElrath, M J, Galbraith R M & Allen, R C Demonstration of alpha₁-antitrypsin by immunofluorescence on paraffin embedded hepatic and pancreatic tissue *J Histochem Cytochem* 27 794-796, 1979
- 16 Milford Ward, A & Underwood, J C E α_1 -antitrypsin deficiency and liver disease in childhood Genetic immunochemical, histological, and ultrastructural diagnosis *J Clin Path* 27 467-472, 1974
- 17 Palmer, P E, Wolfe, H J & Gherardi, G J Hepatic changes in adult α_1 antitrypsin deficiency *Gastroenterology* 65 284-293, 1973
- 18 Palmer, P E De Lellis R A & Wolfe H J Immunohistochemistry of liver in alpha₁ antitrypsin deficiency *Am J Clin Pathol* 62 350-354 1974
- 19 Ray, M B & Desmet, V J Immunofluorescent detection of α_1 -antitrypsin in paraffin embedded liver tissue *J Clin Path* 28 717-721, 1975
- 20 Reintoft, I Periodic acid Schiff positive non glycogenic globules in hepatocytes *Acta Path Microbiol Scand A*, 86 325-329, 1978
- 21 Rygaard, J & Olsen W Toward quantitation of excitation *Ann NY Acad Sci* 177 410-413, 1971
- 22 Sainte-Marie G A paraffin embedding technique for studies employing immunofluorescence *J Histochem Cytochem* 10 250-256 1962
- 23 Sewell M M H A semi quantitative technique using the LKB immunodiffusion apparatus *Science Tools* 14 11-12, 1967
- 24 Sharp, H L Alpha-1-antitrypsin deficiency *Hosp Pract* 6 83-96 1971
- 25 Triger, D R, Millward-Sadler, G H, Czajkowski A A, Trowell J & Wright R Alpha-1 antitrypsin deficiency and liver disease in adults *Quart J Med* 45 351-372, 1976

PRECISION OF HISTOLOGICAL GRADING OF MALIGNANCY

Sources of Variation in a Histological Scoring System for Grading Cancer of the Larynx

NIELS GRÆM, KARIN HELWEG LARSEN and NIELS KEIDING

Pathological Anatomical Institute, Kommunehospitalet, Department of Pathology, Rigshospitalet and Statistical Research Unit, Danish Medical and Social Science Research Councils, Copenhagen, Denmark

Græm N, Helweg Larsen K. & Keiding N. Precision of histological grading of malignancy. Sources of variation in a histological scoring system for grading cancer of the larynx. *Acta path microbiol scand Sect A* 88: 307-317, 1980.

The precision of a grading system based upon average score of 8 items for histological evaluation of malignancy of epidermoid carcinomas of the larynx was studied by letting 6 pathologists examine biopsies from 22 new cases. Exploratory statistical tools as well as a statistical framework (variance component models) for separating and evaluating the noise components are suggested. The order of magnitude of the resulting overall measurement uncertainty allowed discrimination between patients though if a patient is graded by only one pathologist only results at the extremes of the scale of malignancy should be trusted as possible therapeutic guidance. Based upon an analysis of the basic structure of the grading system the single noise components making up the measurement uncertainty were determined. Of greatest importance was noise created by disagreement between the pathologists in their ranking of the patients on the scale of malignancy. Furthermore the pathologists used the individual items differently and certain items seemed to conform little to the scoring system. An attempt to minimize these two last components was performed, however neither calibration of the pathologists nor omission of the deviating items improved the precision significantly.

Key words: Cancer of the larynx, variance component models, histological grading.

Niels Græm, Department of Pathology, Rigshospitalet, Frederik V's Vej 11, DK 2100 Copenhagen Ø, Denmark.

Accepted as submitted 31 III 80.

Histopathological grading has the double purpose of refining and objectifying histopathological diagnosis. Like almost any diagnostic statement, the result of a histopathological grading is only partially correlated to prognosis, but in contrast to laboratory measurements, which are often quite close to ideal objectivity (observer independent), histopathological grading is in addition disturbed by the subjective nature of the procedure, being based upon a subjective interpretation of a complicated image. The subjective factor must be assumed to be more

crucial when the refined statements of histopathological grading are aimed at than for the less subtle traditional histopathological diagnoses.

The important role of the observer in histopathological grading as compared to e.g. laboratory measurements necessitates more detailed definition and evaluation of the precision and accuracy of the method. Of course the final test of any diagnostic procedure is how it correlates to prognosis. In this report, however, we define and evaluate the *intrinsic* precision of histopathological grading in the particular context of epidermoid carcinoma of the larynx.

- 11 Huang, S-N, Minassian H & More, J D Application of immunofluorescent staining on paraffin sections improved by trypsin digestion *Lab Invest* 35 383-390, 1976
- 12 Ishak, K G, Jenis E H & Marshall, M L Cirrhosis of the liver associated with α_1 -antitrypsin deficiency *Arch Pathol* 94 445-455, 1972
- 13 Lillie, R D & Fullmer, H M Histopathological technic and practical histochemistry (4 ed) McGraw-Hill New York 1976 a) p 25-68, b) p 119
- 14 Lindskov, J, Reinicke, V & Clausen P P Pulmonary emphysema and hepatic changes in α_1 -antitrypsin deficiency Investigation of a family *Ugeskr Læg* 140 1551-1555, 1978
- 15 McElraith M J, Galbraith, R M & Allen R C Demonstration of α_1 -antitrypsin by immunofluorescence on paraffin embedded hepatic and pancreatic tissue *J Histochem Cytochem* 27 794-796, 1979
- 16 Milford Ward, A & Underwood, J C E α_1 -antitrypsin deficiency and liver disease in childhood Genetic immunochemical, histological and ultrastructural diagnosis *J Clin Path* 27 467-472, 1974
- 17 Palmer, P E, Wolfe, H J & Gherardi, G J Hepatic changes in adult α_1 -antitrypsin deficiency *Gastroenterology* 65 284-293, 1973
- 18 Palmer, P E, De Lellis, R A & Wolfe, H J Immunohistochemistry of liver in α_1 -antitrypsin deficiency *Am J Clin Pathol* 62 350-354 1974
- 19 Rav, M B & Desmet V J Immunofluorescent detection of α_1 -antitrypsin in paraffin embedded liver tissue *J Clin Path* 28 717-721, 1975
- 20 Reintoft, I Periodic acid Schiff positive non glycolytic globules in hepatocytes *Acta Path Microbiol Scand A*, 86 325-329 1978
- 21 Rygaard J & Olsen W Toward quantitation of excitation *Ann NY Acad Sci* 177 410-413 1971
- 22 Sainte-Marie, G A paraffin embedding technique for studies employing immunofluorescence *J Histochem Cytochem* 10 250-256, 1962
- 23 Sewell M M H A semi-quantitative technique using the LKB immunodiffusion apparatus *Science Tools* 14 11-12, 1967
- 24 Sharp H L α_1 -antitrypsin deficiency *Hosp Pract* 6 83-96, 1971
- 25 Triger, D R, Millward Sadler, G H, Czajkowski A A, Trowell, J & Wright R α_1 -antitrypsin deficiency and liver disease in adults *Quart J Med* 45 351-372, 1976

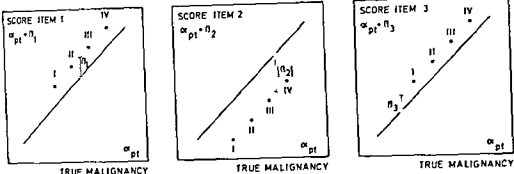


Fig 1 Theoretical score patterns for a perfect scoring system (three items four patients = I, II, III, IV, one pathologist β_1 + β_2 + β_3 = 0)

and agreed on an interpretation of the individual scores as described by Helweg Larsen *et al* (1978)

Statistical Analysis

The statistical evaluation will consist of 2 parts. First an exploratory data analysis investigating the suitability of each of the 8 items, the varying use of the system by the 6 pathologists, and the consistency of the grading in relation to a one dimensional concept of histological malignancy, this forming a natural basis for the use of a simple average of scores as measure of malignancy. Secondly, a definition and assessment of the precision of the grading system should one want to use it routinely. Finally on the basis of these results an attempt to point out some ways to improve the grading system.

RESULTS

Exploratory Analysis of the Structure of the Grading System

The perfect grading system. It is natural to base the use of the average score as an indicator of malignancy upon an assumption of one-dimensional histological malignancy: changes in malignancy level should affect all items in the same way, though it is no requirement that for instance 2 on one item corresponds to 2 on another. Were the true malignancies of a series of patients known we should therefore expect a pattern like that of Fig 1, which indicates how in a perfect grading system the scores on each individual item increase with increasing true malignancy. Further, if an unweighted average is to be used as malignancy index, each item should discriminate equally well between slight and severe cases. This property is indicated by the parallelism of the three lines that could be drawn through the 4 points in each diagram. In addition to this, the reproducibility of the scores should be perfect.

Deviations of the present scoring system from the

idealized pattern. In the actual data the semiquantitative nature of the scoring system with only 4 response categories makes diagrams like those of Fig 1 unfeasible for each pathologist and item. We shall therefore first compare items pooled over pathologists, and secondly pathologists pooled over items. Since the true malignancy is of course an abstraction, we use instead the average score over items and pathologists as reference (abscissa). Fig 2 shows for each item the average score over the 6

responses missing, with a distribution on the items 1–8 of respectively 1, 2, 1, 3, 2, 14, 10 and 2. In the following analysis we treat those as ordinary missing values, and substitute expected values by a routine procedure. The adequacy of that assumption in the context is discussed further below.

It is seen from Fig 2 that items 1, 3, 5 and 7 follow the general pattern determined by the average quite closely. It also appears that the score on item 7 is consistently below the full drawn line, as is indeed permitted by Fig 1. Items 2 and 8 follow the general pattern but much less accurately. Finally, items 4 and 6 are generally scored rather independently of the remaining ones.

In a similar fashion we plot in Fig 3 the average over items of each pathologist's scores for a given patient, again using the overall patient average as reference. First, it is seen that the pathologists agree well in their overall level (most points being close to the identity line), except pathologist F who generally has higher scores than the average opinion. Closer inspection further reveals differences between the pathologists in their ability or willingness to discriminate between the patients. Thus pathologists A and B keep close to the average opinion, whereas C and F discriminate more, and D and E less than the average.

MATERIAL AND METHODS

Biopsies and Histological Grading

The basis of this study is the biopsies from 22 consecutive patients with a new diagnosis of epidermoid carcinoma of the larynx primarily seen at the Department of Otolaryngology Kommunehospitalet Copenhagen during 1977. The biopsies were fixed in formalin and cut in 12 μ m sections of which 9 were stained by haematoxylin-eosin and 3 by van Gieson-alcian.

Immediately after the routine diagnostic procedures the biopsies were graded once by each of 6 pathologists below designated A-F working blindly and independently. The grading was performed according to a histological scoring system for evaluation of malignancy of epidermoid carcinoma of the larynx. The system was

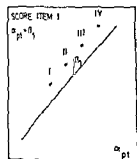
set up by Jakobsson (1973 a and b) and later modified by Lund *et al.* (1976) and is based upon 8 items or questions (Table 1). Items 1, 2, 3 and 4 are Structure, Differentiation, Nuclear polymorphism and Mitoses deal with the tumour cells alone whereas 5, 6, 7 and 8 describing Mode and Stage of invasion, Vascular invasion and Cellular response treat the relations between the tumour cells and the host tissue.

Each of the 8 items has 4 alternative answers which are scored 1, 2, 3 or 4. If the actual histological material is unsuitable for answering a certain item the item is omitted. The average of the scores consequently ranging between 1.00 and 4.00 indicates the malignancy of the tumour.

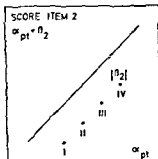
In order to achieve uniformity in the grading the pathologists discussed the system before the investigation.

Table 1. Histological Grading of Malignancy

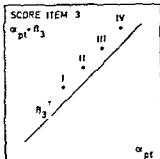
Item number	Tumour cell population	Points			
		1	2	3	4
1	Structure	Papillary and solid	Strands	Small cords and groups of cells	Marked cellular dissociation
2	Differentiation	Highly keratinization	Moderately some keratinization	Poorly Minimum keratinization	Poorly no keratinization
3	Nuclear polymorphism	Few enlarged nuclei	Moderate number of enlarged nuclei	Numerous irregular enlarged nuclei	Anaplastic immature enlarged nuclei
4	Mitoses	Single	Moderate number	Great number	Numerous
	Tumour host relationship	Points			
		1	2	3	4
5	Mode of invasion	Well defined borderline	Cords less marked borderline	Groups of cells no distinct borderline	Diffuse growth
6	Stage of invasion	Possibly	Microcarcinoma (few cords)	Nodular into connective tissue	Massive
7	Vascular invasion	None	Possibly	Few	Numerous
8	Cellular response (plasmolympocytic)	Marked	Moderate	Slight	None



TRUE MALIGNANCY



TRUE MALIGNANCY



TRUE MALIGNANCY

Fig 1 Theoretical score patterns for a perfect scoring system (three items four patients I-IV one pathologist $\beta_1 + \beta_2 + \beta_3 = 0$)

and agreed on an interpretation of the individual scores as described by Helweg Larsen et al (1978)

Statistical Analysis

The statistical evaluation will consist of 2 parts. First an exploratory data analysis investigating the suitability of each of the 8 items, the varying use of the system by the 6 pathologists, and the consistency of the grading in relation to a one-dimensional concept of histological malignancy thus forming a natural basis for the use of a simple average of scores as measure of malignancy. Secondly a definition and assessment of the precision of the grading system should one want to use it routinely. Finally on the basis of these results an attempt to point out some ways to improve the grading system.

RESULTS

Exploratory Analysis of the Structure of the Grading System

The perfect grading system It is natural to base the use of the average score as an indicator of malignancy upon an assumption of one-dimensional histological malignancy changes in malignancy level should affect all items in the same way though it is no requirement that for instance 2 on one item corresponds to 2 on another. Were the true malignancies of a series of patients known we should therefore expect a pattern like that of Fig 1 which indicates how in a perfect grading system the scores on each individual item increase with increasing true malignancy. For each item a line parallel to the three lines that could be drawn through the 4 points in each diagram. In addition to this the reproducibility of the scores should be perfect.

idealized pattern In the actual data the semiquantitative nature of the scoring system with only 4 response categories makes diagrams like those of Fig 1 unfeasible for each pathologist and item. We shall therefore first compare items pooled over pathologists and secondly pathologists pooled over items. Since the true malignancy is of course an abstraction we use instead the average score over items and pathologists as reference (abscissa). Fig 2 shows for each item the average score over the 6 pathologists for each of the 22 patients as ordinate plotted against the estimated true malignancy as just explained (Note: There were 35 out of 1056 responses missing with a distribution on the items 1-8 of respectively 1 2 1 3 2 14 10 and 2). In the following analysis we treat those as ordinary "missing values" and substitute expected values by a routine procedure. The adequacy of that assumption in the context is discussed further below.

It is seen from Fig 2 that items 1, 3, 5 and 7 follow the general pattern determined by the average quite closely. It also appears that the score on item 7 is consistently below the full drawn line as is indeed permitted of Fig 1. Items 2 and 8 follow the general pattern but much less accurately. Finally items 4 and 6 are generally scored rather independently of the remaining ones.

In a similar fashion we plot in Fig 3 the average over items of each pathologist's scores for a given patient against the average

true identity line) except pathologist F who generally has higher scores than the average opinion. Closer inspection further reveals differences between the pathologists in their ability or willingness to discriminate between the patients. Thus pathologists A and B keep close to the average opinion whereas C and F discriminate more and D and E less than the average.

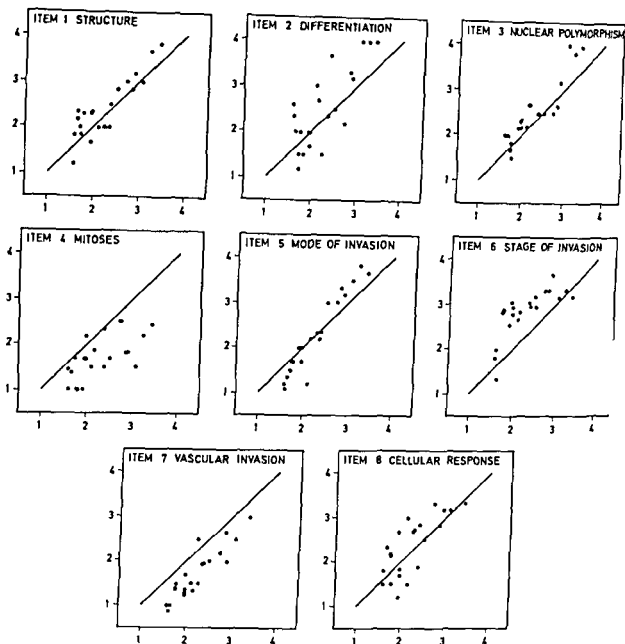


Fig 2 Plots of average score over pathologists for each item (ordinate) against the patient's estimated true malignancy (abscissa), given as the average score over pathologists and items (Each point corresponds to one patient)

Finally we use a similar approach to compare the usage of the items among the pathologists. Fig 4 shows for each pathologist the average score over patients for a given item (indicated by its number) plotted against the average over pathologists and patients. It is seen that the pathologists do not quite agree on the use of the individual items. The extreme parts of the scale are used more than average by pathologists A and B and to some extent by E, and less than average by C. Pathologists D and F seem to use the items differently (larger spread around a straight line). The pathologists in particular disagree on the use of items 4 and 7.

Definition and Assessment of the Precision of the Grading System

We saw in the exploratory part of the analysis above that there were certain variations between the extent to which the various items and the various pathologists conformed to the general pattern. In this section we want to quantify these variations in order to obtain a synthetic measure of the precision of the grading system.

We take the viewpoint that the grading system is given and it is desired to estimate the malignancy level of a new patient. The grading system is to be used by a pathologist belonging to a certain

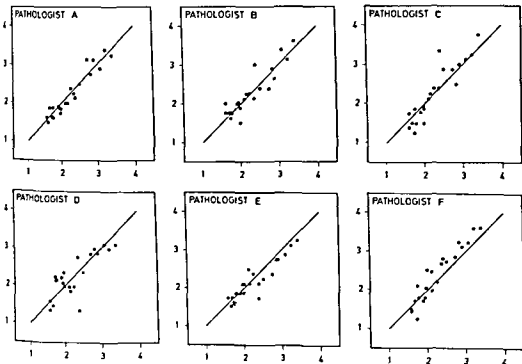


Fig 3 Plots of average score over items for each pathologist (ordinate) against the patient's estimated true malignancy (abscissa)

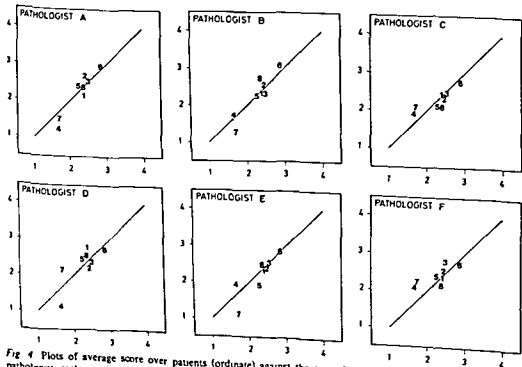


Fig 4 Plots of average score over patients (ordinate) against the general item average (abscissa) One plot per pathologist each point corresponds to an item (indicated by its number)

population of »competent pathologists« from which the 6 present pathologists may be regarded a random sample. This means that if pathologists do not use the items quite the same way, the pathologist-item interaction is an unavoidable »noise« in the system. Similarly, minor disagreement between competent pathologists on the ranking of patients (patient-pathologist interaction) as well as patient-item interaction are unavoidable noise sources.

The statistical model used is a three-way analysis of variance with certain random effects. The present account is based on Jensen (1979) somewhat in line with Nelder (1977). A standard textbook treatment is by Scheffe (1959). We use variance component models primarily because no other available statistical tool can catch and synthesize the various sources of variations inherent in the problem. Although the exposition is phrased in terms of the normal distribution, the emphasis is on identifying and calculating the separate variance terms, which does not depend critically on special distributional assumptions.

The statistical model may be described by the following decomposition of the basic observation which is the score $X_{pt \text{ path } i}$ ($i = 1, 2, 3$ or 4) of the pathologist path on item i , when grading the biopsy of patient pt :

$$X_{pt \text{ path } i} = \alpha_{pt} + \beta_i + U_{\text{path}} + V_{pt \text{ i}} + Y_{pt \text{ path}} + Z_{\text{path } i} + W_{pt \text{ path } i}$$

where α_{pt} and β_i are fixed numbers whereas the U 's [V 's, Y 's, Z 's] are independent normally distributed random variables with zero expectation and constant variance ω_{path} [$\omega_{pt \text{ i}}$, $\omega_{pt \text{ path}}$].

The interpretation of the model is as follows. We agree that a patient pt has a (latent) true malignancy α_{pt} and that the ideal score $\alpha_{pt} + \beta_i$ on item i for patient pt is obtained from the true malignancy by an additive correction β_i (cf. Fig. 1). (We thus adopt the convention that $\sum \beta_i = 0$). Deviations from this ideal additivity, the patient-item interaction are here considered as (random) noise and hence modelled by a random variable $V_{pt \text{ i}}$ whose variance measures the magnitude of the noise.

The general deviation of a pathologist from the true score is also modelled as a random variable U_{path} . This is because we want the analysis to be applicable to a population of pathologists and not only to the 6 specific participants in this study. Similarly, the specific deviations $Y_{pt \text{ path}}$ from true score of pathologist path when studying patient pt as well as the specific deviations $Z_{\text{path } i}$ from true score when pathologist path uses item i are modelled as random noise terms. Finally, even if all the so far mentioned corrections were accounted

for, there would still be the possibility of a second order interaction $W_{pt \text{ path } i}$ which under the present set up also contains the basic measurement uncertainty of the instrument and thus provides a baseline against which to assess the significance of the other noise terms. The estimation of the mean value parameters α_{pt} and β_i (the systematic components) as well as the variance parameters ω_{Λ} (the random components) is obtained fairly directly from a standard analysis of variance. Table 2 shows the ordinary three way (systematic) analysis of variance table as well as the estimates of the patient means α_{pt} and item means $\bar{\alpha} + \beta_i$, $\bar{\alpha} = \sum \alpha_{pt}/22$. (As mentioned above, missing values are filled in by standard prediction methods in the three way anova model. In the »degrees of freedom« column it is indicated in brackets how many degrees of freedom have been sacrificed in each variance component due to missing values.)

The »mean square« column in the anova table contains estimates of parameters σ_{Λ}^2 which are connected to the parameters ω_{Λ} defined above by the relations (cf. Jensen 1979)

$$\omega_{pt \text{ path } i} = \sigma_{pt \text{ path } i}^2$$

$$\omega_{pt \text{ path}} = \frac{1}{n_i} (\sigma_{pt \text{ path}}^2 - \sigma_{pt \text{ path } i}^2)$$

where n_i = number of items = 8 and similarly for $\omega_{pt \text{ i}}$ and $\omega_{\text{path } i}$ and finally

$$\omega_{\text{path}} = \frac{1}{n_i n_{pt}} (\sigma_{\text{path}}^2 - \sigma_{pt \text{ path}}^2 - \sigma_{\text{path } i}^2 + \sigma_{pt \text{ path } i}^2)$$

In this way the parameters ω_{Λ} may be estimated as mentioned in the discussion. A negative estimate may well be interpreted in an alternative statistical framework. The results are shown in Table 3.

We are now ready to compute the measurement uncertainty of the grading system. The patient true malignancy α_{pt} is to be estimated by the patient average \bar{X}_{pt} . We use the decomposition above to calculate the variance (summing the individual independent components) as follows. Using the assumption $\sum \beta_i = 0$ we have

$$\bar{X}_{pt} = \alpha_{pt} + \bar{U} + \bar{V}_{pt} + \bar{Z} + \bar{W}_{pt}$$

where a bar as usual denotes average, thus

$$\bar{V}_{pt} = \frac{1}{n_i} \sum_i V_{pt \text{ i}} = \bar{Z} = \frac{1}{n_{\text{path}} n_i} \sum_{\text{path } i} Z_{\text{path } i}$$

Hence

$$\begin{aligned} \text{Var}(\bar{X}_{pt}) &= \frac{\omega_{\text{path}}}{n_{\text{path}}} + \frac{\omega_{pt \text{ i}}}{n_i} + \frac{\omega_{pt \text{ path}}}{n_{\text{path}}} + \frac{\omega_{\text{path } i}}{n_{\text{path}} n_i} + \frac{\omega_{pt \text{ path } i}}{n_{\text{path}} n_i} \\ &= 0.0304 \end{aligned}$$

corresponding to a standard error of 0.174

TABLE 2 *Three Way Analysis of Variance*

Source of variation	Degrees of freedom (missing values)	Sum of squares	Mean square	F (against residual)	P
Patients	21	309.59	14.742	54.4	< 0.001
Pathologists	5	4.47	0.893	3.30	0.06
Pt. x path	104 (1)	71.65	0.689	2.54	< 0.001
Items	7	148.03	21.147	78.1	< 0.001
Pt. x items	147	151.47	1.030	3.80	< 0.001
Path x items	35	59.64	1.704	6.29	< 0.001
Residual	701 (34)	189.89	0.271		
Total	1020	934.74	0.916		

Patient average scores (ranked)

1.60	1.61	1.69	1.75	1.76	1.79	1.93	1.98	1.99	1.99
2.12	2.17	2.27	2.39	2.41	2.52	2.75	2.85	2.92	3.10
3.25	3.43								

Item average scores

Item	1	2	3	4	5	6	7	8
Item av. score	2.41	2.46	2.51	1.68	2.26	2.85	1.71	2.40

If data from only one pathologist are used (but we still want to include our knowledge regarding the pathologist population variation) we use $\bar{X}_{pt \text{ path}}$ as estimate of α_{pt} and

$$\begin{aligned} \text{Var}(\bar{X}_{pt \text{ path}}) \\ = u_{pa \text{ h}} + u_{pt \text{ pa h}} + \frac{w_{pt} + u_{pa \text{ h}} + w_{p \text{ pa h}}}{n} = 0.103 \\ \text{S.E.} = 0.321 \end{aligned}$$

Table 3 *Estimated Variance Components*

	df	σ^2	w
path	5	0.894	-0.007
pt 1	147	1.030	0.127
pt path	104	0.689	0.052
path 1	35	1.704	0.065
pt path 1	701	0.271	0.271

Attempts to Improve the Precision of the Grading System

Consequences of omitting some items In the exploratory analysis we saw that items 4 and 6 and to a lesser extent items 2 and 8 did not seem to contribute relevantly to the malignancy dimension here considered. In order to assess the consequences of omitting these items we re run the analysis of variance assuming that the grading system has only

Table 4 *Estimated Variance Components when only Items 1 3 5 and 7 Are Retained*

	df	σ^2	w
path	5	3.114	0.016
pt 1	63	0.506	0.042
pt path	104	0.646	0.097
path 1	15	1.281	0.046
pt path 1	302	0.257	0.257

population of »competent pathologists« from which the 6 present pathologists may be regarded a random sample. This means that if pathologists do not use the items quite the same way, the pathologist-item interaction is an unavoidable »noise« in the system. Similarly, minor disagreement between competent pathologists on the ranking of patients (patient-pathologist interaction) as well as patient-item interaction are unavoidable noise sources.

The statistical model used is a three-way analysis of variance with certain random effects. The present account is based on Jensen (1979), somewhat in line with Nelder (1977). A standard textbook treatment is by Scheffe (1959). We use variance component models primarily because no other available statistical tool can catch and synthesize the various sources of variations inherent in the problem. Although the exposition is phrased in terms of the normal distribution, the emphasis is on identifying and calculating the separate variance terms, which does not depend critically on special distributional assumptions.

The statistical model may be described by the following decomposition of the basic observation, which is the score $X_{pi \text{ path } i}$ ($i = 1, 2, 3$ or 4) of the pathologist path on item i when grading the biopsy of patient pt:

$$X_{pi \text{ path } i} = \alpha_{pi} + \beta_i + U_{\text{path}} + V_{pi} + Y_{pi \text{ path}} + Z_{\text{path } i} + W_{pi \text{ path } i}$$

where α_{pi} and β_i are fixed numbers, whereas the U 's [V 's, Y 's] are independent normally distributed random variables with zero expectation and constant variance ω_{path} [ω_{pi} , $\omega_{pi \text{ path}}$].

The interpretation of the model is as follows. We agree that a patient pt has a (latent) true malignancy α_{pi} and that the ideal score $\alpha_{pi} + \beta_i$ on item i for patient pt is obtained from the true malignancy by an additive correction β_i (cf. Fig. 1). (We thus adopt the convention that $\Sigma \beta_i = 0$.) Deviations from this ideal additivity, the patient-item interaction, are here considered as (random) noise and hence modelled by a random variable V_{pi} , whose variance measures the magnitude of the noise.

The general deviation of a pathologist from the true score is also modelled as a random variable U_{path} . This is because we want the analysis to be applicable to a population of pathologists and not only to the 6 specific participants in this study. Similarly, the specific deviations $Y_{pi \text{ path}}$ from true score of pathologist path when studying patient pt as well as the specific deviations $Z_{\text{path } i}$ from true score when pathologist path uses item i are modelled as random noise terms. Finally, even if all the so far mentioned corrections were accounted

for, there would still be the possibility of a second order interaction $W_{pi \text{ path } i}$ which under the present set-up also contains the basic measurement uncertainty of the instrument and thus provides a baseline against which to assess the significance of the other noise terms. The estimation of the mean value parameters α_{pi} and β_i (the systematic components) as well as the variance parameters ω_{λ} (the random components) is obtained fairly directly from a standard analysis of variance. Table 2 shows the ordinary three way (systematic) analysis of variance table as well as the estimates of the patient means α_{pi} and item means $\bar{\alpha} + \beta_i$, $\bar{\alpha} = \Sigma \alpha_{pi}/22$. (As mentioned above, missing values are filled in by standard prediction methods in the three way anova model. In the »degrees of freedom« column it is indicated in brackets how many degrees of freedom have been sacrificed in each variance component due to missing values.)

The »mean square« column in the anova table contains estimates of parameters σ_{λ}^2 which are connected to the parameters ω_{λ} defined above by the relations (cf. Jensen 1979)

$$\omega_{pi \text{ path } i} = \sigma_{pi \text{ path } i}^2$$

$$\omega_{pi \text{ path}} = \frac{1}{n_i} (\sigma_{pi \text{ path}}^2 - \sigma_{pi \text{ path } i}^2)$$

where n_i = number of items = 8 and similarly for ω_{pi} and $\omega_{\text{path } i}$ and finally

$$\omega_{\text{path}} = \frac{1}{n \cdot n_{pi}} (\sigma_{\text{path}}^2 - \sigma_{pi \text{ path}}^2 - \sigma_{\text{path } i}^2 + \sigma_{pi \text{ path } i}^2)$$

In this way the parameters ω_{λ} may be estimated as mentioned in the discussion a negative estimate may well be interpreted in an alternative statistical framework. The results are shown in Table 3.

We are now ready to compute the measurement uncertainty of the grading system. The patient true malignancy α_{pi} is to be estimated by the patient average $\bar{\alpha}_{pi}$. We use the decomposition above to calculate the variance (summing the individual independent components) as follows. Using the assumption $\Sigma \beta_i = 0$ we have

$$\bar{\alpha}_{pi} = \alpha_{pi} + \bar{U} + \bar{V}_{pi} + \bar{Z} + \bar{W}_{pi}$$

where a bar as usual denotes average, thus

$$\bar{V}_{pi} = \frac{1}{n_i} \Sigma V_{pi} \quad \bar{Z} = \frac{1}{n_{\text{path}} \cdot n_i} \Sigma_{\text{path}} \Sigma Z_{\text{path } i}$$

Hence

$$\begin{aligned} \text{Var}(\bar{\alpha}_{pi}) &= \frac{\omega_{\text{path}}}{n_{\text{path}}} + \frac{\omega_{pi}}{n_i} + \frac{\omega_{pi \text{ path } i}}{n_{\text{path}}} + \frac{\omega_{\text{path } i}}{n_{\text{path}} \cdot n_i} + \frac{\omega_{pi \text{ path } i}}{n_{\text{path}} \cdot n_i} \\ &= 0.0304 \end{aligned}$$

corresponding to a standard error of 0.174

$< 2.5 - 1.64 \times 0.32 - 1.98$ should we recommend against 1.64 being the 95 fractile in the standard normal distribution. In the present series of patients this would mean that $11/22 = 50\%$ would be «safely» allocated. If 6 pathologists performed the grading the interval would be narrowed to $2.21 - 2.79$ ($2.50 \pm 1.64 \times 0.174$) so that $17/22 = 77\%$ of the patients were allocated with safety in accordance with the intention.

These examples have important implications. Firstly an evident consequence would be that it is desirable to have several pathologists to grade each patient. (In addition this procedure would be a precaution against a careless extrapolation of the inferences about a population of competent pathologists drawn from the present sample of 6). The second implication is that only the extremes of the scale should be trusted.

The Sources of Variation

The analysis of the basic structure of the scoring system and the subsequent analysis of the variance components have been utilized to localize and quantify the sources of noise in the grading system. Before the discussion of the individual sources it is in structure to consider the decomposition of the basic measurement uncertainty probably best expressed as the variance if one pathologist grades one patient. The estimated malignancy (average score) has a variance given by

$$V(\bar{X}_{p,pa,h}) = \frac{\omega_{p,pa,h} + \omega_{p,pa,h} + \omega_{p,pa,h}}{n} \\ = 0.07 + 0.52 + \frac{1.27 + 0.65 + 2.71}{8} \\ = 0.07 + 0.52 + 0.16 + 0.08 + 0.34 \\ 1.03$$

It follows that the main sources of variation are the general variance (noise) term $\omega_{p,pa,h}/n$ $2.71/8 = 0.34$ and the patient pathologist interaction $\omega_{p,pa,h} = 0.52$. The interactions with items are less important because the estimated malignancy is computed by averaging over 8 items but not averaging over pathologists.

Divergence among the Pathologists in Their Evaluation of the Patients

Slight deviation from the general level and difference in the discrimination between the patients were seen (Fig. 3 and Table 3) but it appeared from the example above that the pathologist-patient interaction has a relatively great weight in the final

computation of the uncertainty of the grading system. This divergence may reflect how the individual pathologist acts in case of doubt which easily may arise as the four scoring categories of each item do not represent well-defined separate entities but rather indistinct parts of a continuum.

Deviation from the general opinion may as suggested by Iversen & Sandnes (1971) reflect the therapeutical philosophy of the pathologist so that a therapeutical optimist instinctively overestimates malignancy and vice versa. Perhaps this effect would become more pronounced if it was known by the pathologists that the grading would have important therapeutical implications unlike the conditions of the present investigation.

Deviations from One dimensionality of Histological Malignancy

In the following considerations it is important to realize the relative role of estimated true malignancy in this study. Our intrinsic comparison has no choice but to use the average score as representing «truth». As an extreme case suppose that in fact only item 1 really represented malignancy while the other seven while highly correlated represented varying degrees of something else. Then any internal comparison would imply that item 1 ought to be omitted.

It was seen from Fig. 2 that items 2, 4, 6 and 8 affect the one-dimensional concept of histological malignancy measured by the present grading system. This becomes even more convincing when it is taken into account that we used the average of all 8 items (including the one under study) as abscissa. From Table 2 it appears that the item average scores differ significantly (range $-1.68 - 2.85$). This is a question of score category definition which does not detract from the consistency of the system; however it should be noted that these differences are ignored when an item which cannot be evaluated and therefore is omitted in the calculation is ascribed a value equal to the average of the remaining items. This inconsistency has been

mentioned to be made in this connection. First this procedure cannot reasonably be

assumed not in itself provide information, an assumption which is perhaps not completely satisfied here. Since only 35 out of 1056 responses were missing here we expect any bias to be rather minor but in series of less suitable biopsies noise may still arise in this way.

TABLE 5 *Estimated Variance Components when Pathologist Main Effects and Pathologist-Item Interactions Are Considered Non-Random*

	df	σ^2	ω
pt 1	147	1.030	0.127
pt path	104	0.689	0.052
pt, path 1	701	0.271	0.271

4 items namely 1, 3, 5 and 7. The results are presented in Table 4. As above we then compute

$$\text{Var}(\bar{X}_{pt}) = 0.0418, \text{ s.e.} = 0.205,$$

$$\text{Var}(\bar{X}_{pt, path}) = 0.200, \text{ s.e.} = 0.447$$

Calibration of pathologists. We consider an idealized case of adjustment, that is, the pathologist main effect (formerly U_{path}) and the pathologist-item interaction (formerly $Z_{path, i}$) now designated Y_{path} resp. $\delta_{path, i}$ can be estimated without error.

The model may then be specified as

$$\begin{aligned} X_{pt, path, i} &= \alpha_{pt} + \beta_i + \gamma_{path} + \delta_{path, i} \\ &+ V_{pt, i} + Y_{pt, path} + W_{pt, path, i} \end{aligned}$$

From the analysis of variance in Table 2 we may now derive the estimated variance components in Table 5. We then get

$$\text{Var}(\bar{X}_{pt}) = \frac{\omega_{pt, i}}{n_i} + \frac{\omega_{pt, path}}{n_{path}} + \frac{\omega_{pt, path, i}}{n_{path} n_i} = 0.0302$$

s.e. 0.174,

$$\text{Var}(\bar{X}_{pt, path}) = \omega_{pt, path} + \frac{\omega_{pt, i} + \omega_{pt, path, i}}{n_i} = 0.102$$

s.e. 0.319

DISCUSSION

Before entering into the details of the results of this investigation let us repeat from the introduction that our only aim here is to study the intrinsic consistency and precision of the grading system. Since we do not know any way of directly observing »true malignancy« the only possible external comparison would be to the observed prognosis. For this to be informative a different study containing many more patients and a considerable follow-up period would be necessary.

Statistical Model

There are several alternative approaches to the definition of analysis of variance models with

random effects. Although the definition in terms of specifying the complete covariance structure (such as »intraclass correlation«) may be the more satisfactory from a statistical point of view, we have here used an error component formulation in the hope that it is more easily accessible for the readers of the present paper. It should however be borne in mind that »negative variances« of all other error components than the residual ($W_{pt, path, i}$) may well be interpreted in the former framework.

In the presentation of the variance component model above, we performed no significance tests to obtain a possible simplified model. First, it is immediately seen from Table 2 that all main effects and first-order interactions are highly significant against the residual given by the second order interaction. We draw one important inference from this fact: Any »rounding error effect« of the integer nature of the basic score would increase the residual variance. Since this is still by far the smallest, that objection against using the normal distribution can reasonably be disregarded. Secondly the question of the negative estimate $\omega_{path} = -0.07$ (first model) may be treated by calculating an approximate standard error ω_{λ} being a linear combination of χ^2 -statistics. This leads to $\omega_{path} = -0.07 \pm 0.04$ meaning that we may well assume $\omega_{path} = 0$ and thus have no need for a further discussion of the alternative statistical framework.

Basic Measurement Uncertainty

It was seen that if data from only one pathologist were used the histological grading was perturbed by a standard error of $\sqrt{0.103} = 0.321$. If 6 pathologists were involved the standard error became 0.174.

Any use of the grading system as therapeutic guidance should consider the relatively good prognosis of epidermoid carcinoma of the larynx treated by radiation alone (Sand Hansen 1975, Jørgensen 1976) as well as the severity of any possible surgical intervention. Lund *et al.* (1977) suggested that »In cases where exploratory operations on the regional lymph nodes are considered the histological score may be the decisive factor«. To illustrate the implications of the measurement uncertainty of the grading system on its use as an aid in such decisions let us assume that it is established that patients with true score greater than 2.5 should be operated while patients with true score less than 2.5 should not. Assume further that we want to make no more than 5% misclassifications in the long run and that only one pathologist performs the grading. Then if the patient's observed average score was $> 2.5 + 1.64 \times 0.32 = 3.02$ we should recommend operation and only if it was

one pathologist grades each patient. One recommendation drawn from the study is that the observer-patient interaction seems so large that each biopsy should be graded by several pathologists.

From a practical point of view the total variability of a grading system like this is composed of the uncertainty of prognostic statements for given levels of malignancy on the one hand and the intrinsic lack of precision on the other. The present paper has only studied the latter source of variation.

We are grateful for several useful discussions on variance component models with Søren Tolver Jensen, Institute of Mathematical Statistics, University of Copenhagen, and we thank Poul T. Boesen, Claus Petri, Carl O. Povlsen and Jørgen Rygaard for their grading of the biopsies and for the inspiring interest they took in the investigation. Jørgen Hilden supplied useful comments on the manuscript.

REFERENCES

- Bergkvist A, Ljungqvist A & Moberger G. Classification of bladder tumours based on the cellular pattern. *Acta Chir Scand* 130: 371-378 1965.
- Bloom H J G & Richardson W W. Histological grading and prognosis in breast cancer. A study of 1489 cases of which 359 have been followed for 15 years. *Brit J Cancer* 11: 359-377 1957.
- Hansen H. Sand. Neoplasma malignum laryngis. Thesis. Polyteknisk Forlag, København 1975.
- Helweg-Larsen K, Græm N, Meistrup-Larsen K J & Meistrup-Larsen U. Clinical relevance of histological grading of cancer of the larynx. *Acta path microbiol scand Sect A* 86: 499-504 1978.
- Iversen O H & Sandnes K. The reliability of pathologists. *Acta path microbiol scand Sect A* 79: 330-334 1971.
- Jakobsson P, Eneroth C M, Killander D, Moberger G & Mårtensson B. Histological classification and grading of malignancy in carcinoma of the larynx. *Acta Radiol Ther Phys Biol* 12: 1-8 1973.
- Jakobsson P. Glottic carcinoma of the larynx: factors influencing prognosis following radiotherapy. Thesis. Stockholm 1973.
- Jensen S T. Varianskomponentmodeller for fuldstændigt balancerede forsøg. Manuscript. Institute of Mathematical Statistics, University of Copenhagen 33 pp 1979.
- Jørgensen K. Carcinoma laryngis. Thesis. Århus 1976.
- Lund C, Søgaard H, Elbrønd O, Jørgensen K & Andersen A P. Epidermoid carcinoma of the larynx. Histological grading in the clinical evaluation. *Acta Radiol Ther Phys Biol* 15: 293-304 1976.
- Lund C, Søgaard H, Jørgensen K, Elbrønd O, Højtm Hansen M & Andersen A P. Histological grading of epidermoid carcinomas in the head and neck. *Danish Medical Bulletin* 24: 162-166 1977.
- Nelder J A. A reformulation of linear models (with discussion). *J Roy Statist Soc A* 140: 48-77 1977.
- Povlsen H E, Taylor C W & Sobin L H. Histological typing of the female genital tract tumours. World Health Organization, Geneva 1975 p 96.
- Scheffe H. The analysis of variance. Wiley, New York 1959.
- Silberberg S G. Reproducibility of the mitosis count in the histological diagnosis of smooth muscle tumours of the uterus. *Hum Pathol* 7: 451-456 1976.

It might be that the items Keratinization Mitoses, Stage of invasion and Cellular response correlate well to clinical malignancy as reported by Jakobsson (1973), but in the grading system they are important sources of noise and main contributors to the patient-item interaction w_{pi} (Table 2 vs 4). In order to increase the precision of the grading we omitted these items (disregarding a possible psychological interactive effect between retained and omitted items), but found that the grading thereby became less precise. The patient-item interaction certainly was reduced to one third (Table 4) of the original value, but at the expense of a doubling of the patient pathologist interaction which in the present example has 4 times (number of items) greater numerical weight in the final calculation of the standard errors (cf example above).

Presumably an imperfect one-dimensionality, which is not surprising remembering the diversity of malignant tumours, also blurs the results of other histological grading systems. This may be expected not only in those employing a single sum or average of scores as the system for grading of breast carcinomas of Bloom & Richardson (1957), but also in grading systems in which the »computation« is performed »within the pathologist« by a complex psychological process e.g. in grading of atypia of bladder tumours (Bergkvist *et al* 1965) and dysplasias of the uterine cervix (Poulsen *et al* 1975).

In order to get an optimal consistency in a grading system analytical diagrams like those of Fig 2 would form a sound basis of the design. Of course it should be remembered that other arithmetical operations than simple addition of score values are possible and that the score values may be weighted differently.

Divergence among the Pathologists in Their Scoring of the Individual Items

It was seen from Fig 4 and Table 3 that the pathologists did not agree in their use of the individual items especially pathologist D and F dissented from the average, and items 4 (Mitoses) and 7 (Vascular invasion) were scored with great disagreement. The divergence on mitotic activity is remarkable as this theoretically might be easily quantitated and as this parameter is often used in grading of malignancy. As pointed out by Silverberg (1976) it might be due to a disagreement on the morphological definition of mitoses. The disagreement on item 7 may have a similar cause. The definition of especially score 2 on this item is vague. While the term »possibly« on item 6 (Stage of invasion) is fairly well understood it has a rather diffuse meaning in case of vascular invasion

as the biopsies contained few and small vessels. Ten out of 35 missing values occurred in item 7. Perhaps it would have been reasonable to drop this item in still more cases, but just the escape option »possibly« may have prevented this. These examples show that the consistency of diagnostic parameters should be secured before they are introduced in routine pathology.

In another attempt to find ways of increasing the precision of the grading system we imagined the pathologists to be calibrated. In principle – given access to a large sample of scorings – one might for each pathologist determine his/her particularities (in the analysis expressed as γ_{path} and δ_{path}) to a standard form. However it was noticed that even perfect adjustment of pathologists would have very limited effect as the basic measurement uncertainty expressed as the standard deviation of $\bar{X}_{pi path}$ was only reduced from 0.321 to 0.319.

Variance due to Preconception

It would be interesting to have further psychological information on how the pathologists make up their minds about a given biopsy – proceeding from the items to a conclusion (such as implicitly assumed when using the grading system) or by first forming a general opinion about »how malignant is this tumour« and subsequently filling in the score values in accordance with the conclusion. Obviously, we do not have such psychological insight. It might however be of interest to point out that the parameter $w_{pi path}$ may be interpreted as the »pure« covariance between the responses on two different items by a given pathologist on a given patient that is for given general levels of the patient, the pathologist and the items and given interactions between patient and items and between pathologist and items.

The highly significant positive intrinsic covariance $w_{pi path}$ between responses on different items on a given patient by a given pathologist may be interpreted as an indication that the pathologists do not score the items independently but at least in some cases proceed from a general impression to the individual item.

CONCLUSION

This paper has defined and discussed methodology for studying consistency and precision of histopathological grading systems taking particularly into account the important observer component in the measurement uncertainty. In the particular example studied, a grading system concerning epidermoid carcinoma of the larynx was seen to be able to discriminate between extreme cases, even if only

SURVIVAL IN IDIOPATHIC GLOMERULONEPHRITIS

MARCUS NYBERG ERNA PETTERSSON GUSTAV TALLQVIST and AMOS PASTERNAK

Central Laboratory of Pathology University of Helsinki IV Department of Medicine University
Central Hospital of Helsinki Department of Pathology Maria Hospital Helsinki and Institute of
Clinical Science University of Tampere Finland

Nyberg M Pettersson E Tallqvist G & Pasternack A Survival in idiopathic glomerulonephritis
Acta path microbiol scand Sect A 88 319-325 1980

Actuarial survival was studied in 285 adult patients with idiopathic glomerulonephritis (GN). Minimum follow up was 7 years. 105 patients had minimal change GN (MC), 22 membranous GN (MGN), 20 acute GN (AGN), 11 mesangial sclerosis GN (MSGN), 28 mesangiocapillary GN (MCGN), 8 crescentic GN (RPGN), 27 unclassifiable GN, 61 focal proliferative GN (FGN) and 3 focal segmental glomerular sclerosis and hyalinosis (FSGSH). Ten year survival was best in FGN (91%) and progressively poorer in MC (90%), AGN (85%), MSGN (83%), MGN (82%), MCGN (62%), unclassifiable GN (37%) and RPGN (16%). One of the three patients with FSGSH died during follow up. At 10 years survival differed significantly ($p < 0.01$) from expected only in MCGN, RPGN and unclassifiable GN. Our results suggest that - because survival was not significantly different from expected in most types of GN - the current classification of GN is only a crude guide to prognosis. The nephrotic syndrome was found to worsen prognosis in MGN and MCGN.

Key words: Glomerulonephritis, nephrotic syndrome, survival, renal biopsy.

Marcus Nyberg, Department of Pathology, University of Helsinki, SF-00290 Helsinki 29, Finland.

Received 13 III 80 Accepted 25 IV 80

Although many clinicopathologic correlation studies of histopathologically-defined glomerulonephritis (GN) have included data on survival only in more recent investigations (Hardwicke & al 1967, Antoine & Faye 1972, Cameron & al 1973, Habib & al 1973, Habib & al 1975, Row & al 1975, survival (Culler & Ederer 1958, Anderson & al 1974) been used that render results from different studies comparable. These investigations however have dealt with only one or a few histopathologic types of GN. Survival of excluded or unclassifiable patients has not been accounted for. To obtain a more complete picture of mortality from idiopathic GN, we believe that survival should be analysed in a comprehensive series that encompasses all histopathologic types including unclassifiable cases. There is only one report of this kind (Cameron 1972) but it

does not describe the age distribution of the patients. A study of children has been published (Habib 1970) for which actuarial survival was analysed later (Cameron 1973) together with data on survival from other clinicopathologic studies by other authors. We have found no study of this kind describing survival in exclusively adult GN patients. Prognosis has been considered to be predictable from the histopathologic type of GN (Habib 1970, Habib 1975, Cameron 1972). However, there are conflicting reports on survival in some types of GN (Cameron 1973), especially in membranous GN (Cameron 1972, Cameron 1973, Legrain & al 1978, Noel & al 1979).

The purpose of this study was to evaluate the relation of the currently used light microscopic classification of GN to long term survival in a comprehensive adult patient population. Survival results were also compared with expected survival in a matched normal population.

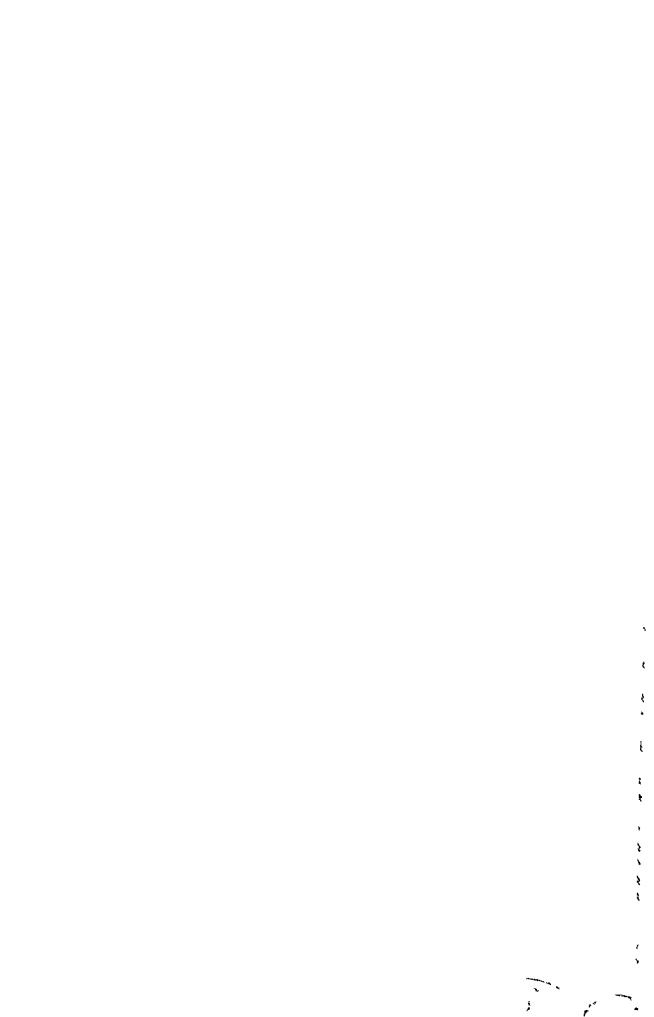


TABLE 1 *Clinical Data*

	Number of patients	Males/ females*	Age (years)			Signs*						Steroid treatment*	Lost to follow up
			mean	median	range	proteinuria	haematuria	proteinuria & haematuria	nephrotic syndrome	renal insufficiency or renal failure	hypertension		
Minimal change	105	48/57	32	29	16-66	31	22	31	19	2	-	19	-
Membranous GN	22	15/7	38	32	16-68	9	-	1	11	3	1	12	-
Acute GN	20	15/5	46	49	26-71	1	4	9	7	8	6	11	-
Acute GN	11	5/6	37	31	16-61	1	3	5	-	2	4	2	1
Mesangial sclerosis	28	16/12	35	33	15-70	8	5	7	10	7	12	10	1
Mesangiocapillary GN	8	6/2	51	52	38-73	-	2	5	2	5	4	4	1
Crescentic GN	27	17/10	44	41	17-76	9	12	11	4	9	7	7	1
Unclassifiable GN	61	30/31	39	39	16-71	14	7	22	1	6	14	11	3
Focal proliferative GN	3	2/1	35	28	27-50	1	1	-	-	-	1	-	-
Focal segmental glomerular sclerosis & hyalinosis	3	2/1	35	28	27-50	1	1	-	-	-	1	-	-
Total series	285	154/131	37	34	15-73	74	56	91	54	42	55	76	7

* Number of patients

MATERIAL AND METHODS

Selection of patients From all percutaneous renal biopsies referred to the Department of Pathology, Maria Hospital, during the period 1959 through 1971, we selected those that were reported, on light microscopy, to be normal or to show changes compatible with or suggestive of GN. These biopsies were then re-examined microscopically without prior knowledge of clinical or histological data. All biopsies were excluded that originally or at re-examination had less than five glomeruli (unrepresentative). Excluded were also all biopsies in which 50 per cent or more of the glomeruli were hyalinised (end stage lesions of uncertain glomerular or non-glomerular origin). The biopsies unrepresentative at re-examination were randomly distributed among histopathological categories at the primary examination. Biopsies from patients with diabetes mellitus, amyloidosis, systemic lupus erythematosus, periarteritis nodosa, and rheumatoid arthritis were also excluded as well as those from patients with a normal biopsy having none of the clinical signs of GN listed below. The remaining biopsies were examined once more and classified according to histological type. After classification of the biopsies, the clinical and laboratory data for each patient at the time of biopsy were collected from the hospital records. The final series comprised 285 patients.

Histological methods The biopsies had been fixed in either formaldehyde or glutaraldehyde. Serial sections 2–3 μ m thick were available for analysis and stained with

made

Criteria of histopathologic classification The classification used was based on light microscopic criteria reported by others (Jones 1957, Ehrenreich & Churg 1968, Churg & al 1970, Habib 1970, White & al 1970, Burkholder 1974, Heptinstall 1974).

A Diffuse lesions (all or most of the glomeruli affected)

Minimal change GN (MC) Glomeruli appear normal with no apparent cellular proliferation or thickening of the glomerular basement membrane (GBM) and no accentuation of the mesangial matrix. No more than one out of 10 glomeruli is globally hyalinised.

Membranous GN (MGN) When stained with H&E, glomeruli show a general thickening of the capillary wall. Staining with PASM reveals conspicuous needle-like protrusions ('spikes') on the epithelial side of the GBM that occur either globally or segmentally in the glomeruli. Mesangium is normal or only slightly increased with no cellular proliferation.

Acute GN (AGN) A normal GBM is seen in combination with a proliferation of mesangial and endothelial cells that narrow or obliterate the capillary lumina. Occasional polymorphonuclear leukocytes may be present in the glomeruli. Mesangial matrix is normal.

Mesangial sclerosis (mesangial proliferative) GN (MSGN) Capillary lumina are normal and patent. Mesangial matrix is increased with or without proliferation of mesangial cells.

Mesangiocapillary (membranoproliferative) GN (MCGN) The GBM appears double-contoured when stained with PASM and it may also stain strongly with PAS. Mesangial matrix is increased, sometimes giving the glomeruli a lobulated appearance. Proliferation of the mesangial cells is present. The GBM may be only slightly affected but the prominent mesangial lobulation distinguishes MCGN from MSGN.

Crescentic (rapidly progressive) GN (RPGN) Epithelial or fibro epithelial crescents appear within Bowman's space in most of the glomeruli, obliterating the glomerular tuft. Unspecific proliferative changes are also seen within the tufts.

B Focal lesions (only some glomeruli affected usually about a third)

Focal proliferative GN (FGN) Glomeruli show at least one of the following changes: cellular proliferation, increased mesangial matrix, capsular adhesion, sclerotic scarring. Occasional crescents may be present as well as one or a few globally hyalinised glomeruli.

Focal segmental glomerular sclerosis and hyalinosis (FSGS) A segmental lesion in one or a few glomeruli shows hyaline material on the luminal side of the capillary wall. Associated with this lesion may be foam cells, minimal cellular proliferation and some sclerosis with or without a capsular adhesion. Some tubular atrophy is present.

C Unclassifiable proliferative GN Glomerular changes are not compatible with any of the aforementioned types.

Clinical and laboratory criteria

Persistent proteinuria more than 0.1 g/l of protein in the urine in repeated specimens.

Haematuria three or more red blood cells per high power field in more than two samples of urine before biopsy.

Nephrotic syndrome proteinuria in excess of 3 g per day in combination with at least two of the following: oedema, hypoproteinaemia (serum protein less than 55 g/l) or hypoalbuminaemia (serum albumin less than 30 g/l), and hypercholesterolaemia (serum cholesterol in excess of 7.5 μ mol/l).

Renal insufficiency serum creatinine in excess of 110 μ mol/l or a creatinine clearance less than 85 ml/min or both.

Hypertension blood pressure higher than 150/100 mmHg regardless of age.

Follow-up and calculation of survival Follow up time was defined as the period between the date of the first representative biopsy and the end of the study or death whichever came first. The last day of the study was not fixed but was chosen to ensure, for all living patients, a minimum follow up time of 7 years. Death when not an actual death, was considered to have happened on the date when chronic haemodialysis was started or on the date of a renal transplantation if not preceded by dialysis (Cameron 1973, Legrain 1978). Survival data were collected from hospital records and from the official

TABLE 1 *Clinical Data*

	Age (years)			Signs*							Lost to follow up		
	Number of patients	Males/ females*	mean	median	range	proteinuria	haematuria	proteinuria & haematuria	nephrotic syndrome	renal insufficiency or renal failure		hypertension	Steroid treatment*
Minimal change	105	48/57	32	29	16-66	31	22	31	19	2	-	19	-
Membranous GN	22	15/7	38	32	16-68	9	-	1	11	3	7	12	-
Acute GN	20	15/5	46	49	26-71	1	4	9	7	8	6	11	-
Mesangial sclerosis	11	5/6	37	31	16-61	1	3	5	-	2	4	2	1
Mesangiocapillary GN	28	16/12	35	33	15-70	8	5	7	10	7	12	10	1
Crescentic GN	8	6/2	51	52	38-73	-	2	5	2	5	4	4	1
Unclassifiable GN	27	17/10	44	41	17-76	9	12	11	4	9	7	7	1
Focal proliferative GN	61	30/31	39	39	16-71	14	7	22	1	6	14	11	3
Focal segmental glomerular sclerosis & hyalinosis	3	2/1	35	28	27-50	1	1	-	-	-	1	-	-
Total series	285	154/131	37	34	15-73	74	56	91	54	42	55	76	7

* Number of patients

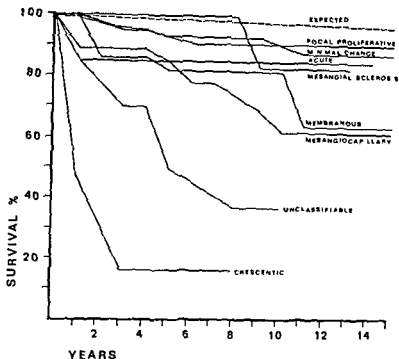


Fig 1 Actuarial survival according to histopathologic type of glomerulonephritis. Expected survival calculated for total series

equally regardless of cause. Expected survival (Ederer & *al* 1961) was calculated from mortality rate tables for the normal population for the period 1961-70 and the year 1977 kindly provided by the Finnish Central Bureau of Statistics. Expected survival rates were adjusted for sex and age in each type of GN.

Of the 285 patients seven were lost to follow-up (Table 1).

RESULTS

Clinical data (Table 1). More women than men had MC, MSGN, and FGN, mean age was highest among patients with RPGN, AGN, and unclassifiable GN. No obvious correlations between clinical signs and the histopathologic type of GN could be found. Of the patients with MC, only those with the nephrotic syndrome had received steroids. In all other groups, some nephrotic and some non-nephrotic patients had been treated with steroids.

Expected survival was almost the same for all types of GN. The survival rates were compared with a single expected survival curve (Fig 1). The survival was best in FGN and MC and progressively poorer in AGN, MSGN, MGN, and RPGN (Fig 1). At 10 years survival was not obtained for crescentic glomerulonephritis (RPGN).

2) In RPGN, no ten year survival could be obtained. In this group, however, a significant difference ($p < 0.01$) from expected was found already after one year of follow-up. No reliable survival curve could be calculated for the three patients with FSGSH. Two of these patients survived with follow-up times of 8.1 and 14.8 years, respectively, the third patient died during the 5th year of follow-up.

At ten years, the nephrotic syndrome correlated significantly ($p < 0.01$) with mortality in patients

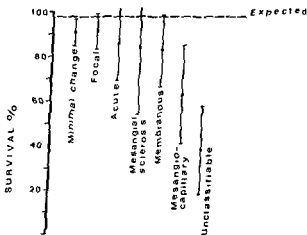


Fig 2 Ten year survival rates ± 2 SE according to histopathologic type of glomerulonephritis. 10 year survival not obtained for crescentic glomerulonephritis (RPGN).

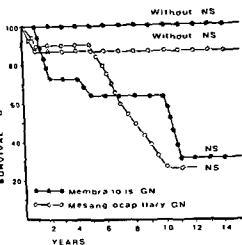


Fig 3 Effect of nephrotic syndrome (NS) on survival in membranous and mesangiocapillary glomerulonephritis

with MGN and MCGN (Fig 3) Survival did not differ, however, between nephrotic and non-nephrotic patients with MC

Fourteen patients with unclassifiable GN had some crescent formation in their biopsies Survival did not differ between these patients and the 13 whose biopsies showed no crescents

DISCUSSION

This study was undertaken to re-evaluate the prognostic value of the current light microscopic classification of idiopathic GN Immunofluorescence and electron microscopic findings were not taken into account Hence, some cases of MGN, because they looked normal on light microscopy (Ehrenreich & Churg 1968, Bariety & al 1970, Tornroth & al 1978, Tallqvist & al 1979) may have been wrongly classified as MC As the short-term prognosis of this variety of MGN is good (Tornroth & al 1978), the effect of this source of error is probably minimal Electron microscopic studies have revealed two types of MCGN type I (subendothelial deposits) and type II (dense intramembranous deposits) (Bariety & al 1971 Habib & al 1973) That these types are not differentiated ultrastructurally in our study is probably of no consequence since actuarial survival is the same in both types (Habib & al 1975, Davis & al 1978)

Our results corroborate earlier observations that there is no consistent correlation between symptoms and histopathologic type of GN or vice versa (Ufab 1970, Cameron 1975)

In our view, possible effects of steroid treatment

on long-term survival cannot be analysed in retrospective studies The inclusion of treated as well as untreated patients in our study conforms with the practice in most other reports

As the occurrence of unrepresentative biopsies was random their exclusion from the study does not, in our opinion, affect the results

In the individual groups, survival was longest in MC and FGN and progressively shorter in AGN, MSGN, MGN, MCGN, unclassifiable GN, and RPGN For his comprehensive series Cameron (1972) reported no or minimal mortality in MC, FGN and MSGN

Our survival curves show the same distribution for all types except MGN Among our patients with MGN, the survival rate was even higher than in MCGN, being about the same as that in AGN and MSGN

In MGN, survival was equal to that in the reports of Legrain & al (1978) and Noel & al (1979) That reports on survival in MGN differ may be due in part to variations in the frequency of the nephrotic syndrome (Table 2) Our results show, in agreement with Habib & al (1973 a) and Legrain & al (1978) that in MGN the nephrotic syndrome has a negative influence on prognosis It may be, however, that in a series in which a high percentage of patients with MGN are nephrotic, biopsies have been obtained only from those with severe and longstanding disease - which might affect the mortality rate Beregi & Varga (1974) performed biopsies on patients with MGN soon after the onset of clinical signs, and the frequency of the nephrotic syndrome in their series was very low (Table 2) But the relation of the nephrotic syndrome to survival in MGN is not without controversy in two of the aforementioned studies (Cameron 1972, Noel & al 1979)

Our survival results agreed with those in all earlier studies (Antoine & Faye 1972, Cameron 1972, Cameron 1973, Cameron & al 1973, Habib & al 1973, Habib & al 1975, Barbiano di Belgiojoso & al 1977, Davis & al 1978, Legrain & al 1978) That the nephrotic syndrome affected mortality in MCGN agrees with earlier reports (Barbiano di Belgiojoso & al 1977, Davis & al 1979)

Other proliferative GN (Cameron 1972) The high mortality in unclassifiable GN can partly be explained by the finding that half of the biopsies

TABLE 2 Frequency of Nephrotic Syndrome (NS) Reported in Membranous Glomerulonephritis

Reference	Patients with NS/all patients	% with NS
Forland & Spargo 1969	19/19	100
Hardwicke & al 1967	40/43	93
Gluck & al 1973	35/38	92
Habib 1970	37/41	90
Habib & al 1973 a	44/50	88
Erwin & al 1973	41/48	85
Row & al 1975	54/66	82
Pollak & al 1968	17/21	81
Cameron 1975	53/69	77
Noel & al 1979	84/116	76
Cameron 1972	30/41	73
Ehrenreich & Churg 1968	44/60	73
Franklin & al 1973	21/32	66
Legrain & al 1978	53/81	65
Beregi & Varga 1974	20/260	8
Present study	11/22	50

showed some crescent formation. The number of crescents has been shown to correlate with survival regardless of type of GN (Zollinger & Mihatsch 1978). In our unclassifiable GN patients mortality was high even in the absence of crescents. However capsular adhesions were found in all of the unclassifiable biopsies in combination with varying proportions of hyalinised glomeruli. Adhesions are thought to represent healed crescents (Zollinger & Mihatsch 1978). Our findings indicate that such lesions may represent a prognostic sign equal in importance to crescent formation.

FSGS has generally been reported to be associated with a poor actuarial survival (Cameron 1972, Cameron & al 1978, Legrain & al 1978). Our series contained too few patients with FSGS for any valid observation. Reported frequencies of FSGS have been variable ranging from 10.4 (Habib 1970) and 6.5 per cent (Cameron 1972) to 1.6 (Velosa & al 1975) and 1.3 per cent (van Acker & al 1975). The low frequency in our series cannot be explained by the misdiagnosis of FSGS as MC or FGN since this would probably have affected the survival rate in these groups.

Conclusion Our results show that the prognosis of GN is fairly good in most types. The only exceptions were MCGN, unclassifiable GN and RPGN which differed significantly from expected. The nephrotic syndrome was found to worsen prognosis in MGN and MCGN, but not in MC. In contrast to conclusions drawn by others (Cameron 1972, Habib 1975) but in agreement with Cameron

(1975) we conclude that the current light microscopic classification of GN is only a relatively crude guide to prognosis. Clinical findings such as the nephrotic syndrome, must also be accounted for.

We are grateful for the technical assistance of Miss Riitta Lusa Laine and Miss Riitta Litmanen. This study was supported by a grant from the Sigrid Juselius Foundation.

REFERENCES

- Anderson R P, Boncheck L I, Grunkemeier G L, Lambert L E, Starr A. The analysis and presentation of surgical results by actuarial methods. *J Surg Res* 16: 224-230, 1974.
- Antoine B, Faye C. The clinical course associated with dense deposits in the kidney basement membranes. *Kidney Int* 1: 420-427, 1972.
- Barbano di Belgiojoso G, Tarantino A, Colasanti G, Bazzi C, Guerra L, Durante A. The prognostic value of some clinical and histological parameters in membranoproliferative glomerulonephritis (MPGN). *Nephron* 19: 250-258, 1977.
- Bariety J, Druet Ph, Lagrue G, Samarcq P, Miller P. Les glomérulopathies «extra membranueuses» (GEM). Etude morphologique en microscopie optique électronique et en immunofluorescence. *Pathol Biol* 18: 5-32, 1970.
- Barrey J, Druet Ph, Lorrat Ph, Lagrue G. Les glomérulonephrites parietoprolifératives (GNPP). Etude histopathologique en microscopie optique électronique et en immunohistochimie de 49 cas. Corrélatons anatomo-cliniques. *Pathol Biol* 19: 259-283, 1971.
- Beregi E, Varga I. Analysis of 260 cases of membranous glomerulonephritis in renal biopsy material. *Clin Nephrol* 2: 215-221, 1974.
- Burkholder P M. Atlas of human glomerular pathology. Harper & Row Publishers, Harperstown, Maryland, N.Y., San Francisco, London, 1974.
- Cameron J S. Bright's disease today: the pathogenesis and treatment of glomerulonephritis - I. *Brit Med J* 4: 87-90, 1972.
- Cameron J S. The natural history of glomerulonephritis. In Black D A K. *Renal Disease*, 3rd ed. Blackwell, Oxford and London, 1973, pp 295-329.
- Cameron J S. Clinicopathological correlates in glomerulonephritis: Problems and limitations. *Clin Nephrol* 4: 1-7, 1975.
- Cameron J S, Ogg C S, White R H R, Glasgow E F. The clinical features and prognosis of patients with normocomplementemic mesangiocapillary glomerulonephritis. *Clin Nephrol* 1: 8-13, 1973.
- Cameron J S, Turner D R, Ogg C S, Chantler C, Williams D G. The long term prognosis of patients with focal segmental glomerulosclerosis. *Clin Nephrol* 10: 213-218, 1978.
- Churg J, Habib R, White R H R. Pathology of the nephrotic syndrome in children. *Lancet* 1: 1299-1302, 1970.

- Cutler S J Ederer F Maximum utilization of the life table method in analyzing survival J Chron Dis 8 699-712 1958
- Davis A E Schneeberger E E Grupe W E McCluskey R T Membranoproliferative glomerulonephritis (MPGN Type 1) and dense deposit disease (DDD) in children Clin Nephrol 9 184-193 1978
- Ederer F Axtell L M Cutler S J The relative survival rate a statistical methodology National Cancer Institute Monograph no 6 101-121 1961
- Ehrensch T Churg J Pathology of membranous nephropathy In Sommers S C (Ed) Pathology Annual Appleton Century Croft New York 1968 pp 145-186
- Ernst D T Donadio J V Holley K E The clinical course of idiopathic membranous nephropathy Mayo Clin Proc 48 697-712 1973
- Forland M Spargo B H Clinicopathological correlations in idiopathic nephrotic syndrome with membranous nephropathy Nephron 6 498-525 1969
- Franklin W A Jennings R B Earle D P Membranous glomerulonephritis Long term serial observations on clinical course and morphology Kidney Int 4 36-56 1973
- Glück M C Gallo G Lowenstein J Membranous glomerulonephritis Evolution of clinical and pathologic features Ann Int Med 78 1-12 1973
- Habbe R Classification anatomique des néphropathies glomérulaires Pad Fortbildungskurse 28 3-47 Karger Basel/München/New York 1970
- Habbe R Classification et corrélations anatomiques des néphropathies glomérulaires Schweiz Med Wschr 105 1749-1758 1975
- Habbe R Kleinknecht C Gubler M C Levy M Idiopathic membranoproliferative glomerulonephritis in children Report of 105 cases Clin Nephrol 7 194-214 1973
- Habbe R Kleinknecht C Gubler M C Extramembranous glomerulonephritis in children Report of 50 cases J Pediatrics 82 754-766 1973 a
- Habbe R Gubler M C Lourai C Mar H Ben Levy M Dense deposit disease A variant of membranoproliferative glomerulonephritis Kidney Int 7 204-215 1975
- Hardwick J Blaisie J D Brewer D B Soothill J F The nephrotic syndrome Proc 3rd Int Congr Nephrol Washington 1966 3 69-82 Karger Basel/New York 1967
- Heptinstall R H Pathology of the Kidney 2nd edition Little Brown & Co Boston 1974
- Jones D B Nephrotic glomerulonephritis Am J Path 33 313-329 1957
- Legrain M Salah H Beaufrès H Flores Esteves L Guedon J Le pronostic des glomerulonephrites chroniques primitives de l'adulte 298 observations anatomocliniques Nouv Presse Méd 7 533-538 1978
- Noel L H Zanetti M Droz D Barbanel C Long term prognosis of idiopathic membranous glomerulonephritis Study of 116 untreated patients Am J Med 66 82-90 1979
- Pollak V E Rosen S Pirani C L Muehrcke R C Kark R M Natural history of lipid nephrosis and of membranous glomerulonephritis Ann Int Med 69 1171-1196 1968
- Row P G Cameron J S Turner D R Evans D J White R H R Ogg C S Chantler C Brown C B Membranous nephropathy Long term follow up and association with neoplasia Q J Med 44 207-239 1975
- Tallqvist G Tornroth T Vantinen T Pasternack A Vacuolization of the glomerular basement membrane Acta path microbiol scand Sect. A 87 411-419 1979
- Tornroth T Tallqvist G Pasternack A Linder E Nonprogressive histologically mild membranous glomerulonephritis appearing in all evolutionary phases as histologically «early» membranous glomerulonephritis Kidney Int 14 511-521 1978
- Van Acker K J Vanden Brande J Hooft H Renal biopsy studies in 150 children with non specific glomerulopathy Acta Paediatr Scand 64 345-354 1975
- Velosa J A Donadio J V Holley K E Focal sclerosing glomerulopathy A clinicopathologic study Mayo Clin Proc 50 121-133 1975
- White R H R Glasgow E F Mills R J Clinicopathological study of nephrotic syndrome in childhood Lancet I 1353-1359 1970
- Zollinger H U Mihatsch M J Renal Pathology in Biopsy Light Electron and Immunofluorescent Microscopy and Clinical Aspects Springer Verlag Berlin Heidelberg New York 1978

THE FINE STRUCTURE OF »DIVIDERS« AND »NON-DIVIDERS« IN PHASE II HUMAN GLIAL CELL CULTURES

E. BLOMQUIST¹, E. ARRO¹, U. BRUNK¹, V. P. COLLINS² and B. A. FREDRIKSSON¹

¹Institute of Pathology¹ University of Uppsala Uppsala and Department of Tumor Pathology²
Institute of Pathology Karolinska Institute Stockholm Sweden

Blomquist, E. Arro, E. Brunk, U. Collins, V. P. & Fredriksson, B. A. The fine structure of »dividers« and »non-dividers« in phase II human glial cell cultures. Acta path microbiol scand Sect A 88 327-337 1980.

A method is described which allows a comparison in the transmission electron microscope (TEM) of cells with different remaining proliferative capacity from one and the same culture. The method takes advantage of a mini-cloning technique employing haptotactic palladium islands in combination with micro dissection and preparation for TEM of islands carrying various numbers of cells after 10 days in culture when all miniclones have become density dependent growth inhibited. By means of this technique non-dividers were compared with miniclones of dividers composed of five to eight cells originating from single cells. Moreover large immotile cells without peripheral ruffling activity known to be non-dividers were compared with small ruffling cells known to be dividers in the reflection interference mode in sparse cultures of living cells and in the TEM mode as whole cell preparations after critical point drying of cells cultured on formvar-coated gold EM grids. Non-dividers proved to contain a moderate number of residual bodies, well developed Golgi areas and often branched or circular mitochondria, they were thinly spread over the substratum with many focal points of contact and large areas of close apposition between cell and substratum.

Key words: Glial cell cultures, ultrastructure.

E. Blomquist, Patologiska institutionen, Uppsala Universitet, Box 553, 751 22 Uppsala, Sweden.

Received 15 iv 80 Accepted 30 iv 80

In recent years it has been clearly shown that any passage of cultured diploid normal cells will include those with proliferative capacity and those with little or no such potential (Merz & Ross 1969; Cristofalo & Sharf 1973; Smith & Hayflick 1974).

As demonstrated during phase I the cells are established *in vitro* in phase II they grow exponentially and in phase III the cultures become impossible to subcultivate due to insufficient proliferation. Normal human glial cells behave in this manner.

to study the relationship between cellular proliferative capacity under various defined conditions and passages of varying age (Blomquist *et al* 1978; Blomquist *et al* 1979; Collins *et al* 1979a).

The human glial cell line U 787 CG can be cultured for a maximum of 48 passages. After about 30 passages the proportion of cells which do not divide within 10 days after subcultivation onto palladium squares on agarose (classified as non-dividers) is 40% while the cells which form miniclones of more than four cells on the haptotactic

THE FINE STRUCTURE OF »DIVIDERS« AND »NON-DIVIDERS« IN PHASE II HUMAN GLIAL CELL CULTURES

E. BLOMQUIST¹, E. ARRO¹, U. BRUNK¹, V. P. COLLINS² and B. A. FREDRIKSSON¹

¹Institute of Pathology¹ University of Uppsala Uppsala and Department of Tumor Pathology²
Institute of Pathology Karolinska Institute Stockholm Sweden

Blomquist, E. Arro, E. Brunk, U. Collins, V. P. & Fredriksson, B. A. The fine structure of »dividers« and »non-dividers« in phase II human glial cell cultures. *Acta path microbiol scand Sect. A* 88 327-337 1980.

A method is described which allows a comparison in the transmission electron microscope (TEM) of cells with different remaining proliferative capacity from one and the same culture. The method takes advantage of a mini-cloning technique employing haptotactic palladium islands in combination with micro-dissection and preparation for TEM of islands carrying various numbers of cells after 10 days in culture when all miniclones have become density dependent growth inhibited. By means of this technique non-dividers were compared with miniclones of dividers composed of five to eight cells originating from single cells. Moreover large immobile cells without peripheral ruffling activity known to be non dividers were compared with small ruffling cells known to be dividers in the reflection interference mode in sparse cultures of living cells and in the TEM mode as whole cell preparations after critical point drying of cells cultured on formvar-coated gold EM grids. Non dividers proved to contain a moderate number of residual bodies, well developed Golgi areas and often branched or circular mitochondria, they were thinly spread over the substratum with many focal points of contact and large areas of close apposition between cell and substratum.

Key words: Glial cell cultures, ultrastructure.

E. Blomquist, Patologiska institutionen, Uppsala Universitet, Box 553, 751 22 Uppsala, Sweden.

Received 15 iv 80 Accepted 30 iv 80

In recent years it has been clearly shown that any asage of cultured diploid normal cells will include those with proliferative capacity and those with little or no such potential (Merz & Ross 1969, Cristofalo & Sharf 1973, Smith & Hayflick 1974).

As defined by Hayflick, the normal life span of a diploid non transformed cell population *in vitro* can be divided into three periods termed phases I, II and III (Hayflick & Moorhead 1961). During phase I the cells are established *in vitro* in phase II they grow exponentially and in phase III the cultures become impossible to subcultivate due to insufficient proliferation. Normal human glial cells behave in this manner.

In earlier studies of cultured glial cells we used a mini-cloning system of small palladium squares on agarose (Hestermark 1978, Blomquist *et al* 1980) to study the relationship between cellular proliferative capacity under various defined conditions and passages of varying age (Blomquist *et al* 1978, Blomquist *et al* 1979, Collins *et al* 1979a).

The human glial cell line, U-787 CG, can be cultured for a maximum of 48 passages. After about 30 passages the proportion of cells which do not divide within 10 days after subcultivation onto palladium squares on agarose (classified as non dividers) is 40% while the cells which form miniclones of more than four cells on the haptotactic

islands number only 10% (Collins *et al* 1979a, Blomquist *et al* 1980)

The non-dividers of this system present a characteristic morphology. They are large, widely and thinly spread and show almost no outward signs of motility in the form of lamella formation or ruffling along their periphery, nor do they translocate (Blomquist *et al* 1978, 1979)

This is in contrast to cells with persisting proliferative capacity, such cells are smaller, less well spread and grow more densely (Blomquist *et al* 1978, Collins *et al* 1979a, 1979b)

So far, it has not been possible to compare known non-dividers with cells retaining proliferative capacity (dividers) in the transmission electron microscope using sectioned material, the proliferative history of individual cells being unknown in ordinary mass cultures. We here describe the application of the haptotactic island system (Carter 1967, Harris 1973, Westermarck 1978) to make this possible

The causes of the phase III phenomenon are at present unknown although diverse hypotheses have been advanced (Hayflick 1977). A detailed study of the morphology of cells which have exhausted their proliferative capacity, together with a comparison with cells from the same culture and passage which have shown proliferative capacity, might give some clues to the mechanisms underlying this phenomenon

MATERIAL AND METHODS

Cell Culture

The experiments were carried out on the glial cell line U 787 CG. The cells were cultured as previously reported (Ponten *et al* 1969). They were grown in Eagle's minimal essential medium supplemented with antibiotics and 10% fetal calf serum in Nunclon® or Falcon® plastic Petri dishes. Cells from passage 30 were subcultivated into plastic dishes with haptotactic islands as described below or into dishes containing carbon stabilized formvar covered EM gold grids as described by Woloszewicz and Porter (1976). The haptotactic island cultures were harvested for EM after 10 days and the gold grid cultures after 3–4 days

Preparation of Haptotactic Islands

Haptotactic islands (7 056 μm^2 squares) were deposited on a layer of 1% agarose as previously described in detail (Blomquist *et al* 1978). The islands were formed with the help of standard (200 mesh) copper grids for electron microscopy

Phase-Contrast and Interference Reflection Microscopy

Cells were seeded out on 25 mm round cover slips. After two days the cover slips were mounted in a Dvorak Stotler chamber filled with pH controlled

culture medium. Sparse cultures of living cells examined and photographed at 37 °C in phase-contrast and interference reflection modes using Kodak ASA Plus-X-film

The interference reflection microscope (Leitz Diavert) is essentially a standard reflected light microscope illuminated by linearly polarized light (50 W mercury light source) with a crossed analyzer in the view optics for the reduction of internal reflections in the microscope. The key accessory is a lambda/4 plate between the objective lens and the object (combined with the new Leitz P1 Apo 40/1.00 immersion objective which circularly polarizes the light reflected from the object to pass the analyzer in the viewing optics)

Transmission Electron Microscopy

A. Cells on haptotactic islands The cells were fixed

..

then at 4 °C for one hour. The medium covering the haptotactic islands was changed for the fixative within any previous rinse. About 800 palladium squares with large, single cells (non-dividers after 10 days) were individually removed from the agarose by means of a thin tungsten needle under a dissecting microscope and transferred to a Beem capsule containing glutaraldehyde fixative. Likewise about 500 palladium squares each with miniclones consisting of 5–8 cells were collected in another Beem capsule. After a brief rinse in 0.15 M Na cacodylate buffer the preparations were post fixed in 1% OsO₄ in 0.15 M Na cacodylate buffer for 90 min at room temperature. The further processing including dehydration and embedding into Epon 812 was carried out in the same capsules. During dehydration the cells were impregnated for 12 h in 1% uranyl acetate in 50% ethanol. The islands were spun down in a Beckman TJ centrifuge between the changes of solution. After polymerization the blocks were cut with a diamond knife on an LKB Ultratome V. The thin sections were collected on formvar covered grids, stained with lead citrate and examined in a Jeol 100 C electron microscope

B. Whole cells on gold grids The gold grids with cultured whole cells were fixed, dehydrated and critically point dried as previously described (Blomquist *et al* 1978) and impregnated

..

..

..

..

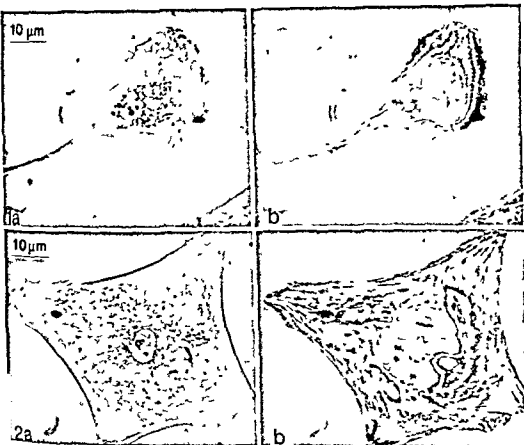
..

equipped with a side entry goniometer. Stereo pairs were photographed at various angles up to 20 °C depending on the magnification

RESULTS

Phase-Contrast and Interference-Reflection Microscopy of Living Cells

The cultures contained a considerable number of large, well spread and immobile cells which have been shown in previous studies to be non-dividers



Figs 1A and 1B Small moule cell of the «dividing» type showing a leading lamella with ruffling activity. In the phase-contrast mode (1A) the thicker perinuclear area containing organelles can easily be differentiated from the peripheral thinner well spread cytoplasm. Note the relatively few small dark areas (arrows mark some of them) in relation to the outer gray zones in the reflection interference mode (1B) indicating focal contacts between the cell and its supporting substratum. The gray zones indicate areas with close apposition between the cell and its substratum.

Figs 2A and 2B Large immotile cell of the «non-dividing» type showing an almost carpet like distribution of stress fibers in the phase-contrast mode (2A) and multiple focal contacts between the cell and its substratum (arrows) in the reflection interference mode (2B). The gray zones (areas of close apposition) are large and irregular. The inner circular zones may represent secondary reflection from within the cell.

Blomquist et al 1978 Collins & Willems 1980). They were intermingled with apparently smaller and less well spread cells presenting a leading edge with ruffling activity a cell form and behaviour demonstrated previously to be associated with entry into and progression through the cell cycle (Brunk et al 1976). In the sparse cultures it was easy to discriminate between these cell types and select typical representatives.

The living cells selected for photography were first identified and photographed in the phase contrast mode and the same cells then immediately studied in the interference mode. Vigor

ously moving cells showed concentric rings of gray areas which were interpreted as areas of close contact (about 30 nm) between the cell and the supporting glass (Fig 1 A and 1 B). However the innermost rings may also result from secondary and higher order of reflections obtained from structures within the cytoplasm or the upper cell surface (Abercrombie & Dunn 1975 Issard & Lochner 1976).

In addition to peripheral gray regions (outer

islands number only 10% (Collins *et al* 1979a Blomquist *et al* 1980)

The non dividers of this system present a characteristic morphology. They are large, widely and thinly spread and show almost no outward signs of motility in the form of lamella formation or ruffling along their periphery, nor do they translocate (Blomquist *et al* 1978, 1979).

This is in contrast to cells with persisting proliferative capacity; such cells are smaller, less well spread and grow more densely (Blomquist *et al* 1978, Collins *et al* 1979a, 1979b).

So far, it has not been possible to compare known non dividers with cells retaining proliferative capacity (dividers) in the transmission electron microscope using sectioned material; the proliferative history of individual cells being unknown in ordinary mass cultures. We here describe the application of the haptotactic island system (Carter 1967, Harris 1973, Westermarck 1978) to make this possible.

The causes of the phase III phenomenon are at present unknown, although diverse hypotheses have been advanced (Hayflick 1977). A detailed study of the morphology of cells which have exhausted their proliferative capacity, together with a comparison with cells from the same culture and passage which have shown proliferative capacity, might give some clues to the mechanisms underlying this phenomenon.

MATERIAL AND METHODS

Cell Culture

The experiments were carried out on the glial cell line U 787 CG. The cells were cultured as previously reported (Ponten *et al* 1969). They were grown in Eagle's minimal essential medium supplemented with antibiotics and 10% fetal calf serum in Nunclon® or Falcon® plastic Petri dishes. Cells from passage 30 were subcultivated into plastic dishes with haptotactic islands as described below, or into dishes containing carbon stabilized formvar covered EM gold grids as described by Woloszewicz and Porter (1976). The haptotactic island cultures were harvested for EM after 10 days and the gold grid cultures after 3–4 days.

Preparation of Haptotactic Islands

Haptotactic islands (7 056 μm^2 squares) were deposited

on culture medium. Sparse cultures of living cells were examined and photographed at 37 °C in phase contrast, and interference reflection modes using Kodak 1 ASA Plus X film.

The interference reflection microscope (Leitz Diavue) is essentially a standard reflected light microscope illuminated by linearly polarized light (50 W mercury light source) with a crossed analyzer in the viewing optics for the reduction of internal reflections in the microscope. The key accessory is a $\lambda/4$ plate between the objective lens and the object (combined with the new Leitz PI Apo 40/1.00 immersion objective which circularly polarizes the light reflected from the object to pass the analyzer in the viewing optics).

Transmission Electron Microscopy

A. Cells on haptotactic islands. The cells were fixed in 2% glutaraldehyde in 0.1 M Na cacodylate (HCl) buffer with 0.1 M sucrose (pH 7.2, total osmolality 510 mOsm, vehicle osmolality 300 mOsm) at 37 °C for 15 min and then at 4 °C for one hour. The medium covering the haptotactic islands was changed for the fixative without any previous rinse. About 800 palladium squares with large single cells (non dividers after 10 days) were individually removed from the agarose by means of a thin tungsten needle under a dissecting microscope and transferred to a Beem capsule containing glutaraldehyde fixative. Likewise about 500 palladium squares, each with miniclones consisting of 5–8 cells, were collected in

room temperature. The further processing, including dehydration and embedding into Epon 812, was carried out in the same capsules. During dehydration the cells were impregnated for 12 h in 1% uranyl acetate in 50% ethanol. The islands were spun down in a Beckman TJ 6 centrifuge between the changes of solution. After polymerization the blocks were cut with a diamond knife on an LKB Ultratome V. The thin sections were collected on formvar covered grids, stained with lead citrate and examined in a Jeol 100 C electron microscope.

B. Whole cells on gold grids. The gold grids with cultured whole cells were fixed, dehydrated and critically point dried as previously described (Blomquist *et al* 1978).

The stereo pairs were prepared on grids equipped with a side entry goniometer. Stereo pairs were photographed at various angles up to 20 °C depending on the magnification.

RESULTS

Phase Contrast and Interference Reflection Microscopy of Living Cells

The cultures contained a considerable number of large, well spread and immobile cells which have been shown in previous studies to be non-dividers.

electron microscopy

Phase Contrast and Interference Reflection Microscopy

Cells were seeded out on 25 mm round cover slips. After two days the cover slips were mounted in a Dvorak Stotler chamber filled with pH controlled



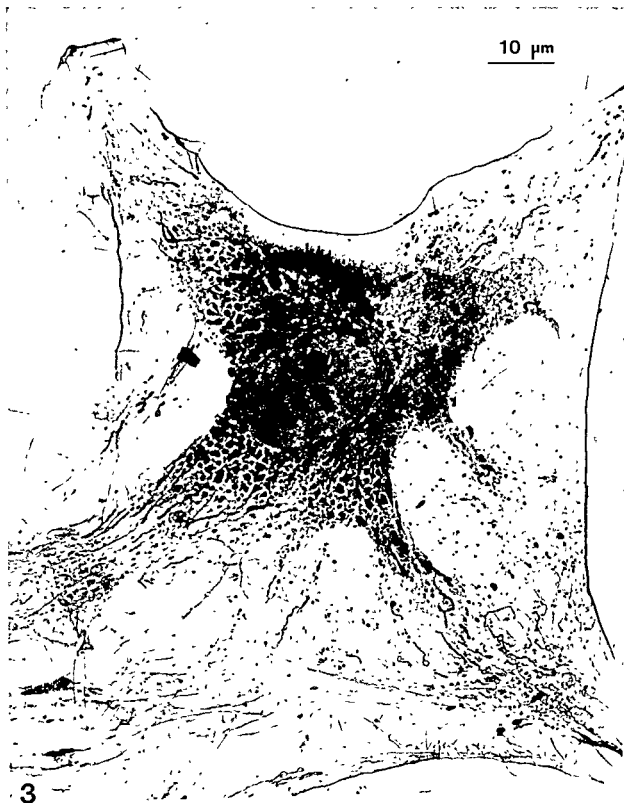


Fig 3 Composite of eight different negatives showing a »non-divider« Note the rather limited, dense and thick perinuclear region containing the majority of mitochondria and residual bodies which contrasts with the large, thinly spread peripheral cytoplasm containing many bundles of microfilaments and relatively few mitochondria and residual bodies

Fig 5 Well spread part of a non-divider showing the degree of irregularity in the relation between mitochondria and the electron dense residual bodies

2 μ m





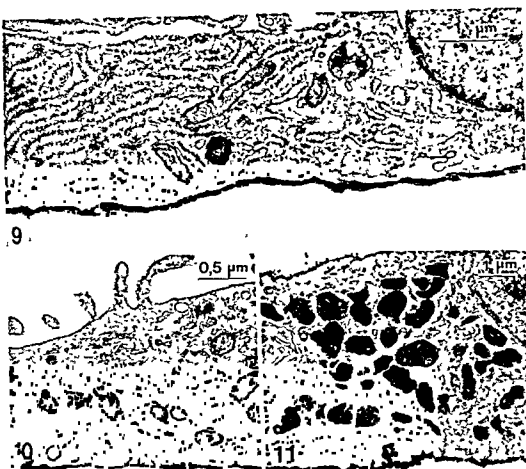


Fig 6 Peripheral thin part of a non-divider with multiple bundles of microfilaments

Fig 7 Stereo pair ($\pm 6^\circ$) of a detail from Fig 4 with a circular mitochondrion enclosing a residual body. Note tiny filaments appearing to connect the residual body with the mitochondrion. Such filaments are seen around many of the free residual bodies too and also along the periphery of the mitochondria. It is not known whether these filaments are real or represent artefacts formed during the inevitable cellprotein transformation during fixation, dehydration and critical point drying.

Fig 8 Parts of three cells in a miniclone (cells retaining dividing capacity). The palladium substratum is arrowed. A specialized area of close contact between the cell and the surface is indicated (arrow heads). Note pinocytotic vesicles originating from the cell surfaces, mainly the lower.

Fig 9 Detail from a cell in a miniclone showing part of the nucleus, endoplasmic reticulum, mitochondria and few residual bodies.

Figs 10 and 11 A divider and a non-divider. Note the difference in the number of residual bodies. Both cells show the perinuclear area. The divider has a few microvilli along its upper cell surface and shows evidence of pinocytotic activity (arrow).

of focal contact (10–15 nm) between the cells and the glass surface (Curtis 1964; Abercrombie & Dunn 1975; Izzard & Lochner 1976; Heath & Dunn 1978). The perinuclear part was in general light gray to white, indicating a region of higher separation (more than 100 nm) between the cell and the glass surface.

The large, immobile and widely spread cells were well endowed with stress fibres (Fig 2A) and had a fairly thin peripheral zone outside the perinuclear area. In the interference reflection mode it was seen that the gray zones were far more pronounced, broader and less regularly arranged than in vigorously moving cells (Fig 2B). It is unknown

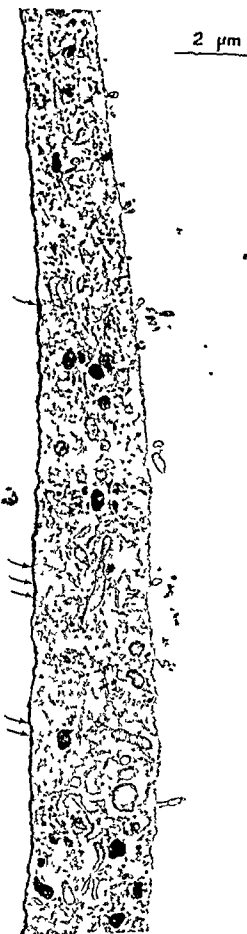


Fig 12 Composite of four micrographs to show a major part of a non divider. Note the extent of the cell and the adherence to the substratum. Groups of pinocytotic vacuoles are forming (arrows) showing that some capacity for endocytosis apparently persists although the cells lie very close to the substratum.

whether the inner, circular gray areas represent zones of close apposition between the cells and the substratum or are due to secondary reflection within the cytoplasm. The immobile cells also showed many black areas representing focal contacts between the cell and the substratum usually in relation to the stress fibres and mostly situated at the periphery of the cells.

Ultrastructure of Whole Cells Grown on Gold Grids

The small cells presented the morphology previously described (Collins *et al* 1978). Large well spread immobile cells were readily identified on the carbon formvar coated gold EM grids. In low magnification (Fig 3) these cells had a highly characteristic morphology with a comparatively thin perinuclear zone occupied by mitochondria and numerous irregularly shaped electron dense organelles outside which the cell was very thinly spread and the cytoplasm contained a few mitochondria of various shapes and sizes as well as bundles of microfilaments (stress fibres). At higher magnifications the morphology of the mitochondria could be studied in detail (Figs 4 and 5). They were often ramified or circular findings which cannot be easily demonstrated in randomly orientated sections as the mitochondria with their branches usually lie horizontal to the substratum and sections in such a plane are understandably few. In the thinly spread area peripheral to the perinuclear zone the cells also contained a number of electron dense irregular organelles resembling residual bodies (Fig 4) some of which showed an intimate relation to mitochondria being occasionally located within a ring shaped part of a mitochondrion as shown in detail in a stereo pair micrograph (Fig 7). In such cases a number of tiny filaments were seen to bridge the gap between the residual body like structure and the inner circumference of the mitochondrion. Other non mitochondria related residual bodies were also surrounded by tiny filaments. For the time being it is hard to say whether these filaments are real structures e.g. related to the microtubecular network as described by Woloszewicz and Porter (1979) or artefacts created during the critical point drying of the cells. The most peripheral regions of the cell were mainly occupied by microfilaments.

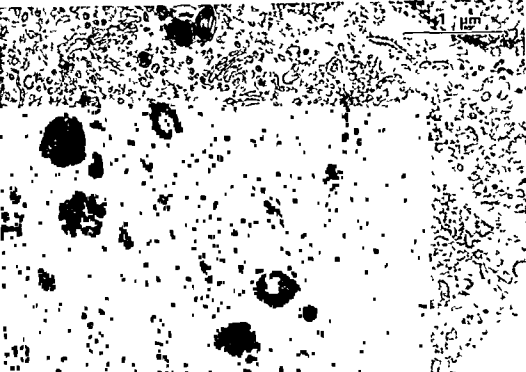


Fig 13 Perinuclear zone of a non divider showing well developed Golgi areas along with smooth and rough endoplasmic reticulum and residual bodies

which were evenly distributed in mat like arrays or arranged in bundles (Fig 6)

Transmission Electron Microscopy of Ultrathin Sections from Embedded Cells

a Miniclones consisting of 5-8 cells The cells showed the same morphological features as have already been described in studies of density dependent growth inhibited cultures from early passages (Brunk *et al* 1973 Collins *et al* 1979c). The cells were essentially monolayered, had few residual bodies and a well developed endoplasmic reticulum. The Golgi zones were well developed with emergent coated vesicles. Autophagosomes occurred occasionally. Micropinocytotic vesicles were chiefly associated with the lower cell surface. Occasional ruffles were registered at the cell borders (Figs 8, 9 and 10).

b Haptotactic islands containing single cells only (non dividers at 10 days) The non-dividers were large and flat and had few microvilli. Occasionally small lamellae could be found at the cell periphery. The endoplasmic reticulum appeared to be less well developed than in the multiplying cells. The Golgi zones however were large and surrounded by

many small vesicles both smooth surfaced and coated. The residual bodies were relatively numerous but far fewer than found in cells which have been kept in a stable monolayer for several weeks (Brunk *et al* 1973 Collins & Brunk 1978). Micropinocytotic vesicles were present both at the upper and the lower surface although less frequently than in the case of the dividers. The cells appeared to adhere closely to the palladium substratum which may restrict the uptake of nutrients by pinocytosis from the lower cell surface (Figs 11, 12 and 13).

DISCUSSION

The micloning technique utilizing haptotactic palladium islands and the subsequent registration during a 10 day period of the potential for proliferative activity of initially single cells under standard culture conditions makes it possible to discriminate between cells lacking proliferative ability and cells retaining the capacity for division (ability to form miniclones of 5 to 8 cells on the $7.056 \mu\text{m}^2$ palladium islands). The combination of this technique with micro-dissection and collection

for embedding in resin and eventual electron microscopy of islands carrying these two types of cells allows us to compare their fine structure

The method described offers an opportunity to analyze populations of cells with defined proliferative or other abilities and known history, and to discriminate between groups of such cells in a way not possible with mass cultures. The findings in morphological studies of the present type should preferably be analyzed with morphometric techniques. Due to the rather complicated and time-consuming procedures employed it was deemed justifiable to limit the present paper to a description of the preparative technique to indicate its usefulness, and to include an account of some of the major differences between dividers and non dividers. Detailed analyses of e.g. differences in pinocytotic activity between the two groups of cells require stereology and statistical evaluation.

In a mass culture non-dividers can be identified by their large size and the fact that they are well spread without the ruffling lamellae characteristic of

in the TEM. They cannot, in such preparations, be compared with the daughter cells of cells which have shown a large proliferative capacity despite the limitation of the factors which are required for cellular proliferation — as is the case in the miniclone system where 5–8 cells have resulted from proliferation on a $7,056 \mu\text{m}^2$ island under otherwise standard conditions.

The most noticeable difference between dividers and non dividers was that the latter, apart from their size, spreading capacity and immobility, contained a highly developed network of microfilaments, often matted but sometimes in the form of stress fibres. The findings are not unlike those obtained when serum starved phase II glial cells (which are blocked in G_1 and also immobile) (Collins *et al* 1978) are examined. The non dividers obviously expand and spread maximally. This is reflected both in the relatively sparse micropinocytotic activity from their lower cell surface and in their reflection-interference pattern showing large areas in close contact with the supporting substratum. Earlier experiments have shown that cells manifest increasing demands for both supporting areas and growth promoting factors in order to be able to divide as they approach phase III and that these parameters can, within certain limits, compensate one another (Blomquist *et al* 1979, Collins *et al* 1979a). It thus seems probable that glial cells become increasingly resistant during continued passage to the aforementioned growth promoting

stimulation, and demand increasing amounts of the necessary factors in order to be able to enter the cell cycle.

The non-dividers showed a somewhat less well developed endoplasmic reticulum, and more numerous large, branched and partially circular mitochondria, than the dividers. Similar observations have been made in phase II glial cells which were growth inhibited by serum starvation (Collins *et al* 1978).

The increasing number of residual bodies in the non-dividers would seem to be merely a reflection of their non-dividing state, since residual bodies rapidly accumulate even in phase II cells if they are blocked in G_1 for long periods (Brunk *et al* 1973, Collins & Brunk 1978). It should be stressed that the non-dividers never contained as many residual bodies as dividers regularly do after some weeks in a non-dividing state (Collins & Brunk 1978). Accordingly, the investigated non-dividers had probably been blocked in G_1 only for a comparatively short time when they were studied. This favours the hypothesis that non-dividers are fragile and rarely survive the somewhat rough subcultivation treatment (Milo 1973). We therefore believe that most of the non-dividers studied became incapable of division probably in relation to the last subcultivation.

The phase III phenomenon — typical of all normal diploid cells which do not transform spontaneously — apparently arises because an increasing fraction of cells in the cultures lose their dividing capacity in the higher passages (Cristofalo & Sharf 1973, Blomquist *et al* 1980). This has been termed «degeneration» or even «terminal differentiation» (Hayflick 1977, Bell *et al* 1978, Kontermann & Bayreuther 1979). Since the non-dividers can survive for a considerable time and at least some of them clearly are only «relative non-dividers» — they may be induced to reenter the cell cycle by an increase in growth promoting factors or substratum area (Blomquist *et al* 1979, Collins *et al* 1979a) — the relationship between the phase III phenomenon and ageing in the complex multicellular organism may be questioned. On theory the phase III phenomenon represents a form of cell growth control. Such a control would prevent unrestricted neoplastic growth by limiting the number of daughter cells which a cell can provoke.

Supported by grants from the Swedish Medical Research Council and the Swedish Cancer Society.

REFERENCES

- Abercrombie M & Dunn G A Adhesions of fibroblasts to substratum during contact inhibition observed by interference reflection microscopy *Exp Cell Res* 97 57-62 1975
- Bell E Marek L F Levinstone D S Merrill C Sher S Young I T & Eden M Loss of division potential in vitro: Ageing or differentiation? *Science* 202 1158-1163 1978
- Blomquist E Arro E Brunk U & Westermark B Plasma membrane motility of cultured human glia cells in phase II and III *Acta Path Microbiol Scand A* 86 257-263 1978
- Blomquist E Arro E Brunk U & Westermark B Growth stimulation of aged cells in culture *Acta Path Microbiol Scand A* 87 393-399 1979
- Blomquist E Westermark B & Pontén J Ageing of human glial cells in culture. Increase in the fraction of non dividers as demonstrated by a micloning technique *Mech Ageing Devel* 12 173-182 1980
- Brunk U Ericsson J L E Pontén J & Westermark B Residual bodies and ageing in cultured human glia cells. Effect of entrance into phase III and prolonged periods of confluence *Exp Cell Res* 79 1-14 1973
- Brunk U Schellens J P M & Westermark B Influence of epidermal growth factor (EGF) on ruffling activity pinocytosis and proliferation of cultured human glia cells *Exp Cell Res* 103 295-302 1976
- Carter S B Haptotactic islands. A method of confining single cells to study individual cell reactions and clone formation *Exp Cell Res* 48 189-193 1967
- Collins V P & Brunk U Quantitation of residual bodies in cultured human glial cells during stationary and logarithmic growth phases *Mech Ageing Devel* 8 139-152 1978
- Collins V P Brunk U Fredriksson B A & Westermark B The fine structure of growing and non growing whole glia cell preparations *Cytobiologie* 18 327-338 1978
- Collins V P Arro E Blomquist E Brunk U Fredriksson B A & Westermark B Cell motility and proliferation in relation to available substratum area serum concentration and culture age. In SEM/1979a (ed O Johari) SEM inc AMF O'Hare Vol III p 411-420
- Collins V P Arro E Brunk U & Westermark B Motility pattern of density growth inhibited glial cells with partially free borders *Europ J Cell Biol* 19 288-293 1979b
- Collins V P Forsby N Brunk U Ericsson J L E & Westermark B Ultrastructural features of cultured human glia and glioma cells *Acta Path Microbiol Scand A* 87 19-28 1979c
- Collins V P & Willems J G M S Identification and characterization of non-dividing cell populations in phase II cultures of human glial cells Submitted for publication
- Cristofalo V J & Sharf B A Cellular senescence and DNA synthesis Thymidine incorporation as a measure of population age in human diploid cells *Exp Cell Res* 76 419-427 1973
- Curtis A S G The mechanism of adhesion of cells to glass. A study by interference reflection microscopy *J Cell Biol* 20 199-215 1964
- Harris A Behaviour of cultured cells on substrata of variable adhesiveness *Exp Cell Res* 77 285-297 1973
- Hayflick L & Moorhead P S The serial cultivation of human diploid cell strains *Exp Cell Res* 25 585-621 1961
- Hayflick L The cellular basis for biological aging. In Finch C & Hayflick L (eds) *Handbook of the biology of ageing* p 159-186 Van Nostrand Reinhold Company New York 1977
- Heath J P & Dunn G A Cell to substratum contacts of chick fibroblasts and their relation to the microfilament system. A correlated interference reflection and high voltage electron microscope study *J Cell Sci* 29 197-212 1978
- Izard C S & Lochner L R Cell to substrate contacts in living fibroblasts: an interference reflection study with an evaluation of the technique *J Cell Sci* 21 129-159 1976
- Kontermann K & Bayreuther K The cellular ageing of rat fibroblasts in vitro is a differentiation process *Gerontology* 25 261-274 1979
- Mertz G S & Ross J D Viability of human diploid cells as a function of *in vitro* age *J Cell Physiol* 74 219-222 1969
- Milo G E Jr Enhancement of senescence in low passage human embryonic lung cells by an agent extracted from phase III cells *Exp Cell Res* 79 143-151 1973
- Pontén J Westermark B & Hugosson R Regulation of proliferation and movement of human glia like cells in culture *Exp Cell Res* 58 393-400 1969
- Smith J R & Hayflick L Variation in the life span of clones derived from human diploid strains *J Cell Biol* 62 48-53 1974
- Valentine R C Shapiro B M & Stadiman E R Regulation of glutamine synthetase XII Electron microscopy of the enzyme from *Escherichia coli* *Biochemistry* 7 2143-2152 1968
- Westermark B Growth control in miclonages of human glial cells *Exp Cell Res* 111 295-299 1978
- Wolosewick J J & Porter K R Stereo high voltage electron microscopy of whole cells of the human diploid line W138 *Am J Anat* 147 303-324 1976
- Wolosewick J J and Porter K R Microtrabecular lattice of the cytoplasmic ground substance. Artifact or reality *J Cell Biol* 82 114-139 1979

BRIEF REPORT

STAINING OF RAT THYROID PARAFOLLICULAR (C) CELLS WITH THE SEVIER MUNGER SILVER TECHNIQUE

Erik Wilander Lisa Juntti Berggren Monahill Lundqvist and Lars Grimelius

Department of Pathology University of Uppsala Uppsala Sweden

Wilander E Juntti Berggren L Lundqvist M & Grimelius L Staining of rat thyroid parafollicular (C-) cells with the Sevier Munger silver technique Acta path microbiol scand Sect A 88 339-340 1980

The argyrophil silver stain of Grimelius and of Sevier Munger was studied in rat thyroid parafollicular (C-) cells after formalin and Bouin fixation. The strongest and most easily reproducible staining reaction was obtained in tissues fixed with Bouin's fluid and stained by the Sevier Munger technique. The identity of the argyrophil cells as the calcitonin containing C-cells was established by re-staining the same sections with calcitonin antibodies according to the method of Sternberger.

Key words: Thyroid parafollicular C-cells silver staining technique

E Wilander Department of Pathology University of Uppsala P.O. Box 553 S-751 22 Uppsala Sweden

Received 7 III 80 Accepted 12 VI 80

Silver stains are often used to identify different types of endocrine cells. The usefulness of these methods, however, is dependent on the examiner's knowledge of the reaction of the individual endocrine cell types to each silver stain. In the present report an argyrophil reaction with the method of Sevier Munger is demonstrated in parafollicular cells of the rat thyroid. The identity of these cells as the calcitonin-containing C-cells was established by re-staining the same sections with calcitonin antibodies according to the indirect immunohistochemical (PAP) method of Sternberger (5).

Materials and methods

Six adult male albino rats (body weight about 250 g) of the Sprague Dawley strain, obtained from Anticimex AB Stockholm, were used. Under general anaesthesia induced with ether, the thyroid gland was carefully removed, fixed in Bouin's fluid or 10% formalin for 24 hours, dehydrated and embedded in paraffin. Sections about 4 μ m thick were cut and stained. Sections displayed a stronger and more reproducible argyrophil reaction in scattered, mostly parafollicular cells than those stained by the method of Grimelius. In the

formalin fixed tissues the argyrophil reactions were weak or negative. Areas of the Bouin-fixed and Sevier Munger stained sections were photographed at a magnification of $\times 250$ and then de-stained with 1% KCN in aqueous solution (2) for about 30 min. The sections were

in the sections as before were photographed again at the same magnification. The calcitonin antibodies employed (a gift from Dr G. Lundqvist) were raised in rabbits after conjugation of synthetic calcitonin to bovine serum albumin. For the present experiments the antibodies were diluted 1:100. Controls as recommended by Goldberg (1) were used.

Sevier Munger technique (Fig. 1). These cells were tissue against. After it was apparent that the argyrophil cells were identical to the cells showing calcitonin-like immuno-reactivity, although the intensity of the staining reaction varied to

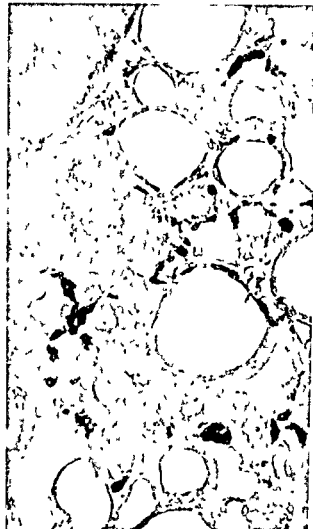


Fig 1 Light microscopic photograph of the rat thyroid gland. Parafollicular cells with heavy black cytoplasmic granulation are seen. Sevier-Munger silver stain $\times 250$.



Fig 2 Photograph of the same area as in Fig 1 after restaining with calcitonin antibodies. The Sevier-Munger stained cells seen in Fig 1 correspond completely to the cells showing calcitonin immunoreactivity. PAP technique $\times 250$.

some extent between individual cells (Fig. 2). The control sections were negative.

The results show that in Bouin fixed rat thyroid tissue both the argyrophil technique of Sevier-Munger and that of Grimelius can be used to identify the calcitonin-containing parafollicular cells of the rat thyroid. With the former method, however, the parafollicular cells are more sharply outlined and more reproducible results can be obtained in quantitative studies, for instance.

Although immuno-cytochemistry with specific antibodies is the most accurate method for visualizing a particular type of endocrine cell, silver stains are often used as well because 1) antibodies are sometimes expensive or difficult to obtain, 2) the hormone content of some endocrine cell types is unknown, and 3) the argyrophil silver techniques are nondiscriminating and

stain several types of endocrine cells (3) and can thus be utilized as screening methods for these cells.

This work was supported by grants from the Swedish Medical Research Council (Project No. 102).

- References** 1. Goldman M. Fluorescent antibody methods. Academic Press, New York, 1968. - 2. Grimelius L. Acta Soc Med Upsalien 73: 243-270, 1968. - 3. Grimelius L & Wilander E. Invest Cell Pathol 3: 3-12, 1980. - 4. Sevier A C & Munger B L. J Neuropathol Exp Neurol 24: 130-135, 1965. - 5. Sternberger L A. Immunocytochemistry. Englewood Cliffs, NJ: Prentice Hall, 1974.

STUDIES ON THE RAT LIVER FOLLOWING IRON OVERLOAD

Electron Microscopical and Histochemical Investigation after Iron Depletion

ROLF HULTCRANTZ¹ BENGT ARBORGH¹ ROMULAD WROBLEWSKI²
and JAN L. E. ERICSSON³

¹Department of Pathology, Karolinska Institutet, Huddinge Hospital, S-141 86 Huddinge, ²Wenner Gren Institute, University of Stockholm, Stockholm and ³Department of Pathology, University of Uppsala, Uppsala, Sweden

Hultcrantz R, Arborgh B, Wroblewski R & Ericsson J L E. Studies on the rat liver following iron overload. Electron microscopical and histochemical investigation after iron depletion. *Acta path. microbiol. scand. Sect. A* 88: 341-353, 1980.

Sprague Dawley rats were given Jectofer injections to obtain iron overload in rat liver Kupffer and parenchymal cells. The release of iron was studied on the light and electron microscopical level by bleeding of the animals. The mobilization of iron was

was demonstrated with X-ray microanalysis at the ultrastructural level and presence of acid phosphatase was revealed using a histochemical method based on precipitation of lead phosphate at sites of enzyme activity in combination with X-ray microanalysis. It was demonstrated that all IP containing cytoplasmic bodies also showed presence of acid phosphatase implying that all of them represented lysosomes. The mechanism of release of iron from Kupffer and parenchymal cells was discussed with special emphasis on the role of the lysosomes and the relationship between their contents and other cellular structures.

Key words: Liver iron overload, ultrastructure, histochemistry.

Rolf Hultcrantz, Department of Pathology, Huddinge Hospital, S-141 86 Huddinge, Sweden.

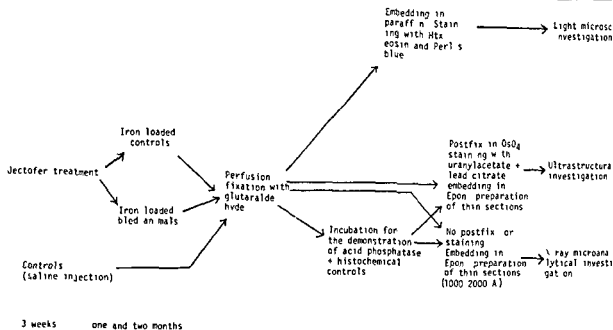
Accepted as submitted 2 v 80

Studies on iron overload in experimental animals have clarified that a substantial part of the excessive iron is stored in the liver (23, 1, 26, 10, 20). Considerable interest has been focused on the processes of uptake and storage (26, 20, 6, 19, 24, 16, 17). In our previous studies we have described the ultrastructural and histochemical basis for the handling of excess iron in the rat liver with special reference to the role of the lysosomal vacuole (13, 14). On the basis of this knowledge it

phologic expressions of turnover, metabolism and release of iron in the overloaded liver.

In order to study the mobilization of iron from the overloaded liver, rats have been bled repeatedly whereby the demand for iron for synthetic purposes in the animals has been greatly enhanced. By this means an experimental model useful to study if and how different types of liver cells are able to release iron has been created. It has further been possible to clarify whether or not different types of lysosomes in these cells react in the same way in a situation of iron demand outside the liver.

Table 1 Short Survey over the Handling of the Investigated Material



MATERIALS AND METHODS

For a short survey see Table 1

Iron Loading

Male Sprague Dawley rats (weighing 200-220 grams) maintained on ordinary diet consisting of pellets containing approximately 260 µg iron/g (R3 Astra Evos Soderstälje Sweden) and water *ad lib* were given intramuscular injections of a citric acid iron sorbitol complex (JECTOFER® Astra Pharmaceutical Company Soderstälje Sweden) 15 times during a three week period the total dose corresponding to 50 mg Fe+++ per 100 g of body weight (these rats are referred to in the following as *iron loaded animals*). Control rats were given intramuscular injections of saline.

Mobilization of Iron from the Liver

After completed injections of iron the rats were divided into two groups each containing 10 animals. One group served as control and received no further treatments. The rats in this group are henceforth referred to as *iron loaded non bled animals*. Thus they constituted the *iron loaded control group*. The experimental group *iron loaded bled animals* was subjected to weekly phlebotomizations in which 1.5 ml peripheral blood/100 g of body weight (corresponding to ~25% of the total blood volume) were withdrawn by puncturing the orbital plexus with a heparinized glass capillary under slight ether anesthesia. Measurements of the hemoglobin were made weekly on the tail. In the control group the animals were measured immediately before phlebotomization. The animals were sacrificed 1 and 2 months after the start of the phlebotomization along with iron loaded controls and the control animals only given saline.

Fixation

All livers were fixed by perfusion. The abdomen was cut open during ether anesthesia and a catheter was inserted into the portal vein and ligated. The inferior caval vein was opened above and below the liver.

buffer containing 0.1 M sucrose as described previously (13). The liver tissue was cut into 1 mm thick cubes at slices and was fixed for 24 hours in the fixative mentioned above.

Preparation for Microscopy

Tissues for light microscopy were embedded in paraffin and stained with hematoxylin eosin and Perls blue.

The material intended for electron microscopy was postfixed in 2% osmium tetroxide buffered cacodylate and embedded in Epon after dehydration in ethanol and propylene oxide. *En bloc* staining with 1% uranyl acetate was performed. Ultrathin sections were prepared on a LKB ultratome V stained with lead citrate and examined in a Jeol 100 C electron microscope.

Demonstration of Acid Phosphatase

The slices fixed in glutaraldehyde for 24 hours were rinsed in 0.1% sucrose in 0.1% cacodylate buffer immersed in 10% DMSO 0.1 M cacodylate buffer and 0.1 M sucrose at pH 7.2 for 24 hours and were then cut into 50 µm thick sections using a Leitz freezing microtome. These sections were incubated for 15, 45, 60 or 90 minutes in a Gomori type medium (2) containing

14% sucrose and were subsequently rinsed in 0.1 M cacodylate buffer. Controls were incubated in media

mode at 100 kV using a take-off angle at 30°. The counting time was 50 sec (14)

RESULTS

described above. Ultrathin sections were cut on an LKB ultratome V, stained with lead citrate and examined in a Jeol 100 C microscope.

X ray Microanalysis

For X ray microanalysis, glutaraldehyde fixed tissues (either as such or incubated for the demonstration of acid phosphatase) were cut in 100–200 nm thick sections which were placed on nylon grids. No post-fixation in osmium staining with uranyl acetate or lead citrate was carried out on this material. Analytical electron microscopy was performed with a Kevex energy dispersive X ray spectrometer in a Jeol C electron microscope provided with a Jeol ASD scanning attachment (14). The tissue was examined in the scanning transmission

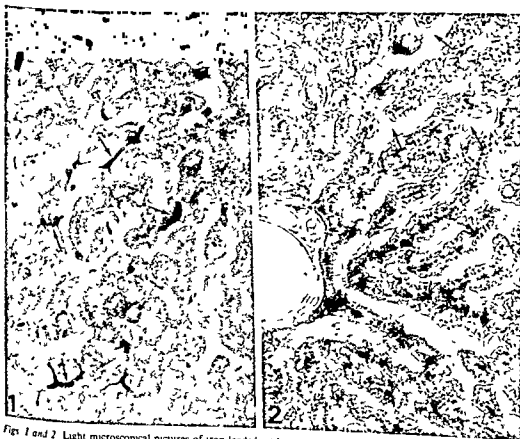
Hemoglobin measurements Following the bleeding, hemoglobin concentration of the blood decreased 10–15%. The hemoglobin concentration in the non bled animals ranged between 155–160 gram hemoglobin/liter.

MORPHOLOGY

Light Microscopy

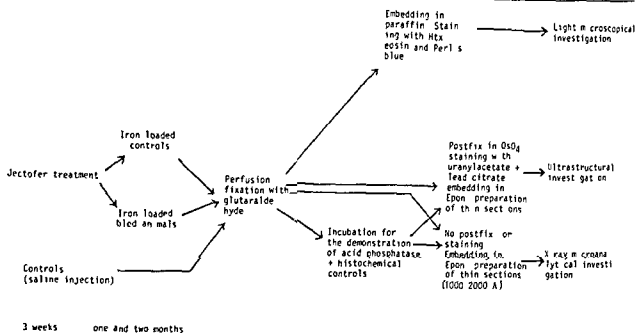
No pathological changes other than those directly dependent on the iron overload (described below) could be demonstrated in the liver tissue from any of the animals.

Iron loaded animals Following completed injection



Figs 1 and 2 Light microscopical pictures of iron loaded rat liver tissue. — — — sections stained for the demonstration of iron. In Figure 1 iron positive pigment in parenchymal cells. Iron positive (arrows). In Figure 2 — showing tissue from a bled animal (arrows). However, in the parenchymal cells, the same iron cells in Figure 1 present. Glutaraldehyde. Perl's blue. $\times 2$

Table 1 Short Survey over the Handling of the Investigated Material



MATERIALS AND METHODS

For a short survey see Table 1

Iron Loading

Male Sprague Dawley rats (weighing 200-220 grams) maintained on ordinary diet consisting of pellets containing approximately 260 µg iron/g (R3 Astra Evos Södertälje Sweden) and water *ad lib* were given intramuscular injections of a citric acid iron sorbitol complex (Jectofer® Astra Pharmaceutical Company Södertälje Sweden) 15 times during a three week period the total dose corresponding to 50 mg Fe+++ per 100 g of body weight (these rats are referred to in the following as *iron loaded animals*). Control rats were given intramuscular injections of saline.

Mobilization of Iron from the Liver

After completed injections of iron the rats were divided into two groups each containing 10 animals. One group served as control and received no further treatments. The rats in this group are henceforth referred to as *iron loaded non bled animals*. Thus they constituted the *iron loaded control group*. The experimental group *iron loaded bled animals* was subjected to weekly phlebotomizations in which 1.5 ml peripheral blood/100 g of body weight (corresponding to ~25% of the total blood volume) were withdrawn by puncturing the orbital plexus with a heparinized glass capillary under slight ether anesthesia. Measurements of the hemoglobin concentrations were carried out weekly on all animals taking a 20 µl blood sample from the tail. In the case of phlebotomized animals hemoglobin was measured immediately before phlebotomization. The animals were sacrificed 1 and 2 months after the start of the phlebotomization along with iron loaded controls and the control animals only given saline.

Fixation

All livers were fixed by perfusion. The abdomen was cut open during ether anesthesia and a catheter was inserted into the portal vein and ligated. The inferior caval vein was opened above and below the liver. Injection of heparin (500 IE/100 g of body weight) was

buffer containing 0.1 M sucrose as described previously (13). The liver tissue was cut into 1 mm thick cubes and slices and was fixed for 24 hours in the fixative mentioned above.

Preparation for Microscopy

Tissues for light microscopy were embedded in paraffin and stained with hematoxylin-eosin and Perl's blue.

The material intended for electron microscopy was postfixated in 2% osmium buffered osmium tetroxide and embedded in Epon after dehydration in ethanol and propylene oxide. *En bloc* staining with 1% uranyl acetate was performed. Ultrathin sections were prepared on a LKB ultratome V, stained with lead citrate and examined in a Jeol 100 C electron microscope.

Demonstration of Acid Phosphatase

The slices fixed in glutaraldehyde for 24 hours were rinsed in 0.1% sucrose in 0.1% cacodylate buffer immersed in 10% DMSO 0.1 M cacodylate buffer and 0.1 M sucrose at pH 7.2 for 24 hours and were then cut into 50 µm thick sections using a Leitz freezing microtome. These sections were incubated for 15, 45, 60 or 90 minutes in a Gomori type medium (2) containing

the Figs 3-6 are electron micrographs of Kupffer cells from nonbled and bled animals. Tissues fixed in glutaraldehyde, thin sections stained with lead citrate. Magnification $\times 30,000$

Fig 3 Non bled one month after completed iron loading. Numerous iron particles (IP) are present both in the cell sap and the lysosomes (Ly)

Fig 4 Bled one month after completed iron loading. Lysosomes are seen to contain IPs. However few IPs are seen in the cell sap. Mi: mitochondrion

Fig 5 Non bled two months after completed iron loading. Large numbers of IPs both in lysosomes and cell sap

Fig 6 Bled two months after completed iron loading. No IPs are present in the lysosomes or in the cell sap and the cell has the appearance of a normal rat liver Kupffer cell. Ly: lysosome. Mi: mitochondrion

tions numerous iron positive granules were present in the liver parenchymal and Kupffer cells with the highest concentration in the periportal regions. Within the parenchymal cells the iron positive granules were most abundant in peribiliary regions

months showed a slight decrease in iron positive pigment in both parenchymal and Kupffer cells (Fig 1). The pigment was still most frequent in the periportal regions. The pigment granules were also most concentrated in peribiliary areas of the parenchymal cells

Iron loaded bled animals Repeated phlebotomies did not result in a more rapid or extensive decrease in the total amount of iron positive pigment in the parenchymal cells than was observed in the non bled group. The same localization with a higher concentration in the periportal regions was also noted. However a drastic reduction in iron pigment was seen in the Kupffer cells and only small numbers of iron granules were seen after two months (Fig 2)

Electron Microscopy

Evidence of cell damage was not obtained in any of the cells studied at the fine structural level

Kupffer Cells

Iron loaded non bled animals Directly after completed

cor
cyt
and
with tightly packed IPs type II bodies with a stretched-out tubular appearance also containing tightly packed IPs and bodies with a typical lysosomal structure. All of these organelles were found to carry acid phosphatase and thus represented lysosomes (14). In the following they are referred to as lysosomes type I, II and III. In addition IPs were found diffusely dispersed in the cell sap

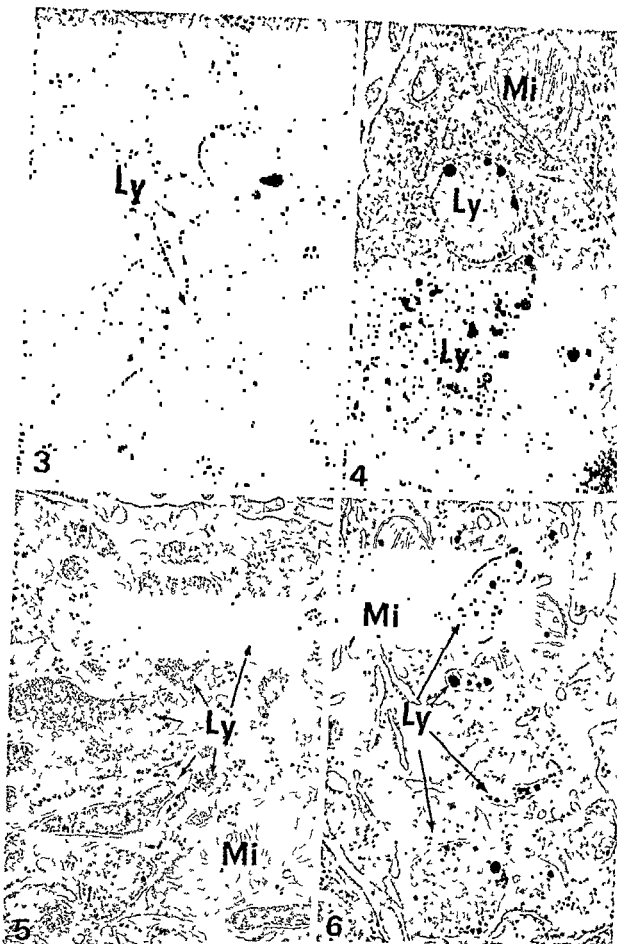
After one month IPs were present both in the cell sap and the three types of lysosomes mentioned above. Type I lysosomes were rarely observed but when present all of them contained IPs though usually in lower concentration than after completed iron loading. IPs were also observed in all type II and III lysosomes. The number of IPs was generally lower than in corresponding elements directly after the loading. Likewise the concentration of IPs in the cell sap was lower (Fig 3)

After two months IPs were seen in all type II bodies and conventional lysosomes

roughly with the amount of intralysosomally located IPs being more frequent in the cells with a high concentration of IP in the lysosomes. In the cells with a low concentration of IPs these particles were characteristically located in the periphery of the lysosomes. IPs were not present in the nucleus, mitochondria, endoplasmic reticulum, the Golgi apparatus or any other part of the cell

Iron loaded bled animals After one month the overall frequency of IPs had diminished considerably compared to the situation immediately after the Jectofer injection and the situation in the non bled group. However some IPs were identified in the majority of the Kupffer cell lysosomes (Fig 4). The latter were usually of conventional type (type III) while type I and type II lysosomes were few or absent. IPs were quite few in the cell sap and were not present in all cells

After two months no clearly identifiable IPs were seen within any membrane bound body or any part of the cell sap. The lysosomal vacuole consisted mainly of two types of elements: namely one with a rather dense matrix and another containing rounded structures with a globular appearance dispersed in a more translucent matrix. Type I and type II lysosomes were not encountered (Fig 6). In general



As Figs 3-6 are electron micrographs of Kupffer cells from nonbled and bled animals. Tissues fixed in glutaraldehyde thin sections stained with lead citrate. Magnification $\times 30\,000$

Fig 3 Non bled one month after completed iron loading. Numerous iron particles (IP) are present both in the cell sap and the lysosomes (Ly).

Fig 4 Bled one month after completed iron loading. Lysosomes are seen to contain IPs. However few IPs are seen in the cell sap. Mi = mitochondrion.

Fig 5 Non bled two months after completed iron loading. Large numbers of IPs both in lysosomes and cell sap.

Fig 6 Bled two months after completed iron loading. No IPs are present in the lysosomes or in the cell sap and the cell has the appearance of a normal rat liver Kupffer cell. Ly = lysosome. Mi = mitochondrion.

ous numerous iron positive granules were present in the liver parenchymal and Kupffer cells with the highest concentration in the periportal regions. Within the parenchymal cells the iron positive granules were most abundant in peribiliary regions.

Iron loaded non bled animals. Compared to the liver tissue obtained immediately after iron loading the livers of the animals sacrificed after one and two months showed a slight decrease in iron positive pigment in both parenchymal and Kupffer cells (Fig 1). The pigment was still most frequent in the periportal regions. The pigment granules were also most concentrated in peribiliary areas of the parenchymal cells.

Iron loaded bled animals. Repeated phlebotomies did not result in a more rapid or extensive decrease in the total amount of iron positive pigment in the parenchymal cells than was observed in the non bled group. The same localization with a higher concentration in the periportal regions was also noted. However a drastic reduction in iron pigment was seen in the Kupffer cells and only small numbers of iron granules were seen after two months (Fig 2).

Electron Microscopy

Evidence of cell damage was not obtained in any of the cells studied at the fine structural level.

Kupffer Cells

Iron loaded non bled animals. Directly after completed iron loading (13) IP's (electron dense iron containing particles) were present in three types of cytoplasmic bodies: type I bodies which were large and rounded with tightly packed IPs; type II bodies with a stretched-out tubular appearance also containing tightly packed IPs and bodies with a typical lysosomal structure. All of these organelles were found to carry acid phosphatase and thus are referred to as lysosomes (14). In the following they are referred to as lysosomes type I, II and III. In addition IPs were found diffusely dispersed in the cell sap.

After one month. IPs were present both in the cell sap and the three types of lysosomes mentioned above. Type I lysosomes were rarely observed but when present all of them contained IPs though usually in lower concentration than after completed iron loading. IPs were also observed in all type II and III lysosomes. The number of IPs was generally lower than in corresponding elements directly after the loading. Likewise the concentration of IPs in the cell sap was lower (Fig 3).

After two months. IPs were seen in all type II bodies and conventional lysosomes and also in the cell sap of all Kupffer cells (Fig 5). The concentration of IPs in the cell sap and within limited bodies varied considerably between different cells. Characteristic type I bodies were lacking in these cells. The concentration of IPs in the cell sap correlated roughly with the amount of intralysosomally located IP's being more frequent in the cells with a high concentration of IP in the lysosomes. In the cells with a low concentration of IPs these particles were characteristically located in the periphery of the lysosomes. IPs were not present in the nucleus, mitochondria, endoplasmic reticulum, the Golgi apparatus or any other part of the cell.

Iron loaded bled animals. After one month the overall frequency of IPs had diminished considerably compared to the situation immediately after the Jectofer injection and the situation in the non bled group. However some IP's were identified in the majority of the Kupffer cell lysosomes (Fig 4). The latter were usually of conventional type (type III) while type I and type II lysosomes were few or absent. IPs were quite few in the cell sap and were not present in all cells.

After two months. No clearly identifiable IPs were seen within any membrane bound body or any part of the cell sap. The lysosomal vacuole consisted mainly of two types of elements: namely one with a rather dense matrix and another containing rounded structures with a globular appearance dispersed in a more translucent matrix. Type I and type II lysosomes were not encountered (Fig 6). In general

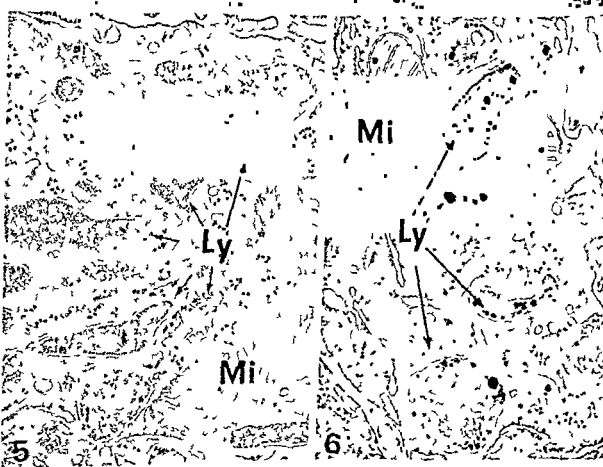
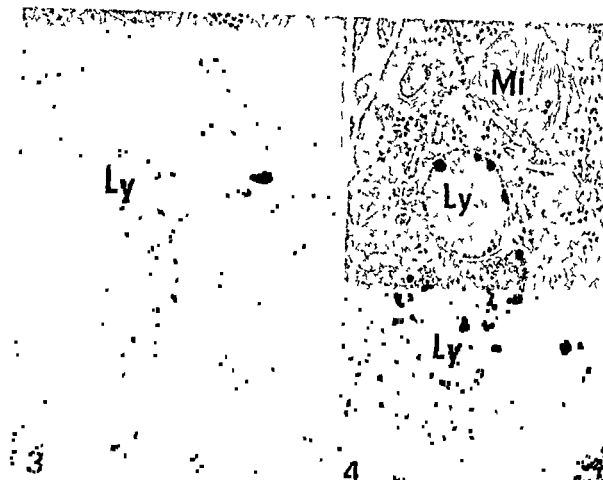


Fig 7 Peribiliary region of two rat liver cells from a non bled animal two months after completed iron loading. The lysosomes are packed with IPs. IPs are also frequent in the cell sap. Bc bile canaliculus. ER endoplasmic reticulum. Go Golgi apparatus. Ly lysosome. Mi mitochondria. P peroxisomes. Glutaraldehyde lead citrate $\times 25\ 000$

Inset IPs are tightly packed in a lysosome but more sparse in the surrounding cell sap $\times 40\ 000$

Fig 8 The appearance of peribiliary regions of three adjacent liver cells from a bled rat (2 months) is illustrated. Numerous IPs are seen both in lysosomes (Ly) and the cell sap. Bc bile canaliculi. Gly glycogen. Go Golgi apparatus. Mi mitochondria. Glutaraldehyde. Staining with lead citrate $\times 30\ 000$

Inset (a) shows a lysosome filled with IPs. IPs are also scattered in the surrounding cell sap. Inset (b) shows an apparent fusion between an IP-containing lysosome and an autophagic vacuole (AV) $\times 40\ 000$

the Kupffer cells and their lysosomal system showed the appearance previously described in the normal rat (27)

Parenchymal Cells

Iron loaded non bled animals Directly after completed iron loading there are three types of IP-containing bodies present in the parenchymal cells: one with a typical lysosome like appearance (peribiliary dense body), one containing no other visible material than IPs and a third body with the appearance of autophagic vacuoles. All of these organelles have been shown to contain acid phosphatase and hence represent lysosomes (14). Great numbers of IPs were observed in the cell sap.

After one month all parenchymal cells showed presence of IPs in the cell sap however not as concentrated as immediately after loading (13). Completely IP filled lysosomes lacking other materials than the granules were no longer present. IPs were usually although not always observed in the other two types of lysosomes described above. Lysosomes lacking IPs were characterized by occurrence of abundant membranous and dense materials and appeared to correspond to residual bodies. In many cases the IP-carrying lysosomes also contained other (degraded) materials.

After two months some IPs were found in all parenchymal cells. The concentration of IPs in the cell sap was not clearly lower than at the one month intervals. IPs were also located in the lysosomes (of conventional type and in the form of autophagic vacuoles). In the latter the IPs were

month intervals. IPs were not demonstrated in any other cellular organelle or compartment than those mentioned above.

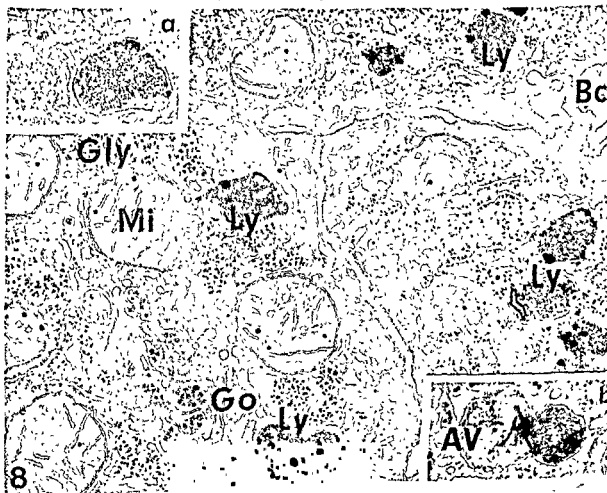
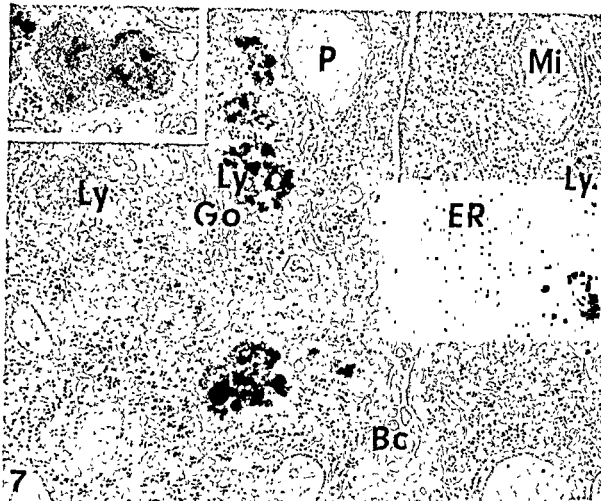
Iron loaded bled animals After one month IPs were seen in all parenchymal cells in the liver lobule in both the cell sap and different types of lysosomes. No clear difference in IP-content in the lysosomes or the cell sap could be demonstrated between this group and the non bled group.

After two months considerable numbers of diffusely distributed IPs were still present in the cell sap. IPs were also observed in membranous bodies but only two varieties namely autophagic vacuoles and lysosomes of the peribiliary dense body type (completely IP filled lysosomes were no longer present) (Fig 8). The IPs were sparse in some lysosomes of the residual body type and also in large irregular bodies containing globular and osmiophilic material and probably representing lysosomes transforming into residual bodies. However in most lysosomes IPs were rather abundant. Sometimes a compartmentalization occurred in the autophagic vacuoles resulting in a separation of the IPs from concomitantly present autophagocytosed matter. There were no signs of fusion between IP-containing bodies and the plasma membranes. However images indicating fusion between IP-containing secondary lysosomes and autophagic vacuoles were seen suggesting that the digestive function of secondary lysosomes was not impaired by the presence of iron loading (Fig 8). No clear difference in the frequency of IPs between the bled and the non bled group was noted in this cell type. This applies both for the cell sap and the lysosomes. No IPs were identified in other fractions than the cell sap or the lysosomal vacuole. Neither was IPs seen outside the cell in the bile capillaries of the space of Disse.

Endothelial and Fat Storing Cells

Like immediately after iron loading no IPs could be discovered in any part of these cells. The same applies for both the bled and non bled animals as well as those in the control groups.

vacuoles (Fig 7) with material such as glycogen and IP separated inside the vacuole. There was no clear difference concerning the concentration of IPs between lysosomes in cells at the one and two



Figs 9-10 Parts of Kupffer cells from a rat which had been given iron two months previously. The cell in *Figure 9* is from a non bled animal and in *Figure 10* from a bled animal. The tissues have been incubated for the demonstration of acid phosphatase. The granular nature of the reaction product in lysosomes makes it hard to detect possible dual occurrence of IPs. Ly lysosome Nu nucleus Glutaraldehyde incubation time 45 min section staining with lead citrate $\times 21\,000$

Fig 11 Liver parenchymal cell from an unbled rat (2 months after completed iron loading). Tissue incubated for the demonstration of acid phosphatase containing several bodies presumed to represent lysosomes. One apparent lysosome (Ly₁) is packed with IPs but does not show clear evidence of final product. Two autophagic vacuoles (AV) contain both reaction product and IPs (arrows) while a lysosome (Ly₂) clearly is covered by lead phosphate precipitate and may contain IPs (these seem to be obscured by the precipitate). M₁ mitochondria. Glutaraldehyde incubation time 45 min section staining with lead citrate $\times 38\,000$

Aut Figs 12-14 show a series of pictures from tissue incubated for the demonstration of acid phosphatase showing the postulated development of an autolysosome through fusion of an autophagosome with a primary lysosome. Glutaraldehyde incubation time 45 min section staining with lead citrate $\times 50\,000$

Fig 12 An autophagic vacuole (AV) containing undegraded glycogen and IPs. The vacuole lacks evidence of reaction for phosphatase

Fig 13 An autophagic vacuole (AV) containing undegraded glycogen and IPs but no reaction product. Adjacent to vacuole is a smaller structure believed to be the equivalence of a primary lysosome (PL) with deposits of lead phosphate precipitate. This lysosome is believed to be in the process of fusing with the autophagic vacuole

14 A lysosome (Ly) showing presence of reaction product and IPs

HISTOCHEMISTRY

Kupffer Cells

Incubation for the demonstration of acid phosphatase resulted in deposition of electron dense reaction product over lysosomal structures often linking the concomitant occurrence of IPs and reaction product hard to substantiate. This applies to most of the IP-containing lysosomes.

Iron loaded non bled animals Reaction product is encountered in all membrane bound bodies here IPs were identified both after one and two months (*Fig 9*). However it was sometimes difficult to identify the IPs in the individual bodies due to the simultaneous presence of reaction product in the lysosomes. Lead phosphate deposits were also observed in the Golgi apparatus.

Iron loaded bled animals Distinct deposits of reaction product were identified over the different types of lysosomal vacuoles both after one and two months. Also in these groups reaction product was seen in the Golgi apparatus. Other portions of the cells lacked precipitates. At the one month interval some reaction product-containing bodies showed presence of IPs while IPs appeared to be lacking in such bodies two months after completed iron loading.

Parenchymal Cells

Iron loaded non bled animals Reaction product was deposited over lysosomal elements in the parenchymal cells. Some of these bodies showed a diffuse heavy deposition of precipitate - in many

instances rendering it difficult or impossible to identify concomitantly occurring IPs. Some IP containing autophagic vacuoles lacked reaction product (*Fig 12*). Images suggesting fusion between lysosomes and such IP-containing autophagic vacuoles were also obtained (*Fig 13* and *14*). Deposition of final reaction product was however observed over other autophagic vacuoles and also in portions of the Golgi apparatus.

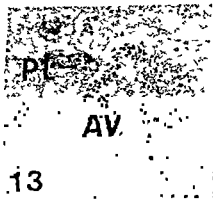
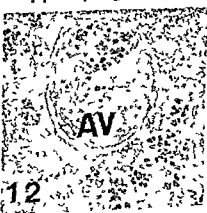
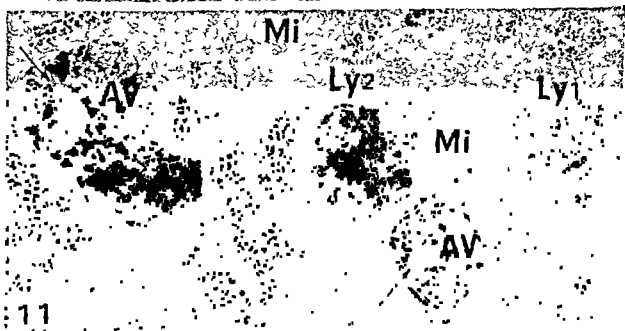
Iron loaded bled animals The lysosomal vacuole showed presence of deposits of reaction product in bodies also containing IPs. However reaction product was also noted in structures where the distinct features of IPs could not be revealed. These structures usually corresponded to somewhat enlarged peribiliary dense bodies lacking recognizable content or sign of autophagy some of them bore resemblance to residual bodies. Reaction product was further deposited over many (but not all) autophagic vacuoles some of which encompassed IPs. Some portions of the Golgi apparatus showed presence of reaction product.

Endothelial and Fat Storing Cells

Lysosomes in endothelial cells of both groups showed a distinct deposition of reaction product. The occasionally encountered fat storing cells also contained bodies covered by precipitates.

Controls

No reaction product was demonstrated in any of the incubated controls.



gs 9-10 Parts of Kupffer cells from a rat which had been given iron two months previously. The cell in Figure 9 is from a non bled animal and in Figure 10 from a bled animal. The tissues have been incubated for the demonstration of acid phosphatase. The granular nature of the reaction product in lysosomes makes it hard to detect possible dual occurrence of IPs. Ly lysosome Nu nucleus Glutaraldehyde incubation time 45 min section staining with lead citrate $\times 21\,000$

Fig 11 Liver parenchymal cell from an unbled rat (2 months after completed iron loading). Tissue incubated for the demonstration of acid phosphatase containing several bodies presumed to represent lysosomes. One apparent lysosome (Ly) is packed with IPs but does not show clear evidence of final product. Two autophagic vacuoles (AV) contain both reaction product and IPs (arrows) while a lysosome (Ly₂) clearly is covered by lead phosphate precipitate and may contain IPs (these seem to be obscured by the precipitate). Mi mitochondria Glutaraldehyde incubation time 45 min, section staining with lead citrate $\times 38\,000$

Fig 12-14 show a series of pictures from tissue incubated for the demonstration of acid phosphatase showing the postulated development of an autolysosome through fusion of an autophagosome with a primary lysosome. Glutaraldehyde incubation time 45 min section staining with lead citrate $\times 50\,000$

Fig 12 An autophagic vacuole (AV) containing undegraded glycogen and IPs. The vacuole lacks evidence of reaction product or phosphatase.

Fig 13 An autophagic vacuole (AV) containing undegraded glycogen and IPs but no reaction product. Adjacent to the vacuole is a smaller structure believed to be the equivalence of a primary lysosome (PL) with deposits of lead phosphate precipitate. This lysosome is believed to be in the process of fusing with the autophagic vacuole.

Fig 14 A lysosome (Ly) showing presence of reaction product and IPs.

HISTOCHEMISTRY

Kupffer Cells

Incubation for the demonstration of acid phosphatase resulted in deposition of electron dense reaction product over lysosomal structures often making the concomitant occurrence of IPs and reaction product hard to substantiate. This applies to most of the IP-containing lysosomes.

Iron loaded non bled animals Reaction product was encountered in all membrane bound bodies where IPs were identified both after one and two months (Fig 9). However it was sometimes difficult to identify the IPs in the individual bodies due to the simultaneous presence of reaction product in the lysosomes. Lead phosphate deposits were also observed in the Golgi apparatus.

Iron loaded bled animals Distinct deposits of reaction product were identified over the different types of lysosomal vacuoles both after one and two months. Also in these groups reaction product was seen in the Golgi apparatus. Other portions of the cells lacked precipitates. At the one month interval some reaction product-containing bodies showed presence of IPs while IPs appeared to be lacking in such bodies two months after completed iron loading.

Parenchymal Cells

Iron loaded non bled animals Reaction product was deposited over lysosomal elements in the parenchymal cells. Some of these bodies showed a diffuse heavy deposition of precipitate - in many

instances rendering it difficult or impossible to identify concomitantly occurring IPs. Some IP-containing autophagic vacuoles lacked reaction product (Fig 12). Images suggesting fusion between lysosomes and such IP-containing autophagic vacuoles were also obtained (Fig 13 and 14). Deposition of final reaction product was however observed over other autophagic vacuoles and also in portions of the Golgi apparatus.

Iron loaded bled animals The lysosomal vacuole showed presence of deposits of reaction product in bodies also containing IPs. However reaction product was also noted in structures where the distinct features of IPs could not be revealed. These structures usually corresponded to somewhat enlarged peribiliary dense bodies lacking recognizable content or sign of autophagy, some of them bore resemblance to residual bodies. Reaction product was further deposited over many (but not all) autophagic vacuoles, some of which encompassed IPs. Some portions of the Golgi apparatus showed presence of reaction product.

Endothelial and Fat Storing Cells

Lysosomes in endothelial cells of both groups showed a distinct deposition of reaction product. The occasionally encountered fat storing cells also contained bodies covered by precipitates.

Controls

No reaction product was demonstrated in any of the incubated controls.

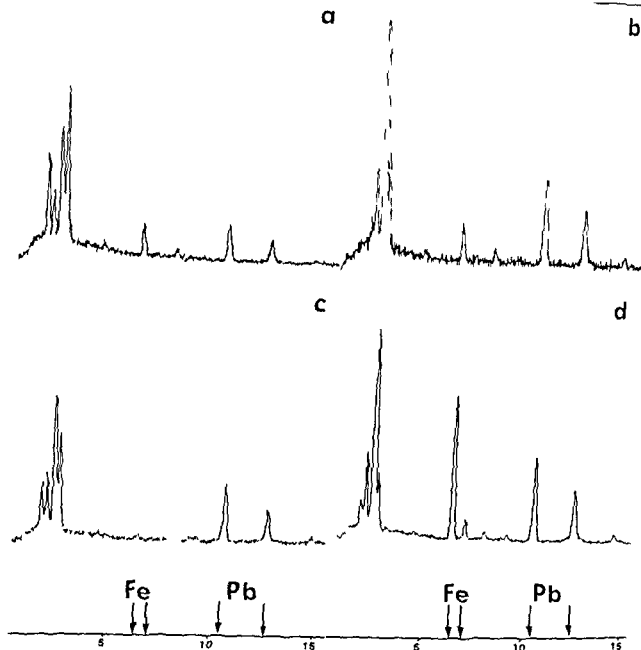


Fig. 15 Energy spectrum obtained from Kupffer and parenchymal cells. A and B show spectra from iron loaded non-bleed Kupffer (a) and parenchymal cell (b) lysosomes. C and D show spectra from Kupffer and parenchymal cell lysosomes of bled animal respectively. Note the absence of iron in the Kupffer cell lysosome from the bled animal. Energy quanta in KeV at which the signals for different elements were recorded: Fe (iron) K α 6.4 K β 7.1 Pb (lead) M α 2.4 La 10.5 L β 12.6 Cl (chlorine) K α 2.5 and P (phosphorous) K α 2.0.

X RAY MICROANALYSIS

The graphs recorded from the different cell types are shown in Figure 15.

The same outcome in the analysis for presence of iron was obtained before and after incubation for the demonstration of acid phosphatase in all instances the following description will therefore only deal with the incubated material.

Kupffer Cells

Iron loaded non-bleed animals In this group all types of lysosomes showed presence of both iron and lead (reaction product) after one and two months. Peaks for lead only were obtained from the Golgi regions. Small peaks indicating presence of iron were obtained from the cytoplasmic ground substance. Signals for iron or lead were not received from any other part of the cells.

Iron loaded bled animals All bodies containing iron gave a positive peak for lead. After two months peaks for iron were not recorded in any Kupffer cell whereas peaks for lead from lysosome like structures were received in the same way as from Kupffer cells of the other groups. Iron and lead were not demonstrated in any other part of the cell. Signals indicating presence of lead only were obtained from the Golgi regions.

Parenchymal Cells

Iron loaded bled and non bled animals No difference in the distribution of iron or lead has been seen in this cell type between the different groups. After one month the peaks for iron were similar to those received immediately after iron loading. After two months some peribiliary dense bodies showed a high concentration of iron (Fig. 15) compared to the bodies investigated previously. Presence of iron was also recorded in the graphs from the cell sap. Signals for lead were also recorded from some Golgi regions but not from any other parts of the cells.

Endothelial Cells and Fat Storing Cells

Only lead – and no iron – was found in the lysosomes analysed in these cell types. No significant signals for lead or iron was received from any other part of the cell.

Controls

No peaks for iron were recorded in the animals only given saline. Peaks for lead were obtained from typical lysosome like structures in all cells.

No peaks for lead were seen in the tissues from the experimental animals used for histochemical controls while the peaks for iron were the same as in liver tissue incubated in the proper medium for the demonstration of acid phosphatase.

DISCUSSION

The present work demonstrates that during the mobilization of iron from the iron loaded rat liver by way of bleeding Kupffer cells show a rapid decrease in and almost complete disappearance of IPs while there is only a limited decline in the IPs present in the parenchymal cells. Depletion of IPs in the latter cells was not noted despite extensive bleeding of the animals. It was further observed that all IP-containing cytoplasmic bodies also showed presence of acid phosphatase one and two months after cessation of iron loading implying that all of these bodies represent lysosomes.

Previous studies by Shoden and Sturgeon (25) concerning the mobilization of iron from the liver

following overload demonstrated – on the light microscopical level – that Kupffer cell hemosiderin was more readily removed than parenchymal cell hemosiderin after administration of saccharated iron oxide followed by bleeding. It has further been shown (9) that iron taken up by reticuloendothelial (Kupffer) cells in the liver is released in an early and a late phase. However if body iron was reduced by phlebotomy the Kupffer cells were able to release most of the excess iron in the early phase. This means that they have the ability to alter their release of iron when there is a need for it. It has likewise been shown (3) that release of iron from reticuloendothelial cells is increased in humans with iron deficiency. However nothing was revealed

when the demand for iron was increased the stored iron was readily released from the Kupffer cells while the endothelially stored iron was retained. Hershko *et al* (11) among others has performed studies on the effects of a chelating agent – desferrioxamine – and demonstrated that administration of this substance mainly results in reduction of the iron overload in parenchymal cells. Bradford *et al* (5) have claimed that ferritin and hemosiderin are released into the bile through reversed pinocytosis by parenchymal cell lysosomes after loading with iron.

In previous papers we have discussed the possible

ways of iron release – following binding of iron – becomes sequestered in lysosomes by way of autophagy as suggested by Trump *et al* (26) among others. In the present study we noted that IPs were present in early autophagic vacuoles along with undegraded glycogen. IPs were demonstrated also in an autophagic vacuole lacking reaction product which appeared to fuse with a structure with heavy deposition of final product. This observation seems to support the idea that IPs are incorporated together with other material from the cell sap in the lysosomal vacuole. The morphological and cytochemical observations have not indicated other ways by which IPs might become associated with the interior of lysosomes. It appears unlikely that iron could become bound to apoferritin in lysosomes since apoferritin is rapidly degraded.

their iron moiety to the blood to become bound in transferrin when needed (9). However, it has also been suggested that ferritin molecules in the cell sap or in membrane bound vacuoles of different cells might be released directly into the blood stream since the serum level of this protein is increased in different iron storage diseases (21). Such release is evidently very difficult to demonstrate morphologically. However, in our pictures we never encountered any evidence for a release of this kind. Furthermore, other macromolecules — such as thorium dioxide particles — that are not degraded by lysosomal enzymes have been shown to remain inside lysosomes of Kupfer cells for up to a year (8, 28). This militates against the idea that reversed endocytosis of lysosomal content had occurred in the Kupfer cells. The occurrence in the peripheral blood of ferritin molecules in various iron storage diseases (21) may possibly be explained by reversed endocytosis in other types of cells. Alternatively, bits of cytoplasm with ferritin in the cell sap or vacuolar elements might become dispatched into the blood stream whereby the ferritin molecules could be set free through lysis of the cytoplasmic fragment.

If not complete ferritin molecules are released from the cells, disappearance of IPs could be explained by separation of the iron moiety from the ferritin molecule. One could then hypothesize the cell sap ferritin is first depleted of its iron molecules and that the lysosomally stored ferritin and hemosiderin molecules subsequently release their iron and become degraded. Another possible way is that the cell sap ferritin is first autophagocytosed in order to be intralysosomally degraded for subsequent release of iron.

The impression obtained from the pictures was that in Kupfer cells of the bled animals, IPs in the cell sap decreased before those in the lysosomes, suggesting that the release of iron commences from the cell sap when the release is increased. However, the evidence obtained did not reveal whether or not this postulated transport occurred through movement of ferritin molecules across the cell membrane or in some other way (such as transfer of iron atoms).

The possible ways for iron transport from the parenchymal cells are (a) release of ferritin molecules of the iron moiety to the blood at the sinusoids and (b) transport to the bile. As regards the release of iron for binding to transferrin in the blood, the same ways are possible as indicated concerning the Kupfer cells. Presence of iron and ferritin molecules in the bile has been demonstrated by Bradford *et al.* (5). Therefore, the transport of iron to the bile can be viewed to occur in at least 3 different ways.

One might be through release of free iron atoms from the cell sap to the bile canaliculus, a second transmembrane movement of ferritin molecules residing in the cell sap and a third reversed endocytosis from lysosomes as suggested by Bradford *et al.* (5).

We have not noticed any signs of reversed endocytosis in the peribiliary regions or elsewhere and we have therefore no evidence to support this theory. The ferritin molecule is too large to be able to be transported through the plasma membrane. Alternatively, transport of iron atoms across the cell membrane into the bile might occur. It should be emphasized, however, that liver parenchymal cells are said to be able to excrete lysosomal content by reversed endocytosis when being under the influence of toxic substances such as arabinoside and vinblastine (15, 18).

The difference in IP content between Kupfer cells in the bled and non bled groups is striking. The fact that the Kupfer cells lose IPs more rapidly than the parenchymal cells in the bled group can be explained in several ways. One possibility is of course that the parenchymal cells have larger stores; if the rate of release is the same from both cell types, the Kupfer cell will evidently be depleted before loss from the parenchymal cell is substantial. This does not seem likely since in the normal rat the Kupfer cells have a volume density of lysosomes that is approximately 50% of that in parenchymal cells (4); furthermore, it appears that the Kupfer cell lysosomes are the ones that increase in volume the most after iron overload, indicating that they initially might store a large portion of the IPs. As was pointed out previously (13), the other possibility would be that the Kupfer cells release iron more readily than the parenchymal cells. Our present findings are compatible with this hypothesis. One possibility is of course that the initially stored Kupfer cell iron becomes redistributed to both parenchymal and hemopoietic cells, resulting in a depletion of iron in Kupfer cells and a continuing overload in the parenchymal cells. In order to prove this redistribution model, one would have to isolate parenchymal and sinusoidal cells after different periods and measure the iron content in both cell types separately.

Supported by a grant from the Swedish Medical Research Council (Project No. C78 12X-01006 14C).

REFERENCES

1. Arborgast B, Å M, Glaumann H & Ericsson J I. E. Studies on iron loading of rat liver by iron

- Effects on the liver and distribution and fate of iron
Lab Invest 30 664-673 1974
- 2 Barka T & Andersson P J Histochemical methods for acid phosphatase using hexazonium pararosanilin as coupler *J Histochem Cytochem* 10 741-753 1962
- 3 Beamish M R Davies A G Eakins J P Jacobs A & Trivett D The measurement of reticuloendothelial iron release using iron-dextran *Br J Haematol* 21 617-622 1971
- 4 Blouin A Bulender R P & Weibel E W Distribution of organelles and membranes between hepatocytes and nonhepatocytes in the rat liver parenchyma A stereological study *J Cell Biol* 72 441-455 1977
- 5 Bradford W P Elchlepp J G Arstila A U Trump B F & Kinney T D Iron metabolism and cell membranes I Relation between ferritin and hemosiderin in bile and biliary excretion of lysosomal contents *Am J Pathol* 56 201-228 1969
- 6 Drysdale J W & Munroe H N Regulation of synthesis and turnover of ferritin in rat liver *J Biol Chem* 241 3630-3637 1966
- 7 Dullmann J Wulfshkel U & Hausmann K Kupffer cells and other liver sinusoidal cells Ed Wisse E Knook P L p 233-244 1978
- 8 Ericsson J L W Unpublished observations 1979
- 9 Flier G Cook J P & Finch C A Storage iron kinetics VII A biological model for reticuloendothelial iron transport *J Clin Invest* 53 1527-1533 1974
- 10 Hausmann K Wulfshkel U Dullmann J & Kuse R Iron storage in macrophages and endothelial cells Histochemistry ultrastructure and clinical significance *Blut* 32 289-295 1976
- 11 Hershko C Cook J D & Finch C A Storage iron kinetics III Study of desferrioxamine action by selective radioiron labels of RE and parenchymal cells *J Lab Clin Med* 81 876-886 1973
- 12 Hicks S J Drysdale J W & Munroe H N Preferential synthesis of ferritin and albumin by different populations of liver polysomes *Science* 164 584-585 1969
- 13 Hulcrant R & Arborgh B Studies on the rat liver following iron overload Fine structural appearance *Acta Pathol Microbiol Scand Sect A* 86 143-155 1978
- 14 Hulcrant R Arborgh B Wroblewski R & Ericsson J L E Studies on the rat liver following iron overload Electron probe X ray microanalysis of acid phosphatase and iron *Am J Pathol* 96 625 1979
- 15 Kerr J F R Liver cell defaecation An electron microscope study of the discharge of lysosomal residual bodies into the intracellular space *J Pathol* 100 99-103 1970
- 16 Lee S S C & Richter G W Biosynthesis of ferritin in rat hepatoma cells and livers I Synthesis and assembly of protein subunits of ferritin *J Biol Chem* 252 2046-2053 1977
- 17 Lee S S C & Richter G W Biosynthesis of ferritin in rat hepatoma cells and livers II Binding of iron by ferritin protein *J Biol Chem* 252 2054-2059 1977
- 18 Marrella L & Glaumann H Increased degradation in rat liver induced by vinblastine II Morphological characterization *Lab Invest* 42 18-27 1980
- 19 Munroe H N & Drysdale J W Role of iron in the regulation of ferritin metabolism *Fed Proc* 29 1469-1473 1970
- 20 Pechet G S Parenteral iron overload Organ and cell distribution in rats *Lab Invest* 20 119-126 1969
- 21 Prieto J Barry M & Sherlock S Serum ferritin in patients with iron overload and with acute and chronic liver diseases *Gastroenterology* 68 525-533 1975
- 22 Redman C M Biosynthesis of serum proteins and ferritin by free and attached ribosomes of rat liver *J Biol Chem* 244 4308-4315 1969
- 23 Richter G W A study of hemosiderosis with aid of electron microscopy *Exp Med* 106 203-217 1957
- 24 Sargenti K S & Munroe H N Association of ferritin with liver cell membrane fractions *Exp Cell Res* 93 15-22 1975
- 25 Shoden A & Sturgeon Ph Iron storage VI Mobilization of iron by bleeding *Haematologia* 2 267-278 1968
- 26 Trump B F Valigorsky J M Arstila A R Mergner W J & Kinney T D The relationship of intracellular pathways of iron metabolism to cellular iron overload and the iron storage diseases Cell sap and cytoacavitary network pathways in relation to lysosomal storage and turnover of iron macromolecules *Am J Pathol* 72 296-335 1973
- 27 Wisse E Observations on the fine structure and peroxidase cytochemistry of normal rat liver Kupffer cells *J Ultrastruct Res* 46 393-426 1974
- 28 Odegaard A Ophus E M & Larsson A Identification of diiodide in human liver cells by electron microscopic X ray microanalysis *J Clin Pathol* 31 893-896 1978

COMPARATIVE SINGLE CELL AND FLOW DNA ANALYSIS IN ASPIRATION BIOPSIES FROM BREAST CARCINOMAS

G AUER and B TRIBUKAIT

Department of Tumor Pathology Karolinska Hospital and Department of Medical Radiobiology
Karolinska Institute Stockholm Sweden

Auer G & Tribukait B. Comparative single cell and flow DNA analysis in aspiration biopsies from breast carcinomas. Acta path. microbiol. scand. Sect. A 88: 355-358, 1980.

The DNA distribution patterns in fine needle aspirates from 17 breast carcinomas were analysed using single cell and flow cytophotometric techniques. A good correlation was observed between the modal DNA values obtained by the two methods. Advantages and disadvantages of the two methods are discussed.

Key words: DNA analyses, human breast carcinoma.

G Auer, Department of Tumor Pathology, Karolinska sjukhuset, S-104 01 Stockholm, Sweden.

Accepted as submitted 8 v 80

Fine needle aspiration biopsy is increasingly used for diagnosis of palpable breast lesions. The main advantage of this technique is its high diagnostic accuracy combined with speed and patient acceptability. Since fine needle biopsy is minimal traumatic it also allows repeated sampling, for example during cytostatic or endocrine treatment of inoperable tumors.

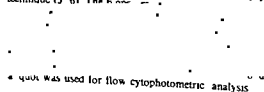
Recent studies have shown that DNA measurements in single morphologically identified breast cancer cells from fine needle aspirates are valuable for the prediction of patient survival (1). In addition a strong correlation between DNA distribution pattern and estrogen receptor (ER) content in breast cancer has been demonstrated indicating that DNA measurements may be used in order to estimate the sensitivity of breast cancer to endocrine therapy in cases in which ER levels cannot be determined with sufficient accuracy, i.e. in premenopausal women (2). It is thus clear that DNA measurements in fine needle aspirates contribute valuable information concerning prognosis and choice of therapy of breast cancer patients.

In the present investigation we studied whether the relatively time-consuming single cell DNA measurements in breast cancer aspirates can be replaced by flow DNA measurements which would decisively facilitate the use of DNA analysis in routine patient work.

MATERIAL AND METHODS

Cell Material

Cell samples from human breast carcinoma were obtained by means of fine needle aspiration biopsy technique (5-6). The biopsy material was



* quartz was used for flow cytophotometric analysis.

Fine Needle Aspiration Biopsy

The technique consists of inserting a thin (0.5-0.7 mm o.d.) needle into a palpable mass, e.g. in the present investigation into a breast tumor, and aspirating cellular

material into the lumen of the needle by negative pressure produced by drawing back the plunger of a 10 ml syringe attached to the needle. During sampling the needle is moved back and forth several times through the tumor mass usually at different angles to the original angle of insertion. The aspirated cell material consists of single cells or clumps of cells. In breast cancer generally the vast majority of the aspirated cells were found to be tumor cells. Small amounts of non tumor cells especially leucocytes, benign mammary epithelial cells, fibroblasts and fat cells are usually admixed with the tumor cells.

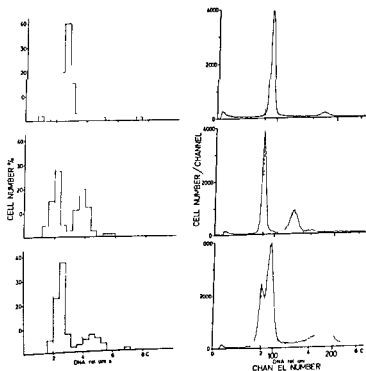
Single Cell Cytophotometry

Smear preparations were fixed in buffered 4% formaldehyde for a minimum of 15 hours and Feulgen stained. Previous studies (7) showed that hydrolysis for 1 hour at 22 °C in 5 M HCL resulted in optimal staining intensities. The nuclear Feulgen DNA in single cells was measured in a rapid scanning - integrating microspectrophotometer developed by T. Caspersson (3, 4). Diploid amounts of DNA were determined by using leucocytes and normal mammary epithelium adventitiously present in all aspirates as internal control. The discrepancies between DNA values of leucocytes with condensed chromatin were partially corrected for by measuring at the «off peak» wave length of 610 nm. Usually 100 tumor cells and 30 control cells were measured per each preparation. Tumor cells could easily be distinguished from normal cells either by their nuclear morphology or by the additional use of phase contrast. All Feulgen DNA values were expressed in relation to their

corresponding staining control which was given the value 2 c denoting the normal diploid DNA content.

Flow Cytophotometry

Flow cytophotometric measurements were performed according to a previously described procedure (8). The cell material from fine needle aspirates was fixed in ice cold ethanol after washing in buffer solution (0.1 M Tris, 0.07 M NaCl, 0.005 M EDTA, pH 7.5). After at least 12 hours fixation the cell material was washed in buffer solution with 1 mg of RNase per ml (RNase A Sigma) added. Single cell nuclei were obtained by subsequent treatment with pepsine (0.5% pepsine Merck No 7180, 1000 Eg) for 10 minutes at 37 °C. After further washing the DNA in the cell nuclei was stained with ethidium bromide (2.5×10^{-5} M, Serva Heidelberg Nr 21238 in Tris EDTA buffer, 386 mOsm). All preparations were checked microscopically. The DNA contents of the cell nuclei were analysed using a rapid flow cytofluorometer ICP 11 (Phywe W. Germany) with a flow rate of up to 1000 cells/sec. The excitation and emission wavelengths were 455-490 nm and 590-630 nm. The output was sorted by a 256 channel analyser (Nuclear Data 100) and was presented as a histogram. The DNA values were expressed in relation to the DNA content of normal diploid human cells. Calculation of the proportion of G₁, S and G₂ + M cells was achieved by automatic integration of cells into corresponding channels in the multichannel analyser. The values were corrected for background noise. On average 30 000-50 000 cells per aspirate were measured.



RESULTS

Fig 1 illustrates three examples of DNA-distribution patterns of breast carcinomas obtained by both single cell and flow cytophotometric technique. It can be seen from the figure that the corresponding DNA-profiles of the first and the second tumor (Fig 1 upper and intermediate curves) are more or less the same. Thus in both the single cell and flow cytophotometric measurements the first tumor exhibits a distinct modal DNA value in the hyperdiploid region of normal mammary epithelial cells and the second tumor exhibits distinct modal DNA values in the diploid and hypotetraploid regions. In the third tumor (Fig 1 lower curves) the single cell DNA profile shows modal DNA values in the hyperdiploid and hypertetraploid regions whereas the flow DNA profile shows DNA values in the diploid hyperdiploid and hypertetraploid region indicating the presence of a large number of diploid normal cells in the aspirate.

Fig 2 illustrates the correlation between modal DNA values of 17 breast carcinomas obtained by single cell and flow cytophotometric measurements. Since flow cytophotometry does not allow discrimination between normal mammary epithelial cells and tumor cells containing DNA amounts corresponding the normal diploid amount only modal DNA values below or above the normal $2c$ value were compared. It is clear from the figure that in

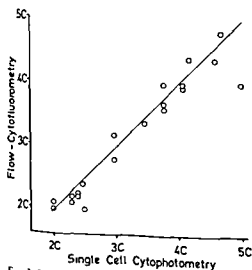


Fig 2 Relationship between modal DNA values (with the exception of those exhibiting values at $2c$ of normal cells) obtained by using single cell and flow cytophotometry. The results comprise measurement in aspirates from 17 breast carcinomas in 3 cases 2 distinct modal DNA values were present.

aspirates from breast carcinomas a good correlation exists between modal DNA values obtained by means of single cell cytophotometric measurements and those obtained by means of flow cytophotometric measurements.

DISCUSSION

Single cell DNA cytophotometry in fine needle aspirates from breast carcinomas has been demonstrated to be valuable for the prediction of the clinical course in the individual patient over and above that reflected by clinical stage and morphological criteria. Patients with tumors in which nearly all cells exhibited DNA values in the near-diploid region were found to have a favourable prognosis whereas in patients with increased and scattered DNA values the prognosis was poor (1).

In the present work we investigated whether single cell DNA analysis in breast cancer aspirates could be replaced by flow DNA analysis. Cytophotometric single cell DNA analysis is still a relatively time-consuming procedure and therefore scarcely suitable in routine clinical work. Flow cytophotometry on the other hand permits rapid DNA measurements of large cell numbers within a minimal time period.

Our results show that the DNA profiles obtained by the two methods are well correlated to each other. It is thus clear that in aspirates from breast tumors single cell DNA measurements can be replaced by flow DNA measurements. Besides rapidity the advantage of the flow technique is the high degree of resolution due to the large number of cells measured. Fine needle aspiration material was found to be especially suitable for flow measurements since the samples are made up of single cells and small cell complexes which means that well preserved cell nuclei can more easily be prepared in comparison with surgical biopsy material. Furthermore fine needle aspirates contain in general mainly tumor cells which minimizes possible alteration of flow DNA profiles due to excessive admixture of normal cells. Yet since breast carcinomas may be composed of tumor cells with DNA amounts corresponding with that found in normal cells e.g. tumor cells with DNA-contents in the normal diploid region the cellular composition of each sample has to be investigated cytologically in order to be able to interpret flow DNA measurements.

REFERENCES

- 1 Auer, G., Caspersson, T. & Wallgren A. DNA content and survival in mammary carcinoma *Acta Cytologica*, in press
- 2 Auer, G., Caspersson, T., Gustafsson, S., Humla, S., Ljung, B.-M., Nordenskjöld, B., Silfverswärd, C. & Wallgren A. Relationship between nuclear DNA distribution and estrogen receptors in human mammary carcinoma *Acta Cytologica* in press
- 3 Caspersson, T. & Lomakka, G. Recent progress in quantitative cytochemistry instrumentation and results. In introduction to quantitative cytochemistry II (Edited by G. L. Wied and G. F. Bahr) p 27-56, New York, Academic Press, 1970
- 4 Caspersson, T. Quantitative tumor cytochemistry - G. H. A. Clowes Memorial Lecture, *Cancer Research* 39 2341-2355, 1979
- 5 Franzen, S. & Zajicek, J. Aspiration biopsy in the diagnosis of palpable lesions of the breast *Acta Radiol. Stockholm* 7 241-262, 1968
- 6 Franzén, S. Thin needle aspiration biopsy in clinical oncology *Front Radiat Ther Oncol* 9 42-47, 1974
- 7 Gaub, J., Auer, G. & Zetterberg, A. Quantitative cytochemical aspects of a combined Feulgen naphthol yellow S staining procedure for the simultaneous determination of nuclear and cytoplasmic proteins and DNA in mammalian cells *Exp Cell Res* 92 323-332, 1975
- 8 Tribukait, B., Gustafson, H. & Espositi, P. Ploidy and proliferation in human bladder tumors as measured by flow cytofluorometric DNA analysis and its relations to histopathology and cytology *Cancer* 43 1742-1751, 1979

BRONCHIOLAR EPITHELIAL LESIONS INDUCED IN THE PREMATURE RABBIT NEONATE BY SHORT PERIODS OF ARTIFICIAL VENTILATION

R NILSSON GERTIE GROSSMANN and B ROBERTSON

Department of Pediatric Pathology and Department of Pediatrics St Goran's Children's Hospital
Karolinska Institutet Stockholm Sweden

Nilsson R Grossmann G & Robertson B Bronchiolar epithelial lesions induced in the premature rabbit neonate by short periods of artificial ventilation Acta path microbiol scand Sect A 88 359-367 1980

Premature newborn rabbits were ventilated with standardized tidal volume (10 ml/kg) or standardized insufflation pressure (35 cm H₂O) for 1-30 min. The lungs of the experimental fetuses were fixed by perfusion of the pulmonary artery and examined by light and electron microscopy with particular reference to the prevalence and ultrastructure of bronchiolar epithelial lesions. Necrosis and desquamation of bronchiolar epithelium were constant findings in fetuses ventilated for 5 min or more and were also present in some of the fetuses ventilated for only 1 min. Since the light microscopic and ultrastructural appearance of these bronchiolar lesions is similar to early stages of human neonatal hyaline membrane disease we conclude that artificially ventilated pre term newborn rabbit might serve as a useful model of this disease.

Key words: Artificial ventilation, bronchiolar epithelial lesions, hyaline membrane disease, IRDS, premature newborn rabbit.

R Nilsson Barnpatologiska forskningslaboratoriet St Goran's Hospital S 112 81 Stockholm Sweden

Accepted as submitted 29 v 80

Necrosis and desquamation of bronchiolar epithelium are regular findings early in the course of the neonatal idiopathic respiratory distress syndrome (IRDS) (Gandy *et al* 1970 Finlay Jones *et al* 1974) and the same type of lesion has been observed in pre term newborn experimental animals subjected to artificial ventilation (Stahlman *et al* 1964 McAdams *et al* 1973 Schwieler and Robertson 1976 Adams *et al* 1978 Cui *et al* 1978 Nilsson *et al* 1978 Nilsson 1979). It therefore seems likely that when infants suffering from severe IRDS are treated with positive pressure ventilation there is a risk that the respirator treatment will aggravate the «endogenous» epithelial lesions. This might in turn lead to the complication known as «broncho pulmonary dysplasia» - a syndrome of chronic pulmonary sequelae which is seen particularly in IRDS patients in whom high peak pressures have been used during

the period of artificial ventilation (Taghizadeh and Reynolds 1976).

Since most previous experimental studies in this field were carried out without adequate standardization of the ventilator treatment there is no precise information about the pathogenesis and early development of the bronchiolar epithelial lesions. We therefore initiated a series of experiments in which premature newborn rabbits were ventilated with a standardized tidal volume (V_T) for defined time periods and the extent of epithelial lesions was assessed by histologic morphometric techniques. In addition the fine structure of the early epithelial lesions was examined by electron microscopy.

MATERIAL AND METHODS

The experiments were carried out on 44 premature rabbit neonates delivered on day 27 of gestation (full term = 31 ± 1 day) (Table 1). The fetuses were obtained by

REFERENCES

- 1 Auer, G., Caspersson, T. & Wallgren A. DNA content and survival in mammary carcinoma *Acta Cytologica*, in press
- 2 Auer, G., Caspersson, T., Gustafsson, S., Humla S., Ljung B-M, Nordenskjöld B, Silfverswärd C & Wallgren A. Relationship between nuclear DNA distribution and estrogen receptors in human mammary carcinoma *Acta Cytologica*, in press
- 3 Caspersson, T. & Lomakka, G. Recent progress in quantitative cytochemistry instrumentation and results. In introduction to quantitative cytochemistry II (Edited by G L Wied and G F Bahr) p 27-56, New York, Academic Press, 1970
- 4 Caspersson T. Quantitative tumor cytochemistry - G H A Clowes Memorial Lecture. *Cancer Research* 39 2341-2355, 1979
- 5 Franzén S & Zajicek, J. Aspiration biopsy in diagnosis of palpable lesions of the breast. *Acta Radiol, Stockholm* 7 241-262, 1968
- 6 Franzén S. Thin needle aspiration biopsy in clinical oncology. *Front Radiat Ther Oncol* 9 42-47, 1974
- 7 Gaub, J., Auer, G. & Zetterberg A. Quantitative cytochemical aspects of a combined Feulgen naphthol yellow S staining procedure for the simultaneous determination of nuclear and cytoplasmic proteins and DNA in mammalian cells. *Exp Cell Res* 92 323-332, 1975
- 8 Tribukait B, Gustafson, H & Esposti P. Ploidy and proliferation in human bladder tumors as measured by flow cytofluorometric DNA analysis and its relations to histopathology and cytology. *Cancer* 43 1742-1751, 1979

E.2 Lung Thorax Compliance and Insufflation Pressure in Premature Rabbit Neonates Delivered on Day 27 of Gestation

Time interval (min)	Number of observations	Compliance (ml/cm H ₂ O/kg)	P vs preceding time interval	Insufflation pressure (cm H ₂ O)	P vs preceding time interval
0-1	20	0.26 ± 0.03		38 ± 3	
2-5	14	0.28 ± 0.05	NS	35 ± 5	NS
6-10	10	0.28 ± 0.05	NS	37 ± 5	NS
26-30	5	0.31 ± 0.05*	NS	33 ± 5	NS

*vs time interval 0-1 min < 0.02

recordings were obtained during intermittent positive pressure ventilation with standardized tidal volume (10 ml/Values are given as $\bar{X} \pm SD$ for various time intervals after the onset of ventilation)

RESULTS

Lung Thorax Compliance

In animals ventilated for more than 1 min, the pressure needed to maintain the standardized V_T increased slightly during the period of observation. In other words, there was a gradual increase in the compliance of the lung thorax system. However, a statistically significant difference was found only between the intervals 0-1 min and 26-30 min (Table 2).

Lung thorax compliance for animals used for electron microscopy was 0.25 ± 0.07 ml/cm O_2 kg ($\bar{X} \pm SD$) after 5 min of artificial ventilation; this value is very close to the compliance value for the corresponding interval in Table 2.

Alveolar Morphometric Findings

In all fetuses there was poor aeration of the alveolar compartment, as verified by low figures for V_A and there was no difference between fetuses

ventilated for various periods of time (Table 3). Epithelial lesions were absent in all non-ventilated fetuses. However, necrosis and desquamation of the bronchiolar epithelium was a constant finding in all fetuses which had been ventilated for 5 min or more. In the group ventilated for only 1 min, pyknotic bronchiolar epithelial cells were found in 2 of 7 fetuses (Table 3, Fig. 1A).

The nature of the individual lesion changed, however, throughout the period of observation. Desquamated cells accumulated in the peripheral airways in later intervals and hyaline membranes made up of cell debris from necrotic epithelium gradually became more prominent (Fig. 1A-C). Figures for I_b representing various periods of artificial ventilation are shown in Table 3.

TABLE 3 Morphometric Data on Alveolar Expansion and Bronchiolar Epithelial Lesions in Premature Rabbit Neonates Delivered on Day 27 of Gestation Related to the Duration of Artificial Ventilation

Duration of ventilation (min)	n	I_a	Bronchiolar epithelial lesions			I_b	P vs preceding time interval
			Number of fetuses				
			with lesions	without lesions			
0	11	0.71 ± 0.25	0	11	0		
1	7	0.79 ± 0.29	2	5	0.16 ± 0.03		
5	6	0.61 ± 0.05	6	0	0.003 ± 0.005	NS	
10	5	0.82 ± 0.26	5	0	0.29 ± 0.11	= 0.002	
30	5	0.76 ± 0.35	5	0	0.27 ± 0.09	= 0.05 NS	

Values are given as $\bar{X} \pm SD$

Table 1 *Survey of the Material*

Period of artificial ventilation (min)	Parameters evaluated			
	Compliance + $I_a + I_b$		Ultrastructure of bronchiolar epithelium	
	n	BW (g $\bar{X} \pm SD$)	n	BW (g $\bar{X} \pm SD$)
0	11	30 \pm 7	5	27 \pm 7
1	7	31 \pm 3		
5	6	30 \pm 2	5	23 \pm 4
10	5	25 \pm 5		
30	5	27 \pm 6		

BW = body weight

hysterotomy under intravenous anesthesia (Ketalar® Parke Davis MI USA) or following sacrifice of the doe by rapid injection of 2 ml sodium pentobarbital (Mebumal vet® 60 mg/ml ACO Sweden) and 5 ml potassium chloride (150 mg/ml). Non ventilated fetuses were killed *in utero* with an intraperitoneal injection of 0.5 ml Mebumal vet®.

Artificial Ventilation

Immediately after delivery the fetuses received intraperitoneal injections of 0.1 ml sodium pentobarbital (6 mg/ml) and 0.1 ml pancuronium bromide (Pavulon® 0.2 mg/ml Organon Holland) for anesthesia and muscle relaxation. They were tracheotomized, kept at 37 °C in a volume constant body plethysmograph and connected to a Harvard Rodent Ventilator 680 set at a frequency of 60/min. In the incubator the fetuses were fixed in dorsal position by ECG electrodes through their paws. Fetuses were included in the study only if the ECG recording revealed cardiac activity throughout the period of ventilation.

Insufflation pressure and pressure in the plethysmograph were registered simultaneously by pressure transducers (EMT 33 or 34 Siemens Elema Solna Sweden or Stathamatham laboratories USA) and recorded on a Mingograph 24B or 81 (Siemens Elema) or on a Polygraph 7B (Grass Incorp USA). Fetuses used for determination of lung thorax compliance and morphometry were ventilated with air with standardized V_T (10 ml/kg) for periods varying between 1 and 30 min. The quasistatic compliance of the lung thorax system was calculated from registrations of V_T and insufflation pressure at end inspiration.

Histologic and Morphometric Techniques

After artificial ventilation the fetuses were killed with intraperitoneal sodium pentobarbital (0.5 ml 60 mg/ml). The lungs were fixed by perfusion of the pulmonary artery with 1 per cent glutaraldehyde and 3.5 per cent formaldehyde in phosphate buffer at a pressure of 65 cm H₂O. During the perfusion procedure (15 min) the air expansion of the lungs was maintained by an endotra-

cheal pressure of 15 cm H₂O. The whole lungs were then embedded in paraffin and sections from the basal portions were stained with hematoxylin and eosin and examined microscopically. By means of the point counting technique (Chalkley 1943) we determined the relative volumes of the alveolar spaces (V_A) and solid parenchyma (V_P) and the alveolar expansion index (I_A) was calculated by the formula (Enhörning *et al* 1973)

$$I_A = \frac{V_A}{V_P}$$

The same sections were then re-examined and the number of high power fields (HPFs) showing evidence of bronchiolar epithelial necrosis were counted and related to the total number of HPFs examined. The index of bronchiolar epithelial lesions (I_b) was calculated according to the formula (Nilsson *et al* 1978)

$$I_b = \frac{\text{No of HPFs with lesion}}{\text{No of HPFs examined}} \times I_A$$

In this calculation I_A is used as a correction factor to compensate for variations in the volume of the alveolar compartment that might influence the spacing of the bronchioles.

To avoid bias the histologic morphometric evaluation of the sections was made without knowledge of the experimental conditions to which the individual fetuses were subjected.

Electron Microscopy

This part of the study was carried out on a separate series of 5 fetuses ventilated for 5 min with a standardized insufflation pressure of 35 cm H₂O and a V_T of 9.0 \pm 2.8 ml/kg ($\bar{X} \pm SD$). Non ventilated fetuses were used as controls (Table 1).

For transmission electron microscopy (TEM) specimens representing marginal parts of the lungs were embedded in Vestopal following dehydration in acetone. Semithin and ultrathin sections were cut with an LKB Ultratome III (LKB produkter AB Bromma Sweden). Areas containing terminal or respiratory bronchioles were first identified by light microscopic examination of 1 μ thick sections stained with toluidin blue. Ultrathin sections from these areas were then stained with uranyl acetate and lead citrate and examined with a Jeol 100S electron microscope.

Specimens for scanning electron microscopy (SEM) were also cut from the marginal portions of the lung. Areas where the cut surface exposed the mucosa of longitudinally oriented terminal and preterminal conducting airways were identified with a conventional dissection microscope. The specimens were dehydrated with ethanol and Freon 113 followed by critical point drying. They were coated with gold (100 Å) and examined with a Cambridge S4 scanning electron microscope with particular reference to the surface structure of the bronchiolar epithelium.

As in the light microscopic study the evaluation of the specimens was made without knowledge of the experimental conditions.

Statistical Evaluation

The Wilcoxon two sample test (two tailed) was used in our statistical calculations.

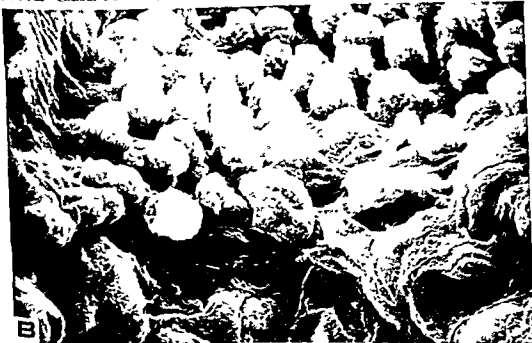


Fig 2 Ultrastructure of bronchiolar epithelium in non ventilated control fetuses showing immature glycogen rich Clara cells bulging into the lumen. There is no evidence of epithelial necrosis

A TEM $\times 4\,800$

B SEM $\times 4\,600$

The exact pathogenesis of the bronchiolar epithelial lesions cannot be deduced from the present data but our morphological observations are concordant with the concept that these lesions reflect shear stress in the airway mucosa secondary to overdistension of preterminal conducting airways in the

surfactant-deficient lung (Hawker *et al* 1967; Robertson 1976; Nilsson *et al* 1980 b). It is of particular interest that similar epithelial lesions develop in premature infants during the early course of IRDS. Gandy *et al* (1970) noted such lesions in infants dying as early as 15 min after birth and

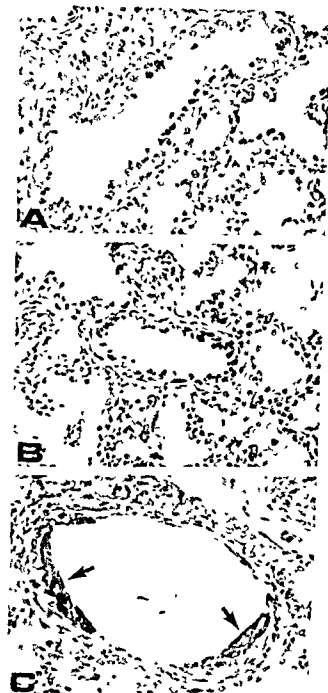


Fig 1 Light microscopic appearance of bronchiolar epithelial lesions induced by positive pressure ventilation. Hematoxylin and eosin $\times 260$

- A Early lesions with pyknosis of individual epithelial cells. This fetus was ventilated for 1 min
- B More advanced lesions with pyknosis and desquamation of epithelial cells. This fetus was ventilated for 5 min
- C Prominent epithelial necrosis with hyaline membrane formation (arrows) in a small bronchiole after 30 min of artificial ventilation

Electron Microscopic Findings (TEM and SEM)

In fetuses killed *in utero* the bronchioles were lined by a regular epithelium, without evidence of

necrosis or desquamation. The epithelium was dominated by non-ciliated cells containing amounts of cytoplasmic glycogen. We interpret these cells as immature Clara cells, as their submicrovilli bulged into the bronchiolar lumen in a cobblestone-like pattern. This pattern was a prominent finding in both SEM and TEM specimens. Ciliated cells were comparatively scarce in the bronchial mucosa (Fig 2).

Epithelial lesions were absent in all unventilated fetuses but present in all those subjected to artificial ventilation.

In general, the ultrastructural appearance of the lesions corresponded well with the light microscopic findings described above. As shown in Fig 3A, 3A, the lesions were characterized by pyknosis of individual cells, or small groups of cells with or without desquamation. Some of the desquamated cells were flattened, elongated, and situated on the surface of apparently intact cuboidal epithelial cells (Fig 3B). These compressed necrotic cells were difficult to identify with certainty in SEM specimens, as flattening of the epithelium is a normal feature in aerated bronchioles (Fig 4). Other necrotic cells, scattered like grains over the mucosal surface, were easily recognized by SEM (Fig 5).

In addition to the bronchiolar lesions, focal necrosis and desquamation of the alveolar epithelium was occasionally observed in some fetuses (Fig 6).

DISCUSSION

Our results show that bronchiolar epithelial lesions develop in premature newborn rabbits after only a few minutes of positive pressure ventilation. These findings are in agreement with earlier observations on premature newborn rhesus monkeys (McAdam *et al* 1973) or lambs (Stahlman *et al* 1964). In those series, however, the methods for artificial ventilation were less standardized than in the present study.

Judged by our morphometric findings, the number of affected bronchioles does not increase after the first 10 minutes, although the character of the individual lesion does change. Moreover, values for I_b representing the 30 min interval in the present study are in the same range as those obtained in previous experiments where the fetuses were ventilated under similar conditions for one hour (Nilsson *et al* 1978). A standardized ventilation period of 10 min has therefore been used in other experimental series in which we analyse the extent to which the development of epithelial lesions depends on variations in V_T and positive end-expiratory pressure (Nilsson *et al* 1980 a, b).

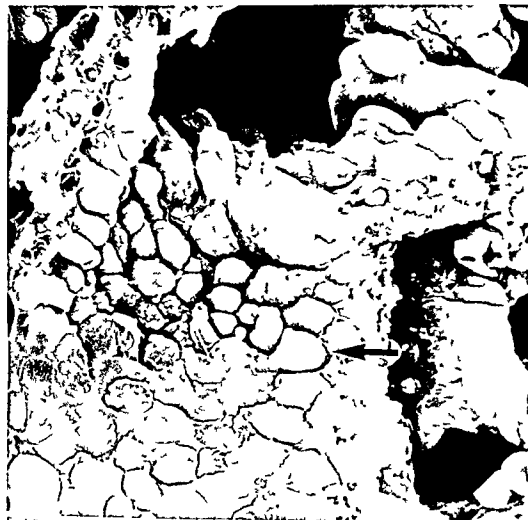


Fig 4 Flattened epithelial cells in the proximal portion of a bronchiole aerated to the level indicated by arrow. The fetus was ventilated for 5 min, but in this field there is no convincing evidence of epithelial necrosis. SEM $\times 2400$.

morphological equivalent of clinical IRDS) especially as this model allows recording of lung mechanics during the course of the experiments.

Financial support was provided by the Swedish Medical Research Council project No. 3351, the Swedish National Association against Heart and Chest Diseases and Kistner Pedagogical Research Fund. We thank Mr. Cor Fox for assistance with English.

REFERENCES

- 1 Adams F H, Towers B, Osher A B, Ikegami M, Fujiwara T & Nozaki M. Effects of tracheal intubation of natural surfactant in premature lambs. *Clinical and autopsy findings*. *Pediatr Res* 12: 841-848, 1978.
- 2 Chalkley H W. Method for the quantitative morphological analysis of tissues. *J Natl Cancer Inst* 4: 47-49, 1943.
- 3 Cruz E, Enhorn G, Robertson B, Sherwood W G & Hill D E. Hyaline membrane disease: Effect of surfactant prophylaxis on lung morphology in premature primates. *Am J Pathol* 92: 581-590, 1978.
- 4 Enhorn G, Grossmann G & Robinson B. Tracheal deposition of surfactant before the first breath. *Am Rev Respir Dis* 107: 921-927, 1973.
- 5 Finlay Jones J M, Papadimitrou J M & Barber R A. Pulmonary hyaline membrane. Light and electron microscopic study of the early stage. *J Pathol* 112: 117-124, 1974.



min Two pyknotic epithelial cells are
type of lesion with multiple necrotic
9)

Finlay-Jones *et al* (1974) reported that necrosis of bronchiolar epithelium can occur »within a few minutes« after delivery even if the infant has only been gasping and no artificial ventilation has been applied

of peripheral airways and it seems likely that bronchiolar and alveolar hyaline membranes develop in

areas where the epithelium has become at least partly desquamated and where the basement membrane is denuded. This hypothesis is supported by the observation that cell debris is a major component of hyaline membranes (Lauweryns 1970). In view of this we share the opinion of McAdams *et al* (1973) that the artificially ventilated pre term fetus might serve as a useful experimental model of neonatal hyaline membrane disease (defined as the



Fig 6 Ultrastructure of alveolar epithelium in premature rabbit neonate ventilated for 5 min. This field shows necrosis and desintegration of a membranous pneumocyte. TEM $\times 9100$

surfactant and the pathogenesis of neonatal bronchiolar lesions induced by artificial ventilation. *Pediat. Res* 12: 249-255, 1978

- 11 Nilsson R Lung compliance and lung morphology following artificial ventilation in the premature and fullterm rabbit neonate. *Scand J resp Dis* 60: 206-214, 1979
- 12 Nilsson R Grossmann G & Robertson B Artificial ventilation of premature newborn rabbits: effects of positive end-expiratory pressure on lung compliance and lung morphology. *Acta Paediatr Scand* 1980 a (in press)
- 13 Nilsson R Grossmann G & Robertson B Pathogenesis of neonatal lung lesions induced by artificial ventilation: evidence against the role of barotrauma. *Respiration* 1980 b (in press)
- 14 Robertson B Current and counter-current theories on lung surfactant. *Scand J resp Dis* 57: 199-207, 1976
- 15 Schwieler G & Robertson B Liquid ventilation in immature newborn rabbits. *Biol Neonate* 29: 343-353, 1976
- 16 Stahlman M Lequire V S Young W C Merrill R E Birmingham R T Payne G A & Gray J Pathophysiology of respiratory distress in newborn lambs. *Am J Dis Child* 108: 375-393, 1964
- 17 Taghizadeh A & Reynolds E O Pathogenesis of bronchopulmonary dysplasia following hyaline membrane disease. *Am J Pathol* 82: 241-264, 1976

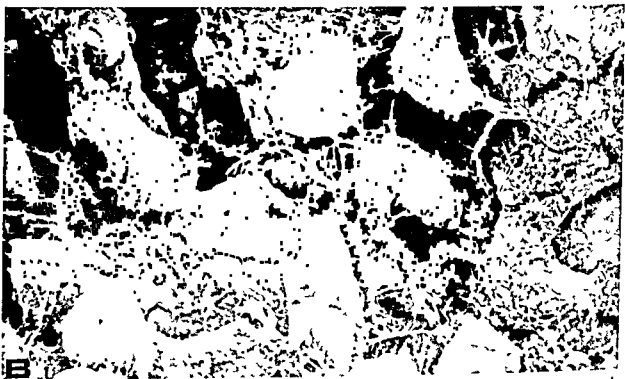


Fig 5 Desquamating bronchiolar epithelial cells in fetus ventilated for 5 min. The necrotic cells have been squeezed out of the epithelial lining and are scattered on the mucosal surface.

A TEM $\times 6\,000$

B SEM $\times 5\,600$

- 6 Gandy G, Jacobson W & Gaudner D. Hyaline membrane disease. I. Cellular changes. *Arch Dis Childh* 45: 289-310 1970.
- 7 Hawker J M, Reynolds E O & Taghizadeh H. Pulmonary surface tension and pathological changes in infants dying after respirator treatment for severe hyaline membrane disease. *Lancet* 2: 75-77 1967.
- 8 Lauweryns J M. Hyaline membrane disease in newborn infants. Macroscopic, radiographic and light and electron microscopic studies. *Human Pathol* 1: 175-204 1970.
- 9 McAdams A J, Coen R, Kleinman L I, Tsang R & Sutherland J. The experimental production of hyaline membranes in premature rhesus monkeys. *Am J Pathol* 70: 277-284 1973.
- 10 Nilsson R, Grossmann G & Robertson B. Lung

THE EFFECT OF FIXATION AND TRYPSINIZATION ON THE IMMUNOHISTOCHEMICAL DEMONSTRATION OF INTRACELLULAR IMMUNOGLOBULIN IN PARAFFIN EMBEDDED MATERIAL

MARIANNE JACOBSEN PER P. CLAUSEN and SUSANNE SMIDT

Department of Pathology Herlev Hospital University of Copenhagen 2730 Herlev Denmark

Jacobsen M Clausen P P & Smidt S The effect of fixation and trypsinization on the immunohistochemical demonstration of intracellular immunoglobulin in paraffin embedded material Acta path microbiol scand Sect A 88 369-376 1980

As found for every 24 hours the fixation time was prolonged. By comparing sections from tissue fixed in buffered formalin and selected fixatives (Lillie's AAF, Bouin's fluid, Clarke's fluid and 96% ethanol 1% acetic acid (E-A)) processed at 4 °C and at 25 °C an increased number of stained immunoglobulin

immunoglobulin containing cells was investigated. Trypsinization of sections from formalin fixed material increased the number of stainable cells substantially. No essential effect was seen on tissue fixed in Lillie's AAF and Bouin's fluid. In contrast trypsin treatment of sections from tissue fixed in Clarke's fluid and E-A completely destroyed the tissue. No differences were observed between different immunoglobulin classes examined as regards the effect of fixation time, fixatives and trypsinization.

Key words: Immunoglobulin, immunoperoxidase, fixation, trypsinization, lymphoid tissue.

Marianne Jacobsen, Department of Pathology, Herlev Hospital, University of Copenhagen, 2730 Herlev, Denmark.

Received 31.1.80 Accepted 4.vi.80

The demonstration of intracellular immunoglobulin on formalin fixed paraffin embedded tissue by the immunoperoxidase staining method was first described by Taylor & Burns in 1974 (22). The method has later on been

from lymphatic tissue with neoplastic or reactive conditions (1, 8, 9, 10, 21).

The results described in these investigations have however not always been concordant and reprodu-

cible (10, 24). It is only possible to compare results based on material which has been prepared in different ways if information is available regarding the influence of the tissue preparation on the

THE EFFECT OF FIXATION AND TRYPSINIZATION ON THE IMMUNOHISTOCHEMICAL DEMONSTRATION OF INTRACELLULAR IMMUNOGLOBULIN IN PARAFFIN EMBEDDED MATERIAL

MARIANNE JACOBSEN, PER P. CLAUSEN and SUSANNE SMIDT

Department of Pathology, Herlev Hospital, University of Copenhagen, 2730 Herlev, Denmark

Jacobsen M, Clausen P P & Smidt S. The effect of fixation and trypsinization on the immunohistochemical demonstration of intracellular immunoglobulin in paraffin embedded material. *Acta path. microbiol. scand. Sect. A* 88: 369-376, 1980.

Using an indirect labelled immunoperoxidase technique the influence of fixation time on the antigenicity of intracellular immunoglobulin in lymphoid tissue fixed in buffered formalin has been investigated. Within a fixation period of 96 hours a decrease of 15% of stainable immunoglobulin containing cells was found. For every 24 hours the fixation time was prolonged. By comparing sections from tissue fixed in buffered formalin and selected fixatives (Lillie's AAF, Bouin's fluid, Clarke's fluid and 96% ethanol, 1% acetic acid (E-A)) processed at 4°C and at 25°C, an increased number of stained immunoglobulin containing cells was found in tissue fixed in Lillie's AAF, Bouin's fluid, Clarke's fluid and E-A processed at 4°C. No difference was found between tissue fixed in buffered formalin and E-A processed at 25°C. In addition the effect of pretreatment of the sections with trypsin on the number of stainable immunoglobulin containing cells was investigated. Trypsinization of sections from formalin fixed material increased the number of stainable cells substantially. No essential effect was seen on tissue fixed in Lillie's AAF and Bouin's fluid. In contrast trypsin treatment of sections from tissue fixed in Clarke's fluid and E-A completely destroyed the tissue. No differences were observed between different immunoglobulin classes examined as regards the effect of fixation time, fixatives and trypsinization.

Key words: Immunoglobulin, immunoperoxidase, fixation, trypsinization, lymphoid tissue.

Marianne Jacobsen, Department of Pathology, Herlev Hospital, University of Copenhagen, 2730 Herlev, Denmark.

Received 31.1.80 Accepted 4.vi.80

The demonstration of intracellular immunoglobulin on formalin fixed paraffin embedded tissue by the immunoperoxidase staining method was first described by *Taylor & Burns* in 1974 (22). The method has later on been employed on materials from multiple myeloma, macroglobulinaemia and reactive plasmacytosis (5, 17, 23, 24), as well as on lymphatic tissue with neoplastic or reactive conditions (1, 8, 9, 10, 21).

The results described in these investigations have, however, not always been concordant and reprodu-

cible (10, 24). It is only possible to compare results based on material which has been prepared in different ways if information is available regarding the influence of the tissue preparation on the antigens to be demonstrated.

The aim of the present investigation is to examine the influence of fixation time and selected fixatives on the demonstration of intracellular immunoglobulin.

Materials and Methods
The tissue material used in this investigation has been evaluated

MATERIAL AND METHODS

Tissues

Lymph nodes removed during cholecystectomy, colectomy and hysterectomy were used

Immediately following the removal the nodes were divided in two parts. One part (the reference specimen) was always fixed for 4 hours in 10% phosphate buffered formalin at room temperature. The other part (the test specimen) was treated according to one of the following procedures:

A Fixation in 10% buffered formalin at room temperature for 4 8 12 18 24 48 72 and 96 hours.

B Fixation for 1 4 8 24 hours at room temperature in the following fixatives Lillies AAF (10 ml 30% neutral formaldehyde solution 5 ml glacial acetic acid 85 ml 99% ethanol) Bouin's fluid (75 ml 12% picric acid aqueous solution 25 ml neutral 30% formaldehyde solution 5 ml glacial acetic acid) and Clarke's fluid (80 ml 99% ethanol 20 ml glacial acetic acid)

C Fixation for 24 hours at 4 °C in 96 % ethanol 1 % glacial acetic acid (E-A)

Following the fixation tissues treated according to A and B were dehydrated in ethanol and xylene at room temperature and embedded in Paraplast® at 58–60 °C. Tissues fixed according to C were either processed as A and B or dehydrated at 4 °C until the last change of xylene after which the temperature was increased to 25 °C and the material was then embedded as described above (19). In cases where the tissue could not be embedded following the dehydration tissue was preserved in 70% ethanol for a maximum of 18 hours until further dehydration.

5 μm serial sections were cut

Trypsinization

In order to examine the effect of pretreatment of the sections with trypsin on the number of stained immunoglobulin containing cells dewaxed sections from lymph nodes fixed for 24 hours in the above mentioned fixatives were incubated for 5-20 min with 0.1% trypsin (Sigma type III) 0.1% calcium chloride in distilled water adjusted to pH 7.8 with 0.1 M NaOH (14).

Arise

Following antisera and lots were used anti lambda (18B) anti kappa (18 C) anti α (18 B) anti γ (28 C) and anti μ (88 C 18 A) (DAKO Denmark) and anti δ (1102 C 1102 L 1104 B) and anti ϵ (1203 E 1203 D) (Behringwerke Hoechst Denmark)

The specificity of the antisera was verified by performance testing on formalin fixed paraffin embedded material from multiple myeloma of known monoclonal protein type

Working dilutions were found by titration. Anti lambda and anti kappa were used in dilutions 1/100-1/102400 anti α γ and μ in dilutions 1/40-1/20480 anti δ and ϵ in dilutions 1/5-1/2560.

Peroxidase
lin (lot 28 A 34
dilution 1/20

For control stainings the immunoglobulin fraction of serum from unimmunized rabbits (lot 38 B) (DAKO) was used in dilution 1/80 (corresponding to the maximum protein concentration of the used antisera).

All antisera were diluted in phosphate buffered saline (PBS) pH 7.2

Staining Procedure

Each set of lymph nodes was stained for lambda kappa α γ μ δ and ϵ chains

Indirect peroxidase labelled antibody technique (6) was used

As control stainings the specific antisera were replaced by 1) immunoglobulin fraction of serum of unimmunized rabbits 2) PBS. In addition the staining of different cell populations by using different antisera served as an inherent control.

In each staining series serial sections from both parts of each lymph node were stained for all the immunoglobulins mentioned.

Counting Method

The number of stained cells was determined by counting all cells with positive intracytoplasmic staining reaction in every second counting unit defined by the

per unit was calculated. In order to evaluate the reproducibility of the counting method used the same section was counted five times and the variation coefficient was calculated to 2% the variation from one serial section to another was less than 4% and the variation from one part of the lymph node to the other part identically processed was less than 4%.

Evaluation

Evaluation of the influence of the fixation time on the number of stained cells was made by expressing the results as a percentage between the number of cells in the test section and in the reference section

The statistical evaluation of corresponding values of fixation time and number of stained cells was made by means of correlation and regression tests. When comparing regression equations the F test of variance was used. The limit for type I error was set at 0.05.

Evaluation of the effect of the different fixatives on the number of stained cells compared to the effect of buffered formalin was performed by counting the number of cells in the sections related to increasing dilution of the primary antisera. The number of cells was semiquantitatively evaluated according to the following scoring system 0 + ++ +++ and ++++ (+ indicating up to 20 cells per unit ++ up to 40 cells per unit +++ up to 60 cells per unit and ++++ more than 60 cells per unit).

A comparative evaluation of the different fixatives at constant fixation time and the effect of pretreatment with trypsin was made by comparing the dilutions which gave the same number of stained cells in the reference section and test section.

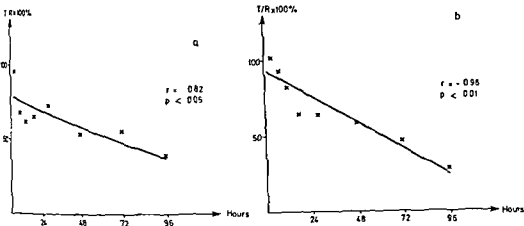


Fig 1 a-b The effect of fixation time on the number of stained immunoglobulin containing cells in formalin fixed paraffin embedded tissue (T = number of cells in test section R = number of cells in reference section) a) light chains b) heavy chains

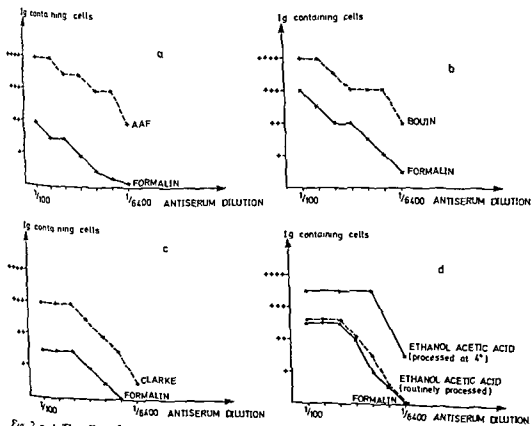


Fig 2 a-d The effect of selected fixatives on the number of stained immunoglobulin (kappa) containing cells in relation to antiserum dilution. Comparison between four hours formalin fixation and four hours fixation in: a) Lillie's AAF b) Bouin's fluid c) Clarke's fluid and d) 24 hours ethanol acetic acid processed either at 4 °C or 25 °C

MATERIAL AND METHODS

Tissues

Lymph nodes removed during cholecystectomy, colectomy and hysterectomy were used

Immediately following the removal, the nodes were divided in two parts. One part (the reference specimen) was always fixed for 4 hours in 10% phosphate buffered formalin at room temperature. The other part (the test specimen) was treated according to one of the following procedures

A Fixation in 10% buffered formalin at room temperature for 4, 8, 12, 18, 24, 48, 72 and 96 hours

B Fixation for 1, 4, 8, 24 hours at room temperature in the following fixatives: Lillie's AAF (10 ml 30% neutral formaldehyde solution, 5 ml glacial acetic acid 85 ml 99% ethanol), Bouin's fluid (75 ml 1.2% picric acid aqueous solution, 25 ml neutral 30% formaldehyde solution, 5 ml glacial acetic acid) and Clarke's fluid (80 ml 99% ethanol, 20 ml glacial acetic acid)

C Fixation for 24 hours at 4°C in 96% ethanol, 1% glacial acetic acid (E-A)

Following the fixation tissues treated according to A and B were dehydrated in ethanol and xylene at room temperature and embedded in Paraplast® at 58-60°C. Tissues fixed according to C, were either processed as A and B or dehydrated at 4°C until the last change of xylene, after which the temperature was increased to 25°C and the material was then embedded as described above (19). In cases where the tissue could not be embedded following the dehydration tissue was preserved in 70% ethanol for a maximum of 18 hours until further dehydration

5 µm serial sections were cut

Trypsinization

In order to examine the effect of pretreatment of the sections with trypsin on the number of stained immunoglobulin containing cells, dewaxed sections from lymph nodes fixed for 24 hours in the above mentioned fixatives were incubated for 5-20 min with 0.1% trypsin (Sigma, type III) 0.1% calcium chloride in distilled water, adjusted to pH 7.8 with 0.1 M NaOH (14)

Antisera

Following antisera and lots were used: anti lambda (18B), anti-kappa (18 C), anti α (18 B), anti γ (28 C) and anti-μ (88 C, 18 A) (DAKO Denmark) and anti δ (1102 C, 1102 L, 1104 B) and anti-ε (1203 E, 1203 D) (Behringwerke, Hoechst, Denmark)

The specificity of the antisera was verified by performance testing on formalin fixed paraffin embedded material from multiple myeloma of known monoclonal protein type

Working dilutions were found by titration. Anti lambda and anti-kappa were used in dilutions 1/100-1/102400, anti-α, γ and μ in dilutions 1/40-1/20480 and δ and ε in dilutions 1/5-1/2560

For control stainings the immunoglobulin fraction of serum from unimmunized rabbits (lot 38 B) (DAKO) was used in dilution 1/80 (corresponding to maximum protein concentration of the used antisera)

All antisera were diluted in phosphate buffered saline (PBS) pH 7.2

Staining Procedure

Each set of lymph nodes was stained for lambda kappa-, α-, γ-, μ-, δ and ε-chains

Indirect peroxidase labelled antibody technique was used

As control stainings the specific antisera were replaced by 1) immunoglobulin fraction of serum unimmunized rabbits, 2) PBS. In addition the staining of different cell populations by using different antisera served as an inherent control

In each staining series, serial sections from both parts of each lymph node were stained for all the immunoglobulins mentioned

Counting Method

The number of stained cells was determined by counting all cells with positive intracytoplasmic staining reaction in every second counting unit, defined by the outer frame of an ocular grid (Leitz 10 × 10 mm (16 squares) with 25 × objective and 10 × ocular. Not less than 25 units were counted (3) and the number of cells per unit was calculated. In order to evaluate the reproducibility of the counting method used the same section was counted five times and the variation coefficient was calculated to 2%, the variation from one serial section to another was less than 4% and the variation from one part of the lymph node to the other part identically processed was less than 4%

Evaluation

Evaluation of the influence of the fixation time on the number of stained cells was made by expressing the results as a percentage between the number of cells in the test section and in the reference section

The statistical evaluation of corresponding values of fixation time and number of stained cells was made by means of correlation and regression tests. When comparing regression equations the F test of variance was used. The limit for type I error was set at 0.05

Evaluation of the effect of the different fixatives on the number of stained cells compared to the effect of buffered formalin was performed by counting the number of cells in the sections related to increasing dilution of the primary antisera. The number of cells was semiquantitatively evaluated according to the following scoring system: 0 +, ++, +++ and ++++ (+ indicating up to 20 cells per unit, ++ up to 40 cells per unit, +++ up to 60 cells per unit and ++++ more than 60 cells per unit)

the same number of stained cells in the reference section and test section

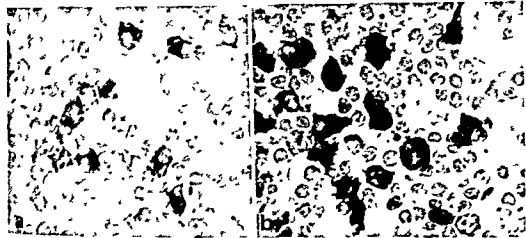


Fig 4 a-b a) Immunoperoxidase staining for IgG of a lymph node fixed in buffered formalin for 24 hours (Counterstained with hematoxylin $\times 800$) b) Adjoining section stained as a with trypsinization of the section before staining (Counterstained with hematoxylin $\times 800$)

The Effect of Trypsinization

Trypsin treatment of sections from tissue fixed in Clarke's fluid and E-A completely destroyed tissue morphology. Trypsinization of sections fixed in Bouin's fluid and Lillie's AAF had no essential influence on tissue morphology or immunoglobulin staining. In contrast trypsinization of sections from formalin fixed material showed a pronounced effect on the immunoglobulin staining. Tissue morphology did not change but the number of stained cells was considerably increased and the staining reaction in trypsin treated sections was more uniform and finely granular (Fig 4 b). Different immunoglobulin classes showed the same reaction pattern.

Following trypsin treatment of formalin fixed tissue immunoglobulin on the surface of the small lymphocytes was to some extent demonstrable and the staining of the connective tissue fibers was slightly more pronounced.

DISCUSSION

Until now only few papers have systematically dealt with the influence of fixation time on the preservation of antigenicity. Kraehenbuhl (15) using glutaraldehyde and formaldehyde described a loss of antigenicity of various antigens including IgA of up to 40% during the first 24 hours of the fixation period. Using formalin as fixative we have likewise for all classes of immunoglobulins demonstrated a high degree of correlation between decrease of stained cells and fixation time.

Thus comparing results obtained by immunohistochemical staining for immunoglobulin in formalin fixed material knowledge of the fixation time used is essential.

The effect of different fixatives on the antigenicity of intracellular immunoglobulin has until recently only been investigated to a limited extent. Table 1 presents a survey of results published within the latest five years including our own results.

Our results are in general in accordance with the previously published results. In addition to Bouin's fluid we found that Lillie's AAF gave good preservation of antigenicity of immunoglobulins, sharp demarcation of the staining reaction as well as satisfactory preservation of tissue morphology. Clarke's fluid likewise gave good antigen preservation but tissue morphology was less satisfactory. Using fixation in E-A at 4 °C and cold processing of the tissue in accordance with Sainte Marie (19) resulted in moderate to good antigen preservation while routine processing gave a less satisfactory result. In both cases however tissue morphology was bad and background staining intense.

The employment of digestion with proteolytic enzymes on sections from formalin fixed and paraffin embedded material was introduced by Huang (13) to increase the antigenicity of

immunofluorescence as by immunoperoxidase technique.

The treatment has been described to result in unmasking of immunoreactive sites with increased number of stained cells, demonstration of surface

RESULTS

The influence of the fixation time on the number of stained cells in formalin fixed material is shown in Fig 1 a and b. The number of stained cells in tissue fixed in formalin for varying time period (T) is related to the number of stained cells in tissue fixed in formalin for 4 hours (R). The number of cells stained for δ and ϵ chains was too small to be taken into account. As the regression equations for the two light chains (κ and λ) and the three heavy chains (α , γ , μ) respectively showed no statistical differences, the results for the light chains and for the heavy chains were pooled.

It is seen that within the fixation time examined there was a decrease of stained cells of 10–20% for every 24 hours the fixation time was prolonged.

The influence of selected fixatives compared to the influence of formalin on the number of stained cells is shown in Fig 2 a–d. All the lymph nodes have been fixed for 4 hours (E–A for 24 hours at 4 °C) and the number of stained cells is correlated to increasing dilution of the primary antisera.

It is seen that tissue fixed in Lillie's AAF, Bouin's fluid, Clarke's fluid and E–A followed by cold processing at all dilutions contained more stained cells than tissue fixed in buffered formalin. In contrast, no substantial difference in the number of stained cells was found in tissue fixed in E–A followed by routine processing compared to tissue fixed in buffered formalin. The different immuno-

globulin classes showed the same pattern of reaction.

In addition to quantitative differences, differences in regard to tissue morphology and quality of the immunoperoxidase staining were found (summarized in Table 1). The morphology of the tissue was good when using Lillie's AAF, Bouin's fluid and buffered formalin, while fixation in E–A and Clarke's fluid led to a rather pronounced shrinkage of the cells, increasing with prolonged fixation time.

The intracytoplasmic staining was homogeneous and granular with well defined cell borders when using Lillie's AAF, Bouin's fluid, Clarke's fluid and E–A (Fig 3). In buffered formalin, a rough granular staining with heterogeneous distribution and ill defined cell borders was found, and this was more pronounced when longer fixation time was used (Fig 4a).

Staining of the extracellular immunoglobulin and surface immunoglobulin on small lymphocytes was to some extent demonstrable when the tissue was fixed in Lillie's AAF, Clarke's fluid or E–A but not in tissue fixed in Bouin's fluid and buffered formalin.

Staining of the connective tissue fibers and background for especially IgG was most pronounced in formalin, Clarke's fluid and E–A fixed tissue, whereas Bouin's fluid and Lillie's AAF fixed tissue showed a weaker connective tissue and background staining.

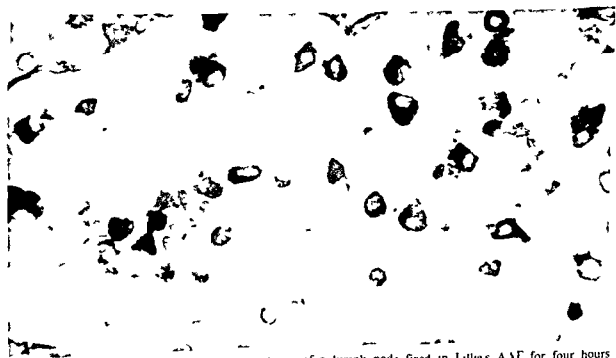


Fig 3 Immunoperoxidase staining for kappa chains of a lymph node fixed in Lillie's AAF for four hours (Counterstained with hematoxylin $\times 800$)

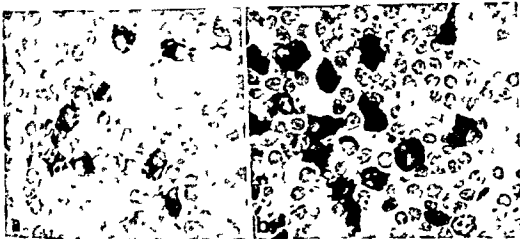


Fig 4 a-b a) Immunoperoxidase staining for IgG of a lymph node fixed in buffered formalin for 24 hours (Counterstained with hematoxylin $\times 800$) b) Adjoining section stained as a, with trypsinization of the section before staining (Counterstained with hematoxylin $\times 800$)

The Effect of Trypsin on

Trypsin treatment of sections from tissue fixed in Clark's fluid and E-A completely destroyed tissue morphology. Trypsinization of sections fixed in Bouin's fluid and Lillie's AAF had no essential influence on tissue morphology or immunoglobulin staining. In contrast trypsinization of sections from formalin fixed material showed a pronounced effect on the immunoglobulin staining. Tissue morphology did not change but the number of stained cells was considerably increased and the staining reaction in trypsin treated sections was more uniform and finely granular (Fig 4 b). Different immunoglobulin classes showed the same reaction pattern.

Following trypsin treatment of formalin fixed tissue immunoglobulin on the surface of the small lymphocytes was to some extent demonstrable and the staining of the connective tissue fibers was slightly more pronounced.

DISCUSSION

Until now only few papers have systematically dealt with the influence of fixation time on the preservation of antigenicity. Kraehenbuhl (15) using glutaraldehyde and formaldehyde described a loss of antigenicity of various antigens including IgA of up to 40% during the first 24 hours of the fixation period. Using formalin as fixative we have likewise for all classes of immunoglobulins demonstrated a high degree of correlation between decrease of stained cells and fixation time.

Thus comparing results obtained by immunohistochemical staining for immunoglobulin in formalin fixed material knowledge of the fixation time used is essential.

The effect of different fixatives on the antigenicity of intracellular immunoglobulin has until recently only been investigated to a limited extent. Table 1 presents a survey of results published within the latest five years including our own results.

Our results are in general in accordance with the previously published results. In addition to Bouin's fluid we found that Lillie's AAF gave good preservation of antigenicity of immunoglobulins, sharp demarcation of the staining reaction as well as satisfactory preservation of tissue morphology. Clarke's fluid likewise gave good antigen preservation but tissue morphology was less satisfactory. Using fixation in E-A at 4°C and cold processing of the tissue in accordance with Sainte Marie (19) resulted in moderate to good antigen preservation while routine processing gave a less satisfactory result. In both cases however tissue morphology was bad and background staining intense.

The employment of digestion with proteolytic enzymes on sections from formalin fixed and paraffin embedded material was introduced by Huang (13) later on trypsin (7, 8, 14), pronase (11) and pepsin (18) have been used in the demonstration of immunoglobulin in paraffin sections as well by immunofluorescence as by immunoperoxidase technique.

The treatment has been described to result in unmasking of immunoreactive sites with increased number of stained cells, demonstration of surface

TABLE 1 *Survey of the Results Obtained by Immunohistochemical Staining for Immunoglobulin in Tissue Fixed in Various Fixatives*

Reference	Fixative	Fixation temp (C)	Hours	Preservation of antigenicity	Definition of staining reaction	Background staining	Tissue morphology
Burns et al (1974)	Abs ethanol Formol saline 10%	4°	24	++ +++	++ +++	strong moderate	++ +++
Kuhlmann (1976)	Buffered formaldehyde 4%	4°	24	+			
	Buffered formaldehyde 1 % + glutaraldehyde 1 %	4°	1-1.5	+			
	Glutaraldehyde 1-1.5 %	4°	1-1.5	+			
	Ethanol 96 % + acetic acid 1 %		10-15	++			
Bosman et al (1977)	Buffered formalin 10 %	25°	3	+			+++
	Bouin's fluid	25°	3	++	+++	weak	+++
	Sublimate formaldehyde Formalin 10 %	25°	3	+++	+++	moderate	++ (<20 ho
	+ glutaraldehyde 6 %	25°	3	0			+
	Zenker's fluid	25°	3	+	+	strong	+++
	Buffered methanol formalin	25°	3	+			+++
	Periodic acid lysine paraformaldehyde	25°	3	++	+	moderate	+++
Dorsett et al * (1977)	Bouin's fluid	25°	6-8	+++	+++	weak	+++
Curran et al (1977)	Buffered paraformaldehyde 4%	4-20°	24	+			
	Buffered formaldehyde 4%	4-20°	24	+			
	Formol saline 10 %	4-20°	24	++			
	Aqueous formaldehyde 4 %	4-20°	24	+++			
	Formalin 10 % + glutaraldehyde 0.5 % + calcium acetate 2 %	4-20°	2-24	+(<2 hours)	+++	strong	+++
	Ethanol 95 %	4°	24	+	+	strong	+
	Diethylpyrocarbonate	55°	3	+++	+++		+++
Jacobsen et al present results	Buffered formalin 10 %	25°	1-96	+	+	moderate	+++
	Lillie's AAF	25°	1-96	+++	+++	weak	+++
	Bouin's fluid	25°	1-96	+++	+++	weak	+++
	Clarke's fluid	25°	1-96	+++	+++	strong	+
	Ethanol 96 % acetic acid 1 % (routinely processed)	4°	74	+	+	strong	+
	Ethanol 96 % acetic acid 1 % (processed at 4°)	4°	24	+++	+	strong	+

+++ good ++ moderate + poor 0 extremely bad * Immunofluorescence

immunoglobulin on small lymphocytes and suppression of background staining to some degree.

In accordance with these observations we have found that trypsin digestion of formalin fixed material caused increased number of demonstrable immunoglobulin containing cells just as surface staining on small lymphocytes to some extent could be revealed. No reduction of background staining was observed.

The mechanism of the demasking effect of trypsinization has not yet been completely clarified.

As explanations increased permeability of the cells (7) or cleavage of cross links between fixative and antigenic determinants (8-14) have been suggested. The latter hypothesis is supported by investigations performed by Takamiya et al (20) who showed that antigenic determinants could be masked by modification of amino groups with

benzyl chloroformate and demasked by treatment with protease

Our results lend support to the latter hypothesis

only when trypsin digestion was used for a limited period

Trypsinization of material fixed in fixatives without formalin caused digestion of the tissue just as trypsinization of formalin fixed material for prolonged periods

In conclusion we want to stress the importance of specifying the fixation time when comparing different results obtained by staining for immunoglobulin on formalin fixed material

In order to obtain a result combining high amount of stained immunoglobulin containing cells with acceptable tissue morphology on paraffin embedded material we suggest fixation in Bouin's fluid or Lillies AAF. It should however be mentioned that Bouin's fixation is not compatible with the use of Methyl Green Pyronin staining for nucleic acids which sometimes is used in characterization of lymphoid cells in tissue sections. Formalin fixation within a limited period is usable and the masking of stainable immunoglobulin containing cells when prolonged fixation has been used can to a great extent be broken by controlled trypsinization of the section

We wish to thank Mrs. Britta Arbjørn for carefully typing the manuscript and Mr. Aksel Ankerstjerne for his technical assistance

REFERENCES

1. Banks P M. Diagnostic applications of an immunoperoxidase method in hematopathology. *J Histochem Cytochem* 27: 1192-1194 1979
2. Bosman F T, Lindeman J, Kuiper G, van der Wal A & Kreunig J. The influence of fixation on immunoperoxidase staining of plasmacells in paraffin sections of intestinal biopsy specimens. *Histochemistry* 53: 57-62 1977
3. Boudreau P, Surjan L & Berdal P. Immunoglobulin systems of human tonsils. I. Control subjects of various ages. Quantification of Ig producing cells, tonsillar morphometry and serum Ig concentrations. *Clin Exp Immunol* 31: 367-381 1978
4. Burns J, Hambridge M & Taylor C R. Intracellular immunoglobulins. A comparative study on three standard tissue processing methods using horseradish peroxidase and fluorochrome conjugates. *J Clin Pathol* 27: 548-551 1974
5. Clausen P P, Jacobsen M, Johansen P & Thomsen N. Immunohistochemical demonstration of intracellular immunoglobulin in formalin

- fixed paraffin embedded sections as staining method in diagnostic work. *Acta path microbiol scand Sect C* 87: 307-312 1979
6. Clausen P P & Thomsen P. Demonstration of hepatitis B surface antigen in liver biopsies. *Acta path microbiol scand Sect A* 86: 383-388 1978
7. Curran R C & Gregory J. The unmasking of antigens in paraffin sections of tissue by trypsin. *Experientia* 33: 1400-1401 1977
8. Curran R C & Gregory J. Demonstration of immunoglobulin in cryostat and paraffin sections of human tonsil by immunofluorescence and immunoperoxidase techniques. *J Clin Pathol* 31: 974-983 1978
9. Curran R C & Jones E L. Immunoglobulin containing cells in human tonsils as demonstrated by immunohistochemistry. *Clin Exp Immunol* 28: 103-115 1977
10. De Lellis R A, Sternberger L A, Mann R B, Banks P M & Nakane P K. Immunoperoxidase technique in diagnostic pathology. *Am J Clin Pathol* 71: 483-488 1979
11. Denk H, Radaskiewicz T & Weirich E. Pronase pretreatment of tissue sections enhances sensitivity of the unlabelled antibody-enzyme (PAP) technique. *J Immunol Methods* 15: 163-167 1977
12. Dorsett B H & Joachim H L. A method for the use of immunofluorescence on paraffin-embedded tissues. *Am J Clin Pathol* 69: 66-72 1978
13. Huang S N. Immunohistochemical demonstration of hepatitis B core and surface antigens in paraffin sections. *Lab Invest* 33: 88-95 1975
14. Huang S N, Minassian H & More J D. Application of immunofluorescent staining on paraffin sections improved by trypsin digestion. *Lab Invest* 35: 383-390 1976
15. Kraehenbuhl J P & Jamieson J D. Localization of intracellular antigens by immunoelectron microscopy. *Int Rev Exp Pathol* 13: 1-53 1974
16. Kuhlmann W D. Cytological localization of antigens. Tissue fixation and processing in immunoenzyme techniques. In: Feldmann G, Druet P, Bignon J & Avrameas S (Ed.) *Immunoenzymatic techniques*. North Holland Publishing Company, Amsterdam-Oxford 1976, pp 91-98
17. Pinkus G S & Sand J W. Specific identification of intracellular immunoglobulin in paraffin sections of multiple myeloma and macroglobulinemia using an immunoperoxidase technique. *Am J Pathol* 87: 47-55 1977
18. Reidy M A. Digestion technique for the reduction of background staining in the immunoperoxidase method. *J Clin Pathol* 30: 88-90 1977
19. Sainte-Marie G. A paraffin embedding technique for studies employing immunofluorescence. *J Histochem Cytochem* 10: 250-256 1962
20. Takamisa H, Bodemer W & Vogt A. Masking of protein antigen by modification of amino groups with carbobenzoxychloride (benzyl chloroformate) and demasking by treatment with nonspecific protease. *J Histochem Cytochem* 26: 914-920 1978

TABLE 1 *Survey of the Results Obtained by Immunohistochemical Staining for Immunoglobulin in Tissue Fixed in Various Fixatives*

Reference	Fixative	Fixation temp (C)	Hours	Preservation of antigenicity	Definition of staining reaction	Background staining	Tissue morphology
Burns et al (1974)	Abs ethanol	4°	24	++	++	strong	++
	Formol saline 10%			+++	+++	moderate	+++
Kuhmann (1976)	Buffered formaldehyde 4%	4°	24	+			
	Buffered formaldehyde 1% + glutaraldehyde 1%	4°	1-1.5	+			
	Glutaraldehyde 1-1.5%	4°	1-1.5	+			
	Ethanol 96% + acetic acid 1%		10-15	++			
Bosman et al (1977)	Buffered formalin 10%	25°	3	+			+++
	Bouin's fluid	25°	3	++	+++	weak	+++
	Sublimate formaldehyde	25°	3	+++	+++	moderate	++ (<20 hours)
	Formalin 10% + glutaraldehyde 6%	25°	3	0			+
	Zenker's fluid	25°	3	+	+	strong	+++
	Buffered methanol formalin	25°	3	+			+++
	Periodic acid lysine paraformaldehyde	25°	3	++	+	moderate	+++
Dorsett et al * (1977)	Bouin's fluid	25°	6-8	+++	+++	weak	+++
Curran et al (1977)	Buffered paraformaldehyde 4%	4-20°	24	+			
	Buffered formaldehyde 4%	4-20°	24	+			
	Formol saline 10%	4-20°	24	++			
	Aqueous formaldehyde 4%	4-20°	24	+++			
	Formalin 10% + glutaraldehyde 0.5% + calcium acetate 2%	4-20°	2-24	++ (<2 hours)	+++	strong	+++
	Ethanol 95%	4°	24	+	+	strong	+
	Diethylpyrocarbonate	55°	3	+++	+++		+++
Jacobsen et al present results	Buffered formalin 10%	25°	1-96	+	+	moderate	+++
	Lillie's AAF	25°	1-96	+++	+++	weak	+++
	Bouin's fluid	25°	1-96	+++	+++	weak	+++
	Clarke's fluid	25°	1-96	+++	+++	strong	+
	Ethanol 96% + acetic acid 1% (routinely processed)	4°	24	+	+	strong	+
	Ethanol 96% + acetic acid 1% (processed at 4°)	4°	24	+++	+	strong	+

+++ good ++ moderate + poor 0 extremely bad * Immunofluorescence

immunoglobulin on small lymphocytes and suppression of background staining to some degree

In accordance with these observations we have found that trypsin digestion of formalin fixed tissue increased number of demonstrable cells as surface extent could be revealed. No such was observed

The mechanism of the demasking effect of trypsinization has not yet been completely clarified

As explanations increased permeability of the cells (7) or cleavage of cross links between fixative and antigenic determinants (8-14) have been suggested. The latter hypothesis is supported by investigations performed by Takamya et al (20) who showed that antigenic determinants could be masked by modification of amino groups with

benzyl chloroformate and demasked by treatment with protease

Our results lend support to the latter hypothesis as we have found that trypsinization had only positive or at least no negative effect on the staining result, when using formalin containing fixatives and only when trypsin digestion was used for a limited period. Trypsinization of material fixed in fixatives without formalin caused digestion of the tissue just as trypsinization of formalin fixed material for prolonged periods.

In conclusion we want to stress the importance of specifying the fixation time when comparing different results obtained by staining for immunoglobulin on formalin fixed material.

In order to obtain a result combining high amount of stained immunoglobulin containing cells with acceptable tissue morphology on paraffin embedded material we suggest fixation in Bouin's fluid or Lillie's AAT. It should however be mentioned that Bouin's fixation is not compatible with the use of Methyl Green Pyronin staining for nucleic acids which sometimes is used in characterization of lymphoid cells in tissue sections. Formalin fixation within a limited period is usable and the masking of stainable immunoglobulin containing cells when prolonged fixation has been used can to a great extent be broken by controlled trypsinization of the section.

We wish to thank Mrs. Britta Arbjørn for carefully typing the manuscript and Mr. Aksel Ankerstjerne for his technical assistance.

REFERENCES

1. Banks P M Diagnostic applications of an immunoperoxidase method in hematopathology *J Histochem Cytochem* 27 1192-1194 1979
2. Bosman F T, Lindeman J, Kuiper G, van der Wal A & Areunis J The influence of fixation on immunoperoxidase staining of plasmacells in paraffin sections of intestinal biopsy specimens *Histochemistry* 53 57-62 1977
3. Brandt Aeg P, Surjan L & Berdal P Immunoglobulin systems of human tonsils I. Control subjects of various ages. Quantification of Ig producing cells, tonsillar morphometry and serum Ig concentrations *Clin Exp Immunol* 31 367-381 1978
4. Burns J, Hambridge M & Taylor C R Intracellular immunoglobulins. A comparative study on three standard tissue processing methods using horseradish peroxidase and fluorochrome conjugates *J Clin Path* 27 548-557 1974
5. Clausen P P, Jacobsen M, Johansen P & Thomsen N Immunohistochemical demonstration of intracellular immunoglobulin in formalin fixed paraffin embedded sections as staining method in diagnostic work *Acta path microbiol scand Sect C* 87 307-312 1979
6. Clausen P P & Thomsen P Demonstration of hepatitis B surface antigen in liver biopsies *Acta path microbiol scand Sect A* 86 383-388 1978
7. Curran R C & Gregory J The unmasking of antigens in paraffin sections of tissue by trypsin *Experientia* 33 1400-1401 1977
8. Curran R C & Gregory J Demonstration of immunoglobulin in cryostat and paraffin sections of human tonsil by immunofluorescence and immunoperoxidase techniques *J Clin Path* 31 974-983 1978
9. Curran R C & Jones E L Immunoglobulin containing cells in human tonsils as demonstrated by immunohistochemistry *Clin Exp Immunol* 28 103-115 1977
10. De Lellis R A, Sternberger L A, Mann R B, Banks P M & Nakane P K Immunoperoxidase techniques in diagnostic pathology *Am J Clin Path* 71 483-488 1979
11. Denk H, Radasiewicz T & Weirich E Pronase pretreatment of tissue sections enhances sensitivity of the unlabelled antibody-enzyme (PAP) technique *J Immunol Methods* 15 163-167 1977
12. Dorsett B H & Joachim H L A method for the use of immunofluorescence on paraffin-embedded tissues *Am J Clin Path* 69 66-72 1978
13. Huang S N Immunohistochemical demonstration of hepatitis B core and surface antigens in paraffin sections *Lab Invest* 33 88-95 1975
14. Huang S N, Minassian H & More J D Application of immunofluorescent staining on paraffin sections improved by trypsin digestion *Lab Invest* 35 383-390 1976
15. Kraehenbuhl J P & Jamieson J D Localization of intracellular antigens by immunoelectron microscopy *Int Rev Exp Path* 13 1-53 1974
16. Kuhlmann W D Cytological localization of antigens. Tissue fixation and processing in immunoenzyme techniques. In: Feldmann G, Druet P, Bignon J & Avrameas S (Eds) *Immunoenzymatic techniques*. North Holland Publishing Company, Amsterdam, 1977
17. Kuhlmann W D Cytological localization of antigens. Tissue fixation and processing in immunoenzyme techniques. In: Feldmann G, Druet P, Bignon J & Avrameas S (Eds) *Immunoenzymatic techniques*. North Holland Publishing Company, Amsterdam, 1977
18. Reading M A digestion technique for the reduction of background staining in the immunoperoxidase method *J Clin Path* 30 88-90 1977
19. Sainte Marie G A paraffin embedding technique for studies employing immunofluorescence *J Histochem Cytochem* 10 250-256 1962
20. Takamiya H, Bodemer W & Vogt A Masking of protein antigen by modification of amino groups with carbobenzoxychloride (benzyl chloroformate) and demasking by treatment with nonspecific protease *J Histochem Cytochem* 26 914-920 1978

- 21 *Taylor C R* An immunohistological study of follicular lymphoma reticulum cell sarcoma and Hodgkin's disease *Europ J Cancer* 12 61-75 1976
- 22 *Taylor C R & Burns J* The demonstration of plasma cells and other immunoglobulin containing cells in formalin fixed paraffin embedded tissues using peroxidase labelled antibody *J Clin Path* 27 14-20 1974
- 23 *Taylor C R & Mason D Y* The immunohistological detection of intracellular immunoglobulin in formalin paraffin sections from multiple myeloma and related conditions using the immunoperoxidase technique *Clin Exp Immunol* 18 417-429 1974
- 24 *Taylor C R Russel R & Chandor S* An immunohistologic study of multiple myeloma and related conditions using an immunoperoxidase method *Am J Clin Path* 70 612-622 1978

ENZYMECYTOCHEMISTRY AND IMMUNOHISTOCHEMISTRY IN MONOCLONAL GAMMOPATHY AND REACTIVE PLASMACYTOSIS

PREBEN JOHANSEN and MOGENS KROGH JENSEN

Departments of Pathology Hematology and Clinical Chemistry Aalborg Hospital and Institute of
Pathology University of Odense

Johansen P & Krogh Jensen M Enzymecytochemistry and immunohistochemistry in monoclonal
gammopathy and reactive plasmacytosis Acta path microbiol scand Sect A 88 377-382 1980

Peripheral blood smears and bone marrow smears from 29 patients with malignant M components (25 with multiple myeloma and 4 with malignant lymphoma) 13 patients with benign monoclonal gammopathy (BMG) and 20 patients with polyclonal reactive plasmacytosis were examined by leucocyte alkaline phosphatase score (LAP-score) and by acid phosphatase score in plasma cells from bone marrow smears Furthermore tissue sections from marrow biopsies from all patients were examined by the three layer unlabelled immunoperoxidase technique to detect cytoplasmic immunoglobulin The LAP score was significantly higher in patients with malignant M-components than in patients with BMG and also higher in IgA and IgG myeloma than in IgA and IgG BMG but the latter difference was not significant Furthermore a significant positive correlation between paraprotein concentration and LAP score was found in multiple myeloma Acid phosphatase score in plasma cells showed no clear distinction between multiple myeloma and BMG Immunohistochemical examination showed a distinct monoclonal pattern in both multiple myeloma and BMG allowing identification of the M-component which in all cases corresponded to the M-component detected by serum examination Cells producing immunoglobulin classes not matching the M-component were more rare in multiple myeloma than in BMG but the difference between the two conditions was quantitative and allowed no clear distinction

Key words Monoclonal gammopathy enzymecytochemistry immunohistochemistry

Preben Johansen Department of Pathology Aalborg Hospital Aalborg Denmark

Accepted as submitted 18 v 80

Prevalence studies have shown that the frequency of serum M-components in the population increases with age In individuals over the age of 80 approximately 5% have M-components (1) The discovery of an M-component always brings about examinations to exclude or confirm a diagnosis of multiple myeloma or malignant lymphoma In the absence of heavy bone marrow infiltration osteolytic skeletal lesions or enlarged lymphoid organs differential diagnosis is difficult between a malignant disease of plasmacytic or lymphocytic origin and the clinical syndrome benign monoclonal gammopathy (2) Criteria such as the

concentration of the monoclonal immunoglobulin fraction presence of Bence Jones protein and depression of other immunoglobulin classes are poor discriminating parameters (9)

Enzymecytochemical studies of plasma cells have demonstrated an increased activity of acid phosphatase in multiple myeloma compared to normal and reactive plasma cells (10 11) Furthermore semi quantitation of cytoplasmic acid phosphatase activity in plasma cells from cases of multiple myeloma and BMG has demonstrated a significantly higher activity of this enzyme in multiple myeloma facilitating a clear distinction between the two conditions (4) Leucocyte alkaline phosphatase

- 21 *Taylor C R* An immunohistological study of follicular lymphoma, reticulum cell sarcoma and Hodgkin's disease *Europ J Cancer* 12 61-75, 1976
- 22 *Taylor C R & Burns, J* The demonstration of plasma cells and other immunoglobulin containing cells in formalin-fixed paraffin-embedded tissues using peroxidase-labelled antibody *J Clin Path* 27 14-20, 1974
- 23 *Taylor, C R & Mason, D Y* The immunohistological detection of intracellular immunoglobulin in formalin paraffin sections from multiple myeloma and related conditions using the immunoperoxidase technique *Clin Exp Immunol* 18 417-429, 1974
- 24 *Taylor, C R, Russel R & Chandor, S* Immunohistologic study of multiple myeloma related conditions, using an immunoperoxidase method *Am J Clin Path* 70 612-622, 1977

ENZYMECYTOCHEMISTRY AND IMMUNOHISTOCHEMISTRY IN MONOCLONAL GAMMOPATHY AND REACTIVE PLASMACYTOSIS

PREBEN JOHANSEN and MOGENS KROGH JENSEN

Departments of Pathology, Hematology and Clinical Chemistry Aalborg Hospital and Institute of Pathology, University of Odense

Johansen P & Krogh Jensen M. Enzymecytochemistry and immunohistochemistry in monoclonal gammopathy and reactive plasmacytosis. *Acta path. microbiol. scand. Sect. A* 89: 377-382, 1980.

Peripheral blood smears and bone marrow smears from 29 patients with malignant M-components (25 with multiple myeloma and 4 with malignant lymphoma), 13 patients with benign monoclonal gammopathy (BMG) and 20 patients with polyclonal reactive plasmacytosis were examined by leucocyte alkaline phosphatase score (LAP score) and by acid phosphatase score in plasma cells from bone marrow smears. Furthermore, tissue sections from marrow biopsies from all patients were examined by the three layer unlabelled immunoperoxidase technique to detect cytoplasmic immunoglobulin. The LAP score was significantly higher in patients with malignant M-components than in patients with BMG and also higher in IgA and IgG myeloma than in IgA and IgG BMG, but the latter difference was not significant. Furthermore, a significant positive correlation between paraprotein concentration and LAP score was found in multiple myeloma. Acid phosphatase score in plasma cells showed no clear distinction between multiple myeloma and BMG. Immunohistochemical examination

distinction than in BMG, but the difference between the two conditions was quantitative and allowed no clear distinction.

Key words: Monoclonal gammopathy, enzymecytochemistry, immunohistochemistry.

Preben Johansen, Department of Pathology, Aalborg Hospital, Aalborg, Denmark.

Accepted as submitted 18 v 80

Prevalence studies have shown that the frequency of serum M-components in the population increases with age. In individuals over the age of 80 approximately 5% have M-components (1). The discovery of an M-component always brings about examinations to exclude or confirm a diagnosis of multiple myeloma or malignant lymphoma. In the absence of heavy bone marrow infiltration, osteolytic skeletal lesions or enlarged lymphoid organs, differential diagnosis is difficult between a malignant disease of plasmacytic or lymphocytic origin and the clinical syndrome, benign monoclonal gammopathy (BMG). Indirect criteria such as the

concentration of the monoclonal immunoglobulin fraction, presence of Bence Jones protein, and depression of other immunoglobulin classes are poor discriminating parameters (9).

Enzymecytochemical studies of plasma cells have demonstrated an increased activity of acid phosphatase in multiple myeloma compared to normal and reactive plasma cells (10, 11). Furthermore, semi-quantitation of cytoplasmic acid phosphatase activity in plasma cells from cases of multiple myeloma and BMG has demonstrated a significantly higher activity of this enzyme in multiple myeloma, facilitating a clear distinction between the two conditions (4). Leucocyte alkaline phosphatase

- 21 *Taylor, C R* An immunohistological study of follicular lymphoma reticulum cell sarcoma and Hodgkin's disease *Europ J Cancer* 12 61-75, 1976
- 22 *Taylor, C R & Burns, J* The demonstration of plasma cells and other immunoglobulin containing cells in formalin-fixed paraffin-embedded tissues using peroxidase labelled antibody *J Clin Path* 27 14-20, 1974
- 23 *Taylor, C R & Mason D Y* The immunohistological detection of intracellular immunoglobulin in formalin paraffin sections from multiple myeloma and related conditions using the immunoperoxidase technique *Clin Exp Immunol* 18 417-429, 1974
- 24 *Taylor C R, Russel, R & Chandor, S* An immunohistologic study of multiple myeloma and related conditions, using an immunoperoxidase method *Am J Clin Path* 70 612-622, 1978

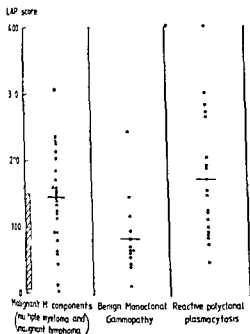


Fig 1 LAP score levels in malignant and benign monoclonal gammopathy and reactive plasmacytosis. The following signatures are used to identify individual immunoglobulin classes: Δ IgA, \square IgG, \circ IgM, \times light chain disease. The hatched area on the interval scale represents the range of LAP scores in the healthy controls.

RESULTS

Fig 1 illustrates the LAP-score levels. The range of LAP-scores from the healthy controls is shown by the hatched area on the interval scale. Patients with

reactive polyclonal plasmacytosis show a high mean LAP score with a considerable variation in individual scores. The mean LAP score in patients with malignant M-components is 146 with a range from 7 to 308 while the mean score in patients with BMG is 87 with a range from 15 to 244; this difference being significant ($P < 0.01$). The LAP score in patients with multiple myeloma of IgA and IgG type is higher than the LAP-score in patients with BMG of the same types, but the difference is not significant. In the BMG group patients with serum M-components of IgM type tended to have lower LAP scores than patients with M-components of IgA and IgG type. Of the four patients with a malignant M-component of IgM type all had malignant lymphomas; the score was elevated in two and in two within the range of the healthy controls. Fig 2 illustrates the correlation between serum paraprotein concentration and LAP-score in patients with multiple myeloma and shows a positive correlation ($r = 0.58$) between the two parameters; this correlation being significant ($P < 0.01$). In patients with BMG of IgA and IgG type LAP-scores also increased with increasing paraprotein concentration while patients with BMG of IgM type showed no correlation between LAP score and paraprotein concentration. All patients with monoclonal gammopathy had normal leucocyte counts at the time of the LAP-score determination. Three patients with multiple myeloma received therapy at the time of blood and bone marrow examination; the LAP-score levels in these cases were all within the range of LAP scores from the controls.

The acid phosphatase scores are illustrated in

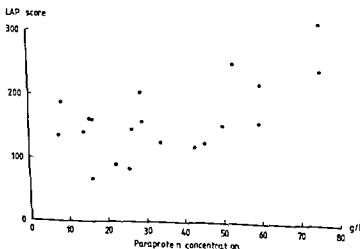


Fig 2 Correlation between LAP-score and paraprotein concentration in patients with multiple myeloma ($r = 0.58$, $P < 0.01$).

activity in neutrophils is also reported to be elevated in patients with multiple myeloma (3, 12) but information is lacking concerning the level of this enzyme in patients with BMG.

Immunocytochemical investigations with special reference to the percentage of cells producing the immunoglobulin matching the serum M component have not revealed a clear distinction between patients with a malignant disease of plasmacytic or lymphocytic origin and BMG (6, 15).

The purpose of this study was to test the difference in cytoplasmic acid phosphatase activity between plasma cells of multiple myeloma and BMG and to see if the level of leucocyte alkaline phosphatase activity (LAP score) allowed a distinction between multiple myeloma and BMG. Further more bone marrow biopsies were examined by immunoperoxidase technique to evaluate the distribution of immunoglobulin producing cells by an immunohistochemical method in these conditions.

MATERIAL AND METHODS

The material consists of 62 consecutive patients from whom peripheral blood smears, bone marrow smears and bone marrow biopsies were examined during a 12 months period (February 1 1978 to January 31 1979). The criteria for entering the study were 1) presence of an M component in serum and/or urine and 2) bone marrow smears with an increased number of plasma cells (more than 3% of nucleated marrow cells). The

sis (20). Multiple myeloma was diagnosed when at least two of the following three criteria were present: 1) M component in serum and/or urine 2) osteolytic skeletal lesions and 3) bone marrow smears with more than 15% plasma cells and/or tissue sections from marrow biopsies showing large solid plasma cell infiltrates. The diagnosis of malignant lymphoma was based on histologic examination of lymphatic tissue (lymph nodes and spleen). Cases with serum M components of IgA and IgG type not fulfilling the criteria for multiple myeloma and cases with IgM serum M components without enlarged lymphoid organs were classified as BMG. Patients in this group have been followed for at least one year without significant increase in the serum M component. Reactive plasmacytosis was diagnosed in patients without a serum M component but with more than

for alkaline phosphatase according to Leucocyte (7). One hundred consecutive neutrophils were counted and the intensity of enzyme activity was graded from 0 to +++++. Simultaneously with each blood smear from a patient a smear from a healthy control was stained and scored. Bone marrow smears were air dried and stained

for acid phosphatase (8). In patients with multiple myeloma BMG with IgA and IgG M components a reactive plasmacytosis the intensity of acid phosphatase activity in individual plasma cells was graded by semiquantitative scoring system from 0 to +++++. The weakest reaction consisted of a diffuse rose cytoplasmic tint with increasing activity a granular reaction occurred the strongest reaction consisted of confluent granular positivity. In each smear the cytoplasmic activity of acid phosphatase was registered in 10 consecutive plasma cells and the result is referred to as the acid phosphatase score. Scoring was not performed in cases with less than 100 plasma cells in the bone marrow smear.

Tissue sections from formalin fixed paraffin embedded bone marrow biopsies (marrow clots or iliac crest biopsies) were examined by the three layer unlabeled immunoperoxidase (PAP) method described in detail elsewhere (5). The method consists of the following steps: 1) sections are deparaffinized and brought to absolute alcohol 2) endogenous peroxidase activity is blocked with H_2O_2 in methanol solution 3) sections are incubated for 30 min with rabbit antihuman immunoglobulin antisera. Working dilutions of antisera in this step were found by titration. In the demonstration of heavy chains concentrations from 1/81 to 1/1001 were used for the demonstration of light chains dilutions from 1/81 to 1/2001 were used 4) incubation with swine antirabbit immunoglobulin in dilution 1/41 5) incubation with rabbit peroxidase antiperoxidase (PAP) complex in dilution 1/101 6) peroxidase activity is developed by incubation with 0.05% 3,3'-diaminobenzidine tetrahydrochloride (Sigma) and 0.01% H_2O_2 in 0.1 M phosphate buffered saline pH 7.6. In steps 3, 4 and 5 antisera contained 20% normal swine serum. Antisera were diluted in phosphate buffered saline pH 7.2. All sections were examined with antisera against human alpha gamma, my heavy chains lambda and kappa light chains. Cases of multiple myeloma without alpha or gamma heavy chains were also examined for the presence of delta and epsilon heavy chains. Antisera against human delta and epsilon heavy chains were purchased from Behringwerke, Hoechst, Denmark, all other antisera were purchased from DAKO, Denmark. In all cases control sections were made by 1) incubation with the immunoglobulin fraction of serum from unimmunized rabbits instead of specific rabbit antiserum 2) incubation with PBS instead of specific rabbit antiserum. Furthermore the varying number of cells stained with each antibody acted as inherent controls. All sections were counterstained with haematoxylin and mounted in Pertex® (Histolab, Bethlehem Trading Ltd).

In each patient the leucocyte count at the time of LAP score determination was recorded.

Qualitative identification of the M component in serum was based on immunoelectrophoresis and the serum concentration of all M components was measured (2).

Statistic analysis of differences in score levels was made by the Mann-Whitney test.



Fig 4 Immunoperoxidase staining of marrow biopsy from a case of BMG with a serum IgA kappa M component showing scattered positive cells (arrows) and a focal infiltrate (upper right) 3 layer unlabelled immunoperoxidase technique for IgA haematoxylin counterstain $\times 512$

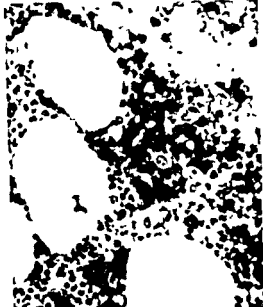


Fig 6 Immunoperoxidase staining of marrow biopsy for IgG from a case of IgG kappa myeloma showing heavy infiltration with only small uninvolved areas 3 layer unlabelled immunoperoxidase technique for IgG haematoxylin counterstain $\times 512$



Fig 5 Same case as Fig 4 stained for IgG showing scattered positive cells (arrows) 3 layer unlabelled immunoperoxidase technique for IgG haematoxylin counterstain $\times 512$

for this elevated LAP-score is unknown. Intercurrent infectious diseases known to cause an elevated LAP score seem unlikely as we find normal leucocyte counts in all patients with M-components corresponding to the findings of *Brook and Dreisbach* (3). In this study we find a significant positive correlation between serum paraprotein concentration and LAP score in patients with multiple myeloma supporting the observation by *Überla et al* (16) who found a positive correlation between LAP score and serum gamma globulin concentration. The reason for this correlation is not known but the finding is of practical importance as the determination of LAP scores in patients with M-components seems to give no further information than can be achieved by determination of serum paraprotein concentration. However it still needs to be known whether an elevated LAP-score precedes a rise in paraprotein concentration. Therefore a patient with an M-component and a high LAP score but without sufficient evidence of multiple myeloma should be followed closely.

Immunocytochemical examination of bone marrow smears in monoclonal gammopathy using immunofluorescence technique has demonstrated a

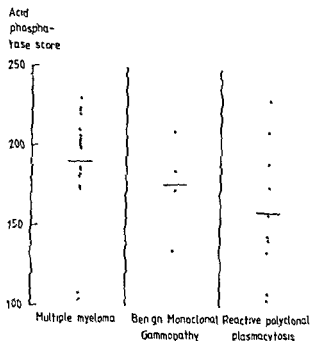


Fig 3 Acid phosphatase score in multiple myeloma benign monoclonal gammopathy with IgA and IgG M-components, and reactive plasmacytosis

Fig 3 The highest mean score is found in patients with multiple myeloma but a considerable overlapping between the three groups exists and the differences in acid phosphatase score are insignificant. The acid phosphatase score did not correlate to serum paraprotein concentration.

Immunohistochemistry

In reactive plasmacytosis the immunoperoxidase-stained bone-marrow sections invariably showed a polyclonal pattern with the presence of an equal number of IgA and IgG producing cells and rare IgM producing cells. In the presence of a serum M-component, whether multiple myeloma or BMG, the immunoperoxidase-stained marrow sections disclosed a plasma cell population, where approximately 80% or more of the cells produced the same immunoglobulin class or the same light chain which always corresponded to the serum and/or urine M-component. In cases of BMG with an IgM serum M component immunoperoxidase staining showed a population of lymphoplasmacytoid cells positive for IgM. These cells occurred singly and in small groups. In multiple myeloma, plasma cells producing immunoglobulin not matching the serum M component were rare while in BMG such cells were more numerous up to approximately 20% (Fig 4 and 5). However, marrow sections from cases of BMG sometimes contained very few cells not matching the serum M-component. In multiple myeloma plasma cell infiltrates tended to be more extensive (Fig 6) but owing to the relative small

samples of marrow-tissue plasma cell infiltrates cases of multiple myeloma could be discrete. For these reasons the differences between multiple myeloma and BMG were only quantitative, allowed no clear distinction. In three of the cases of malignant lymphoma the bone-marrow was infiltrated, and the cytoplasm of the lymphoplasmacytoid cells contained monoclonal immunoglobulin matching the serum M-component. In one of the three cases, marrow involvement was minimal but the monoclonal cytoplasmic immunoglobulin facilitated the recognition of marrow infiltration from malignant lymphoma.

DISCUSSION

Enzyme cytochemical studies of normal and reactive plasma cells and plasma cells in multiple myeloma have revealed an increased activity of acid phosphatase in the latter condition (10, 11). This difference is of little value in clinical practice, as apart from rare cases of nonsecretory myeloma, the differential diagnosis between multiple myeloma and reactive plasma cell hyperplasia is easily made by serologic examination. Of considerable interest is, however, a study by Cassuto *et al* (4) who found a significant difference between multiple myeloma and BMG as regards cytoplasmic activity of acid phosphatase in plasma cells. We, however, cannot confirm this observation. Though we have been able to quantify only a few cases of BMG, our results show a considerable overlapping between the values in the two groups. The mean score is higher in multiple myeloma but the difference is not significant. No major differences seem to exist between the enzyme cytochemical technique in our study and the one by Cassuto *et al* (4), but minor differences may be found in the criteria used to separate multiple myeloma and BMG, as Cassuto *et al* (4) do not specify the criteria in their paper. The cause of the elevated, but in our study not significantly higher, acid phosphatase activity in plasma cells from multiple myeloma is unknown. We find as Löffler (11) no correlation between serum paraprotein concentration and acid phosphatase activity.

We find a significantly higher LAP-score level in patients with malignant M-components than in cases of BMG. In our study this difference is due to the facts that patients with BMG of IgM type all have a LAP-score within the range of the healthy controls and that the LAP score in patients with multiple myeloma of IgG and IgA type is higher than in patients with IgG and IgA BMG. The LAP-score has previously been reported to be elevated in patients with multiple myeloma (1, 12). The reason

shift in the distribution of immunoglobulin producing cells towards the type matching the serum M component. In multiple myeloma usually more than 95% of the immunoglobulin producing cells produce the same immunoglobulin class (6, 15). Though this figure is lower in BMG some overlapping exists and no clear distinction between the two conditions can be made (6, 15). This also holds true for immunohistochemical examination. By immunoperoxidase staining of bone marrow sections in multiple myeloma the light and heavy chain type can easily be achieved and corresponds in the vast majority of cases to the serum M component (5, 13). Contrary to Taylor *et al.* (13, 14) we were able to identify the heavy and light chain type in multiple myeloma as well as in BMG by examination of immunoperoxidase stained tissue sections and in both conditions the result corresponded to the serum examination. Though plasma cells producing immunoglobulin classes not matching the serum M component are generally more numerous in BMG than in multiple myeloma this is not always so and in our experience immunoperoxidase stained bone marrow sections offer no further information for making a distinction between BMG and multiple myeloma. Identification of discrete marrow infiltrates from malignant lymphomas producing monoclonal immunoglobulin is facilitated by the immunoperoxidase technique illustrating the monoclonal cytoplasmic immunoglobulin.

We wish to thank cytotechnologists *Dorthe Thuen* and *Preben Sandahl* for expert technical assistance in performing the enzyme cytochemical and immunohistochemical reactions.

REFERENCES

- 1 Axelsson U, Bachmann R and Hallén J. Frequency of pathological proteins (M components) in 6995 sera from an adult population. *Acta Med Scand* 179: 235-247 1966.
- 2 Blom M and Sørensen D. A turbidimetric continuous flow system for immunochemical quantitation of blood proteins by use of a modified photometer. *Clin Chem* 19: 1148-1151 1973.
- 3 Brook J and Dreisbach P. B. Leucocyte alkaline phosphatase level in multiple myeloma. *J Lab Clin Med* 90: 114-117 1977.
- 4 Cassuto J, P. Hammou J, C. Pastorelli E, Duquardin P and Masseyeff R. Plasma cell acid phosphatase: a discriminative test for benign and malignant monoclonal gammopathy. *Biomedicine* 27: 197-199 1977.
- 5 Clausen P, P. Jacobsen M, Johansen P and Thomsen N. Immunohistochemical demonstration of intracellular immunoglobulin in formalin fixed paraffin embedded sections as staining method in diagnostic work. *Acta path microbiol scand Sect C* 87: 307-312 1979.
- 6 Hjymans W, Schuit H, R. E. and Hulsink E. An immunofluorescence study on intracellular immunoglobulin in human bone marrow cells. *Ann NY Acad Sci* 177: 290-305 1971.
- 7 Leder L. D. *Der Blut Monocyt*. Springer Verlag Berlin Heidelberg New York 1967 p. 225.
- 8 Lennert K. *Malignant lymphomas other than Hodgkin's disease*. Springer Verlag Berlin Heidelberg New York 1978 pp. 79-80.
- 9 Lindstrom F. D. and Dahlstrom U. Multiple myeloma or benign monoclonal gammopathy? A study of differential diagnostic criteria in 44 cases. *Clin Immunol Immunopathol* 10: 168-174 1978.
- 10 Löffler H. and Schubert J. C. F. Cytochemische Unterschiede zwischen Plasmazellen und Myelomzellen. *Klin Wochr* 41: 481-488 1963.
- 11 Löffler H. Unspezifische Esterasen und Saure Phosphatase bei Plasmazytomen. *Blut* 15: 330-332 1967.
- 12 Schumacher K. Die Bedeutung der Alkalischen Leukozyten Phosphatase für Differentialdiagnose und Prognose Maligner Hamoblastosen. *Med Welt* 9: 415-418 1964.
- 13 Taylor C. R. and Mason D. Y. The immunohistological detection of intracellular immunoglobulin in formalin paraffin sections from multiple myeloma and related conditions using the immunoperoxidase technique. *Clin exp Immunol* 18: 417-429 1974.
- 14 Taylor C. R., Russell R. and Stebbings C. An immunohistologic study of multiple myeloma and related conditions using an immunoperoxidase method. *Am J Clin Pathol* 70: 612-622 1978.
- 15 Turesson I. Distribution of immunoglobulin containing cells in bone marrow and lymphoid tissue in patients with monoclonal gammopathy. *Acta Med Scand* 202: 247-255 1978.
- 16 Überla K., Tillings T. and Graf C. Vergleich zweier Bestimmungsmethoden der Alkalischen Leukozyten Phosphatase. *Blut* 15: 13-18 1967.

in Table 1. It is seen that eight weeks of treatment with cimetidine results in a significant increase in N_A (13%) and N_V (15%) and a decrease in \bar{V} (11%). The latter is greater than the median value of CE before and during treatment. No change was found in the value of V_A . Beside alterations of G-cell density the morphology as seen in the light microscope were unchanged before as well as during treatment with cimetidine. Serum gastrin obtained in 26 pairs of patients was increased during treatment but the difference was insignificant.

DISCUSSION

Elevated serum-gastrin caused by vagotomy or histamine H_2 -receptor antagonists is probably induced by reduced gastric acid secretion (9, 21) and must be due to a G-cell change either a hyperplasia and/or hyperfunction. Earlier results after vagotomy are conflicting since in two series G-cell hyperplasia was found (5, 8) whereas in another a decrease of G-cell density was reported (7). A difference in the sensitivity and specificity of the antgastrin may be an explanation of the conflicting results as prerequisite to identification is a content of gastrin.

Several authors have demonstrated ultrastructural changes during stimulation and secretion from the G-cells especially in the granulae (4, 11, 13, 16, 25).

This study shows that cimetidine treatment of duodenal ulcer patients results in a G-cell hyperplasia and that the volume of the individual cell decreases to such an extent that the volume density remains unchanged. Assuming the antral mucosal volume remains the same both before and during treatment then the total G-cell volume will also remain unchanged. Witzel *et al.* (27) also found unchanged volume density during medication of rats with metamizol but they report no calculation of the number of G-cells.

The G-cell hyperplasia after eight weeks of treatment with cimetidine and the elevated levels of serum gastrin even six weeks after withdrawal (6, 10) may be a factor of importance with regard to the frequently rapid recurrence of an ulcer at times presenting as perforation after short term treatment (23, 26). In contrast other authors (3) did not find a higher frequency of re-ulceration after a short successful course of cimetidine compared to a successful course of placebo. It has also been demonstrated that the parietal cell sensitivity to pentagastrin remains unchanged after short term treatment with cimetidine (1).

autonomous function of the increased number of G-cells after cimetidine treatment as a factor in recurrence of the ulcer.

It is concluded that cimetidine treatment of duodenal ulcer patients results in antral gastrin cell hyperplasia without changes in the total G-cell volume and that this hyperplasia may be a factor of importance with regard to the rapid recurrence of many ulcers after cessation of the treatment.

The anti gastrin serum No 2717 was kindly donated by Professor J. F. Rehfeld, Institute of Biochemistry Aarhus University. The authors wish to thank Professor Daniel Andersen, Dept. of Surgical Gastro-enterology Odense University Hospital for his advice and review of the manuscript. The study was supported by grants from the Danish Medical Research Council (Journal No 512 5255 and 512 679).

REFERENCES

1. Aadland E & Berstad. Parietal and chief cell sensitivity to pentagastrin stimulation before and after cimetidine treatment for duodenal ulcer. *Scand J Gastroent* 14: 111-114 1979.
2. Andersen D, Høstrup H & Amdrup E. The Aarhus County Vagotomy Trial II. An interim report on reduction in acid secretion and ulcer recurrence rate following parietal cell vagotomy and selective gastric vagotomy. *World J Surg* 2: 91-100 1978.
3. Bardhan K D, Blum A, Gillespie G, Larkworthy W, Mekel R, Moshal M, Smith P M, Venables C W, Van Tongeren J M H & Watan A. Long term treatment with cimetidine in duodenal ulceration. *Lancet* i: 900-901 1977.
4. Bastie M J, Balas D, Senegas Bala F, Bertrand C, Pradayrol L, Frexinos J & Ribet A. A cytophysiological study of the G-cell secretory cycle in the antrum mucosa of the hamster and of the rat. *Scand J Gastroent* 14: 35-48 1979.
5. Becker H D, Arnold A, Borger H W, Creutzfeldt C, Schafmayer A & Creutzfeldt W. Influence of truncal vagotomy on serum and antral gastrin and G-cells. *Gastroenterology* 72: 811 1977.
6. Buchanan K D, Spencer A, Ardill J & Kennedy T L. Hypergastrinaemia due to cimetidine. *Gut* 19: A 437 1978.
7. Creaghe S B, Greenburg A G, Brown D, Peskin G W & Saik R P. Vagotomy and the antral «G cell». *J Surg Res* 26: 528-531 1979.
8. Delance P, Willems G & deGraf J. Antral gastrin cell proliferation after vagotomy in rats. *Digestion* 18: 27-34 1978.
9. Feldman M, Dickerman R M, McClelland R N, Cooper K A, Walsh J H & Richardson C T. Effect of selective proximal vagotomy on food stimulated gastric acid secretion and gastrin release.

ify an eventual

trin 17 gastrin 34 and component I) with almost equimolar potency (19) The concentrations were expressed in pg/ml Fasting serum gastrin was measured before and at the end of eight weeks of treatment

Tissue preparation Three biopsies were taken approximately 2 cm orally to the pyloric ring in connection with gastro duodenoscopy before and after eight weeks of treatment The biopsies were immediately fixed in 4% methanol free paraformaldehyde pH 7.4 and embedded in paraffin without any attempt at orientating the biopsies Three 5 μ m thick sections were cut at a distance of 25 μ m from each biopsy

Immunohistochemistry The G cells were identified as described earlier (14) by means of the indirect immunoperoxidase technique using anti gastrin serum No 2717 raised in rabbits against synthetic human gastrin I (18) which in radioimmunoassay acts as anti gastrin No 2604 although with a slightly increased cross reaction with cholecystokinin compared to antibody No 2604 (20) 3 amino 9 ethyl carbazol (Sigma Chemical Comp St Louis USA) was used for the development The following controls were employed a) exclusion of the anti gastrin serum b) reaction between anti gastrin serum and gastrin (synthetic human gastrin I Calbiochem Bering Corp USA) 10 μ g per ml diluted anti serum before applying to the sections c) letting the anti gastrin serum react with cholecystokinin octapeptide (Calbiochem Bering Corp USA) 15 μ g per ml diluted anti serum before applying to the sections

Morphometry This was carried out as described earlier (15) where the error of measurement was characterized with regard to between and within observer variation as well as within patient variation and showed that acceptable levels of variation in endoscopic biopsies were reached when a minimum number of about 200 G cell profiles were counted The following variables were estimated 1) volume density (V_v) of G cells which relate the volume of G-cells to that of antrum mucosa volume 2) Numerical density on area (N_A) i.e the number of G cell profiles per antral

mucosal area 3) Numerical density (N_v) i.e the number of G cells per antral mucosal volume and finally 4) Mean G cell volume (\bar{V}) The coefficient of error (CE) was determined for the variable with the greatest variation \bar{V} in every count (15) The proportion between the long and short axis of the G cell profile was determined from randomly selected fields of vision using a Reichert projecting microscope to ensure that this proportion did not change during treatment with cimetidine

Section thickness This was controlled by a Tesatron Electronic Tester (TESA S A Renens Schweiz)

Statistical methods The Wilcoxon test for paired data was used Differences were considered statistically significant when $P < 0.05$

RESULTS

The control staining a) and b) were negative In c) a 10% reduction of the G cell profiles was seen indicating some degree of cross reactivity between anti gastrin and cholecystokinin on the cellular plane In the morphometric analysis 30 pairs of patients fulfilled the minimum number of G-cell counts giving acceptable levels of error (15) only biopsies including muscularis mucosa were used for morphometry The median value of the proportion between the long and short axis of the G-cells was 1.63 (observed range 1.51 to 1.78) before treatment ($n = 179$) and 1.65 (observed range 1.49 to 1.99) during cimetidine treatment ($n = 194$) ($P > 0.1$) indicating the same proportion before and during treatment The median value of CE was 6% before (observed range 3 to 12%) and 6% during treatment (observed range 4 to 11%) The results of the morphometric analysis the fasting serum gastrin and acid secretion before treatment are seen

TABLE 1 Measurements before and during Treatment with Cimetidine

	Before treatment Median (observed range)	During treatment Median (observed range)	
Basal acid output (BAO) (mmol/h)	1.38 (0-9.3)		
Peak acid output (PAO) (mmol/h)	32.9 (10.9-67.9)		
Serum gastrin (pg/ml)	58 (27-165)	71 (39-155)	xx
Volume density of G cells (V_v) (% mucosal volume)	2.42 (1.42-3.21)	2.49 (1.55-4.37)	x
Number of G cells per area (N_A) (cells/mm ²)	294 (152-436)	332 (195-593)	xxx
Numerical density of G cells (N_v) (cells/mm ³)	23687 (11166-34727)	27149 (15492-50481)	xxx
Mean G cell volume (\bar{V}) (μ m ³)	1004 (790-1331)	896 (779-1052)	xxx

x $P > 0.10$ xx $P < 0.10$ xxx $P < 0.01$

n Table 1. It is seen that eight weeks of treatment with cimetidine results in a significant increase in V_A (13%) and N_V (15%) and a decrease in \bar{V} (11%). The latter is greater than the median value of CE before and during treatment. No change was found in the value of V_A . Beside alterations of G-cell density the morphology as seen in the light microscope were unchanged before as well as during treatment with cimetidine. Serum gastrin obtained in 26 pairs of patients was increased during treatment but the difference was insignificant.

DISCUSSION

Elevated serum gastrin caused by vagotomy or histamine H_2 -receptor antagonists is probably in

hyperplasia was found (5-8) whereas in another a decrease of G-cell density was reported (7). A difference in the sensitivity and specificity of the antagastin may be an explanation of the conflicting results as prerequisite to identification is a content of gastrin.

Several authors have demonstrated ultrastructural changes during stimulation and secretion from the G-cells especially in the granulae (4, 11, 13, 16, 25).

This study shows that cimetidine treatment of duodenal ulcer patients results in a G-cell hyperplasia and that the volume of the individual cell decreases to such an extent that the volume density remains unchanged. Assuming the antral mucosal volume remains the same both before and during treatment then the total G-cell volume will also remain unchanged. Wu *et al.* (27) also found unchanged volume density during medication of rats with metiamide but they report no calculation of the number of G-cells.

The G-cell hyperplasia after eight weeks of treatment with cimetidine and the elevated levels of serum gastrin even six weeks after withdrawal (6, 10) may be a factor of importance with regard to the frequently rapid recurrence of an ulcer at times presenting as perforation after short term treatment (23-26). In contrast, other authors (3) did not find a higher frequency of re-ulceration after a short successful course of cimetidine compared to a successful course of placebo. It has also been demonstrated that the parietal cell sensitivity to pentagastrin remains unchanged after short term treatment with cimetidine (1).

Further studies are needed to clarify an eventual

autonomous function of the increased number of G-cells after cimetidine treatment as a factor in recurrence of the ulcer.

It is concluded that cimetidine treatment of duodenal ulcer patients results in antral gastrin cell hyperplasia without changes in the total G-cell volume and that this hyperplasia may be a factor of importance with regard to the rapid recurrence of many ulcers after cessation of the treatment.

The anti gastrin serum No. 2717 was kindly donated by Professor J. F. Rehfeld, Institute of Biochemistry, Aarhus University. The authors wish to thank Professor Daniel Andersen, Dept. of Surgical Gastro-enterology, Odense University Hospital, for his advice and review of the manuscript. The study was supported by grants from the Danish Medical Research Council (Journal No. 512 5255 and 512 679).

REFERENCES

1. Aadland E. & Berstad. Parietal and chief cell sensitivity to pentagastrin stimulation before and after cimetidine treatment for duodenal ulcer. *Scand J Gastroent* 14: 111-114 1979.
2. Andersen D., Høstrup H. & Amdrup E. The Aarhus County Vagotomy Trial II. An interim report on reduction in acid secretion and ulcer recurrence rate following parietal cell vagotomy and selective gastric vagotomy. *World J Surg* 2: 91-100 1978.
3. Bardhan K. D., Blum A., Gillespie G., Larkworthy W., Mekel R., Moshal M., Smith P. M., Venables C. W., Van Tongeren J. M. H. & Watan A. Long term treatment with cimetidine in duodenal ulceration. *Lancet* i: 900-901 1977.
4. Bastie M. J., Balas D., Senegas Bala F., Bertrand C., Pradajol L., Frexinos J. & Ribet A. A cytophysiological study of the G-cell secretory cycle in the antrum mucosa of the hamster and of the rat. *Scand J Gastroent* 14: 35-48 1979.
5. Becker H. D., Arnold A., Borger H. W., Creutzfeldt C., Schafmayer A. & Creutzfeldt W. Influence of truncal vagotomy on serum and antral gastrin and G-cells. *Gastroenterology* 72: 811 1977.
6. Buchanan K. D., Spencer A., Ardill J. & Kennedy T. L. Hypergastrinaemia due to cimetidine. *Gut* 19: A 437 1978.
7. Creaghe S. B., Greenburg A. G., Brown D., Peskin G. W. & Saik R. P. Vagotomy and the antral G-cell. *J Surg Res* 26: 528-531 1979.
8. Deforce P., Willems G. & deGraf J. Antral gastrin cell proliferation after vagotomy in rats. *Digestion* 18: 27-34 1978.
9. Feldman M., Dickerman R. M., McClelland R. N., Cooper K. A., Walsh J. H. & Richardson C. T. Effect of selective proximal vagotomy on food stimulated gastric acid secretion and gastrin release.

- in patients with duodenal ulcer *Gastroenterology* 76 926-931 1979
- 10 Forrester J A H, Fettes M R, McLoughlin K P & Heading R C Effect of long term cimetidine on gastric acid secretion, serum gastrin and gastric emptying *Gut* 20 404-407 1979
- 11 Firssman W G & Orci L Ultrastructure and secretory cycle of the gastrin producing cell *Zellforsch* 101 419-432 1969
- 12 Norman M G, Hansky J & Strickland R G Progressive increase in the functional G cell mass with age in atrophic gastritis *Gut* 14 549-551 1973
- 13 Miyazumi H, Watanabe Y, Sawada Y, Kato A, Shiono A & Kondo A Ultrastructure of G cells and the mechanism of gastrin release before and after vagotomy with pyloroplasty *Arch Histol Jap* 40 51-62 1977
- 14 Nilsen H O, Teglbjærk P S & Håkø F Gastrin and enteroglucagon cells in human antra with special reference to intestinal metaplasia *Scand J Gastroent Suppl* 54 101-103 1979
- 15 Nilsen H O, Halken S & Lorentzen M Quantitative studies of the gastrin producing cells of the human antrum. A methodological study *Acta path microbiol scand Sect A* 88 255-261 1980
- 16 Oliveira M C & Avelly I A morphometric study of the effects of bile on the G cells of the antral mucosa of the dog *World J Surg* 2 223-231 1978
- 17 Pilak J M, Haffbrand A V, Reed P I, Bloom S & Pears A G E Qualitative and quantitative studies of antral and fundic G cells in pernicious anaemia *Scand J Gastroent* 8 361-367 1973
- 18 Rehfeld J F, Stal L & Rubin B Production and evaluation of antibodies for the radioimmunoassay of gastrin *Scand J Clin Lab Invest* 36 221-232 1972
- 19 Rehfeld J F Disturbed islet cell function related to endogenous gastrin release. Studies on insulin secretion and glucose tolerance in pernicious anaemia *J Clin Invest* 58 41-49 1976
- 20 Rehfeld J F Personal communication
- 21 Richardson C T, Walsh J H & Hicks M I The effect of cimetidine, a new histamine H₂ receptor antagonist, on meal stimulated acid secretion, serum gastrin and gastric emptying in patients with duodenal ulcer *Gastroenterology* 71 19-23 1976
- 22 Sark R P, Huseyfel N & Paskin G H Human gastrin responses after ulcer surgery *J Surg Res* 22 352-356 1977
- 23 Saunders J H B & Wormsley A G Long term effects and after effects of treatment of duodenal ulcer with metiamide *Lancet* i 765-767 1977
- 24 Stad L F & Rehfeld J F Determination of gastrin in serum. An evaluation of the reliability of a radioimmunoassay *Scand J Gastroent* 8 101-112 1973
- 25 Track N S, Creutzfeldt C, Arnold R & Creutzfeldt W The antral gastrin producing G cell. Biochemical and ultrastructural responses to feeding *Cell Tiss Res* 194 131-139 1978
- 26 Wallace W A, Orr C M E & Burn A R Perforation of chronic peptic ulcers after cimetidine *Brit Med J* 2 865-866 1977
- 27 Witt L, Heit P U, Hattler F, Olah A J, Varla L, Werner O & Hackl W H Effects of prolonged administration of metiamide on serum gastrin, gastrin content of the antrum and gastric corpus and G cell population in the rat *Gastroenterology* 76 945-949 1979

IN SITU IDENTIFICATION OF INFLAMMATORY CELLS IN MALIGNANT, NON-LYMPHOID HUMAN TUMOURS

J. L. SVENNEVIG

University of Oslo, Institute for Experimental Medical Research and Department of Pathology, Ullevål Hospital, Oslo, Norway

Svennevig J. L. *In situ* identification of inflammatory cells in malignant, non-lymphoid human tumours. Acta path. microbiol. scand. Sect. A 88: 387-395, 1980.

Inflammatory cells (the term is considered to include lymphocytes, plasma cells, macrophages, mast cells and PMN) were identified and quantitated in sections from human carcinomas. Two types of cellular infiltrates are described. In the stroma surrounding the cancer tissue (peritumoural) and to a lesser degree also within the malignant tissue (intratumoural), lymphocytes, plasma cells, macrophages and mast cells dominated, whilst numerous polymorph-nucleated cells (PMN) and aggregates of macrophages characterized central tumour necroses. The demonstration of both T-lymphocytes and macrophages in and around the cancer tissue supports the view that a local immune reaction is initiated by the tumour, and the consistent finding of IgG, IgA and IgM plasma cells at the borders of the carcinomas indicates that plasma cells are also part of an immune response at the tumour site. This view is further supported by the demonstration of an increased proportion of IgG-containing plasma cells in the stroma of colon tumours compared with normal mucosa.

Key words: Inflammatory cells, non-lymphoid tumours.

J. L. Svennevig, Institute for Experimental Medical Research, Ullevål Hospital, Oslo 1, Norway.

Received 13 v 80 Accepted 6 vi 80

Several reports have indicated that a cellular response may take place in and around malignant tumours. The nature of this host response has only been sparsely investigated and it is not proven whether human tumours possess new antigenic characteristics which could explain the induction of local reaction.

Many investigators have been able to demonstrate a positive correlation between the degree of lymphoreticular infiltration and prognosis (Underwood 1974). By analyzing these cell infiltrates, the type of reaction taking place within human tumours may be better understood. Until now most studies have dealt with the *in vitro* characterization of inflammatory cells liberated from the neoplasms. The aim of the present study was to identify the different cell types infiltrating human malignant tumours and to study the distribution of these cells within the tumours and in the peritumoural stroma in contact with the cancer tissue.

MATERIAL AND METHODS

Non-lymphoid tumours from 14 patients undergoing operation in Departments 2 and 3, Ullevål Hospital, were examined. The material included 5 adenocarcinomas of the colon, 3 adenocarcinomas and 1 ductal carcinoma of the breast and 4 bronchial carcinomas (2 squamous cell carcinomas, 1 adenocarcinoma and 1 poorly differentiated carcinoma).

Lymphocytes. Lymphocytes were counted in 6 μ m thick sections.

Stroma. Stroma tissue in contact with the cancer tissue (peritumoural).

T-lymphocytes. Fresh biopsies from all tumours were fixed in formalin-sucrose overnight, then in gum-sucrose overnight and frozen sections were incubated for 22 hours with a naphthyl acetate (Sigma). The method was tested on normal lymph nodes and spleen where it gave distinct red-brownish dots in the cytoplasm of the

lymphocytes in T dependent areas while cells in follicular areas were negative. The ANAE method (Knowles and Holck 1978) was used to identify T cells in sections from all tumours and the number of T cells was expressed as percentage of all lymphocytes.

B lymphocytes This population was included among esterase negative lymphocytes together with null lymphocytes. No specific method for the demonstration of lymphocytes with membrane bound Ig was available when non lymphoid tissues were considered even when these cells could be easily demonstrated in cell suspensions from the same type of tumours (Sjennetig et al 1978, 1979).

Plasma cells IgG, IgA and IgM containing cells were identified in and around the cancer tissue by using the peroxidase antiperoxidase method of Taylor and Burns (1974) on formalin fixed paraffin embedded material. Six μ m thick sections were mounted on gelatine chromalum treated coverslips, deparaffinized (xylol) dehydrated (abs. alcohol) and treated for 17 minutes with a 0.1% pronase (Boehringer Mannheim GmbH) solution. Endogenous peroxidase was blocked by placing the preparations in 3% hydrogen peroxide in methanol for 25 minutes. The sections were then covered with heavy chain specific rabbit anti human IgG, IgA and IgM and with kappa and lambda chain specific antisera (DAKO immunoglobulins A/S) thereafter with swine anti rabbit IgG (DAKO) and finally with soluble complex of horseradish peroxidase and rabbit anti horseradish peroxidase (DAKO) for 30 minutes respectively each step performed at room temperature and followed by a 15 minute wash in trisbuffer pH 7.6.

The reaction was made visible with diaminobenzidine (Sigma) and hydrogen peroxide and the preparations were faintly counterstained with haematoxylin, dehydrated, cleared and mounted in canadabalsam.

The specificity of the antisera was tested on different myelomas where they gave selective staining of cells containing one Ig class and on normal colon mucosa. All preparations were further tested by changing the

heavy chain specific antisera with rabbit Ig (DAKO) with phosphate buffered saline to ensure that no non specific reaction had taken place.

Both plasma cells and lymphocytes were counted corresponding central and peripheral fields in paraffin sections from each tumour and the number of different cell types was given as the average cells per field.

Mast cells The 6 μ m thick sections were deparaffinized, rinsed in alcohol and stained for 10 (5-30) minutes with pinacyanol erythrosinate (Bensley 1952), differentiated in alcohol, rinsed in xylene and mounted in canadabalsam.

This method lead to purple staining of mast cells whereas both epithelial and muscle cells were sky blue with bright blue nuclei.

Macrophages A representative sector of each tumour was fixed in formalin, acetone overnight then in glycerol, sucrose overnight and frozen sections were incubated for 22 hours with a naphthyl butyrate for demonstration of diffuse esterase activity (Sjennetig et al 1979). Monocytes/macrophages were counted in 10 central and peripheral fields selected at random.

RESULTS

In all 14 tumours studied the stroma surrounding the malignant cells contained varying numbers of inflammatory cells and these cell infiltrates were mainly composed of lymphocytes, plasma cells, macrophages, some mast cells and PMN. The majority of PMN were neutrophils except for colorectal carcinomas where a large portion of PMN were eosinophils. There were no evident signs of tumour cell necrosis on the borders between the host cells and the neoplastic cells. All cell types were also found to infiltrate the cancer tissue however the intratumoural cell reaction was sparse compared

TABLE 1 The Number of Inflammatory Cells/Microscopic Field (at Magnification 12.5 \times 40) in and around 14 Human Carcinomas (Mean Value and Range)

		Lymphocytes	Plasma cells	Macrophages	Mast cells	PMN
5 colon carcinomas	Intratumoural	4 (0-8-7)	1.4 (0-3)	9 (1-30)	0.1 (0-0.3)	4 (1-8)
	Peritumoural	35 (20-46)	36 (22-82)	26 (11-46)	4.5 (0.2-14)	10 (2-23)
	Adjacent mucosa	19 (5-35)	56 (29-77)	10 (1-19)	7 (1-16)	10 (2-14)
5 mammary carcinomas	Intratumoural	3.5 (0.6-9)	0.3 (0-0.6)	0.8 (0-2)	0.9 (0-2)	0.2 (0-0.5)
	Peritumoural	25 (2-60)	11 (3-17)	8 (1.5-20)	5 (0.4-7)	1.0 (0-1.6)
4 bronchial carcinomas	Intratumoural	8 (0.8-23)	5.6 (0.8-12)	10 (8-16)	0.1 (0-0.2)	2 (0.5-4)
	Peritumoural	76 (11-150)	53 (31-66)	17 (11-22)	4 (0.8-8)	2.5 (1-4)

th the peritumoural stromal reaction (Table 1) the average number of inflammatory cells found in each tumour was reproducible by repeated counting. Central tumour necroses were frequently found and these areas were dominated by aggregates of PMN and macrophages. Because of necrosis and cell debris it was not possible to quantitate the number of cells in these areas.

There were some differences between the three tumour types studied. All five colon carcinomas which belonged to Dukes stage C contained large numbers of lymphocytes, plasma cells and macrophages (Fig. 1). These cells were mainly found in the stroma between and around the neoplastic tissue (peritumoural) where lymphocytes often formed dense zones in close contact with the cancer tissue. The strongest stromal reaction was seen in the superficial parts of the tumours while the cell infiltrates surrounding groups of cancer cells infiltrating musculature and pericolic fat tissue were sparse.

Large macrophages often contained drops of lipid like material and macrophages were occasionally found diffusely distributed within the malignant tissue (Fig. 1A).

Lymphocytes and plasma cells dominated in colon carcinomas. On an average 33% of the intratumoural and 35% of the peritumoural lymphocytes were T-cells according to the ANAE staining pattern. In some lymphocyte rich areas T cells dominated (Fig. 1B).

Accumulations of IgG and IgA plasma cells were found close to the cords and nests of cancer cells (Fig. 1C-D) while IgM containing plasma cells were most often found as single cells in the stroma. Only a few Ig-containing plasma cells of all three types were found to infiltrate the cancer tissue.

There were no differences with regard to the total number of cells in the 'transitional' mucosa between tumour and normal intestinal wall and the tumour stroma but the tumour stroma was richer in lymphocytes whereas the number of IgA containing plasma cells was decreased. The relative proportion of plasma cells containing IgG was therefore increased in the connective tissue of the tumours compared with the non malignant 'transitional' mucosa adjacent to the tumour and normal mucosa taken at least 8 cm proximally or distally from the tumour (Table 2).

A few single mast cells were located within the neoplastic tissue but the majority of these cells were also found in the peritumoural stroma. The mast cells contained typical metachromatic granules which made the identification of the cells easy (Fig. 1E). Although a significant accumulation of mast cells had taken place at the edges of the colon

TABLE 2 *The Relative Proportion of Plasma Cells with IgG, IgA and IgM in Peritumoural Stroma Mucosa adjacent to Tumour and Normal Mucosa*

	IgG	IgA	IgM
Colon carcinomas	51	40	9
Adjacent mucosa	23	66	11
Normal mucosa	3	93	4
Mammary carcinomas	31	62	7
Bronchial carcinomas	41	36	23

carcinomas the highest number of mast cells was found in the transitional mucosa from the same cases.

Only a few PMN were located within and around the cancer tissue. However large ulcero necrotic areas of various sizes were present in all colon tumours. These areas were dominated by numerous PMN and macrophages, some lymphocytes and cell debris (Fig. 1F). The necroses also contained a few IgG and IgA plasma cells.

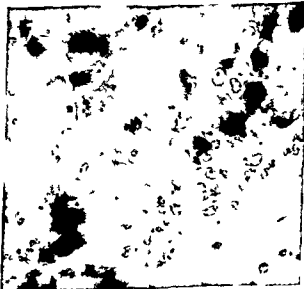
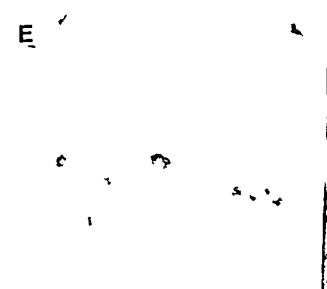
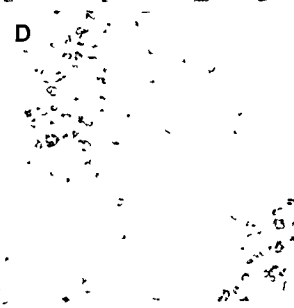
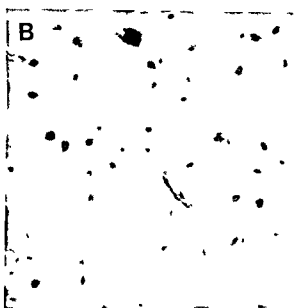
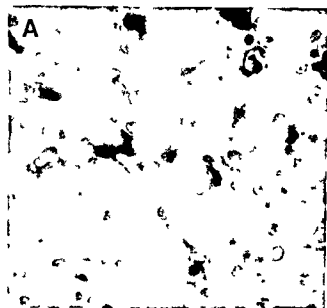
The average number of all cell types identified in and around the colon carcinomas is given in Table 1.

Dense peritumoural cell infiltrates were also present in the four bronchial carcinomas. Similar to the cell infiltrates found in colon tumours, lymphocytes, plasma cells and macrophages dominated except for necrotic areas with numerous PMN. A relatively high number of plasma cells were present in these tumours and the relative proportion of IgG containing plasma cells was comparable with the proportion found in colon tumours (Table 2). Of the lymphocytes on an average 36% had T-cell markers.

Although the morphology was less distinct with regard to the differentiation in a stromal and a neoplastic tissue, the histological picture of the bronchial tumours gave the impression that an evident accumulation of mononuclear cells had taken place at the borders of the cancer tissue.

Mast cells heavily loaded with purple stained granula were numerous in the peritumoural stroma. The cells were oval or spindle shaped and most cells were diffusely distributed in the stroma while some cells were found to line the cancer tissue and the stromal vessels. They were only occasionally seen in necrotic areas of the tumours.

The mildest inflammatory cell reaction was found in mammary carcinomas. In these tumours practically no central tumour necroses were present. Lymphocytes, plasma cells and macrophages were found in the stroma between the cancer cords and around the cancer tissue. The proportion of plasma cells containing IgG was 31% and IgA 62%.



- I Inflammatory cells in and around a colon carcinoma
 Intratumoural infiltration of macrophages and lymphocytes a naphthyl butyrate esterase staining 6 μ m cryostat section \times 500
 Peritumoural lymphocyte zone with ANAE positive T-cells 6 μ m cryostat section \times 1250
 IgG-containing plasma cells lining the cancer tissue (immunoperoxidase 6 μ m paraffin section \times 500
 Neoplastic tissue with groups of IgA-containing plasma cells and lymphocytes Technique as Fig C
 Mast cells lining the cancer tissue Pinacyanol staining 6 μ m paraffin section \times 500
 F Intratumoural necrotic area with aggregates of macrophages and PMN Technique as Fig A

PMN A relatively constant proportion of lymphocytes both in (33%) and around the cancer tissue (38%) had T-cell markers. Most macrophages were diffusely distributed in the connective tissue of the tumours.

Of the plasma cells IgA-containing cells dominated, followed by IgG and IgM. In both mammary and colon tumours there was a slight dominance of lambda chain Ig, whereas plasma cells with kappa chain Ig were most frequent in bronchial tumours.

When the total number of inflammatory cells in the tumours was considered (Table 3) the intratumoural cell infiltration of mammary carcinomas expressed as cells/microscopic field was significantly weaker than the infiltration found in bronchial and colon carcinomas ($p < 0.05$). This was also the case when the intratumoural reaction was expressed as number of inflammatory cells/number of tumour cells in mammary carcinomas on an average 1% of the tumour cells were of an inflammatory nature compared to 6 and 9%

respectively in colon and bronchial carcinomas (Table 3).

The stromal infiltration of inflammatory cells was 6-8 times stronger than the intratumoural infiltration for all three tumour types when the necrotic areas were not considered.

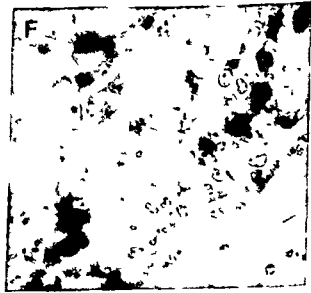
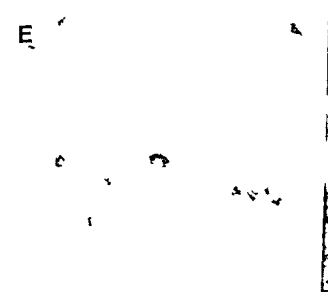
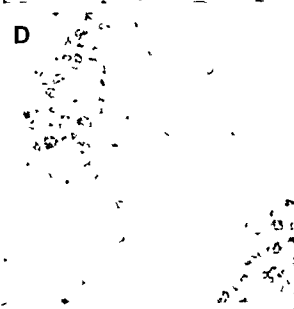
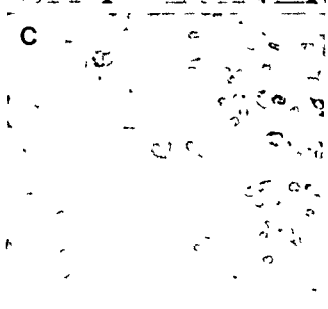
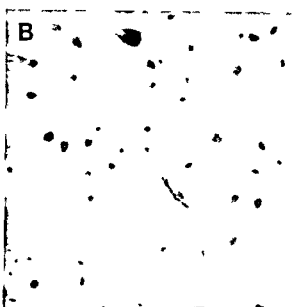
DISCUSSION

The present work represents an attempt to quantify and characterize the inflammatory cells infiltrating and surrounding the malignant tissues in a series of human non lymphoid tumours. By studying the inflammatory cells in corresponding microscopic fields by means of different staining techniques performed on serial tissue sections we were able to analyse the nature of the infiltrates and to compare the local cell reaction of different tumour types.

The infiltrates which are often termed «mononuclear cell infiltrates» or «round cell infiltrates» were composed mainly of lymphocytes, plasma cells and macrophages but varying numbers of mast cells and PMN were also present. Most cells were found in the stroma between and around the cords and nests of cancer cells (peritumoural). No evident signs of cell necrosis were present on the borders between host cells and neoplastic cells and a few inflammatory cells were diffusely distributed among the cancer cells. Even electronmicroscopic studies have failed to demonstrate any cytotoxic effect of inflammatory cells close to neoplastic cells (Carr and Underwood 1974). However in some tumours central necroses were found and these areas were dominated by aggregates of PMN and macrophages. While a marked lymphocyte infiltration may improve prognosis the presence of

TABLE 3 The Total Number of Inflammatory Cells in Areas mainly Composed of Neoplastic Cells and in the Peritumoural Stroma (Mean Value and Range)

Tumour type	Cancer tissue		Peritumoural stroma
	Inflammatory cells	Cancer cells	Inflammatory cells
Colon carcinomas	19 (6-41)	301 (180-529)	112 (83-164)
Mammary carcinomas	6 (3-10)	497 (318-778)	50 (17-94)
Bronchial carcinomas	26 (9-51)	282 (101-356)	153 (59-206)



d Gillespie 1975) and human tumours (Lauder et al 1977)

The accumulation of mast cells in chronic inflammation and around carcinomas was described already by Ehrlich in 1865 (see Selve 1965) but the exact role of the mast cell reaction in malignancies is still not clear. An increase in the number of mast cells has already been shown to take place prior to the development of experimental carcinomas (Cramer and Simpson 1944) and in carcinoma *in situ* (Dunn and Montgomery 1957, Graham and Graham 1966) the mast cell reaction is thus suggested to be associated with a defensive process against cancer (Cramer and Simpson 1944, Fisher and Fisher 1965, Graham and Graham 1966). However the release of granular material from tissue mast cells has been shown to promote tumour growth (Syhen 1945) while heparine binding substance may inhibit tumour growth (Csaba et al 1960).

The distribution pattern of the inflammatory cells in the present series of tumours was comparable to the type of reaction found in autochthonous rat transplants of low antigenic tumours where mononuclear cells tended to scatter around the tumour whereas high antigenic tumours were associated with massive immigration of mononuclear cells which extended throughout the tumour (Kikuchi et al 1976). A similar distribution of lymphocytes and macrophages has been described for growing murine tumours (Wood and Gollahon 1978).

The present study demonstrated that the «round cell» infiltrates surrounding and to a lesser degree infiltrating the malignant human tumours mainly consisted of lymphocytes (including T-cells), plasma cells and macrophages. These cells formed the peri-/intertumoural zones together with a few mast cells and PMN, while PMN and macrophages dominated in central ulcero-necrotic areas. The latter type of reaction may be secondary to the necrosis.

On the basis of these findings and in accordance with some previous reports (Burg and Braun Falco 1972, Elston 1968, Joachim et al 1976, Takahashi 1961) it seems difficult to speak of tumour

quite different mechanisms

REFERENCES

- Bensley S H Pinacyanol erythrosinate as a stain for mast cells *Stain Technol* 27 269-273 1952
- Braathen L R Førre O & Nævig J B An anti human T lymphocyte antiserum *In situ* identification of T cells in the skin of delayed type hypersensitivity reactions chronic photosensitivity dermatitis and mucositis fungoides *Clin Immunol Immunopathol* 13 211-219 1979
- Burg G & Braun Falco O The cellular stromal reaction in malignant melanoma A cytochemical investigation *Arch Derm Forsch* 245 318-333 1972
- Carr I & Underwood J C E The ultrastructure of the local cellular reaction to neoplasia *Internat Rev Cytol* 37 329-347 1974
- Catalona W J Mann R Nime F Potvin C Harris J I Gomolka D & Eggleston J C Identification of complement receptor lymphocytes (B cells) in lymph nodes and tumor infiltrates *J Urol* 114 915-921 1975
- Cramer W & Simpson W L Mast cells in experimental skin carcinogenesis *Cancer Res* 4 601-616 1944
- Csaba G Acs T Horvath C & Kapa E Some new data concerning the biology of tumours The effects of heparine inhibitors on tumour growth *Brit J Cancer* 14 367-375 1960
- Dunn M R & Montgomery P O B A study of the relationship of mast cells to carcinoma *in situ* of the uterine cervix *Lab Invest* 6 542-546 1957
- Eccles S A & Alexander P Macrophage content of tumours in relation to metastatic spread and host immune reaction *Nature* 250 667-669 1974
- Edelson R L Smith R W Frank M M & Green I Identification of subpopulations of mononuclear cells in cutaneous infiltrates I Differentiation between B cells T cells and histiocytes *J Invest Dermatol* 61 82-89 1973
- Elston C W Cellular reaction to choriocarcinoma *J Path* 97 261-268 1968
- Fisher E R & Fisher B Role of mast cells in tumor growth *Arch Pathol* 79 185-191 1965
- Fisher E R Palekar A S Gregorio R M Redmond C & Fisher B Pathological findings from the national surgical adjuvant breast project (protocol no 4) IV Significance of tumor necrosis *Human Path* 9 523-530 1975
- Gersl B Eng L F & Bigbee J W Tumour associated immunoglobulins in pulmonary carcinoma *Cancer Res* 37 4449-4455 1977
- Graham R M & Graham J B Mast cells and cancer of the cervix *Surg Gynecol Obstet* 123 3-9 1966
- Green F H Y Whitehead S & Fox H Abnormalities of the local immune system in intestinal neoplasia a morphological study *J Path* 122 55-62 1977
- Hayry P & Tøttemann T H Cytological and functional analysis of inflammatory infiltrates in human malignant tumours I Composition of the inflammatory infiltrates *Eur J Immunol* 8 866-871 1978
- Hersh E M Gutterman J U Mavligit G M &

tumour necrosis is considered to be an ominous prognostic sign (Fisher *et al* 1975). Except for these necroses which may be explained by insufficiency of blood supply in growing tumours the cells dominating the tumour infiltrates were mainly identical to the cells known to act as mediators of cellular and humoral immunity suggesting that a local host reaction to the neoplastic tissue may take place. The present findings are in agreement with the results of our previous works demonstrating T and B lymphocytes, macrophages and PMN in cell suspensions from different human non lymphoid tumours (Sjennveig *et al* 1978, 1979; Sjennveig and Sjaar 1979).

The significance of lymphocytic infiltrates in human malignant tumours has been discussed for many years. Most but not all studies confirm the prognostic advantage of dense mononuclear cell infiltration (Underwood 1974).

We were able to demonstrate T lymphocytes in all tumours. On an average 35% of the peritumoural and 33% of the intratumoural lymphocytes were T-cells which is in contrast to some previous studies using T-cell antisera (Husby *et al* 1976; Schoorl *et al* 1976). However our findings are in agreement with several works on lymphocytes liberated from human non lymphoid tumours reporting that most often less than half of the tumour lymphocytes were T-cells (Havry and Totterman 1978; Hersh *et al* 1975; Sjennveig *et al* 1978, 1979; Jost *et al* 1977 a, b). The E rosette technique which is the most important marker for T lymphocytes in cell suspensions (Jondal *et al* 1972) may fail when applied on tissue sections (Edelson *et al* 1973; Walker 1976) and well characterized antisera against human T lymphocytes have until recently been difficult to obtain (Braathen *et al* 1979).

By isolating lymphocytes from disaggregated tumours we have previously found that 5–30% (mean 11%) of the lymphocytes had membrane bound immunoglobulin. According to some reports B-cells may be identified in tissue sections by means of immunofluorescence or immunoperoxidase techniques however the term B-cell has also included cells with cytoplasmatic Ig (Husby *et al* 1976). We find it difficult to identify lymphocytes with membrane bound Ig safely in tissues other than lymphoid even when the same technique may be used to identify Ig producing cells (plasma cells) in the same sections. The identification of B lymphocytes by binding AEC rosettes to tissue sections (Catalona *et al* 1975; Siheira *et al* 1972; Singl *et al* 1977) may be useful for lymphoid tissues or when groups of cells are studied but the technique is less suitable for the study of single cells.

The role of plasma cell infiltration in and around malignant tissues has been sparsely investigated and there are conflicting reports with regard to content of plasma cells in human tumours. Gerstl *et al* (1977) were able to demonstrate plasma cells or near tumour tissue in only 6 out of 12 cases of bronchial squamous cell carcinomas while Schoorl *et al* (1976) reported the finding of a small but constant number of plasma cells containing IgA and IgM in a series of breast carcinomas or occasionally were IgG producing cells found. Rognum *et al* (1979) found the number of Ig producing cells significantly increased in the non malignant stroma adjacent to colon carcinomas compared to normal mucosa whereas Weiss Carrington *et al* (1976) and Green *et al* (1977) found the number of plasma cells markedly decreased. In nasopharyngeal carcinomas plasma cells of IgA (Ho *et al* 1978) and IgG (Konorza *et al* 1979) have been reported to dominate.

There are conflicting reports concerning the correlation between the number of plasma cells and the amount of tumour associated Ig (Gerstl *et al* 1977; Hurlman *et al* 1976; Roberts *et al* 1973) and it is still not clear whether tumour bound Ig is associated with an *in situ* expression of humoral immunity (Witz 1977) or whether it may act as a blocking factor of cellular cytotoxicity (Romsdal and Cox 1975).

The relative proportions of IgG, IgA and IgM containing plasma cells in colon mucosa are shown in Table 2. The results are in agreement with the findings of Rognum *et al* (1979) who also found a relative increase of IgG containing plasma cells in the mucosa adjacent to the tumour.

The present study demonstrated a further increase of the portion of IgG producing plasma cells in the tumour stroma and the demonstration of the relatively large portion of IgG-containing plasma cells in the tumour stroma contributes to the view that there exist stimulatory factors bypassing the secretory IgA immune system (Rognum *et al* 1979).

Macrophages were easily identified in the tissue sections by demonstration of their diffuse esterase activity. Other authors have used the Fc receptor (EA rosette binding to tissue sections) as a marker for macrophages (Catalona *et al* 1975; Roubin *et al* 1975; Singl *et al* 1977). These results may be difficult to interpret as other cell types in human tumours may also carry Fc receptors (Tunder *et al* 1974; Vose *et al* 1977 a, b). Although the significance of macrophages in malignant tumours is still under discussion some recent reports emphasize their prognostic significance for both experimental (Eccles and Alexander 1974; Wood

1. I P Tumour bound immunoglobulins *in situ*
expressions of humoral immunity Advanc Cancer
Res 25 95-148 1977

Wood G W & Gillespie G Y Studies on the role of
macrophages in regulation of growth and metastases
of murine chemically induced fibrosarcomas Int J
Cancer 16 1022-1029 1975

Wood G W & Gollahon A A T lymphocytes and
macrophages in primary murine fibrosarcomas at
different stages in their progression Cancer Res 38
1857-1865 1978

- Barsales P B* Lymphocyte content of human solid tumours *Proc Am Assoc Cancer Res* 16 179 1975
- Ho H C Kwan H C & Ng M H* Immunohistochemistry of local immunoglobulin production in nasopharyngeal carcinoma *Brit J Cancer* 37 514-519 1978
- Hurlmann J Lichaa M & O ello L* *In vitro* synthesis of immunoglobulins and other proteins by dysplastic and neoplastic human mammary tissues *Cancer Res* 36 1284-1292 1976
- Husby G Hoagland P M Strickland R G & Williams R C Jr* Tissue T and B cell infiltration of primary and metastatic cancer *J clin Invest* 57 1471-1482 1976
- Joachim H L Dorsett B H & Paluch E* The immune response at the tumor site in lung carcinoma *Cancer* 38 2296-2309 1976
- Jondal M Holm G & Wigzell H* Surface markers on human T and B lymphocytes I A large population of lymphocytes forming non immune rosettes with sheep red blood cells *J Exp Med* 136 207-215 1972
- Kikuchi A Ishii Y Ueno H & Koshiba H* Cell mediated immunity involved in autochthonous tumor rejection in rats *Ann NY Acad Sci* 276 188-206 1976
- Knowles D M H & Holck S* Tissue localization of T lymphocytes by the histochemical demonstration of acid α naphthyl acetate esterase *Lab Invest* 39 70-76 1978
- Konora G Sesterhenn K Krueger G R F & Ablashi D V* Distribution of T and B cells and of immunoglobulin producing cells in tumor tissue of patients with nasopharyngeal carcinoma *J Cancer Res Clin Oncol* 93 195-204 1979
- Lauder I Aherne W Stewart J & Sainsbury R* Macrophage infiltration of breast tumours a prospective study *J clin Path* 30 563-568 1977
- Mueller J del Re G B Buerki H Keller H U Hess M W & Cottier H* Non specific acid esterase activity a criterion for differentiation of T and B lymphocytes in mouse lymph nodes *Europ J Immunol* 5 270 274 1975
- Roberts M M Bass E M Wallace I W J & Stevenson A* Local immunoglobulin production in breast cancer *Brit J Cancer* 27 269 275 1973
- Rognum T O Brandt-aeg P Baklien K & Hognstad J* The effect of the tumor on the lymph node 173 1979
- Romsdal M M & Cox I S* Immunoglobulins and other proteins isolated from the surface of human tumor cells *Collect Pap Ann Symp Fundam Cancer Res* 28 499-521 1975
- Roubin R Cesarini J P Fridman W H Pavie Fischer J & Peter H H* Characterization of the mononuclear cell infiltrate in human malignant melanoma *Int J Cancer* 16 61-73 1975
- Schoorl R de la Riviere A B von dem Borne A E G K & Felikamp Vroom T M* Identification of T and B lymphocytes in human breast cancer by immunohistochemical techniques *Am J Pathol* 101 529-544 1976
- Selye H* The mast cells pp 8 Butterworths Lond (1965)
- Silveira N P A Mendes N F & Tolnai M E* Tissue localization of two populations of human lymphocytes distinguished by membrane receptors *J Immunol* 108 1456-1460 1972
- Stingl G Wolff A Diem E Baumgartner G Knapp W* In situ identification of lymphoreticular cells in benign and malignant infiltrates by membrane receptor sites *J Invest Derm* 69 321-327 1977
- Svennevig J L Closs O Harboe M & Skaar H* Characterization of lymphocytes isolated from non lymphoid human malignant tumours *Scand J Immunol* 7 487-493 1978
- Svennevig J L Lovik M & Skaar H* Isolation and characterization of lymphocytes and macrophages from solid malignant human tumours *Int J Cancer* 23 626-631 1979
- Svennevig J L & Skaar H* Content and distribution of macrophages and lymphocytes in solid malignant human tumours *Int J Cancer* 24 754-758 1979
- Sykes B* Ester sulphuric acids of high molecular weight and mast cells in mesenchymal tumors: histochemical studies on tumorous growth *Acta radiol Suppl* 59 1-99 1945
- Taylor C R & Burns J* The demonstration of plasma cells and other immunoglobulin containing cells in formalin fixed paraffin embedded tissues using peroxidase labelled antibody *J clin Path* 27 14 20 1974
- Tonder O Morse P A Jr & Humphrey L J* Similarities of Fc receptors in human malignant tissue and normal lymphoid tissue *J Immunol* 113 1162-1169 1974
- Underwood J C E* Lymphoreticular infiltration in human tumours: prognostic and biological implications a review *Brit J Cancer* 30 538-548 1974
- Vose B M Vanky F Argov S & Klein E* Natural cytotoxicity in man: activity of lymph node cells and tumour infiltrating lymphocytes *Europ J Immunol* 7 753-757 1977a
- Vose B M Vanky F & Klein E* Human tumour lymphocyte interaction *in vitro* V Comparison of the reactivity of tumour infiltrating blood and lymph node lymphocytes with autologous tumour cells *Int J Cancer* 20 895-902 1977b
- Walker D M* Identification of subpopulations of lymphocytes and macrophages in the infiltrates of lichen planus lesions of skin and oral mucosa *Brit J Dermatol* 94 529-534 1976
- Weisz Carrington P Marshall E P & Lamm M E* Secretory immunoglobulins in colon neoplasms *Amer J Pathol* 85 303-316 1976

ULTRASTRUCTURE OF THE TAIL STUMP SPERM DEFECT IN THE BULL

ERIK BLOM and AKSEL BIRCH ANDERSEN

Statens veterinære Serumlaboratorium and Department of Biophysics, Statens Seruminstitut, Copenhagen, Denmark

Blom E & Birch Andersen A. Ultrastructure of the tail stump sperm defect in the bull. Acta path. microbiol. scand. Sect. A 89: 397-405, 1980.

A characteristic major sperm defect, with about 60% of the sperm cells showing a rudimentary tail stump, was found in two sterile Danish bulls of imported origin. The condition seldom occurs but seems to be widespread and has been observed in several breeds of cattle and in different animal species including man. Electron microscopy of ejaculated sperm and testicular tissue from one of the bulls has shown that a dysfunction of the centriolar apparatus during spermiogenesis is likely to be the cause of the defect. In ejaculated defective sperm the proximal centriole is often found connected with the normally transitory organelle, the centriolar adjunct. In the defective spermids the distal centriole has lost the faculty to form axonemal fibers, so that no tail formation can take place.

Key words: Sperm defect, tail stump, sterility in bulls, spermiogenesis, distal centriole, «dense granules», centriolar adjunct.

E. Blom, Statens veterinære Serumlaboratorium, Bulowsvej 27, DK-1870 Copenhagen V, Denmark.

Accepted as submitted 11 vi 80

In 1964 *Coubrough and Barker* (9, 10) described a characteristic sperm defect found in the semen of three Canadian bulls in which the majority of the sperms showed a rudimentary tail stump while the morphology of the sperm heads was normal. The bulls were of Ayrshire, Shorthorn and Holstein breeds respectively. Eleven years later a similar case was found in a sterile Danish Friesian bull *G*, the dam of which had been inseminated with imported American semen (6).

Recently another Danish case was found in an imported purebred Hereford bull. This bull was also reported totally sterile. For methods used for the evaluation of sperm morphology see ref. 5.

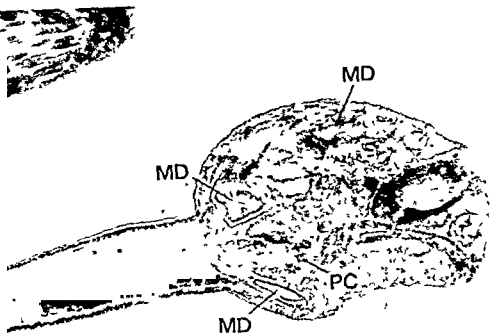
After publication of the first Danish case (6) we were informed of a German case in a Friesian bull (*G. H. Rieck* pers. comm.), a Swedish case in an SRB bull (*I. Settergren* pers. comm.) and an Australian case in a beef bull (*R. L. Fees* pers. comm.). In Brazil a similar defect has been demonstrated in the semen of two inbred sterile Zebu bulls (17).

This particular sperm defect has also been found in the rabbit (14), the stallion and the dog (3). In mice an arrest in the development of the sperm tail has been demonstrated in a new mutant, the «hopsterile» strain (13). This defect may be identical with the tail stump defect found in the other mammals mentioned. In two infertile Italian men a similar «short tail» sperm defect has been reported (2).

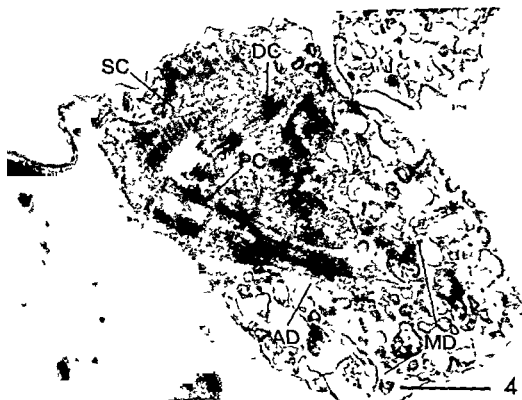
MATERIALS AND METHODS

For electron microscopy an ejaculate was collected when the bull *G* was 21 months old. The semen quality was very poor (Figs. 1 & 2): 60% of the cells showed the tail stump defect, the sperm concentration was low (250 ml/l/ml) and only 10% of the cells were motile. Samples were prefixed shortly after ejaculation by admixture of 7 ml of a solution of 0.1% glutaraldehyde in 3% sodium citrate to 2 ml of the ejaculate. The

3% sodium citrate) Blocks (about 1 mm³) with clusters of



3



4



Figures 1 and 2 Photomicrographs of India ink smears from ejaculates of bull G. More than half of the sperms have rudimentary tail stumps. 450 \times and 1130 \times . (From ref. 6)

cells were cut after solidification of the agar and fixation was continued overnight at 4 $^{\circ}$ C in 3% glutaraldehyde in 0.1 M sodium citrate. After a brief wash in 0.1 M barbiturate buffer pH 7.3 the blocks were fixed for 2 hours at room temperature in 1% osmium tetroxide buffered with barbiturate pH 7.3. *En bloc* treatment for 1 hour with 2% uranyl acetate in the same buffer was used before dehydration through a graded ethanol series. Finally the blocks were embedded in Vestopal W after propylene oxide treatment.

Three months after the first ejaculates were obtained unilateral castration was done (left testis weight 400 g). Small blocks of tissue from the testis and cauda epididymidis were excised and prefixed with 10 minutes after removal in 6% glutaraldehyde in 0.1 M cacodylate buffer pH 7.2. After one hour the blocks were subdivided into pieces of 1–2 mm³ and transferred to fresh 6% glutaraldehyde for 5 hours of continued fixation. The tissue blocks were stored overnight at 4 $^{\circ}$ C

in 0.2 M sucrose in 0.1 M cacodylate buffer pH 7.2 before they were postfixated for 2 hours at room temperature in 1% osmium tetroxide in 0.1 M barbiturate buffer pH 7.3 containing 4.5% sucrose. Finally treatment with uranyl acetate, dehydration and embedding was carried out as described for the ejaculated cells. Sections were cut with glass knives on an LKB ultratome III microtome, stained with magnesium uranyl acetate (12) and lead citrate (16) and examined with a Philips EM 300 electron microscope operated at 60 kV.

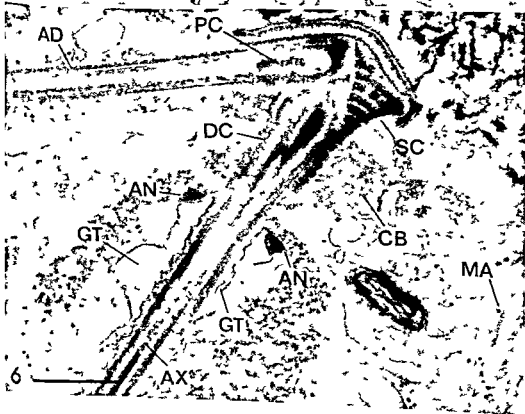
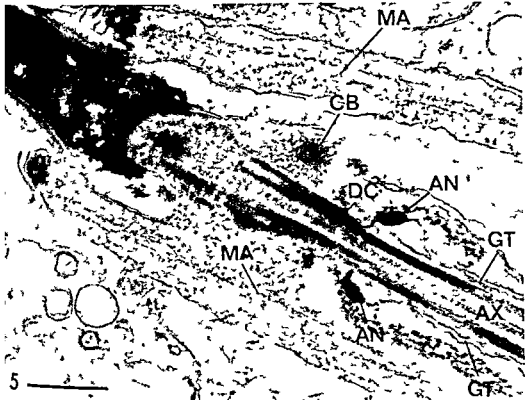
After another five months the bull was slaughtered and tissue from the remaining right testis (weight 410 g) was studied after preparation in the same way as the material from the left testis.

Testis tissue from two normal young bulls, one slaughtered before and one after bull G was fixed and prepared in the same way and used as control material.

Figures 3–9 are electron micrographs of sections of ejaculated sperm cells and spermidis from testis of bull G or from normal control bulls. Sections poststained with uranyl and lead salts. The bar on each micrograph represents 0.5 μ m. The following abbreviations are used throughout: ad = centriolar adjunct, an = annulus, ax = axonemal fibers, ch = chromatoid body, dc = distal centriole, gt = tail guide tube, ma = manchette, md = membranous debris, pc = proximal centriole, sc = segmented column.

Figure 3 Ejaculated cell, bull G. Note the proximal centriole and the membranous debris in the tail stump region. 45 000 \times .

Figure 4 Ejaculated cell, bull G. The centriolar adjunct is present on the proximal centriole. The distal centriole is seen distally to the segmented column. 45 000 \times .



RESULTS

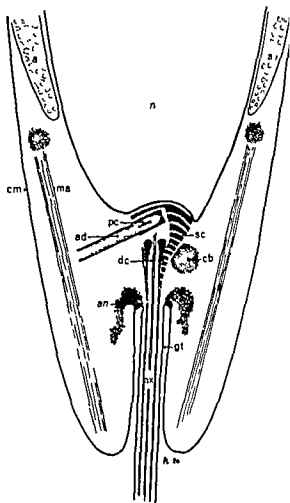
Electron microscopy of sections of *ejaculated sperms* from bull *G* (Fig. 3) clearly demonstrated the contents of the droplet-like rounded body surrounding the implantation region of most of the «tailless» heads. Frequently the normally transitory centriolar adjunct persisted and was attached to the proximal centriole (Fig. 4). Up to this time the centriolar adjunct has never been observed in ejaculated sperm from bulls. In some cases where the tail stump was cut rather peripherally it contained only an accumulation of different types of vesicles and membranous debris. Frequently a mixture of remnants of the capitulum, the segmented columns, and/or dispersed mitochondria together with membranous debris was found to be enclosed by the cell membrane of the tail stump (Fig. 4).

In sections of sperm cells from the *cauda epididymidis* the findings were similar, but the individual tail stumps appeared somewhat larger, as if their contents were not as condensed as demonstrated in the ejaculated cells.

The different phases of spermiogenesis were studied in normal as well as in abnormal testis tissue in order to determine at what stage the pathological material showed deviations from the normal development of spermiids, thus attempting to elucidate the genesis of the tail stump defect.

Through the early phases of spermiogenesis there were no differences between normal and pathological cells. However, from the acrosome phase when the transitory organelle the manchette was present (Fig. 5) differences were noted. In the bull this «manchette phase» as we prefer to call it, most probably includes the stages A_2 and A_3 described in a study on spermiogenesis in the blue fox (1). To our knowledge a similar ultrastructural differentiation in the bull has not been established.

In our normal material the implantation region of a spermid in the «manchette phase» contains the following organelles (Fig. 6 and Text Fig. 1). The proximal centriole with its transitory adjunct is situated distal to the basal plate. The so-called capitulum further contains the segmented column(s) with its implantation plate and the elongated distal centriole situated within the distal parts of the segmented columns. A transitory chromatoid body

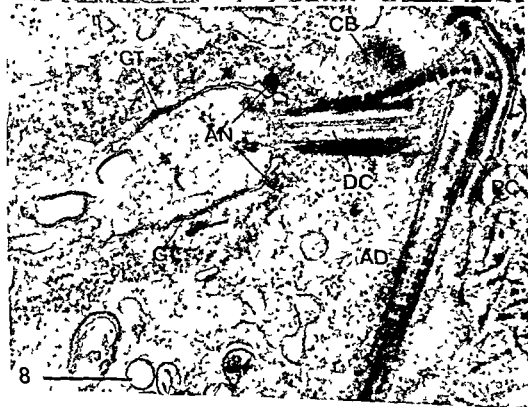
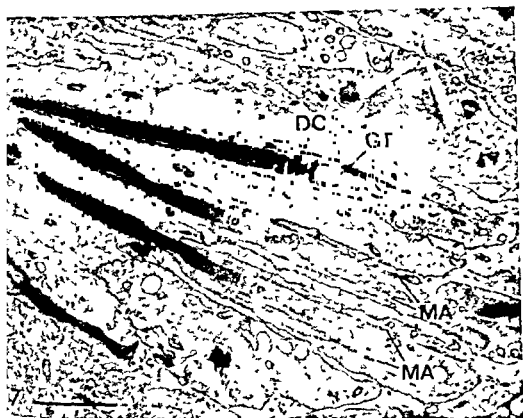


Text Fig. 1 Schematic drawing of the implantation region from a bull spermid in the manchette phase. Note the transitory organelles and the tail guide tube (see text). *a* = acrosome *ad* = centriolar adjunct *an* = annulus and accumulations of granular material *ax* = axonal fibers *cb* = chromatoid body *dc* = distal centriole *gt* = tail guide tube *ma* = manchette *n* = nucleus *pc* = proximal centriole *sc* = segmented column - Lars Blom sec. Erik Blom dir.

is usually present on one or both sides of the capitulum at the level of the distal centriole. In properly oriented sections the annulus is seen as two triangular dense bodies at the distal end of the segmented column. The annulus is at the same time situated at the proximal end of the cell membrane invagination which has at this stage been formed around the tail primordium. This configuration has

Figure 5 Testis normal bull. The implantation region at the manchette stage. Note the presence of distal centriole, axoneme, tail guide tube, annulus, manchette and a chromatoid body. 45 000 \times .

Figure 6 Testis normal bull. The implantation region at the manchette stage. Note the presence of proximal centriole, segmented column, and a chromatoid body. 45 000 \times .



been described as the »tail guide tube« (9) »the cytoplasmic invagination« (15) or the »cytoplasmic canal« (1)

In a favourably oriented section (close to the median axis of the tail) the axoneme can be followed from its base at the distal centriole and the annulus, and as far as the section and the field of view will allow (Figs 5 and 6) The number of axonemal fibers visible depends on the level and the thickness of the section

By light microscopy it was impossible to demonstrate typical pathological changes in the testis tissue from bull *G* However, the ultrastructure of the implantation region did show a pronounced difference between normal and abnormal spermiogenesis, especially from the »manchette phase« and further on Many spermiids in the manchette phase were studied both in sagittal (Fig 7) and in horizontal sections (Figs 8 and 9) In the most successful horizontal sections all the previously mentioned more or less transient organelles the manchette (Fig 9) the centriolar adjunct, the chromatoid body and the distal centriole, could be seen in the section At this stage the detailed morphology within the neck region seemed to be almost identical with that found for normal bulls, but one important difference was noted In the typical abnormal spermiid there was no axoneme formation The »tail« simply terminated as a short »stump« at the end of the distal centriole and no axonemal fibers were present within the tail guide tube which contained only cytoplasmic matrix and some ribosomes (Figs 8 and 9) Sagittal sections of three spermiids in the manchette stage one of them with an empty tail guide tube, are shown in Fig 7

In addition to this main type of abnormality another characteristically abnormal detail was occasionally demonstrated in cells at the later stages of spermiogenesis and in ejaculated sperm from the bull *G* Clusters of 300–500 Å dense granules resembling those described earlier (7) were often seen in association with disorganized accumulations of mitochondria This type of arrangement was usually present in the peripheral cytoplasm of abnormal spermiids or at the periphery of the cytoplasmic droplet of the »tailless« sperm cells

DISCUSSION

The tail stump defect in the bull is a characteristic sterilizing defect which affects only the sperm While the ordinary histological picture of the testis tissue from bull *G* seems normal, the ultrastructural studies have shown that spermiogenesis is never less seriously affected The genesis of the defect linked mainly to the function of the distal centriole in early spermiogenesis i.e. in the formation of axonemal complex

In recent literature on the ultrastructure of mammalian sperm very little information is available on the distal centriole It is an organelle which loses its function during early spermiogenesis and in the mature sperm it is either completely absent or rudimentary, it is, in other words a »partly transitory organelle In the bull sperm the so-called »dense rods« have been identified as rudiments of the distal centriole (4) According to other reports however, the distal centriole does not disappear completely, but persists in a modified form as a so-called »transitional connecting centriole« (18)

The following description has been given of the function of the distal centriole (8) »The earliest events in formation of the tail consist of migration of the centrioles to cell surface in the postnuclear region and polymerization of microtubule proteins on the template provided by the distal centriole A typical 9 + 2 axoneme is formed and the simple flagellum elongates by accretion of microtubule subunits to its distal end« This early stage in the tail formation is illustrated by Fawcett *et al* (11) in their Fig 7, where the tail primordium and the centriolar complex still are situated far from the nucleus

In the present study it was observed that in ejaculated sperm with the tail stump defect could show retention of a typical transitory organelle such as the centriolar adjunct As far as we know the presence of the centriolar adjunct has not been observed previously in bull ejaculates However in normal human ejaculated sperm the presence of the centriolar adjunct is considered a sign of relative immaturity (18) It is therefore tempting to suggest that in the abnormal sperm cells of the present material the normal function of the proximal centriole is also affected

The dense granules found in our sections in the peripheral cytoplasm of abnormal spermiids and in

Figure 7 Testis bull *G* Three spermiids in manchette stage Note the distal centriole and empty tail guide tube in upper cell (see discussion) 8 000 ×

Figure 8 Testis bull *G* Spermiid in manchette stage The proximal centriole and its adjunct is present together with the chromatoid body The distal centriole ends in an empty tail guide tube no axoneme is formed but the annulus is present 45 000 ×



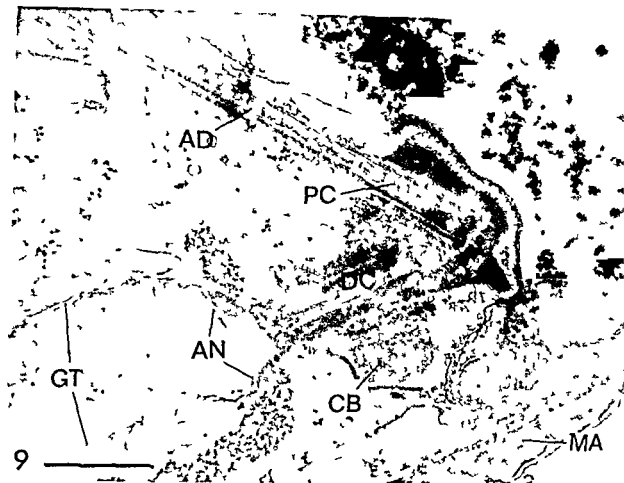


Fig. 9. Testis bull *G*. Spermid in manchette stage. The proximal centriole is seen with its adjunct. A chromatoid body and part of the manchette is also present. Note the distal centriole, the empty tail guide tube, and the annulus. 45 000 \times .

sperm cells morphologically resemble those demonstrated in the pseudodroplet defect in the bull (7). However, in the case of the tail stump defect in bull *G* the axonemal fibers are lacking in the defective spermid and this may have reference to the unorganized accumulation of clusters of mitochondria and dense granules. At present no explanation can be given as to the origin of the dense granules, neither in the pseudodroplet defect nor in the tail stump defect.

It is peculiar that the tail guide tube appears to develop even if no axonemal fibers are formed (Figs 8 and 9). Normally this canal is present at a very early stage in spermiogenesis (1) but how it can possibly develop without a tail primordium is difficult to understand.

Some doubt could probably be raised about the missing axonemes in our illustrations (Figs 8 and 9) of the abnormal spermid. If a tail primordium happens to be cut peripherally in a longitudinal section the tail guide tube will most probably appear empty. However, with one exception our illustrations are from sections close to the median

axis of the neck, because the annulus appears as two well separated dense triangles. Therefore if present some of the axonemal fibers should have been evident in the sections. The one exception is the sagittal section shown in Fig. 7 where the annulus seems to be hit tangentially and where the emptiness of the tail guide tube may therefore be doubtful.

In summary, the tail stump defect may be traced back to some defect(s) at an early stage of spermiogenesis, which seems to originate in abnormal conditions in the centriolar complex causing 1) a retention of the adjunct of the proximal centriole in ejaculated sperm cells and 2) a complete or partial inhibition of the formation of the axoneme by the distal centriole.

REFERENCES

1. Andersen, K. Fine structure of developing spermatids used as a basis for staging of the spermatogenesis in the blue fox (*Alopex lagopus*). *Zbl. Vet. C. Anat. Histol. Embryol.* 7: 164-181, 1978.

- 2 Baccetti B, Burrini A, Pallini V, Renieri T, Rasati F & Menchini Fabris C F The short tailed human spermatozoa. Ultrastructural alterations and dyenin absence. J Submicrosc Cytol 7: 349-359 1975
- 3 Barker C A V Two cases of «tail stump» sperm defect. Proc Society for theriogenology Mobile Alabama 1979
- 4 Blom E Spermatic ultrastructure (bovine). In Williams W W (Ed) Sterility. The diagnostic survey of the infertile couple. Springfield Mass pp 431-440 1964
- 5 Blom E The ultrastructure of some characteristic sperm defects and a proposal for a new classification of the bull spermogram. Atti del 7 Simp Int Zootec Milano 125-139 1972
- 6 Blom E A sterilizing tail stump defect in a Holstein Friesian bull. Nord Vet Med 28: 295-298 1976
- 7 Blom E & Brich Andersen A The ultrastructure of the pseudodroplet-defect in the bull sperm. Proc 6 Int Congr Animal Reprod (Paris) Vol 1: 117-119 1968
- 8 Bloom W & Fawcett D W A Textbook of Histology Saunders Philadelphia 10 edit 1975
- 9 Coubrough R I A study of the testicular histopathology and cytology of infertile bulls. Thesis University of Toronto Canada 144 pp 1964
- 10 Coubrough R I & Barker C A V Spermatozoa. An unusual middle piece abnormality associated with sterility in bulls. Proc 5 Int Congr Animal Reprod (Trento) 5: 219-229 1964
- 11 Fawcett D W, Eddy E M & Philips D M Observations on the fine structure and relationships of the chromatoid body in mammalian spermatogenesis. Biol Reprod 2: 129-153 1970
- 12 Frasca J M & Parks V R A routine technique for double staining ultrathin sections using uranyl and lead salts. J Cell Biol 25: 157-161 1965
- 13 Johnson D R & Hunt D M Hop sterile: a mutant gene affecting sperm tail development in the mouse. J Embryol exp Morph 25: 223-236 1971
- 14 Maqsood M An abnormality of mammalian spermatozoa. Experientia 7: 304 1951
- 15 Ploen L A scheme of rabbit spermatogenesis based upon electron microscopical observations. Z Zellforsch 115: 553-564 1971
- 16 Reynolds E S The use of lead citrate at a high pH as an electron opaque stain in electron microscopy. J Cell Biol 17: 208-212 1963
- 17 Vale Filho V R, Megale F & Garcia O S Mitochondrial sheath defects of spermatozoa and low reproductive efficiency in bulls of the Gyr (*Bos indicus*) breed. Rev Bras de Reproducao Animal 7: 31-39 1977
- 18 Zamboni L & Stefanini M The fine structure of the neck of mammalian spermatozoa. Anat Rec 169: 155-172 1971

LATE EFFECTS OF COLCHICINE ON THE BURSA OF FABRICIUS AFTER NEONATAL APPLICATION ON THE ANAL LIPS OF CHICKENS

TIMO ROMPPANEN and TAPANI E. SORVARI

Department of Pathology University of Kuopio Kuopio Finland

Romppanen T & Sorvari T E Late effects of colchicine on the bursa of Fabricius after neonatal application on the anal lips of chickens Acta path microbiol scand Sect A 88 407-413 1980

One week after the application of colchicine on the anal lips of chickens the bursa of Fabricius was devoid of lymphoid cells and contained only a few epithelial buds all of which were later repopulated with lymphoid cells to form mature lymphoid follicles. After the intraperitoneal injection of cyclophosphamide numerous epithelial buds were found in the bursa and at the age of six weeks only a few of them were populated with lymphoid cells. On week 6 the bursal weights of the chickens treated with colchicine were only about 10% of the normal and about 80% of the bursal weights of the cyclophosphamide treated chickens. The colchicine treatment affected the morphology of the spleen less than the treatment with cyclophosphamide. It is concluded that this new model of chemical bursectomy differs distinctly from the cyclophosphamide model and therefore serves as a new tool in studying bursal function in chicken.

Key words: Bursa of Fabricius, chemical bursectomy, colchicine.

T. Romppanen, Department of Pathology, University of Kuopio, P.O.B. 138, 70101 Kuopio 10, Finland.

Received 21 iv 80 Accepted 14 vi 80

To study the effects of various tissue components of the bursal microenvironment on the maturation of B cell lineage it is necessary to selectively destroy bursal lymphocytes. For this purpose various cell poisons have been applied on the anal lips of the chickens. Recently we described a new model of chemical bursectomy where bursal lymphoid cells were selectively destroyed together with the cells of the follicle associated epithelium by applying colchicine solution on the anal lips of chickens (12). During an observation period of one week no obvious direct effects of colchicine on thymus, spleen or caecal tonsils were seen. Therefore this model of chemical bursectomy seems to differ from the cyclophosphamide model where direct effects on the lymphoid tissues of the spleen, caecal tonsils and thymus has been reported (5-7, 9-11, 13-18). In this report late (1-10 weeks) effects of colchicine on the chicken bursa of Fabricius, spleen

MATERIALS AND METHODS

Laboratory animals. Newly hatched White Leghorn chickens were received from a local hatchery. The chickens were given commercial chicken food and water *ad libitum*.

In this work two groups of non

was given on the day of hatching

TABLE 1 *Body Bursal and Spleen Weights (Mean \pm S D)*

	Untreated	Treatment with colchicine	Treatment with cyclophosphamide
<i>Body weight (g)</i>			
1 week	54.2 \pm 5.2 (20)	57.8 \pm 5.7 (25)***	42.1 \pm 6.0 (10)***
2 weeks	86.3 \pm 14.1 (5)	83.0 \pm 9.4 (5)	
4 weeks	215.5 \pm 24.9 (4)	213.4 \pm 31.4 (7)	187.4 \pm 22.3 (5)
6 weeks	433.0 \pm 5.9 (8)	**362.2 \pm 51.7 (9)*	263.3 \pm 103.8 (9)***
10 weeks	958.5 \pm 121.1 (10)	877.1 \pm 126.1 (18)	
<i>Bursal weight (mg/100 g b w)</i>			
1 week	252.3 \pm 55.1 (20)	***50.6 \pm 18.6 (25)***	93.8 \pm 18.8 (10)***
2 weeks	354.6 \pm 59.8 (5)	***49.7 \pm 28.2 (5)	
4 weeks	747.1 \pm 124.0 (4)	***41.6 \pm 23.5 (7)**	89.8 \pm 24.8 (5)***
6 weeks	592.9 \pm 138.9 (8)	***53.7 \pm 24.7 (9)	67.1 \pm 11.4 (9)***
10 weeks	411.9 \pm 101.8 (10)	***20.5 \pm 10.1 (18)	
<i>Spleen weight (mg/100 g b w)</i>			
1 week	112.1 \pm 37.7 (20)	* 89.0 \pm 19.8 (25)***	47.6 \pm 20.9 (10)***
2 weeks	163.2 \pm 19.7 (5)	134.3 \pm 44.8 (5)	
6 weeks	270.5 \pm 87.0 (8)	203.2 \pm 65.7 (9)	213.4 \pm 58.8 (9)
10 weeks	244.3 \pm 60.2 (10)	235.6 \pm 32.3 (18)	

The numbers in brackets indicate the number of chickens in each group

Marks beneath the values of the colchicine group indicate significant differences when compared to the untreated controls (on the left) or to the cyclophosphamide group (on the right). Marks beneath the values of the cyclophosphamide group indicate significant differences in a comparison to the controls. * $P \leq 0.05$ ** $P \leq 0.01$ *** $P \leq 0.001$

The number of chickens in different experimental groups is presented in Table 1

Tissue sampling The chickens were killed 1, 2, 4, 6 and 10 weeks after hatching with an overdose of ethyl ether. The chickens' their bursae and spleens were weighed. Histological samples were taken from the transversal midline of the bursa, spleen and caecal tonsils, fixed overnight in 4% neutral buffered formaldehyde and embedded in paraffin. Tissue sections six μ thick were stained with Hematoxylin-Eosin-van Gieson.

Hematoxylin and methyl green and pyronin methods

Statistics: Student's *t*-test was employed in comparison of the means

RESULTS

Body bursal and spleen weights The body bursal and spleen weights are presented in Table 1

When the body weights of the chickens treated

TABLE 2 *The Occurrence of Epithelial Buds and Lymphoid Follicles in the Bursa after Colchicine Treatment*

Age of chickens	Total number of bursae	No buds		Buds present		No buds, follicles present		Both buds and follicles	
		n ¹⁾	% ²⁾	n	%	n	%	n	%
1	25	7	28	15	60	1	4	2	8
2	5	2	40	2	40	0	0	1	20
4	7	2	29	0	0	0	0	5	71
6	9	0	0	0	0	1	11	8	89
10	18	0	0	0	0	16	89	2	11

1) Number of bursae

2) Percentage of total number of bursae



Fig 1 Bursa of a one week-old chicken treated with colchicine. No lymphoid follicles present. Small epithelial buds are indicated by arrows (H&E $\times 100$)

Fig 2^a Detail from figure 1. An epithelial bud with rudimentary cortical zone is seen. The open arrow points to the follicle associated epithelium. The closed arrows show the interfollicular surface epithelium (H&E $\times 400$)

Fig 3 Bursa of a two week-old chicken treated with colchicine. A few follicles (F) and epithelial buds (open arrows) are seen. The closed arrow points to a cluster of small lymphocytes around a venule in the bursal stroma (H&E: $\times 100$)

Fig 4 Bursa of a two-week-old control chicken. F = lymphoid follicles, open arrows = follicle associated epithelium, closed arrows = interfollicular surface epithelium (H&E $\times 100$)

TABLE 1 *Body Bursal and Spleen Weights (Mean \pm S D)*

	Untreated	Treatment with colchicine	Treatment with cyclo phosphamide
<i>Body weight (g)</i>			
1 week	54.2 \pm 5.2 (20)	57.8 \pm 5.7 (25)***	42.1 \pm 6.0 (10)***
2 weeks	86.3 \pm 14.1 (5)	83.0 \pm 9.4 (5)	
4 weeks	215.5 \pm 24.9 (4)	213.4 \pm 31.4 (7)	187.4 \pm 22.3 (5)
6 weeks	433.0 \pm 5.9 (8)	**362.2 \pm 51.7 (9)*	263.3 \pm 103.8 (9)***
10 weeks	958.5 \pm 121.1 (10)	877.1 \pm 126.1 (18)	
<i>Bursal weight (mg/100 g b w)</i>			
1 week	252.3 \pm 55.1 (20)	***50.6 \pm 18.6 (25)***	93.8 \pm 18.8 (10)***
2 weeks	354.6 \pm 59.8 (5)	***49.7 \pm 28.2 (5)	
4 weeks	747.1 \pm 124.0 (4)	***41.6 \pm 23.5 (7)**	89.8 \pm 24.8 (5)***
6 weeks	592.9 \pm 138.9 (8)	***53.7 \pm 24.7 (9)	67.1 \pm 11.4 (9)***
10 weeks	411.9 \pm 101.8 (10)	***20.5 \pm 10.1 (18)	
<i>Spleen weight (mg/100 g b w)</i>			
1 week	112.1 \pm 37.7 (20)	* 89.0 \pm 19.8 (25)***	47.6 \pm 20.9 (10)***
2 weeks	163.2 \pm 19.7 (5)	134.3 \pm 44.8 (5)	
6 weeks	270.5 \pm 87.0 (8)	203.2 \pm 65.7 (9)	213.4 \pm 58.8 (9)
10 weeks	244.3 \pm 60.2 (10)	235.6 \pm 32.3 (18)	

The numbers in brackets indicate the number of chickens in each group

Marks beneath the values of the colchicine group indicate significant differences when compared to the untreated controls (on the left) or to the cyclophosphamide group (on the right). Marks beneath the values of the cyclophosphamide group indicate significant differences in a comparison to the controls. * $P \leq 0.05$ ** $P \leq 0.01$ *** $P \leq 0.001$

The number of chickens in different experimental groups is presented in Table 1

Tissue sampling The chickens were killed 1, 2, 4, 6 and 10 weeks after hatching with an overdose of ethyl ether. The chickens, their bursae and spleens were weighed. Histological samples were taken from the transversal midline of the bursa, spleen and caecal tonsils, fixed overnight in 4% neutral buffered formaldehyde and embedded in paraffin. Tissue sections 5 μ thick were stained with Hematoxylin Eosin, van Gieson

Hematoxylin and methyl green and pyronin methods.

Statistics Student's *t* test was employed in comparison of the means.

RESULTS

Body, bursal and spleen weights The body, bursal and spleen weights are presented in Table 1.

When the body weights of the chickens treated

TABLE 2 *The Occurrence of Epithelial Buds and Lymphoid Follicles in the Bursa after Colchicine Treatment*

Age of chickens	Total number of bursae	No buds		Buds present		No buds, follicles present		Both buds and follicles	
		n ¹⁾	% ²⁾	n	%	n	%	n	%
1	25	7	28	15	60	1	4	2	8
2	5	2	40	2	40	0	0	1	20
4	7	2	29	0	0	0	0	5	71
6	9	0	0	0	0	1	11	8	89
10	18	0	0	0	0	16	89	2	11

1) Number of bursae

2) Percentage of total number of bursae



TABEL 3 *The Number (Mean \pm SD) of Lymphoid Follicles and Epithelial Buds in a Cross Bursal Section*

Age of chickens (weeks)	Epithelial buds			Lymphoid follicles		
	Untreated	Colchicine	Cyclophosphamide	Untreated	Colchicine	Cyclophosphamide
1	0 (3)	13 \pm 28 (25)	627 \pm 77 (5)	487 \pm 3 (3)	7 \pm 26 (25) ¹⁾	0 (10)
2	0 (3)	27 \pm 39 (5)		483 \pm 64 (3)	10 \pm 22 (5)	
4	0 (3)	54 \pm 96 (7)	305 \pm 70 (5)	502 \pm 71 (3)	6 \pm 13 (7)	3 \pm 3 (5)
6	0 (3)	30 \pm 29 (9)	417 \pm 97 (9)	652 \pm 68 (3)	30 \pm 30 (9)	7 \pm 9 (9)
10	0 (3)	0.4 \pm 1.4 (18)		592 \pm 83 (3)	16 \pm 22 (18)	

1) In 22 cases 0, remaining 3 cases 7, 90 and 96

The numbers in brackets indicate the number of animals in each group

with colchicine were compared with those of the untreated controls, a significant difference was noticed only on week 6. The body weights of the cyclophosphamide group were significantly lower at weeks 1 and 6, when compared with the other two groups.

In every age group, the bursae of the chickens treated with colchicine were remarkably lighter than those of the untreated controls. The effect of colchicine on the bursal weight appeared to exceed that of cyclophosphamide.

In the colchicine group, the spleens were slightly lighter than those of the untreated control animals, but only on week 1 was this difference significant. On week 1, the chickens treated with cyclophosphamide had spleens which were markedly lighter than in the other two groups.

Histology of the bursa. At the age of 1 week 28% of the bursae in the colchicine group (Table 2) were totally devoid of both lymphoid follicles and epithelial buds, consisting only of fibrous stroma and interfollicular surface epithelium. In 60% of the bursae (Table 2) scattered epithelial buds (mean 13 per section, Table 3) with follicle-associated epithelium were found in the relatively increased bursal stroma (Figures 1 and 2). Practically no lymphoid follicles were observed in the bursae of the colchicine groups whereas in the bursae of the untreated animals they were abundant (mean 487, Table 3). The bursae in the cyclophosphamide group contained numerous epithelial buds thus differing distinctly from the bursae of the colchicine-treated chickens (Table 3).

At the ages of 2, 4 and 6 weeks the number of bursae containing lymphoid follicles increased in the colchicine group (Table 2), indicating a spontaneous lymphoid repopulation. The number of these lymphoid follicles, however, was rather small when compared to the controls (Table 3, Figures 3 and 4). At this time, follicles in different stages of

repopulation were seen in the bursae of the colchicine group. In most follicles the repopulation seemed to begin in the medulla (Figure 5), although cortical accumulation of lymphoid cells was sometimes observed, too. Some lymphoid cells around the buds in the stroma were also observed (Figure 5). In the bursae of the cyclophosphamide-treated chickens numerous epithelial buds were seen, but a repopulated lymphoid follicle only occasionally (Table 3) thus differing from the bursae of the colchicine-treated animals.

At the age of 10 weeks, the bursae of the colchicine-treated chickens contained lymphoid follicles, but practically no epithelial buds (Table 2, Figure 6). The number of the lymphoid follicles remained low, however (Table 3). Numerous lymphoid cells were found diffusely in the stroma as well as aggregated in clusters beneath the interfollicular surface epithelium (Figure 7).

Histology of the spleen and caecal tonsils. After the application of colchicine, the amount of lymphoid cells around the Schweigger-Seidel sheaths seemed to be smaller when compared with the untreated controls, but greater than in the cyclophosphamide group. On week 6, the number of

Fig. 5 Bursa of a four week-old chicken treated with colchicine. The medulla of an epithelial bud is populated with pyroninophilic cells (F) whereas the cortical zone is poorly developed. Note the epithelial buds (B) with few scattered pyroninophilic cells in the medulla and the cortex (Methyl green and pyronin $\times 300$).

Fig. 6 Bursa of a ten week old chicken treated with colchicine. Mature lymphoid follicles (F) are present but no epithelial buds are observed (H&E, $\times 200$).

Fig. 7 Bursa of a ten-week-old chicken treated with colchicine. Lymphoid cells are scattered in the stroma subepithelially or aggregated as a follicle like structure (asterix) (H&E, $\times 400$).

which is in accordance with earlier studies (10-14) and they were more pronounced than those in the colchicine model. It is possible that after the treatment with cyclophosphamide there are not enough suitable lymphoid cells in the chickens to repopulate the bursal epithelial buds unless the chickens are transplanted with bursal cells (14-18).

According to our earlier (12) and present studies colchicine treatment induces a rather selective injury in the bursa affecting the lymphoid cells and the follicular epithelium. This model of chemical bursectomy differs markedly from other models of bursectomy as discussed previously (12) and in this paper and apparently serves as a new tool in studying the development of the B cell lineage in the chicken bursa.

The technical assistance of Mrs. Pirjo Korhovuori, Mrs. Irma Vaananen and Mrs. Raija Pitkanen is gratefully acknowledged.

REFERENCES

- 1 Ackerman G A & Knouff R A Lymphocytopoiesis in the bursa of fabricius. *Amer J Anat* 104 163-206 1959
- 2 Ackerman G A Electron microscopy of the bursa of fabricius of the embryonic chick with particular reference to the lymphoepithelial nodules. *J Cell Biol* 13 127-147 1962
- 3 Ahlquist J & Andersson L Methyl green pyronin staining effects of fixation use in routine pathology. *Stain Technol* 47 17-22 1972
- 4 Glick B Immunity studies in testosteronepropionate injected chicks. *Int Arch Allergy Appl Immunol* 38 93-103 1970
- 5 Glick B Morphological changes and humoral immunity in cyclophosphamide treated chicks. *Transplantation* 11 433-439 1971
- 6 Hiraga T, Sugimura M & Kuro N Effect of cyclophosphamide on the thymus and the bursa of fabricius in chickens. *Jap J Vet Res* 24 87-98 1976
- 7 Hoffman Fe'er G, Hoffman R, Fiedler H &

Losch U Recovery of the bursa of fabricius in chickens after cyclophosphamide treatment. *Int Arch Allergy Appl Immunol* 53 206-213 1977

- 8 Jankovic B D, Isakovic K & Markovic B M & Rajcic M Immunological capacity of the chicken embryo. II Humoral immune responses in embryos and young chickens bursectomized and sham bursectomized at 52-64 h of incubation. *Immunology* 32 689-699 1977
- 9 Lerman S P & Weidman B P The effect of cyclophosphamide on the ontogeny of the humoral immune response in chickens. *J Immunol* 105 614-619 1970
- 10 Linna T J, Frommel D & Good R A Effects of early cyclophosphamide treatment on the development of lymphoid organs and immunological functions in chicken. *Int Arch Allergy Appl Immunol* 42 20-39 1972
- 11 Olah I & Glick B Secretory cell in the medulla of the bursa of fabricius. *Experientia* 34 1642-1643 1979
- 12 Romppanen T & Sorvari T E Chemical bursectomy of chickens with colchicine applied to the anal lips. *Am J Path* 100 193-208 1980
- 13 Sorvari T, Toivanen A & Toivanen P Transplantation of bursal stem cells into cyclophosphamide treated chicks. *Transplantation* 17 584-592 1974
- 14 Sorvari T E & Toivanen A Transplantation of bursal stem cells into cyclophosphamide treated chicks. Lymphoid repopulation of splenic structures. *Scand J Immunol* 5 317-321 1976
- 15 Toivanen P, Toivanen A & Good R A Ontogeny of bursal function in chicken. I Embryonic stem cell for humoral immunity. *J Immunol* 109 1958-1070 1972
- 16 Toivanen P, Toivanen A, Linna T J & Good R A Ontogeny of bursal function in chicken. II Postembryonic stem cell for humoral immunity. *J Immunol* 109 1071-1080 1972
- 17 Toivanen P, Toivanen A & Good R A Ontogeny of bursal function in chicken. III Immunocompetent cell for humoral immunity. *J Exp Med* 136 816-831 1972
- 18 Toivanen P & Toivanen A Bursal and postbursal stem cells in chicken. Functional characteristics. *Eur J Immunol* 3 585-595 1973

TABEL 4 *The Number of Germinal Centers (Mean \pm SD) in a Cross Spleen Section*

Age of chickens (weeks)	Number of germinal centers		
	Untreated	Colchicine	Cyclophosphamide
1	0 (20)	0 (25)	0 (10)
2	0 6 ± 1 (3) (5)	0 (5)	
6	8 3 ± 6 (3) (8)	2 6 ± 3 (4) (9) ¹⁾	0 1 ± 0 (9) (2)
10	7 1 ± 9 (3) (10)	5 1 ± 8 (9) (18) ³⁾	

1) $P \leq 0.05$ when compared to the controls

2) $P \leq 0.01$ when compared to the controls $P \leq 0.05$ when compared to the colchicine group

3) No significant difference in a comparison to the controls

The numbers in brackets indicate the number of animals in each group

germinal centers in a spleen section in the colchicine group was smaller than in untreated controls whereas on week 10 the difference was minimal (Table 4). The cyclophosphamide group distinctly differed from the other two groups because practically no germinal centers were found on week 6.

Caecal tonsils were examined on week 10. In the colchicine treated chickens the amount of germinal centers and lymphoid cells in the stroma was smaller than in untreated controls. The caecal tonsils of the cyclophosphamide treated chickens were not investigated in this study.

DISCUSSION

After treatment with colchicine the bursa contained only a few epithelial buds while after an intraperitoneal injection of cyclophosphamide the number of buds in the bursa approximately equalled the number of follicles in the bursae of untreated control animals. During the observation period all of the few epithelial buds in the colchicine treated bursae were populated by lymphoid cells to form mature histologically normal appearing lymphoid follicles. The number of lymphoid follicles on week 10 however, was only about 3% of that found in the bursal sections of the untreated control animals.

The repopulation of each single epithelial bud by lymphoid cells seemed to take place independently because lymphoid follicles were found in different stages of repopulation. This repopulation resembled either embryonal development of the bursal follicles (1, 2) or states found in the bursae of the cyclophosphamide treated chickens spontaneously (5, 7) or following transplantation with bursal lymphoid cells (14-18). The origin of the repopulating lymphoid cells remains unclear, (1) they can be

descendants of lymphoid cells which survived the initial necrosis caused by colchicine or (2) they can be peripheralized bursal lymphocytes which have returned to bursa or (3) they are lymphocytes from a non bursal site of B cell development (8).

In the colchicine model no acute direct effect on the spleen or caecal tonsils has been demonstrated (12). However, later the spleen weight and amount of lymphoid cells in the periellipsoid area and the number of germinal centers in the spleen

secondary due to total depletion of the lymphoid cells in the bursa. On week 10 increased weight and normalized morphology of the spleens indicated their partial recovery. This injury recovery cycle in the bursa also partially reflected in the spleen in our present model bears some resemblance to that caused by intramuscular testosterone propionate injection (4).

The chickens which received intraperitoneal injections of cyclophosphamide did not gain as much weight as those treated with colchicine, a fact apparently indicating a more serious systemic effect. Besides the total loss of lymphoid cells no other apparent damage was observed histologically in the bursae of the cyclophosphamide treated chickens. Cyclophosphamide did not destroy epithelial buds. As reported in earlier studies (6, 7) in cyclophosphamide treated chickens only a part of numerous epithelial buds are spontaneously populated with lymphoid cells on week 10 while in the present study all of the few buds in the colchicine group were populated. Thus the cyclophosphamide and the colchicine models also differ in their type of spontaneous lymphoid repopulation of the bursa which is less active in the former. The effects of cyclophosphamide on the spleen were evident

which is in accordance with earlier studies (10-14) and they were more pronounced than those in the colchicine model. It is possible that after the treatment with cyclophosphamide there are not enough suitable lymphoid cells in the chickens to repopulate the bursal epithelial buds unless the chickens are transplanted with bursal cells (14-18).

According to our earlier (12) and present studies colchicine treatment induces a rather selective injury in the bursa affecting the lymphoid cells and the follicular epithelium. This model of chemical bursectomy differs markedly from other models of bursectomy as discussed previously (12) and in this paper and apparently serves as a new tool in studying the development of the B cell lineage in the chicken bursa.

The technical assistance of Mrs. Pirjo Kortevaara, Mrs. Irma Vaananen and Mrs. Raija Pukanen is gratefully acknowledged.

REFERENCES

- 1 Ackerman G A & Knouff R A. Lymphocytopoiesis in the bursa of fabricius. *Amer J Anat* 104: 163-206 1959.
- 2 Ackerman G A. Electron microscopy of the bursa of fabricius of the embryonic chick with particular reference to the lymphoepithelial nodules. *J Cell Biol* 13: 127-147 1962.
- 3 Ahlquist J & Andersson L. Methyl green-pyronin staining effects of fixation use in routine pathology. *Scand Technol* 47: 17-22 1972.
- 4 Glick B. Immunity studies in testosteronepropionate injected chicks. *Int Arch Allergy Appl Immunol* 38: 93-103 1970.
- 5 Glick B. Morphological changes and humoral immunity in cyclophosphamide treated chicks. *Transplantation* 11: 433-439 1971.
- 6 Hraga T, Sugimura M & Kuso N. Effect of cyclophosphamide on the thymus and the bursa of fabricius in chickens. *Jap J Vet Res* 24: 87-98 1976.
- 7 Hoffmann Feyer G, Hoffmann R, Fiedler H & Losch U. Recovery of the bursa of fabricius in chickens after cyclophosphamide treatment. *Int Arch Allergy Appl Immunol* 53: 206-213 1977.
- 8 Jankovic B D, Isakovic K & Markovic B M & Rajcevic M. Immunological capacity of the chicken embryo. II. Humoral immune responses in embryos and young chickens bursectomized and sham bursectomized at 52-64 h of incubation. *Immunology* 32: 689-699 1977.
- 9 Lerman S P & Weidanz W P. The effect of cyclophosphamide on the ontogeny of the humoral immune response in chickens. *J Immunol* 105: 614-619 1970.
- 10 Linna T J, Frommel D & Good R A. Effects of early cyclophosphamide treatment on the development of lymphoid organs and immunological functions in chicken. *Int Arch Allergy Appl Immunol* 42: 20-39 1972.
- 11 Olah I & Glick B. Secretory cell in the medulla of the bursa of fabricius. *Experientia* 34: 1642-1643 1979.
- 12 Romppanen T & Sorvari T E. Chemical bursectomy of chickens with colchicine applied to the anal lips. *Am J Path* 100: 193-208 1980.
- 13 Sorvari T, Toivanen A & Toivanen P. Transplantation of bursal stem cells into cyclophosphamide treated chicks. *Transplantation* 17: 583-592 1974.
- 14 Sorvari T E & Toivanen A. Transplantation of bursal stem cells into cyclophosphamide treated chicks. Lymphoid repopulation of splenic structures. *Scand J Immunol* 5: 317-321 1976.
- 15 Toivanen P, Toivanen A & Good R A. Ontogeny of bursal function in chicken. I. Embryonic stem cell for humoral immunity. *J Immunol* 109: 1958-1070 1972.
- 16 Toivanen P, Toivanen A, Linna T J & Good R A. Ontogeny of bursal function in chicken. II. Postembryonic stem cell for humoral immunity. *J Immunol* 109: 1071-1080 1972.
- 17 Toivanen P, Toivanen A & Good R A. Ontogeny of bursal function in chicken. III. Immunocompetent cell for humoral immunity. *J Exp Med* 136: 816-831 1972.
- 18 Toivanen P & Toivanen A. Bursal and postbursal stem cells in chicken. Functional characteristics. *Eur J Immunol* 3: 585-595 1973.

TABEL 4 *The Number of Germinal Centers (Mean \pm SD) in a Cross Spleen Section*

Age of chickens (weeks)	Number of germinal centers		
	Untreated	Colchicine	Cyclophosphamide
1	0 (20)	0 (25)	0 (10)
2	0.6 \pm 1.3 (5)	0 (5)	
6	8.3 \pm 6.3 (8)	2.6 \pm 3.4 (9) ¹⁾	0.1 \pm 0.9 (9) ²⁾
10	7.1 \pm 9.3 (10)	5.1 \pm 8.9 (18) ³⁾	

1) $P \leq 0.05$ when compared to the controls

2) $P \leq 0.01$ when compared to the controls, $P \leq 0.05$ when compared to the colchicine group

3) No significant difference in a comparison to the controls

The numbers in brackets indicate the number of animals in each group

germinal centers in a spleen section in the colchicine group was smaller than in untreated controls, whereas on week 10, the difference was minimal (Table 4). The cyclophosphamide group distinctly differed from the other two groups, because, practically no germinal centers were found on week 6.

Caecal tonsils were examined on week 10. In the colchicine treated chickens, the amount of germinal centers and lymphoid cells in the stroma was smaller than in untreated controls. The caecal tonsils of the cyclophosphamide-treated chickens were not investigated in this study.

DISCUSSION

After treatment with colchicine the bursa contained only a few epithelial buds, while after an intraperitoneal injection of cyclophosphamide the number of buds, the bursa approximately equalled the number of follicles in the bursae of untreated control animals. During the observation period all of the few epithelial buds in the colchicine-treated bursae were populated by lymphoid cells to form mature, histologically normal-appearing lymphoid follicles. The number of lymphoid follicles on week 10 however, was only about 3% of that found in the bursal sections of the untreated control animals.

The repopulation of each single epithelial bud by lymphoid cells seemed to take place independently because lymphoid follicles were found in different stages of repopulation. This repopulation resembled either embryonal development of the bursal follicles (1, 2) or states found in the bursae of the cyclophosphamide-treated chickens spontaneously (5, 7) or following transplantation with bursal lymphoid cells (14-18). The origin of the repopulating lymphoid cells remains unclear, (1) they can be

descendants of lymphoid cells which survived the initial necrosis caused by colchicine, or (2) they can be peripheralized bursal lymphocytes, which have returned to bursa or (3) they are lymphocytes from a non-bursal site of B cell development (8).

In the colchicine model no «acute» direct effects on the spleen or caecal tonsils has been demonstrated (12). However, later, the spleen weight, the amount of lymphoid cells in the periellipsoid area and the number of germinal centers in the spleen as

secondary due to total depletion of the lymphoid cells in the bursa. On week 10, increased weights and normalized morphology of the spleens indicated their partial recovery. This injury-recovery cycle in the bursa, also partially reflected in the spleen in our present model bears some resemblance to that caused by intramuscular testosterone propionate injection (4).

The chickens which received intraperitoneal injections of cyclophosphamide did not gain as much weight as those treated with colchicine, a fact apparently indicating a more serious systemic effect. Besides the total loss of lymphoid cells, no other apparent damage was observed histologically in the bursae of the cyclophosphamide treated chickens. Cyclophosphamide did not destroy epithelial buds. As reported in earlier studies (6, 7) in cyclophosphamide treated chickens, only a part of numerous epithelial buds are spontaneously populated with lymphoid cells on week 10, while in the present study, all of the few buds in the colchicine group were populated. Thus, the cyclophosphamide and the colchicine models also differ in their type of spontaneous lymphoid repopulation of the bursa which is less active in the former. The effects of cyclophosphamide on the spleen were evident

CORRESPONDENCE

HISTOLOGIC TYPING OF BREAST CANCER

See—in a recent monograph (9) and in a brief report (8) which appeared in this Journal *Linell et al* proposed a new classification for breast carcinoma. Their system was elaborated upon on the observation of a large number of mastectomies in which they recorded a stepwise evolution from «radial scars» into carcinomas they called «tubular».

In our opinion an obvious merit of their extensive investigation has been to intend to apply to breast pathology the acception which appears now established for lung carcinoma (Roessle (11)) that cancer seems to arise in scar tissue. They also tried to introduce a concept of dynamic evolution in the process of degeneration suggesting that both histologic type and grade of a tumour does evolve with time. We also have been interested in breast pathology and histologic classification of mammary cancer (17-18). Therefore we would like to comment on some of the basic points of *Linell et al* (8-9) studies.

1) When the authors claim that «tubule formation as a higher degree of differentiation and of better prognosis is nowadays an obsolete idea» they are in contradiction with their own statements (—) «tubule formation is pure in early carcinoma» i.e. in well differentiated

parameters currently in use (19-20).

2) The high percentage of «tubular carcinomas» which reached 21% (8-9) is in profound disagreement with literature data of a 10- to 20 fold lower frequency. This discrepancy is obviously attributable to different histopathological criteria and definition of tubular carcinoma. We (17-18) have already stressed the confusion between true tubular carcinoma and well differentiated infiltrating duct carcinoma or even with other subtypes which has appeared repeatedly (Savino & Koss (12)). So *Hamperl* (6) pointed out that even *Haegensen* misused some terms viz by designating true tubular carcinoma under heading of apocrine carcinoma. Few reports (*Eusebi et al* (2) *Fisher et al* (4)) suggested that true tubular and lobular carcinoma might be two distinct variants of secretory carcinoma the former being the most differentiated of both subtypes. However most authors (*Lagios et al* (7) *Taxy* (14) *Taylor & Norris* (13) *van Bogaert & Mardague* (17-18)) agree with a ductal origin rather than a lobular one.

The most frequent mistake is the confusion with highly

differentiated infiltrating duct carcinoma. Almost all the papers on the subject of true tubular carcinoma agree with the following histopathologic criteria: well-defined tubular structures with angulated contours usually lined by a single layer of bland appearing cells and prominent

lesion they consider a «radial scar» i.e. not yet a carcinoma although it may progress into tubular carcinoma. They believe that malignant degeneration of the «radial scar» may evolve into 5 subtypes according

conceive that with time the degree of differentiation may decrease. It seems rather confusing to name «tubular carcinoma» a tumour which by definition is almost totally devoid of tubules.

3) «Radial scars» are said to be also characterized by

observation might be correct. One could get the wrong impression that elastosis is one of the diagnostic hallmarks. As a matter of fact true tubular carcinoma generally show such changes (*Tobon & Salazar* (15) *Tremblay* (16)) however infiltrating duct and lobular carcinoma (*Azopardo & Laurini* (1) *Martinez Hernandez et al* (10)) scirrhous carcinoma (*Azopardo & Laurini* (1)) and benign breast tissue (*Martinez Hernandez et al* (10)) have been shown to exhibit the same deposits. Moreover studies on this peculiar elastoid substance emphasize that the deposits are found not only in the periductal stroma but also around the blood vessels. The latter topography was not mentioned by *Linell et al* (8-9). Finally *Fisher et al* (3) suggested some association between marked elastica and tumours from patients of older age.

Conclusion. The authors (9) claimed that a new classification system is warranted only when it offers advantages from both a clinical and prognostic point of view. Although we fully agree with their statement their study unfortunately was limited to a 1-3 year follow up. From a pathologist's point of view we feel that their system is based on the misuse of a name «tubular carcinoma» which has been consecrated in a very precise sense. While the authors do recognize all the criteria of

BRIEF REPORT

ESTIMATION OF THE VOLUME OF HUMAN ANTRAL MUCOSA BY MEASURING THE ANTRAL LENGTH ALONG THE LESSER AND GREATER CURVATURE

H Overgaard Nielsen

Institute of Pathology and Department of Surgical Gastroenterology Odense University Hospital Odense
Denmark

Nielsen H O Estimation of the volume of human antral mucosa by measuring the antral length along the lesser and greater curvature Acta path microbiol scand Sect A 89 417-419 1980

A significant positive correlation was found in 11 antrectomy preparations between the product of antral length along the lesser and greater curvatures and the antral mucosal volume (coefficient of correlation 0.9297). This means that the antral mucosal volume can be estimated by measuring the antral length along the curvatures a procedure possible during operation with the organ in situ.

Key words Human antrum curvatures mucosal volume

H Overgaard Nielsen Institute of Pathology Odense University Hospital DK 5000 Odense C Denmark

Accepted as submitted 23 iv 80

The surgical treatment of chronic duodenal ulcer as performed today preserves the antrum. Antrectomy is only the treatment of choice in some cases of recurrent ulcer. This means that direct determination of the antrum area and/or volume can rarely be obtained in duodenal ulcer patients. These parameters can be useful i.e. for determination of the G cell mass and when the antrum size is to be correlated to other parameters. It was therefore considered of interest to report a method for the estimation of antral mucosal volume by means of measurement of the length of the antrum along the lesser and greater curvature.

The antrum was removed after the pylorus had been closed because of early gastric cancer.

After removal the antrum was opened along the greater curvature and placed on a sheet of cork. The border between the antrum and the duodenum was determined by the two sections from the two corners of the pylorus. The antrum was then stripped of its volume determined following the principles of Archimedes by submersion in water. As

Corrected volume of
antral mucosa (ml)

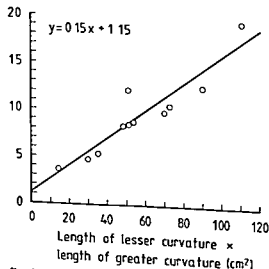


Fig 1 Shows the construction line of regression between antrum mucosa volume and the product of lesser and greater curvature length. The line intercept the Y axis of point 1.15 (ml) and have a slope of 0.15 (ml/cm²).

such lesion in the »radial scar« which they apparently consider as a possible precancerous lesion they use the term to designate a wide range of carcinomas with a progressive loss of tubules. We can hardly agree with their new classification.

References 1 *Azopardi J G & Laurini R N* Cancer 33 174-183 1974 - 2 *Eusebi V Betts C M & Bussolati G* Histopathology 3 407-419 1979 - 3 *Fisher E R Gregorio R M & Fisher B* Cancer 36 1-85 1975 - 4 *Fisher E R Gregorio R M Redmond C & Fisher B* Hum Pathol 8 679-683 1977 - 5 *Flotte Th J Bell D A & Greco M A* Am J Surg Path 4 75-77 1980 - 6 *Hamperl H* Ztschr f Krebsf 81 181-191 1974 - 7 *Lagios M D Rose M R & Margolin F R* Am J Clin Path 73 25-30 1980 - 8 *Linell F & Ljungberg O* Acta path microbiol scand Sect A 88 59-60 1980 - 9 *Linell F Ljungberg O & Andersson I* Acta path microbiol scand Sect A suppl 272 1980 - 10 *Martinez Hernandez A Francis F J & Silverberg S G* Cancer 40 700-706 1977 - 11 *Roessle R* Schweiz Med Wschr 73 1200-1203 1943 - 12 *Savino A & Koss L* Acta Cytol 15 372-374 1971 - 13 *Taylor H B & Norris H J* Cancer 25 687-692 1970 - 14 *Taxy J B* Cancer 36 462-465 1975 - 15 *Tobon H & Salazar H* Arch Pathol Lab Med 101 310-316 1977 - 16 *Tremblay G* Arch Pathol 98 302-307 1974 - 17 *van Bogaert L J & Maldague P* Surg Gynec & Obstet 142 513-518 1976 - 18 *van Bogaert L J & Maldague P* Hum Pathol 9 175-180 1978 - 19 *van Bogaert L J & De Muylder Ch* Anal Quant Cytol 2 55-58 1980 - 20 *van Bogaert L J De Muylder Ch Maldague P & Maisin H* Brit J Cancer (in press)

Experimental Pathology

& Cytology

LOUIS JACQUES VAN BOGAERT
Unit of the Louvain University School of
Medicine Brussels Belgium

Sir - We thank Dr *van Bogaert* for the interest he has shown to our papers and would like to comment on some of his views.

We are glad that Dr *van Bogaert* seems to accept the possibility that tubular carcinomas start in radial scars.

1 Dr *van Bogaert* means that we are in contradiction with our own statements about differentiation. There is no contradiction if one cites also the following sentence: »When the tumours grow larger the progression towards less differentiated structures takes over and the tubules are there only as remnants of the earlier structure of the tumour. To us differentiation means the development of higher differentiated structures in an undifferentiated tumour and progression the development of less differentiated elements in a highly differentiated tumour.

2 »The high percentage of tubular carcinomas is in profound disagreement with literature data. Not at all. As we point out on p. 63 our material contains a big proportion of tumours found at mass screening. The same has been found by other authors cited by us.

Dr *van Bogaert* finds it confusing to use the name »tubular carcinoma 0« for a tumour devoid of tubules. We cannot find it confusing when reading our text.

3 About elastosis: »One could get the wrong impression that elastosis is one of the diagnostic hallmarks. Naturally we mean this is true and the finding of elastosis in all our tubulo ductal carcinomas is one of our histologic arguments for the progression we describe. But elastosis is not pathognomic as stressed on p. 122 where we point out that infiltrating lobular

add that it is impossible in this publication to have a long follow up when we use a *modern* material with many small tumours found at mass screening. We cannot agree that we misuse the name »tubular carcinoma. To us it is not consecrated but subjected to the changing pattern of new knowledge.

To the last sentence: »We can hardly agree with their new classification« we can only say that several correspondents who have gone through their own materials »with new eyes« have agreed with our views.

Department of Pathology
General Hospital
Malmo Sweden

FOIKF LINELL
OTTO LJUNGBERG
INGVAR ANDERSSON

BRIEF REPORT

ESTIMATION OF THE VOLUME OF HUMAN ANTRAL MUCOSA BY MEASURING THE ANTRAL LENGTH ALONG THE LESSER AND GREATER CURVATURE

H Overgaard Nielsen

Institute of Pathology and Department of Surgical Gastroenterology Odense University Hospital Odense Denmark

Nielsen H O Estimation of the volume of human antral mucosa by measuring the antral length along the lesser and greater curvature Acta path microbiol scand Sect A 89 417-419 1980

A significant positive correlation was found in 11 antrectomy preparations between the product of antral length along the lesser and greater curvatures and the antral mucosal volume (coefficient of correlation 0.9297). This means that the antral mucosal volume can be estimated by measuring the antral length along the curvatures a procedure possible during operation with the organ in situ

Key words Human antrum curvatures mucosal volume

H Overgaard Nielsen Institute of Pathology Odense University Hospital DK-5000 Odense C Denmark

Accepted as submitted 23 iv 80

The surgical treatment of chronic duodenal ulcer as performed today preserves the antrum. Antrectomy is only the treatment of choice in a small number of ulcer patients. These parameters can be useful i.e. for determination of the G cell mass and when the antrum size is to be correlated to other parameters. It was therefore considered of interest to report a method for the estimation of antral mucosal volume by means of measurement of the length of the antrum along the lesser and greater curvature.

Corrected volume of antral mucosa (ml)

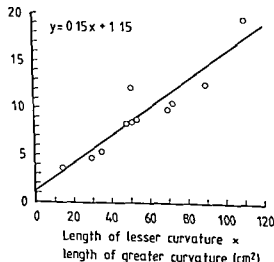


Fig 1 Shows the construction line of regression between antrum mucosa volume and the product of lesser and greater curvature length. The line intercept the y axis of point 1.15 (ml) and have a slope of 0.15 (ml/cm²)

TABLE 1 *Diagnosis Length of Antrum along Lesser and Greater Curvatures and Mucosal Volume in 11 Antrectomy Preparations*

Diagnosis	Antral length lesser curvature (cm) A	Antral length greater curvature (cm) B	Product lesser and greater cur- vature (A × B) (cm ²) C	Antral mucosal volume uncor- rected (ml) D	Submucosal volume (% of uncorrected antral volume) E	Antral mucosal volume corrected (ml) (D-E) F
Recurrent duodenal ulcer	6.0	9.0	54.0	10.5	15.50	8.87
Recurrent duodenal ulcer	6.0	8.5	51.0	14.2	15.02	12.07
Prepyloric ulcer	6.5	7.75	50.4	14.0	38.50	8.61
Prepyloric ulcer	4.0	3.5	14.0	3.9	6.67	3.64
Prepyloric ulcer	6.0	5.0	30.0	5.0	5.00	4.75
Gastric ulcer	5.0	7.0	35.0	6.5	15.20	5.51
Gastric ulcer	10.0	11.0	110.0	28.0	31.10	19.29
Gastric ulcer	6.0	8.0	48.0	10.5	18.95	8.51
Gastric ulcer	8.0	9.0	72.0	11.5	8.70	10.50
Gastric ulcer	9.0	10.0	90.0	13.1	5.80	12.30
Early gastric cancer	7.0	10.0	70.0	11.0	10.00	9.90

the stripped mucosa also includes submucosal tissue the proportion of mucosal and submucosal tissue was determined from three 5 µm thick tissue blocks taken from the stripped mucosa, using the point counting technique (1).

The results are seen in Table 1. A significant positive correlation ($P < 0.001$) with a coefficient of correlation of 0.9297 was found between the product of the antral length along the lesser and greater curvatures and the corrected antral mucosal volume. The linear equation and construction line of regression between these two variables are shown in Fig. 1.

Measurement of the antral length can be performed during operation with the stomach in situ using either a pH electrode to establish the border between the pyloric and fundic mucosae or the border can be estimated by microscopic examination of step wise biopsies taken from the pyloric ring and orally along the lesser and greater curvatures.

References Nielsen H O, Halten S & Lorentzen M. *Acta path microbiol scand Sect A* 88: 255-261, 1980.

ADVICE TO AUTHORS

Usually only articles submitted by Scandinavian authors will be accepted, but the Editorial Board may invite contributions from authors outside Scandinavia.

Submission of a manuscript for publication in this Journal will be held to imply that the work is original, that it has not been published elsewhere and that, if accepted, it will not be published in any other journal without the Editor's written permission. Contributions should usually be in English, but papers in French or German can also be accepted (with English summaries).

The Editorial Board takes no responsibility for contents of or views implied or expressed by the

manuscripts should generally not exceed 4 printed pages and not more than 5 pages of illustrative material. They must contain a summary in English not exceeding 200 words. *Brief reports* for immediate publication must not exceed $1\frac{1}{2}$ printed pages. Such reports will be published as soon as possible after receipt. Manuscripts will be reviewed by appropriate experts. Since manuscripts will not be insured against loss or damage, contributors are expected to retain duplicate copies of all material submitted for publication. Only illustrations of reasonable technical standards will be accepted. If the limit of pages stated above is exceeded and if corrections in the proof are against the manuscript or the tabular and illustrative material unusually extensive and time consuming.

CONTENTS

Vol 88A Fasc 6 1980

Studies on the rat liver following iron overload Electron microscopical and histochemical investigation after iron depletion <i>Rolf Hulicrantz Bengt Arborgh Romulad Wroblewski and Jan L E Ericsson</i>	341
Comparative single cell and flow DNA analysis in aspiration biopsies from breast carcinomas <i>G Auer and B Tribukait</i>	355
Bronchiolar epithelial lesions induced in the premature rabbit neonate by short periods of artificial ventilation <i>R Nilsson Gertie Grossmann and B Robertson</i>	359
The effect of fixation and trypsinization on the immunohistochemical demonstration of intracellular immunoglobulin in paraffin embedded material <i>Marianne Jacobsen Per P Clausen and Susanne Smidth</i>	369
Enzyme cytochemistry and immunohistochemistry in monoclonal gammopathy and reactive plasmacytosis <i>Preben Johansen and Mogens Krogh Jensen</i>	377
The antral gastrin producing cells in duodenal ulcer patients A density study before and during treatment with cimetidine <i>H Overgaard Nielsen K Birger Jensen and L A Christiansen</i>	31
<i>In situ</i> identification of inflammatory cells in malignant non lymphoid human tumours <i>J L Svenesvig</i>	31
Ultrastructure of the tail stump sperm defect in the bull <i>Erik Blom and Aksel Birch Andersen</i>	35
Late effects of colchicine on the bursa of Fabricius after neonatal application on the anal lips of chickens <i>Timo Romppanen and Tapani E Sorvari</i>	40
<hr style="width: 10%; margin: 0 auto;"/>	
<i>Correspondence</i>	}
Histologic typing of breast cancer <i>Louis Jacques van Bogaert</i>	41:
<i>Folke Linell Otto Ljungberg and Ingvar Andersson</i>	41:
<hr style="width: 10%; margin: 0 auto;"/>	
<i>Brief Report</i>	
Estimation of the volume of human antral mucosa by measuring the antral length along the lesser and greater curvature <i>H Overgaard Nielsen</i>	417

